ENERGY AND THE ENVIRONMENT

Abbas Ghassemi, Series Editor

HYDROELECTRIC ENERGY

Renewable Energy and the Environment

Bikash Pandey

Ajoy Karki

CRC Press
Taylor & Francis Group

HYDROELECTRIC ENERGY

Renewable Energy and the Environment

ENERGY AND THE ENVIRONMENT

SERIES EDITOR

Abbas Ghassemi

New Mexico State University

PUBLISHED TITLES

Hydroelectric Energy: Renewable Energy and the Environment
Bikash Pandey and Ajoy Karki

Geologic Fundamentals of Geothermal Energy
David R. Boden

Introduction to Bioenergy
Vaughn Nelson and Kenneth Starcher

Introduction to Renewable Energy, Second Edition
Vaughn Nelson and Kenneth Starcher

Environmental Impacts of Renewable Energy
Frank R. Spellman

Geothermal Energy: Renewable Energy and the Environment, Second Edition
William E. Glassley

Energy Resources: Availability, Management, and Environmental Impacts
Kenneth J. Skipka and Louis Theodore

Finance Policy for Renewable Energy and a Sustainable Environment
Michael Curley

Wind Energy: Renewable Energy and the Environment, Second Edition
Vaughn Nelson

Solar Radiation: Practical Modeling for Renewable Energy Applications
Daryl R. Myers

Solar and Infrared Radiation Measurements
Frank Vignola, Joseph Michalsky, and Thomas Stoffel

Forest-Based Biomass Energy: Concepts and Applications
Frank Spellman

Solar Energy: Renewable Energy and the Environment
Robert Foster, Majid Ghassemi, Alma Cota,
Jeanette Moore, and Vaughn Nelson

HYDROELECTRIC ENERGY

Renewable Energy and the Environment

Bikash Pandey
Ajoy Karki

CRC Press
Taylor & Francis Group
Boca Raton London New York

CRC Press is an imprint of the
Taylor & Francis Group, an **informa** business

CRC Press
Taylor & Francis Group
6000 Broken Sound Parkway NW, Suite 300
Boca Raton, FL 33487-2742

Printed on acid-free paper
Version Date: 20160706

International Standard Book Number-13: 978-1-4398-1167-2 (Hardback)

Library of Congress Cataloging-in-Publication Data

Names: Pandey, Bikash, author. | Karki, Ajoy, author.
Title: Hydroelectric energy : renewable energy and the environment / Bikash Pandey and Ajoy Karki.
Description: Boca Raton, FL : CRC Press, 2017. | Series: Energy and the environment | Includes bibliographical references and index.
Identifiers: LCCN 2016017621 | ISBN 9781439811672 (hardcover : acid-free paper)
Subjects: LCSH: Water-power. | Hydroelectric power plants--Environmental aspects. | Water resources development.
Classification: LCC TK1081 .P34 2017 | DDC 621.31/2134--dc23
LC record available at https://lccn.loc.gov/2016017621

Visit the Taylor & Francis Web site at
http://www.taylorandfrancis.com

and the CRC Press Web site at
http://www.crcpress.com

Contents

Preface

Hydropower generates over 1000 GW globally, producing more than 4000 TWh each year, around 16.5% of the world's total electricity. This makes it by far the largest source of renewable electricity when the world is racing against time to combat climate change by greening its energy supply. Although water wheels were utilized by humans as a source of energy since antiquity, industrial-scale hydropower required the development of modern turbines starting in the first half of the nineteenth century, building on fundamentals of hydraulic machines spelled out by the great mathematician, Euler, half a century earlier. Hydroelectricity saw a period of rapid growth starting late in the nineteenth century with the discovery and proliferation of alternating current, progress in manufacturing and metallurgy, and breakthroughs in civil engineering, which enabled the construction of large dams. By 1940, over 1500 dams supplied 40% of the electricity in the United States. Construction of new hydroelectric projects slowed in the 1960s when concerns began to grow about the social and environmental challenges associated with large dams.

Together with other renewable energy technologies, hydroelectricity has a critical role to play in the ongoing global transition to clean energy. Although starting from a small base and currently contributing only a small fraction to the world's electricity supply, wind and solar energy are growing rapidly, already adding more gigawatts each year than hydroelectricity does. In addition to its own generation, hydroelectricity helps the growth of all renewables by providing energy storage as power grids around the world attempt to integrate ever higher percentages of variable renewable energy. Investment into pumped storage hydroelectricity is expected to grow alongside other renewables.

Hydroelectricity provides an alternative to new investment in coal-based generation for industrializing countries whose power needs are growing rapidly. Coupled with other renewables, hydroelectricity provides these countries a pathway to low-carbon growth. Increased investment into small hydropower features prominently in planned climate actions of most countries both for supplying their grids and for providing electricity in regions of the countries that remain under-electrified. Where resources exist, micro-hydro often provides the lowest cost source of power to remote communities.

The bulk of this book covers the engineering disciplines of civil engineering, hydrology, hydraulics, and mechanical and electrical engineering as they relate to hydroelectricity. The authors, Bikash Pandey and Ajoy Karki, have written different chapters based on their areas of expertise. In addition to technical subjects, they have explored the economics of hydroelectric projects, social and environmental considerations, and engagement with communities necessary for their development.

Chapter 1 probes the history of water power, the development of hydroelectricity, and its continuing relevance today. Chapter 2 goes into the basic physics of how falling water generates power, and describes the main types of modern hydroelectric systems in use today and their major components. Chapter 3 describes how site selection and feasibility studies are carried out. Chapters 4 through 8 explain the principles behind how civil structures of hydroelectric plants are designed, including the intake, headrace, gravel trap, settling basin, forebay, penstock, and the powerhouse. Chapters 9 through 12 explore the design of different types of hydraulic turbines, which are in use and being developed. Chapter 13 focuses on the electrical aspects of hydroelectricity including the workings of generators, controllers, and power transmission and distribution. Chapter 14 discusses the economic analysis of infrastructure projects. Chapter 15 describes the social and environmental challenges of hydroelectric project and participatory processes required for sustainable development.

Taylor & Francis
Taylor & Francis Group
http://taylorandfrancis.com

Acknowledgments

We are indebted to our colleagues at Winrock International and Sanima Hydro & Engineering (P.) Ltd., Nepal, for the insight and feedback they have provided. We especially acknowledge the contribution by Nirmal Raj Joshi, senior engineer, Sanima Hydro & Engineering (P.) Ltd., who proofread the civil engineering chapters and assisted us in preparation of questions at the end of their chapters. Similarly, Chandan Shakya, civil engineer, Sanima Hydro & Engineering (P.) Ltd., has drafted the majority of drawings in this textbook. Last, and far from least, we would like to express our unreserved gratitude to our respective families that have put up with the dozens of weekends we spent working on the book.

Authors

Bikash Pandey is the innovations lead for clean energy at Winrock International, based in Washington, DC. His work experience encompasses 25 years in policy design, review, and implementation of a range of clean/renewable energy and climate change projects in Asia, Africa, and Latin America. His current areas of work include clean energy finance, low emission development, last mile electrification through mini-grids, community-based electrification, and powering agriculture. Mr. Pandey is one of the pioneers of mobilizing independent power producer (IPP) investment into hydroelectricity and establishing a micro-hydro sector in Nepal to electrify rural communities. He has designed hydropower programs and trained practitioners in over a dozen countries in the proper design of hydropower systems. Mr. Pandey is also actively involved in global discussions around sustainable development of hydroelectricity. He participated as a member of the forum that set up the World Commission on Dams. Mr. Pandey holds an MS degree from the Energy and Resources Group at the University of California, Berkeley, and an SB degree in electrical engineering from MIT.

Ajoy Karki is a water resources engineer with over 22 years of experience in management, design, and studies of hydropower, rural electrification, and renewable energy projects. He has worked as a hydropower engineer in 15 countries covering South Asia, Central Asia, and East and West Africa. He completed his MS degree in hydraulic engineering at IHE-UNESCO, The Netherlands, in 2000. He also holds degrees in civil engineering from the University of Iowa and physics (cum laude) from Coe College, Iowa. Mr. Karki has published a number of papers as both the lead author and a coauthor in the *South Asian Energy Journal*, Pakistan; Asian Institute of Technology (AIT), Thailand; World Resource Foundation, UK; and Earthscan, UK. He has also provided extensive training courses in hydropower design in various countries in Asia and Africa, and has prepared training manuals and guidelines such as the *Manual for Survey and Layout Design of Private Micro-Hydropower Plants* for International Centre for Integrated Mountain Development (ICIMOD), Nepal (1999; coauthor).

Taylor & Francis
Taylor & Francis Group
http://taylorandfrancis.com

1 Development of Hydropower

1.1 ANCIENT HISTORY OF WATERPOWER

The history of waterpower dates back more than 2000 years to the use of waterwheels by Greeks and Romans, placed along streams for grinding grains and for irrigation. This first development likely took place during the technically advanced and scientifically minded Hellenistic period between the third and first centuries BC. The British historian of technology M. J. T. Lewis [1] dates the appearance of both the vertical-axle and horizontal water mills to third century BC with Byzantium and Alexandria as the likely places of their invention.

For the first time in human history, waterwheels provided people with the ability to use an inanimate power source for mechanized agricultural processing and basic industrial applications. The smallest grain-grinding water mills of around half a horsepower would mill around 10 times as fast as traditional hand-powered quern-stone milling. The labor savings could be significant. A modest two to three horsepower mill saved the time of 30 to 60 women doing the tedious task of grinding grain by hand [2].

1.1.1 Waterwheel Designs from Ancient Times

Three main water power designs from antiquity have proven durable through the centuries and can be seen today—sometimes still in use in the same or slightly modified form or relatively recently abandoned for more sophisticated machines.

a. Horizontal Norse wheel. The simplest design from ancient times is the vertical shaft Norse wheel, which continues to operate to this day—often with minimal improvement to the ancient technology—in tens of thousands mountainous, rural areas from West Asia to Southeast Asia next to streams where vertical drops of 3–5 m are easily available. Water flows ranging from 30–200 liters per second (lps) are directed from streams along a short canal to develop the drop. The water is accelerated down a steeply inclined wooden chute from the top canal and hits paddles, which are placed obliquely on a wooden hub below the millhouse with a significant velocity. The horizontal runner is connected through the vertical shaft to rotate the top stone grind wheel as shown in the diagram below. This arrangement enables the runner to directly drive the grindstone at a speed of around 100–150 revolutions per minute (RPM) without the need for any gearing. The mills make use of the 1–2 horsepower (hp) produced [3] to grind maize, wheat, millet, barley, and other grains into flour for local consumption (Figure 1.1).

   Although it would seem that this straightforward design should have been the first to be developed and disseminated within the Roman Empire, records covered to date do not show this to be the case. Instead, Wikander [4] notes that there are no certain records of the horizontal wheel technology until the seventh century AD.
b. Undershot waterwheel. A description of the first undershot waterwheels is provided by the first century BC Roman architect and chronicler of Roman technology, Vitruvius. He describes the waterwheel as having its lower end immersed in the watercourse so that the paddles could be driven by the velocity of the running water. Vitruvius's account is of a geared watermill to mill grain that combines two separate Greek inventions of the toothed gear and the waterwheel (Figure 1.2).

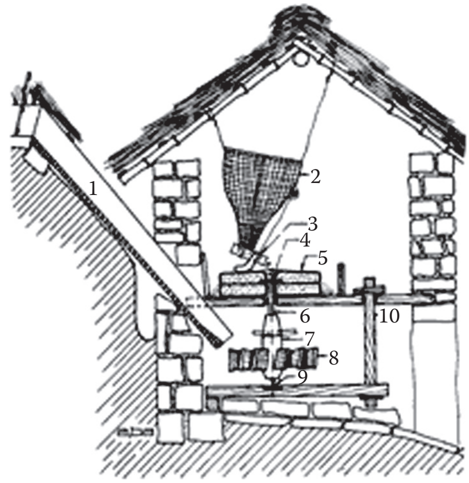

1 Chute, delivering the water to the side of the wheel behind the shaft
2 Hopper (basket)
3 Bird (vibrator to keep the grain moving)
4 Rynd (forged metal piece)
5 Grinding stones
6 Shaft, metal
7 Hub, wood (thick shaft)
8 Wheel or tirl, with obliquely set paddles on thick shaft
9 Metal pin and bottom piece
10 Lever, lifting device to adjust gap between grinding stones

FIGURE 1.1 Traditional horizontal water mill. (From Saubolle, B. R., and Bachmann, A., *Mini Technology I*, Sahayogi Press, Kathmandu, 1978.)

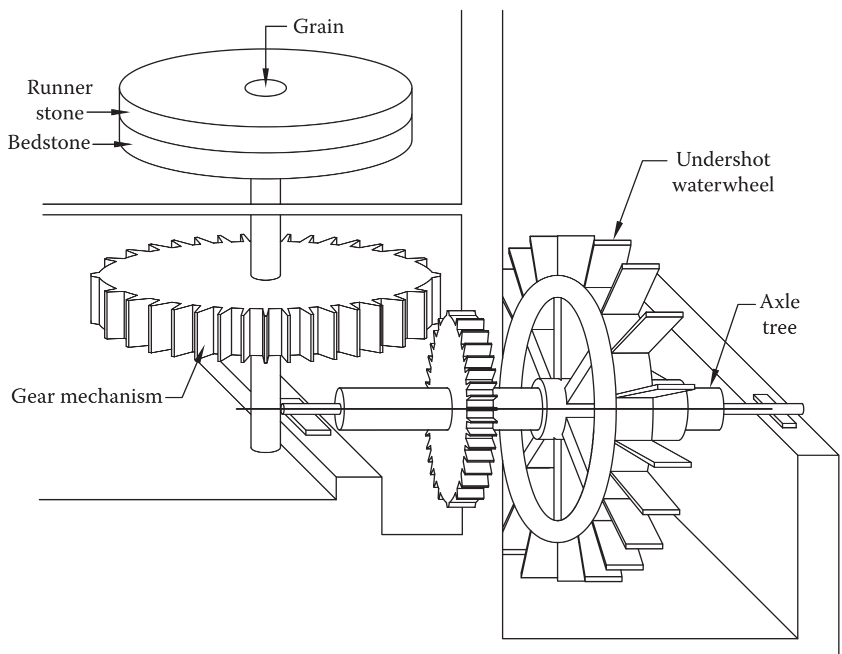

FIGURE 1.2 Roman water-powered grain mill (Vitruvius).

Being a river current machine, the undershot waterwheel gets all of its power from the velocity of the stream and none from water falling from any height. This limits the total power available from an undershot wheel typically to a few horsepower.* As explained in Chapter 9, the power available from the river current is modest compared to utilizing the energy in falling water. For example, the kinetic energy from a stream flowing at 1.5 m/s is equivalent to the potential energy of water dropping only half a meter. The undershot waterwheel would thus require a large "sweep area"—that is, large paddles as well as fast flow of water to produce more than a few horsepower.

Islamic engineers added a number of innovations to overcome the limitations of undershot wheels and significantly increased their output power. They mounted waterwheels on the piers of bridges to take advantage of increased river flow and made adjustments for them to operate at varying water depth. This overcame the problem of paddles ceasing to be immersed in the lower water levels in the dry season when water wheels were fixed to the banks of rivers. They also mounted undershot wheels on the sides of ships moored midstream to achieve this same effect. There are reports that in the 10th century ship mills made of teak and iron installed on the rivers Tigris and Euphrates could produce 10 tons of flour every day.†

Arab engineers used undershot waterwheels to harness energy from the flow of a river for irrigation and water supply by powering a *noria*‡ to lift water into an aqueduct at the top of the wheel. The waterwheel did not drive any gears or millstones in the case of a *noria*, which typically lifted water with pots attached to its outer rim. The diameter of waterwheels driving the *noria* could be as high as 50–80 feet (15–25 m), providing a corresponding level of lift. *Norias* constructed by the 10th century could lift more than 40 lps of water to these heights.

c. Overshot and breast shot wheels. The overshot and breast shot waterwheels were extensively used by the Greeks and Romans for waterpower. These horizontal-axle machines were significantly more powerful than the undershot wheel because they were able to utilize potential energy as the weight of water dropped from a height in addition to kinetic energy from its velocity as the water hit the paddle (Figure 1.3). This additional power output of the waterwheel, which could easily add up to several kilowatts per wheel, was used for grain and saw milling. The Romans also used waterwheels in mining projects—typically reverse overshot waterwheels to dewater deep underground mines.

The best known of the Roman water mills is Barbegal located in present day Arles in Southern France where around the second century AD [4] a series of overshot waterwheels reportedly powered a total of 16 flour mills to grind sufficient grain for an estimated 12,500 individuals [5]. The waterwheels, each of a diameter of around 2.1 m and width of 0.7 m, were constructed in two rows of cascades of eight, one placed below the other as shown in Figure 1.4. Hodge quotes in his article in *Scientific American* (1990) an estimation by Robert Sellin of the University of Bristol, that the total output power of the waterwheels must have been around 2 kW each derived from Sellin's approximation of the total flow in the aqueduct to be 0.3 m^3/s and an efficiency of each waterwheel to be 65%. This estimation is not unreasonable and would put the total cumulative mechanical power output of the 16 waterwheels at around 32 kW—a significant amount of power at a single location for the times.

* From Chapter 12, $P_s = 0.5\rho A_s V_s^3 C_p$ where ρ is the density of water = 1000 kg/m^3, A is the sweep area, V is the water velocity, and C is the coefficient of performance or the efficiency. For example, if the river current is 1.5 m/s, and C is estimated at 20% for a rudimentary machine, the shaft power would be 330 W for every square meter of sweep area where the sweep area is the area of the wheel pushed by the current and would roughly be the area of each paddle.

† http://home.swipnet.se/islam/articles/HistoryofSciences.htm

‡ *Noria* is an Arabic word for a machine using buckets attached to a wheel or a rope, which is used to lift water into an aqueduct and can be powered by animals, wind, or a river.

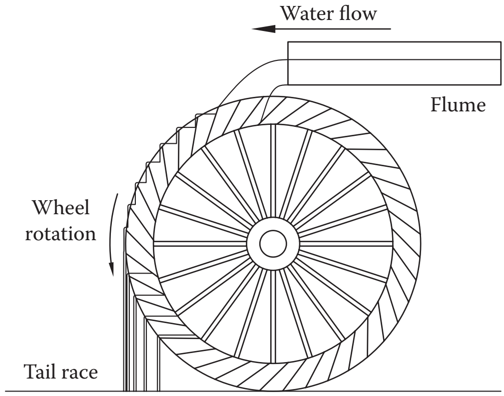

FIGURE 1.3 Overshot waterwheel.

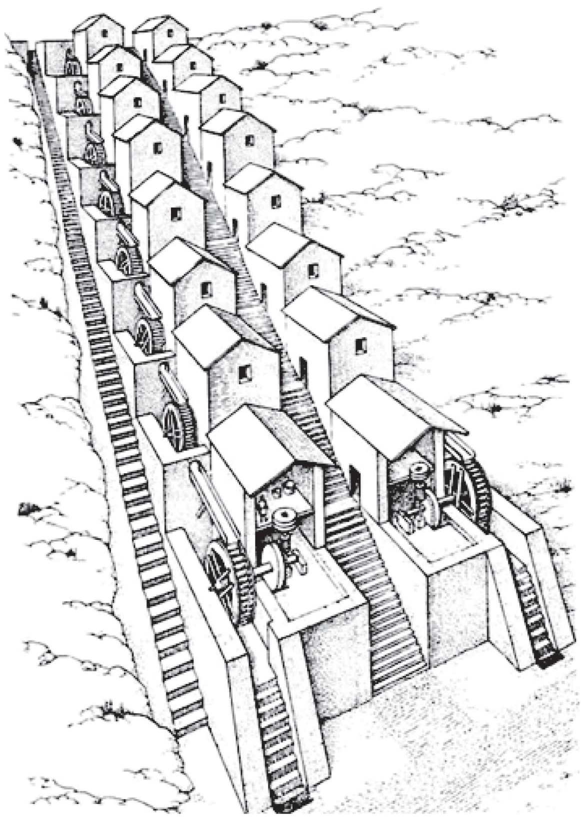

FIGURE 1.4 An artist's representation of water mills of Barbegal. (Courtesy of Connexions, http://cnx.org/contents/bd6bf3d4-a285-48fd-bec9-08aa607cd84e@1.)

Scholars had until recently sought to explain what appeared to be the relatively slow spread of waterpower in antiquity with the dominant discourse that waterpower was not widely used within the Greek and Roman empires on account of the availability of low-cost labor, both slave and free. This view was supported by the writing of Vitrivius, which listed waterpower among those "machines which are rarely employed" when he was describing technological development late in the first century BC. Archaeological findings, such as the Barbegal site in the 1930s, and research particularly after the 1980s point to larger scale adoption, particularly of vertical waterwheels for milling, than had originally been thought. Wikander writes, for example, that the "advent and triumph of the watermill" was already in full swing in different parts of the Roman Empire by the first century AD with some cities having a collegium of water millers by around 200 AD [4]. By the end of the first millennium, water-powered mills for grain, timber, and stone cutting were running in most large settlements in Europe. The Domesday Book recorded 6500 mills in England alone.

1.1.2 Waterpower in Other Parts of the World in Antiquity

There is evidence that water mills spread to parts of the world outside the Roman Empire starting around the third century. The earliest water mills found in Iraq, Arabia, and Iran have been dated between the third and eighth centuries, and there are references to travelers from the Roman Empire engaged in the construction of water mills and baths in India around 325 AD [4]. There is also evidence that applications of waterpower were developed independently outside the Roman Empire.

Some writers have suggested that waterpower was used more extensively in China in ancient times than in Europe and to power more sophisticated applications. This includes the British scientist, historian, and sinologist Joseph Needham, who is known for his writings on the history of Chinese science. Roger Hansen, a current writer on the subject of water mills, summarizes this view as follows: "But while for centuries Europe relied heavily on slave- and donkey-powered mills, in China the waterwheel was a critical power supply … Both the trip hammer and edge runner were not used in Europe until eight centuries later."* These writers have suggested that waterpower was being used widely in China to power trip hammers to mill rice, to grind mineral ore, and to power large bellows to supply oxygen to burn coal and charcoal to smelt ore.

Wikander [4, p. 394] contests the view that hydropower was used more extensively in China than in Europe, arguing that although there is evidence of water-powered trip hammers and bellows being used in China, no certain evidence exists for water-powered grain mills there until the fifth century. He also presents evidence that cam-operated saws and trip hammers were in use in Europe, including water-powered marble saws in Northern Gaul and water-powered stone saws in Asia Minor during the fourth century AD. Lewis [1] presents additional evidence of the use of cam-operated trip hammers in Europe during this period used for pounding grain to flour.

Arab engineers adopted the waterwheel as early as the seventh century and both improved upon it and spread it across the Islamic world for industrial applications, including for grain milling, saw milling, sugar mills, hulling rice, and for lifting water and crushing ore. By the 11th century, it is thought that industrial watermills were in widespread use throughout the Islamic world from North Africa to the Middle East and Central Asia.

Additional evidence in the form of more accurate records of historical development of applications of waterpower in different parts of the world is likely to surface in the coming years given the attention that researchers have recently focused on this subject.

1.2 WATERPOWER'S CONTRIBUTION TO THE INDUSTRIAL REVOLUTION

Waterwheel designs evolved, both in efficiency and size, to meet the accelerated growth in power requirements with the onset of the industrial revolution.

Its ability to produce higher power output meant that the vertical wheel, particularly the overshot wheel, was used to supply motive power to a variety of industrial processes. Between 1000 AD and 1800 AD, a range of applications had already been developed to be powered by vertical waterwheels, including to full cloth, produce hemp, saw wood, pump water, bore pipes, crush ore, and tan leather. As a result of its ability to produce high power output, the vertical waterwheel became the first choice in European heavy industry by the end of the medieval period and remained the mainstay well into the 19th century [2].

* http://www.waterhistory.org/histories/waterwheels/

During the Middle Ages, large wooden waterwheels were developed with a maximum power output of about 50 hp. The modern, large-scale waterwheel owes its development to the British civil engineer John Smeaton, who first built large waterwheels out of cast iron around 1759.* During the industrial revolution, large waterwheels generated tens of kilowatts of power to run cloth mills and mining operations. The largest waterwheels constructed in the 1800s were more than 20 m in diameter and produced several hundred kilowatts of power.

Alongside the steam engine, waterpower played an important role in powering the Industrial Revolution. It gave impetus to the growth of the textile, leather, and machine-shop industries in the early 19th century. Although the steam engine had already been developed, waterpower remained in high demand where resources were available because coal was scarce and difficult to transport and wood was often unsatisfactory as a fuel. Availability of waterpower became a major determinant in the development of early industrial cities in Europe and the United States until the opening of the canals provided cheap coal around the middle of the 19th century. Because waterpower resources were not evenly distributed, it had a major influence on the location of industry and population centers in Europe and America. Availability of waterpower determined the location of textile mill towns in the United States, for example.

1.2.1 Waterwheel to Water Turbine

The waterwheel was used, along with windmills, for close to 2000 years as the first major inanimate prime mover to provide power for industrial applications. This was challenged by the steam engine after James Watt patented the steam engine in 1781. The steam engine gained quick acceptance for industrial applications to expand many of the same sectors that had first been established due to availability of waterpower. In addition, steam engines found application in new sectors, such as for traction engines to pull locomotives, where hydropower could not be used. The steam engine overtook waterwheels as the dominant prime mover in the initial phase of the industrial revolution due to two main reasons: (a) its advantage over waterpower of being able to be sited where it was needed and wherever coal and wood fuel could be transported and (b) the power output of steam engines was quickly scaled up, increasing from the initial patented unit of around 10 hp to 10,000 hp within the relatively short span of a century.

The development of the modern water turbine, starting in the early 19th century and around 50 years after the steam engine, allowed for the development of hydropower as a large-scale source of power to compete with steam engines wherever water resources were available. The turbine, named so by French engineer Claude Burdin, was developed to efficiently extract energy from water through the use of scientific principles, manufacturing methods, and advances in metallurgy developed during the industrial revolution. Using several designs, the modern water turbine was able to generate power efficiently by exploiting hydropower resources covering a large range of head and flow situations.

The waterwheel had been able to make use of larger heads of water and higher water flows by increasing its diameter and width. This put a practical limit on pressure heads and water flows and corresponding output horsepower, which could be utilized for power generation. The large-size wheel also resulted in low speed, which required significant gearing up, especially for electrical power generation. Penstock pipes, which could channel large heads of water to make the entire pressure available right at the turbine, allowed a relatively small runner wheel to transfer a large amount of power to its shaft by rotating at high speed. The first practical modern turbines, known as reaction turbines, were developed to extract power directly from water under pressure in the period 1827–1837, building on the mathematical fundamentals of operation of hydraulic machines developed by Euler in the 1750s. This breakthrough was followed by the development of impulse turbines, which were able to extract power efficiently from high-velocity jets of water hitting the turbine runner. Table 1.1 lists timelines for the development of the most well-known designs of modern

* http://www.ieahydro.org/What_is_hydropower's_history.html

TABLE 1.1
Breakthroughs in Hydropower Development

1827	French engineer Benoit Fourneyron develops a high-efficiency (80%) outward flow, centrifugal water turbine in which water was directed tangentially through the turbine runner, causing it to spin. Fellow French engineer Jean V. Poncelet designs an inward-flow turbine that uses the same principles.
1848	James B. Francis, an English engineer working in the United States, improves on these designs to create a highly efficient inward flow reaction turbine. The Francis has established itself as the most widely used hydropower turbine in the world today.
1878	Lester Allen Pelton develops the Pelton turbine, improving over the Knight wheel, the first efficient impulse turbine design using the split double cup bucket design to convert kinetic energy of water to horsepower, to substitute for steam engines used for gold mining in California.
1880	Grand Rapids, Michigan: Sixteen brush-arc lamps are powered using a water turbine at the Wolverine Chair Factory in the first industrial use of hydropower to generate electricity.
1881	Niagara Falls, New York: A brush dynamo is connected to a turbine in Quigley's flour mill to generate DC power to power machinery and light city street lamps.
1889	Oregon City, Oregon: Willamette Falls station, the first AC hydroelectric plant, transmits single phase power 13 miles to Portland at 4000 volts and steps it down to 50 volts for distribution.
1891	Frankfurt on Main, Germany: The first three-phase hydroelectric system is used for a 175 km, 25,000 volt demonstration line from a plant at Lauffen.
1898	Decew Falls 1 (St. Catherines, Ontario, Canada) transmits power at 22,500 volts, 66 2/3 Hz, two-phase, a distance of 56 km to Hamilton, Ontario.
1914	S. J. Zowski develops a high specific speed reaction (Francis) turbine runner for low head applications.
1919	Viktor Kaplan demonstrates an adjustable blade propeller turbine runner at Podebrady, Czechoslovakia. British company Gilkes patents the Turgo turbine providing an alternative to Francis turbines for small hydropower <10 MW range.
1920	Hydropower provides 25% of U.S. electrical generation. Federal Power Act establishes Federal Power Commission authority to issue licenses for hydro development on public lands.
1929	The Rocky River Plant at New Milford, Connecticut, installs the first major pumped storage hydroelectric plant.
1933	The Tennessee Valley Authority is established.
1937	Power is generated at Hoover Dam, Arizona/Nevada. Bonneville Power Administration is established. Bonneville Dam, the first Federal dam, begins operation on the Columbia River.
1940	1500 hydroelectric facilities provide 40% of electrical generation in the United States. Hydropower capacity tripled since 1920.
1941	Power is generated at Grand Coulee power plant, Washington—the largest hydroelectric plant in the world at 6800 megawatts installed capacity.
1950	The Soviet Union begins construction of large hydropower plants as "Great Building Sites of Communism"—part of a massive postwar industrialization project. Hydroelectric stations completed include Zhighuli (2320 MW, completed 1957) and Volga (2583 MW completed 1961).
1968	The U.S. Wild and Scenic Rivers Act protects rivers in their natural state by excluding them from consideration as hydroelectric power sites.
1974	The Fish and Wildlife Coordination Act ensures equal consideration of fish and wildlife protection in the activities of federal agencies.
1983	Power is generated at Itaipú power plant, Brazil/Paraguay, becoming the largest hydroelectric project in the world at 12,600 megawatts installed capacity.
1986	The Electric Consumers Protection Act amended the Federal Power Act to remove public preference for relicensing actions and gives equal consideration to nonpower values (e.g., energy conservation, fish, wildlife, recreation, etc.) as well as to hydropower values when making license decisions.
1998	The World Commission on Dams is formed as a global multistakeholder process in response to social and environmental conflicts around the building of dams to provide guidelines for better development of water projects. It publishes "Dams and Development: a New Framework for Decision Making" in November 2000.
2008	The Three Gorges Dam project in China, the largest hydroelectric power station in the world goes into operation (final capacity 22,500 MW reached in 2012).

water turbines developed in the 19th and early 20th centuries to efficiently utilize hydropower sites with a wide range of head and flow specifications.

1.2.2 Hydroelectricity

Hydropower grew dramatically all over the world with the invention of the electric generator and particularly after it became possible to generate and transmit alternating current (AC) starting around 1889. The growth in demand for electricity, improvement in turbine efficiency, rapid increase in power output of hydropower turbines, and the civil engineering know-how to build large dams all combined to tremendously expand the role of hydropower in global electricity production. By 1920, hydroelectric plants were generating 25% of the all electricity consumed in the United States, growing to 40% by 1940. The rates of growth of hydropower began to decline starting in the 1960s, when environmental concerns about the damming of rivers, inundating large tracts of land, and displacement of people associated with building large dams slowed the construction of dams in OECD countries. Construction continued to expand in emerging markets in Asia, Latin American, and Africa. Hydropower construction worldwide grew at around 2.7% in 2015 [6].

Table 1.1 lists the breakthroughs in hydropower development, which followed after documentation by French hydraulic and military engineer Bernard Forest de Bélidor in the mid-1770s, in four volumes of *Architecture Hydraulique*, the state of the art in vertical-axis and horizontal-axis waterwheels. Technical progress starting around the first quarter of the 19th century, made it possible for hydropower to establish itself as a major global source of electricity generation within a 100-year period.

Hydropower generates more electricity than any other renewable energy resource with an installed capacity of 1064 GW in 2015 with 3940 TWh generated worldwide and accounting for 16.6% of total global electricity production in that year [7].

Although most countries around the world use hydropower, its use is uneven. This is a function of how hydropower resources are distributed, countries' investment choices in the power sector as well as their ability to mobilize resources. Table 1.2 lists the countries with the largest hydropower production in the world [8].

TABLE 1.2
Largest Producers of Hydropower

	TWh/Year	% of World Generation	% Hydro in Total Domestic Power Supply
People's Republic of China	699	19.6	14.8
Brazil	428	12.0	80.6
Canada	376	10.5	59.0
United States	345	9.7	7.9
Russian Federation	168	4.7	15.9
India	131	3.7	12.4
Norway	122	3.4	95.3
Japan	92	2.6	8.7
Venezuela	84	2.3	68.6
Sweden	67	1.9	44.3
Rest of the world	1054	29.6	13.6
World	3566	100	16.1

Source: International Energy Agency (2013) using 2011 data.

Countries such as Norway, Brazil, Venezuela, and Canada generate the majority of their electricity from hydropower. This is also true of a number of developing countries, such as Laos, Bhutan, Ghana, Ethiopia, Democratic Republic of Congo, Mozambique, Uganda, and Nepal. However, the development of the hydropower sector in developing countries remains small compared to the full potential.

1.2.3 Size Classification

Hydropower plants are often classified based on their size or installed capacity. These classifications, which vary between countries, are used by governments as a basis for their policies to provide tax benefits, feed in tariff to the grid, subsidies, and environmental regulations. This textbook uses the definition given in Table 1.3.

The main differences in application and design of hydropower systems by size classification are as follows:

1. Micro hydropower plants provide electricity to remote rural communities. The communities they serve are generally too remote to be supplied economically by the electricity grid. The engineering design for micro-hydro systems tend to be simple and standardized as far as possible for ease of operation and maintenance by local communities with limited technical support from outside.
2. Mini-hydro and small hydro projects can either supply isolated rural towns or they can be developed to supply power to the grid. Hydropower projects that sell power to the grid are engineered and constructed to be financially viable and to provide commercial returns on investment.
3. Small hydropower plants and some in the medium hydropower range are designed as "run-of-river" (R-o-R) projects. R-o-R projects use a weir to divert water to the intake but do not store water. They tend to have fewer environmental impacts than projects with dams and reservoirs.
4. Large hydropower plants typically involve the construction of a dam to create a reservoir. Some reservoirs are small and are used for storing water to supply daily or weekly peak loads. Other reservoirs are large enough to store water during the rainy months to be available during the dry season and in some cases over multiple years to meet needs in dry years. Reservoirs often serve multiple functions, including irrigation, flood control, and recreation in addition to supplying water to power plants.

TABLE 1.3
Classification of Hydropower by Size

Classification	Size
Micro hydropower	Up to 100 kW
Mini hydropower	Between 100 kW and 1000 kW
Small hydropower[a]	Between 1 MW and 10 MW
Medium hydropower	Between 10 MW and 100 MW
Large hydropower	Larger than 100 MW

[a] Although 10 MW is often used as a threshold for small hydro, definitions are inconsistent across countries. For example, India and China consider small-scale hydro to be ≤25 MW and the United States <30 MW.

Although the basic principles are the same for all hydropower systems, designs become increasingly more complex with size from an engineering perspective. Large hydropower projects often include large dams, underground structures for tunnels and powerhouses, automated control systems to regulate flows and power output as well as dedicated high voltage transmission lines to evacuate the power. Design standards are required to be much higher for larger projects involving dams because the risk of catastrophic failure in terms of loss of lives, property, and investments are potentially enormous. One example of such a high standard is that large dams are typically designed to safely convey extreme flood flows with a return period of 10,000 years or higher.

1.3 DRIVERS OF AND DETERRENTS TO HYDROPOWER DEVELOPMENT

Availability of powerful and efficient hydro turbines covering a range of low to high heads and engineering capability to design and build large dams contributed to rapid growth in the size of hydropower projects, making them the largest power-generating stations in the world by the 1930s. Starting from Western industrialized countries, the technology spread rapidly to Eastern Europe, Latin America, Asia, and Africa. It is estimated that some 50,000 large dams had been built by the end of the 20th century.*

Alongside technological achievements that led to unprecedented development of hydropower also came heated controversies around the construction of large dams. In industrialized countries, the concerns came mainly from (a) environmentalists concerned with damage to riverine ecosystems and riparian habitats and the resulting loss of species and biodiversity from interruption of river flows and flooding of wetlands and forests and (b) stakeholders who valued alternative economic and recreational activities on free-flowing rivers, such as fishing, whitewater rafting, and canoeing.

In developing countries, activists were critical of (a) the role of dams in the displacement of indigenous and local people, loss of biodiversity, and threat to livelihoods of riparian populations dependent on river fish and wetlands and (b) poor governance, corruption, and lack of transparency, leading to misuse of resources, absence of fair compensation to displaced people, and a general impoverishing of project-affected people to supply power to urban populations. These issues are discussed in more detail in Chapter 15.

These considerations led to the first changes in legislation starting in the 1960s in the United States: the Wild and Scenic Rivers Act (1968) and Fish and Wildlife Coordination Act (1974). Similar legislation was enacted in other industrialized countries to protect rivers from additional damming. In response to escalating international controversies over large dams, the World Commission on Dams (WCD) was established in May 1998 as a multistakeholder process that assembled the full spectrum of stakeholders, including representatives of people displaced by dams, environmental and nongovernmental organizations, hydropower companies, and associations of dam builders, multilateral financing organizations such as the World Bank and Asian Development Bank, and governments engaged in the building of large dams. The WCD has proposed guidelines and nonbinding recommendations to achieve better social, environmental, and economic outcomes from the construction of dams and improve their public acceptance.

The environmental controversies of the 1980s and 1990s surrounding large dams did slow down the rate of global hydropower development. Although hydropower continues to supply the largest source of renewable power globally, its growth has remained modest and has in recent years been surpassed by fast-growing new renewable energy technologies, such as solar PV and wind. REN21 2016 estimates that a total of 28 GW of new hydropower was constructed in 2015, an increase of 2.7% over the previous year to reach a total of 1064 GW. The same year saw 50 GW of new solar PV installed, recording a remarkable growth of 28% over the previous year to reach an installed capacity of 277 GW; similarly, 63 GW of new wind energy was installed with a growth of 17% to reach a total global capacity of 433 GW [7].

* http://www.internationalrivers.org/problems-with-big-dams

The countries with the largest installed hydropower capacity are currently China, Brazil, the United States, Canada, Russian Federation, and India, which together account for around 60% of the global capacity. China has around 28% of installed global capacity and also has the most active program of new hydropower construction [7]. Other countries with active hydropower investment programs include Brazil, Turkey, India, Vietnam, Malaysia, Canada, Lao PDR, Colombia, Ethiopia, Democratic Republic of Congo, Bhutan, Indonesia, the Philippines, Myanmar, Nepal, Uganda, Cambodia, Rwanda, and Burundi.

Small hydropower development has been less controversial and has grown relatively faster compared to large hydro. REN21 (2013) estimated that there was around 75 GW of small hydropower (<10 MW) installed around the world as of 2012 [7] and that the sector attracted investment of $5.9 billion in 2011 [6]. Investment into small, mini, and micro hydro projects has been driven in recent years by the fact that they have fewer environmental and social impacts compared to large hydro projects because they are mostly R-o-R and are often the least cost source of power to supply unelectrified remote communities.

Rapid growth in investment into variable renewable power has increased the need for energy storage for system stability. This has increased a trend for co-implementation of pumped storage hydro with solar and wind power. Pumped storage contributes around 145 GW to global capacity with an additional 2.56 GW invested in 2015 [7].

1.3.1 Climate Change

Global climate change has affected hydropower development in several ways. Persistent droughts resulting in reduced output from existing power plants have encouraged some governments to develop alternatives to hydropower generation. Kenya has accelerated investment into geothermal energy, for example, to reduce its reliance on hydropower from 65% of total capacity to 47% by 2015.* At the same time, a significant number of countries include ambitious hydropower targets, especially for small hydro, as part of their climate change mitigation action plans. Countries that have committed to specific targets to invest in hydropower as part of their commitment to combat climate change include Armenia, Austria, Bosnia Herzegovina, Brazil, Bulgaria, Burundi, Canada, China, Egypt, Ethiopia, Finland, France, Haiti, India, Indonesia, Italy, Japan, Korea DPR, Lebanon, Macedonia, Malawi, Malaysia, Morocco, Mozambique, Nepal, Nigeria, the Philippines, Portugal, Russian Federation, Rwanda, South Korea, Spain, Switzerland, Tajikistan, Thailand, Turkey, Uganda, and Vietnam [7].

Hydropower projects are a major beneficiary of carbon financing under the Clean Development Mechanism (CDM).† CDM was designed to provide financing to enable GHG lowering investments in developing countries to become financially attractive over lower cost fossil fuel options. Around one third of the projects registered under the CDM are hydropower projects, and this subsector has the largest share of Certified Emission Reduction credits (CERs) of any renewable energy technology.‡ There has been criticism that hydropower projects, particularly those installed in China and India, are not truly additional§ and should not qualify for carbon financing because the technology is already established and cost-competitive and investment would go forward with or without carbon financing.

Hydropower reservoirs in the tropics can, furthermore, be significant sources of greenhouse gases (GHGs), particularly methane and carbon dioxide from rotting vegetation and other organic matter at their bottom, and be a net contributor to global warming. In extreme cases, in hot climates where the reservoir surface is large compared to its energy production and the vegetation may not

* http://www.kengen.co.ke/sites/default/files/The%20Generator%20Issue%204_Final%202015.pdf
† http://cdm.unfccc.int
‡ www.cdmpipeline.org/ (April 7, 2013)
§ http://carbonmarketwatch.org/category/hydro-power/

TABLE 1.4
Active Micro Hydropower Programs

Country	Number of Systems	kW Generated	Beneficiaries	Programs
Afghanistan	5000	50,000	2.5 million	National Solidarity Program, GIZ/Integration, Remote Hydro Light
Nepal	2900	30,000	1.7 million	AEPC, RERL
Pakistan	340	20,500	290,000	AKRSP, PPAF
Sri Lanka	193	1870	35,000	RERED
Indonesia	63	2130	54,000	IBEKA
Peru	47	1568	30,000	Practical action

have been cleared prior to inundation, the GHG emissions per kilowatt-hour of electricity produced from hydropower can be comparable to that from a fossil fuel power plant or even higher [9].

1.3.2 Hydropower for Energy Access

More than 2 billion people, close to a third of the world's population, do not have access to electricity. In countries in which resources exist, hydropower has provided the most cost-effective power for off-grid rural electrification. Hydropower plants have often started out electrifying isolated communities, including in what are now OECD countries, and have later been connected to a larger grid as the network expanded. More than 6000 stations, in the range of 50 to 500 kW, were operating in Switzerland in 1928. Electrifying mountain communities using small hydropower was a critical component of China's strategy to reach universal electrification. In the early 1990s, it was reported that a third of China's 2300 counties and 40% of the rural townships relied on small hydro schemes (defined as up to 25 MW) for the bulk of their electricity supply [10, p. iv] with most of the projects connected to either the national grid or to regional minigrids.

An estimated 10,000 micro, mini, or small hydro minigrids are functional outside China in developing countries around the world, providing electricity to remote communities in hilly and mountainous areas where hydropower resources exist and the national grid has not yet reached. A number of countries in South Asia, including Nepal, Pakistan, Afghanistan, and Sri Lanka have national programs that provide partial grants for community-managed micro hydropower projects. Achievements of some ongoing active programs are listed in Table 1.4.

NOTES

1. National Solidarity Program, Afghanistan; http://www.nspafghanistan.org/; http://www.ashden.org/winners/giz-integration12; http://www.remotehydrolight.com/
2. Alternative Energy Promotion Centre, Nepal; http://www.aepc.gov.np/
   Renewable Energy for Rural Livelihoods, Nepal; http://www.rerl.org.np/
3. http://www.ashden.org/winners/akrsp
4. Renewable Energy for Rural Economic Development (RERED), Sri Lanka; http://www.energyservices.lk/statistics/community.htm
5. IBEKA; http://www.ashden.org/winners/ibeka12
6. Practical Action; http://www.ashden.org/files/reports/Practical_Action_2007_Technical_report.pdf

REFERENCES

1. Lewis, M. J. T., *Millstone and Hammer: The Origins of Water Power*, University of Hull Press, 1997.
2. Reynolds, T., *Stronger than a Hundred Men, A History of the Vertical Waterwheel*, The Johns Hopkins University Press. Baltimore, MD, 1983.
3. Bachmann, A. and Nakarmi, A. M., *New Himalayan Water Wheels*, Sahayogi Press, Kathmandu, 1983.
4. Wikander, Ö., The water-mill, *Handbook of Ancient Water Technology*, Technology and Change in History, 2, Leiden: Brill, 2000, pp. 371–400.
5. Hodge, A. T., A Roman factory, *Scientific American*, November 1990, pp. 106–111.
6. REN21, *Renewables 2012 Global Status Report*. REN21 Secretariat, Paris, 2012.
7. REN21, *Renewables 2016 Global Status Report*. REN21 Secretariat, Paris, 2016.
8. International Energy Agency, *Key World Energy Statistics*, IEA/OECD. Paris, 2013.
9. REN21, *Renewables 2013 Global Status Report*. REN21 Secretariat, Paris, 2013.
10. Xuemin, C., Recent trends in small hydro power in China, *Water Power and Dam Construction: Small Hydro Supplement*, September, 1994, iv–ix.

2 Basics of Hydropower

2.1 HYDROPOWER TYPES AND THEIR COMPONENTS

Hydropower refers to the generation of power, either mechanical or electrical, using the energy of falling water. The power that can be available from a hydropower plant depends on the volumetric flow of water driving the turbine and its vertical drop in height. The larger the volumetric flow of water, the higher the power generation will be. Similarly, the greater the drop in height of water (which is referred to as "head" in hydropower), the higher the power generation will be.

The mathematical relationship between head, flow, and power is referred to as the "power equation." The derivation of the power equation and its use is discussed next.

2.2 POWER OUTPUT FROM HYDROELECTRIC POWER PLANTS

In the hydropower nomenclature, the volumetric flow of water is referred to as "flow," and the units in SI are m^3/s. Similarly, the vertical height is referred to as the "head," and the SI unit is m. The relationship between power output, flow, and head, which is referred to as the "power equation," is computed as follows:

The potential energy of a body of mass M, falling from a certain height h is expressed as

$$E = M\ g\ h\ [\text{Joules}] \tag{2.1}$$

where g is the acceleration due to gravity. At sea level, the value of g is 9.81 m/s^2. Note that, although the value of g decreases above sea level, because the variation is relatively small, for practical purposes, a value of 9.81 m/s^2 is commonly used regardless of the elevation of the power plant. Also, recall that in physics the basic unit of energy is Joules.

The mass of water is its density (ρ) times its volume (V), or $M = \rho V$.

Thus $E = (\rho V)\ g\ h$ [Joules].

Now divide both sides of the equation by time (t):

$$\frac{E}{t} = \left(\frac{\rho V}{t}\right) gh\,[\text{watt}] \tag{2.2}$$

Note that energy divided by time (E/t) is the power, P, in watts (W), and volume over time (V/t) is the volumetric flow of water (Q) or flow in m^3/s.

Thus, replacing E/t by P and V/t by Q, the power equation becomes

$$P = \rho\ Q\ g\ h\ [W] \tag{2.3}$$

Note that $\rho g = \gamma$, which is the unit weight of water = 9.81 kN/m^3. According to principles of thermodynamics, when energy is changed from one form to another, there will be some losses based on the efficiency of the conversion process or equipment. Hydropower is generated when the potential energy of falling water is first converted into mechanical energy as it rotates the turbine. The turbine shaft, in turn, drives the generator shaft, and the rotating generator converts the mechanical energy into electrical energy. Frictional losses are generated as the water runs down the penstock pipe and in the turbine whereas there are electrical losses in the generator. The overall efficiency of the power plant depends on the efficiency of the penstock pipe, turbine, and generator.

Replacing ρg with γ and taking into account the overall efficiency, the power equation becomes

$$P = \gamma\ Q\ h\ e_o\ [\text{kW}] \tag{2.4}$$

where e_o is the overall efficiency (penstock pipe, turbine, and generator) of the power plant and is "unitless." Note that because the unit for γ is kN/m^3, the unit for P is also kW (instead of watt, used earlier).

Often, the power equation is also expressed as

$$P = Q\ g\ h\ e_o\ [\text{kW}] \tag{2.5}$$

Although their units are different, because the absolute value of both g and γ are the same, neglecting the variation due to elevation, the value for power output (in kW) will be the same.

Often in hydropower, the terms "gross head" and "net head" are also used. Gross head (h_g) is the difference in elevation from the forebay for a run-of-river plant or the water level behind the dam for a storage project to the centerline of the turbine at the powerhouse for impulse turbines, such as Pelton or Turgo. For reaction turbines, such as Francis or Propeller, in which draft tubes are often installed, the downstream water level at the outlet of the draft tube (also referred to as the "tail water level") is used instead of the centerline of the turbine. Major components used in micro hydropower plants are discussed in the next section. Descriptions of various types of turbines used in hydropower plants are provided in Chapter 9.

The net head (h_n) is the pressure head at the entrance to the turbine runner. As the flow travels down the penstock pipe (or through a tunnel in case of some large hydropower plants) there will be some losses (pressure drop or head loss) mainly due to friction between the flowing water and the pipe or tunnel walls as well as bends and other obstructions along the alignment, which also hinder the flow path. These losses will be examined in detail in the headrace and penstock chapters later on. The gross head and net head for a large dam hydropower project with a headrace tunnel and for micro-hydropower plants with reaction and impulse turbines can be seen in Figures 2.1, 2.2, and 2.3, respectively.

As can be seen from Figure 2.1, due to head loss in the tunnel, the normal operation level at the surge shaft will be lower than that at the dam crest level. This is referred to as the head loss in the tunnel ($h_{ltunnel}$). Then, as the flow is conveyed down the penstock pipe into the turbine, there will be

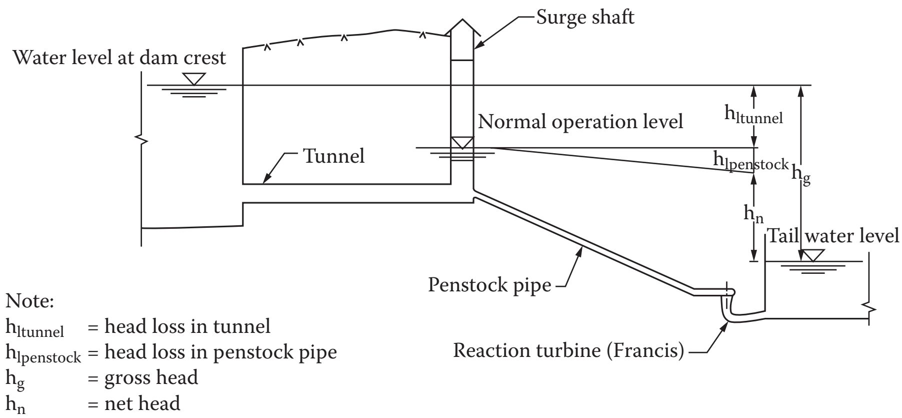

FIGURE 2.1 Gross head in a storage plant with reaction turbine.

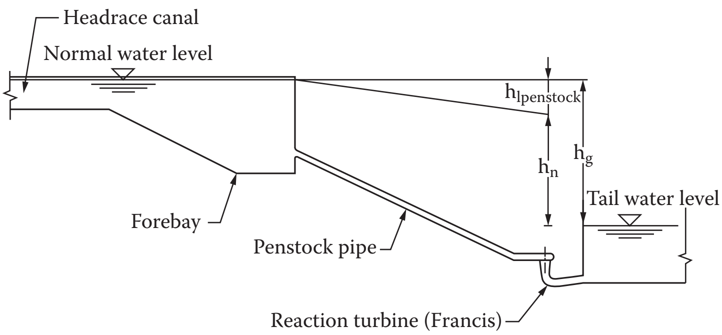

FIGURE 2.2 Gross head in a run-of-river plant with a reaction turbine.

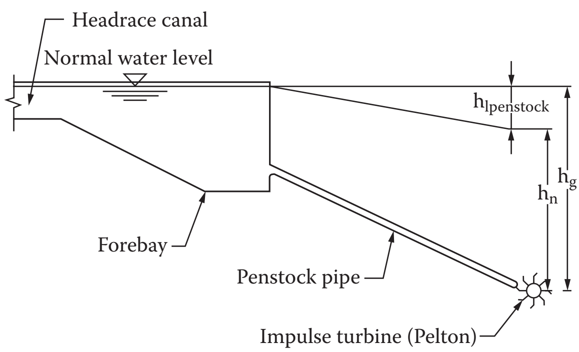

FIGURE 2.3 Gross head in a run-of-river plant with an impulse turbine.

further head loss (i.e., head loss in the penstock). In this case, the gross head will be the difference in elevation between the water level at dam crest level and the tail water level. The net head will be the gross head less the losses in the tunnel and penstock.

Because tunnels are rarely used in micro hydropower plants, instead of a surge shaft, a forebay is constructed at the start of the penstock pipe. If a reaction turbine is installed at the powerhouse, then the gross head will be the difference in elevation between the normal water level at the forebay and the tail water level downstream of the turbine. The net head will then be the gross head less the losses in the penstock pipe ($h_{lpenstock}$).

If an impulse turbine is installed at the powerhouse for a micro hydropower plant, then the gross head will be the difference in elevation between the normal water level at the forebay and the centerline of the turbine runner (the runner is the rotating wheel of the turbine). In an impulse turbine, once the water jet hits the turbine runner, it will not be able to transfer more energy to the turbine. The net head will then be the gross head less the losses in the penstock pipe ($h_{lpenstock}$).

In terms of gross and net head, the power equation can be written as

$$P = \gamma\ Q\ h_g\ e_o \tag{2.6}$$

where e_o is the overall efficiency including that of the penstock pipe.

$$P = \gamma\ Q\ h_n\ e_o \tag{2.7}$$

where e_o is the overall efficiency excluding that of the penstock pipe.

The overall power output efficiency, e_o, is the product of different efficiencies for several components of the hydroelectric system as follows:

$$e_o = e_{penstock} \cdot e_{turbine} \cdot e_{generator} \cdot e_{transformer} \text{ (note that in the case of } h_n, e_{penstock} \text{ is not required)} \quad (2.8)$$

where

$e_{penstock}$ is the efficiency of the penstock. For micro hydroelectric power plants, the efficiency of the penstock is generally in the range of 90%–95%—that is, 0.90–0.95. For larger power plants, the penstock diameter is sized such that the efficiency is optimum, given the plant size and cost–benefit analysis.

$e_{turbine}$ is the efficiency of the turbine. For medium and large hydropower plants, the turbine efficiency can be over 90%, depending on the type of turbine installed. For micro hydroelectric power plants with turbines manufactured at local workshops, the efficiency may be as low as 60%.

$e_{generator}$ is the efficiency of the generator. For medium and large hydropower plants, the generator efficiency can be over 95% whereas for micro hydroelectric power plants the efficiency could be lower, for example, 70%–90%.

$e_{transformer}$ is the efficiency of the transformer. Based on size of the transformer, the efficiency can vary between 95% and 98%.

Thus, at the transformer end, the overall efficiency takes into account individual efficiencies of the penstock pipe, turbine, generator, and transformer. Sometimes in isolated power plants, the losses along the transmission line are also taken into account. In such cases, the transmission line efficiency should also be incorporated. Generally, the transmission line is designed to limit losses to 10% in micro hydroelectric power plants whereas for larger power plants this is based on a detailed optimization study (similar to penstock optimization). In case of a grid-connected power plant, the overall efficiency is based on where the energy meter is installed. For example, if the energy meter is installed at the transformer output end, the overall efficiency should include up to $e_{transformer}$. On the other hand, if an energy meter is installed at the end of the transmission line connecting to the regional or national grid, then the efficiency of the transmission line up to the interconnection point should be included. Generally, the location of the energy meter in a grid-connected system is mutually agreed upon by the power plant owner and the utility buying the electricity.

Example 2.1: Installed Capacity Calculations

During a prefeasibility survey, you have identified a feasible site for a micro hydropower scheme. If you've measured a gross head of 40 m, and from the hydrological analysis, a design flow of 150 l/s appears to be available throughout the year, what would be the likely installed capacity? Assume an overall efficiency of 60%.

Answer:
Given:
Design flow, Q = 150 l/s or 0.15 m^3/s
Gross head, h_g = 40 m
Overall efficiency = 60% or 0.6

Recall the power equation: $P = \gamma\, Q\, h_g\, e_o$ [kW], where $\gamma = 9.81$ KN/m^3
$P = 9.81 \cdot 0.15 \cdot 40 \cdot 0.6$
Or P = 35.3 kW

Therefore, about 35 kW of installed capacity should be available.

Example 2.2: Determination of Design Discharge

A community requires 60 kW of power output to meet their daily electricity needs. If the site survey indicates 100 m of gross head to be available, what design discharge is required to meet the community's electricity needs? Assume an overall efficiency of 55%.

Answer:
Given:
Power output, P = 60 kW
Gross head, h_g = 100 m
Overall efficiency = 55% or 0.55
$P = \gamma\, Q\, h_g\, e_o$ [kW]

$$\text{Or,}\ \ Q = \frac{P}{\gamma h_g e_o} = \frac{60}{9.81 \cdot 100 \cdot 0.55} = 0.111\,\text{m}^3/\text{s}\ \ \text{or 111 l/s}$$

Therefore, a minimum design discharge of 111 l/s should be available in the river to generate 60 kW of installed capacity. Note that if the flow available in the river is less than 111 l/s, then the installed capacity of 60 kW will not be feasible.

2.3 TYPES AND COMPONENTS OF HYDROPOWER

There are two basic types of hydropower plants: namely, run-of-river and storage. The run-of-river power plant diverts available flows from the river into an intake and then to the power plant located at some distance downstream through waterways. In this type of system, water available in the river up to the design flow considered (making allowances for environmental releases downstream) is diverted for power generation. When the flows in the river exceed the design flow for power generation, the excess flow runs downstream over the dam or weir along the river—that is, the river flows are not stored behind the dam at anytime. A schematic figure of a typical run-of-river micro hydropower plant is shown in Figure 2.4.

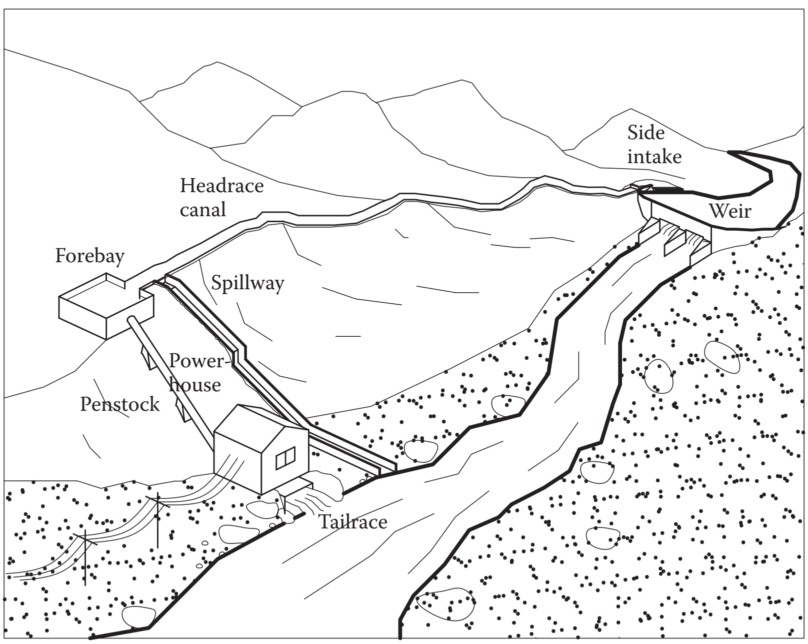

FIGURE 2.4 Typical run-of-river power plant.

FIGURE 2.5 A 183-kW Syange (run-of-river) hydropower plant, Lamjung Nepal (notice that as this is a run-of-river plant, the excess water flows down the weir along the river and the penstock begins close to the intake).

As can be seen from the figure, a micro hydropower plant comprises a diversion intake along with a canal contouring the hill slopes, which conveys the flows into a tank called the "forebay." From the forebay, the flow is routed into a pressure pipe know as the penstock. The penstock leads the flows into the turbine located in the powerhouse. The water that has been used for power generation is then conveyed back into river via a tailrace channel. There are often other structures incorporated in run-of-river hydropower plants, such as a settling basin to remove sand particles in the flow, which are detrimental to the turbines or anchor blocks, and support piers to hold the penstock pipe in place. These components are further described later on in this chapter.

When the topography allows, the penstock can also start from close to the intake as can be seen in the photograph in Figure 2.5.

Various components of the run-of-river hydroelectric power plant are briefly described herein, and their detailed descriptions are provided in the subsequent chapters.

2.3.1 Waterways

The structures that convey the flows from the intake located at the river up to the end of the tailrace are collectively referred to as the waterways—that is, these are structures that provide a path for the water in a hydroelectric power plant.

2.3.2 Dam or Diversion Weir

A dam is a structure built across the river to increase the water level such that the required flow volume can be diverted into the waterways of the hydropower plant for power generation. Generally, for run-of-river plants, the dam has a low-height (as storage is not required) structure and is also referred to as a diversion weir. For large storage type hydropower plants, the dam height can easily be over 100 m. Although there is not a universal definition for "high dam," any dam higher than 15 m and/or with provisions for storage of 1.0 million m^3 is referred to as a high dam by the World Commission on Dams (WCD).

FIGURE 2.6 Typical temporary weir used in micro hydroelectric power plant.

Small hydropower plants that operate on a commercial basis selling electricity to the regional or national grid generally have a permanent weir whereas micro hydroelectric plants in remote communities can be temporary structures comprising brushwood and boulders. Furthermore, for micro (or mini) hydropower plants in which the design discharge is low compared to flow availability in the river throughout the year, a diversion weir may not even be required. However, as the plant capacity increases, such diversion weirs become essential.

In case there are migrating fish that travel upstream of the proposed dam site, typically for spawning during certain seasons, then a fish pass should be incorporated along the dam. For medium or large hydropower projects, many countries require a separate environmental impact assessment (EIA) study before the construction license is awarded. Such an EIA study would identify whether there are migrating fish species across the dam site along with other environmental concerns. Most countries require at least an initial environmental examination (IEE) study as a prerequisite for developing small hydropower plants if not a full EIA. Generally, for micro hydropower plants, neither EIA nor IEE is required. IEE and EIA studies are beyond the scope of this book, and the reader should refer to relevant requirements of the country. With a low diversion weir, provided the upstream and downstream slopes are gentle, fish movement may not be hindered. However, based on site conditions, the presence of migrating fish and possible effects on aquatic life should be verified even for micro hydroelectric plants.

Based on the size of the dam or diversion weir and the design, if permanent, these structures are constructed of mass concrete—often with nominal reinforcement as required. Sometimes, stone masonry weirs are also built in micro, mini, and small hydroelectric plants. Temporary weirs comprising stones and brushwood have also been used traditionally in micro hydroelectric plants (Figure 2.6).

2.3.3 Intake and Headworks

The location from which river water is initially diverted into the waterways of a hydroelectric plant is referred to as the intake. An intake in a run-of-river hydropower plant can be an opening along the riverbank or other types of arrangements that facilitate flow diversion into the waterways of the power plant. A coarse trash rack is generally incorporated at the intake to prevent entry of large boulders and floating debris, such as logs and branches, into the waterways. The coarse trash rack is a structure (often fabricated from mild steel) comprising bars evenly spaced, which allow the river flows to be conveyed from the intake to the waterways but prevent the entry of logs and boulders larger than the bar spacing of the trash rack from entering the intake. The bar spacing of the coarse trash rack is sometimes sized to prevent the entry of fish into the waterways, especially in large dams.

Unless the river flows are constant throughout the year (e.g., regulated flow discharged from a dam upstream), a flow control structure, such as gates, need to be incorporated at the intake.

Structures located at the start of a run-of-river power plant (i.e., at the river or close to it) are collectively referred to as the headworks. The diversion weir, intake, and often gravel trap and settling basin (if they are close to the intake) are components of headworks structures (Figures 2.7 and 2.8).

FIGURE 2.7 Typical side intake used in a small hydroelectric power plant, Nepal.

FIGURE 2.8 A frontal intake used in a micro hydropower plant, Afghanistan.

2.3.4 Headrace

The headrace conveys the water flow from the headworks to the forebay structure. This can either be a canal or a pipe for small hydropower plants. In medium or large hydropower plants, the headrace is sometimes a tunnel. The choice of canal or pipe for the headrace structure depends on the site topography, geology, and costs. If the headrace alignment has a mild slope along stable terrain, an open canal could be appropriate (Figure 2.9). At locations where the alignment needs to cross gullies or depressions on the ground, pipes can be used as headrace along such stretches. Often a combination of both—that is, a canal along stable terrain with mild slopes and pipes to negotiate gullies and crossings—is also used.

On the other hand, in case of difficult terrain with relatively steeper ground profile, a pipe may be required for the headrace. Also, if the headrace alignment is long and any spillage from the canal (e.g., due to rockfall or mudslide from uphill) can cause loss of life or property, a pipe may be suitable. Headrace pipes generally have low pressure such that the longitudinal slope is only sufficient to overcome friction and drive the required flow downstream. Similarly, headrace tunnels in large hydropower plants are also generally designed as low-pressure conduits (Figure 2.10).

FIGURE 2.9 A reinforced concrete headrace canal used in a micro hydropower plant, Indonesia.

FIGURE 2.10 A 22-MW Mai hydropower plant's headrace tunnel near completion, Nepal.

2.3.5 Gravel Trap and Settling Basin

The river can carry boulders, cobbles, gravel, and sediment during the high-flow seasons and especially during floods. The volume of such sediment depends mainly on the discharge that the river carries, its bed slope, and the upstream catchment characteristics, such as geology and vegetation cover. As discussed earlier, although the coarse trash rack at the intake will prevent the entry of large boulders and floating logs into the waterways downstream, and cobbles, gravel, and sediment (i.e., particles that are smaller than the bar spacing of the coarse trash rack) will be conveyed downstream. If such particles are not removed, they will soon fill up the canal and limit the flow as well as abrade the turbine runners (and the penstock pipe to some extent), thereby decreasing their economical life. Thus, such particles need to be removed as early as possible along the waterways of the power plant so that only clean water is conveyed downstream.

As the name denotes, the gravel trap is a basin or pond close to the intake where gravel, cobbles, and other coarse materials are trapped and then removed. In the absence of this structure, gravel can settle along the gentler section of the headrace or in the settling basin. It should be noted that the function of the gravel trap is to remove only the larger particles that enter through the coarse trash rack and not the finer ones (i.e., sediment). Such sediments are removed in a settling basin, which is a larger basin constructed further down the headrace.

The basic operating principle of these basins is that if the cross-sectional area is increased, the flow velocity decreases, which, in turn, decreases the sediment transport capacity of the flow. Thus, the particles are settled in the basins, which then need to be periodically flushed out using control gates. Because fine particles need lower water velocity to settle compared to gravel, the settling basin is always larger than the gravel trap. In some cases, if the topography is suitable, these structures can also be combined together (Figure 2.11). On the other hand, if the river does not carry significant gravel but only fine sediments (such as rivers in the European Alps), a separate gravel trap may not be essential. In the Himalayan rivers, gravel loads can be significant during the rainy seasons (monsoon), and thus, a gravel trap is regularly incorporated in run-of-river hydropower plants.

FIGURE 2.11 Combined gravel trap and settling basin of a 500 kW mini hydroelectric power plant, Nepal.

The gravel trap and/or the settling basin may have to be located some distance downstream from the intake to protect these structures from damage due to floods as well as to provide sufficient head to flush the deposited particles back into the river. In cases in which these structures can't be located immediately downstream of the intake, the headrace canal (or pipe) needs to be sufficiently steep to convey the particles to the basins. Inadequate slope of the headrace upstream of the basins will cause particle deposition along the alignment, thereby reducing flow conveyance capacity and will require frequent maintenance. Because the headrace alignment from the intake to the gravel trap or to the settling basin is steeper compared to the downstream reach, which conveys clean water, some texts also refer to this stretch of the canal as the "intake canal." In case the gravel trap and the settling basin are located at some distance from each other, the headrace slope from the intake to the gravel trap should be steeper than that between the gravel trap and the settling basin.

Gravel trap and settling basins in micro or mini hydroelectric power plants are often built using stone masonry in cement mortar. However, as the required size of these structures increases, reinforced concrete becomes the preferred choice.

2.3.6 Spillway

The spillway is an opening in the headrace canal, gravel trap, settling basin, or the forebay that diverts excess flows and thus allows only the required design flow further downstream (Figure 2.12). Spillways can be gated, generally for larger power plants, or ungated. In ungated spillways, the invert level, or the bottom of the opening, is fixed just above the height required to pass design flow required downstream. Thus, when the water level upstream is higher than the invert level at the spillway, the excess flows are discharged through the spillway. Ungated spillways are also referred to as "overflow spillway weir." Spillways are sometimes also provided along the headrace canal alignment to divert flows in case the downstream reach is blocked or choked, such as due to rockfalls or landslides from above the canal. Spillways that serve such a purpose are also called "escapes" (Figures 2.13 and 2.14).

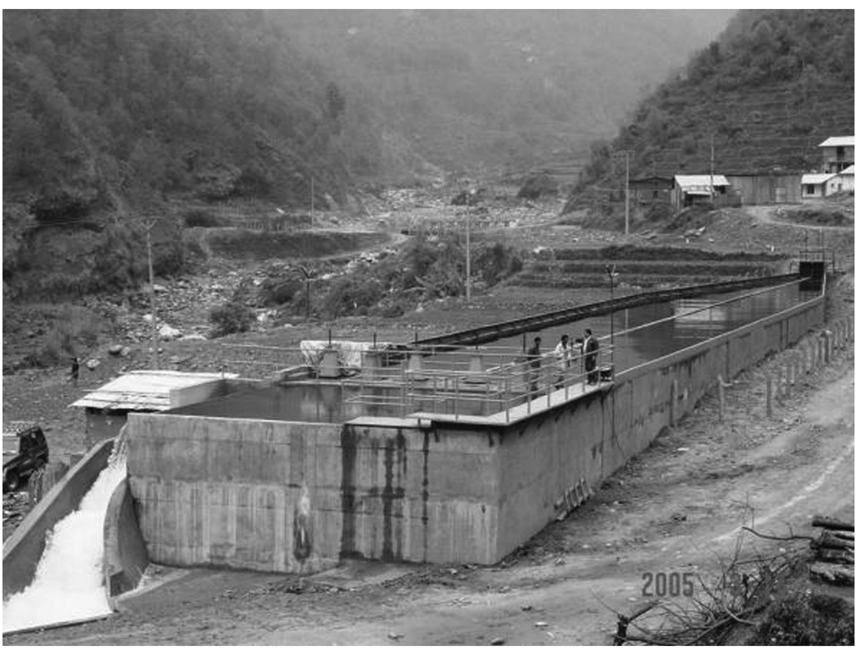

FIGURE 2.12 Settling basin cum forebay of a 2.5 MW small hydropower plant, Nepal (notice overflow spillway at end).

FIGURE 2.13 Spillway located at forebay wall in a micro hydropower plant, Afghanistan.

FIGURE 2.14 Spillway located along an irrigation canal, Afghanistan.

2.3.7 Crossings

In hydropower plants, sometimes water has to be carried across gullies, streams, or other natural depressions due to site topography. Various types of crossing structures are required to convey the flows across such difficult stretches of waterway alignment. Super passages, culverts, siphons, and aqueducts are examples of such crossings (Figures 2.15 and 2.16).

FIGURE 2.15 A penstock crossing for a 3-MW hydropower plant, Nepal.

FIGURE 2.16 An irrigation aqueduct, Nepal.

2.3.8 Forebay

A forebay is a tank that conveys water from the headrace to the penstock pipe. The forebay acts as a transitional structure to transfer water flow from an open channel or low-pressure headrace pipe to pressurized flow in the penstock pipe. Water flow under pressurized conditions is known as "pressure flow" into the penstock. The forebay should provide adequate submergence depth to convey design flow into the penstock pipe and allow for some storage volume for start up of the turbines. This structure should also be sized to accommodate variation in flow into the penstock pipe and turbines

FIGURE 2.17 A typical forebay installed in a micro hydropower plant, Nepal.

at different levels of power output. Sometimes, the forebay serves as a secondary settling basin, especially if the length of the headrace between the upstream settling basin to this structure is long and sediments are likely to enter the headrace stretch in between. An overflow spillway is essential in the forebay to safely spill the entire incoming design flow in the event that the turbines in the powerhouse need to be suddenly closed, such as due to emergency conditions, for example, power failure. A fine trash rack—that is, more closely spaced bars than the coarse trash rack at the intake—is incorporated at the forebay in front of the inlet to the penstock pipe (Figure 2.17). Such a fine trash rack prevents the entry of debris into the penstock pipe, which would be detrimental to the turbine runners.

In cases in which a headrace tunnel is used, the forebay tank is replaced by the surge shaft. The surge shaft serves the same function as the forebay—that is, it acts as a transitional structure to facilitate pressure flow in the penstock pipe—but in addition, it also protects the penstock pipe against surge by providing a free surface for pressure release. Generally, the surge shafts are designed to contain the entire flow even when all turbine units in the powerhouse are simultaneously closed prior to the gate closure at the intake. To ensure this condition, the top level of the surge is set above the static water level at the intake; this allows for an additional margin to accommodate surge height.

Forebay tanks in micro or mini hydroelectric power plants are often built using stone masonry in cement mortar. However, as the sizes increase, reinforced concrete becomes the preferred choice. Surge shafts are almost always built from reinforced concrete.

2.3.9 Penstock Pipe

The penstock is a pipe that conveys water under pressure from the forebay to the turbine. The penstock pipe alignment starts where the ground profile gets steeper to be able to generate the design head with a shorter, and thus less expensive, penstock pipe. Although wooden, concrete, and cast-iron pipes were used for the penstock in the early days of hydropower development, the modern trend is to use mild steel due to availability of high-quality steel throughout most of the world.

Based on the topography, soil type, and costs, penstock pipes can either be buried or placed above ground secured by anchor blocks and support piers. In remote micro hydropower plants, individual sections of penstock pipe are often joined on-site through flanges and gasket arrangements. For larger power plants or more accessible micro hydropower plants, individual lengths of penstock pipe are welded together on-site (Figures 2.18 and 2.19).

FIGURE 2.18 Penstock alignment for a 900-kW plant, Kenya.

FIGURE 2.19 Penstock alignment for a 500-kW mini hydropower plant, Nepal.

2.3.10 Anchor Block

An anchor block is a structure that holds the penstock pipe rigidly and constrains its movement in all directions. Where there are bends along the penstock pipes, there will be hydrostatic forces and dynamic forces to some extent due to flow velocities along with other forces, such as thermal stress due to changes in ambient temperature and lateral earth pressure as a result of change in ground profile. The anchor blocks encase the penstock pipes and transfer all forces on it to the ground and prevent pipe movement. In addition to being located at every bend, in long penstock pipe alignment, anchor blocks may be required at regular intervals even along a straight section, especially to accommodate axial forces and thermal stresses.

In case of buried pipe alignment, anchor blocks are not generally required provided that the forces can be transferred into the ground with sufficient depth of burial.

FIGURE 2.20 Reinforced concrete anchor blocks used in a mini hydropower plant, Nepal.

Based on size, availability of construction materials, and costs, anchor blocks are constructed of stone masonry, plain or plum concrete with nominal reinforcement, reinforced concrete, or a combination of these (Figure 2.20).

2.3.11 Support Pier

Support piers are constructed to support the penstock pipe at regular intervals. They provide intermediate support between anchor blocks to accommodate the weight of the pipe and the water inside it. They are also sometimes referred to as “slide” or “saddle blocks.” Support piers prevent the pipe from sagging along straight sections of the exposed penstock pipe alignment between anchor blocks. If support piers are not incorporated along the penstock alignment, the requirement for the pipe to bear its own weight as well as the weight of the water would result in significantly larger pipe thickness, thereby increasing costs. Thus, the function of the support pier is to resist all vertical forces transmitted by the penstock pipe. Unlike the anchor block, the support pier does not completely restrain pipe movement. It resists vertical movement but allows the pipe to slide along its surface, parallel to the pipe alignment, due to expansion or contraction that occur as a result of changes in ambient temperature.

Based on size, availability of construction materials, and costs, support piers are constructed of stone masonry, plain or plum concrete with nominal reinforcement, reinforced concrete, or a combination of these (Figure 2.21).

FIGURE 2.21 Masonry support piers used in a mini hydropower plant, Nepal.

2.3.12 Powerhouse

The powerhouse is a building that houses the turbine, generator, control panel, and other electromechanical equipment and accessories (Figures 2.22 and 2.23). The function of the powerhouse is to protect the electromechanical equipment from the adverse effects of the weather (rain, heat, cold, etc.) and to provide a sound working environment for the operators. Because the turbines and generators are heavy pieces of equipment, all powerhouses from small to large hydropower plants typically have gantry cranes. Such cranes are used to place or remove turbines and generators on the foundations during installation or for repair and maintenance. In micro hydropower plants, a mobile crane is often used to save costs.

Along with static forces, the machine foundations in the powerhouse need to resist the dynamic forces of the turbines and the generators as a result of rotating parts.

FIGURE 2.22 A powerhouse building of a 900-kW mini hydropower plant, Kenya.

FIGURE 2.23 A powerhouse building for a micro hydropower plant, Indonesia.

2.3.12.1 Inside the Powerhouse

2.3.12.1.1 Turbine

The turbine is a mechanical device that converts the energy of the pressure head of the water and incoming flow from the penstock into mechanical energy by rotating its mass. The type of turbine selected to be used in the power plant depends mainly on the head, volumetric flow, and the number of units that are to be installed. The turbine drives a generator to produce electricity or a direct-drive application, such as a mill or pump (Figures 2.24 and 2.25).

2.3.12.1.2 Generator

The generator converts the rotational mechanical energy of the turbine into electrical energy. The shaft of the rotating turbine is coupled with the generator shaft either directly or via a gear or pulley system. The two principle types of generators used are "synchronous" and "induction" or "asynchronous." The bases for selection of generator type are plant capacity, connection to the grid or isolated use, and the type of loads that are required to be powered by the generator. Both synchronous and induction generators can be single phase or three phase with larger capacity generators normally being three phase.

For small hydropower plants, standard generators can be bought from manufacturers whereas for the very large power plants they have to be custom manufactured (Figures 2.26 and 2.27).

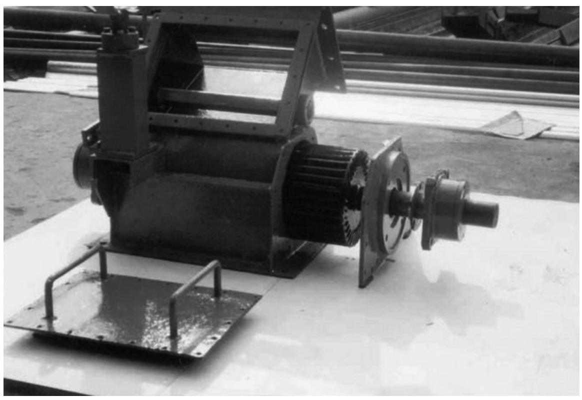

FIGURE 2.24 A cross-flow turbine used in a micro hydropower plant, Nepal.

FIGURE 2.25 A 100-kW Pelton turbine in a workshop, Nepal.

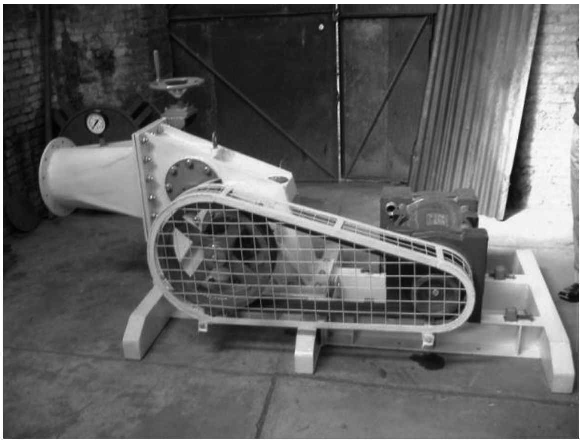

FIGURE 2.26 An induction generator coupled with a cross-flow micro hydro turbine, Nepal.

FIGURE 2.27 An induction generator coupled with a Francis turbine in a micro hydropower plant, Afghanistan.

2.3.12.1.3 Governor

The governor controls the inflows into the turbines based on the demand of the electrical load (Figure 2.28). The governor typically senses the rotational speed (RPM) of the turbine and changes the flow into the turbine such that the RPM remains constant. An increase in RPM denotes an underloading of the turbine and results in the governor restricting the flow to the turbine. A decrease in RPM denotes an overload and results in the governor allowing higher flow to the turbine. In case of emergency measures, such as during a power failure, for example, tripping of the main circuit breaker, the governor will completely close the turbine valve. Flow control by governors is achieved through a hydraulically driven oil pressure system, which regulates the turbine valves. The signals or command for operating the hydraulic system are generated by electronic controls.

On micro hydropower systems, the trend is increasingly in favor of using electronic load controllers (ELC) over mechanical flow control governors. This is because costs are relatively high for smaller capacity mechanical governors and because governors are slower to respond and require regular maintenance. Advantages of electronic load control are faster response, lack of moving parts, and lower cost. ELCs provide control by sensing the electrical frequency or voltage at the

FIGURE 2.28 Turbine governor of a 2.5-MW small hydropower plant, Nepal.

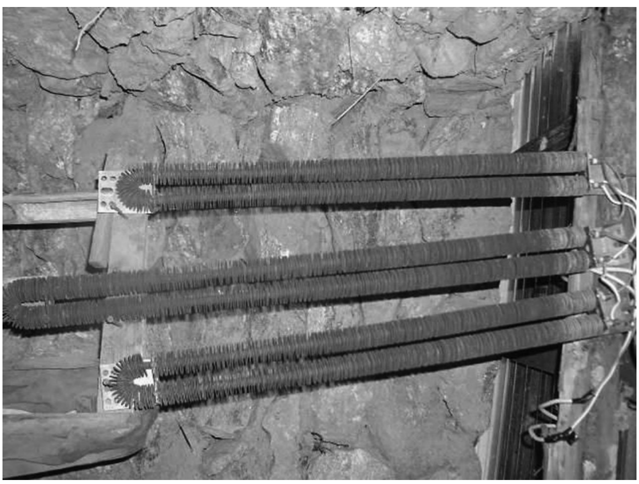

FIGURE 2.29 An air heater ballast of a micro hydropower plant, Nepal.

generator output and diverting more or less power to a dummy ballast load in order to keep these constant (Figure 2.29). The ballast load is either air heaters or immersion heaters in a water tank. With an ELC, the water flow through the turbine and the corresponding power output is kept constant, and any electrical power exceeding the needs of the main load is dumped into the ballast load.

ELCs used with synchronous generators sense the frequency whereas those used with induction generators sense the voltage. In both cases, the control mechanism is to send the required power to the ballast load through electronic switches in order to keep the frequency or voltage at the desired constant level. ELCs used to control induction generators are also called induction generator controllers (IGCs).

2.3.12.1.4 Control Panel

The control panel ensures that the electrical energy generated in the powerhouse meets the specified parameters, such as the voltage and the frequency, before being sent out on the transmission or distribution lines (Figures 2.30 and 2.31). Measurements of the generated electrical power, current, and voltage in each phase as well as the frequency and kilowatt-hours supplied are recorded in the

FIGURE 2.30 Control panel of a micro hydropower plant combined with the ELC.

FIGURE 2.31 Control panel for a mini hydropower plant.

control panel. Although the simplest control panels used in the smaller micro hydropower plants hold little more than voltage and current meters, more sophisticated versions have circuitry for shutting down power supply from the powerhouse in case of overload on the generator and over/under frequency or voltage output and equipment for synchronizing power output from multiple generators and to the grid. Micro hydropower plants generally have the control panel next to the turbine–generator unit as their sizes are small and costs need to be kept at a minimum. Larger hydropower plants generally have a separate control room that houses control panels.

2.3.12.1.5 Transformer

A transformer is used for the purpose of stepping up the voltage output of the generator to transmit power over a long distance (Figure 2.32). The generator inside the powerhouse produces electricity at a relatively low voltage level, for example, 415 V for a micro hydro plant. When the generated electricity needs to be transmitted some distance, to supply the load the voltage level has to be stepped up, typically to 11 kV or 22 kV, in order to minimize transmission losses. In the case of

FIGURE 2.32 An outdoor transformer for a micro hydropower plant, Indonesia.

grid-connected power plants, the generated voltage has to be stepped up to 33 kV or 66 kV or even higher depending on the country's grid code to connect to the grid transmission lines.

Distribution transformers step down the voltage from the transmission line to supply the community via low-voltage distribution networks.

2.3.12.1.6 Tailrace

The tailrace conveys the spent water from the turbine pits back to the river, often into the same river downstream of where the intake is located (Figure 2.33). Occasionally the tailwater is also discharged into another tributary (e.g., interbasin transfer) or into a natural drainage system. Similar to the headrace, either an open canal or a pipe can be used for the tailrace. Based on difference in levels between the turbine pit and the river, the slopes can be higher as energy does not need to be conserved along this stretch. For medium or large hydropower plants with an underground powerhouse, the tailrace can also be a tunnel.

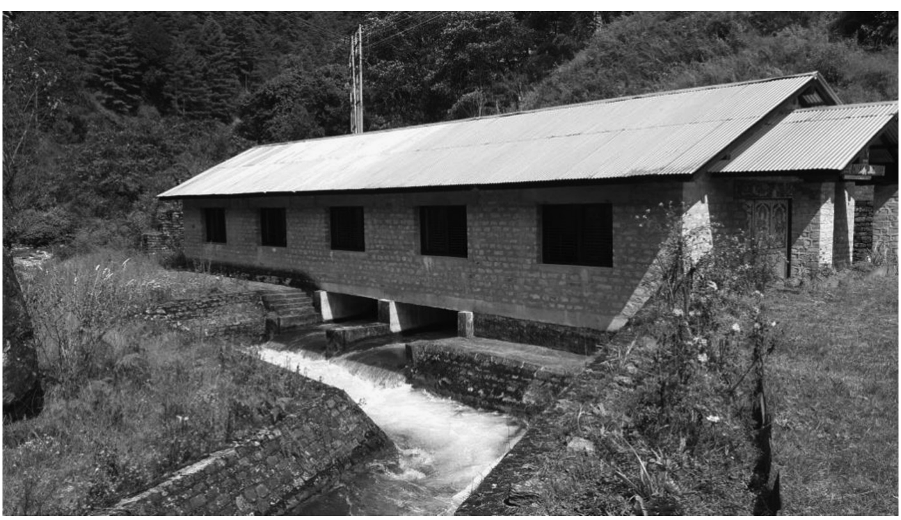

FIGURE 2.33 Tailrace of a 400-kW mini hydropower plant, Nepal.

2.4 STORAGE TYPE HYDROELECTRIC PLANTS

Storage type hydroelectric power plants comprise a dam built across the river to impound large volumes of water. Some dams create reservoirs extending tens of kilometers upstream (Figures 2.34 and 2.35). Hydroelectric power plants associated with large dams do not usually have long waterways as in the case of run-of-river plants. The intake is located at the upstream face of the dam whereas the powerhouse is placed at the foot of the dam. Often large dams are built as part of multipurpose projects generating hydroelectricity in addition to providing irrigation and drinking water along with navigational and recreational facilities.

Some large dams are designed to store flows larger than the annual river water volume. In such large storage projects, the crest of the dam sometimes serves as a multiple lane highway. Smaller dams are designed to store seasonal river flows, such as the volume available during the high-flow season. Some run-of-river power plants have provisions for three to four hours of daily pondage at

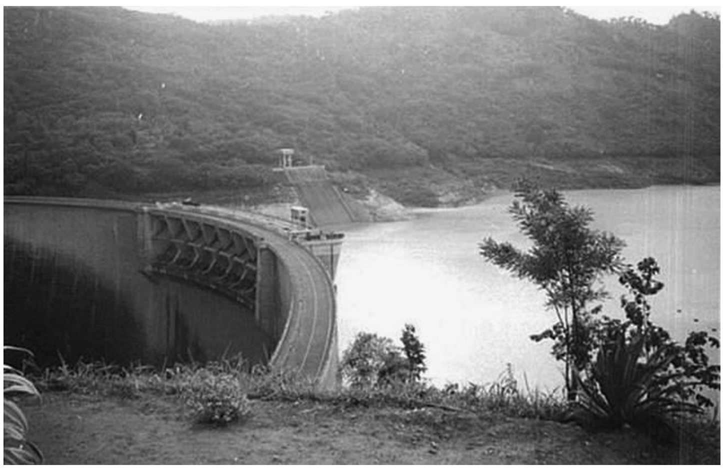

FIGURE 2.34 70-MW Victoria Dam in Sri Lanka.

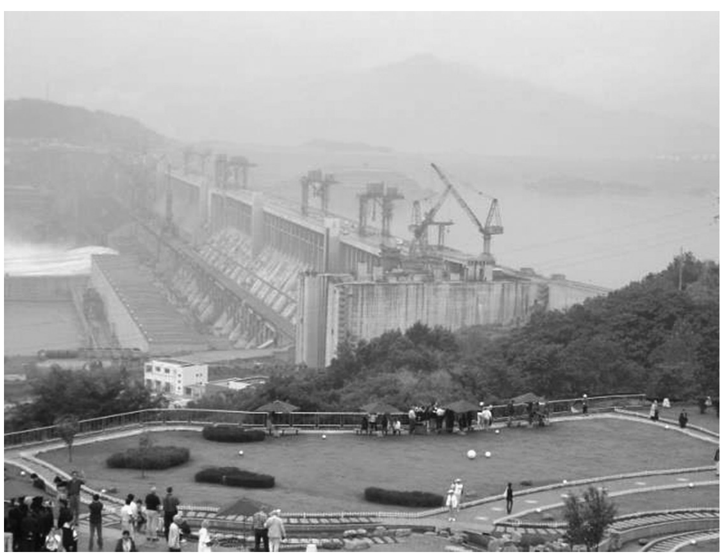

FIGURE 2.35 World's largest Three Gorges Hydropower Plant (22,500 MW), China.

the headworks so that the river flows can be stored during the off-peak hours of the day to supply the full installed capacity during peak demand hours.

EXERCISES

1. For a typical micro hydropower scheme, initial survey and river hydrology indicate that the gross head is 35 m and a design discharge of 120 l/s can be available. On the basis of the gross head and design flow, what installed capacity would you recommend if you expect an overall efficiency of 65%? (Answer: 26.8 kW.)
2. If the penstock efficiency is 95%, generator efficiency is 90%, and the distribution line efficiency is 90%, what is the minimum turbine efficiency required to achieve an overall efficiency of 60%? (Answer: 78%.)
3. If you need to design a 20-kW scheme, and you know that 25 m of head is available, how much flow is needed? Make a reasonable assumption for the overall efficiency. (Answer will depend on assumed efficiency.)
4. For an installed capacity of 35 kW and a design flow of 150 l/s, what is the head required if the overall efficiency is 70%? (Answer: 34.0 m.)
5. Design head at China's Three Gorges Dam, the largest hydropower project in the world, is 80.6 m, and rated power output of each of the 32 turbine generator units is 700 MW. If the efficiency of each of the turbine generator units at full power output is 93.2%, what is the design flow through each turbine? (Answer: 950 m^3/s.)

3 Site Selection and Feasibility Study for Hydropower Projects

3.1 OVERVIEW

Several alternatives may be feasible at a typical hydropower site, and the design engineer or the design team needs to come up with the optimal layout. For large hydropower projects, multiple site visits are made by the design team before finalizing the layout arrangements of the scheme. Technical consideration, such as locating structures and components in suitable and stable areas and protecting relevant structures from floods, together with the need to come up with a cost-effective engineering design makes the selection of hydropower sites an iterative process.

In case of isolated micro hydropower sites in developing countries, in order to keep the costs down, site selection along with survey work are often done at one time. The design engineer may have to decide on the optimal layout of the scheme along with identifying locations of key structures—intake, settling basin, canal and penstock alignments, powerhouse and tailrace—during the first site visit. The design engineer will generally have to do several “walkover surveys” at the site to finalize the scheme layout and locations of structures. These activities may also require discussions with community members to identify landowners whose land will be occupied by the scheme. Sometimes a knowledgeable local resident, for example, a farmer, village chief, or school teacher, may be aware of a potential site nearby and may be a useful source of information.

Once the layout for a micro hydropower scheme is finalized, a topographical survey along the alignment is undertaken, and this forms the basis for the engineering design. Flow measurements at the proposed site are also undertaken in case the river is not gauged—that is, river flow data is not available and if the site visit coincides with the low river flow period. It should be noted that flow measurements during high-flow seasons will not be of much value except to estimate what the annual high flows and the corresponding water levels are likely to be at the intake site. Furthermore, in many developing countries, site visits during the rainy or high-flow season becomes difficult due to poor road conditions. Design of the scheme along with sizing of the components and structures would then be undertaken after the site visit based on topographical survey maps prepared.

Apart from engineering design of the micro hydropower plant, the feasibility study must also address the country’s policies regarding licensing and environmental requirements, subsidies, and other support mechanisms available. The feasibility study for micro hydropower sites in many countries is completed within half a year to a year. Sometimes, the civil works of such plants are built on the basis of the feasibility study alone. In such cases, the detailed engineering design is undertaken by the engineer or technician on-site as the construction work progresses.

The site selection process is more rigorous for hydropower power projects larger than the micro hydro range. Potential sites are often identified through a “desk study” based on studies of published topographical maps, hydrological studies (stream flow records), locations of transmission lines, and other technical parameters. Aerial photographs and satellite images are also becoming widely available and more affordable, and these are also useful resources to have for the desk study.

The topographic maps will show the source river and contours of the area, and with these parameters, the tentative layout of the waterways can be identified and the gross head estimated. In situations in which the stream has been gauged and flow records are available, the design discharge can be arrived at before visiting the site, and the designer can use these two parameters to estimate a tentative installed range for the power capacity. With the installed capacity and waterways layout, a preliminary project cost is also estimated based on prevailing market rates for materials, equipment, and thumb rules.

If the desk study indicates the site to be potentially feasible, then a detailed feasibility study is undertaken. In many countries, a permit or license from the government is required to carry out a survey and site investigation for the feasibility study. In other countries, the government carries out such feasibility studies with the intention of either implementing the power plants on its own or awarding the project to the private sector through a competitive bidding process.

Because the installed capacity of a hydropower plant depends on the available head and flow, it is important that these parameters are measured on-site at the initial stage.

3.2 MEASUREMENT OF HEAD

Once the locations of the forebay and powerhouse are identified, the topographic maps (when available) can indicate what the available head will be. However, it is still important to measure the head on-site for the following reasons:

- Most available topographic maps will not show elevation differences less than 1 m. For low-head micro hydro projects (e.g., 10 m to 20 m gross head) an error of 1 m will be high and will significantly lower the reliability of energy estimates.
- It may be difficult to exactly locate the powerhouse or the machine foundation area in the topographical maps, especially if these maps are of large scale or if there has been significant development in the area (e.g., new houses, bridges, or other infrastructure) after the topographical maps were prepared.
- In some regions or countries, topographical maps may not be available for the project area.

The head of a hydropower plant can be measured using various equipment as follows.

3.2.1 Level Machines, Theodolites, or Total Stations

This is survey equipment used by professional surveyors. The head measured using such equipment is very accurate. For example, the level machine can measure the difference in elevation between two points within 500 m with an error range of less than 1 cm. Theodolites and total stations can measure both difference in elevation between two points as well as the distance between them. The new total stations have a built-in interface facility such that the survey data can be directly downloaded to personal computers, and with the right software, topographical maps can be prepared. If experienced surveyors are available or if site engineers have experience in using such equipment, then a theodolite or total station can be an option to consider or a level machine if only the head needs to be measured. However, in many countries, such equipment is not readily available or is expensive to rent. The use of such survey equipment is beyond the scope of this textbook, and the reader should refer to standard textbooks on topographical surveys (Figures 3.1 and 3.2).

3.2.2 Global Positioning System (GPS)

The global positioning system (GPS) is a network of about 30 satellites orbiting the earth at an altitude of around 20,000 km. The system was developed by the U.S. government for navigation use by the military, but it is now freely available for use by anyone with a GPS device. A GPS device (also called a GPS receiver) locates the satellites that transmit information on their positions and the current time at regular intervals. These signals, traveling at the speed of light, are used by the GPS receiver to calculate how far away each satellite is based on how long it took for the signals to arrive. Based on the time taken for signals from different satellites to reach the GPS receiver, it determines the location of the device—that is, the point of interest recorded in the device (Figures 3.3 and 3.4).

FIGURE 3.1 A level machine mounted on a tripod and staff.

FIGURE 3.2 A digital theodolite.

FIGURE 3.3 GPS satellite orbiting the earth.

FIGURE 3.4 A handheld GPS receiver.

At least three satellites are required to determine location, and with four or more satellites, elevation is also determined. The more the satellites are visible, the higher the accuracy of the location will be. However, with the GPS receiver, the elevation of the desired location may not be very accurate. The error range in the elevation of a point recorded by a GPS receiver can easily be more than 10 m, and the relative difference in elevation between two points, such as the forebay and the powerhouse, can also exceed 10% error. Although GPS receivers are useful to locate the general project area features, such as waterway alignment, load centers, and transmission line layout, they will have limited use in determining the head of a micro hydro project due to high error range. The cost of the GPS receiver ranges from \$100 to \$400 or more, depending on the facilities available. It is also possible to download points recorded in the GPS into a personal computer.

3.2.3 Abney Level

An Abney level is a surveying instrument consisting of a spirit level and a sighting tube attached to a protractor. It is used to measure the angle of inclination of a line from the observer to another point. The observer points the sighting tube to the point of interest and rotates the knob such that the spirit level becomes horizontal. Then the angle can be read from the attached protractor (Figure 3.5).

The ground distance (or slope distance) between the observer and the point of interest can be measured with a tape. Once the slope distance and angle are known, the difference in elevation (or head) and the horizontal distance can be calculated using the following trigonometric equations:

$$\text{Vertical distance} = \text{Ground distance} \times \sin(\text{angle observed}) \tag{3.1}$$

$$\text{Horizontal distance} = \text{Ground distance} \times \cos(\text{angle observed}) \tag{3.2}$$

FIGURE 3.5 Abney level.

If a compass is also used along with an Abney level, then the horizontal angle can also be measured. The cost of this equipment ranges from $100 to $200. It is easy to use and unlike a theodolite or total station, it does not require extensive training.

3.3 MEASUREMENT PROCEDURE

The following equipment and accessories should be ready before the start of the survey:

An Abney level
A 50 m length tape
A stick with a mark at the surveyor's eye level

Once the above Abney level and accessories are available, the following procedure should be adopted:

- Send the helper with the stick to the point of interest.
- Look through the Abney level's telescope and adjust the focus until the mark on the stick is visible.
- Rotate the protractor knob until the spirit level attached to the protractor becomes horizontal. The bubble will be visible and within the edge lines in the telescope's lens.
- Read the angle from the marker next to the rotating knob. This is the inclination angle (θ in Figure 3.6).
- Using the tape, measure the length from where you are standing to where the helper is standing with a stick. This length is the ground length.

Once the ground length (slope length) and angle are known, the difference in elevation (h in Figure 3.6) can be calculated using Equation 3.1.

Example 3.1: Use of Abney Level

An Abney level is used to measure the head from the proposed forebay location to the powerhouse floor level. Six readings were taken as shown in the Table 3.1.

The surveyor started from the forebay area at Station No. 1 and moved downhill. The station is the location from which the observation was made from the Abney level, and the observation station is where the helper stood with the stick. Thus, after recording the readings (angle and length), the surveyor moved to the observation station, and the helper moved further downhill. Observation Station 6 is where the powerhouse is located.

A positive or negative sign should be assigned to differentiate whether the angle is downward or upward. In this case, because the measurement started from the forebay, downward angles are

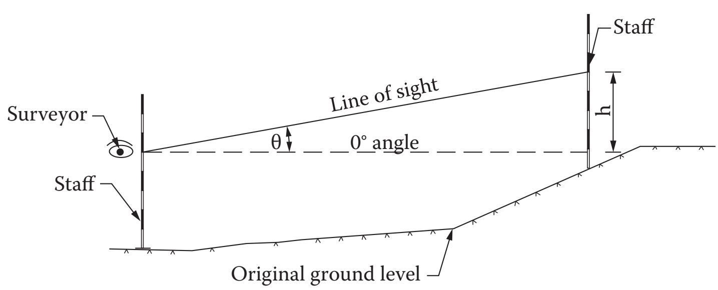

FIGURE 3.6 Measurement with an Abney level.

TABLE 3.1
Head Measurement Using Abney Level

		Observed Values		Calculated Values	
Stn. No.	**Obs. Stn.**	**Vertical Angle (θ)**	**Slope Dist. (m)**	**Hor. Dist. (m)**	**Vert. Dist. (m)**
1	2	30	80	69.28	40.00
2	3	20	65	61.08	22.23
3	4	−5	30	29.89	−2.61
4	5	60	60	30.00	51.96
5	6	45	30	21.21	21.21
Total			265	211.46	132.79

Note: Hor. Dist.: horizontal distance calculated; Obs. Stn.: observation station; Slope Dist.: slope distance measured using tape; Stn. No.: station number; Vert. Dist.: vertical distance calculated; Vertical Angle: angle measured from Abney level.

assigned positive values and the upward angles negative values. As can be seen from the table, when the surveyor is at Station 3 looking at Station 4, the angle is 5° upward. Therefore, a negative value has been assigned in this case. In other words, the elevation of Station 4 is higher than that of Station 3.

Once the angles and slope distances are known, then the vertical and horizontal distances can be calculated using the trigonometric Equations 3.1 and 3.2. The sum of the vertical distance is the gross head. Note that because the angle is upward from Station 3 to Station 4, when calculating the gross head a negative sign is assigned to the angle.

In this example, the sum of the slope distance (265 m) will be the approximate length of the penstock pipe required. The horizontal length will be the length shown in plan in the engineering drawings.

3.3.1 Measurement of River Flows

Often, small streams suitable for micro hydropower projects are not gauged. Therefore, river flow data are not usually available. Therefore, direct spot measurement of the river flows become essential to estimate what the low flows are and how the river flows vary throughout the year. In the absence of flow records, a minimum of one flow measurement per month for at least one year should be performed close to the proposed intake area so that the installed capacity can be finalized and the energy generation can be reliably estimated.

Various flow measurement methods pertinent to micro hydropower projects are described herein.

3.3.2 Flow Measurements Using a Conductivity Meter

A conductivity meter measures the amount of electrical current or conductance in a solution. The meter is equipped with a probe, usually handheld, for field or on-site measurements (Figure 3.7). After the probe is placed in the liquid to be measured, the meter applies voltage between two electrodes inside the probe. Electrical resistance from the solution causes a drop in voltage, which is read by the meter. The meter converts this reading to milli- or micro-Siemens (mS or μS) per centimeter. This value indicates the total dissolved solids. Total dissolved solids is the amount of solids that can pass through a glass-fiber filter.

Flow measurement using conductivity meter is also known as the salt dilution method. This method involves pouring a salt solution some distance upstream and measuring the change in conductivity as the salt wave approaches the gauging location (where the probe is placed). The salt solution changes the conductivity of the river (as the salt wave travels downstream), and this change in conductivity can be related to the river flow if baseline conductivity of the river, the type and amount

FIGURE 3.7 Conductivity meter and probe.

of salt added, and the water temperature are known. As the salt wave passes the measurement location, the conductivity of the river returns to its original level (i.e., baseline conductivity).

Conductivity meters can be used in small, highly turbulent streams with rough, irregular channels for flow measurements of a river. Table salt (sodium chloride, NaCl) is the most commonly used salt because it is inexpensive and widely available.

For accurate results, the following conditions have to be ensured:

- The salt solution poured upstream must be completely mixed throughout the river cross-section before it arrives at the measurement location.
- The stream section should not have large stagnant pools.
- There should not be any inflows into or outflows from the stream between the point at which the salt solution is poured and the measurement location. In other words, the flow at the location where the salt is poured must be equal to the flow that arrives at the measurement location.
- The conductivity meter probe should be submerged in a fairly fast-flowing section of the river.

The advantages of this method are that it is simple and fairly accurate (within ~7%) when used by trained personnel. It is also reliable for a wide range of flows and measurements can generally be taken within 30 minutes. This method can be used in fast-flowing rivers ranging from 25 l/s to about 2.5 m^3/s.

3.3.2.1 Measurement Procedure

The equipment and accessories required are as follows:

1. A conductivity meter covering a range of 0–10,000 micro-Siemens (μS)
2. A thermometer to measure the water temperature
3. Some amount of salt (according to discharge)
4. A weighing machine (to weigh the salt)
5. A stopwatch
6. Graph papers (mm type) and a calculator
7. One bucket
8. Clean stick or stirring rod

3.3.2.2 Discharge Measurement

1. Prepare a salt solution in a bucket by mixing salt and river water, and stir the solution with a clean stick until the salt is completely dissolved. Note that the weight of the salt should be carefully measured (using a weighing machine) and recorded before placing it into the bucket. Also, once such a solution is prepared, care must be taken not to spill any; 50 g to 300 g of salt may be required for each 100 l/s of flow, depending on the baseline conductivity of the flow. For higher baseline conductivity, more salt will be required. Because the river flow is initially unknown, it will have to be estimated in order to apply the above general rule.
2. Turn on the conductivity meter and submerge the probe in a fast-flowing section of the river. Then record the baseline conductivity (i.e., natural conductivity of the river before the addition of the salt solution). Also set the stopwatch so that the time can be measured.
3. Select a place upstream of the measurement location where the salt solution can be quickly dumped. Depending on the turbulence of the flow, this location should be between 50 m and 300 m upstream of the measurement site. If the flow is turbulent upstream (i.e., presence of rapids and falls), 50 m may be adequate; otherwise the distance will have to be increased. The principle is that the cloud of salt solution needs to be completely dispersed in the stream water before it reaches the conductivity measurement location. Similarly, it is necessary to ensure that there are no flow abstractions, additions, or stagnant pools between the measurement site and the upstream location where the salt solution is poured (Figure 3.8).
4. Then send a helper with the salt solution bucket upstream at the chosen location (make sure that the solution is not spilled on the way). Signal the helper to pour the saltwater solution into the stream. The entire solution should be poured quickly and in one go. Slow pouring may cause fluctuations in the conductivity readings and hence less accurate results. Start the stopwatch and note the readings on the conductivity meter as soon as there is an increase in the values from the baseline conductivity (Figure 3.9). The common practice is to note the readings in five-second intervals. It is useful to have two persons to take the readings at the measurement site. One can read the conductivity values every five seconds (using the stopwatch), and the other can record these values. Also, it is helpful to record the readings in a preformatted table (see Table 3.2).

FIGURE 3.8 Pouring the salt solution.

FIGURE 3.9 Readings on the conductivity meter.

The conductivity readings should be taken continuously until the value diminishes back to the baseline conductivity of the stream. Note that sometimes the conductivity values may remain above the baseline value by a few μS for a long time. If this is the case, then the conductivity readings can be stopped because the difference of a few percent in conductivity does not contribute significant additional flows.

5. Measure the temperature of the water in the stream if the conductivity meter does not have provision for temperature adjustment. Also fill in other data, such as weather, date, and time as shown in Table 3.2.
6. Finally, plot the reading on the graph paper with time in seconds on the horizontal axis and conductivity in micro-Siemens (μS) on the vertical axis as shown in Figure 3.10. If the result is not satisfactory (i.e., a smooth-shaped graph according to Figure 3.10e), repeat the measurement with more or less salt, depending on the outcome. Inaccurate graphs and their probable reasons are also presented in Figure 3.10. Therefore, based on the results obtained (i.e., the graph), take remedial measures.
7. After satisfactory results are obtained, take a second set of measurements to verify the first. Note that this will only require about half an hour of additional work on-site and will be cost-effective compared to coming back to the site a second time for flow measurements.

The accuracy of the measurement depends on the calibration of the conductivity meter. The conductivity meter is calibrated by carefully determining the salt constant (k value) for the type of salt used under controlled laboratory conditions. This is discussed in the subsequent section. Note that packet salts should be used rather than loose crystals. This is because packet salts are more homogenous, and loose salt crystals can absorb water and thus lead to errors.

Once a satisfactory graph is obtained, the flow can be calculated as follows:

$$\text{Stream flow,}\quad Q = M \cdot k/A$$

where Q is the flow in l/s, M is mass of the dried salt in mg, and k is the salt constant and is dependent on the nature of salt and water temperature (if the conductivity meter is not of the temperature adjustment type). The units of k are (μS)/(mg/l) or micro-Seimens per milligram per liter. Note that conductivity is the reciprocal of resistivity and micro-Seimen (1 μS) = 1 ohm^{-1} · 10^{-6} and

TABLE 3.2
Flow Measurement Using Conductivity Meter

Sheet: Salt Dilution Measurement Data Input Sheet

Station Name	TangchhaharaKhola, Mustang	Reader	SakundaOjha
Date	Tuesday, March 4, 2014	Estimated discharge (m^3/s)	0.1
Weather	Cloudy	Instrument	Conductivity meter (WTW of Germany)

Gauge Height

At beginning		At end	

Time

At beginning	16:16	At end	16:30
Sampling interval (s)	5 s	Time until first signal (s)	16:19

Distance

Injection point:		Sampling point:	Mixing length (m)	100

Others

Water Temperature (°C)	4.1	Injected salt (g)	1502
Salt constant (K)	1.93	Base level conductivity (µS)	233

S. N.	Conductivity (µS)	S. N.	Conductivity (µS)	S. N.	Conductivity (µS)
1	233	43	298	85	240
2	235	44	294	86	240
3	237	45	290	87	240
4	240	46	288	88	239
5	243	47	287	89	239
6	247	48	286	90	239
7	250	49	283	91	238
8	253	50	280	92	238
9	257	51	279	93	238
10	263	52	273	94	237
11	270	53	273	95	237
12	279	54	272	96	237
13	281	55	271	97	237
14	289	56	271	98	236
15	293	57	268	99	236
16	298	58	266	100	236
17	303	59	265	101	236
18	309	60	264	102	236
19	311	61	262	103	236
20	315	62	261	104	235
21	319	63	260	105	235
22	323	64	258	106	235
23	325	65	255	107	235
24	326	66	255	108	235
25	328	67	254	109	235
26	329	68	254	110	235
27	327	69	252	111	235
28	327	70	251	112	235

(*Continued*)

TABLE 3.2 (CONTINUED)
Flow Measurement Using Conductivity Meter

Sheet: Salt Dilution Measurement Data Input Sheet

Station Name	TangchhaharaKhola, Mustang	Reader	SakundaOjha
Date	Tuesday, March 4, 2014	Estimated discharge (m^3/s)	0.1
Weather	Cloudy Instrument	Conductivity meter (WTW of Germany)	

Gauge Height

At beginning		At end	

Time

At beginning	16:16	At end	16:30
Sampling interval (s)	5 s	Time until first signal (s)	16:19

Distance

Injection point:	Sampling point:	Mixing length (m)	100

Others

Water Temperature (°C)	4.1	Injected salt (g)	1502
Salt constant (K)	1.93	Base level conductivity (μS)	233

S. N.	Conductivity (μS)	S. N.	Conductivity (μS)	S. N.	Conductivity (μS)
29	327	71	250	113	234
30	325	72	250	114	234
31	324	73	249	115	234
32	323	74	248	116	234
33	321	75	247	117	234
34	320	76	246	118	234
35	318	77	245	119	234
36	314	78	244	120	234
37	312	79	243	121	234
38	311	80	243	122	234
39	308	81	242	123	233
40	307	82	242	124	233
41	304	83	241	125	
42	301	84	240	126	

1 Siemen = 1 ohm^{-1}. For determination of k value, refer to Section 3.3.2.3. A is the area of the curve after excluding the area due to base conductivity in (seconds × μS).

A can be calculated from the following formula:

$$A = (\Sigma C(t) - N \cdot C_0) \cdot T$$

where $\Sigma C(t)$ = sum of conductivity values (μS), N = number of observations, C_0 = base conductivity (μS), and T = time interval (seconds). The units in the equation Q = Mk/A are checked below:

$$[mg \cdot (\mu S / (mg/l))/(sec \cdot \mu S) = l/s]$$

Because the final units are l/s for the flow (Q), the units match.

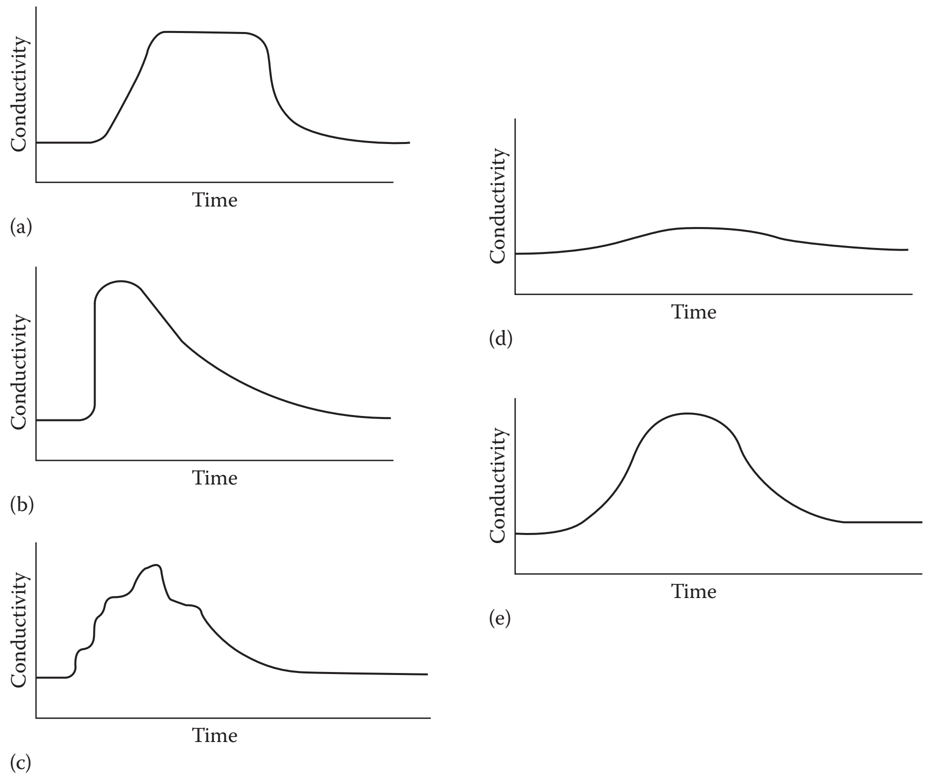

FIGURE 3.10 Conductivity graphs for various conditions: (a) meter saturated, change scale or use less salt; (b) badly skewed curve, use longer distance; (c) uneven reading, salt not mixed, use longer distance; (d) insufficient response compared to base level; and (e) perfect.

Example 3.2: Flow Calculation Using Conductivity Meter Results

Data obtained from a site using a conductivity meter is presented in Table 3.2.

AREA (A) UNDER THE CURVE

M = 1,502,000 mg
K = 1.934 μS/(mg/l)
ΣC(t) = 32,861 μS
N = 124
C_0 = 233 μS/cm
T = 5 s

Now,

$$
\begin{aligned}
A &= (32,861 - 124 \cdot 233) \cdot 5 \\
&= 3969 \cdot 5 \\
&= 19,845\ \mathrm{s} \times \mu\mathrm{S}
\end{aligned}
$$

Note that the area here is the area under the graph of conductivity in μS in the vertical axis and time in seconds in the horizontal axis excluding the baseline conductivity (i.e., conductivity measure before pouring the salt solution upstream). Hence, the units of area under the graph are

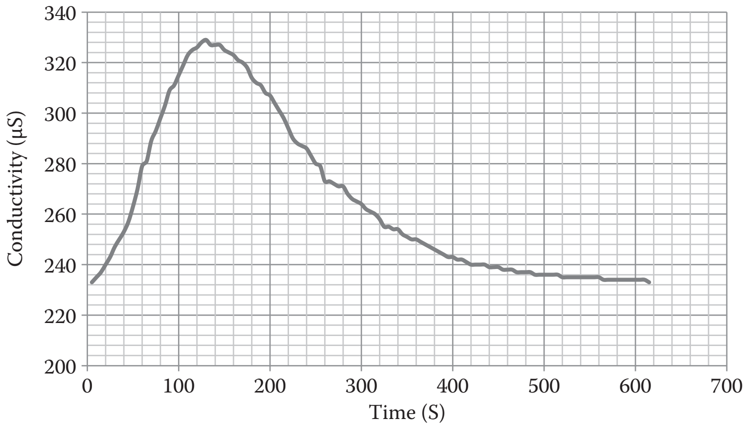

FIGURE 3.11 Graph of conductivity over time (based on data from Table 3.2).

µS Sec. The graph of the conductivity readings over time for this example is also presented in Figure 3.11.

Note that the shape of the graph is similar to that of the ideal case (Figure 3.10e).

DISCHARGE

$$Q = 1{,}502{,}000 \cdot 1.93 / 19{,}845$$
$$= 146 \text{ lps}$$

Therefore the river flow is 146 lps.

3.3.2.3 Determination of K Value

The following equipment is required to determine the K value:

1. Conductivity meter
2. Weighing machine
3. Bucket (10–20 l)
4. Graduated cylinder (1 l)
5. Pipette
6. Stirring rod
7. Salt (of the type that will be used for flow measurement)

Once all equipment is ready, adopt the following procedure:

1. Pour about 10 l of tap or river water in the bucket. Use the graduated cylinder to measure the exact volume of water.
2. Using the weighing machine, weigh about 200 g of salt and note the exact weight. Pour about 1 l (1000 ml) of tap water into the graduated cylinder and note the exact volume. Pour the salt in the water and stir with a stirring rod until it is completely dissolved. Now, the concentration of salt in the calibration solution is 200 g/1000 ml = 200 mg/ml (assuming that exactly 200 g of salt was added into 1000 ml of water).
3. Measure the temperature and the base conductivity of the water in the bucket and note them in the field book.

4. Take 10 ml of the above-calibrated solution (i.e., 10 ml·200 mg/ml = 2000 mg of salt) in a pipette and inject it into the bucket. Stir the saltwater solution to ensure proper mixing and then note the conductivity reading. Note that once the saltwater has been completely mixed in the bucket, the readings will not fluctuate. Therefore, after adding the calibrated solution in the bucket, it must be stirred well, and measurements should be taken once there is no fluctuation. Note that, in this case, the concentration in the bucket is 2000 mg/10.01 l = 199.8 mg/l. Note that the volume in the bucket is 10.01 l because 10 l of water was initially placed in the bucket and then 10 ml of salt solution was added. The volume of the salt solution should also be included in the total volume calculation because this could be significant as more and more salt solution is added.
5. Repeat Step 4 about 10 times so that there are adequate data to calculate the salt constant.
6. Now plot the conductivity values (μS) in the vertical axis and the cumulative salt concentration (mg/l) in the horizontal axis. Then draw a best-fit line joining the 10 data points. Determine the slope of this line—that is, the rise in conductivity over the rise in salt concentration, which is the value for the salt constant (k value).

Note that if the conductivity meter is not of the temperature compensating type, then the calibration method presented above should be repeated at various temperatures, and then the change in k value with change in temperature can be determined. If the procedure is repeated three to four times for temperatures between 5°C to 20°C, it should be adequate because this range should cover most of the cases on-site.

Alternatively, the salt constant at different temperatures can be calculated using the following equation:

$$K = k/(1 + \alpha\Delta T)$$

where K = salt constant at temperature T, K = salt constant at temperature t, α = temperature compensation slope for salt (for table salt, its value is 0.0214), and ΔT = Change in temperature (T − t).

An example is presented below to further illustrate the calibration of the conductivity meter.

Example 3.3: Conductivity Meter Calibration

Project Name: Tangchhahara Small Hydroelectric Project

Location	Kothethati
Date	Tuesday, March 04, 2014
Time	3:22:00 PM
Temperature in °C	4.7
Meter type	Conductivity meter (WTW Germany)
Place	Near powerhouse
Salt	Table salt (NaCl)
Calibration solution	200 g of salt in 1 l of water
Calibration quantity of water in liters	10

Amount of Solution Added, ml	Total Volume in Bucket, ml	Cumulative Salt Concentration, mg/l	Conductivity, μS
0	10,000	0.00	233
10	10,010	199.80	628
20	10,020	399.20	1014
30	10,030	598.21	1391
40	10,040	796.81	1769

(*Continued*)

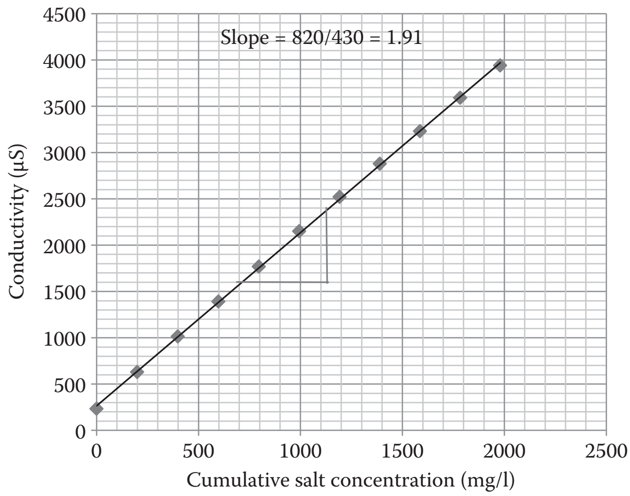

FIGURE 3.12 Conductivity meter calibration.

Amount of Solution Added, ml	Total Volume in Bucket, ml	Cumulative Salt Concentration, mg/l	Conductivity, μS
50	10,050	995.02	2150
60	10,060	1192.84	2520
70	10,070	1390.27	2879
80	10,080	1587.30	3230
90	10,090	1783.94	3590
100	10,100	1980.20	3940

Now plot the salt concentration in the bucket (mg/l) on the horizontal axis and conductivity (μS) on the vertical axis and draw the best-fit line as shown in Figure 3.12.

As can be seen from Figure 3.12, the slope of the line is 1.91. Therefore the salt constant k at 4.7°C is 1.91 μS/(mg/l).

Now, salt constant at temperature 4.1°C = $1.91/(1 + 0.0214 \cdot (4.7 - 4.1) = 1.93$.

3.3.3 Flow Measurements Using a Current Meter

A current meter is a mechanical device with revolving cups or a propeller attached to a shaft (Figure 3.13). These cups or propellers revolve when the instrument is immersed in flowing water because of flow velocity. The revolving frequency is dependent on flow velocity—that is, the higher the flow velocity, the faster the revolution. With the correlation between the revolutions of the cups or propeller, the flow velocity can be determined. If the cross-section area of the river is known at the discharge measurement point, then in principle, the river discharge can be calculated using average velocity determined.

Discharge measurement by conductivity meter is not practical for large rivers due to the large volumes of salt required and increased likelihood of intermittent stagnant pools along a short stretch. Thus, for rivers with flows larger than 2.5 m^3/s, an alternative method of flow measurement (than conductivity meter) is required. The current meter is a suitable method of flow measurement for rivers with relatively higher flows.

As there is a direct correlation between the frequency of revolution and flow velocity, the flow velocity can be calculated from the current meter using the correlation equation. This current meter

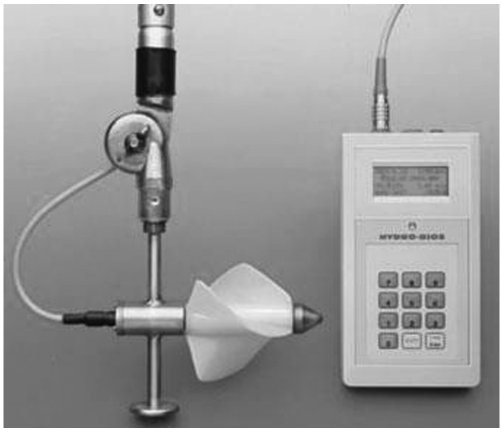

FIGURE 3.13 Current meter.

is most suitable for flow measurement in the velocity range between 0.2 m/s and 5 m/s where the accuracy can be as high as 98%.

A current meter is the most commonly used instrument to measure the velocity at a point in the flow cross-section. It generally consists of a rotating element, which rotates due to the reaction of the stream current with an angular velocity proportional to the stream velocity. During flow measurement using a current meter, the river section is divided into a number of strips (trapezoidal and triangular), and velocity corresponding to each strip is determined by using a current meter.

3.3.3.1 Flow Measurement Procedure

3.3.3.1.1 Selection of Measurement Location

As far as possible, a straight portion of river with a comparatively uniform flow section should be selected for flow measurement. Moreover, a stretch with a backwater effect should be avoided. A typical measurement location is shown in Figure 3.14.

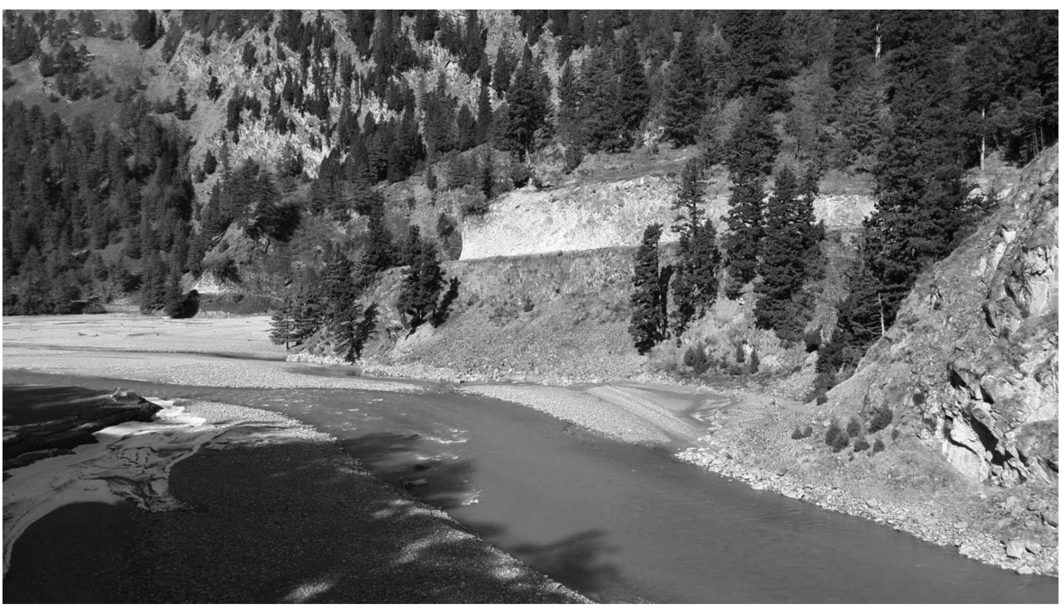

FIGURE 3.14 Appropriate flow measurement location.

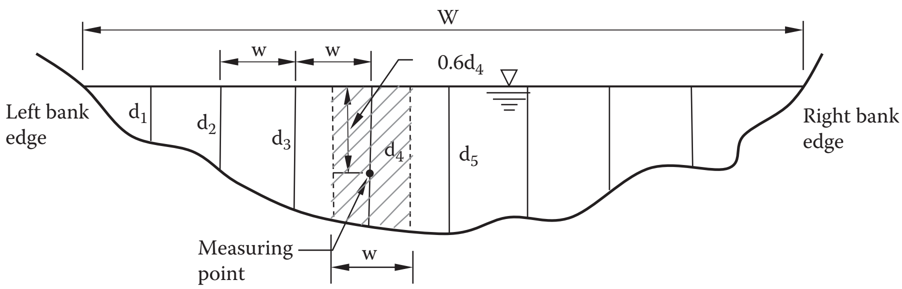

FIGURE 3.15 River cross-section.

3.3.3.1.2 Segment Division

The entire width of the river should be divided into equal segment width, w, as shown in Figure 3.15. It is recommended that the river cross-section be divided into at least 15 segments so that measurement accuracy is increased. The segment width should generally be between 0.5 m and 1.0 m.

A typical river cross-section for flow velocity measurement and flow calculation is shown in Figure 3.15, and notations used are as follows:

W = width of river
w = width of measurement segments (all equal)
$d_1, d_2, d_3, \ldots$ = depths of flow of measurement segments

3.3.3.1.3 Measurement

If flow depth is below 0.75 m, a current meter mounted on a graduated wading rod should be placed at the end of each segment at a depth of 0.6 times the water depth from the surface (see Figure 3.15), and the readings should be recorded (e.g., d_1, d_2, d_3). And if flow depth is above 0.75 m, two readings should be taken 0.2 and 0.8 times the flow depth from the surface; the average of these values yield the flow velocity at the section.

Note that the cup or propeller of the current meter should be facing the upstream side of the wading rod, and care should be taken not to disturb flow during the measurement process—that is, the recorder should stand downstream from the wading rod.

The number of revolutions in 30 to 40 seconds time should be recorded. Based on the type of current meter, the number of revolutions can be counted either via a sound emitted (e.g., beep or click) through a headphone or via a mechanical or digital counter mounted on the current meter.

3.3.3.1.4 Parameter Calculation

The frequency of revolution is the number of revolutions per second and can be found by dividing the number of revolutions recorded by the time period in seconds. Then flow velocity of the segment can be found from the correlation equation:

$$v = a \cdot N + b$$

where v = segment velocity m/s, N = frequency of revolution rps, a = constant based on N and provided by the equipment manufacturer or determined through calibration in a standard hydraulic laboratory, b = constant based on N and provided by the equipment manufacturer or determined through calibration in a standard hydraulic laboratory.

Area of the segment can be found by multiplying segment width, w, and segment depth (in Figure 3.15 d_4 in hatched area segment).

Then the flow through the hatched segment in Figure 3.15, is $w \cdot d_4 \cdot v_4$ (v_4 flow velocity through Segment 4). Thus, calculating the flow of each segment and adding all flows will result in total river flow at the time of measurement. At least three sets of measurements should be taken during flow measurement to avoid error. If all measurements are within a 5% range, the average should be used as the estimated flow. If the deviation is larger than 5%, the measurement should be repeated until the three sets of measurements are within the 5% range.

It should be noted that current meters displaying the direct value of velocity are also available in the market. If such a current meter is used, the velocity calculation will not be necessary.

A form for recording the measured data and flow calculation is presented here, and an example of flow data recording and calculation is shown in Table 3.3.

TABLE 3.3
Data Recorded and Flow Calculation Example

Flow Data Recording and Calculation By Current Meter

Date:	10/26/2070	River width (W):	21 m
Instrument:		Segment width (w):	1 m
River:	Mai Khola	Revolution duration (t):	40 s
Location:	Chisapani-9, Gunmune, Illam	Last calibrated date:	

Segment	Distance, m	Depth, m	Area, m^2	Number of Revolutions	Rev/s (N)	Velocity, m/s	Discharge, m^3/s
1.00	0	0					
2.00	1.00	0.39	0.44	52.00	1.30	0.33	0.14
3.00	2.00	0.60	0.60	50.00	1.25	0.32	0.19
4.00	3.00	0.75	0.75	102.0	2.55	0.65	0.49
5.00	4.00	0.69	0.69	91.00	2.28	0.58	0.40
6.00	5.00	0.62	0.62	118.00	2.95	0.75	0.47
7.00	6.00	0.64	0.64	92.00	2.30	0.59	0.38
8.00	7.00	0.61	0.61	120.00	3.00	0.77	0.47
9.00	8.00	0.65	0.65	108.00	2.70	0.69	0.45
10.00	9.00	0.59	0.59	106.00	2.65	0.68	0.40
11.00	10.00	0.62	0.62	170.00	4.25	1.09	0.67
12.00	11.00	0.56	0.56	131.00	3.28	0.84	0.47
13.00	12.00	0.52	0.52	102.00	2.55	0.65	0.34
14.00	13.00	0.55	0.55	117.00	2.93	0.75	0.41
15.00	14.00	0.54	0.54	96.00	2.40	0.61	0.33
16.00	15.00	0.48	0.48	115.00	2.88	0.73	0.35
17.00	16.00	0.55	0.55	86.00	2.15	0.55	0.30
18.00	17.00	0.47	0.47	67.00	1.68	0.43	0.20
19.00	18.00	0.33	0.33	70.00	1.75	0.45	0.15
20.00	19.00	0.27	0.27	92.00	2.30	0.59	0.16
21.00	20.00	0.22	0.22	34.00	0.85	0.21	0.05
22.00	21.00	0.13	0.25	18.00	0.45	0.11	0.03
							6.84

Correlation Equation aN + b

Correlation Coefficient	**a**	**b**	
	0.2473	0.00123	for N < 1.74
	0.2568	−0.0042	for N ≥ 1.74

Note: The segment velocity should be kept in the velocity column if the current meter gives it directly.

Calculation of Segment 4 flow is shown below.
Known:

Depth (d_4) = 0.75 m
Segment width (w) = 1 m
Revolution duration (t_4) = 40 s
Number of revolutions (R_4) = 102

Correlation coefficient (provided by equipment supplier in the owner's handbook and confirmed by calibration)

$$\begin{aligned}(a, b) &= (0.2473,\ 0.00123) \text{ for } N < 1.74 \\ &= (0.2568,\ -0.0042) \text{ for } N \geq 1.74\end{aligned}$$

Calculation:

$$\begin{aligned}\text{Frequency of revolution } (N_4) &= R_4/t_4 \\ &= 102/40 \\ &= 2.55 \text{ rps}\end{aligned}$$

$$\begin{aligned}\text{As } N > 0.84\text{, formula for segment velocity } (v_4) &= 0.2568 \cdot N_4 - 0.0042 \\ &= 0.2568 \cdot 2.55 - 0.0042 \\ &= 0.65 \text{ m/s}\end{aligned}$$

$$\begin{aligned}\text{Segment flow } (q_4) &= w \cdot d_4 \cdot v_4 \\ &= 1 \cdot 0.75 \cdot 0.65 \\ &= 0.49 \text{ m}^3/\text{s}\end{aligned}$$

Similarly, discharge of each segment is calculated and totaled to come up with the river flow of 6.84 m^3/s.

3.3.3.2 Calibration of Current Meter

Calibration of the current meter should be done at least once every six months by a standard laboratory for consistency and accuracy of flow measurement. During calibration, a wide range of velocities and a sufficient number of measurements need to be taken as recommended by the manufacturer. The laboratory then issues a certificate of calibration with the date and other technical parameters.

3.4 FLOW MEASUREMENT USING FLOAT METHOD

Float measurement is a simple method to measure flows in small rivers. In this method, any object that floats in water is released at the surface of the river, and its velocity is estimated by recording the time required for it to travel a certain distance. Thus, the surface flow velocity can be obtained by dividing the length of the river stretch that the floating object has traveled by the time taken. This value should be multiplied by following the correction factor to obtain the mean flow velocity of the river at the measurement location.

And the discharge can be calculated by using the following equation:

$$Q = AkV$$

where Q = discharge of the river in m^3/s, A = cross-section area of the stretch (m^2; computation of cross-section was discussed earlier), V = float velocity or velocity of the floating object (m/s), and k = coefficient to correct the surface velocity.

Equipment for float method measurement are as follows:

1. A measuring tape
2. One stopwatch
3. 5–10 floats

Floats can be orange peel, a water-soaked block of wood, or other natural material that sinks at least halfway into the water, is visible from shore, will not be moved by wind, and is nonpolluting (Figure 3.16).

3.4.1 Float Method Procedure

1. Measure and mark two points, at least two to three channel widths apart, at the channel cross-section. If stationing stakes are still in place, one or two may be left in the ground to serve as markers.
2. Two observers are best. One tosses the float into the channel above the marker and calls out when it crosses the upstream point. Toss each float a different distance from the bank to get a rough average of velocities.
3. The downstream observer starts the timer, sighting across the stream from the lower point. When the float passes it, stop the watch and record the time. Repeat the procedure five to 10 times. Average the values to get the mean surface velocity.
4. Multiply the previously measured cross-sectional area with the surface velocity and the coefficient (k) based on flow depth according to Table 3.4 (Q = AkV).

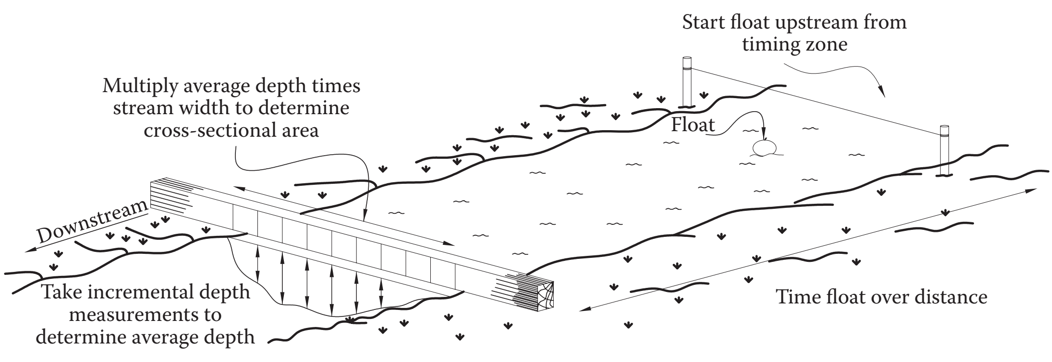

FIGURE 3.16 The float method of estimating flow.

TABLE 3.4
Coefficients to Correct Surface Float Velocities to Mean Channel Velocities

Average Depth in Reach		
Feet (ft)	**Meters (m)**	**Coefficient (k)**
1	0.3048	0.66
2	0.6096	0.68
3	0.9144	0.70
4	1.2192	0.72
5	1.5240	0.74
6	1.8288	0.76
9	2.7432	0.77
12	3.6576	0.78
15	4.5720	0.79
>20	>6.0960	0.80

3.5 SIZING OF A MICRO OR MINI HYDROPOWER PLANT

Sizing of a run-of-river hydropower plant depends on the head and flow available. Once the location of the intake and the powerhouse are known, the gross head will also be known. As discussed earlier, the river flows are likely to vary over the months. Thus, based on financial analysis of the proposed project at various design flows, the demand for power and energy at the load centers and whether the power plant is to be grid connected as well as other country or site-specific variables, the installed capacity is decided. Example 3.4 illustrates how a tentative range of installed capacity can be reached based on a topographic map and basic hydrological data available.

Example 3.4: Sizing of Tinekhu Small Hydropower Project

A topographic map with a tentative layout of a small hydropower project in Tinekhu River, Nepal, is shown in Figure 3.17. An intake (headworks) has been located tentatively at the right bank of the river at an elevation of 1398 m above mean sea level (amsl). At this stage, it is assumed that there is adequate space for the gravel trap and settling basin close to the intake. Then a 2046-m-long headrace pipe will be needed to convey the flow to the forebay. The elevation of the forebay is at 1387 amsl. The 11-m difference in elevation between the intake and the forebay allows for the head loss in the gravel trap, settling basin, and through the headrace pipe. Calculations of such losses will be dealt with in later chapters. From the forebay a 960-m-long penstock pipe will convey the design discharge into the turbines in the powerhouse. The ground elevation of the powerhouse (or tentative turbine centerline) is 985 amsl. Thus, the gross head of the scheme is 402 m (i.e., 1387 m − 985 m). Note that the four corners shown in the topographic map are the license boundaries given by the concerned government authority based on the layout submitted.

Once a tentative layout is sketched on the topographic map, a site visit should be undertaken to verify the following:

- Ensure that the intake location is suitable. If not, the intake location should be adjusted based on ground conditions.
- Find suitable locations for key structures, such as the gravel trap, settling basin, forebay, and the powerhouse.
- Finalize the waterway layout according to site conditions. For example, if the canal route is through an existing house (not shown in the topographic map), then the alignment would have to be readjusted.
- If possible, undertake flow measurement at the proposed intake location.

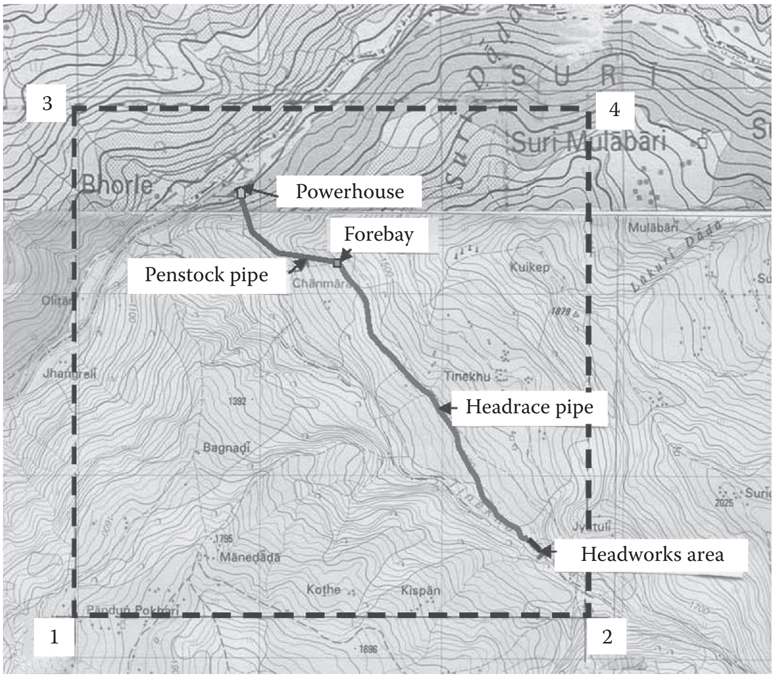

FIGURE 3.17 Tinekhu small hydropower site, Nepal, identified based on study of topographic map.

Thus, the tentative layout done on the topographic map during the desk study is finalized after a site visit. Based on the size of the project and site conditions, this may require a number of site visits. Note that for micro hydropower, due to simplicity of the project and limited funds available, generally one or two visits are made to finalize the layout.

Once the layout is finalized, the installed capacity is determined based on flows available in the river and their variations throughout the year. The mean monthly flows estimated at the intake of the Tinekhu Small Hydropower Project based on hydrological data available and flow measurements are provided in Table 3.5.

The mean monthly flows of the Tinekhu Small Hydropower Project is also shown graphically in Figure 3.18. A plot of river flows over a time series is also known as a "hydrograph."

As can be seen from Figure 3.18 and Table 3.5, the river flows are low from November to May and increase from June when the monsoon rainy season starts in Nepal. The hydrograph would look quite different for a snow-fed river or for a river at a geographic location in North America where the lowest flow may be experienced during the summer months. Based on the flows available for the Tinekhu Small Hydropower Project, the installed capacity has been determined as follows:

- Recall that the gross head available is 402 m.
- As can be seen from Table 3.5, the mean monthly flows vary from 122 l/s in March to 3300 l/s in August. Therefore, the selected design discharge should be between 122 l/s

TABLE 3.5
Mean Monthly Flows Available at the Proposed Intake Site of the Tinekhu Small Hydropower Project

Month	Jan	Feb	Mar	Apr	May	Jun	Jul	Aug	Sep	Oct	Nov	Dec
Flow (l/s)	236	175	122	146	231	1200	2400	3300	1700	700	427	325

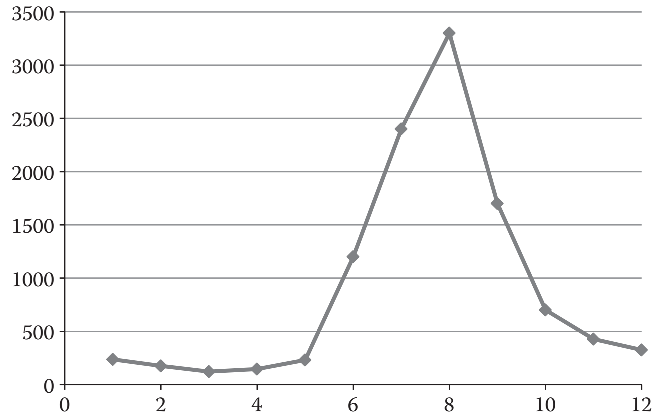

FIGURE 3.18 Mean monthly flow hydrograph of Tinekhu River.

and 3300 l/s. Note that if 122 l/s is selected as the design discharge, then the installed capacity will be available throughout the year as this is the least monthly flow. This may result in undersizing the plant capacity as most of the river discharge will not be used for power generation for the rest of the year. On the other hand, if 3300 l/s is selected as the design discharge, then this flow would only be available for about one month in a year, and for the remaining 11 months, the installed capacity cannot be generated. In this case, the plant installed capacity may have been overestimated. At this stage, to select the design discharge, it is often useful to derive a flow duration curve based on the data available. Derivation of flow duration curve is discussed hereafter.

3.5.1 Flow Duration Curve

Once the river flows for power generation are available, a flow duration curve (FDC) can be prepared. FDC indicates flow available for power generation as percentage of time during the year. For example, in the case of the Tinekhu Small Hydropower Project, 122 l/s is available throughout the year or 122 l/s is exceeded 100% of the time. Similarly, 3300 l/s is available for only one month a year, or one 12th of the time, which is 8.33% exceedance. Once flow data is available to prepare an FDC, the data needs to be ranked in ascending order. Then, based on the nature of the data available (daily, weekly, or monthly), the percentage exceedance can be calculated. For example, if data is available on a weekly basis, then the highest weekly flow available will be 1.92% exceedance (i.e., 100 × 1/52). Based on the mean monthly flows available for the Tinekhu Small Hydropower Project, the flow exceedance is calculated as shown in Table 3.6.

Based on the mean monthly flows available and their corresponding percentage of exceedance, a flow duration curve can be prepared as shown in Figure 3.19.

As can be seen from Figure 3.19, the slope of the FDC changes sharply once the flow exceedance decreases below 45%. For exceedance between 100% and 45%, the slope of the FDC is relatively low. Once the flow exceedance decreases below 45% (note that the corresponding flows will increase), the slope of the FDC increases. This indicates that flow exceedance below 45% will result in marginally lower energy generation. In other words, if a higher design discharge corresponding to a value lower than 45% exceedance is selected, then for each additional 1.0 l/s of discharge, the incremental annual energy available will fall increasingly lower. The optimal design discharge can be estimated based on the FDC alone, using this technique.

In the case of the Tinukhe Small Hydropower Project, the 45% exceedance flow is about 520 l/s. Thus, the optimum design discharge based on FDC alone would be 520 l/s. However, in this case, the developer decided to select a design discharge of 350 l/s. This was done to stay within an

TABLE 3.6
Flow Exceedance at the Intake Site of the Tinekhu Small Hydropower Project

Rank	Flow l/s (Month)	Months Exceeded	% Exceedance
1	122 (March)	12	12/12 = 100%
2	146 (April)	11	11/12 = 91.67%
3	175 (Feb)	10	10/12 = 83.33%
4	231 (May)	9	9/12 = 75.0%
5	236 (Jan)	8	8/12 = 66.67%
6	325 (Dec)	7	7/12 = 58.33%
7	427 (Nov)	6	6/12 = 50.0%
8	700 (Oct)	5	5/12 = 41.67%
9	1200 (Jun)	4	4/12 = 33.33%
10	1700 (Sep)	3	3/12 = 25%
11	2400 (Jul)	2	2/12 = 16.67%
12	3300 (Aug)	1	1/12 = 8.33%

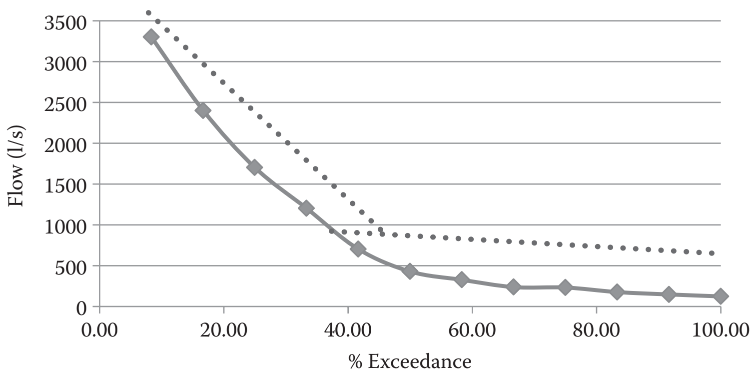

FIGURE 3.19 Flow duration curve (FDC) of the Tinekhu Small Hydropower Project.

installed capacity threshold of less than 1.0 MW to take advantage of simpler licensing requirements and to avoid paying an annual royalty, which is levied by the government on larger plants.

At 350 l/s design discharge and 402 m gross head, assuming overall system efficiency of 72%, the installed capacity will be 990 kW or just below 1.0 MW. The 72% overall efficiency allows for losses along the penstock pipe, generating units, transformer, and transmission line up to the interconnection point at the utility's grid (2.8 km away). Note that 350 l/s is about 55% exceedance flow. In this example, the environmental release has not been considered yet. Based on recommendations of the environmental studies, some flows will have to be released downstream of the intake along the river. This environmental release will decrease the power and energy outputs during the low-flow months when river discharge is less than 350 l/s plus the recommended environmental release.

If 670 l/s was selected as the design discharge, then at 72% overall efficiency the project would have an installed capacity of about 1870 kW or 1.87 MW.

From this example, it can be seen that although the FDC can be useful to estimate the installed capacity, the developer may decide on a different capacity based on the country's policies, such as those pertaining to taxes, royalty and license fees, funds available, and other factors.

3.6 SITE SELECTION

As discussed earlier, selecting a suitable site for hydropower development depends on the available stream flow and the topography of the site. The range of river flows available during the year determines the design discharge that can be used for power generation whereas the topography determines the gross head available as well as feasible waterways alignments. Satellite images such as Google Earth can also be useful in sketching out a tentative layout of hydropower projects at the start of the desk study (Figure 3.20).

Site selection and sizing for large and especially storage type hydropower projects is a multidisciplinary task and is beyond the scope of this textbook. For micro to small run-of-river (RoR) hydropower plants, the general methodology is as follows.

3.6.1 Market Study and Licensing

The first step is to ascertain the market for the generated electricity. Some questions that need to be answered are the following:

- For a grid-connected potential hydroelectric power plant, is the utility interested in buying the generated electrical energy, and if so, what are the terms and conditions?
- In the case of isolated micro hydropower plants, who are the customers, what is their ability to pay for electricity, and what are the load characteristics? Given their potentially large community development benefits, isolated plants are often eligible for grants or loans from the local government, central government departments, NGOs, or donor organizations. The market study and feasibility analysis must thus take into account the contribution from these additional actors as well.

The market opportunities for large hydropower plants are ascertained during the desk study phase. The size and profile of the load for potential isolated micro hydropower plants need to be estimated through discussions with prospective users during the field visit whereas determining financing available requires discussions with various stakeholders, such as banks, donor and government line agencies, and reviewing country-specific policies (e.g., rural or renewable energy policy, subsidy policy).

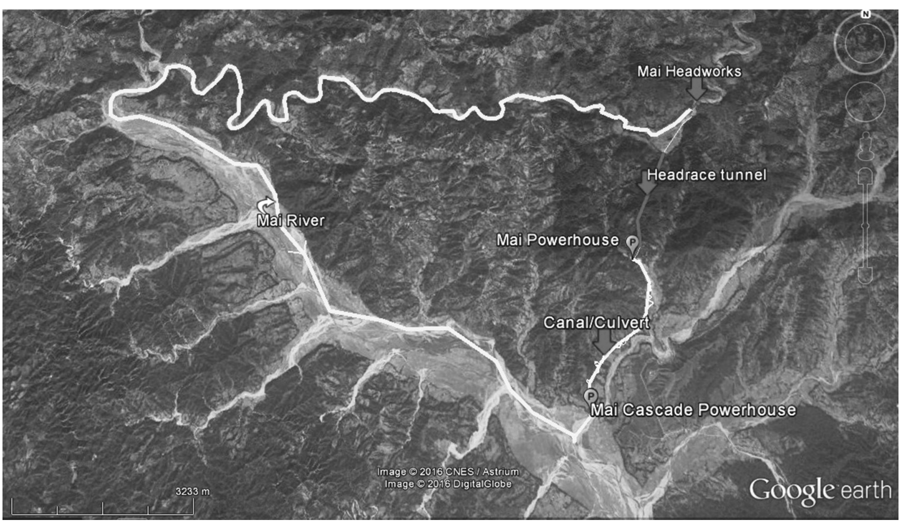

FIGURE 3.20 A potential hydropower site layout on a Google Earth satellite image.

Any permits or licenses required for the survey of potential hydropower sites need to be obtained from the relevant authorities before embarking on the field trip. A completed desk study may be one of the requirements for submitting the license or permit application. Even when a desk study is not required, the developer or the investor may commission this to first evaluate whether investment for a full feasibility study is justified. In case the desk study indicates the site to be infeasible, costs for a further detailed feasibility study can be avoided.

An example of sizing of an isolated micro hydropower plant based on demand for electricity by the community is discussed in Example 3.5.

Example 3.5: Determining Installed Capacity for an Isolated Power Plant

A remote community with 150 households is considering building a micro hydropower plant to meet its electricity needs. The national electricity grid is not likely to reach the community for at least another 10 years, and therefore, the power plant will have to be run on isolated mode. Based on a household survey, the demand for electricity in the community is estimated to be as follows:

Domestic demand: 300 W/household, which includes a few light bulbs, a television set, and a mobile charging outlet.
Computer center: One at the center of the town, which will require 300 W.
Photocopying service: An entrepreneur is considering providing this service. Power requirement is estimated at 500 W.

The community also requires some agro-processing facilities as follows:

One rice-milling plant, which requires about 10 kW of power
One corn-/wheat-grinding plant, which requires 7.5 kW of power
One oil-expelling plant, which requires 7.5 kW of power

Based on the above information/data the plant size needs to be determined.

During the evening to nighttime, all households will have their lights on, and most of the television sets will be turned on. Therefore, based on the domestic demand alone, the power requirement will be the following:

$$300 \text{ W/household} \cdot 150 \text{ households} = 45{,}000 \text{ W or } 45 \text{ kW}$$

$$\text{The total agro-processing demand} = 10 \text{ kW} + 7.5 \text{ kW} + 7.5 \text{ kW} = 25 \text{ kW}$$

If the community agrees to operate agro-processing plants only during the daytime and not in the evening, then the required installed capacity for domestic demand of 45 kW should be adequate to meet this need as well. During the daytime, there will be limited lighting demand, and at most, some households will have their television sets turned on. Furthermore, it is unlikely that all three agro-processing plants will be operated at the same time. Most likely, only one of the three will be in use at any time.

If the community decides to use the computer center and photocopying services during the daytime only, then the installed capacity of 45 kW should still be adequate. On the other hand, if the community members would like to use such services during the evenings or nighttime, then the capacity would have to be increased by about 1.0 kW.

Another issue to consider is that the demand will certainly increase over time due to an increase in number of households and increased commercial activities. It is important to make allowances for growth in future demand as once the capacity is fixed the plant size cannot be increased. However, a high allowance for future demand will make the power plant expensive at present. Therefore, the decision as to how much allocation is to be made for future demand depends on (a) the funds available with the community and/or funding agency, (b) the expected growth in demand by the mideconomic life of the plant, and (c) the installed capacity feasible given the river flows and gross head available.

In this example, the domestic demand is 45 kW, and if the computer center and photocopying machines are to be operated during the evenings, then another 1.0 kW should be added—that is, installed capacity = 46 kW. If 10% allocation is made for future growth (4.6 kW), then the installed capacity of this power plant should be around 50 kW.

Finalizing the design of an isolated micro hydropower plant is often an iterative exercise between estimating the demand and confirming the hydrological resources available to meet that demand. Once the first estimation of demand has been completed, the next step is to check whether there is a potential site nearby that can generate the required power. Note that after a tentative layout has been identified, the gross head will be fixed. Thus, the capacity will depend on the river flows available. Because the river flows can vary over the months, the selected design flow will have to take into consideration both the total demand of the community and the percentage flow exceedance.

If the river flows are lower than required to generate 50 kW power output for most months of the year, additional discussions will be needed with the community to see if their needs can be met with a smaller power plant. It could well be that the community will agree to restrict their power use to an average of 200 W per household in place of the originally estimated 300 W by using more efficient lamps or fewer appliances concurrently. This would reduce the required size of the power plant to closer to 35 kW. In the event that much less flow is available than what is required to meet the needs of the community, the surveyors may have to identify a different site that can produce more power, or the decision may have to be made to not build the micro hydropower plant at all in case there is a serious mismatch between demand and the power at available sites. An additional factor to consider is the design guidelines issued by agencies that may be providing grants or loans for the project. In Nepal, isolated micro hydropower plants must be designed such that the installed capacity can be generated for at least 11 months of the year—that is, the design flow is exceeded 91.67% of the time (i.e., 11 months exceedance flow) in order to qualify for government subsidy. This rule is designed to ensure that the community demand can be met 11 months of the year, and rationing of power would have to be done for one month at most.

Example 3.6: Determination of Installed Capacity for a Typical Micro Hydroelectric Power Plant Feasibility Study

The site survey for the micro hydropower plant in Example 3.5 indicates that a gross head of 70 m is available.

The hydrological study shows mean monthly flows as shown in Table 3.7.

Estimate the potential power output each month on the basis of the mean monthly flows and the corresponding energy output in kWh. Assume an overall efficiency of 65%. Then recommend a suitable installed capacity.

$$\text{Recall the power equation } P = \gamma Q h e_o$$

where P = power output in kW, γ = 9.81 kN/m^3 (unit weight of water), Q = the mean monthly flows above in m^3/s, h = 70 m (given), and e_o is the overall efficiency = 65% or 0.65.

TABLE 3.7
Mean Monthly Flow Estimates at Proposed Intake Site

Month	Jan	Feb	Mar	Apr	May	Jun	Jul	Aug	Sep	Oct	Nov	Dec
Flows (l/s)	200	190	170	160	150	300	500	400	350	300	270	250

Instead of establishing the flow duration curve (FDC) based on the mean monthly flows, the mean monthly power and mean monthly energy can also be estimated. For example, the mean monthly power output for January is

$$P = 9.81 \cdot 0.200 \cdot 70 \cdot 0.65 = 89.3 \text{ kW}$$

The corresponding energy available in January is $89.27 \cdot 30 \cdot 24 = 64{,}275$ kWh or 64.3 MWh. Similarly, the mean monthly power and energy output for the rest of the months are shown in Table 3.8.

Note that in Table 3.8, the energy produced each month is calculated based on an assumption of 30 days for simplicity. If the actual number of days in the month are used, the energy output will be slightly different but will not change the analysis.

A plot of months versus mean monthly flow and the corresponding monthly power output is shown in Figure 3.21.

Because the power output of a hydropower plant is directly proportional to the flows available (for a given head), the flow hydrograph and the power graph are parallel. Note that the month of

TABLE 3.8
Mean Monthly Power and Energy Output

Month	Flows (l/s)	Power Output (kW)	Energy (MWh)
Jan	200	89.27	64.3
Feb	190	84.81	61.1
Mar	170	75.88	54.6
April	160	71.42	51.4
May	150	66.95	48.2
Jun	300	133.91	96.4
Jul	500	223.18	160.7
Aug	400	178.54	128.6
Sep	350	156.22	112.5
Oct	300	133.91	96.4
Nov	250	111.59	80.3
Dec	220	98.20	70.7

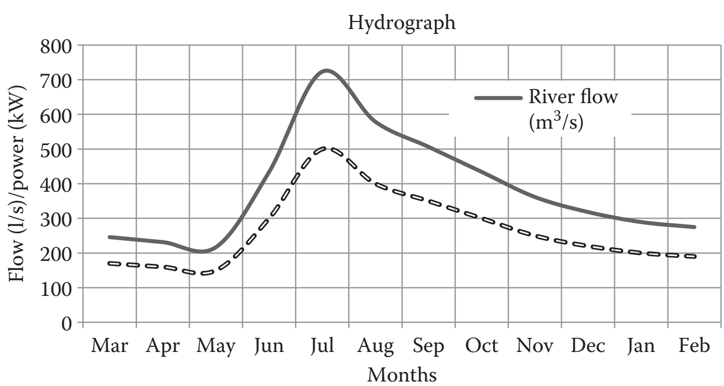

FIGURE 3.21 Mean monthly flow and power output.

March is used as the first month in the hydrograph so that the high flows are in the middle with low flows at the sides.

As can be seen from Figure 3.21 and Table 3.5, based on the flows available, the average monthly power output varies from 67 kW in May, which is the least mean monthly flow or 100% exceedance flow, to 223 kW during the highest monthly flows in July (8.33% exceedance). A suitable design for installed capacity will depend on the following factors:

1. If the installed capacity is to be guaranteed throughout the year, then it should be limited to 67 kW. This capacity is called firm power as it is available throughout the year. Because in this example the demand for power in the community is 50 kW, the installed capacity should be fixed at 50 kW even though the firm power available would be higher. If the demand was higher and the community was willing to accept some power cuts for one month, then the capacity corresponding to 11 month exceedance flow would be 71 kW.
2. If all of the generated electricity can be sold, such as in case of a grid-connected power plant, then a cost–benefit analysis should be undertaken to optimize the installed capacity. Example 3.5 illustrates this process.

Example 3.7: Change in Project Cost and Sales of Energy Generated

In the earlier Example 3.5, assume the Project cost to be US$1500 per kW of installed capacity and that all of the generated electricity can be sold to the grid at 6 US Cents per kWh. On the basis of these assumptions, recommend an appropriate installed capacity.

First, the corresponding annual energy should be estimated for each installed capacity considered. For example, if the capacity of the power plant was designed to be consistent with the least mean monthly flow in May, the power output would be 67.0 kW and the corresponding annual energy generation would be $67.0 \cdot 12 \cdot 30 \cdot 24 = 578{,}448$ kWh or 578.45 MWh. Design to coincide with the April flow, which is the second lowest mean monthly flow (or 11-month exceedance flow), would result in the power output being 71.4 kW and the corresponding annual energy generation at this installed capacity would be $(71.4 \cdot 11 + 67.0) \cdot 30 \cdot 24 = 613{,}692$ kWh or 613.7 MWh.

The annual energy available for the various installed capacities (based on available monthly flows) can be calculated as discussed above and converted into revenues at US 6 cents per kWh of energy generated. The corresponding project costs are calculated assuming construction cost of US$1500/kW. However, it should be noted that although the project costs are incurred during the construction phase, revenue benefits accrue every year throughout the plant's economic life. Thus, the costs should be annuitized (i.e., brought to equivalent annual cost) to compare it with annual revenues. In this example, the plant's generation license has been provided by the government for 35 years. A discount rate of 10% has been used to annuitize the project costs. Then the installed capacity that results in the highest ratio of gross annual revenue/annuitized project costs should be selected as the first estimate for the design capacity. This is generally followed by a more rigorous financial and economic analysis, Chapter 14. Annual energy, gross annual revenues, project costs, and gross annual revenue/annuitized project costs are presented in Table 3.9.

As can be seen from Table 3.9, the ratio of gross annual revenue/annuitized project cost is highest for the least installed capacity of about 67 kW, implying that marginal annual revenue is less than the marginal cost for any additional increase in installed capacity beyond 67 kW. This is because as the capacity of the power plant is increased, the percentage of time the flow available for power generation at that installed capacity decreases. It may seem surprising that the best revenue to annual cost ratio results for the smallest capacity design option for the power project. This counterintuitive conclusion is a direct result of assuming fixed construction cost per kilowatt in this example and neglecting any economy of scale benefits. In real life, the per kW construction cost declines with size and a repeat of the analysis above with realistic costs will indeed provide a different optimal project size at which the ratio of revenue to annual cost is the highest.

TABLE 3.9
Financial Parameters for Selection of Installed Capacity

Month	Q, l/s	P, kW	Annual Energy, MWh	Gross Annual Revenue, US$	Project Cost, US$	Annuitized Project Cost, US$	Gross Annual Revenue/Annuitized Project Cost
Jan	200	89.3	730	43,771	133,907	13,885	3.15
Feb	190	84.8	704	42,229	127,211	13,190	3.20
Mar	170	75.9	646	38,758	113,821	11,802	3.28
Apr	160	71.4	614	36,830	107,125	11,108	3.32
May	150	67.0	578	34,709	100,430	10,414	3.33
Jun	300	133.9	913	54,762	200,860	20,827	2.63
Jul	500	223.2	1025	61,511	334,766	34,712	1.77
Aug	400	178.5	993	59,583	267,813	27,769	2.15
Sep	350	156.2	961	57,655	234,336	24,298	2.37
Oct	300	133.9	913	54,762	200,860	20,827	2.63
Nov	250	111.6	832	49,942	167,383	17,356	2.88
Dec	220	98.2	775	46,471	147,297	15,273	3.04

3.6.2 Site Selection and Layout

Selection of a suitable site and designing an optimum layout is different for each hydropower plant as no two sites are identical. However, the general principles of site selection and scheme layout are similar for all sites. The requirements for suitable sites and the procedures for identifying them during a field visit are briefly discussed herein:

- It should be possible to divert part of the flows away from the river at the intake with minimal weir/dam height. For example, if the river flows through a deep gorge, it may not be feasible to divert the flows away from the banks without building an excessively high dam.
- A suitable waterways alignment should exist downstream from the intake to provide the head. The topography must be favorable for a relatively short headrace alignment, penstock along steeper ground profile, and a short tailrace alignment from the powerhouse. If a desk study was undertaken earlier, the tentative layout considered during this phase is confirmed and/or updated during the field visit.
- Land ownership along the waterways alignment should be identified. Private land may have to be purchased through negotiations, and government land may have to be acquired on a long-term lease based on the prevailing laws of the country.
- It should be possible to site a powerhouse at a location safe from flood impacts, such as on a high terrace along the riverbank or on a stable, accessible location along a cliff with minimal excavation works.
- The waterways alignment and the locations of key structures, such as the settling basin, forebay, anchor blocks, and powerhouse, should be on stable ground. If some parts of the alignment must be placed along unstable ground, geotechnical engineering measures to stabilize the slopes, such as provisions for retaining walls, maybe feasible. Similarly, with aqueducts, siphons, and level crossings, short gullies along the waterways alignment can be negotiated. However, if large lengths of the alignment are along unstable grounds and/or there are too many crossings, the site although technically viable—that is, with favorable head and flow conditions—may not be financially viable.

- Other factors that need to be considered are the following:
  - Accessibility and ease of construction: Can equipment and construction materials be transported to the site, or will a new access road be required? Which of the alternative layout arrangements considered can be built in a shorter time period?
  - Transmission line: In case of a grid-connected scheme, how far is the interconnection point?
  - Load centers: In case of isolated scheme, how far are the load centers?
  - Other site-specific issues, such as avoiding an alignment that requires significant farmland or areas that have cultural, religious, or archaeological values, should be taken into account.

Specification of a suitable intake, waterways alignment, powerhouse, and other key components along with their design basis are discussed in detail in subsequent chapters.

3.6.3 Feasibility Study

The feasibility study is started once the necessary permits and licenses are obtained to survey a potential site after the market for the electricity generated is confirmed to exist. A desk study is undertaken as a first step to confirm the existence of potential sites and often as the basis for applying for licenses and permits. As stated earlier, site investigations, finalization of the layout arrangement of the power plant, and the determination of the optimal installed capacity are iterative processes carried out during the feasibility study. In the case of small-scale isolated micro hydropower plants supplying electricity to a few households, the number of steps to arrive at the design is reduced. The feasibility study process for power plants in the larger than micro hydropower range are summarized as follows:

- During the first field visit, the general layout arrangement envisioned in the desk study phase is updated based on site conditions, and a detailed topographic survey is carried out.
- Once the topographic maps are ready, based on the survey, the general layout arrangement is further updated based on the topography, lengths of waterways required, and ground levels.
- Based on flow measurements taken during the field trip and available hydrological records for the stream, a tentative range of flow available for power generation is arrived at by preparing a flow duration curve (FDC) as discussed earlier. When estimating flows for power generation, downstream flow release requirements for environmental reasons should also be taken into consideration. Using the computed flow range, the power output range is then estimated as the head will have been relatively fixed once the location of the forebay and the powerhouse are finalized.
- From the range of flow available for power generation, some discrete design flows, and thus the installed capacities, are selected, and a corresponding preliminary cost for a power plant for each design flow is calculated. Similarly, the annual energy generation for the selected design flow is also calculated. The installed capacity is selected based on cost–benefit analysis to arrive at an optimum return on investment as discussed in Chapter 14.
- Once the installed capacity is tentatively fixed as above, individual components, such as the headworks and intake, gravel trap, settling basin, forebay, penstock pipe, anchor blocks, support piers, powerhouse, and tailrace, are designed. During this design process, the installed capacity will have to be updated and refined given the results of analysis. For example, a detailed hydrological analysis may indicate that the powerhouse would have to be shifted at a higher elevation to minimize flood risks, which would, in turn, decrease the installed power capacity. During this component design process, the design team members

may have to make a number of field visits to take additional flow measurements, collect soil samples, or perform in situ tests to determine foundation design parameters or to record existing flora and fauna, including endangered species for environmental studies. Although environmental studies, such as the initial environmental examination (IEE) or environmental impact assessment (EIA), are often carried out by an independent team, it is useful to compile such environment-related information during the feasibility study so that the two studies are well coordinated.

- The sizing of the electromechanical equipments and accessories (cables in the powerhouse, earthing, etc.) is undertaken by the electrical and mechanical engineers on the design team. Prospective equipment suppliers are contacted for information on the number of electromechanical units, equipment size, weight, and other parameters required. The powerhouse layout along with the design of the machine foundations are then undertaken based on the dimensions of the equipment and other parameters, including weight, rotational speed of the generating units, etc., by the civil, hydraulic, and structural engineering members of the design team. Thus coordination among the team members becomes essential to design the powerhouse. It should be noted that for micro hydropower plants in developing countries, due to cost considerations, one or two engineers typically undertake the entire feasibility study.
- Once the installed capacity is finalized and the individual components are designed, a final field visit may be required, depending on size of the scheme and budget available for quality assurance purposes and to verify the design from a construction viewpoint.
- Once the design is completed, the cost estimates will have to be updated along with the financial analysis because during the design process a number of cost parameters, for example, volume of works and rates, will have changed. Similarly, a construction schedule will have to be prepared to estimate the time required for implementing the project (see Figure 3.6).
- Along with the technical design, an environmental study will have to be carried out based on the size of the power plant and the prevailing laws of the country. Several inputs from the environmental study will need to be incorporated to update the design, such as provisions for fish pass along the weir and ecological flow requirements, which will not be available to flow through the turbine.

The composition of the design team and the number of site visits required depend mostly on the size of the proposed power project. In the case of a professionally designed small hydropower project, the composition of a typical design team could be as shown in Table 3.10.

The above design team is assisted by a survey team that is responsible for carrying out site surveys and preparing detailed topographical maps. The feasibility study and design of large hydropower projects will typically require several design teams rather than individual engineers, such as a hydraulic design team and structural design team with corresponding team leaders. On the other hand, for micro hydropower projects with limited budget allocation, one or two engineers may take the entire responsibility for the feasibility study and subsequent supervision during construction.

The contents of a typical feasibility study for a small hydropower project are listed in Table 3.11.

As can be seen from the small hydroelectric power feasibility study requirements, the document needs to cover a range of issues as it needs to address the requirements of the various stakeholders, including the client and other potential investors, local populations that could benefit and/or be negatively impacted, financial institutions (e.g., banks), interested contractors, the utility that will purchase the generated electricity as well as government institutions responsible for awarding permits, licenses, and environmental clearances. Feasibility studies of small hydroelectric projects are often undertaken as a requirement to seek loan financing from commercial banks for construction if such studies demonstrate their financial viability. In such cases, the feasibility studies must be a comprehensive “bankable” document—that is, the document should be thorough and convincing

TABLE 3.10
Typical Design Team Composition and Responsibility

S. N.	Position	Responsibility
1	Team leader – hydropower or civil engineer	Finalization of the project layout, overall coordination and quality assurance of the study, and supervision of the design team
2	Hydraulic engineer	Assist the team leader in selecting the project layout and undertake hydraulic design of the headworks and waterways, including the penstock pipe
3	Civil engineer	Assist the hydraulic and structural engineers in estimating the civil works costs and prepare a detailed bill of quantities (BoQ)
4	Structural engineer	Structural design of the headworks, powerhouse, and other key components of the project
5	Geologist/ geotechnical specialist	Assist the design team in selecting general layout arrangements for the project to ensure stable locations and recommend design measures (e.g., foundations and retaining walls) to address specific site instability issues
6	Environmental specialist	Ensure that all potential negative environmental impacts due to project implementation are identified and adequately addressed and all required environmental standards in accordance with the country's legal requirements are met
7	Economist and/or financial analyst	Appraise the financial/economic viability of the project, including estimation of revenue streams, internal rate of return, net present value, and other parameters
8	Electrical engineer	Select appropriate generators and other electrical equipment for the project and design protection system, design switch yard, and transmission/distribution line for the power plant
9	Mechanical engineer	Select appropriate turbines, flywheels, and other mechanical equipment (e.g., control valves) and design gates, stop logs, trash racks, and other steelworks

TABLE 3.11
Contents of a Typical Small Hydropower Feasibility Study Document

S. N.	Contents	Description
1	Executive summary	Overall summary of the feasibility study along with the salient features of the proposed project
2	Introduction/ background	Background to the study and project area, such as location, accessibility, and grid availability, client's requirements, country context, personnel involved, and structure of the report
3	Market conditions	General description of electricity market conditions in the region or country
		Description of how the generated electricity is to be utilized, such as through sales to the regional/local grid under a power purchase agreement (PPA) or directly to consumers by the power plant
		Prevailing buy-back rates and consumer tariff
4	Methodology	How the feasibility study was undertaken, such as detailed survey, site visits, soil tests, and rock drilling as necessary for foundation design
5	River hydrology	Description of the river basin, catchment area, precipitation, estimate of river discharges, derivation of flood duration curve, and flood flows for different return period
6	Site description	General description of the site, including possible alternative waterways alignment and selection of the most appropriate layout
		Estimation of the range of power output technically
7	Environmental and social issues	Possible environmental impacts of the projects and how these are to be mitigated, minimum downstream release, compliance with the environmental regulations of the country, including a full environmental impact assessment (EIA) or and initial environmental examination (IEE) as required

(*Continued*)

TABLE 3.11 (CONTINUED)
Contents of a Typical Small Hydropower Feasibility Study Document

S. N.	Contents	Description
		Need for public and private land acquisition, conflict with irrigation, and potential impacts on forests or farmlands and households that fall along the proposed waterway or at the location of the power plant Expected benefits to the local population from electricity access or increased irrigation Consultations that took place with the local communities and authorities during the course of the study, including potentially affected persons
8	Technical design and optimization	Selecting the optimum installed capacity of the power plant based on gross head, flow duration curve, environmental release downstream, and buy-back rates or other prevailing market conditions for sales of electricity generated Estimates of weekly, monthly, and annual energy generation based on available flow as well as expected power plant shut down for annual repair and maintenance Sizing of the waterways components from the headworks to the tailrace and their detailed description Sizing of electromechanical equipment, design of protection systems and switchyard and distribution or transmission line
9	Construction schedule and project cost estimates	Estimates of the construction period required for implementing the project and a detailed schedule taking into account site-specific features, such as weather, festivals, and seasonal availability of laborers Estimation of project cost based on the technical design and prevailing market rates for equipment, labor, and construction materials (e.g., cement, reinforcement bars) For the civil works, based on the engineering drawings prepared, a detailed bill of quantities (BoQ) to estimate the costs Quotations from prospective suppliers are used for estimating costs of electromechanical equipment and accessories
10	Project financial analysis	Financial analysis based on annual revenue of the project and its annual operation and maintenance costs Analysis includes loan repayment schedule and cash flow analysis to evaluate the financial viability and bankability of the project Internal rate of return (IRR), net present value (NPV), and other financial parameters to demonstrate attractiveness of the investment[a]
11	Management issues	Discussions of possible contract packages, such as turnkey, unit rates basis, or cost plus pricing Description of the operation and management aspects of the power plant, such as staffing requirements, record keeping and billing, number of shifts, spare parts, and stocks to be maintained
12	Conclusions and recommendations	Conclusions of the feasibility study—that is, how technically and financially viable is the project? Discussions on the recommendation for the next stage, such as acquiring a government license, communicating with banks, preparing tender documents, and going into construction and description of any other studies and investigations required, for example, continuing flow measurements due to paucity of data or further soil tests
13	Appendices	Any secondary information that supports or corroborates the analysis and findings of the feasibility study, such as the following: Stream flow records, soil test results, design calculations, site photographs, etc. Engineering drawings prepared for the feasibility study are either included in the appendices or as a separate volume

[a] Note that for large hydropower projects that are to be developed by public sector agencies, an economic analysis is undertaken to include the secondary benefits, such as irrigation and flood control, from the projects. These aspects are further discussed under economic analysis in Chapter 14.

enough for the banks to agree to provide loan financing. It should be noted that the content of a small hydropower feasibility study shown in Table 3.2 is not exhaustive because there may be additional country-specific requirements by the government and financing agencies.

For micro hydropower plants, often the agencies responsible for deciding funding applications need to know at what subsidy amount the power plant would be financially viable—that is, be able to bear the operation and maintenance costs of the power plant throughout its economic life without further support.

Obviously, for micro hydropower projects, the feasibility study requirements would be much less than for small hydro whereas for large hydro it would be more elaborate than what has been discussed above.

3.7 PROJECT IMPLEMENTATION SCHEDULE

As part of the feasibility study, the designer needs to prepare a project implementation schedule. Such a schedule will show the important milestones of the project, which are then used to prepare cash outlays for construction and payment for equipment ordered and labor and construction materials requirements at various times.

The project implementation schedule needs to be realistic enough and should take local site conditions into account as follows:

- Weather conditions: In some areas, it may not be possible to take up significant construction activities during the winter due to cold weather. Similarly, during the heavy rainy season, transport of materials at the site and construction work both will be difficult in tropical regions.
- Festivals: Labor arrangement may not be feasible during regional or national holidays and festivals.
- Performance and availability of construction equipment, materials, and contractors or project staff: If there are experienced contractors in the country who have built a number of hydropower plants, the construction period could be shortened.
- Site access and facilities: Is there an existing road access to the intake, powerhouse, and the waterways or will one have to be constructed? Is electricity available near the campsite, or do diesel or gas generators need to be provisioned for?
- Availability of funds: Can the funds be made realistically available for the construction schedule envisaged?

A typical project implementation schedule is presented in Figure 3.22.

As can be seen from Figure 3.6, a total time period of 31 months from the approval of the feasibility study is estimated for completion of the project, including just over eight months for preparatory works, such as tender documents, land acquisition, and award of construction contract. It should be noted that due to site-specific conditions during construction, it may not be possible to completely adhere to this schedule and meet the milestones—that is, there are likely to be some adjustments in the individual activities even when the implementation period remains the same. The construction management team at the site or the site engineer for smaller projects needs to continuously update the schedule to ensure timely completion. A number of construction activities will be carried out concurrently, and the construction supervision team along with the contractor need to avoid delays due to lack of logistic support or other site-specific conditions, especially along the critical path activities. For example, if adequate stocks of cement and reinforcement bars are not maintained, concrete works can be delayed. Similarly, if the generating equipment and the transmission line cables are not ordered on time, there could be delays in installation and subsequent commissioning.

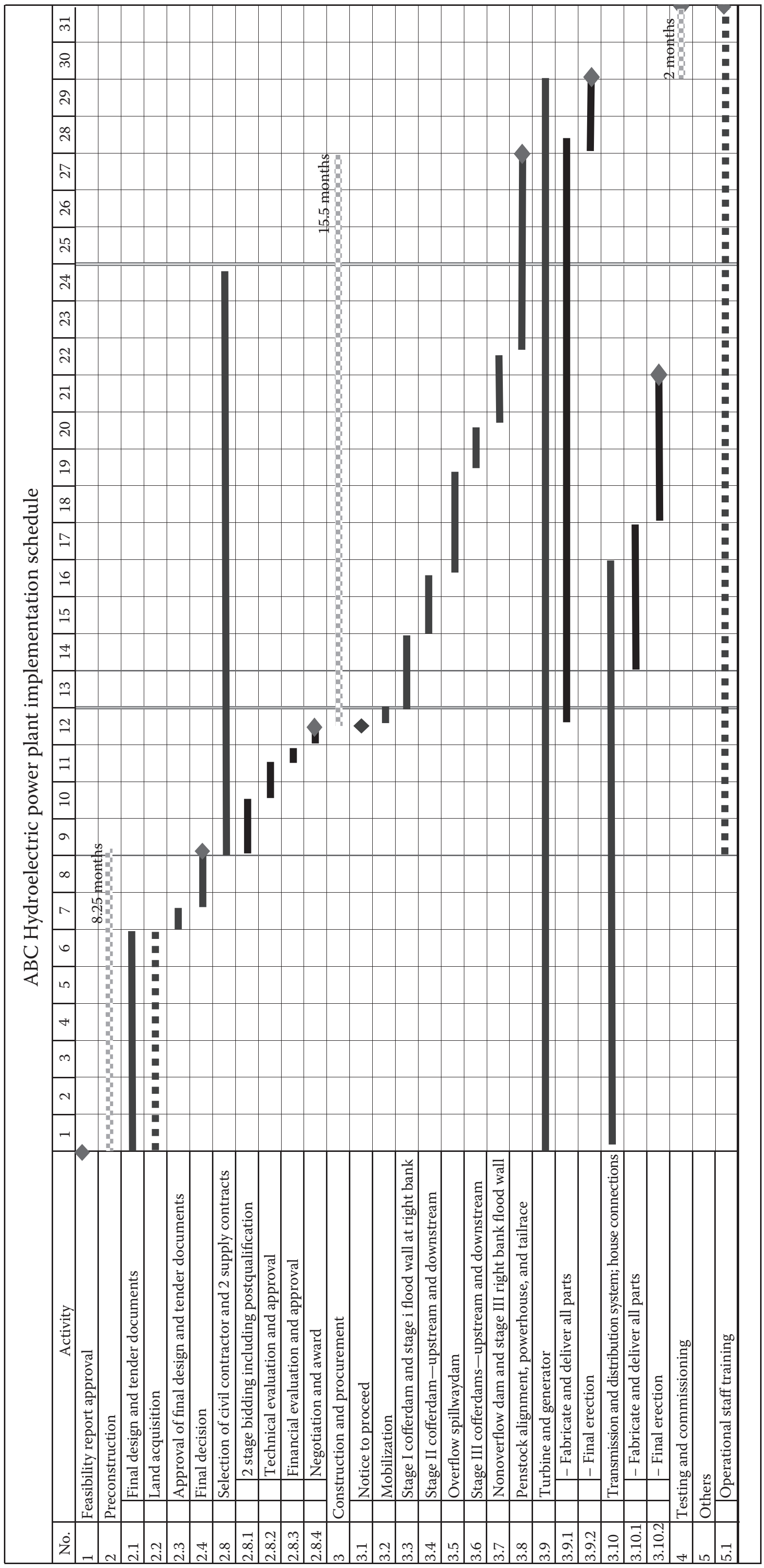

FIGURE 3.22 Typical implementation schedule for a small hydroelectric power plant.

During the actual construction phase, detailed construction schedules are prepared even on a daily or weekly basis, depending on plant size to plan for procurement of construction equipment and labor arrangements.

EXERCISES

1. For the mean monthly flows given in the table below,
   a. Prepare a hydrograph and a flow duration curve (FDC).
   b. If the site has a gross head of 150 m, what is the firm power available? Make reasonable assumptions for the overall efficiency.
   c. What would be the plant capacity based on 11 months exceedance flow?

   Mean monthly flows available at proposed intake site of a potential hydropower plant:

Month	Jan	Feb	Mar	Apr	May	Jun	Jul	Aug	Sep	Oct	Nov	Dec
Flow	236	175	122	146	231	1200	2400	3300	1700	700	427	325
(l/s)	190	140	98	130	185	950	1900	2500	1450	585	375	285

2. Assume that the above site will be an isolated micro hydropower plant. The demand for electricity in the community is as follows:
   a. Domestic demand: A hundred households want 500 W/household, and another 400 households want 250 W/household. The households will use electricity throughout the year on average for six hours a day (evening and nighttime).
   b. Commercial loads are expected to be around 40 kW. Commercial loads would be turned on only during the daytime (average eight hours/day throughout the year) when domestic loads are not required.
   c. Agro-processing facilities proposed are the following:

      Two rice mills, each requiring 10 kW. Operation time: three months a year at eight hours/day

      Two grinding mills, each requiring 7.5 kW. Operation time: four months a year at eight hours/day

      One oil-expelling mill requiring 7.5 kW. Operation time: two months a year at eight hours/day

      These three agro-processing plants will be used at separate months because harvest seasons are different—that is, only one agro-processing plant will be used in a given month

   Based on the data provided, (a) propose the installed capacity of the micro hydropower plant and (b) prepare a monthly energy table.

4 Intake and Diversion Works

4.1 OVERVIEW

As discussed in Chapter 2, the headworks for a run-of-river hydropower plant comprise a diversion weir, intake openings, flood protection walls, and other river training works. As the name denotes, "headworks" refers to structures built at the start or "head" of a hydropower plant. If the gravel trap and settling basin are also close to the river, these structures are also collectively referred to as the headworks. Some literature also uses the term "headworks" to geographically differentiate the intake area from the waterways and the powerhouse downstream. In case of a storage type hydropower plant with the powerhouse immediately downstream of the dam, the term headworks would have no meaning.

For a run-of-river hydroelectric power plant, the intake, along with the diversion, river training, and flood protection works, need to be designed for the following conditions:

i. It should be possible to divert the design flow into the intake when there is sufficient discharge in the river—that is, when the available river discharge less the environmental release is equal to or larger than the design flow.
ii. The design should minimize entry of sediment, especially bed load and floating debris, such as twigs and logs.
iii. The design should restrict entry of excess flow during floods, and the structures at the headworks should remain safe and operational during the maximum design flood considered.
iv. The design should address all environmental concerns, such as providing safe passages across the diversion weir in case there are migrating fish species along the river stretch.

No two hydropower sites are exactly the same even when immediately downstream of each other in the same river basin, for example, cascade sites. The river width, gradient, and topography will always be different. Thus, the designs of hydropower plants, especially the civil structures, are site specific. The specificity of designs is particularly relevant in the case of headworks design as it needs to be based on accurately understanding the nature of the river during both normal and flood conditions as well as principles of hydraulics. Furthermore, the design engineer or the design team also need to be able to address the four conditions listed above. Hydropower plants with poorly designed headworks may operate adequately in the beginning, but after a few years or after a flood event larger than the annual flood, there will be substantial damage to the structures. Sometimes in large hydropower plants, scaled physical models are also constructed in laboratories to test the performance of the headworks designs (Box 4.1).

For waterways structures downstream, flood flows should not generally be a major concern because these would have been dealt with at the headworks. The headrace route is generally aligned away from the river as early as possible to avoid exposure to flood risks. Thus, the waterways structures downstream of the headworks need to be principally designed to safely convey the design flow.

The major maintenance requirements at the intake or the headworks generally include the following:

a. Repair of gates and other control structures that have been damaged by floods
b. Removal of trash from the trash rack at the intake
c. Removal of sediments and debris deposited upstream of the gravel trap and/or the settling basin
d. Repair of the weir surface or the downstream apron due to scouring action by the river

FIGURE 4.1 Flood damage at partially completed headworks structure, Nepal.

Sometimes, large floods can occur during the construction phase of a hydropower power plant. If the headworks is only partly completed prior to the onset of a flood, there can be considerable damage to the structure as can be seen from the photograph in Figure 4.1. Note the logs that have been deposited at the intake, and part of the river flow has come around the floodwall outside the main river course.

4.2 TYPES OF INTAKE

Various types of intakes are used in hydropower plants to divert water from the river. As discussed earlier, the type of intake used for a particular site depends on the nature of the river and the topography. Sometimes, the choice of intake is also based on the experience that the design engineer has, especially when two types of intake appear feasible.

Types of intake structures can be distinguished either by their layout arrangements or by the method used to divert water from the river. Three basic types of intakes used in run-of-river hydropower plants are as follows:

i. Side intake: The intake is located at the side of the river along one of the banks.
ii. Frontal intake: The intake faces the river flow sometimes even perpendicular to the flow.
iii. Bottom intake: The intake withdraws water from the riverbed and conveys it directly into the headrace.

Some headworks designs combine different types of intakes, such as a side intake along with a bottom intake.

4.2.1 Side Intake

Side intakes, as the name denotes, divert water from the side (bank) of the river. An opening along the wall on the riverbank usually acts as the intake while the wall itself also protects the downstream structures from flood impacts. Often a weir or a dam is built across the river downstream of the intake to raise the water level and facilitate flow diversion toward the intake. Side intakes are simple and easy to construct, operate, and maintain. In principle, they are similar to traditional irrigation intakes built by farmers in many parts of the world.

A flow control structure, such as gates, are often incorporated either at the intake opening, or if this area is vulnerable to flood impact, then they are located at some distance downstream along the headrace structure.

A typical side intake for a small hydropower plant is shown in Figures 4.2 and 4.3. In Figure 4.2, the river flows are diverted from the right bank of the river though the side intake and then conveyed to the gravel trap via a covered canal (box culvert).

FIGURE 4.2 Side intake of 2.5-MW Sun Koshi Hydropower Plant, Nepal.

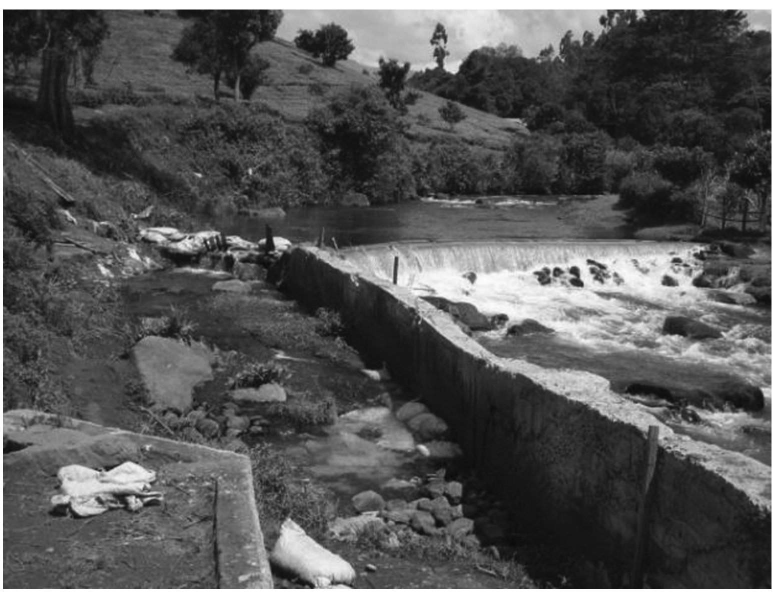

FIGURE 4.3 Side intake under construction, Kenya.

FIGURE 4.4 A typical bottom intake of a micro hydropower plant, Nepal.

4.2.2 Bottom Intake

The bottom intake consists of a trench built across the river at its bed, which withdraws the water. It is also known as a Tyrolean or trench intake. The lower portion of the river flow drops into the bottom intake, and the flow is conveyed toward the headrace. The bottom intake is covered with a coarse trash rack (grill-like bars) on top to prevent the trench from being blocked by large boulders. This type of intake is suitable across high gradient rivers that do not carry significant sediments, such as in the Alpine areas of Europe, where they are widely used. Bottom intakes are susceptible to being blocked by sediments or bed load because they divert the bottom portion of the river water, which has higher sediment concentration. Sometimes allowance is made for surplus flow so that continual flushing of sediments is feasible—that is, in the case that bottom intakes are used in rivers with relatively high sediment loads as can be seen in Figure 4.4. One of the trash racks has fallen down the trench during the high-flow season when repair work is not feasible. Because the intake trench was oversized, it was possible, in this particular case, to withdraw the required flow into the headrace downstream from the functioning portion of the intake. However, it should be noted that with an oversized intake, the size of the spillway has to be proportionally increased, and the conveyance structures (canal, culvert, or pipe) upstream of the spillway need to be oversized as well.

BOX 4.1 HYDROLAB

Hydrolab is a company in Nepal that undertakes research and model studies in hydropower and other areas related to water. Building any water resources project along the rivers in the Himalayan region poses serious challenges given the sheer complexity of such rivers in terms of flow hydraulics and sediment transport capacity. A river with a flow of a few cubic meters per second in the dry season swells tremendously to more than a hundredfold in volume along with an even larger nonlinear increase in sediment-carrying capacity during the rainy season. The flow is often uncontrolled and unpredictable, and the normal theory of hydraulics alone is not sufficient to predict its behavior. Thus, often comprehensive experimental research and hydraulic model studies are required to physically verify the performance of the proposed design structures before they are actually constructed on-site. Hydrolab provides such services in the Himalayan region, namely Nepal, India, and Bhutan (Hydro Lab Pvt. Ltd., Pulchowk, P.O. Box 21093, Kathmandu, Nepal. Website: www.hydrolab.org).

Physical hydraulic model studies.

Sediment analyses in the laboratory. Website: www.hydrolab.org.

4.2.3 Frontal Intake

The opening in a frontal intake faces the river flow as can be seen in Figures 4.5 and 4.6. The intake itself is generally located along the riverbank. These types of intake are more vulnerable to being hit by boulders that the river may carry during floods. This type of intake is suitable in situations in which the river does not carry large boulders even during high floods. Sometimes, when an intake has to be located along a narrow valley with high cliffs along the riverbanks, then a frontal intake may be the only choice because there will be no space to construct a side intake.

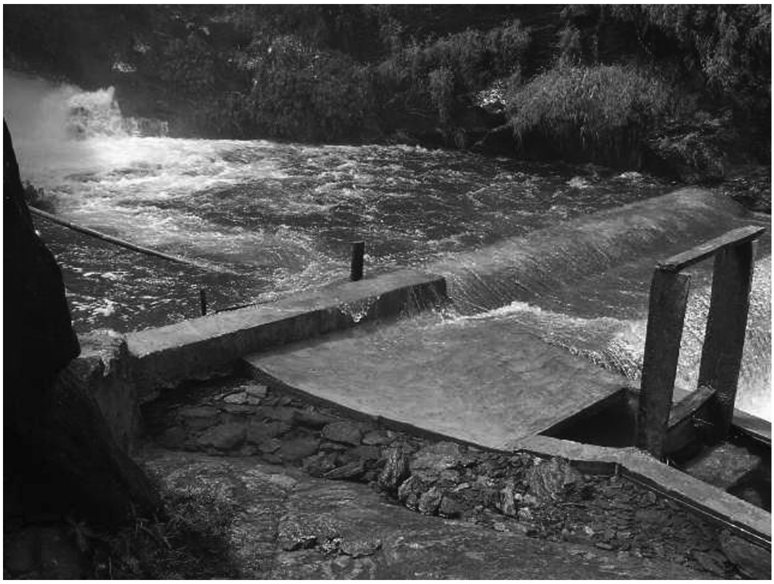

FIGURE 4.5 A frontal intake of a mini plant in the Panjshir Hydropower Plant in Nepal.

FIGURE 4.6 A temporary weir built from boulders and brushwood to divert water into the intake of a micro hydroelectric power plant, Nepal.

Similar to a side intake, flow control structures, such as gates, are often incorporated in frontal intakes either at the intake opening or, if this area is vulnerable to flood impacts, then at some distance downstream along the headrace. Note that in the case of the Nepalese mini hydropower plant (Figure 4.6), the gate is located at some distance downstream from the intake to protect it from boulder impacts. In case the water level needs to be raised to divert flows into the frontal intake, a weir is constructed across the river, similar to the case of the side intake. Thus, apart from orientation of the intake, the design principles for both side intake and the bottom intake are similar.

4.2.4 Diversion Weir

A weir is a small dam constructed across the river to raise the water level at the intake to divert water flow into the waterways of the hydropower plant. A weir or a dam becomes essential if the required flow volume cannot be diverted toward a side intake or a frontal intake without raising the river water level, especially during the low-flow season. For a bottom intake, a diversion weir is not required because the water level need not be raised in order to channel the flows into the trench at the riverbed. The dimensions of the bottom intake (width, depth, and length) are fixed such that the required flow can be conveyed (dropped) into the trench during the low-flow season.

Based on the size of the hydropower plant and funds available, weirs can be of temporary, semipermanent, or permanent type. For example, many weirs installed for diversion of water flow to waterwheels or small community micro hydropower plants (5–10 kW) in remote mountain areas around the world utilize temporary construction. These are generally comprised of boulders and brushwood placed across the river as can be seen in Figure 4.7. Such weirs are almost always destroyed during flood flows. However, during the annual floods, the water level in the river is high enough, and thus flows can be diverted into the intake even in the absence of a weir. As the flood recedes, the villagers get together and reconstruct another "temporary" weir, which will last until the next high-flow season.

A gabion weir is an example of a semipermanent construction. It uses wire cages filled with boulders to raise the water level at the intake. In rivers that do not carry large boulders during the floods, when adequately designed, this type of weir can be a cost-effective solution for micro or mini hydropower plants.

FIGURE 4.7 500-kW Jhankre mini hydropower plant, Nepal, with a semipermanent gabion weir.

A gabion weir has been used in the 500-kW Jhankre mini hydropower plant as shown in the photograph in Figure 4.8. A cross-section through this weir is shown in Figure 4.9. The intake of this power plant is located on the left bank of the river below a 15-m-high waterfall. A gabion weir is constructed across a wide pool below the waterfall, which raises the water level such that the required flow of 455 l/s can be diverted into the intake. As can be seen from the sectional view of the weir, three layers of gabions are used to construct the weir. The bottom gabion box is 3 m long and 1 m high, the middle one is 2 m × 1 m, and the topmost gabion box is 1 m × 1 m. The exposed surface of the gabions are covered with 150 mm of plain concrete, which protects the gabion wires from being nicked by cobbles and gravels carried by the river flows during floods. This is required to protect the gabion cages because the entire box becomes unstable and the packed stones can start falling apart if even a few of the wires are cut or broken. Once the flood season (i.e., monsoon in this case) is over, the damaged plain concrete topping is repaired by the power plant staff. As can be seen from the sectional view of the weir, the upstream face of the gabions is lined with a heavy-grade polythene sheet to minimize seepage. Furthermore, boulder/stone backfill is placed upstream of the polythene sheet to prevent it from being damaged.

Since its commissioning in 1994, the Jhankre weir has survived a number of floods albeit with regular maintenance work, which has comprised replacing the plain cement concrete on the exposed surface. Gabion weirs can be significantly damaged during floods but are often subsequently repaired. The photograph in Figure 4.9 shows an example of a partially damaged gabion weir.

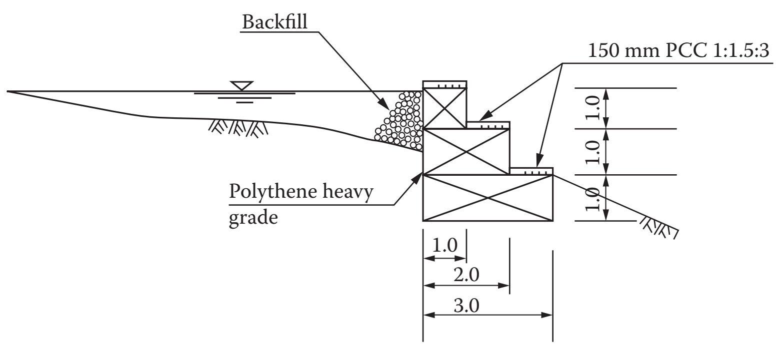

FIGURE 4.8 Section through the Jhankre mini hydro weir.

FIGURE 4.9 Partially damaged gabion weir placed across the river, Nepal.

Modern permanent weirs or dams are generally constructed of high-grade concrete. The downstream weir profile is often "ogee shaped" to safely accommodate the designed flood flow without negative pressure on the surface, which causes excessive cavitations (Figure 4.10). For large dams, roller compacted concrete (RCC) is usually the preferred choice in concrete gravity dams. RCC dams are constructed by compacting concrete in layers by driving heavy rollers on the freshly poured concrete surface. In fast flowing steep gradient rivers such as in the Himalayas, some boulder lined weirs have also been built and they seem to function satisfactorily (Box 4.2).

Seepage control on concrete weirs is achieved by providing cutoff walls and adequate weir length. The downstream reach of the weir can be susceptible to erosion and scour due to high velocity of the flow as it reaches its toe. Scour protection measures are provided at the downstream end of the weir. Concrete aprons or boulder ripraps are used for this purpose based on availability of boulders. Stilling basins may be required to dissipate the energy of the flow over the weir or small dam in case their heights exceed 2–3 m. The design of stilling basins is extensively covered in the *USBR Design of Small Dam*, and the reader should refer to this manual for additional details.

A temporary weir is the preferred option for micro-hydro schemes. In planning a weir, attention must be given to the geomorphology of the river, and any changes that may be taking place. At the proposed weir location, the design engineer should ascertain whether the river is eroding (a general lowering of the river-bed), aggrading (a general building up of the riverbed), or shifting its course. The headworks design, and in particular the choice of weir, must take account of possible future changes. When it becomes apparent that a weir is required, the following factors should be considered for both permanent and temporary weirs:

- If a weir across part of the river length is sufficient, then it should not be extended across the entire width. Apart from adding extra cost it also encourages sediment deposition upstream of the weir.
- The weir height should be as low as possible (i.e., weir crest level = h_r, should be just sufficient to maintain the water level in the intake). This makes the structure more stable, less susceptible to flood damage, and also minimizes sediment deposition.
- A permanent weir must be stable against sliding, overturning, and sinking (i.e., bearing pressure within allowable range for given ground conditions).

FIGURE 4.10 A low-height concrete weir with an undersluice and a side intake for a 14-MW hydroelectric power plant in Nepal.

BOX 4.2 BOULDER-LINED WEIR

A boulder-lined weir was constructed in the 60-MW Khimti hydroelectric plant in Nepal based on Norwegian experience. Because there is significant boulder movement along the Khimti River during the high flows, design of a conventional concrete weir would have been both expensive and also require high annual maintenance costs. Thus, a boulder-lined weir with two thin central reinforced concrete walls extending below the riverbed level was constructed (Figure 4.11). The vertical concrete walls were covered with large boulders, and the gaps between the boulders were filled with high-grade plain concrete (see photographs in Figures 4.11 and 4.12). Since its commissioning in 2000, the Khimti weir has been functioning satisfactorily.

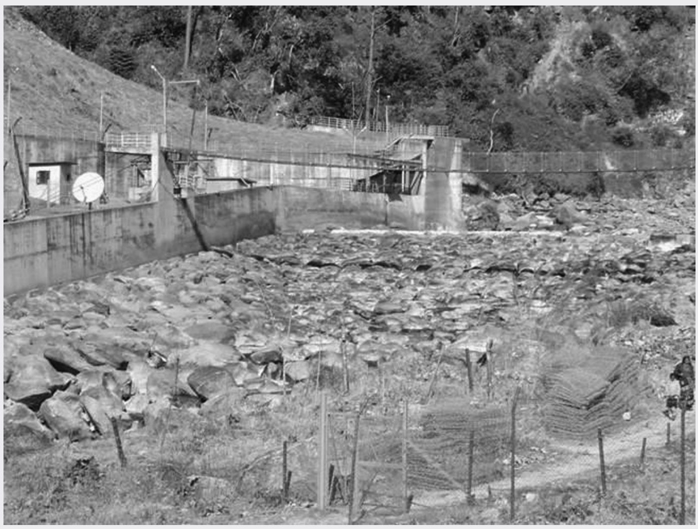

FIGURE 4.11 Boulder-lined, low-height diversion weir 60 MW Khimti, Nepal.

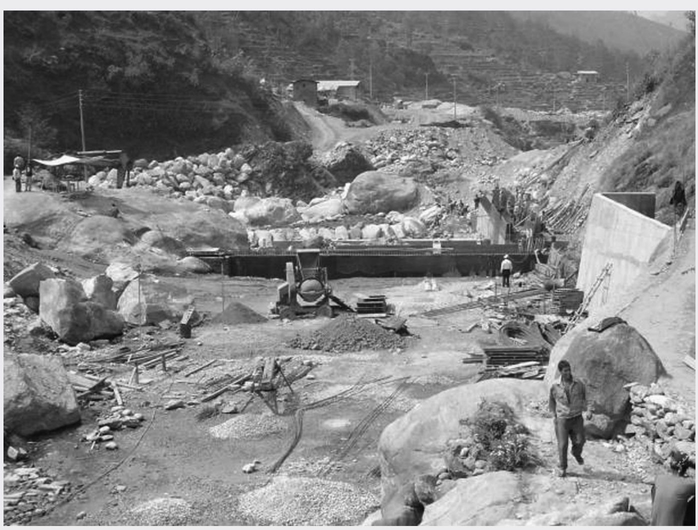

FIGURE 4.12 Boulder diversion weir under construction 2.5 MW Sun Koshi Hydropower Plant, Nepal.

Based on the Khimti experience, the 2.5-MW Sunkoshi project constructed a similar boulder-lined weir. The design comprises a number of reinforced vertical cutoff walls filled with large boulders. Similar to the Khimti plant, the gaps between the boulders were filled with high-grade concrete (C35). The reinforced concrete cutoff walls serve two purposes: (a) They provide seepage control, and (b) they hold the boulders together between the walls. Substantial energy in the flow over the boulder-lined weir is dissipated due to rough boulder surface—this reduces the dimensions of the stilling basin downstream, and in the case of the Sunkoshi Plant, the need for a stilling basin was eliminated.

Apart from being low cost, another advantage of a boulder-lined weir is that it blends well with the environment in rivers that have significant boulder movement.

4.3 TRASH RACKS FOR INTAKES

The trash racks for intakes can be manufactured from flat steel, angles, tees, or round bars welded together at fixed intervals. The trash rack at the intake is also known as a coarse trash rack because the bar spacing is wider here compared to the trash rack at the forebay. For intakes, the function of the trash rack is to stop boulders, cobbles, floating logs, and branches from entering the headrace. Coarse trash racks are not designed to exclude gravel and sediment. This is handled by the gravel trap and the settling basin. It should be noted that coarse trash racks for bottom intakes should be more robust than those for side or frontal intake because they are more directly impacted by boulders and other bed load materials.

The size of the trash rack for frontal and side intake should be designed for water velocity of approximately 0.6 m/s (a lower velocity is generally uneconomic whereas high velocity tends to attract bed load and debris and results in increased head loss). For bottom intakes, the velocity through the trash rack can be much higher because flow conditions are often supercritical as water drops into the trench below.

Depending on the length and width of the opening, the nature of the sediment load and the required flow, a clear spacing of 50 mm to 200 mm is the range typically adopted for trash racks used in mini or small hydropower plants.

4.3.1 Orifice Design

A side intake often includes an orifice or an opening along the intake wall along the riverbank, downstream of the trash rack, through which water is initially drawn into the headrace. Such an orifice when adequately designed allows the required flow to enter the intake but limits excessive flows during floods when the river water level is high. A design that ensures submerged flow conditions through the orifice, as shown in Figure 4.13, will limit entry of excessive flows into the intake. The gates at the intake can sometimes serve the function of the orifice whereas, in other cases, such gates are placed after the orifice opening.

In poorly designed intakes, the side intake is sometimes just a continuation of the headrace canal up to the riverbank without an orifice or gate to control excess flow entering the canal during floods. Such excess flow can damage the headrace canal and other structures downstream. Furthermore, together with excess flows, the sediment entry into the waterways will also increase. If the intake must be located in a flood plain or is susceptible to damage from boulders, then the permanent orifice structure can be located further downstream at a safe location. In the case of micro hydroelectric power plants in developing countries where labor costs are low compared to the cost of cement and other construction materials, the canal upstream of the orifice and the intake along the flood plains are often of a temporary nature, requiring repairs or rebuilding after every rainy season.

The discharge through an orifice for submerged conditions can be calculated as

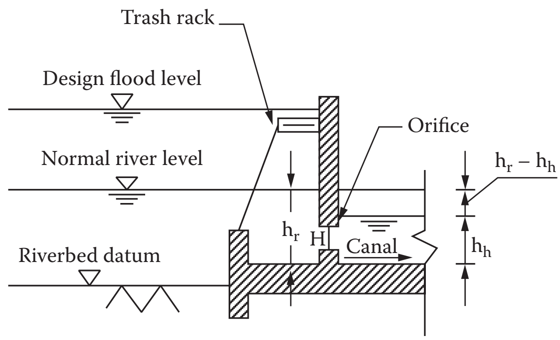

FIGURE 4.13 Typical section through an orifice intake.

$$Q = AC\sqrt{2g(h_r - h_h)}$$

where A is the area of the orifice opening in m^2 and C is the coefficient of orifice, which depends on the shape of the orifice. For roughly finished and sharp-edged concrete or masonry orifice structure, C will be around 0.6, and for carefully finished structures with smooth edges, it can be as high as 0.8 [1]. g is the acceleration due to gravity = 9.81 m/s^2 at sea level. h_r is the water level at the river from an arbitrary datum. h_h is the water level along the headrace canal from the same datum as in case of h_r. H is the orifice height.

The design procedure is as follows [1]:

- Assume a weir height based on flow diversion requirements and site conditions. The weir height sets the normal water level in the river (weir height = h_r)—that is, as long as the required diversion flow is available in the river, the water level in the river will be at least equal to h_r.
- Assume a practical orifice height based on design flow and site conditions. Sediment entry (especially bed load) into the intake can be minimized if the invert level of the orifice opening is set above the riverbed level as can be seen from Figure 4.14.
- Choose an appropriate weir profile based on size of the scheme and locally available masonry skills. For example, for micro hydropower a roughly finished masonry structure may be appropriate due to lack of skilled labor (C = 0.6) whereas larger hydroelectric plants will be able to construct a more complicated profile resulting in higher values of the orifice constant (C).
- Assume a water level at the entrance of the headrace canal based on site conditions but ensuring that this level is above the orifice height (i.e., h_h > H in Figure 4.14) so that submerged conditions apply. Note that initially the water level in the headrace canal is

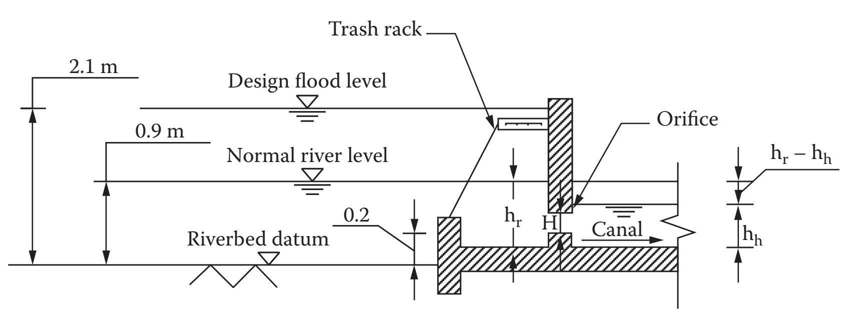

FIGURE 4.14 Orifice intake for Example 4.1.

unknown and thus needs to be assumed. Later, when the headrace canal is designed and the water level becomes known, then the orifice size will have to be revised accordingly.

- Now the only unknown in the orifice equation is the required orifice opening area and can be computed. Often additional allowance of 5%–10% is made in the orifice opening to allow for head loss at the coarse trash rack in front of the orifice as well as possible partial blockages from leaves and other floating debris.
- Once the required orifice area is determined, either the length or height (H) should be chosen based on site conditions. It is generally more practical to select the height and then calculate the required length.
- Once the orifice dimensions have been finalized, the flow through the orifice during flood conditions should be calculated (based on expected water levels during flood flows), and the spillway downstream should be sized accordingly to spill the excess flows. Spillway sizing is covered in Chapter 5.
  - Normal river water level (h_r) is set by weir height:

$$Q = AC\sqrt{2g(h_r - h_h)}$$

  - Canal height h_h is set when sizing headrace. Ensure orifice is submerged during normal depth (i.e., during design flow) in the canal.

C is the coefficient of discharge or the weir constant. For roughly finished masonry or concrete, C = 0.6. For a carefully finished opening (sharp edged), C = 0.8.

Refer to Table 4.1 [2] for orifice constant.

- Repeat calculations for flood flow condition
- Size initial headrace canal to accommodate flood flow
- Locate spillway as close as possible and size its capacity to spill the entire flood flow.

TABLE 4.1
Weir Coefficient for Various Weir Profiles

Profile of weir crest		C_w
	Broad; sharp edges	1.5
	Broad; round edges	1.6
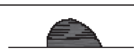	Round overall	2.1
	Sharp edges	1.9
	Rounded	2.2
	Roof-shaped	2.3

Source: Harvey, A. and Brown, A., *Micro-Hydro Design Manual: A Guide to Small-Scale Water Power Schemes*, ITDG Publishing, London, 1993.

Example 4.1

- Choose an appropriate orifice for design flow of 400 l/s. The weir height has been set at 0.9 m above the riverbed level. The estimated flood level (~1 in 20 years) is 2.1 m above the riverbed level. Also size a spillway to spill excess flows during the flood. See Figure 4.15 for the sectional view of the orifice along with the dimensions.
  - $Q = (0.40)\cdot 1.15 = 0.46\ m^3/s$ (with 15% additional flow to account for subsequent losses along the headrace)

    Set V = 1.1 m/s

    $$\text{Orifice Area (A)} = \frac{Q}{V} = \frac{0.46}{1.1} = 0.42\ m^2$$

    Set orifice height = 0.4 m, calculate width, W

    $$W = \frac{A}{H} = \frac{0.42}{0.4} = 1.05\ m$$

    Set W = 1.1 m

    Set bottom of orifice 0.2 m above datum to minimize entry of bed load.
  - Set water level at headrace canal h_h = 0.7 m above the datum—that is, 0.1 m above top of orifice to ensure submerged conditions.

    The calculated dimensions are presented in Figure 4.15.

    Recall the orifice equation:

    $$Q = AC\sqrt{2g(h_r - h_h)}$$

  - Given: C = 0.6 for roughly finished masonry

    With

    $$h_r - h_h = 0.9 - 0.7 = 0.2\ m$$

  - $Q = 0.52\ m^3/s$
  - OK!

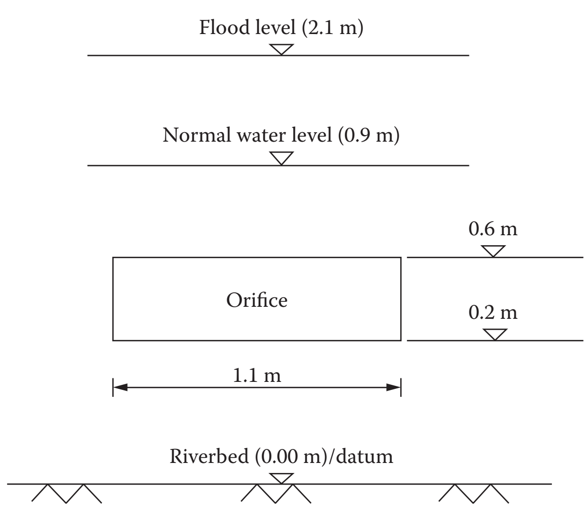

FIGURE 4.15 Orifice dimensions and levels calculated for Example 4.1.

Check velocity

$$V = \frac{Q}{A} = \frac{0.52}{0.44} = 1.19 \text{ m/s}$$

- Velocity is in acceptable range
- Flood conditions

Assume same water level in canal (although with higher flow in the canal during floods, the water level in the canal will be higher).

$$Q_{flood} = 0.44 \cdot 0.6\sqrt{2 \cdot 9.81(2.1 - 0.7)} = 1.38 \text{ m}^3/\text{s}$$

Note that the actual flood flow will be less as the canal water level will be higher downstream. Thus, for the calculated flood flow of 1.38 m^3/s, the corresponding water level in the canal downstream should be calculated. Because the canal water level will be higher than assumed earlier, the driving head ($h_r - h_h$) will be lower, and thus, the flood flow will also be lower. A few iterations may have to be performed to come up with a closer estimate of the flood flows through the orifice.

4.3.2 Use of Gates at Orifice

From Example 4.1, it is clear that an intake orifice sized to withdraw design flow during the low-flow season can convey significant excess flows during high river flow months. Although, such excess flows can be discharged from a downstream spillway, the conveyance structures upstream of this spillway will have to be oversized. Furthermore, excess flows into the intake will also bring in more sediment and thus overload the gravel trap and settling basin. Note that the spillway will discharge the water from the surface level, which is relatively cleaner, and the water that is conveyed along the waterways further downstream will have high sediment concentration. To avoid this, a gate can be placed at the orifice. During the high-flow season, the gate can be partially closed so that the orifice area becomes smaller as the flow through it is reduced.

Discharge through a partially opened gate depends on the type of gate, upstream water level (e.g., flood level), gate opening, and the downstream water level (e.g., water level in the headrace canal downstream). Figure 4.16 shows a vertical gate installed behind an orifice. The equation for flow through an orifice is also applicable for gates. However, the coefficient of discharge will be different depending on the water levels and gate opening [3].

Note that in Figure 4.17, y_1 is upstream water depth, b is the gate opening height, and y_3 is the downstream water level. The chart in Figure 4.18 shows how the coefficient of discharge (C_d) varies in relation to y_1, b, and y_3. Once the coefficient of discharge is determined from the chart, the orifice

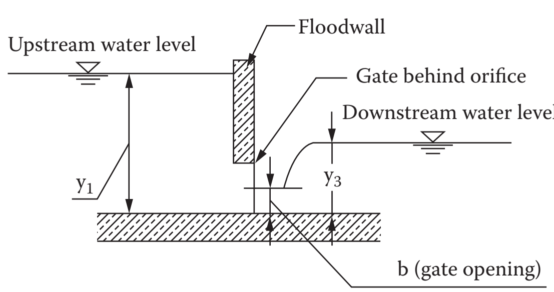

FIGURE 4.16 Vertical gate installed behind an orifice.

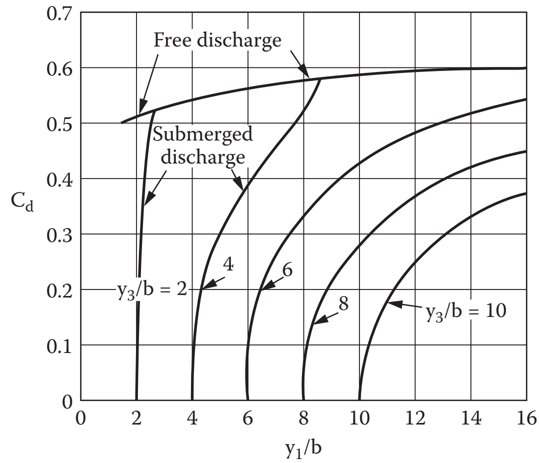

FIGURE 4.17 Coefficient of discharge for free and submerged flow under a vertical lift gate. (From J. Lewin, *Hydraulic Gates and Valves in Free Surface Flows and Submerged Outlets*, Thomas Telford Publications, 1995.)

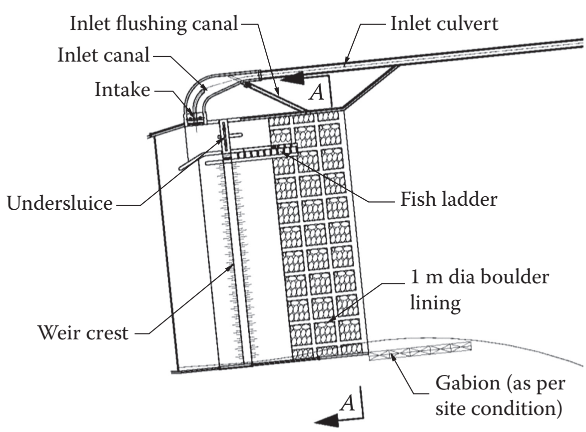

FIGURE 4.18 Plan of headworks with flood protection walls for Example 4.3.

equation can be used to determine the flow through the gate. Note that instead of C in the earlier submerged orifice equation, C_d should be used.

As can be seen from Figure 4.18, for a high value of y_1/b or high flood level and small gate opening, the flow through the gate will be free flow initially. This is because the flow will be supercritical at high head at the river side and small gate opening. This would result in a hydraulic jump further downstream of the headrace canal, and then the flow would be subcritical with a higher water level.

In micro and small hydropower plants, vertical gates are often used as they are economical and easy to operate, especially when the flows are low. In large hydropower plants, radial gates are also used to control flows in the waterways. The calculations for flows through the radial gates are similar to vertical gates, but the determination of the discharge coefficient is based on different charts. Sizing of radial gates is beyond the scope of this textbook, and the reader should refer to other literature.

Example 4.2

Calculate the flow through the orifice in Example 4.1 for flood flow conditions (flood level = 2.10 m above the riverbed level) if the gate opening at the orifice is 0.30 m. Assume downstream water level to be 1.2 m above the riverbed level.

Recall that the orifice opening in Example 4.1 was 0.4 m high and 1.1 m wide. Gate opening, b = 0.30 m. The flood water was at 2.1 m high from the datum. Note that the datum was assumed at the riverbed level or 0.2 m below the invert of the orifice to minimize entry of bed load. Therefore, y_1 = 2.1 m – 0.2 m = 1.9 m, and similarly, downstream water level y_3 = 1.2 m – 0.2 m = 1.0 m.

Thus, $y_3/b = 1.0/0.30 = 3.3$ and $y_1/b = 1.9/0.3 = 6.3$

Now with known y_3/b and y_1/b values, from the chart in Figure 4.18, $C_d = 0.52$ (approximately).

If the gate is opened 0.3 m, then the effective area will be $A = 0.3 \cdot 1.1 = 0.33\ m^2$.

Thus, flow through the gate will be

$$Q = 0.33 \cdot 0.52\sqrt{2 \cdot 9.81(2.1 - 1.2)} = 0.72\ m^3/s$$

Now for this flow of 0.72 m^3/s, the downstream water level in the headrace canal should be verified as a final check. Calculating water levels in the headrace canal is covered in Chapter 5. If the water level is not close to 1.2 m as assumed, then the calculations should be repeated with the new water level. Also, note that the gate would have to be further closed to divert only 0.40 m^3/s, which is the design discharge.

4.4 RIVER TRAINING WORKS

A flood protection wall along the riverbank may be required if there is a high probability of flood damage to the initial headrace and other structures, such as the gravel trap and settling basin. Such walls are also called river training structures because they confine the river channel. The wall height should be greater than or at least equal to the design flood level. Such walls also contain the floodwater between them and prevent scouring of the river banks near the weir area.

The foundation of any river training walls must be protected from undermining by the river. This can be done by one of the following methods:

- Founding the wall on rock or large boulders. For gabion walls, it may be necessary to first build up a level base using stone masonry or mass concrete, especially if the river carries boulders during floods.
- Founding the wall below possible scour depth.

On alluvial rivers (i.e., deep deposition of sand and cobbles), gabion flood protection walls are usually more appropriate for a micro hydro scheme. This is because the ground of alluvial rivers tends to change, and flexible structures can cope better in such conditions. Gabion walls may require annual maintenance (especially after a monsoon), and therefore, skilled manpower should either be available at site or some local people should be trained during the construction phase. Gabion walls can also serve the function of retaining walls and stabilize the slopes behind it. If slopes at the alluvial riverbank are unstable, then gabion walls can also be designed as retaining walls. On stable riverbanks, such as along exposed bedrock, a masonry wall can be built provided that the river does not carry large boulders that could damage masonry structures. In large hydropower and irrigation projects, concrete flood barrier walls are typically used, but usually such solutions are not economically justifiable for smaller micro hydro schemes.

4.4.1 Head Over Weir

As stated earlier, placing a weir across the river raises the water level. Any excess flow that is not withdrawn into the intake flows over the weir. The discharge over the weir is given by the following equation:

$$Q = C_w \cdot L_{weir} \cdot (h_{overtop})^{1.5}$$

where Q = discharge over the weir in m^3, L_{weir} = Length of weir in m, $h_{overtop}$ = head over the weir crest level in m, and C_w = Weir coefficient, which varies according to the weir profile. C_w for different weir profiles is shown in Table 4.1. In micro hydro, the weir is usually broad with round edges for which C_w is 1.6.

The weir equation is also useful in calculating the flood levels at the intake if the flood discharge is known or can be calculated based on the river hydrology. Once the flood levels are known, the flood protection walls at the riverbank can be designed. For known discharge over the weir, the head over the weir (and hence the water level at the intake) can be calculated by rewriting the weir equation as follows:

$$h_{overtop} = [Q/(C_w \cdot L_{weir})]^{0.667}$$

Example 4.3

A broad-crested weir 1.4 m high and 20 m wide has been placed across the river. The design flood has been estimated to be 75 m^3/s. What should be the height of the floodwalls at the river bank to contain the flood flows within the river width?

First calculate the head over the weir:

$$h_{overtop} = [Q/(C_w \cdot L_{weir})]^{0.667}$$

where Q = 75 m^3/s, L_{weir} = 20 m (20 m wide weir), C_w = 1.6 as the shape is broad crested, and $h_{overtop} = [75/(1.6 \cdot 20)]^{0.667} = 1.76$ m.

With allowance for some freeboard, the floodwalls should be around 2.0 m. Figure 4.18 shows the plan view of the headworks structure along with flood protection walls and Figure 4.19 shows the sectional view.

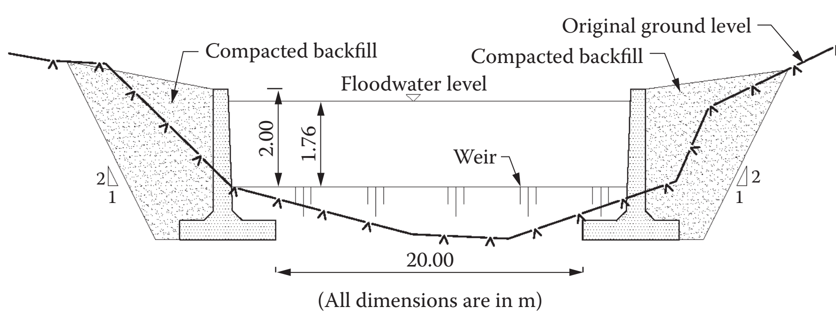

FIGURE 4.19 Headworks Section A-A for Example 4.3.

EXERCISES

1. The figure below shows the cross-section of a weir along with an orifice intake. The weir is 22 m long, and the annual floodwater level is 1.5 m above the crest of the weir. Assuming round overall weir profile ($C_w = 2.1$), calculate the flood flow down the weir assuming that the gate at the orifice opening is closed.

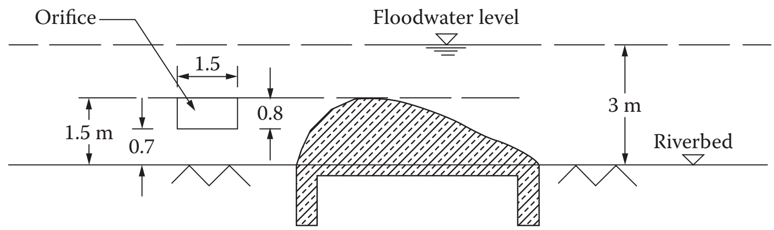

2. For Exercise 1, calculate the flow through the orifice, assuming
   a. There is no gate installed behind the orifice.
   b. A vertical gate is installed behind the orifice, and it is half open.
   c. If the required design discharge is 1.0 m^3/s, what should the gate opening be?
   (Assume roughly finished and sharp-edged concrete orifice and the water level at the headrace canal to be 1.6 m from the riverbed level for all cases.)
3. Hydrological analysis indicates that the 100-year return period flood is about 180 m^3/s. If the headworks structures are designed to be safe against the 100-year return period flood, how high should the flood protection walls have to be from the riverbed level?

REFERENCES

1. ITDG, *Civil Works Guidelines for Micro Hydropower in Nepal*, BPC Hydroconsult and Intermediate Technology Development Group, Kathmandu, Nepal, 2002.
2. Harvey, A. and Brown, A., *Micro-Hydro Design Manual: A Guide to Small-Scale Water Power Schemes*, ITDG Publishing, London, 1993.
3. Lewin, J., *Hydraulic Gates and Valves in Free Surface Flows and Submerged Outlets*. Thomas Telford Publications, London, 1995.

5 Headrace

5.1 OVERVIEW

The water conveyance system that connects the intake and the forebay of a run-of-river hydropower plant is referred to as a headrace. Canals, pipes, tunnels, or other conduits, such as box culverts, are used as headraces in hydropower plants. The headrace dimensions (canal width and depth or pipe diameter) and the longitudinal slopes are sized such that the required flow can be conveyed by gravity. In case of large run-of-river hydropower plants, the headrace may also be comprised of a tunnel (referred to as a headrace tunnel). In such cases, a surge shaft is used instead of the forebay as discussed in Chapter 2. The flows along the headrace pipes or tunnels in a hydropower plant are either open-channel type (upper part of the pipe or tunnel is empty, and thus there is atmospheric pressure on the water surface) or have low pressure if flowing full.

In case of a reservoir type or large dam hydropower plant with the powerhouse either inside the dam or at its toe, the headrace is not required (Figure 5.1). The high dam height creates the head required, and the discharge is conveyed through a penstock pipe laid across the dam directly to the turbines. It should be noted that the initial length of the headrace from the intake to the gravel trap or the settling basin is also sometimes referred to as the intake canal, approach canal, or the power canal. In this textbook, the entire length of the canal from the intake to the forebay is referred to as the headrace canal.

The headrace alignment is kept as mild as possible based on site topography, taking into account the location of the forebay, the flow required to be conveyed, and the type of material used. This is because the steeper the headrace alignment, the more the head loss as the drop in elevation (or head) between the start and end of the headrace does not contribute to power generation. In case of a headrace pipe or tunnel, either low-pressure or open-canal (part flow along the pipe or tunnel) systems are adopted to maintain the required water level at the downstream structure such as the forebay or the surge shaft. Therefore, the headrace pipes or tunnels are generally not subjected to significant hydraulic pressure.

In mini hydropower plants, a headrace canal is usually the preferred choice when the alignment is along stable and gently sloping terrain (Figure 5.2). As pipes are generally more expensive than canals, they are used along difficult terrain, such as to cross cliffs, gullies, or streams. Thus, a combination of both a canal along stable terrain with mild slopes and pipes to negotiate gullies and crossings are used.

In large hydropower plants, tunnels are used as headraces for the following reasons (Figure 5.3):

a. The headrace length can be minimized with a tunnel compared to a surface canal.
b. Even when the ground surface is unstable (e.g., prone to landslides and rockfalls), the tunnel along sound bedrock will be stable and not prone to structural damages.
c. Acquiring a large parcel of land for the canal or pipe alignment is avoided.
d. Security measures are not required.

5.2 BASIC CRITERIA FOR HEADRACE SIZING

Once the type of headrace (canal or pipe) has been decided, the next steps are to determine the dimensions and the longitudinal slope. The longitudinal slope is based on (a) the ground profile

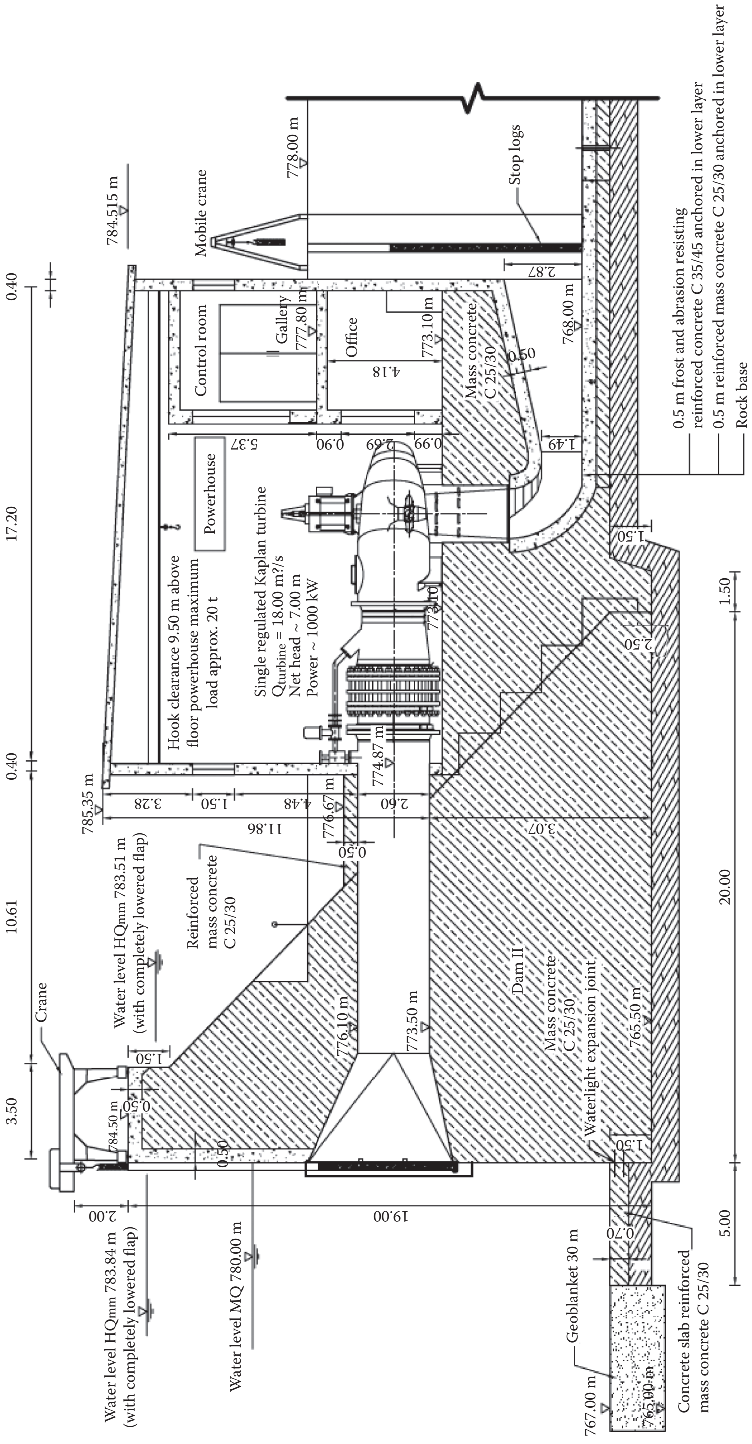

FIGURE 5.1 A typical storage-type hydropower plant with the penstock laid across the dam to the turbine. Note the lack of headrace in this case.

FIGURE 5.2 A typical cement masonry–lined headrace canal in a micro hydropower plant.

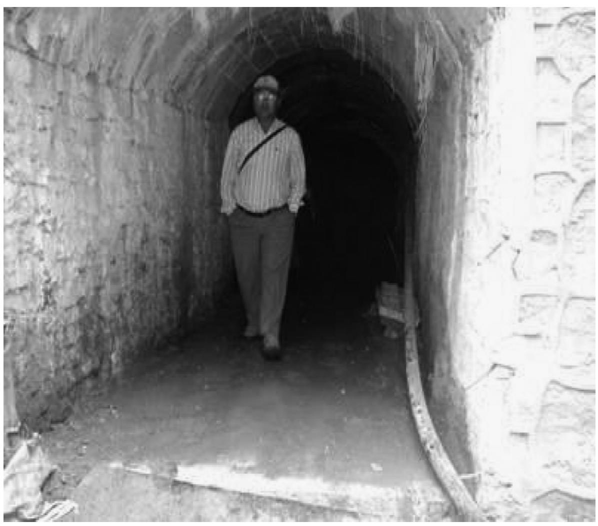

FIGURE 5.3 An under-construction headrace tunnel in a 3.0 MW Chaku hydropower plant, Nepal.

along the headrace alignment and (b) the location of the forebay. Thus, the design engineer may not have much flexibility in fixing the ground slope.

After the ground slope is fixed, the canal or pipe dimensions are sized based on velocity criteria. For a fixed flow in a headrace pipe or canal, the smaller the headrace dimensions, the higher the velocity will be. The velocity criteria in the headrace are determined by the type of material used and the stretch of the headrace alignment. The underlying principles in setting the velocity in the headrace are the following:

i. The velocity should not be excessively high such that it erodes the headrace canal bed and walls or the internal surface of the headrace pipe. Such limiting velocity depends on the type of headrace materials used. Velocity criteria based on headrace materials used can be seen in Table 5.1. These values can also be found in standard hydraulic textbooks.

TABLE 5.1
Roughness Coefficient and Allowable Maximum Velocity for Various Canal Types

Channel Type	Description	n	Max. Velocity (m/s)
Earth channel	Clay, with stones and sand, after aging	0.02	0.8
	Gravelly or sandy loams, maintained with minimum vegetation	0.03	0.4
	Lined with coarse stones, maintained with minimum vegetation	0.04	1
	For canals less than 1 m deep, use the equation in the note for *n* value		
	Vegetated (useful to stabilize soil);		
	water depth 0.7 m	0.05	0.8
	water depth 0.3 m	0.07	0.8
	Heavily overgrown water depth 0.3 m	0.15	1
Masonry channel	Stone masonry in mud mortar, dry stone masonry	0.035	1
	Stone masonry in cement mortar using rounded stones	0.03	
	1:4 cement sand mortar		1.5
	1:3 cement sand mortar		2.5
	Stone masonry in cement mortar using split stones (dressed)	0.02	
	1:4 cement sand mortar		2
	1:3 cement sand mortar		3
	with 1:2 pointing		5
Concrete channel	According to finish	0.013–0.017	
	1:3:6 plain concrete		1.5
	1:2:4 plain concrete		2
	1:1.5:3 reinforced concrete		3
	1:1:2 reinforced concrete		5
Cement plaster		0.013	
	1:3		3
	1:2		5
Mountain streams	Dominant bed material		
	Gravel (up to 60 mm)	0.03	
	Cobbles (up to 200 mm)	0.04	
	Boulders (up to 600 mm)	0.05	
	Large boulders (>600 mm)	0.07	

Source: BPC Hydroconsult and Intermediate Technology Development Group, *Civil Works Guidelines for Micro-Hydropower in Nepal*, ITDG Nepal 2002; A. Harvey et al., *Micro-Hydro Design Manual: A Guide to Small Scale Water Power Schemes*, ITDG Publishing, London, 1993.

Note: Roughness effect for shallow channels research at Wageningen University in the Netherlands demonstrated that the roughness is increased for channels under 1 m in depth because of the turbulence created by the side and bed surfaces. The research showed that the following equations can be used to find the roughness coefficient. H is the depth of water. Well-maintained channels with little vegetation: $n = 0.03/\sqrt{H}$ where $H < 1$ m; channels with short vegetation: $n = 0.04/\sqrt{H}$ where $H < 1$ m; heavily overgrown channels: $n = 0.08/\sqrt{H}$ where $H < 1$ m. In practice, it is sensible to maintain short vegetation in order to protect the banks of canals; n can therefore be found from the equation $n = 0.04/\sqrt{H}$ where $H < 1$ m.

ii. The velocity should not be too low such that the sediment in the flows is deposited along the canal bed. For example, the velocity in the initial headrace length needs to be high enough to carry gravel and sediment up to the gravel trap. The velocity in the reach between the gravel trap and the settling basin should be high enough to carry sediment that is to be settled in the settling basin—that is, sediments should not be deposited along the headrace canal. It should be noted that the gravel size that can enter the intake depends on the coarse trash rack bar spacing at the intake. If the coarse trash rack bar spacing is 75 mm, then the maximum size of gravel that can enter the intake will also be 75 mm, and the longitudinal slope of the initial stretch of the headrace should be sufficiently sized to achieve the required water velocity to transport gravel of this size to the gravel trap.

iii. The headrace reach between the settling basin and forebay will carry sediment-free flow, and thus, the velocity can be lowered accordingly; however, in case of an earthen canal, the velocity should not be too low such that aquatic plants can be sustained that would decrease the effective cross-sectional area of the canal and increase the channel roughness—both of which will lower the canal's conveyance capacity. A minimum velocity of 0.4 m/s should be maintained to prevent the growth of such aquatic plants.

5.2.1 Other Considerations for Headrace Canals

a. The canal should be able to carry the design flow with adequate freeboard. Freeboard is the difference in elevation between the top of the canal walls and the design water level. When the river water level is high, such as during the rainy season (or snow melt period), flows higher than the design flow can enter the intake. Even when there are control gates at the intake, higher flows can enter the headrace, such as during flash floods, which are sudden events, and the operators may not have adequate time to lower the gates. Another possibility causing the entry of excessive flows into the intake is malfunction of gates during high river water at the intake. Spillways located appropriately along the headrace canal are required to spill such excess flows. Such spillways may also be required if there are possibilities of rockfalls or earth slides from the uphill slopes that would block the canal. In case of blockages, spillways located upstream from such unstable areas but close to a gully or stream can safely discharge the entire incoming flows.

b. Head loss and seepage along the canal alignment should be minimized. The longitudinal slope of the canal should be just sufficient to safely convey the required flow for given site conditions without depositing sediment at its bed. It should be noted that the higher the longitudinal slope, the higher the head loss will be. The choice of appropriate construction materials (earth, cement mortar, or reinforced concrete canals, etc.) based on flow volume and the ground conditions will control seepage. For example, a cement-lined canal will have less seepage than an earthen canal under similar conditions although construction costs will be higher for lined canals.

c. The canal shape can be either rectangular or trapezoidal based on site conditions and flows required to be conveyed. For example, if the headrace alignment is along a narrow cliff, then it may have to be of relatively low width compared to its height. For large flows along an alignment where the width is not a constraint, a trapezoidal canal may be cost-effective (Figure 5.4). In such a canal, more flows can be accommodated compared to a rectangular canal with the same bed width, or for each unit of additional flow depth from the canal bed, the marginal increase in flow will be higher. Furthermore, part of the load from the side walls can be absorbed by the ground, and thus, thin lining sections would suffice provided that the side walls rest on well compacted backfill. In an ideal condition, the optimum cross-sectional shape for a canal is a semicircle because it can convey the maximum flow for a given cross-sectional area. As it is generally not practical to construct semicircular canals (unless lining is prefabricated at a workshop and brought to the site), a trapezoidal shape is used because it roughly resembles a semicircle and is easier to construct. For smaller flows, generally a trapezoidal-shaped canal may not be cost-effective as its construction is more complicated than a rectangular one. Recommended side slopes for different canal types based on ground conditions are shown in Table 5.2.

d. The selected canal alignment should be along stable grounds. Furthermore, the hill slopes above and below the alignment should also be stable. If the hill slopes above are unstable,

FIGURE 5.4 A trapezoidal stone masonry in cement mortar headrace canal.

TABLE 5.2
Allowable Side Slopes for Trapezoidal Canals in Various Soil Types and Linings

S. N.	Type of Soil	Z
1	Very light, loose sand to average sandy soil	2:1 to 3:1
2	Sandy loam	1.5:1 to 2:1 (in cutting) 2:1 (in filling)
3	Sandy gravel/murum	1.5:1 (in cutting) 1.5:1 to 2:1 (in filling)
4	Black cotton	1.5:1 to 2.5:1 (in cutting) 2:1 to 3.5:1 (in filling)
5	Clayey soil	1.5:1 to 2:1 (in cutting) 1.5:1 to 2.5:1 (in filling)
6	Rock	0.25:1 to 0.5:1

Source: Indian Standard (IS) 10430:2000.

then debris could fall into the canal or any landslide above could sweep away part of the canal length. On the other hand, instability along the downhill stretch undermines the canal foundation and can cause structural damage. Keeping the areas above and below the canal alignment dry, such as by constructing catch drains and routing surface runoff to nearby natural gullies, will also significantly contribute to decreasing problems associated with instability.

e. Various materials can be used to construct headrace canal based on site conditions and flow volume. The types of headrace canal that are generally used in hydropower plants are briefly described below.

5.2.1.1 Earthen Canal

Earthen canals (also referred to as unlined canals) are simple to construct on grounds that are stable and have mild slopes and good soil cover (Figure 5.5). They are constructed by excavating the ground surface to come up with the required dimensions. These canals have trapezoidal walls as unlined earthen canals cannot be stable at a vertical slope. Compared to lined canals, earthen canals

FIGURE 5.5 An unlined headrace canal used in a micro hydropower plant.

have milder slopes. This type of canal should not be selected if any seepage or overflow can trigger slope instability, such as soil erosion or landslides. In isolated micro hydropower plants where the headrace alignment is on stable ground and where any seepage or overflow from the canal will not contribute toward slope instability, earthen canals could be a cost-effective option. Often irrigation canals along plain land or river terraces are unlined. In hydropower plants, the flows along unlined canals will pick up some sediment, and thus a settling basin will be required at the end of the canal. Dry stone lining in such canals will add strength and to some extent reduce seepage. There are also geotextiles available in the market, which when properly laid along the canal surface and well protected, will completely prevent seepages.

5.2.1.2 Stone Masonry Canal

Canals constructed of stone masonry in mud mortar are also frequently used in mini hydropower plants, especially in developing countries. These are less vulnerable to erosion than earthen canals and will have relatively less seepage. Where stones are easily available (such as along riverbanks), they may be cost-effective because the cross-section of this type of canal can be made smaller than the earthen canal. This is because a higher velocity can be allowed in stone masonry canals than in earthen canals where such high velocities would cause erosion along the bed and sides.

Stone masonry in cement mortar canals are also used in hydropower plants. Compared to stone masonry in mud mortar canals with similar flows and along similar terrain, cement masonry canals will have significantly less seepages. Such canals can be appropriate along headrace alignment that has porous-type soils. Where larger flows are involved along with installed capacities in the range of a few MW, stone masonry with cement lining can be the preferred choice. Because cement would have to be brought to the site, for remote micro hydropower plants, located at some distance from the closest road head, the need for a long cement-lined masonry canal can significantly increase construction costs.

5.2.1.3 Concrete Canals

Among the conventional headrace canals used in hydropower plants, concrete canals generally are the most expensive ones. They need to be reinforced as concrete is weak in tension, and their construction requires a skilled workforce and equipment (Figure 5.6). Thus, in micro hydropower plants in developing countries, these types of canals are not frequently used. The advantage of reinforced concrete canals is that they are relatively flexible and can accommodate some ground movement and thus have a higher probability of remaining mostly intact in the event that a short stretch of the alignment is swept away by a landslide. In mini hydropower plants, if a short stretch of the headrace alignment is along unstable terrain or ground that is susceptible to landslides, then a reinforced concrete canal may be essential. Another advantage with concrete canals is that full seepage control can be achieved.

In micro hydropower plants, polyvinyl chloride (PVC) and high density polyethylene (HDPE) pipes are preferred instead of concrete canals as they are more economical and flexible and thus serve the same purpose—that is, to convey flows through a short stretch of unstable terrain (Figure 5.7). The use of plastic pipes as headrace is discussed further in this chapter.

f. Finally, any engineering design must take the costs of the structures into consideration. Thus, the design of a headrace canal will require a number of iterations to come up with optimum shape and type along with an appropriate alignment. This may require a preliminary design with various alternatives considered to come up with the least-cost option. Furthermore, a number of canal types and dimensions may have to be combined on the same project based on site conditions. For example, along fairly stable headrace alignment, a masonry-lined canal, mud, or cement mortar based on site conditions may be appropriate whereas along short stretch of unstable terrain, such as through an old landslide deposit, a reinforced concrete canal could become essential. Similarly, where the longitudinal slope is mild, the canal dimension will be large and even an earthen canal can be suitable (if along stable ground with low discharge), but along steeper

FIGURE 5.6 A reinforced concrete headrace canal with a side spillway, Indonesia.

FIGURE 5.7 A HDPE headrace pipe used to cross steep hill slopes, Nepal.

slopes of the alignment, a lined canal with smaller dimensions (keeping the velocity within limit) could be appropriate.

5.3 HEADRACE CANAL DESIGN

The basic criteria for selecting the type of headrace canal have been discussed earlier. The following section elaborates the headrace canal design procedure.

5.3.1 Manning's Equation

Although there are other equations that are also used in open channel flows (i.e., channels where the flow is due to gravity), Manning's equation is commonly used, especially in uniform open canals. Manning's equation in terms of flow and velocity is written as follows:

$$Q = \frac{1}{n} AR^{2/3}\sqrt{S}$$

Or

$$V = \frac{1}{n} R^{2/3}\sqrt{S}$$

where Q (m^3/s) = flow in the canal; V (m/s) = velocity in the canal; n (unit less) = the roughness coefficient of the canal, which depends on the materials used to construct the canal. This is also sometimes referred to as Manning's n. For a smooth-surface canal (e.g., well-plastered canal bed and walls) the value of n will be low whereas it would be higher along rough surfaces. The value of n

for different types of canals can be seen in Table 5.1. A (m^2) = cross-sectional area of the canal up to the water level. S (unit less) = slope of the energy grade line. This is an imaginary line along the canal longitudinal section that follows the water level plus the velocity head. The invert slope of the canal is used for S for long-length uniform canals because it becomes parallel to the energy grade line. P (m) = wetted perimeter of the canal. This is the total length at the bottom (canal bed) and the two sides of the canal up to the water surface level. R (m) = hydraulic radius. R = A/P.

In hydraulics, the term *velocity head* is frequently used and is denoted as follows:

$$\text{Velocity head} = \frac{V^2}{2g}$$

where V is the flow velocity, and g is acceleration due to gravity as discussed in the earlier chapter.

As can be seen from Manning's equation, the flow in an open channel is dependent on its cross-sectional area, shape, longitudinal slope, and roughness. The larger the cross-sectional area or longitudinal slope, the higher the discharge will be. For a given cross-sectional area and wetted perimeter, the shape that results in higher hydraulic radius will convey higher flows. On the other hand, the higher the roughness coefficient or Manning's *n*, the lower the flow will be.

5.3.2 Headrace Canal Design Procedure

The headrace canal design procedure is as follows:

1. First, the type of canal appropriate for given site conditions should be decided.
2. Then, for the selected canal type, a suitable velocity (V) and roughness coefficient should be selected using Table 5.1.
3. The required flow (Q) to be conveyed by the headrace will have been fixed earlier based on river hydrology and installed capacity, and other allowances, such as flushing requirements from the downstream settling basin. Now that both Q and V are known, the required cross-sectional area of the canal "A" can be calculated as follows:

   $$A = Q/V$$

   where the units for Q and V are m^3/s and m/s, respectively. Then the units for area will be m^2.
4. In case a trapezoidal canal is selected, Table 5.2 should be used to fix the canal side slope (Z) based on soil type. Note that in Table 5.2, Z is the ratio of the horizontal length by the vertical height of the canal side wall—that is, for a vertical side wall, z = 0.

   Note that the values for Z in Table 5.2 are minimum ones for depths (cutting or filling) up to 6 m. Thus, small values for Z should not be used as this would result in steeper side slopes leading to potential stability problems. For example, a canal in ordinary gravel can have side slopes Z = 1.5:1 but not 1:1 as the recommended side slope is Z = 1.25:1, or for every 1.25 m of horizontal length, the vertical length should be limited to 1.0 m. Lined canals, such as stone masonry or concrete, can have vertical slopes provided that the wall thickness is sufficient to take the water pressure inside and loads due to soil pressure from outside. As discussed earlier, trapezoidal canals can also be lined using masonry or concrete slabs to minimize seepages. Such lining would be thin (100 mm to 300 mm, depending on depth of water and other site conditions, such as ground water) and need not take up any soil pressure as the slopes would have been selected to be stable on their own. Thus, lined trapezoidal canals can be cost-effective when a large volume of flow needs to be conveyed over long distances. The slope of the canal walls in such cases depends on the type of soil in which they are to be built. For depth//height in excess of 6.0 m, detailed slope stability analysis should be performed.

5. For a given side slope (Z), the optimum canal dimensions can be derived using the following equations:

$$X = 2\sqrt{(1+Z^2)} - 2Z$$

where X is an intermediate parameter used to derive the other parameters B, H, and T below.

$$H = \sqrt{\frac{A}{X+Z}}$$

where H is canal height up to the water level.

$$B = XH$$

where B is canal bed width.

$$T = B + (2HZ)$$

where T is the top width of the canal up to the water surface level.

In the above equations, the units for T, B, and Z are in m. In the case of a rectangular canal, $Z = 0$, which results in $X = 2$.

Thus, $H = \sqrt{\frac{A}{2}}$, and $T = B = 2 \cdot H$. Therefore, for a rectangular canal, hydraulically optimum shape is achieved when the width (B) is twice the height (H). Note that for a rectangular canal, $B = 2H$ is closest to a semicircle, which has the highest hydraulic radius (R) for fixed area (A) and wetted perimeter (P).

If an optimum canal shape is not possible due to site-specific conditions (such as narrow width along a cliff), then either the width or the height should be selected to suit the conditions. Then, the other dimension can be calculated. Note that optimum canal dimensions can be achieved in case there is some flexibility in choosing the canal slope—that is, after the dimensions have been optimized, the corresponding canal slope is calculated using Manning's equation. In case the canal slope is fixed, such as when the headrace alignment traverses through a fixed route, then it may not be feasible to optimize the dimensions, especially in case of trapezoidal canals. Optimum trapezoidal canal dimensions for various side slopes are also given in Table 5.3. Canal hydraulic parameters for various canal shapes corresponding to Figure 5.8 are shown in Table 5.4.

6. The flow in an open canal is stable if the velocity is less than the critical velocity. The critical velocity is calculated as follows:

$$\text{Critical velocity } V_c = \sqrt{\frac{Ag}{T}}.$$

Note that for a rectangular canal, $T = B$, and thus,

$$V_c = \sqrt{Hg}.$$

To ensure stable and uniform flow in a headrace canal, the flow velocity should be limited to 80% of critical velocity—that is, $V = 0.8\ V_c$.

TABLE 5.3
Optimum Trapezoidal Canal Dimensions for Given Cross-Sectional Area and Side Slope

Side Slope	$\frac{H}{\sqrt{A}}$	$\frac{B}{\sqrt{A}}$	$\frac{T}{\sqrt{A}}$	$\frac{P}{\sqrt{A}}$	$\frac{R}{\sqrt{A}}$
0.5:1	0.759	0.938	1.698	2.640	0.379
1:1	0.739	0.612	2.092	2.705	0.370
1.5:1	0.689	0.417	2.483	2.905	0.344
2:1	0.636	0.300	2.844	3.145	0.318
2.5:1	0.589	0.227	3.169	3.395	0.295
3:1	0.549	0.174	3502	3.645	0.275

Note: H, B, T, P, R, and A have been defined earlier while discussing Manning's equation.

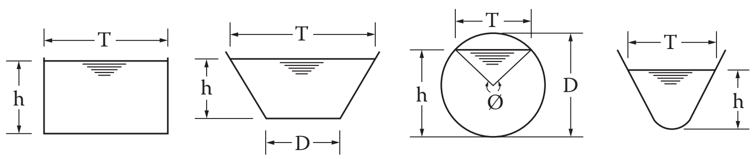

FIGURE 5.8 Various canal geometries.

TABLE 5.4
Canal Hydraulic Parameters for Various Shapes

Parameter	Rectangular	Trapezoidal (z Side Slope)	Circular	Parabolic T-Top Width
Area, A	b·h	(b + zh)h	$\frac{1}{8}(\phi - \sin\phi)D^2$	$\frac{2}{3}Th$
Wetter perimeter, P	b + 2h	$b + 2h\sqrt{1+z^2}$	$\frac{1}{2}\phi D$	$b + \frac{8h^2}{3T}$
Top width of section, T	b = T	b + 2zh	$2\sqrt{h(D-h)}$	T
Hydraulic radius, R	$\frac{bh}{b+2h}$	$\frac{(b+zh)h}{b+2h\sqrt{1+z^2}}$	$\frac{1}{4}\left(1-\frac{\sin\phi}{\phi}\right)D$	$\frac{2T^2h}{3T^2+8h^2}$

7. The wetted perimeter (P) for a trapezoidal canal is calculated using the following equation:

$$P = B + 2H\sqrt{(1+Z^2)}.$$

Note that, for a rectangular canal, Z = 0, and thus, P = B + 2H.

8. Once the area and perimeter is known, the hydraulic radius (R) can be determined as follows:

$$R = A/P$$

9. The required slope (S) of the energy grade line (and thus the canal longitudinal slope for long uniform canals) can now be found from Manning's equation: $S = (nV/R^{0.667})^2$. Now all dimensions required for the construction of the canal are known.

10. The head loss along the canal is the length of the canal times the slope, or canal $H_{loss} = L_c S$ where L_c = the length of the canal section. Thus, the elevation of the canal bed at the downstream end should be lowered by canal H_{loss} from the elevation at the start. Often, the slope S is fixed in the beginning, such as when the canal route has been finalized at the site. In such situations, for the required flow and canal type proposed, velocities should be calculated for various cross-sectional areas (assumed by trail and error). Then the cross-sectional area that results in the flow velocity that is less than the allowable maximum velocity for the design flow should be selected. The dimensions should, of course, also be practical to suit ground conditions.

    With a fixed design flow (Q), ground slope (S), Manning's roughness coefficient *n* based on the canal type considered, an appropriate canal side slope (Z) should be chosen. Then either the bed width (B) or canal height (H) should be selected, and the other dimensions calculated using Manning's equation rewritten in terms of side slope, canal bed width, and height as follows:

$$Q = \frac{(BH + ZH^2)^{5/3}\sqrt{S}}{n[B + 2H\sqrt{(1 + Z^2)}]^{2/3}}.$$

    Note that the above equation needs to be solved for B or H by trial and error. From Table 5.1, the velocity for the canal type considered should be checked to ensure that it is within the allowable limit. Furthermore, as mentioned earlier, the velocity should be checked to ensure that it is less than 80% of the critical velocity.

11. Finally, the size of the largest particle that can be transported along the canal should be calculated: A simplified version of Shield's equation as follows can be used for this.

$$d = 11\ RS$$

    where d = the maximum size of particle transported in a canal in m, R is the hydraulic radius in m, and S is the canal bed slope.

    Any particle of less than size d calculated above will be carried along the canal by the flow whereas larger particles will be deposited along the canal bed. Thus, the required transport capacity of the canal designed should be verified based on its location as well as the particle size to be settled along the gravel trap or the settling basin. It should be ensured that there will be no deposition of sediment along the canal bed.

12. Once the size of the canal for a given design flow has been determined, some freeboard or free space above the design water level should be allowed for. Such freeboards are required for the flowing reasons:

    - There may be some variation in the canal dimensions due to slight deviations in construction, or the roughness may vary by some percentage from the estimates.
    - Some additional flows may enter the headrace canal, such as when the gates upstream are opened to higher depths than required.
    - Large boulders may fall in the canal, and they would raise the water level locally.

    The general rule for freeboard allowance in hydropower plants are as follows:

    - 300 mm for design flows less than 500 1/s. Sometimes, for smaller flows, freeboard is also limited to half the design water depth (0.5 H).
    - 400 mm for design flows from 500 1/s to 1000 1/s.

For larger flows, freeboard should be decided based on detailed risk analysis and cost repercussions for the site conditions. For example, along the stable reach of the canal where some overflow will not cause stability problems, a smaller freeboard can be acceptable. On the other hand, along unstable terrain a larger freeboard will be required.

13. During floods, if larger flows can enter the headrace canal, then this stretch of the canal should be able to accommodate such flows. If possible, the flood flows should be accommodated in the canal using not more than 50% of the freeboard.
14. The design of the headrace canal is an iterative process. Coming up with an optimum design requires trial and error with various canal types and dimensions. Where long lengths are involved, to keep costs down, different types of canals may be required even in the same hydropower project to suit the ground conditions.

    From a construction perspective, a canal width of less than 300 mm should be avoided. Such canals can be difficult to construct (especially for stone masonry) and can also be easily blocked. Furthermore, it will be difficult to maintain narrow canals—that is, a person with a spade should be able to get into the canal when cleaning is required.

    Various canal shapes and corresponding formula to calculate area, perimeter, top width, and hydraulic radius are shown in Figure 5.8 and Table 5.4.

Example 5.1: Headrace Canal Sizing

Design a stone masonry in cement mortar canal to convey a flow of 460 l/s. A topographical survey indicates that the longitudinal slope along the canal alignment would be 1:1200.

Given:

$Q = 460$ l/s $= 0.46$ m^3/s
$S = 1/1200$
Canal type: stone masonry in cement mortar
$n = 0.020$ for dressed stone masonry (from Table 4.1)

Because 460 l/s is relatively high discharge, try a trapezoidal canal to minimize construction material volume (cement, sand, and stones). From Table 5.2, choose Z = 0.5 (lh/2 v).

Set the bottom width (B) = 0.6 m.

Now use the following form of Manning's equation where only the water depth, H, is unknown:

$$Q = \frac{(BH + ZH^2)^{5/3}\sqrt{S}}{n[B + 2H\sqrt{(1+Z^2)}]^{2/3}}$$

$$0.460 = \frac{(0.60H + 0.5H^2)^{5/3}\sqrt{1/1200}}{0.020[0.60 + 2H\sqrt{(1+0.5^2)}]^{2/3}}$$

By a trial and error method, the above equation is balanced when H = 0.63 m for a flow of 460 l/s.

Therefore, the water depth will be about 0.63 m. Now check that the velocity is less than the maximum allowable velocity of 2.0 m/s from Table 4.1.

$$V = Q/A \text{ or } V = 0.460/(BH + ZH^2) \text{ or } V = 0.460/(0.60\cdot 0.63 + 0.5\cdot 0.63^2) \text{ or}$$
$$V = 0.80 \text{ m/s} < 2.0 \text{ m/s OK.}$$

Now check for critical velocity: $V_c = \sqrt{\frac{Ag}{T}}$ for a trapezoidal canal; recall that T = B + 2HZ = 0.6 + 2·0.63·0.5 = 1.23 m

$$V_c = \sqrt{\frac{(0.60 \cdot 0.63 + 0.5 \cdot 0.63^2) \cdot 9.81}{1.23}} = 2.14 \text{ m/s.}$$

0.8 V_c = 1.72 m/s; thus, the actual velocity of 0.8 m/s is less than the critical velocity.

Thus, the headrace canal of width, B = 0.6 m along with side slopes Z = 0.5 will be suitable. The water depth in the canal will be about 0.63 m.

Allow a freeboard of 0.3 m. Thus, the total canal depth will be 0.63 m + 0.3 m = 0.93 m or say 0.95 m.

Example 5.2: Rectangular Canal Sizing

Calculate the water depth (H) required in case a rectangular headrace canal is designed for the parameters given in Example 5.1, assuming canal width (B) = 0.6 m.

Given:

Q = 460 l/s = 0.46 m^3/s
Canal width, B = 0.6 m
S = 1/1200
Canal type: stone masonry in cement mortar
n = 0.020 for dressed stone masonry

Recall Manning's equation:

$$Q = \frac{1}{n} AR^{2/3} \sqrt{S},$$

which for a rectangular canal can be written as

$$Q = \frac{1}{n} BH \left(\frac{BH}{B + 2H} \right)^{2/3} \sqrt{S}$$

or

$$\frac{1}{0.020} 0.6H \left(\frac{0.6H}{0.6 + 2H} \right)^{2/3} \sqrt{1/1200} = 0.46 \text{ m}^3\text{/s}$$

By trial and error, for H = 1.35 m, the flow Q will be 0.458 m^3/s or 0.46 m^3/s.

Example 5.3: Transport Capacity in Headrace Canal

What is the maximum particle size that the headrace canal in Example 5.2 can carry?

$$\text{Area, } A = B \cdot H = 0.60 \cdot 1.35 = 0.81 \text{ m}^2$$

$$\text{Wetted perimeter, } P = B + 2H = 0.60 + 2 \cdot 1.35 = 3.3 \text{ m}$$

$$\text{Hydraulic radius, } R = \frac{A}{P} = \frac{0.81}{3.3} = 0.245 \text{ m}$$

$$S = 1/1200$$

Recall the equation d = 11 RS where d is the maximum particle size that the flow can carry.

Therefore, $d = 11 \cdot 0.245 \cdot (1/1200) = 0.0024$ m or 2.4 mm.

In this example, the maximum particle size the headrace canal can carry during design flow condition is just over 2 mm. Thus, this headrace canal would be suitable if it is located between the gravel trap and the settling basin, which is designed to settle particles up to 2 mm diameter.

Example 5.4: Optimum Rectangular Headrace Canal

Design an optimum rectangular canal for the parameters given in Examples 5.1 and 5.2.

Note that a different value for the bed width will result in different flow depth (H). Recall that dimensions for a rectangular canal are optimum when B = 2H.

In Example 5.2, the canal cross-sectional area, $A = 0.6 \cdot 1.35 = 0.81$ m.

Because B = 2H, $A = 2H \cdot H = 2H^2$; therefore, $2H^2 = 0.81$ m or H = 0.64 m, and B = 2H = 1.28 m.

Thus, a canal with 0.64 m width and 1.28 m height (up to the water surface level) would be optimum.

Now verify that this canal can accommodate 460 l/s of flow using Manning's equation:

$$Q = \frac{1}{0.020} 1.28 \cdot 0.64 \left(\frac{1.28 \cdot 0.64}{1.28 + 2 \cdot 0.64} \right)^{2/3} \sqrt{1/1200} = 0.55 \text{ m}^3/\text{s}$$

The canal dimensions calculated above can convey 0.55 m^3/s or 550 l/s of flow, which is more than the required flow of 460 l/s. This is because the canal width has now been increased whereas the height has decreased, which results in lower wetted perimeter and thus higher hydraulic radius compared to Example 5.2. Note that R = 0.32 m in this case, and R was 0.245 m in Example 5.2.

The dimensions can be further reduced by trial and error maintaining the B = 2H criteria. By trial and error an optimum headrace canal for the above parameters will have dimensions of B = 1.26 m and H = 0.63 m.

5.4 SPILLWAYS

5.4.1 Location of Spillways

As mentioned earlier, spillways are required in headrace canals to spill excess flows during high river flows and in case of obstruction in the canals. Similarly, spillways are also required at the forebay to spill the entire design flow in case of sudden closure of the turbines at the powerhouse (Figure 5.9).

The excess flows that are discharged via a spillway should be safely diverted into the stream, nearby gully, or other safe areas such that they do not cause any erosion or damage to other structures. Sometimes, this may require the construction of a channel to reach a natural watercourse. Locating spillways close to a gully will save the cost of channel construction.

5.4.2 Spillway Design

Where water is ponding (pool of still water) at a downstream regulator, such as in a forebay, the design of spillways can be based on the weir equation discussed in Chapter 4.

$$Q_{spillway} = C_w L_{spillway} (h_{overtop})^{1.5}$$

FIGURE 5.9 A spillway located at the forebay end wall.

where $Q_{spillway}$ = discharge over the spillway in m^3/s, $L_{spillway}$ = length of the spillway in m, $h_{overtop}$ = head over the spillway in m (i.e., height of water over the spillway), and C_w = a coefficient (similar to weir coefficient), which varies according to the spillway profile. C_w for different weir profiles is shown in Table 4.1 in Chapter 4.

The design procedures are as follows:

- Calculate the flow through the intake during floods as discussed in Chapter 4. The spillway should be sized such that the entire flood flow can be diverted away from the canal. This is because the hydropower plant could be closed during a flood, or there could be an obstruction in the canal.
- Choose a spillway profile and determine C_w.
- Spillway crest level should be placed about 0.05 m above normal canal water level to ensure that part of the design is not spilled. The required length of the spillway should be calculated for the chosen $h_{overtop}$ and flood flow.

Where there is no ponding immediately downstream, such as in the headrace canal, the spillway length calculated using the weir equation should be doubled. This increase in length accounts for the gradual decrease in head over the spillway until the required level is reached at the downstream end of the spillway. In this case, only the excess flow ($Q_{flood} - Q_{design}$) should be accounted for as the portion of the flow below the spillway level will be conveyed downstream. Spillway design calculations are provided in Example 5.5.

Example 5.5: Design of a Headrace Canal and a Spillway

Design a headrace canal to convey a flow of 285 l/s. Site conditions indicate that the canal would be stable if stone masonry in mud mortar is used. The expected flow through the intake during a 20-year return flood is about 480 l/s. Design an adequate spillway along the headrace canal assuming no pondage immediately downstream.

Design procedure:

Canal type: stone masonry in mud mortar
$Q = 0.285\ m^3/s$
From Table 5.1:

Roughness coefficient, $n = 0.035$

Choose $V = 1.0\ m/s$

From Table 5.1, for gravelly earth, select side slope, $Z = 0.50$ (1h/2v).
Cross-sectional area,

$$A = 0.285/1.0 = 0.285\ m^2$$

$$X = 2\sqrt{1+Z^2} - 2Z$$
$$X = 2\sqrt{(1+0.5^2)} - 2\cdot 0.50$$
$$X = 1.236$$

Calculate the water depth in the canal, H:

$$H = \sqrt{\frac{A}{(X+Z)}}$$
$$H = \sqrt{\frac{0.285}{(1.236+0.5)}}$$
$$H = 0.405\ m$$

Calculate the bed width,

$$B = HX$$
$$B = 0.405\cdot 1.236$$
$$B = 0.50\ m$$

Calculate the top width up to the design water level, T:

$$T = B + (2HZ)$$
$$T = 0.50 + (2\cdot 0.405\cdot 0.5)$$
$$T = 0.905\ m$$

Check if $V < 0.8\ V_c$

$$V_c = \sqrt{\frac{Ag}{T}}$$

$$V_c = 1.76\ m/s$$

$$0.8\ V_c = 1.41\ m/s > V = 1.0\ m/s\ \text{OK}$$

Calculate the wetted perimeter, P:

$$P = B + 2H\sqrt{(1+Z^2)}$$

Or

$$P = 0.50 + 2 \cdot 0.405\sqrt{(1+0.5^2)}$$
$$P = 1.406 \text{ m}$$

Calculate the hydraulic radius, R:

R = A/P = 0285/1.406 = 0.230 m

Calculate the required canal bed slope, S:

$$S = \sqrt{\left(\frac{nV}{R^{0.667}}\right)^2}$$

Or

$$S = \sqrt{\left(\frac{0.035 \cdot 1}{0.23^{0.667}}\right)^2}$$

S = 0.0103 or 1:97 (i.e., 1 m of drop in 97 m of horizontal canal length)
Finally, allow 300 mm of freeboard. The canal dimensions can be seen in Figure 5.10.
Check the flow depth for maximum flood flow in the canal.

$$Q = \frac{(BH + ZH^2)^{\frac{5}{3}}\sqrt{S}}{n[B + 2H\sqrt{1+Z^2}]^{\frac{2}{3}}}$$

$$0.480 = \frac{(0.5H + 0.5^2)^{5/3}\sqrt{0.0103}}{0.035[0.5 + 2H\sqrt{(1+0.5^2)}]^{2/3}}$$

By the trial-and-error method, the above equation is balanced when H = 0.55 m. Therefore, the flood flow occupies 50% of the freeboard, and the head on the spillway (hovertop) will be 100 mm.

Check the size of particle that will settle in the canal at a velocity of 1.0 m/s.

$$\begin{aligned} D &= 11 \text{ RS} \\ &= 11 \cdot 0.203 \cdot 0.0103 \\ &= 23 \text{ mm} \end{aligned}$$

Thus, particles larger than 23 mm would settle in this headrace canal. Therefore, to avoid deposition upstream of the settling basin, the gravel trap must be designed to remove all particles greater than 23 mm.

5.4.3 Design of Spillway

Note that two conditions need to be checked as follows:

1. The spillway must be able to convey the entire flood flow of 480 l/s in case the headrace canal downstream gets obstructed (ponding case).
2. The spillway should be able to spill the excess flow (480 l/s − 285 l/s) when there is no obstruction downstream.

The calculated maximum spillway length should then be used in the design.

Calculations
Choose a broad-crested weir with round edges profile, so $C_w = 1.6$
Case 1:

$Q_{spillway} = 480$ l/s
$h_{overtop} = 100$ mm calculated earlier.

Now calculate the length of the spillway,

$$L_{spillway} = Q_{spillway}/C_w \cdot (h_{overtop})^{1.5}$$
$$L_{spillway} = 0.480/1.6 \cdot (0.1)^{1.5} = 9.5\,\text{m}$$

Case 2:

$$Q_{spillway} = 480 - 285 = 0.1951/\text{s}$$
$$L_{spillway} = 2Q_{spillway}/C_w \cdot (h_{overtop})^{1.5}$$
$$L_{spillway} = 2 \cdot 0.195/1.6 \cdot (0.1)^{1.5} = 7.7\,\text{m}$$

Therefore, a spillway length of 9.5 m is required for the above canal (Case 1).

5.5 HEADRACE PIPE

5.5.1 General

Pipes may be required along the headrace alignment where slopes are unstable and where landslides may occur. Although masonry and concrete canals can minimize seepage-induced landslides, they are rigid structures and in the event of slope failures, such canals can be swept away. These canals will also crack if there are slope movements. Where soil instability problems are expected, flexible pipes may be an appropriate solution provided that the required pipe length is not too long. Another case for the use of flexible pipes is when the entire hillside is slowly sliding (i.e., mass movement is occurring) and part of the headrace alignment needs to traverse over it.

5.5.2 Design Criteria

The design criteria for headrace pipes are similar to those of headrace canals. Specifically, the design should address the following issues:

- The pipe diameter should be such that for the ground slope of the alignment, it should be able to convey the design flow. If there is a possibility of flood flows entering into the pipe, provisions should be made for spilling such excess flows.

- The inlet to each section of headrace pipe should be protected with a trash rack so that debris does not get in and block the pipe. The spacing of the trash rack bars should be no more than one third of the pipe diameter.
- Where a section of headrace pipe ends in an unlined canal, a masonry transition structure is recommended to avoid scour by the high velocity flow coming out of the pipe.
- Headrace pipes are efficient when they are flowing full, but if the head on the pipe exceeds the rated pipe head (i.e., allowable head on the pipe) break pressure tanks need to be provided. Such tanks dissipate the head over the pipe and avoid the need to use a higher pipe rating (i.e., pipes with thick walls). Break pressure tanks should be provided with lockable covers, so that debris cannot get in and block the pipe.
- As far as possible, the pipe alignment should be such that it is always sloping downhill. This ensures that there is always a positive head over the pipe, and the risk of it being blocked is also reduced.
- If there is a need for inverted siphons (or the pipe needs to go uphill for some length due to the ground profile), air release valves should be provided at high points along the alignment. Similarly, flush-out valves should also be provided at low points to flush sediment from the pipes and hence prevent them from being clogged.

Note that PVC and HDPE pipes should always be buried. A minimum buried depth of 1 m with sieved soil 150 mm to 300 mm around the pipe is recommended. The use of sieved soil ensures that the pipe is not punctured by pointed rocks during compaction, distributes the loads evenly, and prevents future differential settlements above the pipe. The 1 m depth minimizes the overburden loads over the pipe, such as when people or cattle walk over it. Also, in areas where freezing is expected during midwinter, 1 m is usually sufficient to be below the frost line.

At inlet and outlet sections of a headrace pipe, it is recommended to provide inlet and outlet structures of stone masonry or concrete.

5.5.3 Design Procedure

The design procedure (i.e., selection of an appropriate pipe diameter) for a headrace pipe is as follows:

1. Choose a standard pipe size based on what is available locally, such that the velocity V is less than 3 m/s (to minimize wall abrasion and to avoid excessive head loss) and greater than 0.6 m/s (to avoid fine sediment being deposited in the pipe). In general, for HDPE pipes, a velocity of 2.5 m/s to 3.0 m/s can be economical.
2. Calculate the actual velocity:

$$V = 4Q/\Pi d^2$$

   where V is velocity in m/s, Q is design flow in m^3/s, and d is the pipe internal diameter in m.
3. At the entrance of the headrace pipe, set the submergence head as follows:

$$h_s = 1.5V^2/2g$$

   where h_s is the submergence head or the vertical distance from the water surface level to the crown of the pipe or the head from the crown of the pipe. If the submergence head is less than required, then the pipe will not be able to convey the design flow (Q) because air will be drawn into it. Based on Figure 5.11a and the pipe arrangement at the inlet select $K_{entrance}$.
4. Calculate the head loss in the pipe length based on the inlet, wall friction, bends, valves, and exit losses as follows:

$$\text{Total head loss} = \text{wall loss} + \text{turbulence losses}$$

The wall losses result from the friction between the flow and the pipe wall. Wall losses are calculated as follows:

First determine the roughness value, k, in mm from Table 5.4. Note that the values of k in this table are based on normal age (5–15 years) or condition.

Then use the Moody chart in Figure 5.10 to find the corresponding friction factor f for the selected pipe material, diameter, and the design flow. The wall loss can now be calculated from the following equation:

$$h_{\text{wall loss}} = f\,(LV^2/d \cdot 2g)$$

In terms of the flow, diameter and length, this equation can also be rewritten as

$$h_{\text{wall loss}} = fLQ^2/12d^5$$

Turbulence losses are calculated as follows:

$$h_{\text{turb loss}} = V_2/2g\,(K_{\text{entrance}} + K_{\text{bend}} + K_{\text{contraction}} + K_{\text{valve}})$$

where head loss coefficients, K, are as shown in Table 5.5.

Note that HDPE pipes can be bent (manually) without causing any damage if the bend radius is at least 50 times the pipe diameter. This should be done wherever possible, because

a. it avoids the need for mitered bends
b. it avoids the need for anchor blocks to restrain bend forces
c. at such large radius, K_{bend} becomes negligible.

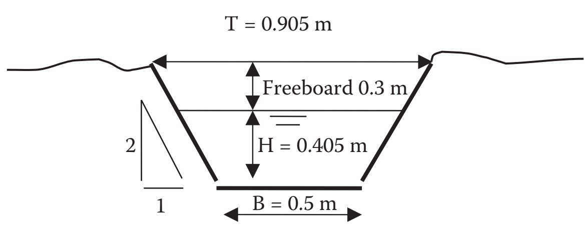

FIGURE 5.10 Headrace canal dimensions for Example 5.5.

TABLE 5.5
Roughness Values for Different Types of Pipes

Pipe Material	Roughness, k (mm)
Smooth pipes, HDPE (heat welded at site), PVC or glass fiber	0.06
Mild steel	
Uncoated	0.10
Galvanized	0.15
Concrete	0.15

Source: A. Harvey et al., *Micro-Hydro Design Manual: A Guide to Small Scale Water Power Schemes*, ITDG Publishing, London, 1993.

Where a long radius bend is not possible, a sharper bend is required, and the value of K_{bend} should be taken from Table 5.5. Mitered bends are normally be used for steel and HDPE pipelines. These are fabricated by cutting the pipe at an angle (maximum 15°) and then welding the ends together to create a bend of up to 30°. For bends of more than 30°, two or more mitered joints are required.

5. Check if the total head loss for the design flow is less than the loss in head due to the pipe gradient (S) and that the pipe profile is below the hydraulic grade line everywhere. If not, repeat the calculation with larger pipe diameter.
6. Determine the water level at the control structure at the end of the pipe, such as the break pressure tank, gravel trap, or the settling basin. Allow 10% margin by assuming that the

Entrance profile

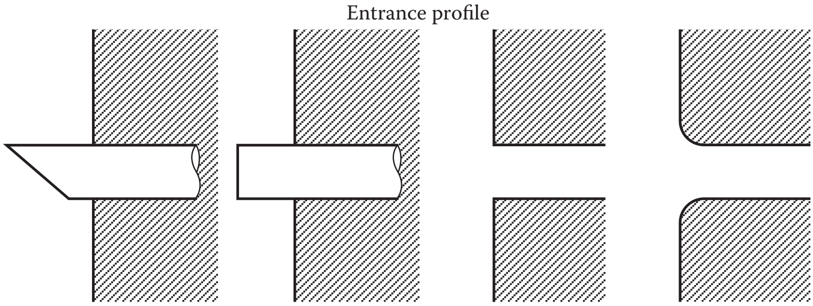

$K_{entrance}$	1	0.8	0.5	0.2

(a)

Bend profile

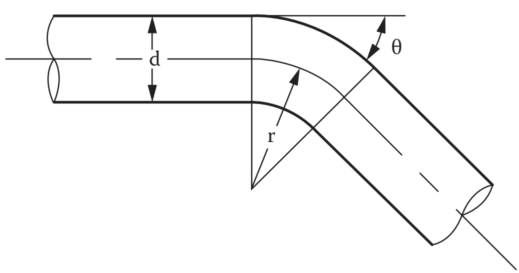

r/d	1	2	3	4	MITERED*
K_{bend} (θ = 20°)	0.20	0.15	0.12	0.10	0.10
K_{bend} (θ = 45°)	0.40	0.30	0.25	0.20	0.22
K_{bend} (θ = 90°)	0.75	0.50	0.25	0.20	0.45

* Mitered bends with r/d = 1.5, maximum 30° per mitered joint.

(b)

FIGURE 5.11 Turbulence losses in pipes. (a) Head loss coefficient for intakes ($K_{entrance}$). (b) Head loss coefficient for intakes (K_{bend}). (From ITDG, *Civil Works Guidelines for Micro Hydropower in Nepal*, BPC Hydroconsult and Intermediate Technology Development Group, Kathmandu, Nepal, 2002.)

total head loss is 10% higher than calculated (i.e., water level is 10% lower than calculated). This is to allow for uncertainties, such as the wall losses being higher than assumed.

7. Repeat the calculations with higher submergence head due to flood flows and calculate the corresponding losses and pipe flow. The excess flow will have to be spilled from a control structure (gravel trap, settling basin, etc.) at the end of the pipe.

Example 5.6: Design of a Headrace Pipe

From the topographical survey, the headrace alignment from the settling basin to the forebay needs to be laid on a 1:500 slope to convey a flow 250 l/s. The total pipe length required is 190 m. Estimate the pipe diameter in case of HDPE pipe. Assume that there are no bends along the pipe alignment.

Given:

$Q = 250$ l/s or $0.25\ m^3/s$
$S = 1:500$
Pipe length, $l = 190$ m
Type = HDPE, and thus $k = 0.06$ mm (Table 5.4)

Try $V = 2.5$ m/s.
Then $A = Q/V = 0.25/2.5 = 0.10\ m^2$

The corresponding diameter $D = \sqrt{\dfrac{4Q}{\Pi V}} = \sqrt{\dfrac{4 \cdot 0.25}{\Pi \cdot 2.5}} = 0.36$ m

$k/d = 0.06/360 = 0.00017$ and $1.2\ Q/D = 0.83$, and from the Moody chart in Figure 5.12, the corresponding friction factor $f = 0.013$.

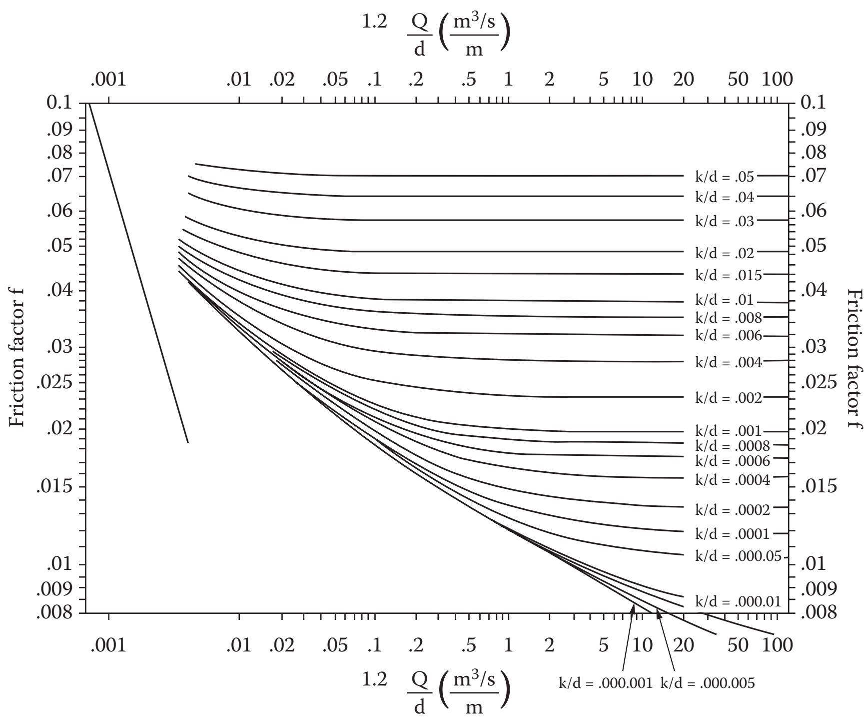

FIGURE 5.12 Moody chart. (From Harvey, A. and Brown, A. *Micro-Hydro Design Manual: A Guide to Small-Scale Water Power Schemes*, ITDG Publishing, London, 1993.)

$$h_{wall\ loss} = f\frac{lV^2}{2g} = 0.013\frac{190 \cdot 2.5^2}{2 \cdot 9.81} = 0.787\ \text{m or say } 0.79\ \text{m}$$

Thus, a HDPE pipe of internal diameter 360 mm will result in a head loss of 0.79 m. Therefore, the pipe will have to be laid on a ground slope of 0.79/190 = 0.0041 or ~1:240 slope, which is much steeper than the 1:500 slope available. Thus, a larger pipe diameter will be required.

Thus, try a larger diameter in proportion to the square root of head loss ratio of $\left(\frac{500}{240}\right)^{0.5} = 1.44$ or D = $1.44 \cdot 0.36$ = 0.52 m.

With a 520 mm internal diameter HDPE pipe, the flow velocity will be 1.18 m/s, and the friction factor f will be 0.0125, resulting in a head loss of 0.323 m, which corresponds to a 1:588 slope, which is slightly milder than the required slope of 1:500. Thus, a slightly smaller pipe diameter will result in the required head loss of 0.38 m, which corresponds to 1:500 slope for a pipe length of 190 m (i.e., 190/500 = 0.38). By trial and error, the required pipe diameter comes out to be 0.505 m or 505 mm when only friction losses along the pipe length are considered.

Because HDPE pipes come in discrete diameters, 505 mm diameter pipe may not be available in the market. In this case, the designer should consult with the manufacturers (or review their catalogues) and select the closest diameter that is above 505 mm, for example, 510 mm or 520 mm. Also note that if there are bends along the alignment, these should be accounted for, and thus the head loss would be higher, or a larger pipe diameter would be required to come up with similar head loss.

Example 5.7: Water Levels Upstream and Downstream of Headrace Pipe

In Example 5.4, if the design water level at the settling basin is 1235 m above mean sea level (amsl), what would be the design water level in the forebay? Suggest the level at which the headrace pipe should be placed in the settling basin. Assume HDPE pipe with an internal diameter of 505 mm is available in the market.

Note that there will be some head loss as the flow enters from the settling basin to the forebay. Assume that the pipe is flushed to the wall at the settling basin. Thus, $K_{entrance}$ = 0.5 (Table 4.5).

$$V = \frac{Q}{A} = \frac{4Q}{\Pi D^2} = \frac{4 \cdot 0.250}{\Pi \cdot 0.505^2} = 1.25\ \text{m/s}$$

$$\text{Entrance loss} = \frac{K_{entrance} \cdot V^2}{2g} = \frac{0.5 \cdot 1.25^2}{2 \cdot 9.81} = 0.0398\ \text{m or say } 0.04\ \text{m}$$

Friction loss along the pipe length from Example 5.5 above = 0.38 m.

Finally, as the flow in the headrace pipe enters the forebay, there will be some exit loss. The maximum loss, assuming that the velocity in the forebay is negligible, will be as follows:

$$\text{Exit loss} = \frac{V^2}{2g} = \frac{1.25^2}{2 \cdot 9.81} = 0.08\ \text{m;}$$

this exit loss results as the flow velocity in the pipe becomes almost nil in the forebay.

Therefore, total loss will be entrance loss + friction loss + exit loss or 0.04 m + 0.38 m + 0.08 m = 0.50 m. Thus, the water level at the forebay will be 0.5 m below that of the settling basin or at 1235 m – 0.5 m = 1234.5 m.

The headrace pipe should be well below the settling basin water surface level to ensure that there is no air entrainment during design flow condition. Recall that the minimum submergence head is given by

$$h_{submergence} = \frac{1.5\,V^2}{2g} = \frac{1.5 \cdot 1.25^2}{2 \cdot 9.81} = 0.12 \text{ m}$$

Thus, the headrace pipe (the crown or the top level) should be at least 0.12 m or 120 mm below the settling basin water surface level. This corresponds to an elevation of 1235 m – 0.12 m = 1234.88 m or lower. Note that a larger submergence depth is not detrimental in a headrace pipe if the downstream outlet level is fixed (i.e., the total head difference is fixed), but if the depth is less, it will not be possible to convey the required design flow. Furthermore, as discussed earlier, in such conditions air will also enter into the pipe causing local surges.

EXERCISES

1. Design a rectangular stone masonry in a cement mortar (1:4) headrace canal to convey a flow of 450 l/s to the gravel trap, which is 100 m downstream. The maximum flow into the intake during design flood is estimated at 1100 l/s. The average ground slope up to the gravel trap is 1:200. Design an adequate spillway along the headrace canal assuming no pondage immediately downstream. What is the largest particle size that the headrace canal can transport up to the gravel trap? What should be the minimum spacing of the coarse trash rack at the intake?
2. For Question 1 above, design a trapezoidal canal assuming clayey soil. The entire canal alignment will be excavated (on cut).
3. A flow 580 l/s is to be conveyed from the gravel trap to the settling basin, which is 200 m downstream. The water level in the gravel trap will be at 1298.5 m. Design a trapezoidal-shaped stone masonry canal in cement mortar (1:4) to convey the flow from the gravel trap to the settling basin assuming 1:480 ground slope. What will the water level be at the settling basin? What is the largest particle size that the headrace canal can transport up to the settling basin?
4. The normal water level at the weir is 1300 m, and at the gravel trap 150 m downstream it is 1298.5 m. The required design discharge up to the gravel trap is 300 l/s. What HDPE pipe diameter would you recommend to convey this design flow? Neglect minor losses.
5. In the above Question 4, if the water level during design flood is 1304 m, what would be the flow in the HDPE pipe? Design a spillway at the gravel trap to spill the entire design flood.
6. A rectangular canal has the following properties:
   Type: stone masonry in cement mortar (1:3)
   Width: 1.5 m
   Total height: 1.0 m

   At what bed slope should the canal be constructed to convey a flow of (a) 400 l/s and (b) 800 l/s with 300 mm freeboard?

   If the ground slope is 1:1000, what is the maximum conveyance capacity of the canal (i.e., canal flowing full)? What is the conveyance capacity of the canal if 300 mm is of freeboard is to be provided?

REFERENCES

1. ITDG, *Civil Works Guidelines for Micro Hydropower in Nepal*, BPC Hydroconsult and Intermediate Technology Development Group, Kathmandu, Nepal, 2002.
2. Harvey, A. and Brown, A., *Micro-Hydro Design Manual: A Guide to Small-Scale Water Power Schemes*, ITDG Publishing, London, 1993.
3. Indian Standard (IS) 10430:2000.

6 Gravel Trap, Settling Basin, and Forebay

6.1 OVERVIEW

Depending on the geology, rainfall, and hydrology in the catchment area, all rivers will carry some quantity of sediment downstream. Based on the catchment characteristics, the sediment carried by the river varies both in size and quantity. For example, rivers flowing down the Himalayas along steep slopes carry large boulders during heavy rainfall that occurs during the annual monsoon period. All rivers will carry some fine sediment, especially during the high flow period, such as the rainy season or when there is substantial snow melt during the summer. River flows free from sediment at all times are possible only if the intake is located downstream of a large dam (which will have settled such sediment) or if coming down from the tailrace of an upstream run-of-river hydropower plant with a well-designed (and operating) settling basin.

Unless the flows from the tailrace of an upstream project are to be used for power generation, intakes for run-of-river hydropower plants should be located and designed to limit the amount of sediment entering the waterways system. However, even a well-designed intake cannot entirely eliminate sediment but can minimize their entry into the waterways downstream and prevent entry of boulders and cobbles. As discussed in the earlier chapters, gravel and finer sediments smaller than the clear spacing between the coarse trash rack bars at the intake can enter into the waterways.

Large particles can block the headrace, reduce its capacity, and also require more maintenance work. On the other hand, when suspended sediments are not removed, they can cause severe wear and tear on the turbine runner blades as the flow velocity at the runner is high. Wearing of the runner reduces its efficiency and will eventually lead to its complete failure. In either case, maintenance is necessary, requiring high expenditure in terms of replaced parts, skilled labor-hours, and in loss of power production. There are abundant examples of turbine runners completely destroyed within a few years after installation that either lacked or had a poorly designed settling basin.

The rate of wear of turbine parts due to sediment abrasion is governed by the following factors:

- Concentration of suspended particles
- Hardness of particles
- Size of particles
- Shape of particles
- Resistance of turbine runner (type of alloys used in preparing the runner)
- Turbine head

It is not necessary to exclude all sediment at the settling basin. This is practically impossible and would not be economically viable as well. A small concentration of fine sediment is often permissible as will be discussed later. The design should be such that the size and concentration of sediment passing through the settling basin are within acceptable limits.

6.1.1 Functions of the Structures

When the flow velocity decreases, its sediment transport capacity also decreases causing suspended sediment to settle along the bottom surface. For a constant flow, the velocity decreases when the cross-sectional area increases. Therefore, gravel traps and settling basins are made wider than the headrace canal or pipe.

As the name denotes, the function of the gravel trap is to settle gravel and coarse sediment that enter into the intake along with the incoming flows. Many rivers in the Himalayas will not only carry gravel but also large boulders during monsoon. In other areas, such as the European Alps, most rivers only carry some fine sediment, and there is no gravel movement even during the high flow seasons. In such cases, a gravel trap will not be required—that is, a settling basin alone would suffice. If a gravel trap is not incorporated in hydropower plants that withdraw water from rivers that carry gravel during floods, these will settle along the gentler sections of the headrace or in the settling basin. Gravel deposited along the headrace may require frequent maintenance work, and as mentioned earlier, its conveyance capacity will also be reduced. It will be difficult to flush large gravel that is deposited in the settling basin because it is generally designed to flush finer sediment only.

A settling basin is a water tank or a basin whose function is to settle suspended particles that enter into the waterways of a hydropower plant along with the incoming flows. As mentioned earlier, rivers are never free from sediment, and thus, all run-of-river hydro schemes should have settling basins unless they tap into a tailrace of upstream power plants (with a well-designed and functioning settling basin). For a storage-type power plant, the reservoir upstream of the dam acts as a settling basin.

A forebay is a tank located at the end of the headrace and the beginning of the penstock pipe. The flow in the headrace is either open channel (atmospheric) or low pressure, and that in the penstock will be fully pressurized. A transitional tank will be required to convert the open-channel or low-pressure flow into full-pressure flow. The forebay is such a structure that allows for the transition from open-channel to pressure-flow conditions. Other functions of the forebay are the following:

- To provide the required submergence flow depth into the penstock pipes: Unless there is some minimum water depth above the penstock inlet (called submergence head), the required flow will not pass through it even when this flow volume is continuously coming into the forebay. When submergence head is less than required, less than the design flow will enter into the penstock along with air, and the balance of the incoming flow would spill through the spillway.
- To provide some storage for start up of the turbines: When the turbine valves are opened, the water volume in the forebay will bring the operational system into steady state quickly. As a general rule, a minimum of 15 s of design flow storage volume is provided above the penstock pipe in the forebay.
- To provide escape route for the flows in case of sudden turbine valve closure at the powerhouse: The forebay is the first control structure upstream of the powerhouse from where it will be possible to spill flows when the turbines need to be shut down quickly, such as during emergency conditions.

The water level at the forebay determines the operational head of the hydropower scheme. The head upstream of the forebay does not contribute toward power generation. Thus, as discussed in Chapter 5, the slope along the headrace alignment from the intake to the forebay is fixed such that it is just sufficient to convey the design flow and prevent deposition of sediments.

6.1.2 Location of Structure

The gravel trap and the settling basin should be located as close to the intake as possible. The sooner the gravel and sediment are removed from the incoming flows, the lesser the problems will be further downstream.

Combining the gravel trap, settling basin, and forebay will minimize construction costs. Sometimes, either the gravel trap and the settling basin (Figure 6.1) or the settling basin and the forebay are combined, but the topographic conditions are rarely appropriate to be able to combine all three structures.

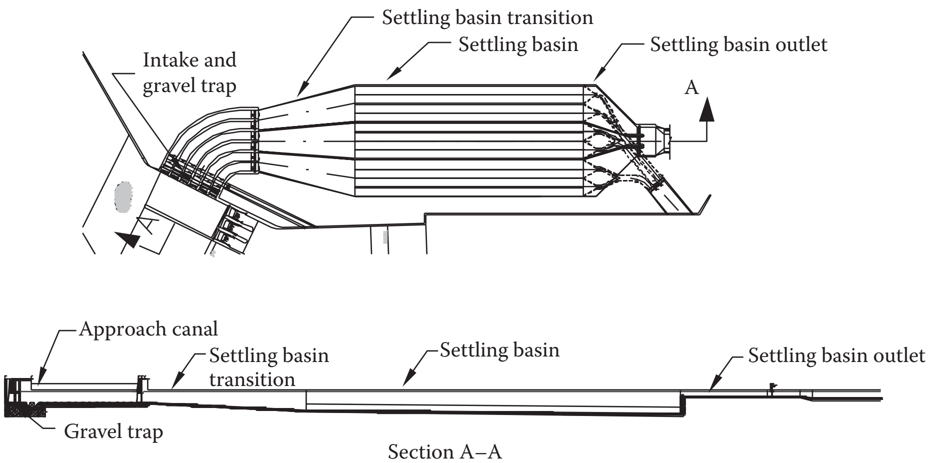

FIGURE 6.1 Plan and section of a combined gravel trap and setting basin.

Selection of an appropriate gravel trap or settling basin site is governed by the following criteria:

- The location should be such that it is possible to flush the gravel or the sediment and spill excess flow from the basin without causing erosion problems or damage to other structures. There must be sufficient head to flush the sediment and drain the basin even during high water level in the river. This flushing head criteria is important because there will be more gravel and sediment in the river during high flows when the river water level will also be high, thus decreasing the available flushing head. Gravel is more abrasive than fine sediments and will cause more wear and tear along the upstream headrace reach. Often, the canal bed and walls upstream of the gravel trap need to be lined with high-strength concrete (or even steel) to prevent abrasion of the canal bed and walls. Therefore, it is important to locate the gravel trap at the first location where gravel can be flushed during high water level in the river.
- The settling basin should be located as close to the headworks as possible, especially if it is separate from the forebay. The earlier the sediment is removed, the less the maintenance of the headrace. Furthermore, the headrace alignment downstream of the settling basin can be gentler (hence less loss in the available head) because the flow will be sediment free. A location close to the intake also allows easy discharge of sediment back to the river. From an operational viewpoint, it will also be easier for the operator/helper to combine work at the intake, such as cleaning the coarse trash rack and flushing of the settling basin.
- There needs to be adequate space to construct the structures as designed. Note that especially the settling basin can be a relatively wide and long structure. Therefore, locating this structure on fairly level ground minimizes excavation costs.

The forebay is located immediately uphill of the transition area where the ground profile changes from level to steep. The following additional factors should be considered before deciding whether a site is suitable for a forebay:

- It should be possible to spill the entire design flow from the forebay without causing erosion or instability problems. Ideally, if this structure can be located close to a gully, it may be possible to safely divert the spillway flows into it. In the worst case, a pipe parallel to the penstock may be required to discharge the spill the flow into the river or the tailrace.
- Similar to the settling basin, there needs to be adequate space to construct this structure as designed. However, the forebay is usually smaller in size.

TABLE 6.1
Coefficients C and n for Himalayan Region to Calculate Sediment Transport Capacity

Catchment Elevation (amsl)	C	n
70 to 2000 m	1.02	0.052
2000 to 4000 m	1.15	0.039
4000 to 6000 m	1.28	0.031

6.2 SEDIMENT TRANSPORT CAPACITY OF RIVER

The transport capacity of a stream flow depends mainly on the nature of the river basin and rainfall characteristics. The catchment characteristics, such as type of soil, presence of vegetation, and presence of landslides influence the type of sediments carried by the river. The geological condition will define the mineral composition of the sediments. The intensity, duration, and chemical composition of rainfall will also affect the quantity and quality of sediment carried by the river.

A simple transport capacity estimate can be obtained by using the following empirical relationship:

$$T = C(AR)^n$$

where T = sediment transported by river flow, A = drainage area in km^2, R = mean rainfall in the catchment area in mm, C = coefficient of drainage area, and n = coefficient of rainfall characteristics.

Table 6.1 presents typical values for C and n in the Himalayan region. Note that these coefficients will be different in other regions.

6.3 THEORY OF SEDIMENTATION

Stokes' law describes how a particle will fall in still water. The velocity of falling particle increases until the viscous drag force is balanced by its weight, and thereafter, it falls with a uniform velocity. This velocity is called terminal velocity or settling velocity. This velocity depends upon different factors, such as temperature, the Reynolds number, density, and shape of particle [1].

6.3.1 Stokes Law

Consider a particle of diameter d and specific gravity ρ_p. Let the specific gravity of water be ρ, and acceleration due to gravity be g. If a particle is suspended in water, it initially has two forces acting upon it:

a. Force of gravity:

$$Fp = \rho_p gVp.$$

b. The buoyant force is quantified by Archimedes principle as

$$F_b = \rho_w gVp$$

here Vp = volume of particle.

As the density of the particle differs from that of the water, a net force is exerted, and the particle is accelerated in the direction of the force:

$$F_{net} = F_p - F_b = F(\rho_p - \rho_w)gVp.$$

This net force becomes the driving force and will initiate the motion of the particle. Once the motion has been initiated, a third force is created due to viscosity of water. This force, called the *drag force* is

$$F_{net} = \frac{C_D A_p \rho_w w^2}{2}$$

where C_D = drag coefficient, which depends on the Reynolds number and temperature. A_p = projected area of the particle. w = velocity of falling particle. Note that the unit for the drag force is Newton (n).

Because the drag force acts in the opposite direction to the driving force and increases as the square of the velocity, acceleration occurs at a decreasing rate until a steady velocity is reached at a point at which the drag force equals the driving force:

$$(\rho_p - \rho_w) g Vp = \frac{C_D A_p \rho_w w^2}{2}.$$

For spherical particles,

$$V_p = \frac{\pi d^3}{6} \quad \text{and} \quad A_p = \frac{\pi d^2}{4}.$$

Thus, $w^2 = \frac{4g(\rho_p - \rho_w)}{3C_D \rho_w} d.$

Expressions for C_D change with characteristics of different flow regimes. For laminar, transition, and turbulent flow, the values of C_D are the following:

$$C_D = \frac{24}{R_e} \text{ (Laminar)}$$

$$C_D = \frac{24}{R_e} + \frac{3}{R_e^{1/2}} + 0.34 \text{ (Transition)}$$

$$C_D = 24 \text{ (Turbulent)}$$

where R_e is the Reynolds number [2]:

$$R_e = \frac{\rho_w w d}{\mu}$$

A Reynolds number less than 1.0 indicate laminar flow, and values greater than 10 indicate turbulent flow. Intermediate values indicate transitional flow.

For laminar flow, terminal settling velocity equation becomes the following:

$$w = \frac{(\rho_p - \rho_w) g}{18 \mu} d^2 \tag{6.1}$$

This equation is known as the *Stokes equation*.

6.3.2 Settling Velocity

As described above, the settling velocity is a function of the particle's Reynolds number. Generally, for small particles (laminar approximation), it can be calculated with Stokes' law. For larger particles (turbulent particle Reynolds numbers apply), fall velocity is calculated with the turbulent drag law. Dietrich compiled a large amount of published data to which he empirically fitted settling velocity curves. Ferguson and Church (2006) analytically combined the expressions for Stokes flow and a turbulent drag law into a single equation that works for all sizes of sediment and successfully tested them against the data of Dietrich [3]. Their equation is

$$w_s = \frac{RgD^2}{C_1\nu + (0.75C_2RgD^3)^{(0.5)}}$$

where w_s is the sediment settling velocity, g is acceleration due to gravity, and D is mean sediment diameter.

ν is the kinematic viscosity of water, which is approximately $1.0 \cdot 10^{-6}$ m²/s for water at 20°C.

C_1 and C_2 are constants related to the shape and smoothness of the grains.

Constant	Smooth Spheres	Natural Grains: Sieve Diameters	Natural Grains: Nominal Diameters	Limit for Ultra-Angular Grains
C_1	18	18	20	24
C_2	0.4	1.0	1.1	1.2

The expression for fall velocity can be simplified so that it can be solved only in terms of D. We use the sieve diameters for natural grains, g = 9.8, and values given above for ν and R. From these parameters, the fall velocity is given by the expression:

$$w_s = \frac{16.17D^2}{1.8 \cdot 10^{-5} + (12.1275D^3)^{(0.5)}}$$

6.3.3 Temperature Correction

The settling velocity calculated above is standardized at temperature of 10°C. For other temperatures, the following relationship can be used to estimate the settling velocity:

$$V_t = V_s \frac{3T + 70}{100}$$

where V_s is settling velocity at 10°C, and V_t is velocity of particle other than 10°C.

6.3.4 Turbulence in Settling Basin

Due to flow velocity in the settling basin, the particle that has already settled in the basin tends to rise upward. Due to this, the settling efficiency decreases. The shear velocity accounts for such phenomenon. This effect is more predominant in shallow basins where the depth of flow is low compared to the width of basin. Figure 6.2 shows this condition.

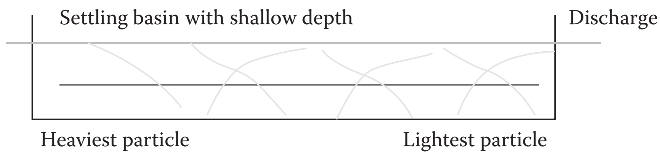

FIGURE 6.2 Basin with shallow depth.

The uplift velocity of flow can be estimated by using the empirical formula

$$u_* = \frac{nV\sqrt{g}}{R^{1/6}} \tag{6.2}$$

where u_* is lifting velocity of flow, n = Manning roughness of bed material, V = longitudinal flow velocity, and R = hydraulic mean radius.

6.3.5 Theory of Sediment Transport

The sediment in flowing water can be separated in three parts (Figure 6.3). These are bed load, suspended load, and dissolved load. For flushing of sediments, bed load is the major concern.

6.3.6 Mechanics of Sediment Transport (Tractive Force Theory)

When water flows in a channel, it exerts drag force on the wetted perimeter (channel side walls and bed). This force is called tractive force, shear force, or drag force.

Consider a particle without cohesion (i.e., c = 0), such as sand or gravel in the bed of a channel (Figure 6.4). Let the channel length be L and cross-sectional area be A.

The weight of water in this reach = $\gamma_w \cdot L \cdot A$.

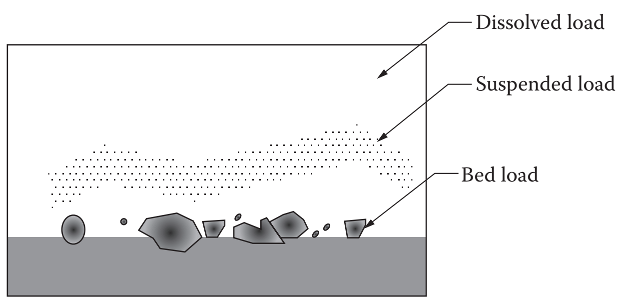

FIGURE 6.3 Various types of sediments transported by river water.

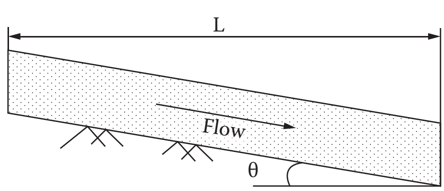

FIGURE 6.4 Forces on column of water.

Horizontal component of this weight = $\gamma_w \cdot L \cdot A \cdot \sin\theta = \gamma_w \cdot L \cdot A \cdot S$, where S is slope of channel, which is very small.

Average tractive force per unit of wetted area = Tractive force/wetted area

$$\tau = \frac{\gamma_w \cdot L \cdot A}{P \cdot L}$$

$\tau = \gamma_w RS$ because A/P = R.

Thus, the average tractive force $\gamma_w RS$.

This force is exerted on the bed particles. As the force increases, at some point, the particle tends to move. The shearing force at this stage is called critical tractive force.

6.3.6.1 Shield's Formula

Shield provided a semitheoretical approach to find the bed movement. According to the theory, the bed particle moved when the drag force exerted by the fluid on the particle is just equal to or greater than the resistance force offered by the particle to its movement.

The drag force is given by

$$F_d = C_D A_p \rho v^2/2 \text{ for spherical particles.}$$

$$F_d = KC_D d_p^2 \rho v^2/2 \text{ for other shaped particles,} \tag{6.3}$$

where K = factor depending on the shape of the particle, C_D = drag coefficient = f_1/R_e, d_p = diameter of the particle, and v = velocity of flow.

The velocity at the boundary of the channel is expressed by the Karman–Prandtl equation:

$$\frac{V_o}{V_*} = f_2\left(\frac{Vd}{\nu}\right) \tag{6.4}$$

$$V_o = f_2 V_* R_e$$

where shear friction velocity = $V_* = \sqrt{\dfrac{\tau_c}{\rho_w}}$,

where ν = kinematic viscosity of flowing water, and R_e = Reynolds number.

Substituting the value of C_d and V_o in Equation 6.3, we have

$$F_d = k\frac{f_1}{R_e} d_p^2 \rho \frac{(f_2 V \cdot R_e)^2}{2}.$$

Or

$$F_d = \frac{kf_1 f_2 \rho}{2} V_*^2 d_p^2.$$

Now, the particle resistance is the function of its net weight and internal friction of particle and boundary

$$Fp = K' \cdot \text{weight of particle}$$

$$\text{Or} \quad F_p = K'(\rho_p - \rho)gd^3$$

$$\text{Or} \quad F_p = K(s-1)\gamma d^3 \tag{6.5}$$

where K = factor depending upon the shape and friction, and s = specific gravity of particle = $\rho_p/\rho w$.

At equilibrium condition, the drag force is equal to the resistance force or $F_d = F_p$

$$\text{Or} \quad Kf_1f_2dp^2\rho V_*^2 R_e/2 = K(s-1)\gamma d^3$$

When all the factors are summed up in one side, the equation becomes

$$\frac{\tau_c}{\gamma_w d(s-1)} = F \cdot R_e.$$

The dimensionless number on the right side is called Shield's entrainment function.

$$F_s = F \cdot R_e$$

Based on experiments, Shield plotted a curve between F and R_e as shown in Figure 6.5.

For d > 6 mm, $F_s = 0.056$; thus,

$$\tau_c = 0.056 \cdot \gamma_w d(s-1).$$

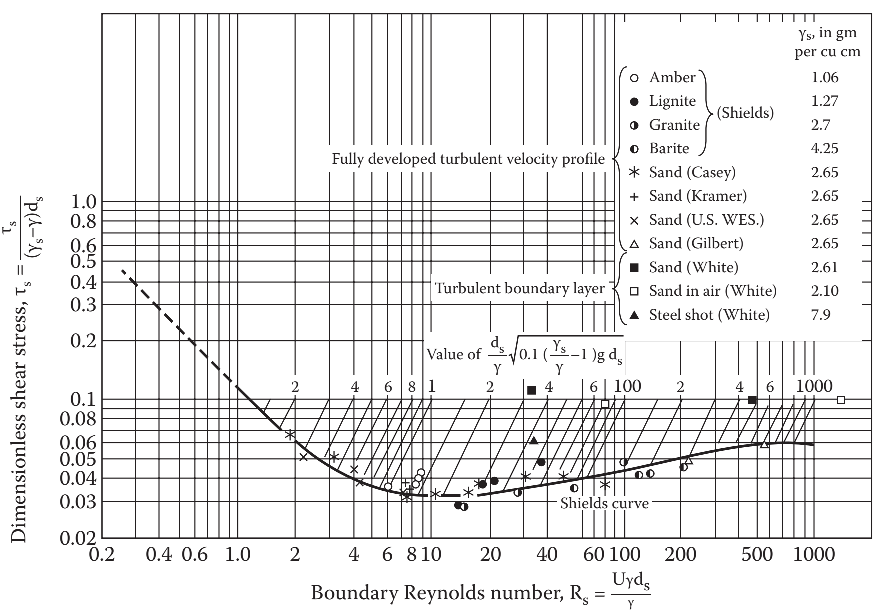

FIGURE 6.5 Shield's curve.

As the average tractive force on bed is given by

$$\tau_o = \gamma_w RS$$

we get

$$\gamma_w RS = 0.056\gamma_w d(s - 1)$$

using s = 2.65, we get

$$d \geq 11\ RS.$$

6.4 GRAVEL TRAP

A gravel trap is required unless, as discussed earlier, the river does not carry such gravel and cobbles during the high flow seasons. In the absence of a gravel trap, the settling basin must be close to the intake and be able to flush relatively larger particles that enter the basin. Gravel traps differ from settling basins in that they handle coarse material that enters near the bed rather than suspended material that needs to be settled. The main design principle for a gravel trap is that the velocity through it should be less than required to move the smallest size of gravel to be removed. The largest size allowed to enter into the intake can be controlled by the spacing of the coarse trash rack bars. In general, gravel traps should settle particles larger than 2 mm diameter. Smaller-sized particles will be settled and removed in the settling basin.

6.4.1 Components of Gravel Trap

A gravel trap consists of a chamber in which the velocity of flow is maintained relatively low so that the particle can settle without much turbulence. A flushing mechanism to flush the settled particles back to the river is also provided. Many times, a spillway is incorporated along the wall of gravel trap to spill excess water. Figure 6.6 shows a typical intake and gravel trap arrangement in

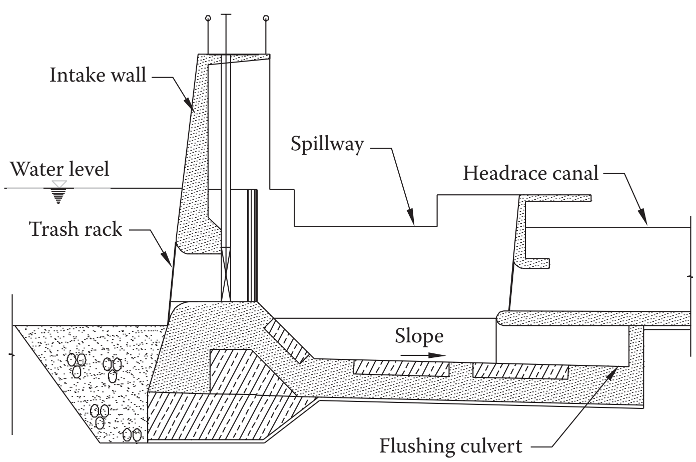

FIGURE 6.6 Gravel trap just after the intake. A spillway is incorporated to spill excess water and maintain water level.

FIGURE 6.7 Large sediments deposited in the gravel trap.

a hydropower plant. Figure 6.7 shows a photograph of a small hydropower gravel trap that is being repaired. Note the size of the stones deposited and the spillway of the gravel trap.

6.4.2 Types of Gravel Trap

Gravel traps can be classified on the basis of their shapes and their location.

a. Rectangular and hopper-type gravel traps:

   A gravel trap can be constructed in a rectangular shape or a hopper shape as shown in Figure 6.8. Due to simplicity of construction and ease of calculations, the rectangular shape is adopted in most of the small hydro plants.

   The hopper shape of the gravel trap helps to flush the sediment more effectively. But the shape is complicated, and hence, more rigorous calculation should be done for such types of gravel trap. Sometimes, a gravel trap is constructed in rectangular shape and triangular stone masonry is constructed on the side of the walls to give the hopper shape.

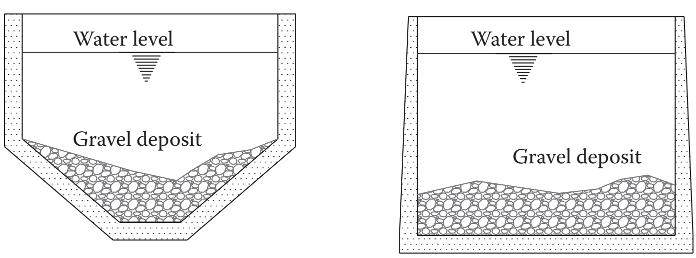

FIGURE 6.8 A hopper-shaped and a rectangular-shaped gravel trap.

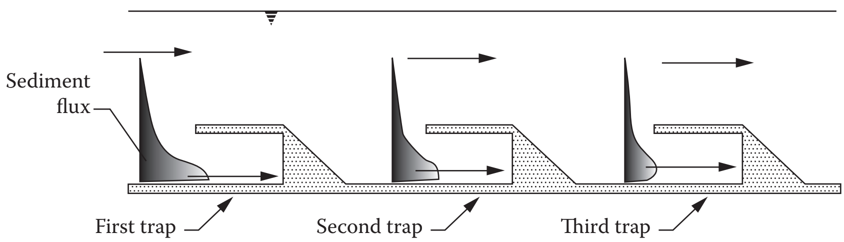

FIGURE 6.9 Gravel trap in series.

b. Single and series gravel trap

When sediment load is heavy, a series of gravel traps can be adopted. Owing to the opposite profile of fluid flow and sediment density, a series gravel trap tends to increase the velocity at the bottom of gravel trap and transport the sediments to the flushing zone more effectively. This concept is shown in Figure 6.9.

6.4.3 Design Criteria of Gravel Trap

The following criteria should be used for the design of the gravel trap [4]:

- To be able to trap particles down to 2 mm diameter, the velocity in the gravel trap should be limited to 0.6 m/s. The critical velocity of flow is given by

$$V_{cr} = a\sqrt{d_{mm}} \tag{6.6}$$

V_{cr} = Critical velocity in m/s
a = coefficient whose value is 0.44 for particle size greater than 1 mm
d = diameter of particle in mm

- If the gravel trap is hopper shaped, the floor slopes should be about 30° (1:1.7). Such an arrangement will facilitate easy flushing of gravel. If it is not possible to construct such a shape, the floor should slope toward the flushing end with a longitudinal slope of 2%–5%.
- The length of the gravel trap is given by

$$L = V \cdot t_{set}$$

where V = velocity of flow, t_{set} = settling time of particle = h/w, h = depth of flow, and w = settling velocity.

- Whenever possible, the length of the gravel trap should also be at least three times the width of the headrace canal or 2 m, whichever is larger. Note that this is a general rule of thumb, but if a significant bed load can enter the intake, then a longer length may be required. Because studies regarding the movement of gravel in rivers are rare (rarer than sediment studies), it is usually difficult to estimate the storage required in a gravel trap. Note that the storage must be provided below the normal flow depth.
- To minimize blockage of the headrace or damage due to abrasion in the headrace, gravel traps should be located as close to the intake as possible.
- The flushing channel of the gravel trap should be at least twice the opening of trash rack at intake to avoid clogging of flushing channel.

Gravel traps can be emptied via flushing gates or by lifting stop logs (i.e., wooden planks). Because gravel enters the intake only during high flows, incorporating stop logs is generally more convenient and economic.

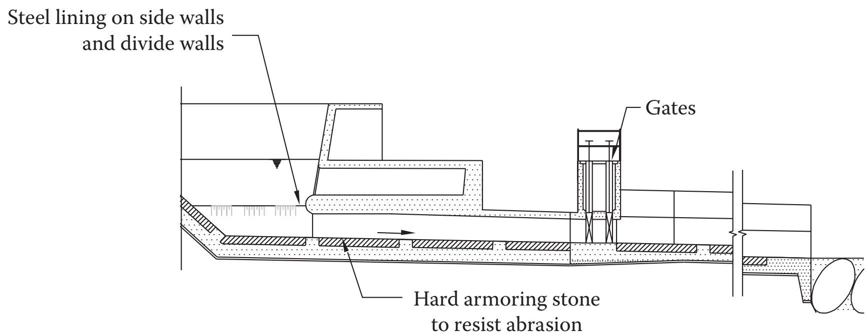

FIGURE 6.10 Gravel trap and flushing protected against abrasion by steel and hard stone lining.

6.4.4 Practical Considerations

As heavy sediments are settled and flushed in the gravel trap, high abrasion on the slab and walls of gravel trap is a common problem. To prevent this, the following methods can be adopted:

- Steel lining
- High-strength concrete for construction
- Adoption of admixture to increase hardness of concrete
- Hard stone armoring as shown in Figure 6.10

6.5 SETTLING BASIN

Suspended sediment that is not settled in the gravel trap is trapped in the settling basin. The basic principle of settling is that the greater the basin surface area and the lower the through velocity, the smaller the particles that can settle. A settling basin has a significantly larger cross-sectional area than the headrace canal, and therefore, the flow velocity is lower, which allows the settling of the suspended materials. The main concept is that as the flow moves from inlet to outlet, the sediments will settle gradually.

A well-designed settling basin will trap most of the suspended sediments, and an undersized settling basin will not trap the lighter particles. Similarly, a shallow settling basin will uplift the settled particle reducing the efficiency of the settling basin. The effect of the size of the settling basin on its efficiency for a given flow is shown in Figure 6.11.

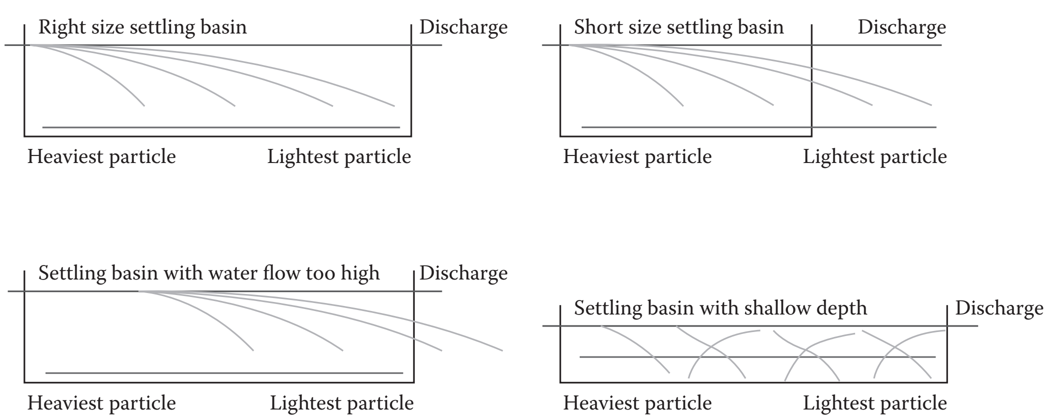

FIGURE 6.11 Different size of settling basin and its effect on settling capacity.

Sedimentation in a settling basin is studied as a two-dimensional problem. However, in reality, the three-dimensional flow field will affect the sedimentation process. Due to a complex flow field, several types of water currents may occur in the sedimentation basin, such as the following:

- Density currents are caused by the weight of the sediment particles, their concentration, and the temperature of the water in the basin.
- Eddy currents are produced by the flow of the water coming into the tank and leaving the tank. The currents can be beneficial in that they promote flocculation of the particles. However, water currents also tend to distribute the flow unevenly throughout the basin, and as a result, particles do not settle out at an even rate. Some of the water current problems can be reduced by good design of the basin. Installation of baffles helps prevent currents from short-circuiting in the basin.

6.5.1 Components of Settling Basin

The settling basin has three distinct zones: the inlet, settling, and outlet zones. These are discussed below.

6.5.1.1 Inlet Zone

This is the initial zone in which the transition from the canal to the settling basin occurs, and there is a gradual expansion in the basin width.

The design of the inlet is important to the efficiency of the basin. For high hydraulic efficiency and effective use of the basin, the inlet should distribute the inflow and suspended sediment over the full cross-sectional area as it reached the settling zone.

Various research data show that horizontal velocity variations across the width of a rectangular tank affect the hydraulic efficiency considerably more than velocity variations in depth. Therefore, attention needs to be given to uniform flow distribution in the horizontal plane. The following methods are used in the inlet zone to achieve a good flow distribution:

- Gradual expansion in the range of 7° to 10° gives a smooth transition. In small schemes, up to 11° of transition (1:5) is used. This will allow an even flow distribution at the beginning of the settling zone. The vertical expansion ratio can be higher at about 1:2 (a = 27°). The smaller angle of transition also allows for lower head loss.

  When the inlet transition cannot be maintained at an angle of 7° to 10° due to space requirements, the inlet transition may be made shorter using guide walls so that the opening angle between the two guide walls is small for separation of flow as can be seen in Figure 6.12. Such guide walls are called tranquilizers. Similarly, the clogging of floating material should be taken into account while designing such tranquilizers.

Other options when using shorter inlet transitions are the following:

- Provide a weir at the beginning of the settling zone
- Provide troughs with slots or orifices in walls or bottom
- Provide baffle walls

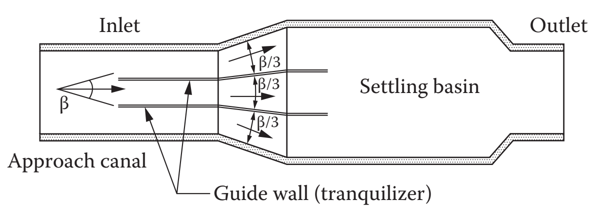

FIGURE 6.12 Inlet transition with tranquilizer.

Note that orifices or baffle walls are often used in water treatment facilities where extremely low velocity is required, but these methods are rarely used in hydropower schemes.

6.5.1.2 Settling Zone

As the sectional area of the flow increases, its velocity gradually decreases, and the suspended particle starts to settle down. This zone of the basin is called the settling zone. The particles are settled, stored, and flushed in this zone. The length of this zone is longer than the inlet or the outlet zones. It should be noted that long, narrow basins perform better than short, wide basins.

Typical aspect ratio of settling basin:

Description	Ratio
Length/breadth (L/B)	4–10
Depth/width (D/B)	1–1.5
Preferred depth of basin (D)	3–5 m

Basin shape can also be improved by subdivision with a longitudinal divide wall because this doubles the L/B ratio for a given basin length. Also the longitudinal divide wall can assist in the operation of the scheme. For example, the sediment in one chamber (sub-basin) can be flushed while the other is in operation, producing half the power output. Without the subdivision, the plant would have to be closed during flushing.

Provision for flushing the stored sediment should be at the end of the settling basin. A floor slope of 1:20 to 1:51 in the settling zone facilitates flushing.

6.5.1.3 Outlet Zone

This forms the transition from the settling zone to the headrace. The transition can be more abrupt than the inlet expansion (i.e., horizontally 1:2 or $\alpha = 26.5°$ as shown in Figure 6.13, and vertically 1:1 as shown in Figure 6.14. Note that if the settling basin is combined with the forebay, then this zone is not necessary—that is, the forebay structure can be directly downstream of the settling zone.

The operating water level of the settling basin is generally controlled at the outlet, sometimes by a weir, which may be designed to operate as submerged in order to conserve head (Figures 6.15 and 6.16).

6.5.1.3.1 Storage Zone

In this zone, the sediments get deposited. The volume required for this zone depends on the sediment concentration of the flow and flushing frequency.

6.5.1.3.2 Flushing Arrangement

Another important component of the settling basin is the flushing arrangement. The flushing arrangement may be the intermittent type or continuous. The flushing arrangement should be designed to carry all the deposited material with minimum disturbance to the flow in as little a time as possible (Figure 6.17).

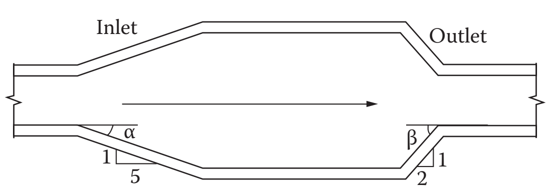

FIGURE 6.13 Expansion and contraction ratio in settling basin.

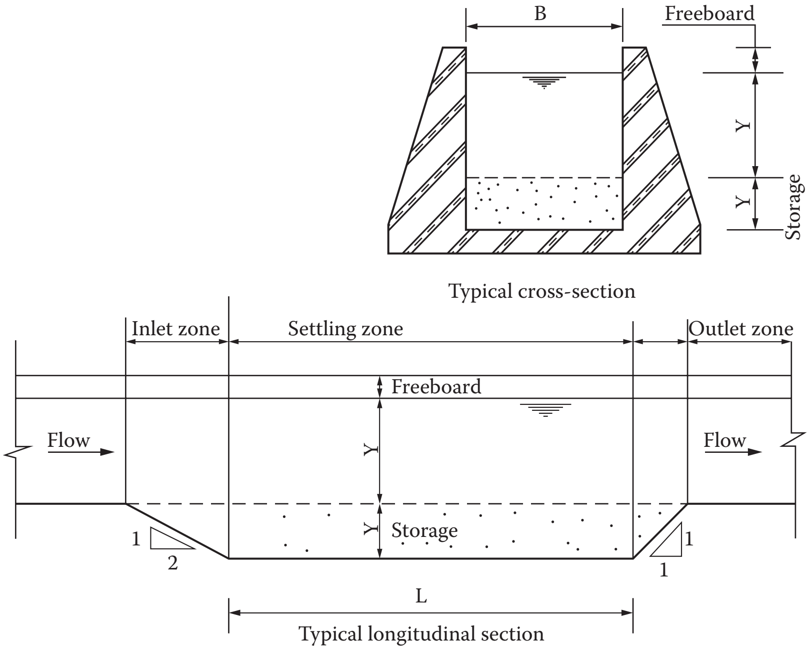

FIGURE 6.14 Typical cross-section and longitudinal section of a settling basin.

FIGURE 6.15 Settling basin inlet and settling zone.

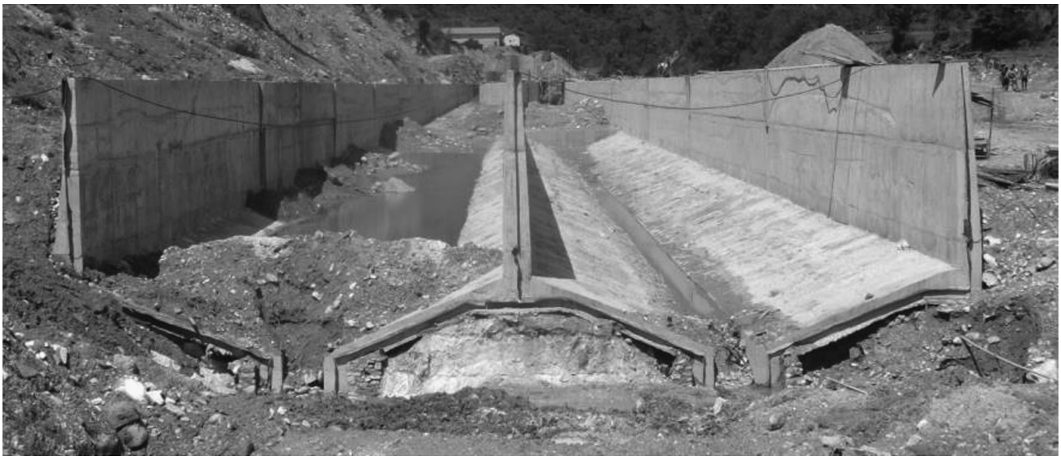

FIGURE 6.16 Settling basin main body during construction.

FIGURE 6.17 Flushing culvert and gates of settling basin (under construction).

6.5.2 Types of Settling Basin

Settling basins can also be classified on the basis of their flushing arrangement as follows:

a. Intermittent flushing
b. Continuous flushing

a. Intermittent Flushing

The settling basin with intermittent flushing operates by letting sediment deposit until the storage volume is filled up. Then, after the water level is reduced and debris deposite, the basin is cleaned using the gravity flushing method. During flushing, water can be stopped or, in the case of multiple chambers, flow into the chamber being flushed when it is stopped, allowing partial power to be generated during flushing (through inflows from other chambers).

b. Continuous Flushing

In continuous flushing, the settling of sediment and flushing of the deposited sediments occur simultaneously. A small volume of water is flushed out along with sediments in this arrangement. Hence 10%–30% higher discharge is abstracted from intake to account for this flushing. Because flushing requirements are more frequent during the high-flow seasons, additional flows would be available in the river.

6.5.3 Selection of Type of Settling Basin

The selection of settling basin type depends upon following factors:

6.5.3.1 Ease of Operation

The continuous-flushing settling basin can work without any human intervention. Hence when headwork lies in remote parts, such a mechanism may be preferred over the intermittent basin.

6.5.3.2 Water Availability

Continuous flushing requires a continuous supply of water for flushing as well. Hence, where water is abundant, such a method may be preferred.

6.5.3.3 Cost of Construction

The cost of construction is the major factor for the choice of settling basin. The following factors should be considered from a financial perspective:

- The continuous flushing arrangement requires a larger approach canal to accommodate extra water for flushing. Furthermore, the conveyance structures from the intake to the settling basin also need to be oversized.
- The intermittent flushing arrangement requires a deeper settling basin to store the sediments. Generally, a hopper-type basin is preferred in intermittent flushing for ease of flushing. Such hopper construction requires a more advanced construction methodology.

6.5.3.4 Power Requirement

The settling basin should provide continuous water to the power plant to produce electricity throughout the day. The intermittent system requires water to be stopped periodically for the flushing operation. Hence, at least two chambers need to be provided in an intermittent system so that at least half the power output can be produced during the flushing operation. On the other hand, with a continuous flushing system, full power can be generated while sediments are being flushed out.

6.5.4 Design Criteria

Continuous flushing mechanisms are not usually incorporated in small hydropower schemes due to the complexity of the design. For larger hydropower plants, continuous flushing mechanisms are often incorporated. Therefore, only the design of intermittent settling basins is discussed hereafter.

6.5.4.1 Settling Capacity

As discussed earlier, the length and width of the basin must be large enough to settle a large percentage of the fine sediment to fall out of suspension and be deposited on the bed. The sediment concentration passing out from the basin should be within acceptable limits. The geometry of the inlet, the width of the basin, and any curvature must be such as to cause minimum turbulence, which will lower the efficiency.

6.5.4.2 Storage Capacity

The basin should be able to store the settled particles for some time unless it is designed for continuous flushing. As discussed earlier, storage capacity depends on the sediment concentration expected in the river flows during high-flow season and how often the basins will be flushed—that is, flushing frequency.

6.5.4.3 Flushing Capacity

The basin should be able to be operated so as to remove the stored particles from it. This is done by opening gates or valves and flushing the sediment along with the incoming flow in the basin. The bed gradient must be steep enough to create velocities capable of removing all the sediment during flushing.

6.5.5 Basic Principles for Design of Settling Basin

The theory behind the design of a settling basin has already been presented earlier. For simplicity and to understand the design principle, the concept of the ideal basin needs to be understood. Such an ideal basin is shown in Figure 6.18. Consider a particle entering the ideal settling basin on the water surface at point X (i.e., the beginning of the settling zone). This particle will have two velocity components; one is the horizontal component due to the momentum of flow, and the second is the vertical component due to its weight.

Let,

L = length of the settling zone (m)
B = width of the settling zone (m)
Y = mean water depth in the settling zone (m), also called hydraulic depth
t = time for particle to travel the length L (s)

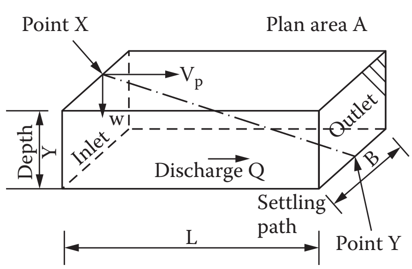

FIGURE 6.18 Ideal settling basin.

V_p = horizontal velocity component of the particle (m/s)
w = vertical velocity component of the particle (ms)—that is, the fall velocity, which was discussed earlier
Q = discharge (m^3/s)

Then the following equations must hold for the particle to reach the end of the settling basin (point Y):

$$y = w\ t \tag{6.7}$$

$$L = V_p\ t \tag{6.8}$$

$$Q = B\ V_p\ y \tag{6.9}$$

Substituting for y, V_p, and t from Equations 6.7 and 6.8 into Equation 6.9 results in

$$Q = BLw$$

$$\text{Or } w = Q/A\ t$$

Therefore, for a given discharge Q, the plan area of the settling basin can theoretically be determined for settling of a particle with fall velocity w. The ratio is also called surface overflow rate (SOR). However, in practice, a larger basin area is required because of the following factors:

- The turbulence of the water in the basin
- Imperfect flow distribution at the entrance
- The need to converge (sometimes curve) the flow toward the exit. Therefore in real basins, the through velocity is limited to reduce turbulence, and the required plan area is about twice the area calculated for an ideal basin

6.5.6 Fall Velocity of Sediment and Particle Size

The fall velocity, w, characterizes the ability of particles of various sizes to settle down under gravity. For a discrete particle, this value depends on its size, density, shape, and temperature of water.

Figure 6.19 shows the fall velocity in water, w, as a function of the particle diameter for reference quartz spheres [5]. This figure can be used to estimate w for the calculations required in the design of the basin. Note that the temperature effect becomes less for larger diameter particles.

In micro hydropower schemes, the settling basin is designed in theory to trap 100% of particles greater than a certain size. The largest particle size that is designed to settle in the basin is called d_{limit}. However, in practice, a certain percentage of such particles will escape the settling basin as is discussed later in this chapter.

A lower proportion of particles smaller than d_{limit} will be trapped. However, the smaller particles passing though the basin will not cause significant abrasion damage to the turbine.

For small schemes, the following procedure is recommended for the selection of d_{limit}:

- Low head schemes, h < 10 m: d_{limit} = 0.2 mm to 0.5 mm
- Medium head schemes, 10 m < h < 100 m: d_{limit} = 0.2 to 0.3 mm
- High head schemes, h > 100 m: d_{limit} = 0.1 to 0.2 mm

where h is the gross head.

The following factors should be used when deciding on the value of d_{limit}:

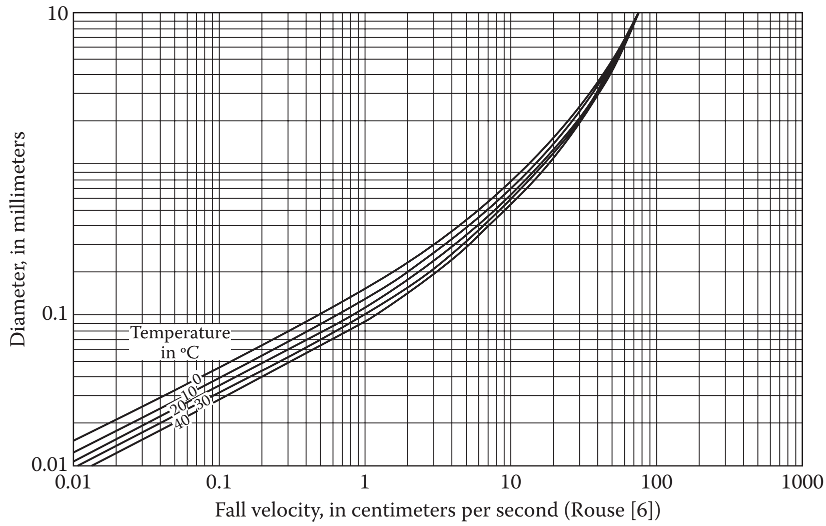

FIGURE 6.19 Fall velocity of quartz sphere in still water.

- If most particles are highly abrasive (quartz sand or minerals), then the lower limiting values should be used. If the particles are softer, less abrasive substances, then the higher limiting values may be acceptable. Hardness values for various particles are given in Figure 6.19. The harder the mineral, the more abrasion is caused on the turbine runner.
- Cross-flow turbines are relatively less sensitive to soft impurities, such as silt and clays. Other types, such as the Francis turbines, are more sensitive to any kind of suspended matter. Pelton turbines fall in the intermediate range.

For example, d_{limit} = 0.2 mm should be selected in a case in which h = 50 m, suspended particles are mostly pure quartz or similar minerals, and a Francis turbine is used.

It should be noted that for larger hydropower projects, the manufacturers provide d_{limit} and acceptable concentration, and the settling basin is sized accordingly (Figure 6.20; Ref. [7]).

10	Diamond
9	Corundum
8	Topaz
7	Quartz
6	Feldspar
5	Apatite
4	Fluorite
3	Calcite
2	Gypsum
1	Talc

FIGURE 6.20 Moh's scale of hardness. (From *Engineering Geology and Rock Engineering: Handbook No. 2*, Norwegian Group for Rock Mechanics, Oslo, 2002.)

6.5.7 Settling Basin Design

The area required for the settling basin and its plan shape are calculated as follows:

1. Using the criteria discussed, determine what the range of the scheme is (i.e., low, medium, or high head) and decide on the corresponding minimum particle size to be settled—that is, d_{limit}.
2. Using Figure 6.19, for the selected d_{limit}, determine the fall velocity, w.
3. Calculate the required basin surface area using the following equation: $A_s = \frac{Q}{(w - u_*)}$

$$u_* = \frac{n\,V\sqrt{g}}{R^{1/6}}$$

   where u_* is uplift velocity, and R is hydraulic mean radius of the flow.
4. With the basin area calculated above, fix either the length, L, or the width, B, according to site conditions and calculate the other dimension such that 4 < L/B < 10.
5. Calculate critical horizontal velocity

$$V_{cr} = 0.44\sqrt{d}$$

   For d = 0.3 mm, $V_{cr} < 0.24$ m/s
6. Find depth required by using $B \cdot y = Q/V_{cr}$

Increase the length of basin by 30%–50%, depending upon the economic factors.

6.5.8 Efficiency of Settling Basin

Vetter's equation is commonly used in the design of settling basins to estimate the settling for the particle size considered (i.e., d_{limit}). The Vetter's equation to determine settling efficiency is [5]

$$\eta = 1 - e^{-\left(\frac{WA_s}{Q}\right)} \tag{6.10}$$

where η = efficiency of basin, A_s = surface area of settling basin, Q = discharge, and W = fall velocity of particle.

A 90% settling efficiency for particle size based on head as discussed earlier would be appropriate when using Vetter's equation to size (or verify) settling basin in micro hydro schemes. The desired efficiency of the settling basin is achieved by finding the surface area of the settling zone and then dimensioning the area considering the criteria mentioned earlier.

6.5.9 Camp's Method

Based on a series of experiments, Camp has published an equation to find the surface area of the settling basin. Camp's equation to find the settling velocity is

$$w = w_0 - 0.04\,V_{mc}$$

where w = settling velocity of sand in flowing water (m/s), $V_{mc} = 0.44 \cdot d^{1/2}$ critical mean flow velocity (m/s), d = design particle size (mm), and w_0 = settling velocity of sand in quiescent water (m/s).

Note that multiple chambers will not be required for small flows, but this arrangement will enhance the settling efficiency and allow partial power generation instead of complete plant shutdown.

6.5.10 Storage Design

The concentration of suspended particles in the flow can be expressed as follows:

$$\text{Concentration (C)} = \text{kg of suspended matter/volume of water}$$

The sediment carried by water can be estimated using Equation 6.1. When data are unavailable, $C = 2\ \text{kg/m}^3$ for the design of settling basins.

The sediment storage requirement in a settling basin is calculated as follows:

1. Calculate the sediment load using the following equation:

$$S_{load} = Q\ T\ C$$

where S_{load} = sediment load in kg stored in the basin, Q = discharge in m^3/s, T = sediment emptying frequency in seconds, and C = sediment concentration of the incoming flow in kg/m^3.

A reasonable emptying frequency (T) for micro hydropower plants could be about once to twice daily during high flow, which generally results in less than once a week during the low-flow season when the sediment concentration is low. As discussed earlier, large hydropower plants often have continuous flushing systems.

2. The next step is to calculate the volume of the sediment using the following equation:

$$V_{sediment} = S_{load}/S_{density} \cdot S_{factor}$$

where $V_{sediment}$ = volume of sediment stored in the basin in m^3. $S_{density}$ = density of sediment in kg/m^3, about 2600 kg/m^3. P_{factor} = packing factor of sediment submerged in water.

When submerged in water, particles occupy more space than when dry. This is measured in terms of packing factor, which is the ratio of unit volume of dry sediment to unit volume of wet sediment (i.e., volume of 1 m^3 of dry sediment divided by the volume of this sediment when submerged). The packing factor for submerged sediment is about 0.5 (i.e., the volume of dry sediment is doubled when submerged).

Below the settling zone must be the capacity to store the calculated volume of sediment, $V_{sediment}$. This storage space is achieved by increasing the depth of the basin as follows:

$$Y_{storage} = V_{sediment}/A$$

where $Y_{storage}$ is the storage depth in the settling basin below the hydraulic depth (y) discussed earlier, and A is the plan area. The hydraulic depth and the storage depth are also shown in Figure 6.3.

6.5.11 Flushing Design

As the operation starts, deposition of sediment also starts in the settling basin. The deposition mainly consists of fine sediment as can be seen in Figure 6.21. This sediment should be removed from the basin as quickly as possible for uninterrupted operation of the power plant. There are various ways of removing the stored sediment from the settling basin. The main philosophy of designing flushing

FIGURE 6.21 Sediments deposited in settling basin.

is the use of sediment transport theory. The transport capacity of the flow depends upon the velocity and depth of flow—that is, the energy head of flow.

a. Channel Section for Flushing

The mass of sediment transported by the flow can be estimated using

$$m = \frac{(V_f - 0.35)^3}{h^2}$$

where m = mass of sediment transported (kg), V_f = flushing velocity m/s, and H_f = depth of flow during flushing, m.

The culvert used to pass the sediment out of the settling basin can be designed using the orifice flow formula and providing adequate slope so that no deposition occurs in the channel.

b. Vertical Flush Pipe Method

An appropriate method for micro hydro settling basins is the vertical flush pipe. This uses a detachable vertical mild steel pipe over a hole in the basin floor. A drainpipe is fixed below the basin floor to convey the flow out of the basin. When the vertical flush pipe is lifted, the water stored in the basin and the incoming flow along with the sediment are drained through the hole. Apart from being simple, the other advantage of this system is that it can spill some excess flow, such as during floods when the water level in the basin is above the normal level. The diameter of the flush pipe is governed by the following criteria [5]:

i. Overflow Capacity

It needs to spill the excess flood flow that enters the basin. This is governed by the weir equation, in which the perimeter of the pipe is used for the length as follows:

$$Q_{flood} = \pi d C_w h_{flood}^{3/2}$$

where Q_{flood} is the expected flood flow in the basin, and h_{flood} is the depth of water above the vertical pipe during Q_{flood}. This is the height between the top of the vertical flush pipe and the top of the settling basin wall.

C_w is the weir coefficient for a sharp-edged weir, which is around 1.9. The reason for using the sharp-edged weir coefficient is because the pipe thickness is small compared to the head.

In terms of the pipe diameter, the above equation can be rewritten as follows:

$$d = \frac{Q_{flood}}{1.9\pi h_{flood}^{3/2}}$$

To ensure draining of excess flow and to prevent spilling of the design flow, the height of the vertical flush pipe should be such that the top level is 50 mm above the design water level. Also note that if the settling basin is combined with the forebay, it may be more important to size the flush pipe diameter such that it is able to spill the design flow. This is because if the turbine valve is closed during emergencies, the entire design flow will have to be spilled from the forebay until the operator reaches the intake or other control structures upstream of the forebay.

The pipe should be able to divert both the incoming flow and the water volume in the basin, thus emptying it. This is based on the following equations:

$$1.5\ Q_{design} = CAh_{basin} + h_{flush}$$

$$\text{Or } 1.5\ Q_{design} = CAh_{flush}$$

$$\text{or } Q_{design} = CA\ h_{flush}$$

where Q_{design} is the design flow. Q_{design} is multiplied by 1.5 in the first equation to ensure that there is a draw down in the water level inside the basin during flushing (i.e., both the incoming flow and the flow in the basin can be drained). C is the orifice coefficient = 2.76 (applies only when the total pipe length is less than 6 m). h_{basin} is the depth of water in the basin during the design flow prior to flushing. h_{flush} is the flushing head when basin is empty. This is the difference in level between the floor of the basin and the flush pipe outlet as can be seen in Figure 6.22.

A is the area of the pipe section.

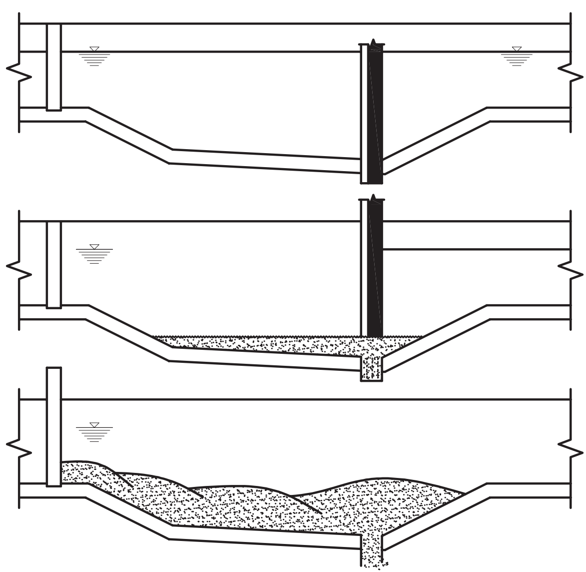

FIGURE 6.22 Vertical flush pipe in settling basin.

The second equation ensures that the design flow can be discharged through the system when the basin is empty. It is important to check this condition, especially if the h_{flush} is low.

In terms of the pipe diameter, the above two equations can be rewritten as follows:

$$d = \frac{6Q_{design}}{\pi C(h_{basin} + h_{flush})}$$

$$\text{or } d = \frac{4Q_{design}}{\pi h_{flush}}$$

Note that these equations assume that there is free pipe flow at the outlet and the pipe diameter is constant (vertical and horizontal pipes of the system have the same diameter).

All of the above three equations should be used to size the diameter of the flush pipe. The pipe should be sized using the equation that results in the largest diameter.

6.6 FOREBAY

A forebay is a small reservoir that stores water for a certain period of time (Figure 6.23). It is generally located at the place from where the flow regime changes from a nonpressurized to a pressurized system. In a micro hydropower scheme, this is the beginning of penstock pipe. Basically, a forebay serves for the following purpose:

- It allows transition from open channel to pressurized conditions.
- It releases the surge pressure that comes from pressurized conditions.
- It serves as water storage while there is down surge in the penstock.
- It also serves as a secondary settling basin as the velocity of flow is small in forebay.

Note: Surge pressures are discussed in Chapter 7.

FIGURE 6.23 Forebay with surface spillway and a flushing pipe.

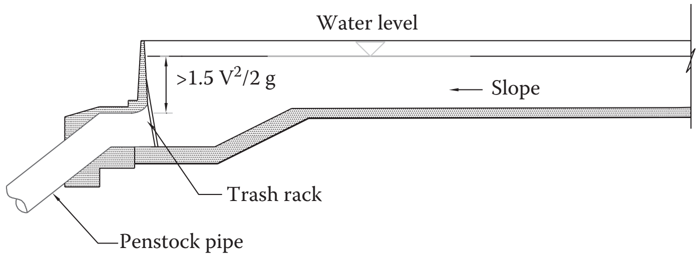

FIGURE 6.24 Schematic drawing of a forebay

6.6.1 Components of Forebay

A forebay essentially consists of a tank to hold water for a certain period of time. Generally, a fine trash rack is provided at the outlet to prevent trash from entering inside the penstock.

6.6.2 Design Criteria

A forebay should be sized in such a way that a person can get in and clean it (Figure 6.24). The depth of a forebay should be greater than the submergence head required. The submergence head can be calculated using

$$h = 1.5\frac{v^2}{2g} \tag{6.11}$$

where h is submergence head, and v is velocity of flow in the penstock.

6.7 SPILLWAY

If excess flows cannot be spilled from the upstream headrace portion, such as due to lack of a suitable area (or if a pipe is used), a spillway should also be incorporated at the settling basin. The spillway should be sized to spill the entire flow expected during the high-flow season. The spillway serves by letting water overflow through it when there is rejection of load in the power plant or when the plant is suddenly closed. Note that the design of spillways was covered in Chapter 5.

However, in the case in which there is a vertical flush pipe sized to divert the expected high flows, a separate spillway is not necessary.

6.8 STRUCTURAL DESIGN OF SETTLING BASIN AND FOREBAY

The settling basin is founded on ground. Hence, a good stable foundation is preferred for construction of this structure. When a good foundation condition is not available, a foundation improvement technique should be used. At least the topsoil should be removed for the foundation. Where bedrock can be reached, the structure should be anchored to the rock. The structural design of such structure should be done in two steps.

In the first part, assessment of the bearing pressure in the foundation should be done. The loads that should be considered are

- Dead load
- Earth pressure
- Overburden pressure
- Hydrostatic load
- Uplift forces
- Silt load
- Seismic load

When there are multiple chambers and provision for independent operation of each chamber is made, load combination should account for an empty and nonempty case of each chamber. The foundation should be designed such that, even in the worst case, the bearing pressures are within an allowable limit and there is no tensile force developed on any part of the foundation. However, in larger projects, small tension is allowed for economic reasons. But even in such a case, the tension should not cause cracks on the concrete.

In the second part, the reinforcement should be calculated using the principle of structural analysis. It is common practice to consider the unit length of the basin for analysis of foundation and reinforcement design. The reinforcement can be calculated either considering the settling basin and forebay as an open water tank structure or, in the worst case, when there is risk of differential settlement, the structure should be designed as slabs. The deflection of the structure should be checked and should be within the permissible limit set by the code of practice. Structural analysis is a vast topic and beyond the scope of this textbook. Standard textbooks should be referred to for details on structural analysis of water-retaining structures.

Example 6.1

Design a gravel trap, settling basin, and a forebay for a power plant with a design discharge of 1.33 m^3/s. The design head of the project is 200 m. The suspended sediment concentration is 8000 ppm, and bed load concentration is 3 kg/m^3. Assume headrace canal width upstream of the settling basin to be 1.7 m.

Step	Calculation	Remarks
1	Note that the design discharge is $Q = 1.33\ m^3/s$. For flushing, we will require additional discharge. Allow additional 10% discharge for gravel trap flushing and another 10% for settling basin flushing. The total discharge is then 20% additional to the design discharge $Qt = 1.33 \cdot 1.20$ $= 1.60\ m^3/s$	
2	Design of gravel trap The gravel trap is designed to remove particle size greater than 5 mm.	$D = 5$ mm
2.1	Critical velocity of flow to be maintained for settlement particle is $V_{cr} = a\sqrt{d_{mm}}$ Or $V_{cr} = 0.44\sqrt{5}$ Or $V_{cr} = 0.98$ m/s > 0.6 m/s Thus, the flow velocity is adopted $V_{cr} = 0.6$ m/s	$V_{cr} = 0.6$ m/s

(Continued)

Step	Calculation	Remarks
2.2	Settling velocity of 5 mm particle is given the form w = 30 cm/s Or w = 0.30 m/s	Figure 6.20 w = 0.3 m/s
2.3	Calculation of hydraulic dimension Let width of gravel trap B = 2.30 m, then flow depth in gravel trap is given by $Q_t = V_{cr} \cdot B \cdot D$ Or $D = \frac{Q_t}{V_{cr} \cdot B}$ Or $D = \frac{1.60}{0.6 \cdot 2.3}$ Or D = 1.16 m Length of gravel trap is given by $L = D\frac{V_{cr}}{w}$ Or $L = 1.16\ \frac{0.6}{0.3}$ Or L = 2.32 m Minimum length of gravel trap = three times of headrace canal width or 2 m because the width of headrace canal is 1.70 m (this should be calculated using the bed slope and Manning's equation). $\text{Minimum width} = 3 \cdot 1.7 \text{ or } 2\text{ m}$ $= 5.10\text{ m}$ Hence, set the length of gravel trap as 5.50 m.	B = 2.30 m D = 1.20 m L = 5.10 m Free board = 0.3 m
2.4	Design of spillway The length of spillway to spill the excess discharge is given by the equation $Q_s = C_d L H^{3/2}$ To calculate the length of spillway, we must know the discharge that may enter the gravel trap during a flood. Let us assume that at the 20-year return period flood, 4.0 m^3/s flow enters the gravel trap. i.e., $Q_f = 4.0$ m^3/s Hence, excess flow is given by $Qe = Qf - Qt$ $= 4.0 - 1.60$ $= 2.4\ m^3/s$ This flow should be spilled from the spillway. Let spillway length be 4.0 m. The depth of spillway required will be given by Or $H = \left(\frac{Q_s}{C_d L H^{3/2}}\right)^{2/3}$ Or $H = \left(\frac{2.4}{1.65 \cdot 4.0}\right)^{2/3}$ Or H = 0.51 m	L_{spill} = 3.0 m H_{spill} = 1.20 m
2.5	Design for sediment deposition Given bed load concentration C = 3 kg/m^3 Let flushing interval be 2 hours (when C = 3 kg/m^3)	Flushing duration = 2 hours D_{sed} = 1.20 m

(*Continued*)

Step	Calculation	Remarks
	Hence, the volume of bed load deposited in 2 hours will be $$V_{sed} = \frac{QCT}{\rho}$$ The density of bed load is 2600 kg/m^3 Or $V_{sed} = \frac{1.6 \cdot 3 \cdot 2 \cdot 60 \cdot 60}{2600}$ Or V_{sed} = 13.29 m^3 The depth required to deposit this sediment is $$D_{sed} = \frac{V_{sed}}{L \cdot B}$$ $$D_{sed} = \frac{13.29}{5.1 \cdot 2.3}$$ D_{sed} = 1.13 m Therefore, the total wall height = flow depth (D) + Sediment deposition depth (D_{sed}) + Spillway depth (H) Or total wall height required = 1.16 + 1.13 + 0.51 = 2.80 m. If 0.2 m of freeboard is allowed over the water level at the gravel trap, the wall height will be 3.0 m. Note that the spillway invert level needs to be at 1.16 + 1.13 + 0.20 = 2.59 m from the bed level of the gravel trap.	
3	Design of settling basin Consider 10% flushing discharge for settling basin. Let the settling basin be designed with two chambers. Hence, each chamber is served for half of the discharge. $Q_{st} = 1.33 \cdot 1.2 = 1.46$ m^3/s $Q_s = Q_{st}/2 = 1.37/2 = 0.73$ m^3/s	
3.1	Critical velocity of flow to be maintained for particle to be settled assuming 0.2 mm size particle is $$V_{cr} = a\sqrt{d_{mm}}$$ Or, $V_{cr} = 0.44\sqrt{0.2}$ Or, V_{cr} = 0.20 m/s (the flow velocity should be maintained between 0.1 and 0.4 m/s)	From Figure 6.20
3.2	Fall velocity of 0.2 mm grain $$\begin{aligned} w &= 2.20 \text{ cm/s} \\ &= 0.022 \text{ m/s (from Figure 6.20)} \end{aligned}$$ Using Camp's equation, the fall velocity will be $w = w_0 - 0.04\, V_{mc}$ $$w_o = \frac{(\rho_p - \rho_w)g}{18\,\mu} d^2$$ $$w_o = \frac{(2600-1000)\cdot 9.81}{18 \cdot 1.15 \cdot 10^{-3}} \cdot \left(\frac{0.2}{1000}\right)^2$$ w_o = 0.03 m/s w_o = 3.03 cm/s Now $\mu = 1.15 \cdot 10^{-3}$ N_s/m^2 $w = w_0 - 0.04\, V_{mc}$ or $w = 0.03 - 0.04 \cdot 0.2$ or w = 0.022 m/s	W = 0.022 m/s

(*Continued*)

Step	Calculation	Remarks
3.3	Calculation of hydraulic dimension Using Vetter's efficiency equation and considering 90% trap efficiency, we can calculate surface overflow rate (A_s) $\eta = 1 - e^{-\left(\frac{WA_s}{Q}\right)}$ Or $0.9 = 1 - e^{-\left(\frac{0.022 \cdot A_s}{0.73}\right)}$ Or $A_s = 76.40\ m^2$ Consider width of each basin B = 2.8 m Then, length of basin $L = A_s/B$ L = 76.4/2.8 L = 27.29 m (say 28 m) Now for flow depth of basin, $D = \frac{Q_t}{V_{cr} \cdot B}$ Or $D = \frac{0.73}{0.2 \cdot 2.8}$ Or D = 1.30 m Check aspect ratio L/B = 28/2.8 = 10.0 OK! Let freeboard be 0.3 m	L = 28 m B = 2.5 m D = 1.40 m Freeboard = 0.3 m
3.4	Calculation of sediment deposition depth The bed load concentration C = 8000 ppm Let flushing interval be 8 hours Hence, the volume of bed load deposited in 2 hours will be $V_{sed} = \frac{QCT}{\rho}$ The density of bed load is 2600 kg/m^3 Or $V_{sed} = \frac{0.73 \cdot 8000 \cdot 8 \cdot 60 \cdot 60}{2600 \cdot 1000}$ Or $V_{sed} = 64.69\ m^3$ The sediment will not be in compact form. The loose sediment will occupy more volume. Let the packing factor f = 0.5. $V'_{sed} = \frac{V_{sed}}{f}$ $V'_{sed} = \frac{64.69}{0.5}$ $V'_{sed} = 129.38\ m^3$ The depth required to deposit this sediment is $D_{sed} = \frac{V'_{sed}}{L \cdot B}$ $D_{sed} = \frac{129.38}{28 \cdot 2.8}$ $D_{sed} = 1.65$ m (say 1.70 m)	Flushing duration = 8 hours $D_{sed} = 1.70$ m

(*Continued*)

Step	Calculation	Remarks
	Total depth of settling basin $Dt = D + D_{sed} + \text{Free board}$ $= 1.4 + 1.7 + 0.3$ $= 3.40\,m$ Check aspect ratio D/B = 3.4/2.8 = 1.21 OK!	
3.5	Horizontal and vertical Let the approach canal width be the same as gravel trap width—that is, 2.30 m Adopt expansion ratio of 1:5 in inlet and 1:3 in outlet of settling basin. The vertical transition is 1:2. Note that the horizontal transition and vertical transition need not end at same point. Adopt 1:100 bed slope. The basin is tapered near the flushing outlet to achieve better flushing.	
4	Designed settling basin	

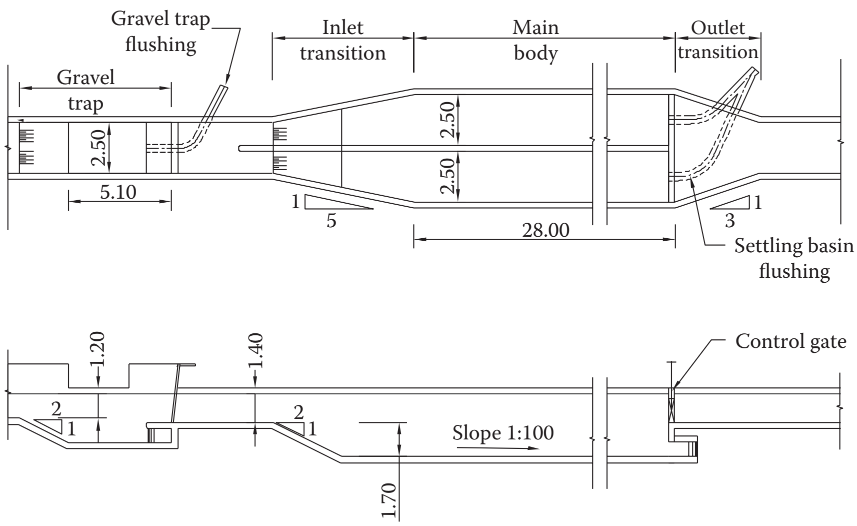

EXERCISES

1. Design a forebay for Example 6.1. Make reasonable assumptions for any missing data.
2. A settling basin has the following dimensions:
   - Design flow = 350 l/s
   - Gross head = 160 m
   - No. of chambers = 2
   - Width per chamber = 1.5 m
   - Settling zone length = 12 m
   - Flow depth = 1.8 m
   - Design sediment concentration, C = 3.5 kg/m^3
     a. Estimate the settling efficiency for d_{limit} = 2 mm, 3 mm, and 5 mm. Assume 10% additional flow allowance into the settling basin.
     b. For d_{limit} = 2 mm, what should be the storage depth assuming flushing frequency of 8 hours and 12 hours?

c. Can the basin dimensions be further optimized keeping the overall volume the same? If so, propose the optimized dimensions.

3. Design a gravel trap for the data provided in Question 2. Assume the incoming headrace canal into the gravel trap to be 0.8 m wide.
4. Design a hollow pipe flushing system for the settling basin in Question 2.

REFERENCES

1. Miedema, S. A. and Vlasblom, W. J., *Theory of Hopper Sedimentation*, WODCON XIV, Amsterdam, 1995.
2. Robertson, J. A. and Crowe, C. T., *Engineering Fluid Mechanics*, Third Edition, Houghton Mifflin, Boston, 1985.
3. Ferguson, R. I. and Church, M., A simple universal equation for grain settling velocity, *Journal of Sedimentary Research*, 74(6), 933–937, 2006.
4. Harvey, A. and Brown, A., *Micro-Hydro Design Manual: A Guide to Small-Scale Water Power Schemes*, ITDG Publishing, London, 1993.
5. ITDG, *Civil Works Guidelines for Micro-Hydropower in Nepal*, BPC Hydroconsult and Intermediate Technology Development Group, Kathmandu, Nepal, 2002.
6. Rouse, H., *Nomogram for the Settling Velocity of Spheres*, Cooperative Research Laboratory, Soil Conservation Service, California Institute of Technology, 1937.
7. *Engineering Geology and Rock Engineering: Handbook No. 2*, Norwegian Group for Rock Mechanics, Oslo, 2002.

7 Penstocks

7.1 OVERVIEW

A penstock is a pipe that conveys the flow from the forebay to the turbine. The penstock pipe starts downstream of the forebay where the ground profile is much steeper than the headrace alignment. The potential energy of the water at the forebay is converted into kinetic energy at the turbine via the penstock pipe. Because the flow is conveyed under pressure, it is important for the pipe design to be safe. Cases have been reported in which the penstock pipes have burst. Because the penstock is on steep ground slopes, such a pipe burst can instantaneously cause landslides and other stability problems. Furthermore, penstock installation is often challenging and requires safe and careful work as shown in Figure 7.1. Sometimes a long pipeline is used to convey water from the headworks to the forebay; in such cases, the penstock is referred to as the headrace pipe.

The penstock pipe usually constitutes a significant portion of the construction cost. Therefore, it is necessary to optimize the design. This involves a careful choice of pipe material, such as mild steel or HDPE; an economical diameter such that the head loss is within acceptable limits; and wall thickness, so the pipe is safe for the design head and any surge effect that may result from sudden blockage of the flow.

7.2 SELECTION OF THE PENSTOCK ALIGNMENT

Selection of the penstock alignment on-site should be based on the following criteria.

7.2.1 Forebay Location

The penstock starts at the forebay. The forebay location should be chosen to optimize the lengths of the headrace and penstock while achieving the required power output from the scheme. The penstock pipe is generally more expensive than the headrace canal. Therefore, in most cases, the forebay location should be chosen to give the minimum penstock length but, at the same time, also conserving head. However, sometimes a longer penstock may be economical, such as to avoid the need for the headrace to cross an unstable slope.

7.2.2 Practical Ground Slope

An ideal ground slope for the penstock alignment is between 1:1 and 1:2 (V:H). The flatter the ground slope, the less economic the penstock because a longer pipe length is required for a lower head. Although a steep slope minimizes the penstock length, it will be difficult to manually lay the penstock; construction of support piers and anchor blocks is required if the slope is larger than 1:1. Therefore, for penstock alignments on slopes steeper than 1:1, the added site installation cost may outweigh the savings made on the pipe costs.

A penstock profile that starts at a gentle slope and then becomes steeper should be avoided because of the risks of negative surges causing subatmospheric pressure. The ground profile should be measured as accurately as possible. An Abney level can be used for smaller hydro projects, and for larger schemes, more precise equipment, such as a theodolite or total station should be used. This is because, if the prefabricated bends do not fit on-site due to survey errors, additional costs and time will be required to amend these, especially if the site is located at a remote area and the

FIGURE 7.1 Penstock alignments in different terrain.

pipes are to be flange-connected. Note that some slight adjustment can be made if the pipes are to be welded on-site.

Additionally, errors in the design head calculation (due to survey errors) will result in either oversizing or undersizing the electromechanical units, which will also increase the project cost, either in terms of lost power production or in extra cost for the oversized units.

7.2.3 Minimum Number of Bends

Bends increase the head loss and require additional anchor blocks. Therefore, the selected alignment should be as straight as possible, both in plan and elevation. Note that small bends can be avoided by varying the support pier heights for the exposed section and the trench depth for the buried section.

7.2.4 Space for Powerhouse Area

The chosen alignment should be such that it is possible to construct a powerhouse at the end of the penstock. A river terrace well above the flood level is ideal for the powerhouse area. A route that is otherwise suitable for the penstock alignment but does not allow for the construction of the powerhouse is inappropriate.

7.2.5 Stability

Because the penstock alignment is on steep ground slopes and the pipe is under pressure, it is important for the alignment to be on stable ground. Any ground movement can damage the pipe, support piers, and anchor blocks, and in case of pipe bursts, unstable slopes will cause further erosion and landslides. Adequate drainage facilitates (e.g., drain canals) for surface water should be provided along the pipe alignment. Note that a pipe alignment that is dry will have less stability problems.

7.2.6 Other Site-Specific Conditions

Apart from the above criteria, there may be other site-specific conditions that dictate the penstock alignment. For example, if the alignment crosses a local trail, this section should either be buried or high enough above the ground such that people and cattle can walk underneath.

7.3 PROFILE OF THE SELECTED ALIGNMENT

Based on the site survey, a plan and profile of the penstock alignment should be prepared at the design office as follows:

- The ground profile should first be drawn using an appropriate scale. The same scale should be used for both horizontal and vertical lengths so that the bend angles are true angles, which minimizes the likelihood of errors. If the alignment also has horizontal bends, then a plan view should also be prepared to show horizontal bend angles.
- Once the ground profile has been prepared, the penstock pipe should be drawn on it such that the number of bends is kept to a minimum. In general for above ground alignment, the support pier height should be minimized unless some of them need to be increased to avoid small angle bends. Similarly, excavation should be minimized for the buried section unless deeper trenches are required at short sections to avoid small angle bends. Optimizing the alignment will require some iterations. An example of a penstock profile is shown in Figure 7.2.
- For aboveground penstock sections, a minimum ground clearance of 300 mm is recommended to keep the pipe dry and for ease of maintenance, such as painting.
- For buried penstock sections, a minimum soil cover of 1 m is recommended as in the case of HDPE headrace pipe, and the trench details should be similar to those shown in Figure 7.3.

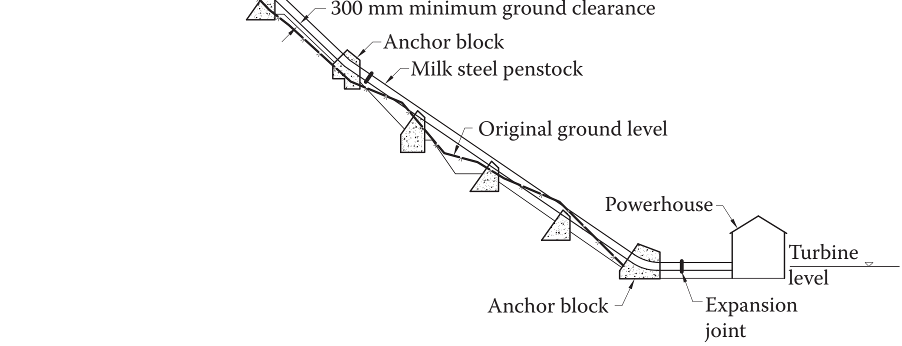

FIGURE 7.2 Typical penstock profile.

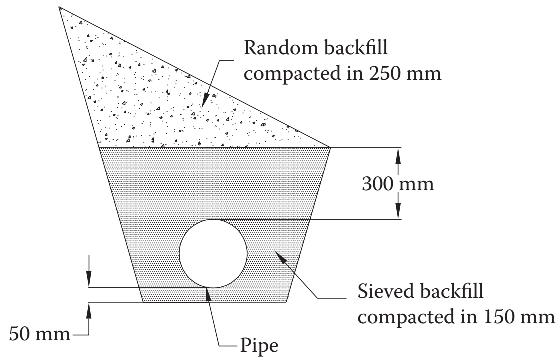

FIGURE 7.3 Typical buried section.

7.4 SELECTION OF PIPE

7.4.1 Pipe Materials

The most commonly used penstock pipe materials are mild steel and HDPE. Rigid or unplasticized PVC (uPVC) and glass reinforced plastic (GRP) are other options that have been sometimes used in countries such as Peru, Sri Lanka, and Nepal. The decision as to which pipe material to use for the penstock is based on the flow required, head and surge pressure, durability, allowable head loss, ease of transportation, ease of fabrication, and the cost of material [1].

7.4.1.1 Steel

Due to high strength and durability, the most used material in pipe is mild steel. Such steel pipes are usually made of plate steel with longitudinal joints by welding. In the past, steel plates were joined by riveting, which has now been replaced by welding technology. It should be noted that high strength steels are difficult to weld, and hence, mild steel is preferred. Steel pipes less than 3 m in diameter have a shipping length of about 4 to 8 m. Pipes with larger diameter are delivered to the site in segments due to transportation limitation. Such segments are then joined by welding.

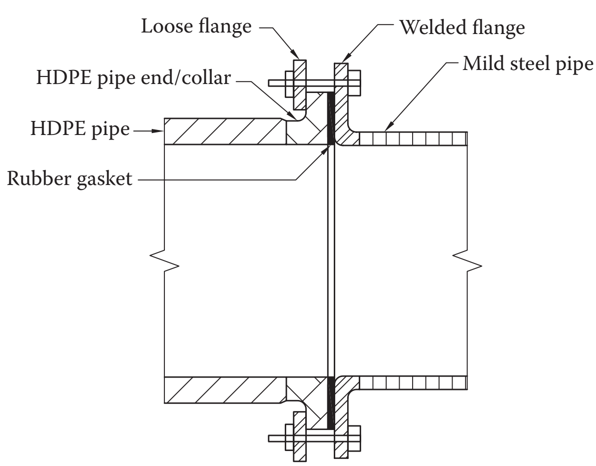

FIGURE 7.4 Typical steel–HDPE pipe coupling.

7.4.1.2 HDPE

For long penstock alignments, low-strength pipe, such as HDPE, can be used for the upstream length where the head is relatively low. After the stress in pipe exceeds the allowable stress, steel can then continue. Standard couplings are available to join HDPE and mild steel pipes as shown in Figure 7.4.

7.4.1.3 GRP

The use of GRP in hydropower projects has been successfully tested. GRP is light in weight but has very high compressive and tensile strength compared to steel. It is resistant to change in pH of water and chemically inert. Due to the lower value of elasticity, the water hammer effect is considerably low in GRP pipes. However, GRP is weak in shear strength. By laying multiple layers of fiber on top of one another with each layer oriented in various preferred directions, the stiffness and strength properties of the overall material can be increased. However, there are some health risks during production and laying of GRP pipes. When resins are cured, chemical vapors are released, which causes irritation to mucous membranes and the respiratory tract. Further manufacture of GRP components (grinding, cutting, sawing) releases emission of fine dusts and chips containing glass particles, which affects people's health and functionality of machines and equipment. Hence, strict safety regulations should be adopted while using GRP pipes during production and installation.

Pipe Material	Specific Gravity	Compressive Strength (Mpa)	Tensile Strength (Mpa)	Young's Modulus of Elasticity (Mpa)
Mild steel	7.85	408	250	205,000
HDPE	0.95	22	20–32	1000
PVC	1.3	65	55	2750
GRP	1.5	150–350	100–300	24,000

7.4.2 Pipe Diameter

Once the penstock alignment and pipe material have been decided on, the design involves choosing the diameter and pipe thickness. When selecting an appropriate pipe diameter, the most important parameter is velocity of flow. The following points should be noticed when selecting the pipe diameter:

1. Friction loss along the pipe
2. Abrasion
3. Cost of the penstock
4. Governing condition of the turbine/cost of turbine governor
5. Limitation of pipe manufacturer

For practical purposes, pipe diameter can be selected such that the velocity is between 2.5 m/s and 3.5 m/s. In general, a velocity lower than 2.5 m/s results in an uneconomically large diameter. Similarly, if the velocity exceeds 3.5 m/s, the head loss can be excessive and hence uneconomical in the long run due to loss in power output. Furthermore, it must be noticed that higher velocities in the penstock will result in high surge pressure. In any case, the final pipe diameter selection should be based on results of head loss calculations and their implications on loss of annual energy or annual revenue, especially as the plant size gets larger.

7.4.2.1 Head Loss along the Pipe

The frictional loss in pipeline can be divided into two categories—that is, major loss due to frictional resistance along the pipe length and minor losses at the entrance and bends. The permissible head loss can be determined by economic analysis by comparing the amount of energy gained by reducing the head loss. The economic analysis should also involve cost for repair and maintenance. As we increase the diameter of pipe, head loss decreases, and the cost of pipe increases. By iterating with multiple pipes of different diameter, an economic diameter can be determined.

7.4.2.2 Abrasion

All water conveyed in the pipe contains sediment particles. At high velocity, such particles start to scour the pipe material depending upon (a) the particle size, (b) the hardness of the particle, and (c) hardness of the pipe material. Hence, a limiting velocity of 3–5 m/s is generally adopted. For clean water, the velocity may be as high as 8 m/s. It must be noticed that higher velocity not only scours pipe materials, but also damages the turbine runner.

7.4.2.3 Cost of Penstock

The major factor determining the diameter of pipe is its cost of installation and operation. Economic analysis should be done to arrive at the best diameter for which the cost of power will be minimum during the entire life of the project. The cost of a turbine governor should also be added to get the realistic economic indicators.

7.4.2.4 Governing Condition of the Turbine/Cost of Turbine Governor

While operating the power plant, two cases are encountered that limit the diameter of pipe. These are (a) the startup condition in which there is the possibility of drawing excess water than can be supplied causing subnormal pressure and (b) the stopping condition when the plant is stopped suddenly or there is a change in load, causing water hammer phenomenon [2]. These two cases are also called governing conditions.

At the initial moment, the pressure head accelerating the water column in the penstock is the entire head H, which decreases as soon as the moment has started. Part of the pressure energy is converted into kinetic energy, and part is lost to overcome wall friction.

The accelerating head is thus He = Gross head losses.

Because head loss and velocity head is negligibly small, assuming a uniform rate of acceleration under constant accelerating head is also very small.

By Newton's second law, pressure force on the water column in the pipe line = mass · acceleration

$$\gamma aH = \frac{\gamma aL}{g} \cdot \frac{dv}{dt}.$$

Or

$$H = \frac{L}{g} \cdot \frac{dv}{dt}. \tag{7.1}$$

This is also called Euler's equation.

Where a is pipe sectional area, L is length of pipe, and V is flow velocity.

Considering uniform acceleration, the time required for stationary water column to attain velocity v may be written as

$$\frac{dv}{dt} = \frac{v}{T_a}. \tag{7.2}$$

From Equations 7.1 and 7.2,

$$T_a = \frac{Lv}{gH}. \tag{7.3}$$

The time of the opening of the valve should be greater than the time of accelerating. If the time of opening is less than the time required for acceleration, excessively high hydrodynamic forces will rupture the pipe, governing device, and turbines. The equation also indicates that the long and high-velocity pipe requires a long opening time to design the governor. And there is limiting value of velocity up to which this mechanical component can be designed. Thus, the velocity in pipe has a limiting value, which, in turn, determines the diameter of pipe.

7.4.2.5 Limitation of Pipe Manufacturers

There are limits imposed by the equipment of manufacturers to supply the pipe. Similarly, transportation and erecting of large pipes also imposes limitations to the diameter of pipe.

7.4.3 Pipe Optimization

Optimization of pipe is a method to find the size of pipe that gives the maximum benefit over the lifetime of the plant operation. To reach the optimum diameter of pipe, a set of pipes with different diameters are taken. As the diameter increases, the total energy output increases, but the cost of pipe increases too. When we plot the cost of pipe and the cost of power lost due to head loss against these diameters, we get the most economic diameter of pipe.

7.4.3.1 Procedure to Select the Pipe Diameter

7.4.3.1.1 Choose a Diameter of Pipe

For steel penstocks, it may be economical to choose the diameter so that there is no wastage from standard size steel sheets. For HDPE or PVC, available sizes must be selected. Pipes are normally specified by outside diameter, so two times the wall thickness must be subtracted to obtain the internal diameter.

7.4.3.1.2 Calculate the Actual Velocity

$$V = \frac{4Q}{\pi d^2}$$

where V is velocity in m/s, Q is design flow in m^3/s, and d is the pipe internal diameter in m.

The permissible velocity in penstock pipe by USBR is given by

$$V = 0.125\sqrt{2gH}$$

V = permissible velocity, m/s
H = rated head, m

7.4.3.1.3 Calculate the Head Loss in the Pipe

The head loss in the length based on the inlet, wall friction, bends, valves, and exit loss.

Total head loss = friction loss + turbulence losses. The formulas to calculate head loss are described below.

7.4.3.1.4 Frictional Loss

The frictional loss in the pipe depends upon the pipe surface and is given by (Figure 7.5)

$$H_L = \frac{flv^2}{2gD}$$

where the friction factor (f) depends upon the pipe relative roughness (k/D) and the velocity in the pipe (Table 7.1).

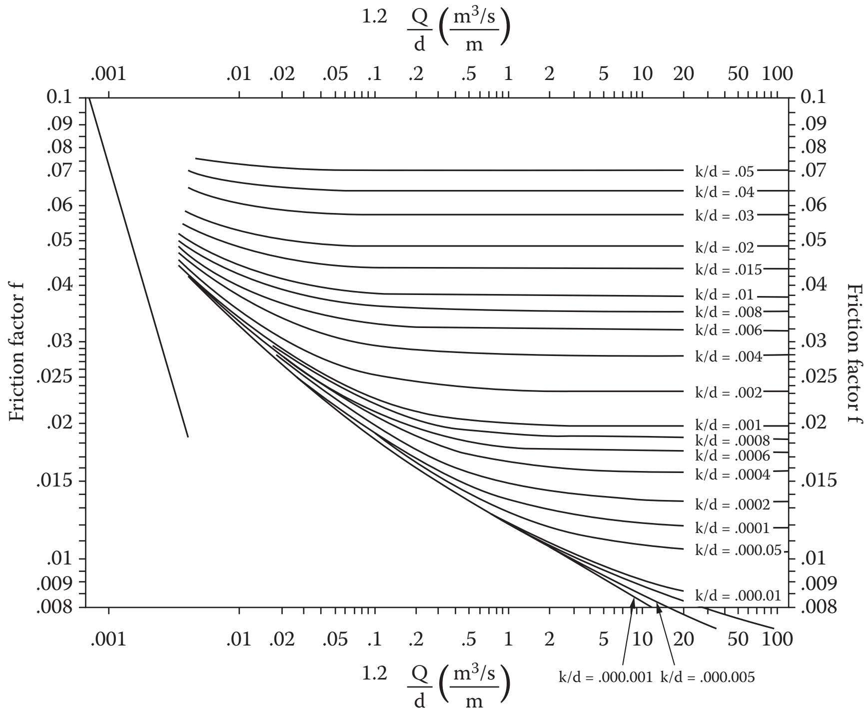

FIGURE 7.5 Moody's chart. (From ITDG, *Civil Works Guidelines for Micro Hydropower in Nepal*, BPC Hydroconsult and Intermediate Technology Development Group, Kathmandu, Nepal, 2002.)

TABLE 7.1
Roughness Value of Different Pipe Materials

Material	Roughness Value, k (mm)
Smooth pipes PVC, HDPE, MDPE, glass fiber	0.06
Concrete	0.15
Mild steel uncoated, galvanized	0.06, 0.15

7.4.3.1.5 Entrance Loss

$$H_L = K\frac{v^2}{2g}$$

where K is given as follows: Sharp edge entrance = 0.5, rounded entrance (r/D = 0.1) = 0.1, and bell mouth = 0.05.

7.4.3.1.6 Sudden Expansion Loss

$$H_L = K\frac{v^2}{2g}$$

where $K = \left(1 - \frac{A_2}{A_1}\right)^2$

A_1 = cross-section area of flow incoming from A_2 = cross-section area of flow going to V_2 = velocity in cross-section 2.

7.4.3.1.7 Gradual Expansion Loss

$$H_L = K\frac{v^2}{2g}$$

where K is determined from the Figure 7.6.

7.4.3.1.8 Sudden Contraction Loss

$$H_L = K\frac{v^2}{2g}$$

where $K = 0.5\left(1 - \frac{A_2}{A_1}\right)^2$

A_1 = cross-section area of flow incoming from A_2 = cross-section area of flow going to V_2 = velocity in cross-section 2.

7.4.3.1.9 Gradual Contraction Loss

$$H_L = K\frac{v^2}{2g}$$

where K is determined from Figure 7.7.

$$H_L = K\frac{v^2}{2g}$$

where K is determined from Figure 7.8.

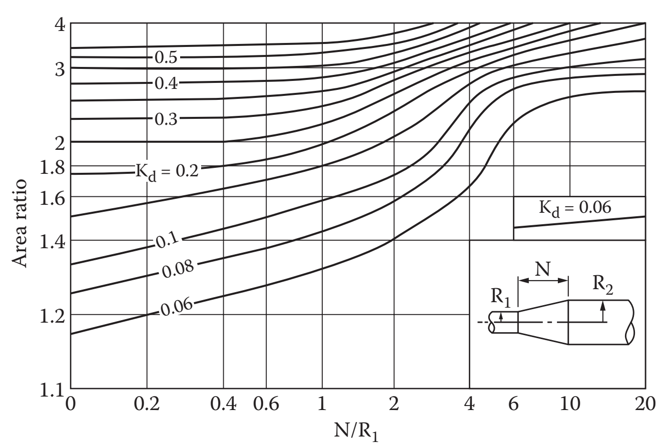

FIGURE 7.6 Gradual expansion loss coefficients.

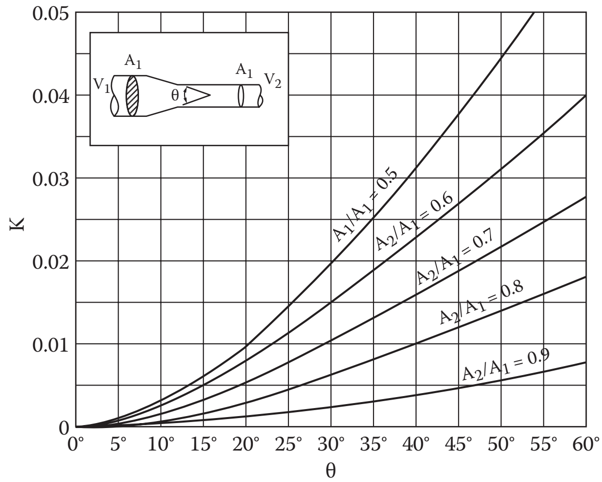

FIGURE 7.7 Gradual contraction loss coefficients.

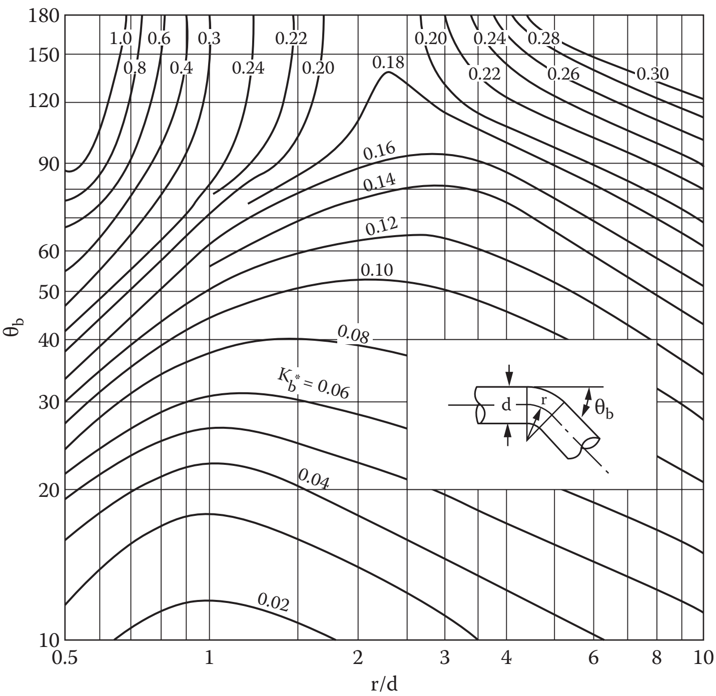

FIGURE 7.8 Bend loss coefficients.

In general, ensure that total head loss for the design flow is between 5% and 10% of the gross head—that is, 95% to 90% penstock efficiency. If the head loss is higher than 10% of the gross head, repeat calculations with larger diameter. Similarly, if the head loss is less than 5%, the pipe diameter may be uneconomic; therefore, repeat calculations using smaller diameters.

Note that in exceptional cases, a less efficient penstock may be more economical, such as when the power demand is limited, the penstock is long and there is abundant flow in the river even during the low-flow season. In such cases, a higher flow can be allowed in a smaller pipe allowing a higher

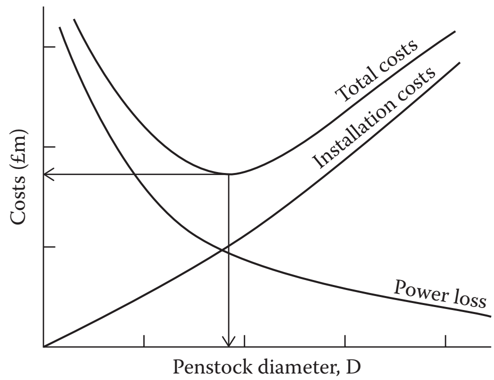

FIGURE 7.9 Penstock optimization curves.

head loss. Hence, savings can be made in the cost of pipes. Similarly, a more efficient penstock pipe could be selected when the power demand is high or higher rates per unit are offered by the utility (in case of grid-connected plant), and there is limited flow available in the river for power generation. However, these approaches should be justified by a detailed economic analysis.

7.4.3.2 Calculate Thickness of Pipe

The thickness of pipe is calculated by calculating stress in the pipe due to topographic head and surge head. Additional thickness is added to allow for corrosion of pipe (2–3 mm). The safety of pipe should also be checked for negative pressure. The overall safety factor should be above three, depending upon the risk and associated cost.

7.4.3.3 Calculate the Cost

Calculate the cost of energy loss due to head loss and the total cost of the pipe. Also calculate the total cost of the pipe installation (i.e., sum of pipe cost and energy loss) for each size of pipes. The diameter that gives the least cost should then be selected. The cost is graphically shown in Figure 7.9.

7.4.3.4 Select the Pipe

The final step is to select the pipe that gives minimum total cost. The pipe that will be available in the market easily will be more cheaper than the pipe with special diameters.

7.5 SURGE PRESSURE IN PENSTOCK

7.5.1 General

The thickness of the penstock pipe is determined by the gross and surge heads of the scheme. It is therefore important to have some understanding of the concept of surge before calculating the pipe wall thickness.

A sudden blockage of water or rapid change in velocity in the penstock (or any pipe that has pressure flow) results in very high instantaneous pressure. This high pressure is known as surge pressure or often referred to as water hammer. Surge pressure travels as positive and negative waves throughout the length of the penstock pipe. Water hammer occurs as the surge wave travels from the source or the origin of the disturbance along the pipeline until it strikes some boundary condition (such as a valve or other obstruction) and is then reflected or refracted. If the pipe is strong enough to withstand the initial surge effect, the pressure will ultimately dissipate through friction losses in the water and pipe wall as well as through the forebay. The speed of the surge wave (wave velocity) is dependent on such factors as the bulk modulus of water, flexibility of the pipe, and the ratio of pipe diameter to wall thickness.

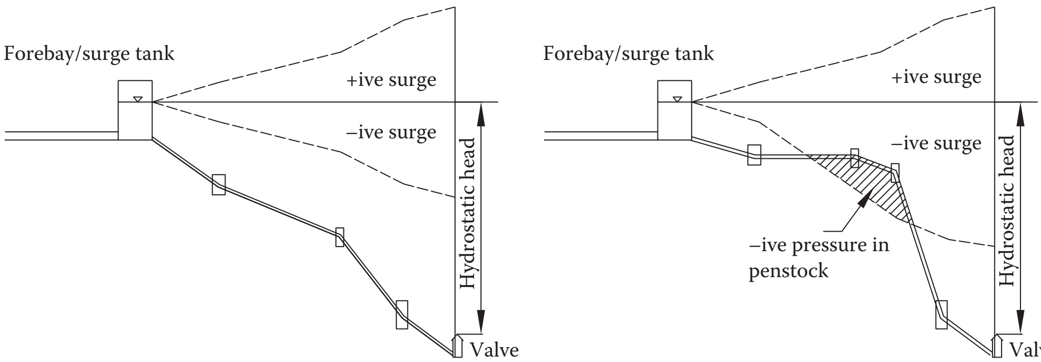

FIGURE 7.10 Surge pressure in penstock.

In hydropower schemes, positive surge characteristics are different for different types of turbines. Surge head calculations for the two most common turbines are discussed here. Note that these calculations are based on the initial (i.e., undampened) positive surge head. In practice, there will be some damping of the surge pressure as the wave travels along the pipe, and while the pressure fluctuation is uniform in the lower portion, it diminishes gradually to zero at the forebay as shown in Figure 7.10. However, the pipe is normally designed for static head plus constant positive surge over the full penstock length.

Note that the negative surge can produce dangerous negative (subatmospheric) pressure in a penstock if the profile is as in Figure 7.10. Once the negative pressure reaches 10 m, the water column separates, and subsequent rejoining will cause high positive surge pressure sufficient to burst the penstock. Subatmospheric pressures less than 10 m can cause inward collapse of the pipe wall, so it should also be avoided [4]. If there is any possibility of negative pressure, the pipe wall thickness must be checked for buckling.

From the Euler equation, we have

$$H = \frac{L}{g} \cdot \frac{\Delta v}{\Delta t}$$

where H is the surge head. Suppose the gate valve is being closed; then the water column deaccelerates during time Δt. Δv denotes the change in velocity. In case of complete closure, $\Delta v = v - 0 = v$. In case of partial closure $\Delta v = v - v1$.

The expression $\frac{L}{\Delta t} = a$ denotes the rate of deacceleration of the water column. It also indicates the celerity of the pressure wave induced by deacceleration of water column. Thus,

$$H = a\frac{\Delta v}{g}.$$

The velocity a is the same as the velocity of sound in the water and is given by the relationship

$$a = \sqrt{\frac{K}{\rho}}$$

where K (= $2.07 \cdot 10^9$ N/m^2) is the bulk modulus of water, and ρ is the density of water. The value of a is about 1440 for water.

The velocity of the water hammer is less for elastic pipes. The velocity in elastic pipe is given by

$$a = \sqrt{\frac{K}{\rho\left(1+\frac{KD}{Et}\right)}}$$

where E is elasticity of pipe material, D is diameter of pipe, and t is thickness of pipe.

When turbine gates are closed, pressure waves travel upward toward the forebay. The waves are then reflected back from the forebay to the turbine. The time of one complete cycle is called critical time. It is expressed as [4]

$$T_c = \frac{2L}{a}.$$

If the closure time is less than given by the above equation, then the surge head is approximately given by $H = a\frac{v}{g}$. However, if the closure time is greater than the critical time, then the negative pressure waves will be superimposed on the positive waves, and the full pressure will not be realized. The water hammer pressure (H′) developed by the gradual closure of valve is given by

$$H' = \frac{T}{T_c}H.$$

7.5.2 Pelton Turbine

For a Pelton turbine, use the following method to calculate the surge head:

1. First calculate the pressure wave velocity a using the equation below.

$$a = \frac{1440}{\sqrt{\left(1+\frac{2150D}{Et}\right)}}\ \text{m/s}$$

   where $K = 2.07 \cdot 10^9$ N/m^2, E is Young's modulus in N/mm^2 of the pipe, and d is the pipe diameter (mm). t is the nominal wall thickness (mm), not $t_{effective}$.
2. Then calculate the surge head (h_{surge}) using the following equation: $h_{surge} = av/g \cdot 1/n$ where n is the total no. of nozzles in the turbine(s).

   Note that in a Pelton turbine, it is highly unlikely for more than one nozzle to be blocked instantaneously. Therefore, the surge head is divided by the number of nozzles (n). For example, if a penstock empties into two Pelton turbines with two nozzles on each turbine, n = 4.

   The velocity in the penstock (V) is $V = \frac{4Q}{\pi d^2}$.
3. Now calculate the total head: $h_{total} = h_{gross} + h_{surge}$.
4. As a precaution, calculate the critical time, T_c, from the following equation: $T_c = (2L)/a$ where T_c is the critical time in seconds, L is the length of penstock in m, and a is the wave velocity calculated earlier.

If the turbine valve closure time, T, is less than T_c, then the surge pressure wave is significantly high. Similarly, the longer T is compared to T_c, the lower the surge effect.

Note that this calculation is based on the assumption that the penstock diameter, material, and wall thickness are uniform. If any of these parameters vary, then separate calculations should be done for each section.

Also note that when $T = T_c$, the peak surge pressure is felt by the valve at the end of the penstock. If a pressure gauge is not installed upstream of the valve, a valve closure time of twice the critical time (i.e., $T > 2T_c$) is recommended.

The design engineer should inform the turbine manufacturer of the closure time (T) so that, if possible, the manufacturer can choose the thread size and shaft diameter such that it will be difficult to close the valve in less than twice the calculated closure time. The operator at the powerhouse should be made aware of this closure time and the consequences of rapid valve closure.

If the gross head of the scheme is more than 50 m, it is recommended that a pressure gauge be placed just upstream of the valve. Compared to the cost of the turbine and the penstock, the cost of such a device is low and is worth the investment. When the operator closes or opens the valve, his speed should be such that there is no observable change in the pressure gauge reading.

7.5.3 Cross-Flow Turbine

In a cross-flow turbine, instantaneous blockage of water is not possible because there is no obstruction at the end of the manifold (i.e., cross-flow turbine has a rectangular bore opening instead of a nozzle). Therefore, surge pressure can develop only if the runner valve is closed rapidly. For a cross-flow turbine use the following method to calculate the surge head:

1. Calculate the pressure wave velocity

$$a = \frac{1440}{\sqrt{\left(1 + \frac{2150D}{Et}\right)}}, \text{ m/s.}$$

2. Now calculate the critical time T_c, similar to the Pelton turbine case: $T_c = (2L)/a$
3. Choose a closure time, T (in seconds), such that: $T > 2T_c$

   Similar to the Pelton turbine case, the design engineer should inform the turbine manufacturer of the closure time (T), and the operator at the powerhouse should be made aware of this closure time.
4. Now calculate the parameter k using the following equation:

$$k = \left(\frac{LV}{g \cdot h_{gross} \cdot t}\right)^2.$$

5. Calculate surge head by substituting the value of k in the equation below:

$$h_{surge} = \left(\frac{k}{2} \pm \sqrt{k + \frac{k^2}{4}}\right) h_{gross}.$$

If k is less than 0.01 (i.e., closure time T is long enough), then the following simplified equation can also be used:

$$h_{surge} = h_{gross}\sqrt{k}.$$

Note that if the valve is closed instantaneously, the entire length of the penstock will experience a peak pressure as follows:

$$h_{surge} = av/g \text{ (i.e., same as in the case of Pelton turbine with one nozzle).}$$

However, in practice, it will take at least five to 10 seconds for the operator to close the valve; therefore, in a cross-flow turbine, instantaneous surge pressure is not a problem.

If the gross head of the scheme is more than 50 m, a pressure gauge should be placed upstream of the valve to control its closing/opening speed, as in the case of a Pelton turbine.

7.5.4 Quick Method for Small Schemes with Cross-Flow Turbines

For small micro hydro schemes using cross-flow turbines (such as milling schemes) in which the power output is less than 20 kW and the gross head is less than 20 m, this quick method may be used by adding 20% to the gross head to allow for the surge head—that is, $h_{surge} = 1.2 \cdot h_{gross}$. This results in a more conservative value for the surge head, but its contribution to the increase in the thickness would be insignificant because the h_{gross} is low.

7.6 PIPE WALL THICKNESS

The pipe shell is designed for positive internal and negative surge pressure, external loadings during construction, and operation and transportation requirements.

7.6.1 Positive Internal Pressure

The thickness required to resist the internal hoop pressure is given by the relationship:

$$t = \frac{PR}{f\eta} + \varepsilon$$

where t = thickness of pipe, P = internal pressure, R = internal radius of pipe in cm, f = allowable stress, η = welding joint efficiency, and ε = corrosion allowance.

However, in practice, the following design procedure is adopted.

Once the surge head has been determined, the nominal wall thickness (t) can be calculated as follows:

1. If the pipe is mild steel, it is subject to corrosion and welding or rolling defects. Its effective thickness, $t_{effective}$, will therefore be less than the nominal thickness. Therefore, for mild steel, assume a nominal thickness (t), and to calculate $t_{effective}$, use the following guidelines [5]:
   a. Use a safety factor of 1.1 to allow for welding defects.
   b. Use safety factor of 1.2 to allow for rolling inaccuracy of the flat sheets.
   c. Because mild steel pipe is subject to corrosion.

   The recommended penstock design life is 10 years for schemes up to 20 kW, 15 years for schemes of 20–50 kW, and 20 years for schemes of 50–100 kW. These figures may be adjusted on the basis of a financial analysis. For example, the effective thickness of a 3-mm-thick mild steel pipe designed for a 10-year life is

$$t_{effective} = \frac{3}{1.1 \cdot 1.2} = 1.27.$$

From this example, it is clear that if a mild steel pipe is used, the nominal wall thickness (t) should be at least 3 mm.

Note that this does not apply for HDPE pipes: Their effective thickness is the nominal wall thickness of the pipe. A low-temperature correction factor may apply to PVC pipes; refer to the pipe manufacturer: If the temperatures are subzero, $t_{effective}$ may be as low as 0.5 t. Apart from protection from ultraviolet degradation, this is another reason to bury PVC pipes at high altitude.

2. Now calculate the safety factor (SF) from the following equation [4]:

$$SF = \frac{200\, t_{effective} S}{h_{total} d}$$

where $t_{effective}$ is the effective thickness, and d is the internal diameter of the pipe. Note that the same units (m or mm) should be used for both $t_{effective}$ and d because they cancel out in the above equation.

S is the ultimate tensile strength of the pipe material in N/mm^2.

h_{total} is the total head on the penstock as follows:

$$h_{total} = h_{gross} + h_{surge}.$$

For mild steel or PVC pipes, if SF < 3.5, reject this penstock option and repeat the calculation for the thicker walled option. However, SF ≥ 2.5 can be accepted for steel pipes if the surge head has been calculated accurately and all of the following conditions are met:

a. There are experienced staff on-site who have installed penstock pipes of similar pressures and materials.
b. Slow-closing valves are incorporated at the powerhouse and the design is such that a sudden stoppage of the entire flow is not possible.
c. Damage and safety risks are minimal. For example, even if the pipe bursts, it will not cause landslides or other instability problems in the short run.
d. Careful pressure testing to total head has been performed before commissioning.

For HDPE pipes, HDPE pipes are available in discrete thicknesses based on the pressure ratings (kg/cm^2) or static heads. The designer should set SF ≥ 1.5 and calculate $t_{effective}$ (note that $t = t_{effective}$ for HDPE). Then from the manufacturer's catalogue the actual thickness should be chosen such that it is equal to or larger than the calculated $t_{effective}$. The safety factor should then be checked using the actual thickness. For HDPE pipes, it is recommended that the safety factor always be at least equal to 1.5.

7.6.2 Negative Internal Pressure

The pipe wall thickness should be checked for buckling if the negative surge can produce negative internal pressure in the pipe. The shape of the negative surge pressure profile cannot be accurately determined. It can be approximately calculated by assuming it is horizontal in the lower half of the penstock and diminishes gradually in the upper half to zero at the forebay.

In order to provide an adequate factor of safety against buckling, the minimum pipe wall thickness is given by

$$t_{effective} \geq d\left(\frac{FP}{2E}\right)^{0.33}$$

where $t_{effective}$ is the effective pipe wall thickness in mm, d is the pipe internal diameter in mm, F is the factor of safety against buckling (two for buried penstock and four for exposed penstock), P is the negative pressure in N/mm^2 (10 m head = 0.1 N/mm^2), and E is Young's modulus for the pipe material in N/mm^2.

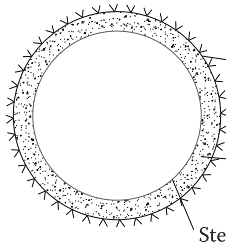

FIGURE 7.11 Steel penstock inside tunnel.

If the steel quality is uncertain, it is best to ask for samples and have them independently tested at laboratories. Properties of PVC and HDPE vary considerably; they should be confirmed from manufacturers' catalogues or by laboratory tests.

7.6.3 Transportation Requirements

Minimum plate thickness of the pipe shell is required to account for the possibility of deformation during transport. The minimum thickness recommended by USBR is given by

$$t = \frac{D + 800}{400}$$

where t = minimum thickness of pipe shell in mm, and D = internal diameter of pipe in mm.

7.6.4 Embedded Penstock

The penstock may be embedded inside a concrete casing, or it may be used as a steel lining in vertical and inclined shafts in tunnels. In the case of tunnels, the space between the rock surface and steel should be filled with concrete, and perfect contact is made by extensive grouting. Such contact creates structural interaction, and thus, a part of the load is transmitted to the rock, and the hoop stress in the pipe is much lower (Figure 7.11).

7.7 PENSTOCK ACCESSORIES

7.7.1 Air Vents and Air Valves

Air vents and air valves are provided on the immediate downstream side of the control gate or valve and in vertical bends to release air that may get trapped inside the penstock. Such air pockets can drastically reduce the transmitting capacity of the penstock. Air inlets serve the purpose of admitting air into the pipes when the control gate or valve is closed and the penstock is drained, thus avoiding collapse of the pipe due to vacuum excessive negative pressure [6]. Similarly, when the penstock is being filled up, these vents allow proper escape of air from the pipes where the pipe has bends as shown in Figure 7.12. USBR suggests the capacity of the air vent to be designed as a conduit to pass 25% of design discharge.

7.7.2 Drain Pipes

Sometimes, the pipes have to be installed in inverted positions as shown in Figure 7.13. To drain the pipe for inspection and maintenance, valves should be installed at the lowest point. Such valves are put in pairs to avoid any leakage and also for the maintenance of the valve itself.

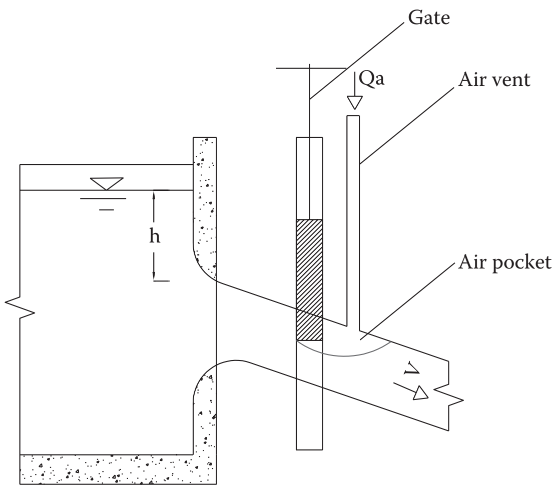

FIGURE 7.12 Air vent near forebay.

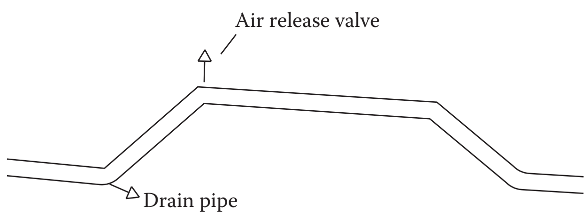

FIGURE 7.13 Location of air release valve and drain pipes.

7.7.3 Pressure Relief Valves

During quick closing of a wicket gate, there is a rapid rise in pressure causing a surge in penstock. The surge pressure can be decreased by installing pressure relief valves. When the gate is closed, this valve automatically opens when it detects an increase in pressure; thus, the water in the penstock continues to move regardless of closure. The downside is that water is wasted from this valve. Therefore, it must be designed to close gradually when it detects closure of the wicket gates.

7.7.4 Bends and Branches

The inclusion of bends in the pipes is required as dictated by topography. The bend in a pipe generates a large impulse due to change in momentum. To keep those forces to a minimum, bend angles should be preferably less than 10°. To achieve hydraulically smooth flow, the bends and branches in pipelines should be bent with a radius not less than three to five times the diameter of pipe.

7.8 PIPE JOINTING

7.8.1 General

Individual mild steel penstock pipes can be joined on-site by two conventional methods, namely site welding and via flanges. Each of these methods has its own advantages and disadvantages as discussed in Table 7.2.

TABLE 7.2
Comparison between Site Welding and Flange Connection

Pipe-Joining Method	Advantage	Disadvantage	General Recommendations and Comments
Site welding	Easy to fabricate at workshop because flanges do not have to be welded at pipe ends. A properly welded pipe will not leak and requires less maintenance.	Higher degree of precision work required on-site to weld the pipe ends. Improper welds can cause leaks and the pipe can burst at high heads. Need to transport a welding machine and a generator at site. Also requires supply of gas/diesel to site.	Difficult logistics if the site is more than a day's walk from the road head. Generally not economic for small schemes and/or short penstock lengths. Select this option only if the site staff are experienced, the site is less than a day's walk from the road head, and the penstock length is more than 50 m.
Flange connection	Easy to install on-site. Site installation work involves placing a gasket between the flanges and bolting them.	Fabrication cost is high welded at ends. Also there is some wastage because the flange is prepared by removing the central disc of a diameter equal to the external pipe diameter. The pipe alignment and the bends cannot be adjusted on-site. Can leak if the bolts are not well tightened or if gaskets are of poor quality. Higher risk of vandalism because the bolts can be removed.	Flange connection is appropriate for schemes that are located more than a day's walk from the road head and/or have a relatively short penstock length. Minimum flange thickness should be at least twice the penstock wall thickness or 8 mm, whichever is larger. A minimum bolt diameter of 12 mm is recommended. A minimum gasket thickness of 5 mm is recommended. Should be above ground.

Source: ITDG, *Civil Works Guidelines for Micro-Hydropower in Nepal*, BPC Hydroconsult and Intermediate Technology Development Group, Kathmandu, Nepal, 2002.

7.8.2 Site Welding

This involves transporting a welding machine and diesel or gas to the site, then joining the pipes by welding together the ends as shown in Figure 7.14.

7.8.3 Flange Connection

This involves welding flanges (that have bolt holes) at both ends of the pipes in the workshop, then joining them on-site by bolting them together. A rubber gasket should be placed between the flanges for tightness and to prevent leakage.

7.8.4 HDPE and PVC Pipes

For HDPE pipes, the best method of joining them is by heat welding. Although special flanges are available to connect HDPE pipes, they are generally more expensive than the cost incurred in heat welding them. HPDE pipes are available in rolls for small diameter (up to 50 mm), and for larger diameter they are available in discrete lengths (3 m to 6 m).

PVC pipes with small diameter (up to 200 mm) have sockets at one end such that another pipe can be inserted inside after applying the solution at the ends. Larger diameter PVC pipes are joined with a coupler, which is a short pipe section with an inside diameter equal to the outside diameter of the pipes to be joined. The solution is applied on the connecting surfaces of both the coupler and the pipes and then joined together.

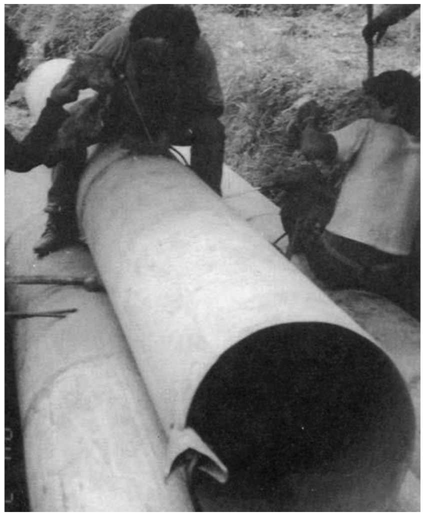

FIGURE 7.14 Site welding of penstock pipe.

7.9 PIPE LENGTHS

Mild steel pipes can be manufactured at the workshop in almost any length required. PVC and HDPE pipes are available in fixed lengths (3 m to 6 m). Although shorter pipes are easy to transport, additional costs will have to be incurred in joining them on-site (more flanges or welding work). It should be noted that, unlike cement bags, animals (mules and yaks) do not usually carry penstock pipes because of the shapes and lengths involved.

Sometimes, due to the weight involved, the only option for transporting the generator and turbine to a remote site is by a helicopter. In such cases, it may be possible to transport the penstock pipes in the same trip with the current transport helicopter.

7.9.1 Mild Steel Pipe

The following factors should be considered when sizing mild steel pipes.

1. In general, pipes longer than 6 m should not be manufactured because they will be difficult to transport on trucks.
2. If the pipes need to be carried by porters from the road head, the weight should be such that an individual length can be carried by one or two porters. For example, if the pipe weight is about 50 kg, usually one porter can carry it. Similarly, two porters may be to able carry up to 90 kg. Therefore, it is optimum to size pipes accordingly, especially if the penstock length is long and the site is located more than a day's walk from the road head.
3. For flat, rolled pipes, the manufacturing costs will be less if the pipe length is a multiple of the available steel plate width. For example, if pipes are rolled from 1.2 m wide plates, lengths of 1.2 m, 2.4 m, or 3.6 m, etc., will lower manufacturing costs.

7.9.2 HDPE and PVC Pipes

As mentioned earlier, these pipes are manufactured in the factory at fixed lengths, but they can be cut in half or one third of the length for ease of transportation. However, a PVC pipe with a socket at one end should not be cut because rejoining will not be possible without a special collar. The following factors should be considered when determining the length of HDPE and PVC pipes.

7.10 EXPOSED VERSUS BURIED PENSTOCK

HDPE and PVC pipes should always be buried. This minimizes thermal movement and protects the pipe against impact, vandalism, and ultraviolet degradation. Flanged steel pipe should be above ground. This is because the gaskets may need to be replaced during the life of the scheme. Mild steel penstock with welded joints can be either buried or above ground. However, maintenance of buried pipe is difficult; therefore, the original painting and backfilling must be carefully supervised to ensure that corrosion does not reduce the life of the penstock. Sometimes part of the penstock alignment may be above ground and part buried. In such cases, it is best to make the transition at an anchor block; otherwise, careful detailing is required. An example of such detailing at the transition is the use of a retaining masonry wall with a larger diameter mild steel pipe through which the penstock comes out and can accommodate thermal expansion and contraction (Figure 7.15). An expansion joint should normally be used immediately downstream of the retaining wall. The advantages and disadvantages of buried penstock pipes are given below.

For buried pipes, a minimum cover of 1 m should be provided in all cases (i.e., HDPE, PVC, and mild steel pipes). Buried pipes do not require support piers, and the savings made on the piers may equal or even exceed the cost of excavation and backfill. Because this is a site-specific case, a cost calculation should be done if buried mild steel pipe is being considered. Both exposed and buried penstock pipes require anchor blocks at significant bends. However, for relatively low head and flow as well as small bend angles, the 1 m depth of well-compacted soil cover on buried pipe may be adequate. The nature of the terrain and the soil depth may also govern whether to bury or expose the penstock pipe. Buried penstock is not practicable on routes steeper than 30° because the backfill will be unstable. Where topsoil is thin or rock is exposed, the costs involved in excavating the rock may make burial of the pipe very difficult.

7.10.1 Expansion Joints

Penstock pipes are subjected to temperature variations due to changes in the ambient temperature. When the ambient temperature is high, pipes will expand, and when it drops, the pipes will contract. Such thermal expansion causes stresses in the pipes.

An aboveground penstock is subjected to greater temperature variations, resulting in higher thermal expansion. The thermal expansion or contraction is highest when the penstock is empty, such as

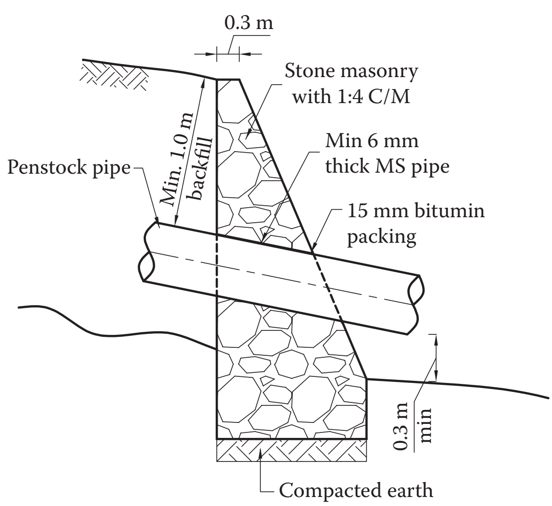

FIGURE 7.15 Transition from buried to exposed penstock.

during installation or repair work. The temperature variation is relatively low when the pipe is full because the flow of water with fairly constant temperature prevents the pipe from rapidly heating up. As long as pipes are free to move at one end, thermal expansion does not cause additional stresses. However, a penstock pipe section between two anchor blocks is kept fixed at both ends. In such a case, thermal expansion could cause additional stresses, and the pipe can even buckle. Therefore, provision must be made for the penstock pipe to expand and contract by installing an expansion joint in a penstock pipe section between two anchor blocks. The most common type of expansion joint used is of the sliding type. This is shown in Figure 7.16. Such an expansion joint is placed between two consecutive pipe lengths and bolted to them. The stay rings are tightened, which compresses the packing and prevents leaking. Jute or other similar type of fiber is used for packing. When the pipes expand or contract, the change in lengths is accommodated inside the joint section because there is a gap between the pipes. An advantage of an expansion joint is that it reduces the size of the anchor blocks because they will not need to withstand forces due to pipe expansion. Another advantage is that they can accommodate slight angular pipe misalignment. Expansion joint requirements for various penstock conditions are discussed below.

7.10.1.1 Mild Steel Pipes

An expansion joint should always be incorporated immediately downstream of the forebay and immediately downstream of each anchor block for both aboveground and buried steel pipe. One is also recommended immediately downstream of a transition from buried to above ground pipe.

7.10.1.2 HDPE Pipes

Expansion joints are not necessary for HDPE penstock pipes provided that they are buried (which should always be the case). This is because HDPE pipes are flexible and can bend to accommodate the expansion effects due to the differences in temperature between installation and operational phases.

7.10.1.3 PVC Pipes

PVC pipes with glued joints require provision for expansion at the same locations as for steel pipes.

7.10.1.4 Sizing of Expansion Joints

The sliding surface of the expansion joints should be machine finished (such as in a lathe machine) to a tolerance of about 0.1 mm. The recommended thickness of the steel parts (retainer and stay ring) is about twice the thickness of a well-designed penstock pipe.

The gap in the expansion joint should be about twice the calculated maximum pipe expansion length.

The maximum expansion length is calculated using the following equation:

$$\Delta L = \alpha(T_{hot} - T_{cold})L$$

where

ΔL = pipe expansion length in m as shown in Figure 7.16.

α = coefficient of linear expansion in m/m °C of the pipe, which depends on the pipe material. This coefficient relates to the length that a material will expand per 1°C increase of temperature. Different materials expand at different rates.

T_{hot} = highest temperature in °C that the pipe will experience. Note that this can even be during midsummer afternoon when the pipe is empty (either during installation or repair work).

T_{cold} = lowest temperature in °C that the pipe will experience. This can be during winter when the water temperature is just above the freezing point. Note that if freezing temperatures are expected, the pipe should either be emptied or provision should be made for constant flow.

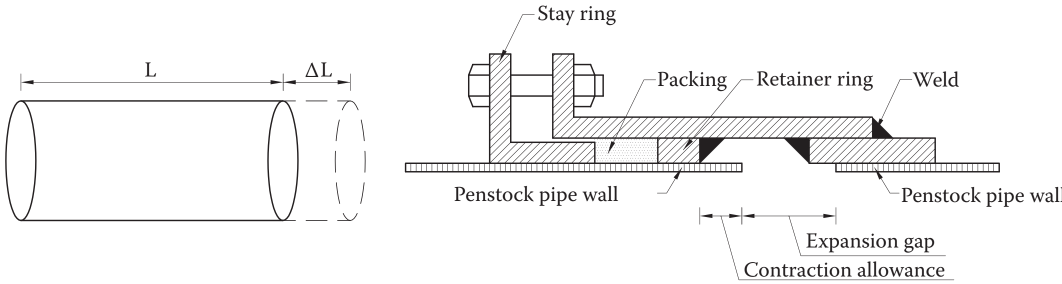

FIGURE 7.16 Expansion joints.

If the water in the penstock stagnates during freezing temperature, ice will form inside the pipe and could burst it because when water freezes, the volume expands.

L = pipe length in m. Because it may be difficult to determine when the expansion joint will be installed on-site, the manufacturer should be asked to allow an expansion gap of 2 ΔL. Then, during installation, the temperature should be noted and the gap left accordingly.

7.11 PAINTING

Because mild steel pipes are subjected to corrosion, appropriate coats of paint should be applied before dispatching them to site. Proper painting of mild steel pipes significantly increases their useful lives.

The pipes should be sandblasted if possible; otherwise they should be thoroughly cleaned using a wire brush and a piece of cloth. Prior to painting, the pipe surface should be clean from oil, dust, and other particles. When applying subsequent coats of paint, the previous coat must be dry.

The following coats of paint are recommended:

7.11.1 Outside Surface of Aboveground Mild Steel Pipes

First two coats of primer should be applied on the pipe surface. Red oxide zinc chromate primer is appropriate for this purpose. Then another two coats of high-quality polyurethane enamel paint should be applied on top of the primer.

7.11.2 Outside Surface Pipe Which Will Be Buried or Cast into Anchor Blocks

Two coats of primer similar to aboveground pipe should be applied. Then, another two coats of high-build bituminous paint should be applied over the primer. An extra coat of bituminous paint should be provided at transition areas, which are more prone to corrosion.

7.11.3 Inside Surface of Pipes

For small-diameter pipes, it may not be possible to paint the inside surface. However, whenever possible, the inside surface should be painted with two coats of good-quality red lead primer. If there is a doubt about the quality of paint, the supplier's specifications should be checked prior to its use. Note that paintwork is not required for HDPE or PVC pipes. Any paintwork damaged during transport and installation must be made good so that the full number of coats is present everywhere. This is especially important for buried pipes.

7.12 INSTALLATION

The following procedure should be used:

a. The centerline of the penstock should be set out using a cord and pegs along the selected route.
b. A line should be marked by spreading lime on the surface of the ground to replace the cord. Then the positions of anchor blocks and support piers should be marked to the required spacing for exposed pipes and excavation carried out along this line as required.
c. For buried pipes, the penstock is installed in the excavated trench and backfilled. The backfill should be rammed in layers and a slight hump above the level of the ground helps to keep the alignment dry. An improperly backfilled penstock alignment can quickly become the route for drainage water down the hillside. However, note that backfill should be completed only after the pipe has been pressure tested.
d. For exposed pipes, the anchors and supports should be constructed. The pipe should be cast into the anchors and placed on one support pier at a time. No further supports or anchors should be built until the pipe is secured to the previous anchor block or support pier. For both site-welded and flange-connected pipes, the end should protrude from the last support block with adequate margin (~300 mm) so that either the flange or the weld line does not lie on the support pier during thermal expansion or contraction. If more than one pipe section needs to be welded between the support piers, temporary supports should be used as shown in Figure 7.17. Flange-connected pipes should be joined and the bolts tightened as the installation progresses.

The installation of the penstock should start from the machine foundation and proceed upstream. This avoids any misalignment between the penstock and the turbine housing. Because the turbine needs to be firmly fixed to the machine foundation, there is almost no tolerance at this end after the machine foundation has been constructed. Furthermore, the pipe sections below the expansion joints can slide down if installation proceeds downstream from the forebay. Minor pipe deviation can be adjusted at the forebay wall, but such adjustment is not feasible at the machine foundation. For micro hydro schemes, laying of penstock in discrete lengths is not recommended because this can lead to misalignment of the pipes [3].

FIGURE 7.17 Temporary support for site welding work.

Penstock pipes should be pressure tested at the factory before transport to site. For schemes in which the head is more than 15 m, the completed penstock should also be pressure tested during the commissioning phase. If feasible, such pressure test should include the surge head (i.e., pressure test at h_{total}). This can be done by simulating the expected surge head at the forebay using a manual pressure pump. If any leakage is noticed, the section should be repaired, such as by tightening the bolts, changing faulty gaskets, or welding. For buried pipe alignment, the backfill should only be completed after successful pressure testing; however, if there are any minor bends without anchor blocks, these must be backfilled before pressure testing. Once the pipe trench is backfilled, it will be difficult and time consuming to re-excavate and identify the leaking section.

7.13 MAINTENANCE

Aboveground mild steel penstocks should be repainted every 3 to 4 years, depending on the conditions. Nuts, bolts, and gaskets of flange-connected mild steel pipes should be checked annually, loose bolts should be tightened, and damaged gaskets should be replaced. A visual check for flange leaks should be carried out monthly. For buried penstock sections, signs of leakage, such as the sudden appearance of springs along the alignment (especially during winter) and moist ground where the area was previously dry, should be checked. If any leakage is noticed, the penstock should be drained and carefully excavated for repair of the leaking section.

7.14 CHECKLIST FOR PENSTOCK WORK

a. Decide on the penstock material. When in doubt, compare the costs of all available options.
b. Is the alignment on practical ground slope? Is there adequate space for the powerhouse area at the end of the penstock alignment? Have the bends been minimized?
c. For mild steel pipes, decide on flange connection or site welding. Also be sure to specify appropriate coats of paint.
d. If a buried penstock alignment is being considered, compare the advantages and disadvantages.
e. Is the pipe diameter such that the head loss is between 5% and 10%?
f. Has allowance been made for surge effects while sizing the penstock wall thickness?
g. Is the safety factor sufficient? Are the pipe lengths and weights such that they are transportable and portable?

Example 7.1: Sizing of Expansion Joints

A mild steel penstock pipe is 60 m long between the first and second anchor blocks. The steel temperature during installation was measured at 48.0°C, and the lowest temperature during the winter can be –5.0°C during winter. What expansion gap should be allowed?

Here, $\alpha = 12 \cdot 10^{-6}$ m/m °C
$T_{hot} = 48.0°C$
$T_{cold} = -5.0°C$
$L = 60.0$ m
$\Delta L = \alpha\, a(T_{hot} - T_{cold})L$
or $\Delta L = 12 \cdot 10^{-6}\,(48.0 - (5.0)) \cdot 60.0$
or $\Delta L = 0.038$ m
or $\Delta L = 38$ mm

Therefore a minimum expansion gap of 38 · 2 = 76 mm or say 80 mm should be provided.
If the temperature during installation is 20°C,

$L = 12 \cdot 10^{-6}(40 - 20) \cdot 45$
or $L = 0.011$ m
or $L = 11$ mm

Therefore, during installation, an expansion gap of 11 mm · 2 = 22 mm should be provided.

Example 7.2

A penstock is to be designed for 3 m/s of discharge with a head of 50 m. There are three bends with angles of 20°, 42°, and 20°. Design the penstock with steel if the turbine is the cross-flow type and the length of the penstock is 140 m.

Pipe Diameter Calculation

Steps	Calculations	Result
Step 1 Calculate the internal pipe diameter:	Set V = 3.5 m/s As, $Q = A \cdot V$ $= \pi D^2/4 \cdot V$ Or $D = \sqrt{\frac{4Q}{\pi V}}$ $D = \sqrt{\frac{4 \cdot 3}{\pi \cdot 3.5}}$ D = 1.04 m Select pipe with 1.0 m Actual velocity V = Q/A Or $V = \frac{4Q}{\pi d^2}$ $V = \frac{4 \cdot 3}{\pi \cdot 1^2}$ = 3.82 m/s (less than max permissible velocity. ok)	D = 1.00 m V = 3.82 m/s
Step 2 Calculate friction factor	Roughness of pipe, k = 0.06 mm $k/D = 0.06/1000 = 6 \cdot 10^{-5}$ 1.2 Q/D = 1.2 · 3/1 = 3.6 From Moody's chart, f = 0.012	f = 0.012
Step 3 Calculate head loss	(a) Friction loss $H1 = \frac{flv^2}{2gD}$ $H1 = \frac{0.012 \cdot 140 \cdot 3.82^2}{2 \cdot 9.81 \cdot 1}$ = 1.25 m (b) Inlet loss $H2 = K\frac{v^2}{2g}$ Assume sharp edge entrance, K = 0.5 $H2 = 0.5\frac{3.82^2}{2 \cdot 9.81}$ = 0.372 m	Hl = 1.719 m

(*Continued*)

	(c) Bend loss $$H3 = \sum k \frac{v^2}{2g}$$ Assume the radius of bend to be 2D = 2 · 1 = 2 m i.e., r/D = 2 For 20° bend: K1 = 0.05 For 42° bend: K2 = 0.08 $$H3 = (0.05 + 0.08)\frac{3.82^2}{2 \cdot 9.81}$$ H3 = 0.097 m Total head loss $$H1 = H1 + H2 + H3$$ $$= 1.25 + 0.372 + 0.097$$ $$= 1.719 \text{ m}$$
Step 4 Calculate surge head and critical closure time	$$a = \frac{1440}{\sqrt{\left(1 + \frac{2150D}{Et}\right)}}$$ Assume thickness of pipe to be 16 mm $$a = \frac{1440}{\sqrt{\left(1 + \frac{2150 \cdot 1000}{2 \cdot 10^5 \cdot 16}\right)}}$$ $$a = 1114 \text{ m/s}$$ Critical closure time is given by 2L/a = 2 · 140/1114 = 0.25 s Chose closure time to be 5 s. Now, for cross-flow turbines $$k = \left(\frac{LV}{g \cdot h_{gross} \cdot t}\right)^2$$ $$k = \left(\frac{140 \cdot 3.82}{9.81 \cdot 50 \cdot 5}\right)^2$$ k = 0.047 $$h_{surge} = \left(\frac{k}{2} \pm \sqrt{k + \frac{k}{4}^2}\right) h_{gross}$$ $H_{upsurge}$ = 12.15 m $H_{downsurge}$ = −9.78 m H_{max} = 50 + 11.40 = 62.16 m H_{min} = 50 − 10.38 = 40.22 m

(*Continued*)

Step 5 Check safety factor of pipe thickness	Effective thickness of pipe allowing 1.5 mm for corrosion during its lifetime $t_{effective} = \frac{t}{1.1 \cdot 1.2} - 1.5$ $t_{effective} = \frac{16}{1.1 \cdot 1.2} - 1.5$ $t_{effective} = 10.62$ mm Safety factor is given by $SF = \frac{200 t_{effective} S}{h_{total} d}$ $SF = \frac{200 \cdot 10.62 \cdot 320}{62.16 \cdot 1000}$ SF = 10.93 > 3 hence ok! (for optimization, thickness should be decreased, and recalculation shall be done)

EXERCISE

With the required data given below, design the penstock and optimize it to get the most economic diameter for the power plant:

Q = 450 lps
$h_{gross} = 180$ m
Bends: 10 vertical bends, θ = 69°, 23°, 26°, 37°, 40°, 2°, 3°, 12°, 8°, and 3°, all mitered.
Material: Penstock material: mild steel, flat rolled, and site welded
Length: 550 m long.
Minimum tensile strength of pipe, S = 400 N/mm^2
Turbine type: Three Pelton turbines with two nozzles in each turbine, therefore n = 3 · 2 = 6.
Overall efficiency = 80%
Lifespan of the project = 15 years
Price of electricity generated = \$0.04/kWhr
Price of steel = \$1000/ton

Assume suitable data whenever necessary.

(Hint: Calculate the required pipe diameter and wall thickness. Note that because the penstock is long, it will be economic to decrease the thickness at lower heads.)

REFERENCES

1. IIT, *Guidelines for Small Hydro Development*, Indian Institute of Technology, Roorkee, 2011.
2. Nigam, P. S., *Handbook of Hydro Electric Engineering*, Roorkee Press, 2008.
3. ITDG, *Civil Works Guidelines for Micro Hydropower in Nepal*, BPC Hydroconsult and Intermediate Technology Development Group, Kathmandu, Nepal, 2002.
4. Mosonyi, E., *High Head Power Plants*, Akademiai Kiado, Budapest, 1991.
5. Harvey, A. and Brown, A., *Micro-Hydro Design Manual: A Guide to Small-Scale Water Power Schemes*, ITDG Publishing, London, 1993.
6. *Technical Standards for Gates and Penstocks*, Hydraulic Gate and Penstock Association, Tokyo, n.d.

8 Powerhouse

8.1 OVERVIEW

The powerhouse accommodates electromechanical equipment, such as the turbine, generator, and control panels. Sometimes in micro hydro power plants, agro-processing units are also incorporated. The main function of the powerhouse building is to protect the electromechanical equipment from adverse weather as well as possible mishandling or vandalism of the equipment by unauthorized persons. The powerhouse should have adequate space such that all equipment can fit in and be accessed without difficulty. The generators, turbines, and other accessories need to be securely fixed on the machine foundation in the powerhouse. This requires a careful design because the equipment generates dynamic forces, and even a slight displacement can cause excessive stresses on various parts and lead to equipment malfunction.

8.2 CLASSIFICATION OF THE POWERHOUSE

Depending upon the location, the powerhouse can be classified as a surface or underground type. The underground powerhouse is built inside the Earth's surface by excavating a cavity. This type of powerhouse requires sound rock. In case of a surface powerhouse, the superstructure is founded above the ground and only the foundation is below the surface. Sometimes, there are also cases in which the machine hall is built underground and the control bay is kept over ground.

Powerhouses can also be classified according to type of water passage provided. For example, in some cases, the powerhouse is built just downstream of a forebay or a reservoir. Such powerhouses draw water directly from the reservoir or the forebay and exclude the penstock pipes. In many large dams, the powerhouse is located at the toe and often inside the dam. In small hydropower projects, the powerhouse is built some distance from the forebay, and water is conveyed to the turbines inside the powerhouse via a penstock pipe.

8.3 EQUIPMENT AND ACCESSORIES IN THE POWERHOUSE

The equipment and accessories required in the powerhouse depend on the size and type of generating machines that have to be accommodated. They also depend on the location of the powerhouse and the layout design that the manufacturer offers [1]. Powerhouse equipment and their functions are briefly described below.

Turbine: This is the equipment that converts the kinetic energy of water in the penstock into mechanical energy. The flowing water rotates the turbine runner, which, in turn, rotates the generator shaft. The type of turbine applicable for a particular hydropower site mainly depends on the available net head and design discharge. Sometimes, more than one type of turbine can be feasible for a given site. In such cases, selection of the turbine is done on the basis of the cost and the corresponding efficiency (for the various turbines considered). Detailed descriptions of turbines and their selection process can be seen in Chapter 9.

Generator: The generator converts the mechanical energy of the turbine into electrical energy. The physical dimensions of the generator depend on its capacity (i.e., power to be produced), type, and rotational speed (RPM). As the turbine shaft is connected to the generator shaft, the layout of the generator also depends on the layout of the turbine, for example, whether the turbine shaft is horizontal or vertical. In a pulley driven system (e.g., belt drive), the generator may be placed on a different level than the turbine. Detailed descriptions of the generator and its selection process can be seen in Chapter 13.

8.3.1 Other Components and Accessories

Apart from the turbine and generator, there are also other components and accessories in the powerhouse. The main components used in micro to small hydropower plants are briefly discussed below.

Inlet valve: This valve is required to control the flows coming from the penstock pipe into the turbine. It is also required for ease of turbine maintenance. This valve facilitates maintenance of the turbine without having to empty the penstock pipe, thus saving stored water volume and eliminating additional time required to refill the penstock pipe. As the pressure at the upstream face of the inlet valve will be very high when fully closed, a bypass is generally provided in the valve that equalizes the pressure when opening it.

Governor: The governor regulates flows into the turbine to match with the fluctuation in demand for power. Based on the power demand, the governor controls the inflows into the turbines. In case of micro hydropower plants, electronic load controllers (ELC) are used instead of the governor. After meeting the power demand of the load center, the ELC diverts additional unused power generated into a ballast. Descriptions of the governor and ELC are provided in Chapters 12 and 13.

Electronic load controller (ELC) and ballast: In small hydropower schemes, such as isolated micro hydro systems, instead of providing costly servomotors and governors for load control, a simple electronic circuit is provided that senses the change in load demand and diverts the unused power to a heat sink (e.g., ballast comprising immersion heaters in a water bank). Thus, power plants with ELC run on constant flow.

Large hydropower plants will have further components in the powerhouse, such as oil purification systems, air compressors, cooling water pumps, a backup power supply, and a separate workshop for equipment maintenance work.

8.4 LAYOUT OF POWERHOUSE

The powerhouse has to accommodate different mechanical and electrical equipment. Some of this equipment is housed in the machine hall, and other equipment is located in the control bay. Basically, the dimensions of the powerhouse depend on the following factors:

a. Dimension and design of electrical and mechanical accessories
b. Orientation of turbine—that is, whether it is of a horizontal or vertical axis type
c. Requirement of space, such as clearance area for efficient operation and maintenance of the generating equipment—the height of the powerhouse is determined by the clearance required to lift a turbine–generator unit while other units are in operation
d. Dewatering and other arrangements
e. Civil engineering consideration, such as column, beam, and wall thickness required; ventilation; and security

The final layout of the powerhouse is fixed after a number of iterations. From an economic design perspective, the following factors should be considered while sizing a powerhouse:

a. Cost of the civil structure of the powerhouse can be very high; thus, effort should be made to make the building as compact as possible. As the span or height of the powerhouse increases, the bending moment increases in geometric ratio requiring larger supports—that is, the beam and columns.

b. From an ease-of-construction perspective, each turbine–generator unit should be founded on a separate block. This also helps to reduce vibrations in the powerhouse. Proper joint locations in transverse and longitudinal directions should be provided. When fixing such joints, concrete pouring capacity (by volume) should be estimated. As a large quantity of concrete and steel are required for the machine foundations, these joints help to construct the blocks separately.
c. Excavation required to construct the powerhouse should be kept to a minimum.

8.4.1 Arrangement of Turbines and Generator

The powerhouse geometry primarily depends on the types of turbine and generator. Different types of geometrical configurations are used based on site conditions and type of units. The main objective should be to minimize the plinth area of the powerhouse. However, construction technology needs to be more advanced as the powerhouse size decreases. Similarly, advanced planning is required to ensure that the powerhouse is efficient and comfortable for operation of the equipment as well as their maintenance, including safe movement of operators inside the building [2].

Some of the common layouts of powerhouse buildings are described below:

Linear layout: This is the most popular layout of the powerhouse due its simplicity and ease of construction. In this layout, each machine is arranged in a single horizontal row, parallel to each other. The machines are either aligned parallel or oblique to the powerhouse walls. Figure 8.1 shows an example of a linear arrangement.

Circular layout: In this layout, the units are arranged in a circular pattern to maximize the use of space. Here, the penstock splits into radial pipes that connect to the turbines. Lifting equipment should be designed in a circular pattern in this layout. Figure 8.2 shows an example of a circular layout. Although this type of layout is compact, it is not commonly used as circular gantry cranes are not widely available.

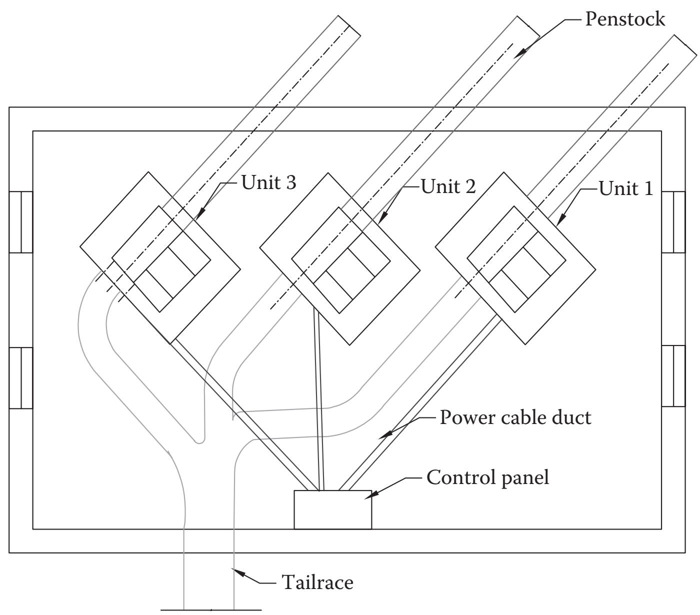

FIGURE 8.1 Linear layout of powerhouse with units kept oblique to the face of the powerhouse.

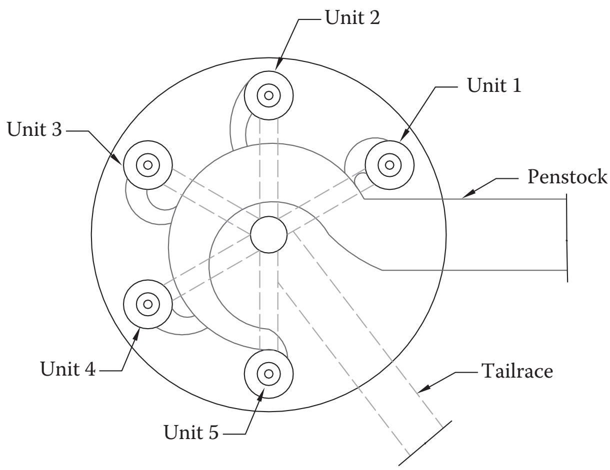

FIGURE 8.2 Circular layout with five units.

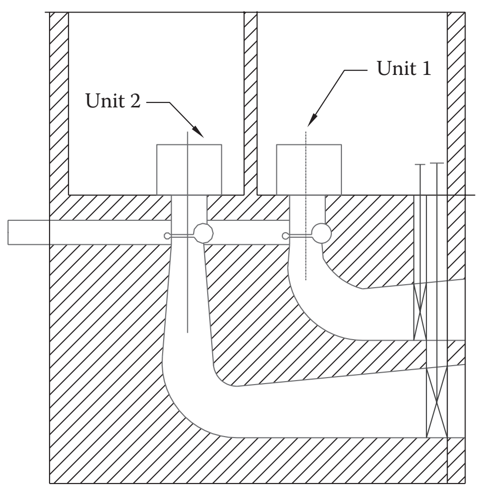

FIGURE 8.3 Multirow layout with two units.

Multirow layout: In this layout, two or more units are installed in a single row. The axis of the turbine is kept the same, and the draft tube is located at different levels as can be seen in Figure 8.3. For vertical axis turbine–generator units, this arrangement can save space requirements.

8.5 COMPONENTS OF POWERHOUSE STRUCTURE

The powerhouse can be broadly divided into three components based on hydraulic and structural functions. These are the following:

Substructure: This is the foundation of the powerhouse, which transfers all superimposed loads to the Earth's surface. The substructure may also embed parts of the turbine to convey water to the tailrace. For example, in reaction turbines, the substructure houses the draft tube.

Intermediate structure: The intermediate structure houses the spiral case in reaction turbines and manifold water jets and spear valves in Pelton turbines.

Superstructure: This part of the powerhouse has no hydraulic function. An overhead crane, roofing, ventilation, and lighting systems are part of the superstructure. In smaller schemes, the cost of the superstructure can be brought down by constructing it in a similar manner as other houses in the local community. For example, instead of a gantry crane, which is attached along the longitudinal beams of the powerhouse, a mobile crane is used in micro hydropower plants. Gantry cranes require larger columns and beams in the powerhouse to accommodate their own weight along with the weight of the turbine–generator parts that they need to lift.

8.6 SITE SELECTION OF THE POWERHOUSE

The location of the powerhouse is governed by the penstock alignment because this building must be located at the end of the penstock. Apart from this, the following criteria are recommended for locating the powerhouse:

- The powerhouse should be safe from not only annual floods, but also rare flood events. Discussions should be held with the local residents to ensure that floodwaters have not reached the proposed powerhouse site within at least the past 20 years. For smaller schemes (micro hydro), it is recommended that the powerhouse be above the 50-year flood level, and for larger schemes, the powerhouse should be protected at least up to the 100-year flood level.
- The tailrace length should be kept as short as possible.
- The proposed location should be accessible throughout the year. In small isolated schemes, the powerhouse should be located close to the community that it serves, provided that the penstock alignment and other parameters are feasible and economical. This will reduce the transmission line cost, and if agro-processing units are also installed in the powerhouse, the community will not have to carry their grain for a long distance.
- The powerhouse should be located on level ground to minimize excavation work. As far as possible, the powerhouse should be founded on stable rock. As an enormous load has to be transferred to the ground from the machine foundations, there is a risk of settlement and foundation failure.
- Geological investigation should be done with all available technologies to avoid any surprises during excavation. A dry location with sound bedrock should be selected.
- Larger schemes should be away from the settlement as far as possible to reduce risk of environmental hazards. However, the powerhouse should be accessible year round.

8.7 DESIGN OF THE POWERHOUSE

8.7.1 General

As discussed earlier, the powerhouse should be as compact as possible without compromising the efficiency of equipment and space required. The space inside the powerhouse should be well lit and ventilated. In smaller community electrification schemes, it is economical and appropriate to construct a powerhouse building similar to other local houses in the community. This type of construction will require nominal supervision. Additionally, windows should be provided for ventilation. Placing a few transparent fiberglass sheets (skylights) in the roof will provide additional illumination in the powerhouse. Flood walls may have to be constructed to prevent entry of water into the powerhouse, especially when it is close to the riverbank.

The design of the powerhouse consists of two stages. In the first stage, the size of the powerhouse is fixed. This comprises sizing the turbine and generator, fixing the location of the control panel and other accessories, and sizing of the control room. Architectural and functional aspects, such as access to different equipment, sometimes on different floor levels; ventilation; lighting systems; and drainage systems of the powerhouse are also finalized at this stage. A thorough understanding of the different fields of engineering is required to finalize equipment arrangements and the plinth area of the powerhouse, especially as the plant size increases. In large power plants, this first stage activity is often done by a multidisciplinary team.

In the second stage, structural design of the powerhouse building is carried out. The design of the superstructure frame (columns and beams), slabs, roof, and machine foundations are undertaken in this stage. The structural design should ensure that the powerhouse structure will be stable against all possible adverse loading conditions (e.g., earthquakes, hurricanes, landslides based on site conditions) throughout its lifetime.

8.7.2 Sizing of the Powerhouse

The overall size of the powerhouse depends mainly upon the size of the turbine. The plan area of the powerhouse should be determined on the following basis [3]:

- The sizes of the electromechanical equipment should be obtained from the manufacturer.
- All required equipment should be drawn to scale and placed on the proposed powerhouse plan area in conjunction with the penstock alignment and the branching arrangement. This may require a few trials to determine the optimum layout.
- Adequate lighting and ventilation should be provided. Note that the door and windows need to be located such that they do not obstruct access to the equipment. This requires coordinating the locations of the equipment, windows, and door.
- Adequate space should be provided such that all equipment is easily accessible. In micro hydropower plants, there should be a clear spacing of at least 1 m around each item of equipment that has moving parts (such as the generator, turbine, and the belt drive). In plants in which agro-processing or other milling equipment is installed, the community members will regularly visit the powerhouse (to process their grains or saw wood). Therefore, additional space is required so that the powerhouse does not become overcrowded and become a potential area for accidents. It is recommended that such additional space is provided as a lobby at the entrance and the equipment placed further beyond. A lobby large enough for five people to wait with their grain (about 3 m by 3 m) may be adequate in the case of an agro-processing mill. For larger power plants, clear spacing between generating units is recommended by the manufacturer.

8.7.3 Examples of Powerhouse Layout

- *Typical Micro Hydropower Plant Powerhouse:* As discussed earlier, micro hydropower powerhouses are simple one-story buildings similar to rural houses. They generally house one or two generating units and other electromechanical accessories. A photograph of a micro hydro powerhouse can be seen in Figure 8.4.

  A plan layout and a sectional view of a typical micro hydropower with a single unit of a horizontal axis Francis turbine can be seen in Figure 8.5.
- *Vertical Axis Francis Turbine for Large Hydropower Plant:* An example of a powerhouse layout with vertical axis Francis turbines is shown from Figures 8.6 through 8.9. This is based on the 22-MW Sanima Mai hydropower plant in Nepal where the powerhouse houses three sets of vertical axis Francis turbines. The design discharge for this plant is 23 m^3/s, and the net head is 120 m.

Figure 8.10 shows a photograph of the front view of the Mai hydropower powerhouse. Note the large entrance door that has been provided for ease of transportation of generating equipment into

FIGURE 8.4 500-kW Tagabi micro hydro powerhouse, Kenya.

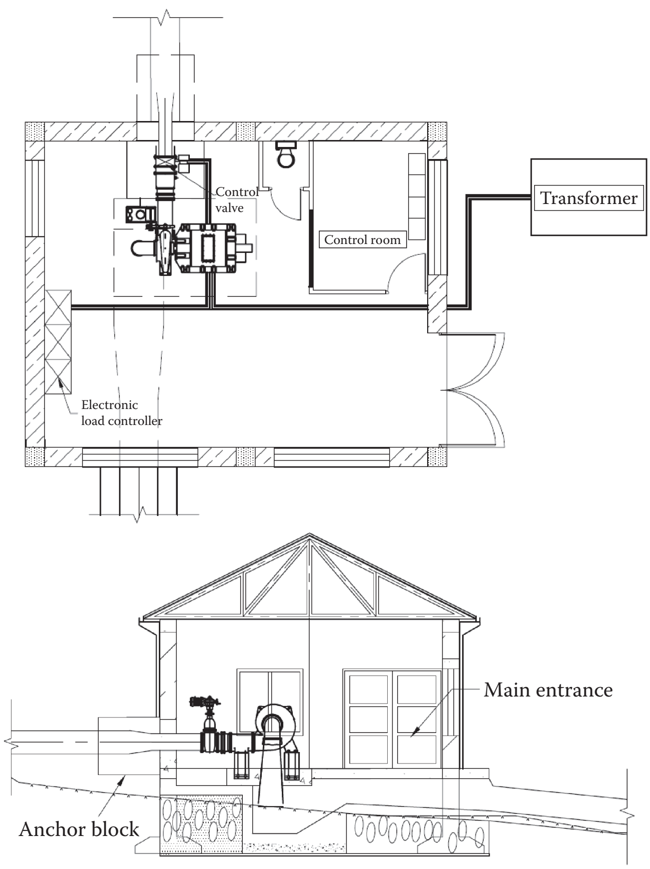

FIGURE 8.5 Plan and sectional view of a typical micro hydropower plant.

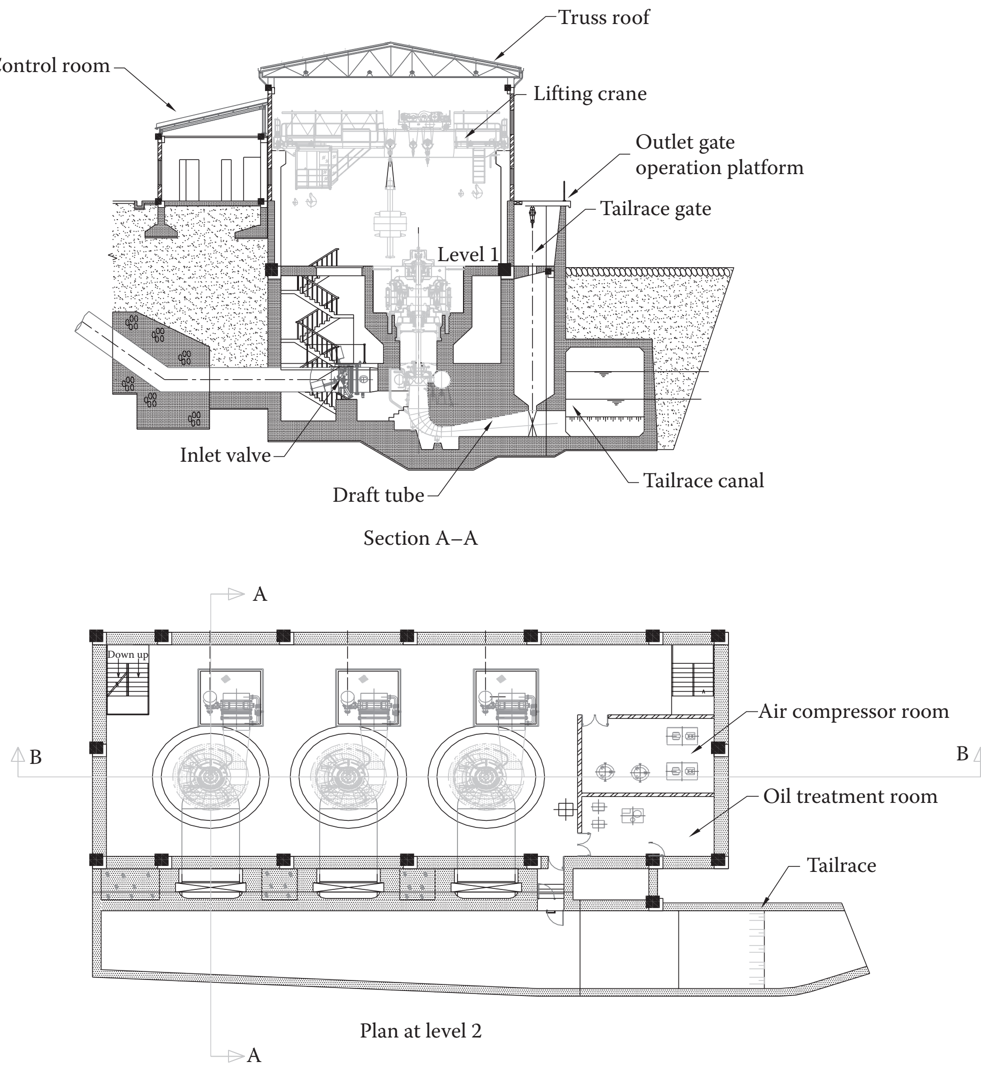

FIGURE 8.6 Powerhouse pan at turbine floor level.

the powerhouse building. Similarly, Figure 8.11 shows the generator floor of the Mai hydropower powerhouse. All equipment is delivered on the generator floor and then placed at the required locations using the gantry crane (moving crane).

8.8 DESIGN OF MACHINE FOUNDATION

The turbine and generator of the powerhouse needs to be well-anchored into the machine foundation, which should withstand all forces that this equipment exerts. The machine foundation transmits static and dynamic loads from the equipment to the Earth's surface. The machine foundation needs to also dampen any vibrations due to the rotation of the machine's moving parts (Figure 8.12).

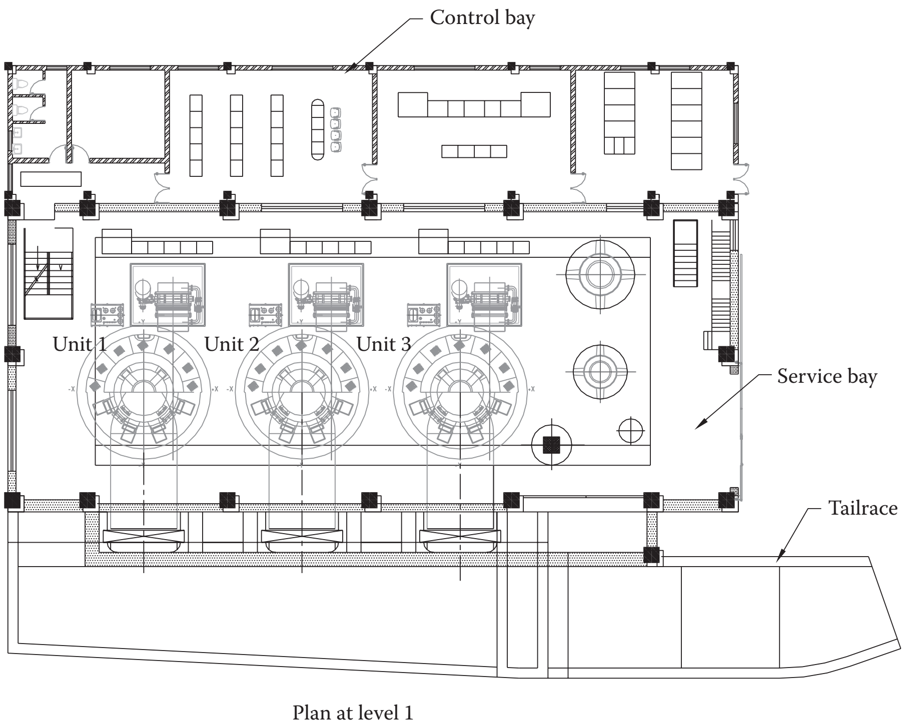

FIGURE 8.7 Powerhouse plan at generator floor level.

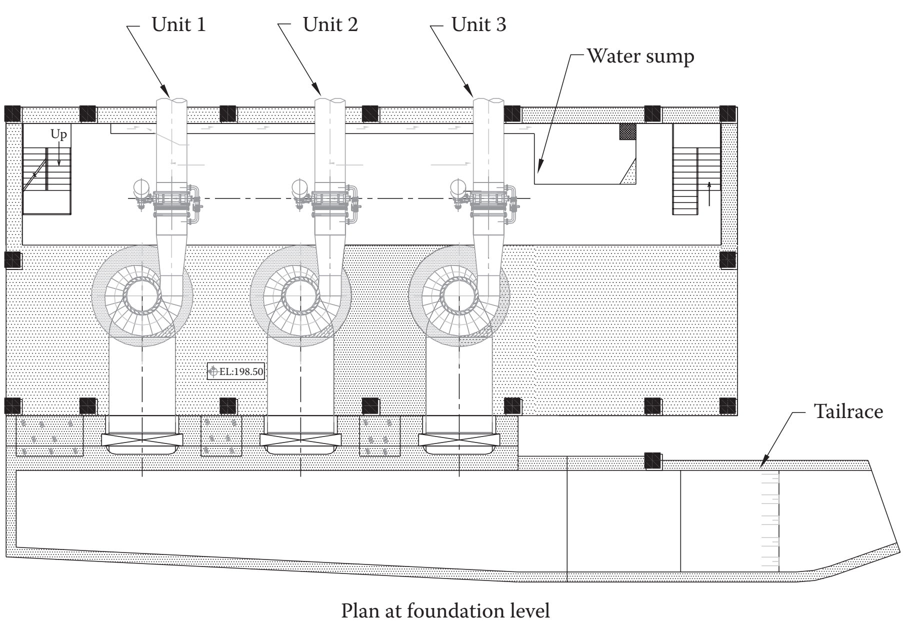

FIGURE 8.8 Powerhouse plan at foundation level.

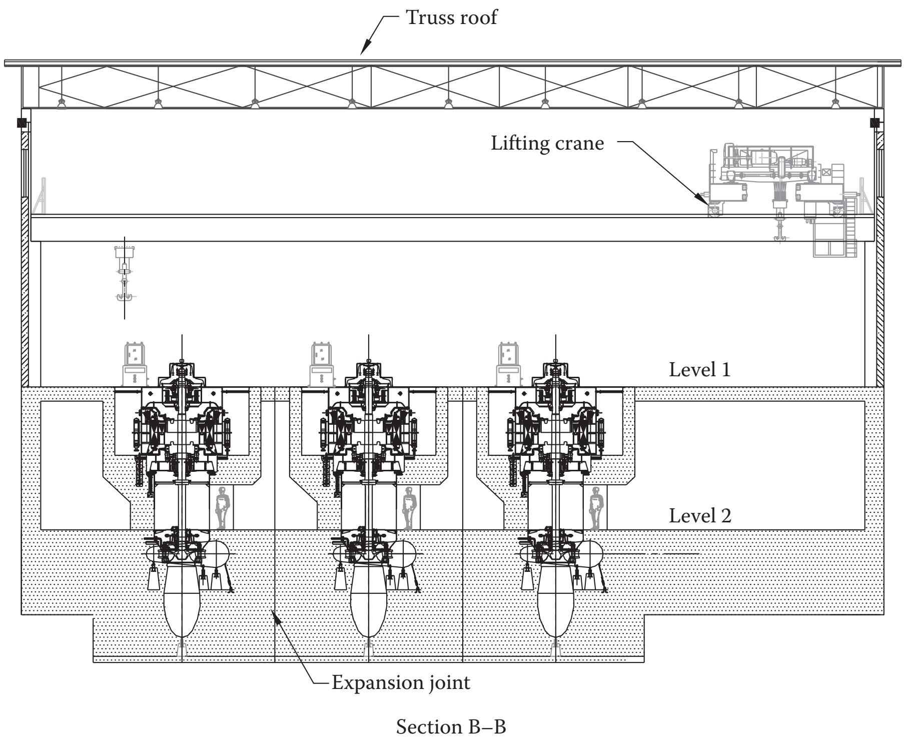

FIGURE 8.9 Powerhouse longitudinal sectional view.

FIGURE 8.10 Powerhouse of Mai hydropower plant.

FIGURE 8.11 Generator floor level of Mai hydropower plant's powerhouse.

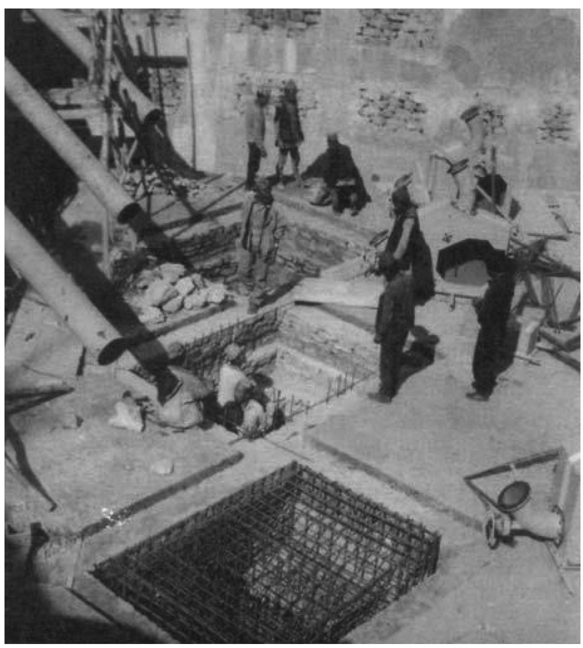

FIGURE 8.12 Machine foundation under construction.

8.8.1 General Guideline for Machine Foundation

The following factors should be considered when designing a powerhouse machine foundation:

- The foundation should be constructed in nonexpansive soil. The foundation pressure should be less than the bearing capacity of the soil. If this condition cannot be met, other alternatives, such as use of piles, should be considered.
- Foundation settlement should be within permissible limits such that the structural elements (beams, columns, etc.) do not get overstressed due to such settlements. For this, it is desirable to construct each unit as a separate block. This will prevent differential settlement and thus avoid overstresses. However, this arrangement will result in relatively larger structural elements (deeper beams and wider columns) as the load has to be distributed among fewer numbers of frame elements.
- The dynamic load is applied repetitively over a very long period, but its magnitude is small, and therefore, the soil behavior can generally be assumed to be elastic.
- Because a homogeneous and rigid structure is required, the machine foundation should be constructed of reinforced concrete.
- The foundation block should be heavier than the weight of the machines it supports.
- Holding-down bolts should be strong enough to resist maximum vibration.
- A suitable medium between the base plate of the generating equipment and the foundation block should be provided to reduce vibration (e.g., a shock-absorbing mechanism).

8.8.2 Stability of Machine Foundation

After deciding on the layout of the powerhouse, it is necessary to check the stability of the powerhouse building and the machine foundation. For micro and small hydropower plants, only two-dimensional analyses are performed due to ease of calculation. This approach results in relatively larger dimensions. Rigorous three-dimensional analyses are performed for larger projects to reach more economic dimensions.

The major forces acting on the machine foundations are the following:

- The thrust due to hydrostatic force, including surge pressure.
- Dead and live load from superstructure.
- Impact and breaking load due to the motion of lifting cranes.
- The vertical force due to the weight of the foundation block, the turbine, and the generator.
- Dynamic forces generated by the rotation of turbines. These rotations create rotational shear forces due to the torque generated. Dynamic loads from air compressors, oil treatment plant, pumps, etc., should also be considered if the forces generated are of significant magnitude.
- Horizontal force due to earth pressure. In smaller schemes, soil pressure is not considered.
- Forces due to wind and snow.
- Seismic forces.
- Temperature loads.

The foundation should be safe against the combination of all the probable forces. The safety factor for overturning, sliding, and bearing should be checked. The bearing pressure should not exceed the safe bearing pressure of the soil, and there should not be any tensile force in the foundation—that is, bearing pressure should be non-negative. The minimum safety factors listed in Table 8.1 should be ensured when designing the powerhouse foundations for micro hydropower plants.

TABLE 8.1
Minimum Safety Factor

Safety Factor	Normal Loading	Extreme Loading
Overturning	1.2	1.1
Sliding	1.5	1.2

The safety factor should be calculated using the following equations:

$$\text{Safety factor for overturning:}\ \ SF = \frac{\sum \text{Resisting moment}}{\sum \text{Overturning moment}}$$

$$\text{Safety factor for sliding:}\ \ SF = \frac{f.\sum \text{Vertical forces}}{\sum \text{Horizontal forces}} \quad \text{where f = friction factor}$$

$$\text{Bearing pressure:}\ \ p = \frac{\sum V}{A}.\left(1 \pm \frac{6.e}{b}\right)$$

where ΣV = sum of vertical forces, e = eccentricity of resultant force, b = length of foundation, and A = base area of foundation.

8.8.3 Vibration in Powerhouse

The turbines and generators are designed to rotate at high speed. Therefore, even small eccentricity in the axis of the turbine or generator shaft results in large vibrations, which will eventually result in failure of the equipment (e.g., breaking of the turbine–generator shafts). Therefore, the manufacturer of this equipment generally specifies the maximum amplitude of the vibration that can occur. These amplitudes and frequencies have to be damped by the weight of the machine foundation. These vibrations can have multiple consequences, such as the following:

- Fatigue failure of concrete
- Development and propagation of cracks on foundation and walls
- Shear failure of foundation soil

Table 8.2 provides how vibration is perceived at different levels.

When multiple units are housed in the powerhouse, providing expansion joints for each unit will have the following benefits:

- Reduction in calculation efforts and more predictable estimates of forces.
- As a huge volume of concrete work is required for the machine foundation, separating each unit will ease the construction works—that is, make it easier to manage pour volumes.

Sometimes up to two units are placed in the same machine foundation block. However, if the number of units is more than two, it is more practical to put each unit in a separate foundation block.

TABLE 8.2
Vibration and Human Perception of Motion

Approximate Vibration Level (mm/s)	Degree of Perception
0.10	Not felt
0.15	Threshold of perception
0.35	Barely noticeable
1.00	Noticeable
2.20	Easily noticeable
6.00	Strongly noticeable

8.8.4 Analysis of Vibration and Empirical Design Methods

The vibration forces acting in a powerhouse are the following:

I. Pressure surge due to water hammer
II. Draft tube surges
III. Vibration due to error in turbine–generator alignment resulting in eccentricity
IV. Unbalanced rotating parts
V. Vibration due to turbine runner blades
VI. Secondary vibration due to rotating parts, such as the compressor or pumps

Due to the complex geometry of the powerhouse substructure, it is very difficult to perform dynamic analysis. Hence, various empirical rules have been given by different authorities for design of powerhouse foundations. For example, USBR recommendations are the following:

a. The volume of concrete in the substructure (in cubic feet) should be not less than two times the generating capacity of the machine in KW.
b. The weight of the concrete in the generator support and scroll case encasement should be greater than twice the weight of the rotating parts.

For large schemes, even when such empirical criteria are met, the design engineers will want to perform further analysis. When such analysis is done without using software, the system is simplified, and minor forces are neglected. Example 8.1 shows a typical machine foundation analysis done using spreadsheet calculations.

Modern structural software can be used for more realistic analysis of vibration problems. This is outside the scope of this book. Readers should refer to topics on structural dynamics for a more in depth description of how vibration forces are modeled.

8.9 DESIGN OF SUPERSTRUCTURE

The superstructure includes the frame to support the roof, lifting mechanism, and other accessories of the powerhouse. Some general guidelines for design follow.

- For micro hydropower plants, the superstructure should be constructed using local material as much as possible. For example, the powerhouse can be constructed employing local technologies (e.g., load-bearing walls of stone or brick masonry in mud mortar and wooden truss with corrugated iron sheet [CGI], slates, or a thatched roof).

- There should be adequate ventilation and lighting arrangements. This can be done by providing sufficient and well-placed windows.
- The floor of the powerhouse should be damp proof. This can be achieved by providing 300–500 mm thick concrete on the base of the powerhouse floor.
- All the equipment should be easily accessible.
- A provision for a lifting mechanism should be provided to lift heavy equipment.
- To avoid vibration, if the machine foundation has been separated by expansion joints, twin columns should be used to isolate each of the foundations completely.

8.9.1 Analysis and Design of Superstructure

There are several types of forces acting on the superstructure of the powerhouse. The design loads mentioned in machine foundations are equally valid for design of superstructure. The forces that should be considered are the following:

I. Dead loads of beams, columns, slabs, roof, truss, crane rail, etc.
II. Live load due to movement of cranes, humans, machines, etc.
III. Wind load on the powerhouse exterior walls and roof
IV. Temperature load
V. Seismic load

Using these forces, analysis should be carried out for design forces, namely, deflection, bending moment, shear force, and torsion. Using computer software for such analysis is becoming increasingly common. The software makes three-dimensional analyses easily possible. Once the analysis is completed, the structural elements have to be designed to resist the forces complying with applicable codes. If software is not available, a conventional method of analysis can be done by analyzing frames in transverse and longitudinal directions separately.

8.10 CONSTRUCTION OF POWERHOUSE

After all the design has been finalized and drawings have been prepared, the construction of the powerhouse structure can commence. Careful planning is required before the start of construction. Strict safety rules should be followed, and a procedure for documentation should be in place. It should be noted that powerhouse and tailrace construction can occur simultaneously in many projects.

8.10.1 Construction Sequence of Powerhouse

The construction sequence of a powerhouse structure is given below:

1. Excavate to line and level.
2. Install grounding/earthing system.
3. Primary concreting of powerhouse base.
4. Laying of embedded parts and concreting of powerhouse substructure. Spiral case, draft tubes, etc., along with the number of pipes for the cooling system, air ducts, and wire ducts have to be placed during this phase. Therefore, careful examination should be done before pouring of concrete.
5. Construction of superstructure. In this phase, beams, columns, slabs, stairs, walls, and other required structural elements are constructed. Generally, concrete or steel is used for construction of superstructure. The roof is also installed during this phase.
6. Lifting equipment (gantry crane) is installed.

7. Turbine and generator are now fixed above the machine foundation. Secondary concrete is poured to snugly fix the turbine and generators to the foundations. Electrical systems are then laid out.
8. Finishing is done to make the powerhouse architecturally attractive.
9. Installation of safety equipment is done for emergencies, such as fire and other hazards.
10. Finally, testing and commissioning takes place, after which the powerhouse comes into operation.

8.10.2 Guideline for Concrete Works

- The general guidelines followed for structural elements should be strictly adhered to when concreting the powerhouse structure.
- Planning should be done beforehand to locate the position of joints by estimating the capacity of concrete volume that can be done in a single pour.
- Location of expansion joints, contraction joints, etc., should be well defined in the drawings.
- Weather conditions should be noted, and proper preventive methods should be undertaken if weather conditions are unfavorable for concrete works.
- When concreting the foundation, the surface below should be dry. For example, in case of ground water table, constant pumping out of water will be required during concrete works.

Example 8.1: Stability Analysis of a Machine Foundation

Check the stability of a machine foundation for a Pelton turbine with the following parameters:

Length of foundation, L1	5.00	m
Length of foundation, L2	3.00	m
Length of foundation, L3	5.00	m
Height of foundation, H1	3.00	m
Height of foundation, H2	4.00	m
Breadth of foundation, B1	6.00	m
Breadth of turbine foundation turbine, B2	3.00	m
Total length of foundation	13.00	m
Total height of foundation	7.00	m
Discharge in pipe, Q	24.000	m^3/s
Diameter of pipe, d	2.60	m
Thickness of pipe, t	25	mm
Length of penstock, L	300.00	m
Gross head, H_{gross}	121.00	m
Weight of turbine	19.62	
Weight of generator	15.00	
Weight of foundation	12,558.00	
Deduction for turbine hole	−828.00	
Dynamic loads for turbine	19.62	
Dynamic loads for generator	15.00	

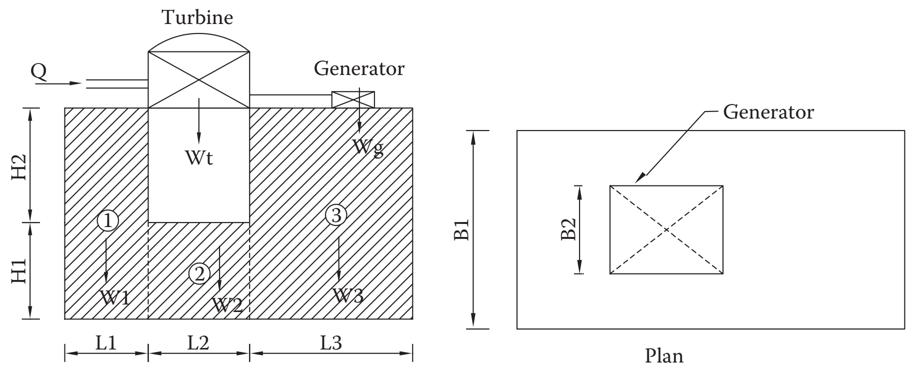

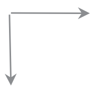

Assumed positive axis

Design Steps (Simplified Analysis)

Step	Calculations	Results/References
1	Calculation of surge head Water velocity in pipe, v = Q/A 4.52 m/s Wave velocity is given by $a = \dfrac{1440}{\sqrt{1+\left(\dfrac{2150\cdot d}{E\cdot t}\right)}}$ m/s $= 989.46$ where d = diameter of pipe in mm, E = Young's modulus of elasticity = $2\cdot 10^5$ N/mm^2, t = thickness of pipe in mm = 25 mm Critical time is given by $T_c = 2L/a = 0.61$ s where L = length of penstock with Number of turbines = 3 Number of jet valve in each turbine, n (for Pelton) = 2 Valve closure time, T = 5 s Surge in Pelton turbine with Pelton, H_{surge} $= \dfrac{av}{g}\cdot\dfrac{1}{n}$ $= 75.99$ m Total head, $H = H_{surge} + H_{gross} = 121 + 75.99 = 196.99$ m	Total design head = 196.99 m

(*Continued*)

2 Force calculations

a. Hydrostatic force = $g_w \cdot H = 9.81 \cdot 196.99 = 1932.47$ kN (direction is +x)
   g_w = unit weight of water
b. Torque generated due to turbine = 10.27 kN (direction is +y) (data provided by machine supplier)
c. Torque generated due to generator = $2 \cdot \pi/60 \cdot dN/dT \cdot wt = 7.85$ kN (direction is +y)
   dN/dT to be provided by manufacturer of turbine. Generally, it varies from 2.8 to 10.4.
d. Weight of turbine, $W_t = 19.62$ kN (direction +y) (data provided by machine supplier)
e. Weight of generator, $W_g = 15.00$ kN (direction +y) (data provided by machine supplier)
f. Weight of foundation = $(L1 + L2 + L3) \cdot B1 \cdot (H1 + H2) \cdot gc =$ 12,558 kN (direction +y)
g. Deduction for turbine hole = $L2 \cdot B2 \cdot (H2) \cdot gc = -828.00$ kN (+y)
   G_c = unit weight of concrete = 23 kN/m^3
h. Dynamic loads for turbine = 100% of self weight = 19.62 kN (+y) (assumed values)
i. Dynamic loads for generator = 100% of self weight = 15.00 kN (+y)

(assumed values)

3 Stability analysis

Force Description	**Lever Arm**
Overturning force	
Hydrostatic force = 1,932.47 kN	H1 + H2 + Hp = 4 + 6 + 1 = 11 m
Resisting forces	
Weight of turbine = 19.62	L2/2 + L3 = 6.50 m
Weight of generator = 15.00	L4/2 = 2.50 m
(provided by machine supplier)	
Weight of foundation = 12,558.00	Total length/2 = 13/2 = 6.50 m
Deduction for turbine hole = −828.00	L2/2 + L3 = 6.50 m
Dynamic loads for turbine = 19.62	L2/2 + L3 = 6.50 m
Dynamic loads for generator = 15.00	L4/2 = 2.50 m

(*Continued*)

$$\sum \text{overturning force} = 1932.47\ \text{kN}$$

$$\sum \text{overturning moment} = 1932.47 \cdot 11 = 21,257.14\ \text{kNm}$$

$$\sum \text{resisting force} = 10.27 + 7.85 + 19.62 + 15.00 + 12,558.00 - 828.00 + 19.62 + 15.00$$

$$= 11,817.37$$

$$\sum \text{resisting moment} = 10.27 \cdot 6.50 + 7.85 \cdot 2.50 + 19.62 \cdot 6.50 + 15.00 \cdot 2.50 + 12,558.00$$

$$\cdot 6.5 - 828.00 \cdot 6.5 + 19.62 \cdot 6.5 + 15.00 \cdot 2.50 = 87,456.89\ \text{kNm}$$

$$\text{Factor of safety for sliding} = \frac{\mu \cdot \sum \text{resisting forces}}{\sum \text{overturning forces}} = \frac{11,817.37\ \text{kN}}{1932.47\ \text{kN}} = 3.97$$

μ = coefficient of friction = 0.65 assumed

$$\text{Factor of safety for sliding} = \frac{\sum \text{resisting moment}}{\sum \text{overturning moment}} = \frac{87,456.89\ \text{kNm}}{21,257.14\ \text{kNm}} = 4.11$$

Bearing pressure

$$\text{Eccentricity} = \frac{L}{2} - \frac{\sum M}{V} = \frac{13}{2} - \frac{(87,456.89 - 21,257.14)}{11,817.37} = 0.90\ \text{m}$$

Corner bearing pressure $\frac{V}{L \cdot B}\left(1 \pm \frac{6e}{L(\text{or } B)}\right)$ = 214.30, 88.71, 187.57, 15.44 kN/m^2 (bearing pressure at four corners)

Generally, minimum factor of safety is taken as 1.5 for nonseismic cases and 1.2 for seismic cases. The bearing pressure below 250 kN/m^2 is acceptable for gravel-mixed soil. As can be seen from the calculations, the machine foundation is safe against overturning and sliding, and bearing pressure is below 250 kN/m^2. Thus, the design of the structure is adequate although the dimensions could be further reduced.

A detailed analysis of a machine foundation structure (including seismic load) done using a spreadsheet is shown in Example 8.2.

Example 8.2: Detailed Stability Analysis of Machine Foundation

Geometry of the structure	
Length of foundation, L1	5.00 m
Length of foundation, L2	3.00 m
Length of foundation, L3	5.00 m
Height of foundation, H1	3.00 m
Height of foundation, H2	4.00 m
Breadth of foundation, B1	6.00 m
Breadth of foundation turbine, B2	3.00 m
Total length of foundation	13.00 m
Total height of foundation	7.00 m
Loads	
Discharge in pipe, Q	24.000 m^3/s
Diameter of pipe, D	2.60 m
Thickness of pipe, t	25 mm
Length of penstock, L	300.00 m
Geographical head, H gross	121.00 m
Height of penstock from foundation level, Hp	1.00 m
Turbine properties	
Weight of turbine, Wt	19.62 kN
Weight of generator, Wg	15.00 kN
Distance of generator from left corner, L4	5.00 m
Rotation speed of turbine, c	50 rev/min
Diameter of turbine, Dt	3.00 m
Turbine type	PELTON
Number of turbines	3
Number of jet valve in each turbine, n (for pelton)	2
Valve closure time, T	5 sec
dN/dT	5

should be >1.22 sec

Calculations

Step 1 Calculate surge head

Water velocity in pipe, v = Q/A — 4.52 m/s

Wave velocity — 989.46

$$a = \frac{1440}{\sqrt{1 + \left(\frac{2150 \cdot d}{E \cdot t}\right)}} \text{ m/s}$$

Critical time of valve closure, Tc = 2L/a — 0.61 sec

a. Surge head for Pelton turbine, hsurge = av/g · 1/n — 75.99 m

b. Surge head for Francis turbine

$$K = \left[\frac{L \cdot V}{g \cdot hgross \cdot T}\right]^2 \quad 0.0522 \text{ m}$$

$$hsurge = \left[\frac{k}{2} \pm \sqrt{k + \frac{k^2}{2}}\right] \cdot hgros. \quad 30.99 \text{ m}$$

Surge head, Hs — 75.99 m

Total head, H = Hsurge + Hgross — 196.99 m

Soil properties		
Angle made by soil with horizontal	0.00	deg
Angle of internal friction	30.00	deg
Coefficient of active earth pressure	0.33	
Unit weight of soil, γs	18.00	kN/m^3
Unit weight of concrete, γc	23.00	kN/m^3
Unit weight of water, γw	9.81	kN/m^3
Friction coefficient, μ	0.65	
Safe bearing capacity of the soil	500.00	kN/m^2
Modulus of elasticity of penstock, E	2.0E + 05	kN/m^2
Coefficients		
Percentage of passive pressure to	0%	
Dynamic loads (% of self wt)	1	
Horizontal seismic coeff.	0.15	
Vertical seismic coeff.	0.07	
Uplift coefficient	0.75	

Result			
Factor of safety		*Bearing*	
1. Sliding	1.94	Maximum	261.25
2. Overturning	2.65	Minimum	41.76

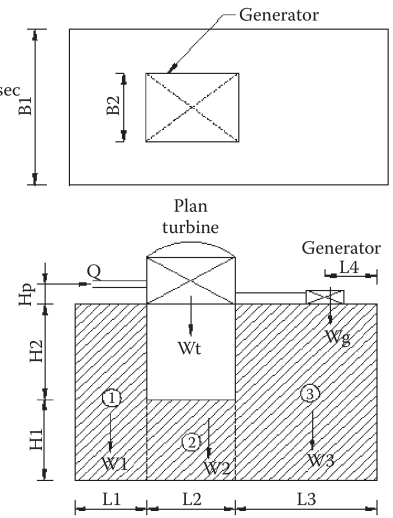

	1 Primary load cases definition	Formula	Intensity of force	Direction
P1	Hydrostatic force	gw · H	1932.47	+x
P2	Torque vertical due to turbine	??	10.27	
P3	Torque vertical due to generator	2 · π/60 · dN/dT · wt	7.85	+y
	2 Dead and dynamic loads			
D1	Weight of turbine	Wt	19.62	+y
D2	Weight of generator	Wg	15.00	+y
W1	Weight of foundation	(L1 + L2 + L3)*B1*(H1 + H2)*γc	12,558.00	+y
W2	Deduction for turbine hole	L2*B2 (H2)*gc	−828.00	+y
D3	Dynamic loads for turbine	100% of self weight	19.62	+y
D4	Dynamic loads for generator	100% of self weight	15.00	+y
	3 Seismic load in normal operation			
S1	Horizontal seismic force(+x)	coeff*(D1+D2+W1+W	1731.16	+/−x
S2	Vertical seismic force: uplift	coeff*(D1+D2+W1+W	865.58	+/−y
S3	Horizontal seismic force(−x)	coeff*(D1+D2+W1+W	1731.16	+/−x
S4	Vertical seismic force: bearing	coeff*(D1+D2+W1+W	865.58	+/−y
	4 Combination			
C1	Normal operation	D1+D2+D3+D4+W1+W2+P1+P2+P3		
C2	Normal operation + seismic: bearing(+x)	D1+D2+D3+D4+W1+W2+P1+P2+P3+S1+S4		
C3	Normal operation + seismic: uplift(+x)	D1+D2+D3+D4+W1+W2+P1+P2+P3+S1+S2		
C4	Normal operation + seismic: bearing(−x)	D1+D2+D3+D4+W1+W2+P1+P2+P3+S3+S4		
C5	Normal operation + seismic: uplift(−x)	D1+D2+D3+D4+W1+W2+P1+P2+P3+S3+S2		

Note: dN/sT to be g

* as per IS code

(*Continued*)

Step 3 Stability analysis

Moment shall be taken at toe of riverside

	Descriptions	Force		Moment arm		Moments		Remarks
		Horizontal KN	Vertical KN	X m	Y m	Overturning KNm	Resisting KNm	
Primary load								
P1	Hydrostatic force	1932.47			11.00	21257.14		
P2	Torque vertical due to turbine		10.27	6.50			66.77	
P3	Torque vertical due to generator		7.85	2.50			51.05	
Dead and dynamic loads								
D1	Weight of turbine		19.62	6.50			127.53	
D2	Weight of generator		15.00	2.50			37.50	
W1	Weight of foundation		12,558.00	6.5			81,627.00	
W2	Deduction for turbine hole		−828.00	6.50			5382.00	
D3	Dynamic loads for turbine		19.62	6.50			127.53	
D4	Dynamic loads for generator		15.00	2.50			37.50	
				11,799.24				
Seismic load								
S1	Horizontal seismic force(+x)	1731.16			3.50	6059.07		
S2	Vertical seismic force: uplift		−865.58	6.50		5626.28		
S3	Horizontal seismic force(−x)	−1731.16			3.50		6059.07	
S4	Vertical seismic force: bearing		865.58	6.50			5626.28	
Load combinations								
C1	D1+D2+D3+D4+W1+W2+P1+P2+P3	1932.47	11,817.37			21,257.14	87,456.89	
C2	D1+D2+D3+D4+W1+W2+P1+P2+P3+S1+S4	3663.63	12,682.95			27,316.22	93,083.17	
C3	D1+D2+D3+D4+W1+W2+P1+P2+P3+S1+S2	3663.63	10,951.79			32,942.50	87,456.89	
C4	D1+D2+D3+D4+W1+W2+P1+P2+P3+S3+S4	201.30	12,682.95			21,257.14	99,142.24	
C5	D1+D2+D3+D4+W1+W2+P1+P2+P3+S3+S2	201.30	10,951.79			26,883.43	93,515.96	

Result of all cases

Case		Eccentricity	Factor of safety		Bearing pressure			
			Slide	Overtum	At coner 1	At coner 2	At coner 3	At coner 4
C1	Normal operation	0.90	3.97	4.11	214.30	88.71	287.57	15.44
C2	Normal operation + seismic: bearing(+x)	1.31	2.25	3.41	361.25	63.95	376.35	−51.14
C3	Normal operation + seismic: uplift(+x)	1.52	1.94	2.65	239.06	41.76	354.15	−73.34
C4	Normal operation + seismic: bearing(+x)	0.36	40.95	4.66	189.55	135.65	220.99	104.22
C5	Normal operation + seismic: uplift(+x)	0.42	35.36	3.48	167.35	113.46	198.79	82.02

8.11 TAILRACE

8.11.1 General

The tailrace is a channel or a pipe that conveys water from the turbine, after generating power, back into the stream—generally, the same stream from which the water was initially withdrawn.

Often, inadequate attention is given to the design and construction of the tailrace because the flow at this stage does not contribute toward power production. However, such a practice can result in inadequate depth of the tailrace pit or erosion of slopes, which could threaten the powerhouse structure.

8.11.2 Design of Tailrace

The following factors should be considered when designing the tailrace:

- The tailwater level at the outlet river should be verified in the same way as the water level at the intake. High and low flow levels should be recorded. Provisions should be made so that backflow into the powerhouse does not occur during high flow in the stream. To prevent such backflows, gates may have to be installed in the tailrace canal.
- The exit of the tailrace must be arranged so that there is no danger of erosion either by the river or by the flow from the tailrace. Ideally, the discharge point should be onto bedrock or large boulders. In erodible riverbed materials, a stilling basin may be required to dissipate the energy from a steep tailrace channel.
- The tailrace canal should be designed in the same way as any hydraulic canal using Manning's equation. If a pipe is used, the design procedure is same as that for a headrace pipe.
- The structural analysis of the tailrace should be done considering all the hydrostatic, hydrodynamic, earth pressure, and seismic loads. In smaller schemes, instead of a reinforced concrete canal, stone masonry in cement mortar can also be used.

EXERCISES

1. Discuss the advantages and disadvantages of various types of layouts of powerhouses. Sketch options that you would consider for turbine generator arrangement when three units are to be branched off from the penstock pipe.
2. What essential equipment is required in a micro hydro powerhouse? What key additional equipment is required in a large hydropower plant?
3. What main factors need to be considered when deciding on the number of turbines in the powerhouse?
4. Redesign the machine foundation in Example 8.1 (change the dimensions) such that the safety factors against overturning and sliding are close to 1.5 and maximum bearing pressure is less than 250 kN/m^2. Make reasonable assumptions for any missing data.

REFERENCES

1. Mosonyi, E., *High Head Power Plants*, Akademiai Kiado, Budapest, 1991.
2. Nigam, P. S., *Handbook of Hydro Electric Engineering*, Roorkee Press, 2008.
3. Kumar, A. and Singal, S. K., *Standards/Manuals/Guidelines for Small Hydro Development* (Version 2), Indian Institute of Technology Roorkee, 2013.

9 Hydraulic Turbines

9.1 BASIC THEORY

Hydraulic turbines convert the energy in falling and moving water, its potential and kinetic energy, to rotational mechanical power. In the example of a simplified hydropower system, as depicted in Figure 9.1, the forebay tank provides water to the inclined penstock pipe, which carries it down to a nozzle where it comes out as a jet. The nozzle transforms the potential energy of the column of water in the penstock pipe to kinetic energy conveyed by the high-velocity jet. This energy is transferred to the turbine runner when the jet of water hits its buckets and loses its kinetic energy in the process.

Bernoulli's equation, which derives from the conservation of energy, states that, for a nonviscous, incompressible fluid in steady flow, the sum of pressure and potential and kinetic energies per unit volume is constant at any point in the system.

Bernoulli's equation is a special form of Euler's equation derived along a fluid flow streamline and can be expressed, as shown below, by three terms:

Pressure energy + Kinetic energy + Potential energy = Constant

Once the friction loss in the penstock pipe, h_{loss}, is added, Bernoulli's equation between the surface of the forebay, labeled "0," and the inlet to the nozzle, labeled "1," can be stated as follows:

$$\frac{p_0}{\rho g} + \frac{v_0^2}{2g} + z_0 = \frac{p_1}{\rho g} + \frac{v_1^2}{2g} + z_1 + h_{loss} \tag{9.1}$$

p_0 (pressure head at the surface of the forebay tank) = 0 at atmospheric pressure.
p_1 is the pressure head at the inlet of the nozzle.
v_0 (velocity of water in the forebay tank) = 0 because the water there is almost still.
v_1 is the water velocity in the penstock pipe right before the nozzle.
z_0 is the height to water surface in the forebay.
z_1 is the height of the nozzle centerline.
$z_0 - z_1$ is the gross head, H_{gross}, available.
g is acceleration due to gravity.
h_{loss} is the frictional head loss in the penstock pipe.
$H_{gross} - h_{loss} = H_{net}$ is the net head available to the turbine after subtracting losses in the penstock pipe.

Substituting these into Equation 9.1:

$$\frac{p_1}{\rho g} + \frac{v_1^2}{2g} = H_{gross} - h_{loss} = H_{net}$$

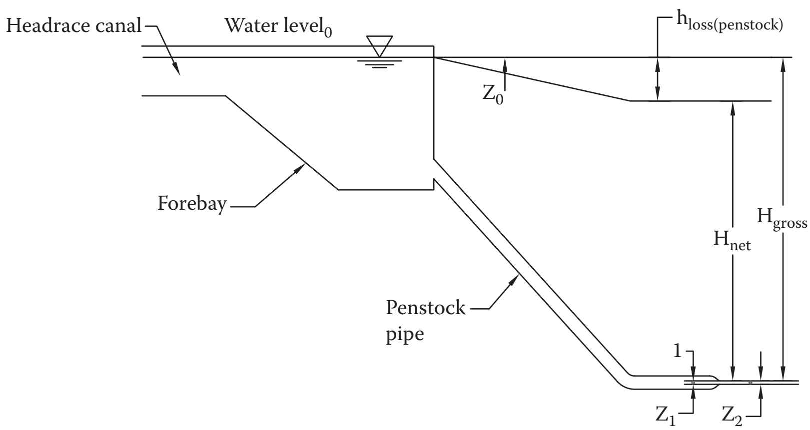

FIGURE 9.1 Basic hydropower system.

A similar equation can be written between the inlet of the nozzle and the water jet as it comes out of the nozzle, labeled "2" in Figure 9.1.

$$\frac{p_1}{\rho g} + \frac{v_1^2}{2g} + z_1 = \frac{p_2}{\rho g} + \frac{v_2^2}{2g} + z_2 \tag{9.2}$$

$p_2 = 0$ because "2" is at atmospheric pressure.
v_2 is the velocity of the jet, and $z_1 = z_2$; therefore,

$$\frac{p_1}{\rho g} + \frac{v_1^2}{2g} = \frac{v_2^2}{2g}$$

Combining the results of the applications of Bernoulli's equation gives:

$$\frac{v_2^2}{2g} = H_{net}$$

and

$$v_2 = \sqrt{2 \cdot g \cdot H_{net}}. \tag{9.3}$$

The result of applying Bernoulli's equation demonstrates that other than the losses in the penstock, assuming negligible losses in the nozzle, all the potential energy of the water is transformed into kinetic energy as the water comes out the nozzle. For this particular configuration, it is this kinetic energy, which is transferred via the water jet to the turbine runner. Impulse turbines, such as Pelton and Turgo, are designed to efficiently extract energy from the velocity of the water jet and transform it to mechanical energy.

9.1.1 Turbine Power Output

If the impulse turbine were 100% efficient in converting the kinetic energy of the water to mechanical energy, the energy transferred to the turbine would be

$$E = 0.5\ mv^2.$$

Power, P, available to the turbine is the rate at which the energy is transferred to the runner:

$$P = \frac{dE}{dt} = 0.5\left(v^2 \cdot \frac{dm}{dt} + m \cdot \frac{dv^2}{dt}\right) \text{ using the product rule for derivatives.}$$

v^2 is equal to $2 \cdot g \cdot H_{net}$ from Equation 9.3 and is thus a constant, resulting in $\frac{dv^2}{dt} = 0$.
So the second term can be removed from the equation.

The first term, $\frac{dm}{dt}$, is the rate of change of mass and is equal to ρQ where ρ is the density of water expressed in kg/m^3 and Q is the rate of flow of water in m^3/s.

Therefore,

$$P = 0.5\ \rho Q \cdot (2gH_{net})$$

Substituting $\rho = 1000\ kg/m^3$ for the density of water,

$$P = 0.5\ 1000 \cdot Q \cdot 2g \cdot H_{net}$$

$$P = 1000\ Q \cdot g \cdot H_{net}\ [W] \text{ with units in Watts.}$$

Once an efficiency coefficient, e_0, is included to signify the ratio of energy input to energy output of the turbine and the result divided by 1000 to convert the units to kW, this gets back to the power equation from Chapter 2, which shows that power output of the turbine (in kW) is equal to the product of the flow Q (in m^3/s), net head "h" (m), the constant "g," and the turbine efficiency e_0.

$$P = Q \cdot g \cdot h \cdot e_0 [kW] \tag{9.4}$$

In practice, there are additional losses, resulting from friction and turbulence, as the nozzle converts water pressure into a high-velocity jet. This is generally accounted for with a velocity coefficient, C_v, which is introduced into Equation 9.3 to give

$$v_2 = C_v \cdot \sqrt{2 \cdot g \cdot H_{net}} \tag{9.5}$$

Example 9.1

Calculate the power produced by an impulse turbine with an efficiency of 88% if the elevation of the reservoir surface in Figure 9.1 is 1400 m, the nozzle is at an elevation of 1050 m and produces a water jet of diameter 170 mm, and the length of the penstock pipe is 870 m. Assume the velocity coefficient of the nozzle is 0.98 and the head loss from friction in the penstock pipe is equal to 2% of its length.

$$H_{gross} = z_0 - z_1 = 1400\ m - 1050\ m = 350\ m$$

$h_{loss} = 0.02 \cdot 870\ m = 17.4\ m$ is the frictional loss resulting in loss of pressure head in the penstock pipe as the water flows through it.

$$H_{net} = H_{gross} - h_{loss} = 350\ m - 17.4\ m = 332.6\ m.$$

From Equation 9.5,

$$v_2 = C_v \cdot \sqrt{2gH_{net}} = 0.98 \cdot \sqrt{2 \cdot 9.81 \cdot 332.6} = 79.2\ m/s$$

The flow of water through the nozzle can be computed by multiplying the calculated velocity of the water jet with its cross-section area.

$$\text{Area of nozzle } A = \frac{1}{4}\pi d^2 = 0.25 \cdot 3.14 \cdot 0.17^2 = 0.0227 \text{ m}^2$$

$$Q = v_2 \cdot A = 79.2 \text{ m/s} \cdot 0.0227 \text{ m}^2 = 1.80 \text{ m}^3\text{/s}$$

Once the flow of water hitting the turbine in m^3/s, the net head in meters, and the efficiency of the turbine are known, the power produced in kW can be calculated using Equation 9.4:

$$P = Q \cdot g \cdot H_{net} \cdot e_0 = 1.80 \cdot 9.81 \cdot 332.6 \cdot 0.88 = 5.2 \text{ MW}$$

The following section examines how the kinetic energy of the jet of water is transferred to the runner of the turbine to produce mechanical power.

9.1.2 Transfer of Energy to the Runner

Understanding how the energy carried by the water is efficiently converted to mechanical energy by the turbine requires an appreciation for how energy gets transferred to the runner, the rotating part of the hydraulic turbine.

Imagine a jet of water of area "A" and velocity "V" striking a flat plate moving in the direction of the jet at a velocity "u" as shown in Figure 9.2.

Because the jet has a velocity (V – u) relative to the plate, imagine the plate as stationary and being impinged by a relative discharge of

$$Q_r = A(V - u)$$

where A is the cross-sectional area of the jet, and (V – u) is the relative velocity of the jet as seen by the plate.

According to Newton's second law, the force of the jet hitting the plate is equal to the rate of change of momentum of the water as it hits the plate in the direction of motion of the plate and splashes off to the side. This linear momentum equation can be written as

$$F = \text{mass of water striking the plate/sec} \times \text{change in velocity of water jet}$$

Examining each of the two terms,

Mass of water striking the moving plate per second = $\rho A(V - u)$, where ρ is the density of water.

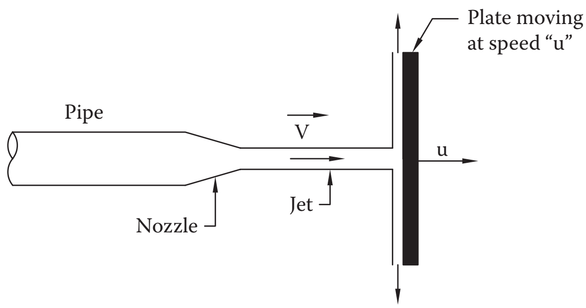

FIGURE 9.2 Jet striking a moving flat plate.

Change in velocity of the jet in the direction of motion of the plate
= (Initial relative velocity of the jet as it strikes the plate
− final velocity of jet in the direction of motion) = (V − u) − 0 = (V − u).

And combine them to calculate the force:

$$F = \rho A(V - u) \cdot (V - u) = \rho A(V - u)^2$$

From the force and the velocity of the plate, calculate the rate of work done on the plate:

$$\text{Work done on the plate per second} = \text{Force} \times \text{Velocity} = \rho A(V - u)^2 \cdot u$$

This gives us the power transferred to the plate, which is defined as work done per second.

The force and work done will next be computed on a series of flat plates moving at a constant velocity "u" away from the jet but in the same direction as might be expected if the plates were mounted on the circumference of the runner wheel of a turbine as seen in Figure 9.3. As one plate on the runner moves away, another moves into its place to be hit by the jet.

The main difference between the two cases—the jet striking a single moving plate versus striking a series of moving plates—lies in how the mass of water striking the plates per second is calculated. In the case of the single plate, there is a clear difference between the mass per second of water contained in the jet, ρAV, and the mass per second of water striking the plate, ρA(V − u), as calculated above. The jet can be thought to be chasing the plate, which is moving away from it with a different rate of water hitting it depending on the speed of the plate. For example, all the flow from the jet hits the plate when it is not moving and u = 0. And if the plate were moving at the same velocity as the jet, u = V, none of the flow from the jet would hit the plate at all.

In the case of a series of plates with one coming in front of the jet to take the place right after the other, the full flow of water from the jet will always be intercepted by one or another plate following it, and the rate at which water hits the runner is equal to the flow of the jet: ρAV.

Using the linear momentum equation, the force of the jet hitting each of the plates in turn is

F = Rate of change of momentum in the direction of motion
= mass of water striking each plate/sec × change in velocity of water jet

The difference from the case of the single plate is that now the mass of water striking the plates per second = ρAV.

Change in velocity of the jet in the direction of motion of the plate remains
= (Initial relative velocity of the jet as it strikes the plate
− final velocity of jet in the direction of motion) = (V − u) − 0 = (V − u).

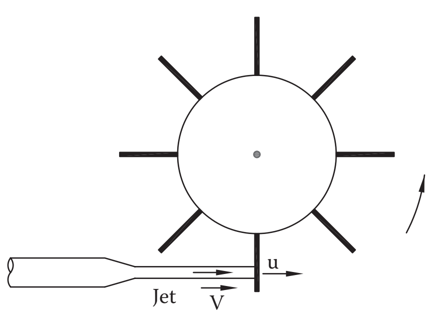

FIGURE 9.3 Jet striking flat plates mounted on a wheel.

The force is now calculated to be

$$F = \rho aV \cdot (V - u) = \rho aV(V - u)$$

And the rate of work done becomes

$$\text{Work done on the plates per second} = \text{Force} \times \text{Velocity} = \rho aV(V - u) \cdot u$$

The input energy carried by the water is its kinetic energy:

$$\begin{aligned}\text{Energy input per second} &= \text{Kinetic energy of jet per second} = 0.5\ \text{Mass/sec} \cdot V^2 \\ &= 0.5\ \rho AV.V^2 = 0.5\ \rho AV^3\end{aligned}$$

The efficiency with which the jet is able to transfer energy to the plates is the ratio of the work done to the input energy:

$$\text{Efficiency} = \eta = \frac{\text{Work done per second}}{\text{Energy Input per second}} = \frac{\rho AuV(V - u)}{0.5\ \rho AV^3} = \frac{2u(V - u)}{V^2}$$

The plate velocity "u" at which the energy of the jet is most efficiently being transferred to get work done on the plates can be found by differentiating and setting $\frac{d\eta}{du} = 0$

$$\frac{d\eta}{du} = \frac{2}{V^2}\left\{\frac{du}{du}(V - u) + u\frac{d(V - u)}{du}\right\} = \frac{2}{V^2}(V - 2u) = 0$$

This shows that at the point of maximum efficiency of energy transfer, V = 2u—that is, each flat plate is moving away as a result of the impact at half the velocity of the jet.

Replacing u for 0.5 V in the expression for η shows that at this velocity the maximum efficiency, $\eta_{max} = 0.5$.

This analysis provides a basic understanding of how the kinetic energy carried by the water jet gets transferred to a rotating water wheel. This wheel shown in Figure 9.3 with flat plates for buckets is able to achieve an efficiency of up to 50%. After hitting the plates and transferring its energy, the jet of water exits tangentially, or at right angles, to the direction of motion of the plates.

Example 9.2

A jet of 50 mm diameter transforms the potential energy of water of net head 50 m to kinetic energy. The turbine runner is made from a number of flat plates attached to the circumference of a wheel, which the jet strikes perpendicularly.

a. Calculate the velocity of the water jet.
b. Calculate the force on the series of plates assuming they are moving away at the same speed as the jet velocity; calculate the power transferred to the runner in this case.
c. Calculate the force on a series of plates in the case when they are not moving, and calculate the power transferred to the runner in this case.
d. Calculate the force on plates moving away at half the jet velocity and the power transferred to the runner.
e. Calculate the power transferred to the runner when the plates are moving away at a quarter of the jet velocity.
f. Calculate the difference in turbine efficiency between the cases (d) and (e) and compare with the efficiency in cases (b) and (c)—that is, u = 0.5 V and when u = 0.25 V, V, or 0.

Solution:

a. $V_{jet} = \sqrt{2 \cdot g \cdot H} = \sqrt{2 \cdot 9.81 \cdot 50} = 31.32\ ms^{-1}$
b. When u = V, $F_x = \rho AV(V - u) = 0$. The runner offers no resistance to the jet, and there is no force exerted on the plates when the plate speed is the same as the jet velocity. Thus the force, power transferred, and efficiency are all equal to zero.
c. When u = 0, $F_x = \rho AV(V - u) = \rho AV^2$.

$$F = 1000\ kg.m^{-3} \cdot \frac{\pi}{4} \cdot (0.05)^2 \cdot (31.32)^2 = 1926.2\ N$$

In this case, the runner offers plenty of resistance to the jet, and thus there is significant force on it. However, there is no work done on the runner, and no power is transferred to it by the jet because the runner is not moving.

Work done on the runner per second or power transferred to the runner, $P = F \cdot u = 0$, when u = 0.

d. When u = 0.5 V, $F_x = \rho AV(V - u) = 1000\ kgm^{-3} \cdot \frac{\pi}{4} \cdot (0.05)^2 \cdot 31.32 \cdot (31.32 - 0.5 \cdot 31.32) =$ 963.1 N. The force on the runner plates is half as much when u = 0.5 V compared to when u = 0 as calculated in (c). Despite the lower force, as per theory, the maximum power must be transferred to the runner when u = 0.5 V.

$$P = F \cdot u = 963.1\ N \cdot 0.5 \cdot 31.32 = 15.1\ kW$$

e. When the plates are moving at quarter of the speed of the jet, u = 0.25 V, the power transferred to the runner can be expected to be somewhat reduced from (d):

$$P = \rho AuV(V - u) = 1000\ kgm^{-3} \cdot \frac{\pi}{4} \cdot (0.05)^2 \cdot 0.25 \cdot 31.32 \cdot 31.32 \cdot (31.32 - 0.25 \cdot 31.32) = 11.3\ kW$$

f. $\eta = \frac{\text{Power Output}}{\text{Power Input}}$

Efficiency can be calculated by dividing the power output by the power input from the jet.

$$\text{Power Input} = 0.5\ \rho AV^3 = 0.5 \cdot 1000\ kgm^{-3} \cdot \frac{\pi}{4} \cdot (0.05)^2 \cdot 31.32^3 = 30.2\ kW$$

$$\eta_{(u=0.5\,V)} = \frac{15.1}{30.2} = 50\%$$

$$\eta_{(u=0.25\,V)} = \frac{11.3}{30.2} = 37.5\%$$

$$\eta_{(u=0\ \text{or}\ V)} = \frac{0}{30.2} = 0\%$$

9.1.3 Improving Efficiency of Energy Transfer

In practice, hydraulic turbines achieve significantly higher than 50% efficiency of energy transfer. They do this through the use of optimally shaped runner plates, which are also called vanes or buckets.

This section examines the force of a jet, power transferred, and efficiency of the turbine with curved plates. After hitting these vanes, the jet turns and exits at an angle θ as shown in Figure 9.4.

The incoming jet has a relative velocity of $V_r = V - u$. Assuming no friction on the polished inside surface of the curved vane, the relative exit velocity also has the same magnitude, V – u at an angle θ with the negative x-axis.

The effect of the jet turning in the vane and exiting at an angle θ can be reflected in the second term of the linear momentum equation from Section 9.1.2:

$$\begin{aligned}\text{Change of velocity of the jet} &= \text{Initial relative velocity of the jet as it strikes the vane}\\ &\quad - \text{final velocity of jet in the direction of motion}\\ &= [(V-u) - \{-(V-u)\cos\theta\}]\end{aligned}$$

The force of the jet striking each vane in turn is now

$$F = \text{mass/sec} \times \text{change in velocity of the jet} = \rho AV\,[(V-u) - \{-(V-u)\cos\theta\}] = \rho AV\,(V-u)\,(1+\cos\theta)$$

$$\text{Work done on the plates per second} = F \cdot u = \rho AV\,(V-u)\,(1+\cos\theta)\cdot u$$

$$\text{Energy input per second} = \text{Kinetic energy of jet per second} = 0.5\,\rho AV^3$$

$$\text{Efficiency} = \eta = \frac{\text{Work done per second}}{\text{Energy Input per second}} = \frac{\rho AV\cdot(V-u)(1+\cos\theta)\cdot u}{0.5\,\rho AV^3}$$

$$\eta = \frac{2u(V-u)(1+\cos\theta)}{V^2} \tag{9.6}$$

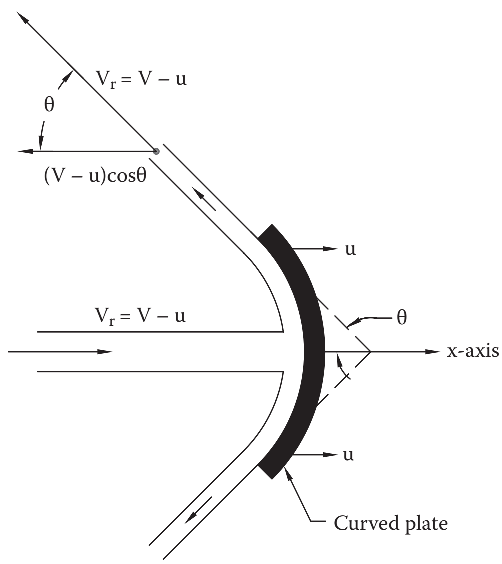

FIGURE 9.4 Jet striking center of curved moving plate.

Differentiating and setting $\frac{d\eta}{du} = 0$ can be used to calculate the plate velocity u at which the energy of the jet is most efficiently transferred to it:

$$\frac{d\eta}{du} = \frac{2}{V^2}(V - 2u)(1 + \cos\theta) = 0$$

Because $(1 + \cos\theta) \neq 0$, once again the maximum efficiency results when u = 0.5 V.

By substituting this value into Equation 9.6, the theoretical maximum efficiency can be written as

$$\eta_{max} = 0.5\ (1 + \cos\theta) \tag{9.7}$$

Equation 9.7 shows that, depending on the angle θ, the maximum efficiency using curved vanes can increase significantly from the case of the flat plates on the wheel.

In the case when θ = 0—that is, when the vanes are semicircular in shape and the jet turns and goes straight back after being deflected through 180°, $\eta_{max} = 0.5 \cdot (1 + 1) = 1$; the theoretical potential efficiency jumps from 50% with the flat plates to 100% with the semicircular bucket.

This doubling of potential efficiency has been achieved by utilizing not only the force of the jet hitting the bucket in the direction it is moving, but adding to it the force of the jet exiting the bucket in the opposite direction. The two force vectors resulting from the jet striking the bucket, as per Newton's second law, and from the jet leaving the bucket, as per Newton's third law, are aligned and simultaneously push the bucket in its direction of motion.

Using fully semicircular-shaped buckets in an attempt to maximize efficiency runs the risk of interference between the outgoing water jet and the bucket in front of it. In order to avoid the potential for such interference, the angle of deflection on buckets is designed to be less than 180° and typically kept at 160° to 165° with θ ranging correspondingly from 15° to 20°. This avoids the risk of jet interference without significantly reducing the maximum theoretical hydraulic efficiency, which remains in the high 90s.

It is reassuring to see that in the case where θ = 90°, as in the case when the bucket is a flat plate, Equation 9.7 gets back to the earlier result:

$$\eta_{max} = 0.5 \cdot (1 + 0) = 50\%.$$

This lower maximum efficiency when using a flat plate results from the fact that the jet exits the plate tangentially to the direction of motion, contributing no additional force on the plate in the direction of motion, and hence no additional torque on the wheel, as it does so.

Example 9.3

For the runner in Example 9.2, calculate the maximum power transferred to the turbine and maximum efficiency of this transfer, when the jet hits the center of a series of curved vanes, which are moving at a speed of 0.5 V, and exits at an angle of deflection of 165°.

$$\theta = 180° - 165° = 15°$$

Work done on the plates per second = $F \cdot u = \rho AV \cdot (V - u)\ (1 + \cos\theta) \cdot u = 1000\ \text{kgm}^{-3} \cdot \frac{\pi}{4} \cdot (0.05)^2 \cdot 31.32(31.32 - 0.5 \cdot 31.32) \cdot (1 + \cos(180° - 165°) \cdot 0.5 \cdot 31.32 = 29.65\ \text{kW}$

$$\eta = \frac{29.65}{30.2} = 98\%$$

The actual hydraulic efficiency of a turbine will be lower due to friction of the water flowing on the inside of the vanes. Additional efficiency losses result from windage and mechanical losses of the spinning runner.

9.1.4 Velocity Triangles

The examples above show that to compute how efficiently energy is transferred when water strikes moving curved blades requires an analysis of changes in velocity vectors, both magnitude and direction, at entry and exit as the water interacts with the blades. Vector diagrams, also called velocity triangles, give a graphical representation of the changes in velocity as water flows past moving curved blades.

Velocity triangles are useful to analyze the performance of all categories of turbines and pumps with differing blade shapes and runner designs. They typically incorporate the three velocity vectors: the absolute velocity of the water jet, the velocity of the vane, and the relative velocity of the jet to that of the vane. To carry out this analysis, two vector triangles, one each at the inlet and outlet, are generally drawn to graphically depict the changes in velocity as the water strikes the vane and exits it.

In order for energy to be transferred between a moving fluid and a moving runner blade of a hydraulic machine, the runner blade must cause the fluid to change its velocity. The runner blade can accelerate the fluid by imparting energy to it as in the case of a pump. In the case of the water turbine, on which this textbook is focused, the runner blade slows down the fluid and extracts energy from it in the process. The energy exchange that takes place between the moving fluid and the blades of the water turbine can be seen in the difference between the inlet and exit velocity triangles. The parameters derived using these velocity triangles can be used to calculate: (a) force on the blade, (b) work done on the blade, (c) torque on the runner wheel, (d) work done per second on the runner wheel, and (e) hydraulic efficiency of the machine.

The sides of the velocity triangle are comprised of the absolute velocity of the water jet, $\mathbf{V}$, the peripheral velocity of the vane, $\mathbf{u}$, and the relative velocity of the water to that of the vane, $\mathbf{V_r}$. A stationary observer outside the runner observes the absolute velocity $\mathbf{V}$ of the moving jet whereas an imaginary observer sitting on the moving vane observes the relative velocity of the jet as the vector difference between the absolute velocity of the jet and the peripheral velocity of the vane.

The three velocities can be represented by the vector relationship with vectors depicted in bold font:

$$\mathbf{V} = \mathbf{u} + \mathbf{V_r} \tag{9.8}$$

The velocity triangle is a graphical representation of this vector equation and can be drawn as shown in Figure 9.5 using the following steps:

a. Let the horizontal line AB represent the peripheral velocity, $\mathbf{u}$.
b. Draw AC, with its length representing the absolute jet velocity $\mathbf{V}$, at an angle, α, with the horizontal line, AB.
c. The line BC connecting the ends of the two vectors would then represent the relative velocity: $\mathbf{V_r} = \mathbf{V} - \mathbf{u}$. For the loss of energy due to impact of the jet on the vane to be zero, referred to as shock-less entry, BC must be tangential to the vane.

The angle α, which is the angle between the absolute velocity of the jet and the peripheral velocity of the blade, is known as the *guide vane angle* whereas the angle ABC between the relative velocity of the jet and peripheral velocity, which is assigned to be β, is called the *blade angle* or *vane angle*.

Utilizing the guide vane angle α, the absolute jet velocity **V** can be resolved into its two components:

i. The tangential component in the same direction as u is called the *velocity of whirl*, V_w, where $V_w = V \cos \alpha$.
ii. The radial component perpendicular to the direction of u is called the *velocity of flow*, V_f, where $V_f = V \sin \alpha$.

The shapes of turbine blades are designed to accommodate the requirements of different categories of site conditions and corresponding specifications that hydropower projects must meet. These shapes are reflected in the inlet and outlet velocity triangles as a range of angles α and β. Higher head sites with low flows require "impulse" type turbines with blades designed to allow nearly tangential flow at both the inlet and outlet. The tangential velocity is high for these turbine types with nozzles typically directing water jets at a small angle, α. As the flows become larger, runners are designed to admit a large quantity of water into the rotor and require a higher radial velocity of flow. Such turbines fall in the "reaction" type categories and they typically have guide vanes placed to produce a larger angle α at the inlet.

Figure 9.5 depicts three different shapes of velocity triangles for different blade angles: β is obtuse (> π/2), acute (< π/2), or at a right angle (= π/2). The triangles themselves can represent either inlet or outlet velocity triangles depending on whether the velocity vectors being referred to are at the inlet to or outlet from the vane.

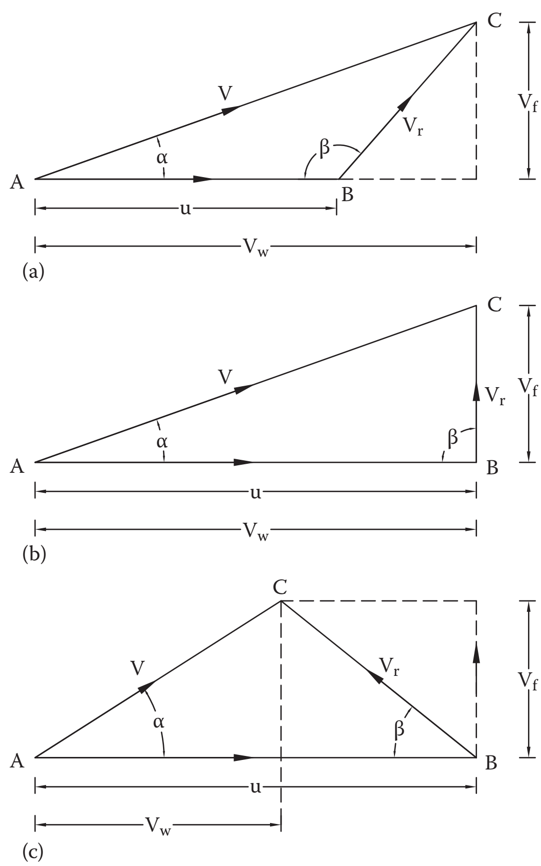

FIGURE 9.5 Velocity triangles for different blade angles: (a) β > π/2; (b) β = π/2; (c) β < π/2.

TABLE 9.1
Velocities of Flow and Whirl for Different Blade Angles

β > π/2 (Low Speed)	β = π/2 (Medium Speed)	β < π/2 (High Speed)
$V_f = V \sin \alpha$	$V_f = V \sin \alpha = V_r$	$V_f = V \sin \alpha$
$V_w = V \cos \alpha = u + V_r \cos (180 - \beta)$	$V_w = V \cos \alpha = u$	$V_w = V \cos \alpha = u - V_r \cos \beta$

As can be seen from Figure 9.5, an obtuse β applies to turbine runners with lower speed rotors as indicated by the relative shorter length of u versus V whereas an acute β pertains to turbines with a high rotor speed, u.

Table 9.1 lists the relationships for the velocity of flow, V_f, and velocity of whirl, V_w, for the three conditions of the blade angle, β.

As a first direct application, velocity triangles are used to analyze how a jet impinging on a moving curved vane transfers energy to it. As with the case of the flat plate above, the case of a single moving vane is examined first, and that analysis is followed with the case of multiple vanes mounted on a wheel.

Figure 9.6 depicts both the inlet and outlet velocity triangles for a curved asymmetrical vane moving in the x-direction with a velocity u. Suffixes 1 and 2 are used to denote vectors and angles used in the inlet and outlet velocity triangles, respectively.

A jet of water with velocity V_1 strikes the bottom edge of the vane, moves through its inner surface, and exits from the bottom edge.

In Figure 9.6, for the inlet and outlet velocity triangles:

V_1, V_2 = *Absolute velocities* of the water at entry to and exit from the blade.
u_1, u_2 = *Peripheral velocities* of the blade at the inlet and outlet.
V_{r1}, V_{r2} = *Relative velocities* of water with respect to the blade at entry and exit (relative velocities must be tangential to the vane to avoid energy losses).
α_1, α_2 = *Guide vane angles* at entry and exit; angles made by absolute jet velocities with direction of peripheral velocities.
β_1, β_2 = *Blade angles* at inlet and outlet; angles made by relative jet velocities with the negative direction of peripheral velocities at inlet and outlet.
V_{f1}, V_{f2} = *Velocities of flow* at inlet and outlet (components of the absolute velocities normal to direction of motion, u).
V_{w1}, V_{w2} = *Velocities of whirl* (tangential component of absolute velocities in the direction of u).

In this particular case of impulse type turbines,

- Peripheral velocities are the same at inlet and outlet: $u_1 = u_2 = u$.
- The relative velocities are equal as long as friction inside the blade is small: $V_{r1} = V_{r2}$.

The expressions for the force imparted to the vane and the power produced are similar to the case of the flat plate and consistent with the linear momentum equation.

F_x = mass of water striking the plate per sec × change in velocity of water jet in the direction of motion

$$P = \text{Work done on the plate per second} = \text{Force} \times \text{velocity} = F_x \cdot u$$

For a single vane moving away from the jet of water, the first term in the force equation will be the relative discharge impinging on it = $\rho A V_{r1}$.

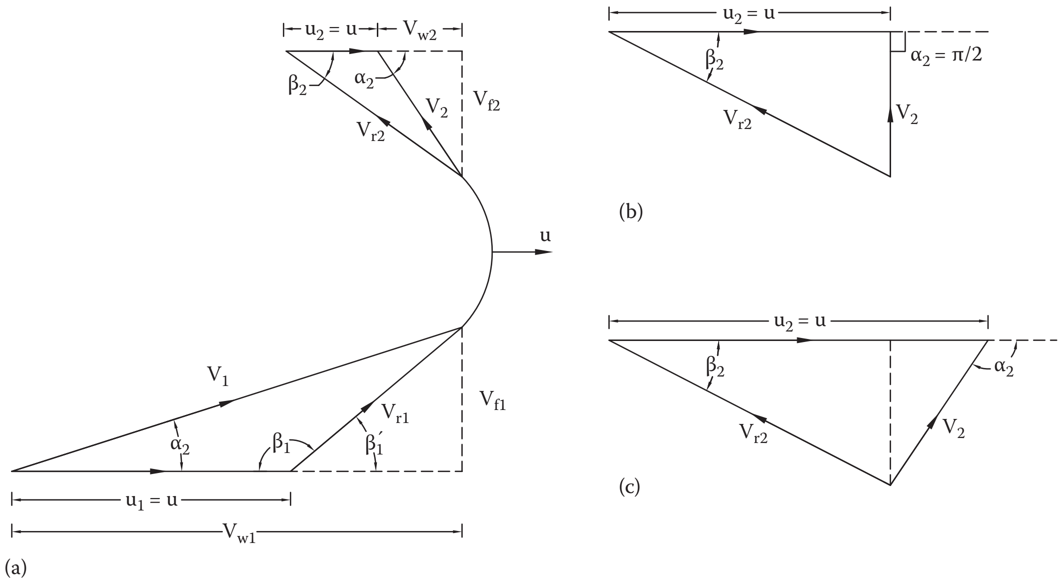

FIGURE 9.6 Inlet and outlet velocity triangles for a curved vane (impulse turbine). (a) $\alpha_2 < \pi/2$; (b) $\alpha_2 = \pi/2$; (c) $\alpha_2 > \pi/2$

The change in velocity in the direction of motion $V_w = V_{w1} - V_{w2}$.

It can be seen from Figure 9.6 that V_{w2} is in a direction opposite to u when $\alpha_2 < 90°$; zero when $\alpha_2 = 90°$; and in the same direction as u when $\alpha_2 > 90°$.

The equations for F_x and P can thus be written as

$$F_x = \rho A V_{r1}(V_{w1} \pm V_{w2}) \tag{9.9}$$

$$P = \rho A V_{r1}(V_{w1} \pm V_{w2})u \tag{9.10}$$

For the situation in which the water strikes a series of vanes tangentially, for example, when they are mounted on a rotating wheel, it can be noted that all the discharge will be striking one or another vane. The mass of water that strikes the vanes is thus equal to $Q = AV_1$ rather than AV_{r1}, and the above equations become

$$F_x = \rho A V_1(V_{w1} \pm V_{w2}) \tag{9.11}$$

$$P = \rho A V_1(V_{w1} \pm V_{w2})u \tag{9.12}$$

in the case of water impinging on a series of vanes one after the other.

The expression for work done per second in Equation 9.12 can also be expressed per unit weight of water striking the vanes.

$$\text{Work done per second per N of fluid} = \frac{\rho A V_1(V_{w1} + V_{w2})u}{\text{Weight of fluid}} = \frac{\rho A V_1(V_{w1} + V_{w2})u}{\rho A V_1 g} = \frac{1}{g}(V_{w1} + V_{w2})u \tag{9.13}$$

This last formulation allows calculation of the power transferred to the runner per N of water and bucket efficiency using velocity triangles even without knowing the size of the jet.

Example 9.4

A jet of water with an area of 0.015 m² and velocity of 20 m/s strikes a curved blade, moving at a velocity of 9 m/s at a guide vane angle of 20°. The exit blade angle of the water is 40° compared to the direction of motion of the vane. (a) Calculate the inlet blade angle to ensure that the water impinges without shock. (b) Calculate the force exerted by the water on the blade in its direction of motion. Neglect friction along the blade.

For the water to hit the blade without shock, the relative velocity V_{r1} will be tangential to the blade. The inlet and outlet velocity triangles can be used as shown in Figure 9.6 to carry out the calculations.

a. From the inlet velocity triangle:

$$V_{w1} = V_1 \cos\alpha_1 = 20\cdot\cos 20 = 18.79 \text{ m/s}$$

$$V_{f1} = V_1 \sin\alpha_1 = 20\cdot\sin 20 = 6.84 \text{ m/s}$$

$$\tan\beta_1' = \frac{V_{f1}}{V_{w1} - u} = \frac{6.84}{18.79 - 9} = 0.6987;\ \beta_1' = 34.93°$$

Where β_1' is the supplementary angle to the inlet blade angle β_1; thus,

$$\beta_1 = 180° - 34.93° = 145.07°$$

b. Force on the blade and the work done per second on it by the water jet can be calculated by making use of Equations 9.9 and 9.10:

$$F_x = \rho A V_{r1}(V_{w1} \pm V_{w2})$$

$$P = \rho A V_{r1}(V_{w1} \pm V_{w2})u$$

The magnitudes of V_{r1} and V_{w2} can be computed by making use of the inlet and outlet velocity triangles. From the inlet triangle,

$$V_{r1} = \frac{V_{f1}}{\sin\beta_1'} = \frac{6.84}{\sin 34.93} = 11.95\frac{\text{m}}{\text{s}} = V_{r2};\ \text{if no friction is assumed}$$

From the outlet velocity triangle,

$$V_{w2} + u = V_{r2}\cos\beta_2;$$

$$V_{w2} = V_{r2}\cos\beta_2 - u = 11.95\cdot\cos 40 - 9 = 0.15 \text{ m/s}$$

Inserting the value of V_{w2} into the equations gives

$$F_x = \rho A V_{r1}(V_{w1} + V_{w2}) = 1000\cdot 0.015\cdot 11.95\cdot(18.79 + 0.15) = 3395 \text{ N}$$

$$P = \rho A V_{r1}(V_{w1} + V_{w2})\,u = 3395\cdot\frac{9\text{ m}}{\text{s}} = 30{,}553 \text{ W} = 30.55\,\text{kW}$$

The positive sign for V_{w2} is used here because $\alpha_2 < 90°$.

Example 9.5

A Pelton runner is operating under the following conditions: Velocity of jet = 100 m/s, diameter of jet = 100 mm, diameter of runner = 2.0 m, speed of runner = 450 RPM, bucket angle at outlet = 15°. Assuming negligible mechanical losses of the runner and zero friction inside the bucket, find (a) the force of the jet on the bucket, (b) work done on the bucket per second, (c) bucket efficiency.

$$V_1 = 100 \text{ m/s}$$

$$d_1 = 0.1 \text{ m}$$

$$D = 2.0 \text{ m}$$

$$N = 450 \text{ RPM}$$

$$\beta_2 = 15°$$

$$\omega = \frac{2\pi}{60} \cdot \text{speed of runner} = \frac{2 \cdot \pi \cdot 450}{60} = 47.12 \text{ radian/s}$$

Peripheral speed of the bucket:

$$u = \omega \cdot r = 47.12 \cdot 1 \text{ m} = 47.12 \text{ m/s}$$

The peripheral velocity of the runner is the same as the velocity of the bucket and can be used for both the inlet and outlet triangles:

$$u = u_1 = u_2 = 47.12 \text{ m/s}$$

The inlet velocity triangle is a straight line for a Pelton turbine (see Figure 9.7). Because the guide vane angle, $\alpha_1 = 0$, the vectors $\mathbf{V_1}$ and $\mathbf{u}$ are aligned, and V_{r1} can be calculated as the arithmetic difference between their magnitudes:

$$V_{r1} = V_1 - u_1 = 100 - 47.12 = 52.88 \text{ m/s.}$$

Alignment of $\mathbf{V_1}$ and $\mathbf{u}$ also means that velocity of flow is zero and velocity of whirl is equal in magnitude to V_1.

$$V_{w1} = V_1 = 100 \text{ m/s}$$

From the outlet velocity triangle,
$V_{r2} = V_{r1} = 52.88$ m/s; when it is assumed that friction in the bucket to the water jet is negligible.

$$V_{w2} = V_{r2} \cos \beta_2 - u_2 = 52.88 \cdot \cos 15 - 47.12 = 3.95 \text{ m/s}$$

Force on the bucket, $F = \rho a V_1 (V_{w1} + V_{w2}) = 1000 \cdot \frac{\pi}{4} \cdot (0.1)^2 \cdot 100 \cdot (100 + 3.95) = 81.64 \text{ kN}$

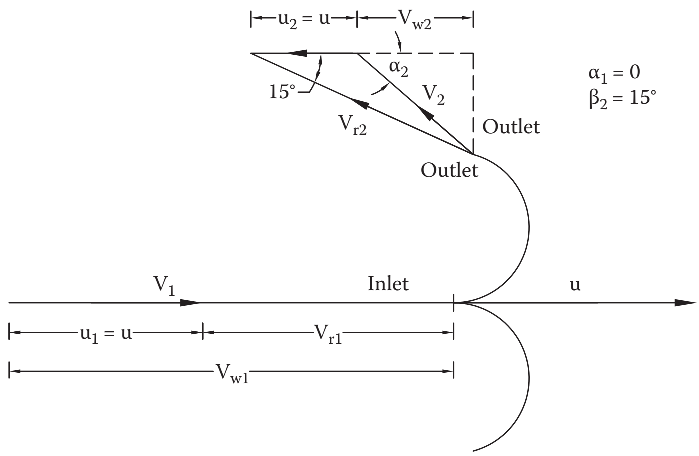

FIGURE 9.7 Inlet and outlet velocity triangles for Pelton bucket.

a. Work done per second (Power), $P = F \cdot u = 81.64\,\text{kN} \cdot 47.12\frac{m}{s} = 3.84\,\text{MW}$
b. Efficiency of the bucket:

$$\eta = \frac{\text{Power delivered}}{\text{Power Input}} = \frac{u(\rho A V_1)(V_{w1}+V_{w2})}{0.5(\rho A V_1)V_1^2} = \frac{2u(V_{w1}+V_{w2})}{V_1^2} = \frac{2 \cdot 47.12 \cdot (100+3.95)}{100^2} = 98\%$$

Example 9.6

A jet of water with velocity of 50 m/s strikes a series of curved vanes moving at a speed of 24 m/s. The jet makes an angle of 20° at entry and 130° at exit. Use velocity triangles to calculate

a. Relative velocity angles (blade angles) at entry and exit
b. Work done per second per N of water
c. Efficiency

$$V_1 = 50\ \text{ms}^{-1}$$

$$u_1 = u_2 = u = 24\ \text{ms}^{-1}$$

$$\alpha_1 = 20°$$

$$\alpha_2 = 180° - 130° = 50°$$

The inlet and outlet velocity triangles in Figure 9.6 can be used to calculate the blade angles.

a. From the inlet velocity triangle,

$$\tan\beta_1' = \frac{V_{f1}}{V_{w1}-u_1} = \frac{V_1\sin\alpha_1}{V_1\cos\alpha_1 - u} = \frac{50\cdot\sin 20}{50\cdot\cos 20 - 24} = \frac{17.10}{22.98} = 0.7440$$

$$\beta_1' = \tan^{-1}0.7440 = 36.65°$$

$\beta_1 = 180° - 36.65° = 143.35°$ is the angle of relative velocity at entry.

$$V_{r1} = \frac{V_{f1}}{\sin\beta_1'} = \frac{17.10}{0.5969} = 28.65\frac{m}{s} = V_{r2} \text{ assuming no friction}$$

Using the sine rule in the outlet triangle,

$$\frac{V_{r2}}{\sin\alpha_2'} = \frac{u_2}{\sin(180 - \alpha_2' - \beta_2)} = \frac{u_2}{\sin(\alpha_2 - \beta_2)}$$

$$\frac{V_{r2}}{\sin 130} = \frac{u_2}{\sin(50 - \beta_2)}$$

$$\sin(50 - \beta_2) = \frac{24}{28.65} \cdot \sin 130 = 0.6418$$

$$50 - \beta_2 = 39.92$$

$\beta_2 = 10.08°$ is the blade angle at exit.

$$\text{Work done per second per N on the wheel} = \frac{1}{g} \cdot (V_{w1} + V_{w2}) \cdot u$$

$$V_{w1} = V_1 \cos\alpha_1 = 50 \cdot \cos 20 = 46.98 \text{ m/s}$$

$$V_{w2} = V_{r2} \cos\beta_2 - u_2 = 28.65 \cdot \cos 10.08 - 24 = 4.21 \text{ m/s}$$

$$\text{Work done per second per N of water} = \frac{1}{9.81} \cdot (46.98 + 4.21) \cdot 24 = 125.3 \text{ Nm}$$

$$\text{Energy delivered by the water per N} = \frac{1}{2g} V_1^2 = \frac{1}{2 \cdot 9.81} \cdot 50^2 = 127.5 \text{ Nm}$$

$$\eta = \frac{\text{Work done per second per N of water}}{\text{Energy delivered per N of water}} = \frac{125.3}{127.5} = 98.3\%$$

9.1.4.1 Velocity Triangles for Reaction Turbines

Velocity triangles were used in the examples above to calculate the force and work done per second on blades of impulse turbines that were struck by a jet of water. The rate of change in the linear momentum of the high-velocity water jet is the source of the force on the runner, which rotates at atmospheric pressure.

Unlike the impulse turbine, the runner of a reaction turbine utilizes both pressure and kinetic energies carried by the water to produce mechanical rotational energy. The water acting on the runner blades is under pressure, above atmospheric, and the runner passages are always completely filled with water. As the water flows past the stationary parts of the turbine, not all of the pressure energy is transformed to kinetic energy. Thus, the flow velocity at the runner inlet is comparatively low in reaction turbines even at high heads. There is both change in direction and slowing down of the velocity as the water flows through the moving rotor and gives up its energy to it. In addition, there is a reduction in the water pressure between the inlet and outlet of the runner. Reaction turbines, which include the Francis, Kaplan, and Propeller, will be explored in detail in Chapter 11.

The angular momentum equation is more suitable than the linear momentum equation to understand how power is transferred from swirling water to a rotating runner. The runner of the reaction turbine experiences torque and work done on it per second resulting from changes in the angular momentum of the water.

Angular momentum is the rotational analog of linear momentum. It is defined as the product of the moment of inertia, I, and angular velocity, ω.

$$L = I\omega$$

Consider a point mass, m, rotating along a circle of radius, r, with an angular velocity ω with unit radians per second. Angular velocity denotes the rotational speed and is related to the speed of a rotating wheel in units of revolutions per minute (RPM) whereas its vector direction is perpendicular to the plane of rotation (Figure 9.8).

$$N = \frac{60}{2\pi}\omega$$

The magnitude of the linear velocity of the mass can be calculated by multiplying angular momentum with its radius from the axis of rotation and its direction is tangential to its circular path:

$$v = \omega \cdot r$$

The moment of inertia of the mass is expressed as $I = m \cdot r^2$.

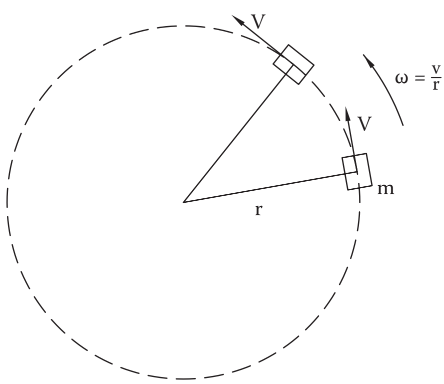

FIGURE 9.8 Angular velocity.

Substituting “v/r” for “ω” in the expression for angular momentum,

$$L = m \cdot r^2 \cdot \frac{v}{r} = r \cdot mv$$

It can be seen that the magnitude of the angular momentum, L, of the point source is its linear momentum multiplied by the radius, r.

Angular momentum, which is also known as moment of momentum or rotational momentum, is a vector, similar to linear momentum.

Torque, τ, is the time derivative of the angular momentum and is the analog of force in the angular form of Newton’s second law:

$$\tau = \frac{dL}{dt}$$

The moment of momentum theorem states that in steady-state flow the *torque on the rotor equals the time rate of change of angular momentum of the fluid as it passes through the runner.*

This theorem can be used to compute how power is transferred from flowing water to the runner using velocity triangles.

The peripheral speeds, u_1 and u_2, at the inlet and outlet triangles can be expressed as

$$u_1 = \omega \cdot r_1$$

$$u_2 = \omega \cdot r_2$$

$$= \rho Q \cdot V_1 \cos \alpha_1 = \rho Q \cdot V_{w1}$$

The product $\rho \cdot Q$ of water density and flow rate of water is the mass of water per second flowing past the rotor. $V_1 \cos \alpha_1$, the component of the velocity of the incoming jet, V_1, parallel to u_1, is the velocity of whirl, V_{w1}.

$$\text{Momentum of water per second at outlet} = \rho Q \cdot (-V_2 \cos \alpha_2) = -\rho Q \cdot V_{w2}.$$

The negative sign is used when V_{w2} is in the opposite direction of V_{w1}.

Because angular momentum = linear momentum × radius

$$\text{Angular momentum per second at inlet} = \rho Q \cdot V_{w1} \cdot r_1$$

$$\text{Angular momentum per second at outlet} = \rho Q \cdot V_{w2} \cdot r_2$$

Torque on the wheel created by the jet = rate of change of angular momentum.

$$\tau = \rho Q \cdot V_{w1} \cdot r_1 - (-\rho Q \cdot V_{w2} \cdot r_2) = \rho Q (V_{w1} \cdot r_1 + V_{w2} \cdot r_2) \tag{9.14}$$

Work done per second on the wheel = $\tau \cdot \omega = \rho Q \cdot (V_{w1} \cdot \omega r_1 + V_{w2} \cdot \omega r_2) = \rho Q \cdot (V_{w1} \cdot u_1 + V_{w2} \cdot u_2)$.

This power equation is referred to as the *Euler power equation for a water turbine.*

If the guide vane angle in the outlet triangle, α_2, is obtuse, the sign on the second term $V_{w2} \cdot u_2$ becomes negative, and the expression for work done per second becomes:

$$\text{Work done per second on the wheel} = \rho Q (V_{w1} \cdot u_1 - V_{w2} \cdot u_2)$$

In the general case, the expression for work done per second or power is written as

$$P = \rho Q(V_{w1} \cdot u_1 \pm V_{w2} \cdot u_2) \tag{9.15}$$

Power output when expressed per unit weight of water striking the vanes:

$$\text{Work done per second per N of fluid} = \frac{\rho Q(V_{w1} \cdot u_1 + V_{w2} \cdot u_2)}{\text{Weight of fluid}} = \frac{\rho Q(V_{w1} \cdot u_1 + V_{w2} \cdot u_2)}{\rho Q g}$$

$$= \frac{1}{g}(V_{w1} \cdot u_1 + V_{w2} \cdot u_2) \tag{9.16}$$

Equation 9.16 can be used to calculate the power transferred to the rotor per N of water by utilizing velocity triangles without need to know the water flow.

Hydraulic efficiency can be computed using the basic relationship:

$$\text{Efficiency} = \eta = \frac{\text{Work done per second}}{\text{Energy input per second}}$$

Equations 9.15 and 9.16 give the work done per second on the runner. However the energy input is not only kinetic energy, which could be computed from the absolute velocity V_1. The energy input to the runner is a combination of kinetic energy and pressure energy, in the case of reaction turbines, and so the power supplied by the water to the runner must also take into account the pressure energy.

Hydraulic efficiency for reaction turbines is thus often stated as the ratio of power transferred to the runner to the power supplied by the water:

$$\eta_h = \frac{\text{Power transferred to the runner}}{\text{Power supplied by the water}} = \frac{\rho Q(V_{w1} \cdot u_1 - V_{w2} \cdot u_2)}{\rho Q g H} = \frac{(V_{w1} \cdot u_1 - V_{w2} \cdot u_2)}{gH} \tag{9.17}$$

Once the flow term cancels out, the efficiency can be thought of as a ratio of heads: The numerator is known as the Euler head, and the denominator is the net head. The net head available to the rotor is defined as the difference between total head at the end of the penstock or just before the turbine and any residual head at the tailrace [1].

This topic is addressed in more detail in the chapter on reaction turbines (Chapter 11).

The blades of reaction turbines are almost always shaped such that the tangential or whirling velocity at the outlet becomes zero—that is, $V_{w2} = 0$. This is desired to minimize any residual kinetic energy of the water as it exits the runner [1]. The outflow velocity is radial when this happens, with $\alpha_2 = 90°$, and the Euler power equations simplify to

$$P = \rho Q(V_{w1} \cdot u_1) \tag{9.18}$$

$$\text{Work done per second per N of fluid} = \frac{1}{g}(V_{w1} \cdot u_1) \tag{9.19}$$

$$\eta_h = \frac{(V_{w1} \cdot u_1)}{gH} \tag{9.20}$$

Another simplification, which is usually possible to make, is that, neglecting friction, the flow velocity remains constant from the inlet of the blade to the outlet—that is, $V_{f1} = V_{f2}$—and equals the velocity at the inlet of the draft tube.

Example 9.7

Calculate the work done per second per N of water on the rotor of an inward flow reaction turbine operating at a peripheral velocity at the inlet of 20 m/s, an inlet guide vane angle of 30°, and blade angle of 135°. Find the net head available to the turbine if the hydraulic efficiency is 95%.

Given:

$$\alpha_1 = 30°$$

$$\beta_1 = 135°$$

$$\alpha_2 = 90°$$

From the inlet triangle (see Figure 9.9):

$$V_{w1} = V_1 \cos \alpha_1 = V_1 \cos 30 = 0.866\ V_1$$

$$V_{f1} = V_1 \sin \alpha_1 = 0.5\ V_1$$

$$V_{r1} = \frac{V_{f1}}{\sin \beta_1'} = \frac{0.5\ V_1}{\sin 45} = 0.7071\ V_1$$

$$V_{w1} - u_1 = V_{r1} \cos \beta_1' = 0.7071\ V_1^* \cos 45 = 0.5\ V_1$$

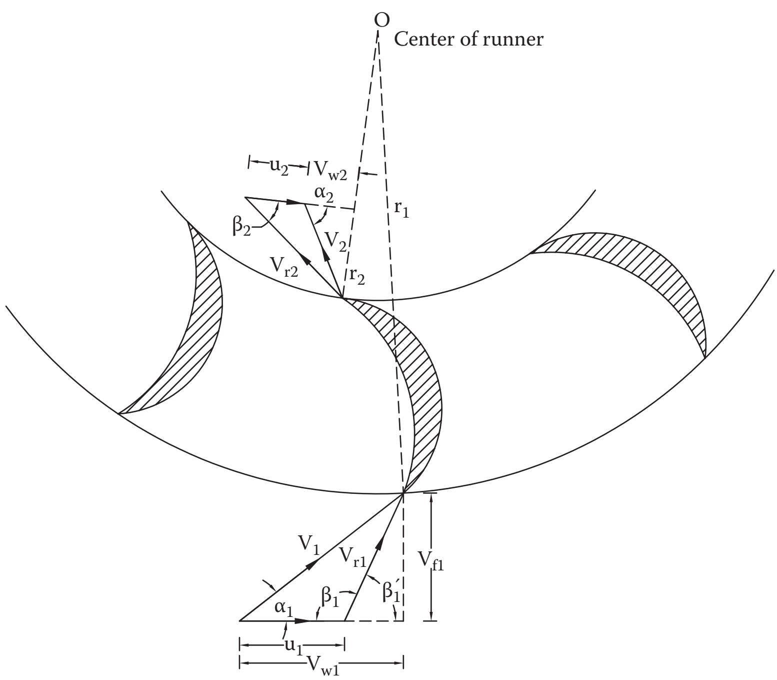

FIGURE 9.9 Velocity triangles for an inward flow reaction turbine.

This can be rewritten and the value of V_{w1} substituted to get

$$u_1 = V_{w1} - 0.5\ V_1 = 0.866\ V_1 - 0.5\ V_1 = 0.366\ V_1$$

Because the peripheral velocity is 20 m/s,

$$V_1 = 20/0.366 = 54.6 \text{ m/s}$$

$$V_{w1} = 0.866 \cdot V_1 = 47.3 \text{ m/s}$$

Because $V_{w2} = 0$

$$\text{Work done per second per N of water} = \frac{1}{g}(V_{w1} \cdot u_1) = \frac{1}{9.81}(47.3 \cdot 20) = 96.4$$

$$\eta_h = \frac{(V_{w1} \cdot u_1)}{gH} = \frac{47.3 \cdot 20}{9.81 \cdot H}$$

Because the efficiency is given to be 0.95, $H = \dfrac{47.3 \cdot 20}{9.81 \cdot 0.95} = 101.5\,\text{m}$

$$H = 101.5 \text{ m}$$

9.2 TYPES OF TURBINES

A range of types of turbines are available with one or more types suited for a particular application depending on the head and flow characteristics available at the site. The power equation, Equation 9.4, makes clear that the power inherent in falling water depends on the two key parameters head (H) and flow (Q). The power output and speed for each turbine can be calculated from these two site parameters plus the specifications of the selected turbine.

There are two broad conventional categories of water turbines: impulse and reaction turbines. Water current turbines and very low head turbines fall into a third, relatively new, category, which has been growing in importance in recent years and is described in Chapter 12. Impulse turbines are typically used at sites where a high head of water is available. They first transform water pressure to kinetic energy by forcing the water through a nozzle and increasing its velocity. The high-velocity jet of water coming from the nozzle hits the turbine runner,* transferring energy and making it rotate and losing most of its energy in the process. The runner of an impulse turbine rotates in air at normal atmospheric pressure. Impulse turbines include the Pelton, Turgo, and cross-flow and are analyzed in detail in Chapter 10.

Table 9.2 shows turbine types used at different ranges of heads.

The table shows that Peltons are used in high head applications, and Kaplan and propeller turbines cover the low head range. Francis, Banki-Michell, and Turgo turbines cover the middle head sites. It is clear from the table that most turbine types cover a fairly wide range of heads. In addition to head, an additional parameter, the flow Q, needs to be known before the choice of turbine can be narrowed down for a particular site. The turbine application chart in Figure 9.10 shows the head and

* A runner refers to a hydraulic device that rotates while it converts the energy from water to mechanical power. In addition to the runner, other elements of the turbine are the housing, jets, vanes, valves, etc.

TABLE 9.2
Suitable Head Ranges by Turbine Types

Hydro Turbine Type	Head (H) Range in Meters	Site Types Covered by Head
River current and VLH	$0 < H < 5$	No head, very low head
Kaplan and propeller	$2 < H < 70$	Low, medium
Banki-Michell (cross-flow)	$5 < H < 200$	Low, medium
Francis	$20 < H < 700$	Low, medium, high
Turgo	$50 < H < 250$	Medium
Pelton	$50 < H < 2000$	Medium, high, very high

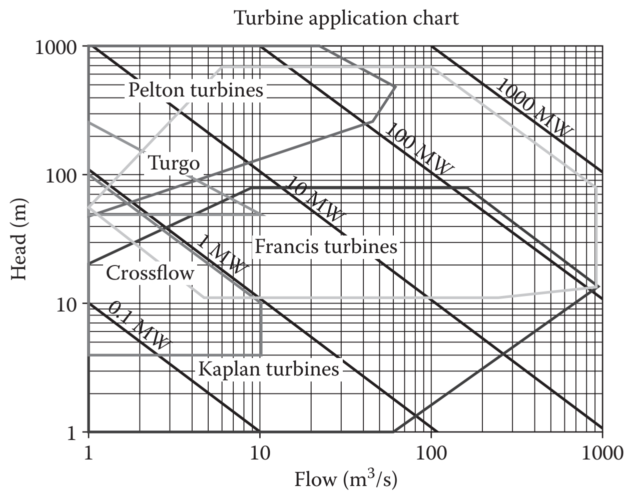

FIGURE 9.10 Head and flow regimes for turbine types. (From https://upload.wikimedia.org/wikipedia/commons/b/bf/Water_Turbine_Chart.png.)

flow regimes covered by turbine types from a number of different manufacturers. The chart shows, for example, that although a Pelton turbine is generally suitable for a high head application, it may not be suitable if the site has a large flow at the same time. Francis turbines cover a broad application range for both head and flow. Kaplan turbines cover the high flow and low head range.

Application charts will also show head and flow regimes for distinct power output ranges. For example, Figure 9.11a shows a turbine selection chart covering mini hydropower in the 1 kW to 500 kW range from a number of manufacturers. Figure 9.11b shows the chart for the manufacturer Ossberger covering the company's namesake Ossberger turbine, which is a cross-flow design as well as Pelton and Kaplan, which the company also manufactures. Ossberger cross-flow turbines are available for sites up to 200 m of head and flows as high as 50 m^3/s. They cover a larger head and flow range than most other manufacturers of cross-flow turbines.

Turbines are also classified depending on the way water flows inside the machines with the categories generally found in the literature including (a) tangential flow, (b) radial flow, (c) radial-axial flow, and (d) axial flow turbines.

a. Tangential or peripheral flow turbines have water flowing tangential to the rotation of the runner. The best example is the Pelton turbine.
b. Radial flow turbines have the water flowing along the radius of the runner. Early Francis turbines used to be inward radial flow.

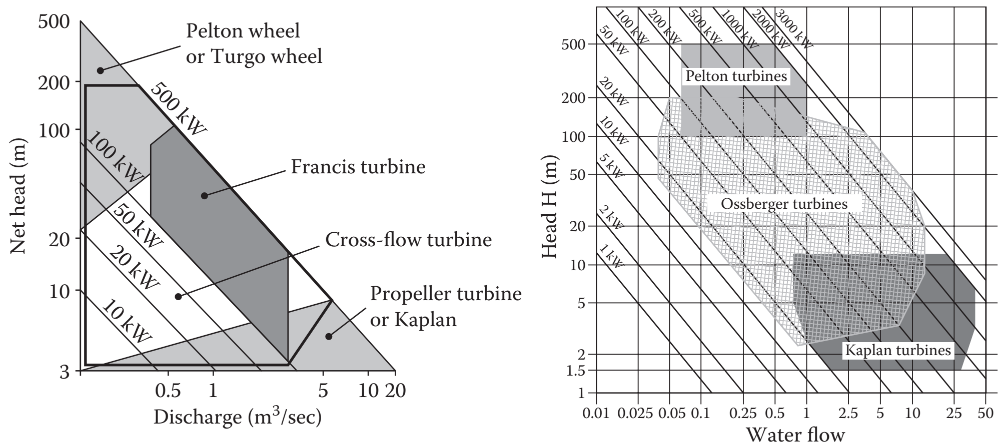

(a) Chart for 1-500 kW mini-hydro turbines (b) Ossberger turbine chart

FIGURE 9.11 Turbine application charts for mini hydropower: (a) Chart for 1–500 kW mini hydro turbines (From http://cdn.intechopen.com/pdfs-wm/40550.pdf.) and (b) Ossberger turbine chart. (From http://www.ossberger.de/cms/pt/hydro/ossberger-turbine/envelope/.)

c. Radial–axial flow turbines have water enter the runner radially at the inlet and exit along the axis at the outlet. Modern Francis turbines are radial–axial flow.
d. Axial flow turbines have water both entering and exiting parallel to the axis. Kaplan and propeller turbines are examples of axial flow turbines.

The runner of a tangential flow turbine rotates in air, and a few of the buckets interact with the high-velocity water jet at any time. Tangential flow turbines are classified under the impulse turbine category. Radial flow, radial–axial flow, and axial flow turbines all fall under the reaction turbine category. The runners of these types of turbines rotate in water, and the water flows continuously past all their blades.

9.2.1 Specific Speed

In addition to the head and flow, a third factor important in the selection of a turbine for a particular hydropower site is its optimal rotational speed at the available head. The expression “specific speed” incorporates the three parameters that determine the choice of a turbine—head, power (which incorporates the flow parameter through the power equation), and speed—into a single number.

Every turbine has a particular speed at a given head at which it produces its maximum efficiency. This highest efficiency is achieved when water flows most smoothly around the turbine blades and passages at this speed. If the head were to be changed, the optimal speed would also change, but the flow pattern of the water would need to remain similar to maintain its best efficiency. Larger or smaller turbines of the same design would have the same optimal speed at the same head. The specific speed has conventionally been defined as the optimal speed of a particular type of turbine with a capacity of 1 metric horsepower at a head of 1 m and is expressed, in metric units, using Equation 9.21:

$$N_s = N\frac{\sqrt{P}}{H^{5/4}} \tag{9.21}$$

N = operating RPM of the turbine
P = turbine power output in metric hp
H = net head (m)

TABLE 9.3
Specific Speeds for Various Turbine Types

Turbine Type	N_s
Pelton	10–50
Turgo	20–70
Cross-flow	20–80
Francis	80–400
Propeller and Kaplan	340–1200

The units are mixed, however, with the metric horsepower* being used to denote power rather than kilowatts for historical reasons. This metric-specific speed, as it is known, has the units of RPM.$hp^{0.5}m^{-1.25}$.

The equation for the specific speed using kW for power is

$$N_s = 1.166\ N\frac{\sqrt{P}}{H^{5/4}}$$ and its unit would be RPM.$kW^{0.5}m^{-1.25}$.

Its unusual units mean that the value of the specific speed changes depending on the particular system of units being used. The specific speed in imperial units has the units of RPM.$hp^{0.5}ft^{-1.25}$, for example, and there is a conversion factor of 4.446 between it and the metric specific speed [2].

The specific speed computed by entering the characteristics of a particular site location for a potential hydropower project can be used for a first screening to see which turbine types may be most suitable. From the system designer's perspective, larger specific speeds are desirable when selecting turbines because for the same head and rated power it is possible to use a smaller, faster rotating turbine. Turbines that can run efficiently at high RPM have the added advantage that they can drive alternators via a direct coupling, thus avoiding the expense of drives to increase the speed or the use of expensive, lower speed alternators. The limiting factor is the geometry of turbines. The higher specific speed turbines have more complex geometries and have been the latest to be developed.

Given that it is desirable for the operating RPM of all turbines to stay within a fairly narrow band, most suitable-for-driving alternators with minimal or no gearing can infer from the specific speed of a turbine type indicate the head and flow characteristics it is most suitable for. Because H is in the denominator and P is the numerator, turbines with lower specific speeds are suited for high head and low flow applications, and those with high specific speeds are suited for sites with low heads and high power or large flow. Turbines that are suitable for sites with both high head and high power output or both low head and low power outputs will have a medium specific speed.

Table 9.3 lists ranges for specific speeds for different hydropower turbine types. It shows that Pelton turbines have a low specific speed; Turgo, cross-flow, and Francis turbines have medium specific speeds; and Kaplan and propeller turbines have the highest specific speeds.

To determine which turbine type might be suitable for a particular hydropower site, the specific speed is first computed using the head, power, and desired speed. The likely result when checking the specific speed against Table 9.3 is that more than one turbine type may potentially be suitable for the site. The designer will then examine the manufacturer's turbine application charts to narrow down turbine types and check availability from suppliers. If the type of turbine most suitable is not available or is too expensive, the designer can try out other turbine types that are more easily available and affordable. Example 9.8 demonstrates the flexibility that the designer can exercise either by trying out different turbine types or opting to operate in a different range of RPM to utilize available

* The metric horsepower is defined as 75 kgf-m per second and is approximately equivalent to 735.5 W.

turbines. The actual type of turbine that is selected for the project, particularly for small hydropower installations, will ultimately depend on availability and price.

Example 9.8

Which turbine types would be most suitable for a 50-kW power project for which the net head is 40 m and must drive a generator at 1500 RPM?

The simplest configuration would have the turbine running at 1500 RPM and driving the generator through a direct coupling.

N = 1500 RPM
P = 50 kW
H = 40 m

A turbine that would fit this characteristic using the formula above has specific speed of

$$N_s = 1.166 \cdot 1500 \cdot \frac{\sqrt{50}}{40^{1.25}}$$

$$N_s = 122.9$$

This specific speed, based on the site characteristics, recommends selection of a Francis turbine for this particular site.

Francis turbines require relatively sophisticated design and casting capability to fabricate and are not readily available in some less developed markets where the simpler cross-flow turbines might be locally manufactured and readily available at a lower cost for the 50-kW plant under consideration. The designer might check if a locally fabricated cross-flow turbine is suitable for this application by adjusting the system design so that the specific speed falls within its range.

One possibility is to reduce the RPM and bring the specific speed down to the level at which the cross-flow turbine might operate. If a speed of 750 RPM is acceptable—that is, 50% of 1500 RPM, this reduces the specific speed N_s to half, or to 61.5, which falls firmly within the specific speed of the cross-flow turbine. A drive system using belts and pulleys or a gear box would be required to double the RPM to drive the generator at the required speed of 1500 RPM.

There is also the option of using two turbines in place of one to reduce the specific speed if the designer wants to avoid investing in a drive system. With 25 kW output per turbine, $N_s = 87$. Although this is higher than the range given above for the cross-flow, an inquiry with the local turbine manufacturer will make clear if the company manufactures a turbine to meet the site conditions. Most turbine companies manufacture a standard set of machines that cover the different subregimes of head, flow, and speed. Even if a suitable 25-kW turbine is available, the designer could conclude that using two turbines does not provide a good solution because the cost of having two generators that require synchronizing results in higher overall costs.

Could the designer alternatively select a Pelton turbine for this site? In order to come within the specific speed range of a Pelton turbine (12–50) the RPM would need to be reduced even further.

At N = 600 RPM,

$$N_s = 1.166 \cdot 600 \cdot \frac{\sqrt{50}}{40^{1.25}}$$

$N_s = 49$, which does just fit into the range of the multijet Pelton.

The analysis above shows how, by comparing the specific speed for different system designs, the designer can examine different choices of turbines suitable for the site before carrying out detailed calculations or contacting the supplier.

9.2.2 Similar Turbines

Similarity laws allow turbine designers to predict the behavior of a full-size turbine based on model studies. The operational modes of turbines of the same type are said to be similar when in addition to being geometrically similar their velocity triangles are similar. This requires the corresponding angles to be the same and the ratio of velocities at corresponding points must be constant. For two turbines of the same type but different sizes, D_1 and D_2, which operate at heads H_1 and H_2, the ratios of speed and discharges can be calculated to ensure that their modes of operation are deemed to be similar.

Given the variation in geometric shapes of different turbines, proportional relationships will be used to describe how velocities, flow, and speed depend on head and diameter of the rotor.

Both the velocity of the water jet and the peripheral velocity of the runner are proportional to the square root of the head:

$$V \alpha \sqrt{H};\ u \alpha \sqrt{H}$$

The area is proportional to the square of the runner diameter,

$$A \alpha D^2$$

Because flow Q = V.A; Q can be expressed proportionally as $Q \alpha D^2 \sqrt{H}$.

This can be written as an equation for the discharge ratio between the two turbines as

$$\frac{Q_1}{Q_2} = \left(\frac{D_1}{D_2}\right)^2 \sqrt{\frac{H_1}{H_2}} \tag{9.22}$$

Because the peripheral speed of the runner $u = \frac{\pi DN}{60}$, and it is known that $u \alpha \sqrt{H}$, a proportional relationship between ND and H can be expressed as

$$ND \alpha \sqrt{H}$$

This can be written as an equation for the speed ratio between the two turbines as

Speed ratio:

$$\frac{N_1}{N_2} = \frac{D_2}{D_1} \sqrt{\frac{H_1}{H_2}} \tag{9.23}$$

Substituting the proportionality between flow Q and head H gives, in turn, $ND \alpha \frac{Q}{D^2}$ which can be written as an important relationship:

$$\frac{Q}{ND^3} = \text{constant} \tag{9.24}$$

Example 9.9

A quarter-scale turbine model is tested under a head of 5.5 m. The full-scale turbine will be working under a head of 65 m and RPM of 395. At what speed should the model be run? If the model produces 40 kW using a flow of 0.85 m^3/s, how much power can the full-size turbine be expected to produce assuming that the full-size turbine is 5% more efficient than the model? Compare the specific speed of the full-scale turbine with that of the model.

From Equation 9.23,

$$\frac{N_1}{395} = \frac{4}{1}\sqrt{\frac{5.5}{65}}$$

$$N_1 = 395 \cdot 1.16 = 459.60 \text{ RPM}$$

From Equation 9.22,

$$\frac{Q_1}{Q_2} = \left(\frac{D_1}{D_2}\right)^2 \sqrt{\frac{H_1}{H_2}} = \left(\frac{1}{4}\right)^2 \sqrt{\frac{5.5}{65}} = 0.0182$$

$$Q_2 = \frac{Q_1}{0.0182} = \frac{0.85}{0.0182} = 46.75 \text{ m}^3\text{s}^{-1}$$

The power equation, Equation 9.4, can be used to calculate the efficiency of the model:

$$P = Q \cdot g \cdot h \cdot e_0 [\text{kW}]$$

$$\eta_{\text{model}} = \frac{P}{Q \cdot g \cdot H} = \frac{40}{0.85 \cdot 9.81 \cdot 5.5} = 87.22\%$$

Because the actual turbine is an additional 5% more efficient than the model,

$$\eta_{\text{turbine}} = 87.22\% + 5.0\% = 92.22\%$$

$$P_{\text{turbine}} = 46.75 \cdot 9.81 \cdot 65 \cdot 92.22\% = 27.49 \text{ MW}$$

Specific speed for the model:

$$N_{\text{s-model}} = 1.166\,N\frac{\sqrt{P}}{H^{5/4}} = 1.166 \cdot 459.6 \cdot \frac{\sqrt{40}}{5.5^{1.25}} = 402.40$$

Specific speed for the full-size turbine:

$$N_{\text{s-turbine}} = 1.166\,N\frac{\sqrt{P}}{H^{5/4}} = 1.166 \cdot 395 \cdot \frac{\sqrt{27490}}{65^{1.25}} = 413.75$$

The difference in specific speeds between the model and the full-size turbine comes about due to the difference in efficiency between them and would disappear if the model was as efficient as the actual turbine [3].

EXERCISES

1. Calculate the overall efficiency, “water to wire,” of an operating hydropower plant when the elevation of the surface of the reservoir is recorded at 903 m, the tailrace is at an elevation of 735 m, flow of water exiting the turbine is measured at 610 l/s in the tailrace and power output measured at the generator is 688 kW. (Answer 68.4%.)
2. Assume that the friction loss in the penstock in Exercise 1 is 8.5 m when the average velocity of water in the penstock is 4.2 ms^{-1}. Assuming that an impulse turbine is being used with a nozzle, calculate gross head, net head, velocity of jet coming out of the nozzle, and pressure head at the inlet of the nozzle. (Answer: 168 m; 159.5 m; 55.9 ms^{-1}; 158.6 m.)
3. At what velocity does a single flat plate moving away from a jet in a straight line in the same direction as the jet experience the maximum transfer of power? What is the maximum transfer of power at this optimal velocity expressed in terms of the jet velocity V and jet area “a.” (Answer: u = 1/3 V; $P = \frac{4}{27}\rho a V^3$.)
4. A jet of water with velocity 30 m/s strikes a single curved plate, which is moving at 10 m/s. The jet makes an angle of 30° at the inlet and 120° at the outlet with the direction of motion of the plate. Use velocity triangles to calculate the angles that the relative velocities make (i.e., vane angles) at the inlet and outlet. (Answer: 43.2°; 36.7°.)
5. A Pelton runner with a diameter of 640 mm is struck with a jet of water of diameter 50 mm and velocity of 54 m/s. The buckets attached to the circumference of the runner have an exit bucket angle of 15°. The relative velocity of the jet is reduced by 10% as a result of friction while it passes through the bucket.
   a. Calculate the force on the buckets when the runner is rotating at a speed of 750 RPM. Calculate the power transferred to the runner from the jet, assuming no mechanical losses of the runner, and the bucket efficiency. (Answer: 5722 N; 143.8 kW; 93%.)
   b. Calculate the peripheral velocity of the runner, the force of the jet on the bucket, power transferred to the runner, and bucket efficiency when the speed of the runner increases to 1000 RPM. (Answer: 33.5 m/s; 4061 N; 136 kW; 88%.)
6. The inlet of a Francis runner has a peripheral velocity of 25 m/s and whirl velocity of 40 m/s. The flow velocity is constant at 5 m/s. Calculate: (a) the guide vane angle at the inlet; (b) blade angle at the inlet; (c) blade vane angle at the outlet if there is no whirl at exit and the ratio of inlet to outlet diameters of the runner is 2. (Answer: 14°; 162°; 22°.)
7. Compare the specific speeds of two turbines whose nameplates read (a) H = 235 m, P = 150 kW; N = 1500 RPM and (b) H = 35 m, Q = 0.25 m^3/s, η = 75%, N = 600 RPM and speculate which turbine types they might be based on the specific speeds. (Answer: 23 RPM.$kW^{0.5}.m^{-1.25}$, Pelton; 76 RPM.$kW^{0.5}.m^{-1.25}$, cross-flow or Turgo.)
8. Confirm that the conversion between the metric specific speed and the imperial specific speed for the same turbine specifications are different by a factor of 4.446. Which is the larger of the two specific speeds?
9. A fifth-scale turbine model is being tested under a head of 2 m. The full-scale turbine will be required to operate at 100 m of head and 1000 RPM. At what speed should the model be tested? (Answer: 707 RPM.)
10. A turbine model with diameter of 0.40 m is found to have the best efficiency at a speed of 380 RPM when tested at a head of 5.0 m; the flow through the model is measured at 120 l/s. Find the optimal speed, discharge, and power output of the full-scale turbine of the same type with a diameter of 2.5 m when operating at a head of 120 m. Assume an efficiency of 93% for the full-size turbine. (Answer: 297.9 RPM, 22.96 m^3/s, 25.13 MW.)

REFERENCES

1. Subramanya, K., *Hydraulic Machines*. Tata McGraw-Hill Education, New Delhi, 2013.
2. Inversin, A. R., *Micro-hydropower Source Book*. NRECA International Foundation, Arlington, VA, 1986.
3. Krivchenko, G., *Hydraulic Machines: Turbines and Pumps*. CRC Press, Boca Raton, FL, 1994.

10 Impulse Turbines

Impulse turbines direct high-velocity jets at runner blades to convert kinetic energy to shaft power. Nozzles are used to transform the potential energy of the water to kinetic energy carried by the jets. Only a few of the blades of the runner interact with each jet at any time, and the discharge through an impulse turbine is largely independent of the speed of rotation of the runner. Other features that distinguish impulse turbines from reaction turbines are that (a) the change in water pressure occurs in the nozzles of the machine and not along the turbine rotor and (b) impingement of the jet on the runner and its rotation both take place at atmospheric pressure.

Pelton turbines are the most widely used among impulse turbines covering a remarkable range from less than a kilowatt to single units producing hundreds of megawatts. In addition to Peltons, this chapter explores the Turgo and cross-flow impulse turbines, which cover the micro hydro to small hydro range from 1 kW typically up to 5 MW. The Pelton and Turgo are tangential flow turbines with jets striking the periphery of the runner and exiting from the sides whereas the cross-flow is a radial flow turbine with the water flowing along the radius toward the shaft of the runner after striking the first set of blades.

10.1 PELTON TURBINES

Pelton turbines utilize high-velocity jets from one or more nozzles to strike buckets on a spinning runner. There are typically between 20 and 25 buckets mounted on the periphery of the runner shown in Figure 10.1. The buckets have the shape of two half bowls joined together with a sharp ridge between them. When the turbine is operating efficiently, upon hitting the bucket the jet loses most of its energy, and the exit velocity of the water is small. In addition to the runner and the shaft on which it is mounted, other key components of the Pelton turbine are nozzles, which accelerate the pressurized water from the penstock pipes to produce the water jets; spear valves located inside the nozzles to control the size of the jets; deflectors to interrupt the jet if required to slow down the runner quickly; and a turbine housing to both position the nozzles correctly with respect to the runner and to contain the exhaust water.

Pelton turbines are used at high head sites that other hydraulic turbines are unable to cover. For large hydropower plants, this is typically above several hundred meters and can go to over 1500 m. For micro, mini, and small hydropower projects, Pelton turbines are found at relatively lower heads, starting at around 30 m and going to a maximum of 300 m. Using multiple jets, Pelton turbines can have an overlap at lower heads with Francis, Turgo, and cross-flow turbines, as the application charts in Figures 9.10 and 9.11 show. The next section introduces the basic calculations for sizing the turbine based on head and flow available at the site, the number of nozzles that the Pelton turbine requires to accommodate available discharge and the speed at which it operates.

10.1.1 Basic Calculations

In the case of the Pelton bucket shown in Figure 10.2, the velocity of the water jet V_1 is tangential to the runner and in the same direction as the velocity of the bucket. Thus, the velocity vectors line up, and the velocity triangle at the inlet becomes a straight line.

Inlet Velocity Triangle

Velocity of the jet relative to the bucket, $\mathbf{V_{r1}} = \mathbf{V_1} - \mathbf{u_1}$.

Velocity of whirl is equal to the jet velocity: $V_{w1} = V_1 \cos \alpha_1 = V_1$.

The guide vane angle is equal to zero: $\alpha_1 = 0°$, and the vane angle $\beta_1 = 180°$.

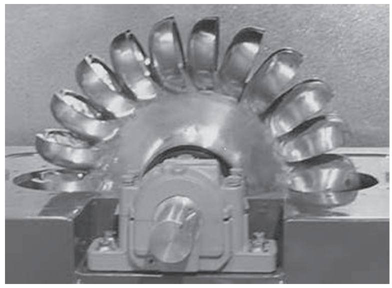

(a)

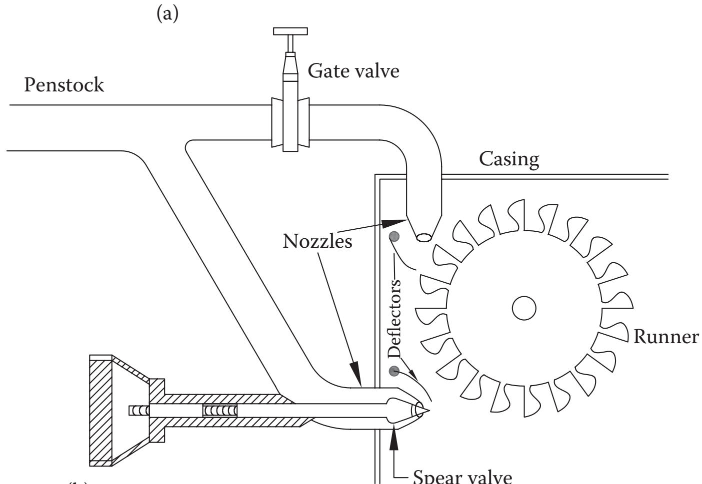

(b)

FIGURE 10.1 Pelton turbine (a) manganese bronze runner. (From Canyon Hydro, Deming, WA.) (b) Components of a Pelton turbine.

Outlet Velocity Triangle

$$V_{r2} \cos \beta_2 = u_2 + V_{w2}$$

Peripheral velocity of the runner is the same for both inlet and outlet triangles:

$$u_1 = u_2 = u$$

β_2 is the vane angle, also known as the bucket angle, made by the relative velocity of the jet as it leaves the bucket with the negative direction of motion of the bucket. The angle through which the impinging jet is turned around after it hits the bucket is referred to as the *deflection angle*, ϕ, and as can be seen in Figure 10.2, it is the supplement of the vane angle.

Force by the jet on the runner can be expressed as

$$F = \rho A V_1 (V_{w1} + V_{w2}),$$

Work done by the jet on the runner per second:

$$P = F \cdot u = \rho A V_1 (V_{w1} + V_{w2}) \cdot u;$$

from Equations 9.11 and 9.12 in the previous chapter.

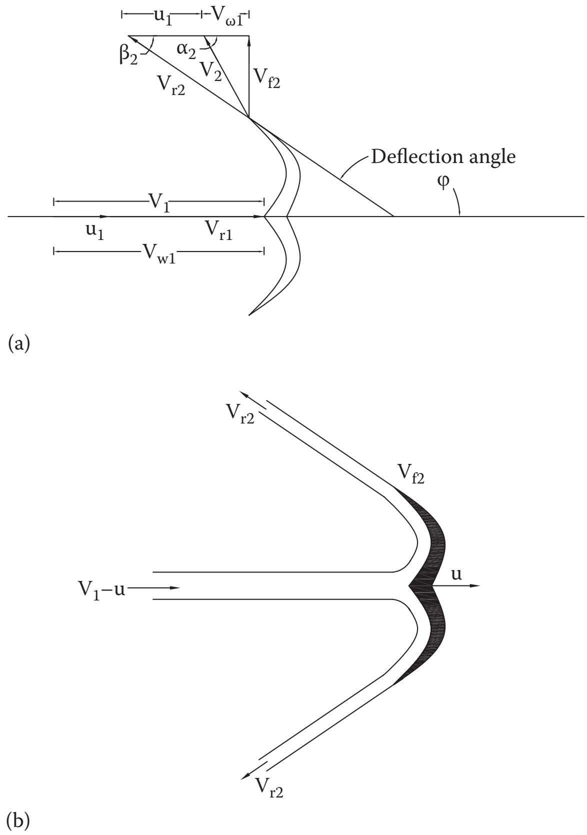

FIGURE 10.2 Flow into a Pelton bucket. (a) Velocity triangle and (b) velocities relative to the bucket.

Substituting the values for V_{w1} and V_{w2} from the velocity triangles:

$$V_{w1} = V_1 = V_{r1} + u$$

$$V_{w2} = V_{r2} \cos \beta_2 - u$$

$V_{r2} = V_{r1}$, assuming zero friction on the inside surface of the bucket; however, assuming a factor ζ (zeta) for friction, this can be written as: $V_{r2} = \zeta V_{r1}$ and $V_{w2} = \zeta V_{r1} \cos \beta_2 - u$.

$$V_{w1} + V_{w2} = V_{r1} + u + \zeta V_{r1} \cos \beta_2 - u = V_{r1}(1 + \zeta \cos \beta_2) = (V_1 - u)(1 + \zeta \cos \beta_2)$$

Hydraulic efficiency,

$$\eta_h = \frac{\text{Work done per second}}{\text{Energy of water jet per second}} = \frac{\rho a V_1 (V_{w1} + V_{w2}) \cdot u}{0.5\ \rho a V_1 \cdot V_1^2} = \frac{2u(V_{w1} + V_{w2})}{V_1^2}$$

$$\eta_h = \frac{2u(V_1 - u)(1 + \zeta \cos \beta_2)}{V_1^2} \tag{10.1}$$

This is consistent with Equation 9.6 in the previous chapter.

The runner speed, u, at which the hydraulic efficiency is highest can be determined by differentiating and setting to zero:

$$\frac{d\eta}{du} = \frac{2(1+\zeta\cos\beta_2)}{V_1^2}\cdot(V_1 - 2u) = 0$$

Because

$$(1 + \zeta\cos\beta_2) \neq 0, \quad u = 0.5\,V_1 \tag{10.2}$$

This is consistent with the earlier finding that the Pelton runner operates at its highest efficiency when its speed is half that of the jet velocity. Equation 10.2 shows this to be true even after taking friction into account. The maximum efficiency can be seen to be

$$\eta_{max} = 0.5(1 + \zeta\cos\beta_2) \tag{10.3}$$

As discussed in Chapter 9, the maximum efficiency occurs when $\beta = 0$—that is, when the bucket is a semicircle and the angle of deflection is 180°. For such a bucket design, η_{max} is seen to be close to 100% if friction on the surface can be minimized—that is, ζ brought close to 1.0.

It is interesting to examine what happens to the water jet once it leaves the bucket.

As shown above, when the turbine is operating efficiently, the speed of the jet V_1 is around twice the peripheral speed of the bucket u. In a Pelton bucket, the jet is split by the ridge and flows around the cups to emerge from the sides of the bucket. If the inside of the bucket is smooth and the friction losses are minimal, the water would leave the buckets at about the same velocity that it enters: $V_1 - u$.

When $V_1 = 2u$,

$$V_1 - u = 2u - u = u.$$

It can thus be seen that when the bucket is moving away from the jet with a velocity of u, the water is also coming out of the bucket with a speed of u, relative to the bucket velocity but in the reverse direction. However, relative to the turbine housing, the absolute velocity of water coming out of the bucket is close to zero with its energy having been largely transferred to the bucket.

An absolute velocity of zero represents an ideal situation efficiency-wise in which all the kinetic energy of the jet is removed by the bucket and the water falls out of the runner under its own weight. In practice, the water does need some speed so that it can get out of the way of the next bucket. The buckets are designed to have a small blade angle β of between 10° and 15° to give the water a slight velocity to leave the bucket from the sides without hitting the back of the next bucket. Because any significant speed of the water leaving the bucket represents wasted energy, this velocity needs to be kept to a minimum. The residual energy in the exit water is known as *discharge loss*.

At $\beta_2 = 15°$, at an idealized $\zeta = 1$ of zero friction,

$$\eta_{max} = 0.5\,(1+\zeta\cos\beta_2) = 98\%.$$

Although ζ can be as high as 0.98 for a well-engineered and highly polished bucket, it is typically down to 0.85 or less for locally manufactured Pelton runners used for micro hydropower projects [1].

Example 10.1

Calculate the maximum hydraulic efficiency of a Pelton runner made at a small workshop assuming a friction factor of 0.85 and bucket angle of 15°.

From Equation 10.3,

$$\eta_{max} = 0.5\ (1 + \zeta \cos \beta_2)$$

$$\eta_{max} = 0.5\ (1 + 0.85 \cos 15°) = 0.91$$

Additional inefficiencies will result from friction losses in the nozzle as well as friction in the bearings and rotor windage losses.

10.1.2 Nozzles

Equation 9.3 shows that the velocity of the jet coming out of the nozzle pushed by a net head, H, is

$$V_j = \sqrt{2gH}$$

where "g" is the acceleration due to gravity = 9.81 ms^{-2}, and H is the net head in meters.

The frictional losses at the nozzle can be accounted for by including the factor C_v in the equation above.

$$V_j = C_v\sqrt{2gH} \tag{10.4}$$

where C_v, the coefficient of velocity for the nozzle, is usually between 0.95 and 0.99.

The water flow from the nozzle Q_{noz} is affected by C_v, which reduces the velocity of the jet. Along with slowing down the jet, the coefficient of velocity, C_v, results directly in energy loss in the nozzle due to friction and turbulence. Because the energy of the jet is all kinetic energy: 0.5 mv^2, the energy loss is proportional to C_v^2.

The range of C_v values, 0.95 to 0.99, translates to inefficiencies in energy conversion ranging from 2% to 10% on account of the nozzle alone. In the case of Example 10.1, using a low-efficiency nozzle with 10% losses added to inefficiency of the runner, the turbine efficiency would come down to 81% or lower. Energy losses in a well-designed nozzle can start out in the 4% to 6% range, but these losses can increase substantially to more than 30% if the nozzle is allowed to wear out.

In addition to impacting the velocity, quantified by C_v, the nozzle also contracts the jet, reducing it to a minimum diameter, called the *vena contracta*, as it emerges from the nozzle. The contraction coefficient C_c, which is defined as the ratio of the cross-section area of the jet at the *vena contracta* to the area of the nozzle opening, can range widely depending on the type of nozzle.

10.1.2.1 Spear Valves

Flow through the nozzle can be regulated through the use of a spear valve, also known as a needle valve. The spear valve, shown in Figure 10.3c, is a spear-shaped needle in the middle of the nozzle, which can be moved different distances into the nozzle to control its effective diameter, starting from the full nozzle diameter to zero as shown in the diagram. The regulation is done automatically on all but the smallest installations through the use of a governor that monitors the speed of the turbine and keeps it constant by varying the flow that strikes the runner by moving the spear valve.

When the turbine has more than one nozzle, cost savings can be achieved by equipping only one of the nozzles with a spear valve and installing fixed nozzles on the others. The single spear valve would, in this case, have to provide sufficient regulation over the range of available flow. In situations in which there is wide variation in flow, turbines usually require more than one nozzle with a spear valve.

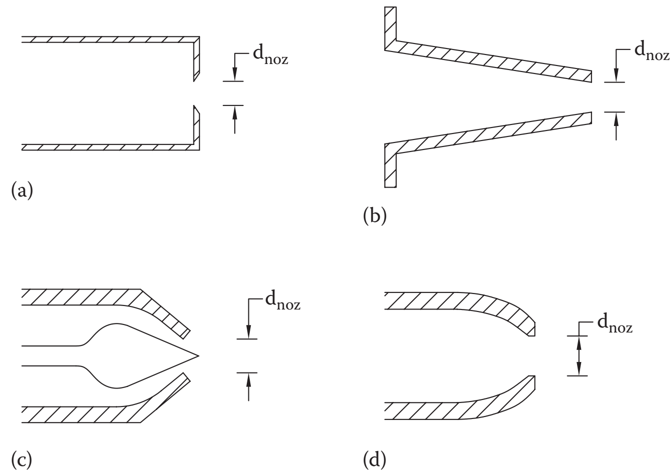

FIGURE 10.3 Nozzles with and without a spear valve. (a) Fixed diameter, sharp-edged orifice; (b) fixed tapered nozzle; (c) nozzle with spear valve; and (d) fixed rounded nozzle.

Well-designed spear valves will have a C_v of 0.97–0.98 [1], corresponding to an efficiency of 94%–96% from full flow down to a quarter flow or less. It is this almost constant performance of the spear valve over a range of flows that ensures high part-flow efficiency for the Pelton turbine.

The effective diameter of the jet emerging from a spear valve can be expressed as follows [1]:

$$D_{jet} = \sqrt{2\sin\frac{\alpha}{2}\cdot(2sd_{noz} - s^2\sin\alpha)} \tag{10.5}$$

where d_{noz} is the diameter of the nozzle, "α" is the spear angle in degrees, and "s" is the distance traveled by the spear into the nozzle in the same unit as D_{jet}. Table 10.1 shows the percentage flow for different values of "s."

When s = 0, the spear is sitting in the nozzle, and flow = 0.

s_{max} will provide the design flow.

For example, if $\alpha = 50°$, and $d_{noz} = 54$ mm, and $s_{max} = 25$ mm.

$$D_{jet} = \sqrt{2\sin\frac{50°}{2}\cdot(2s\cdot 54 - s^2\cdot\sin 50°)}$$

TABLE 10.1
Percentage Flow for Different Spear Valve Settings

s (mm)	D_{jet} (mm)	% Jet Area or % Flow
0	0	0%
5	20.98	23%
10	29.12	45%
15	34.98	65%
20	39.58	83%
25	43.33	100%
30	46.43	115%
35	49.01	128%

Low-cost micro hydro Pelton turbines often use fixed nozzles to avoid the additional expense of a spear valve to control the size of the jet. Jet sizes can be varied in the wet and dry seasons to account for different amounts of flow available by changing the size of the orifice of the fixed nozzle or turning the flow on or off through one or more nozzles in a multinozzle system using a gate valve or butterfly valve. In a situation in which there is plenty of water flow all year round, another alternative low-cost arrangement is to use a deflector between the fixed nozzle and the runner to deflect the portion of the jet that is not required for power production.

Hydropower installations using turbines without spear valves or governors often use an electronic load controller (ELC) to provide system load control. An ELC (see Chapter 13) puts constant electrical load on the turbine and generator, and any generated power that is not required by the main load is diverted to a dummy ballast load. In addition to keeping the turbine speed constant, the ELC removes the need to adjust the flow and power output of the turbine as the main load varies. The spear valve becomes optional because the flow into the turbine can be left constant. With either method of control, use of a deflector or ELC, there must be sufficient water available to "waste." These control systems are appropriate in run-of-river systems in which water does not need to be stored in a reservoir for use during low-flow periods or during peak hour usage.

10.1.3 Runner

10.1.3.1 Bucket Design

Pelton runners are typically cast, either with the full runner cast as a single piece or with buckets cast individually and welded or bolted on to a central disc. High-efficiency turbine runners are cast as a single piece of stainless steel. Cast iron, brass, and bronze are also frequently used for casting turbine buckets, especially those manufactured in small workshops in developing countries. High-efficiency Pelton bucket shapes are often proprietary to the manufacturing companies and are not available in the public domain. A number of design manuals are now available that provide basic shapes and dimensions for buckets for the manufacture of low-cost runners. Thake [1] provides dimensions of a scalable Pelton bucket with all dimensions given as a percentage of the runner diameter.

10.1.3.2 RPM of the Runner as a Function of Net Head and Runner Diameter

Equation 10.2 shows that, in theory, energy is transferred from the jet to the bucket most efficiently when the bucket is moving away from it at half the speed of the jet. In practice, the optimal peripheral speed of the runner is always slightly less than half the velocity of the jet, and the ratio of the bucket to jet speed can be anywhere between 0.42 and 0.48. This text will use a standard value of 0.46 for the optimal ratio of speeds unless specified otherwise.

The reasons for the maximum efficiency occurring at a somewhat lower runner speed have to do with a combination of factors: (a) higher exit velocity of water from a slower bucket is able to get away more cleanly without hitting the following bucket; (b) an effective increase in the diameter of the runner (PCD) and a resulting lower optimal RPM as the jet gets pushed slightly outward once the bucket begins to cut into it; and (c) friction of bearings and windage* losses of the runner, both of which increase with speed.

Assuming

$C_v = 0.97$,
$u = 0.46\ V_j$ at maximum efficiency.

* Windage is the drag on the runner resulting from the movement of buckets through the air and water spray inside the turbine housing.

And by definition,

$$u = \frac{D}{2} \cdot \omega$$

where u is the speed of the runner, V_j is the velocity of the jet, D is the pitch circle diameter (PCD) of the Pelton wheel, and ω is the angular velocity of the runner. The PCD is defined as the diameter of the circle of which the centerline of the jets are tangents as shown in Figure 10.4.

$$\omega = 2\pi \cdot f = 2\pi \cdot \frac{N}{60}$$

where f is the revolutions of the runner per second, and N is the runner speed in rev/min.

The runner speed N can be calculated:

$$N = \frac{30}{\pi} \cdot \omega = \frac{30}{\pi} \cdot \frac{u}{D} \cdot 2 = 60 \cdot 0.46 \cdot 0.97 \cdot \frac{\sqrt{2gH}}{\pi D}$$

$$N = 27 \cdot \frac{\sqrt{2gH}}{\pi D} \tag{10.6}$$

Substituting for acceleration due to gravity, g, and π, gives

$$N = 38 \cdot \frac{\sqrt{H_{net}}}{D} \tag{10.7}$$

Or alternatively,

$$D = 38 \cdot \frac{\sqrt{H}}{N} \tag{10.8}$$

where N = runner speed (RPM), H = net head (m), and D = runner diameter (PCD) (m).

Equations 10.7 and 10.8 show first that the runner speed is dependent only on the net head and the runner diameter and not on the power output or the flow. Second, they show that the speed of

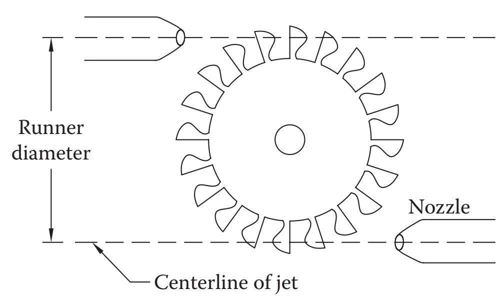

FIGURE 10.4 Runner PCD.

the runner and its diameter have an inverse relationship such that for a given net head, a smaller diameter runner will rotate with higher speed, and a higher diameter runner will rotate with a proportionately lower speed. This is consistent with Equation 9.20.

Example 10.2

For a net head of 100 m, and a runner diameter of 250 mm, find the optimal speed of the Pelton runner.

Assuming $C_v = 0.97$, and optimal efficiency of the runner results when u = 0.46 V,

$$V_j = C_v \cdot \sqrt{2 \cdot 9.81 \cdot 100} = 43.0\,\text{ms}^{-1}$$

$$u = 0.46 \cdot 43\frac{m}{s} = 20.0\frac{m}{s}$$

$$\omega = \frac{u}{r} = \frac{20\frac{m}{s}}{0.125\,m} = \frac{158.1}{s}$$

$$f = \frac{\omega}{2\pi} = 25.2 \text{ revolutions per second} = 1512 \text{ RPM.}$$

The example shows that a turbine runner of 250 mm diameter can be used at a site with a net head of 100 m to directly drive a 1500 RPM generator. Chapter 14 will show how this corresponds to a four-pole generator specified to operate at 50 Hz.

Large turbines with a uniquely specified runner diameter will typically be designed and constructed to run at an optimally efficient speed for a particular site. Small hydropower turbines, on the other hand, are often available in a series of fixed runner sizes and the designer will need to select the runner diameter that best meets the requirements of the site. The designer must, of course, take into consideration any reduction in efficiency when selecting the standard size turbine. Figure 10.5 shows turbine efficiency plotted against the ratio of bucket speed to the jet speed on the x-axis. Although the runner performance remains good close to the optimal ratio u = 0.46 V,

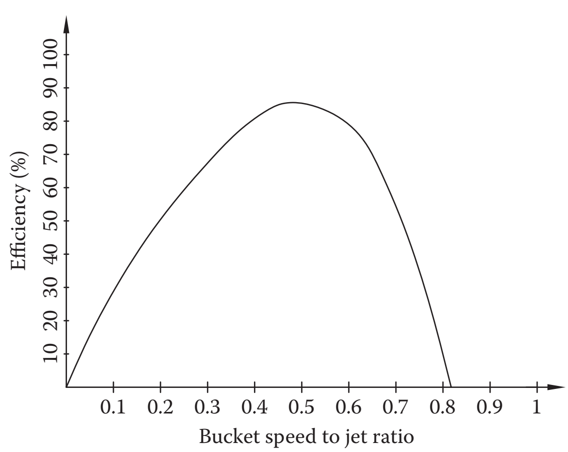

FIGURE 10.5 Pelton runner efficiency curve.

efficiency can drop quite rapidly, especially when the runner is operating at a significantly higher speed than optimal.

The runner efficiency curve, Figure 10.5, provides insight into potentially poor turbine performance as the result of mismatch between the runner diameter and the head available at the hydropower site. Such a mismatch could be the consequence of design error or result from a turbine being moved to a site different from which it was originally designed for. Sometimes micro hydropower turbines are found to be operating at a much lower net head than what they were designed for on account of an undersized penstock pipe. To compensate, the installed turbine could be running inefficiently at a higher speed ratio than is optimal. The combination of reduced net head and inefficient operation of the turbine can result in significantly lower power output than designed. Once the actual net head and turbine diameter are measured, a possible fix for the mismatch is to increase the speed ratio of the drive system to allow the turbine to operate at its optimal speed.

Inefficiencies can also result when there is a mismatch between the turbine output and the load placed on it. An overloaded turbine will be operating at a speed lower than optimal. This can happen during the dry season for hydropower projects serving isolated loads. Another feature of some standalone mini hydropower installations is overloading on the system after some years of operation on account of the gradual increase in appliances such as refrigerators, televisions, rice cookers, and in some cases, air conditioners, that consumers connect to the system.

Whether the cause is reduced power supply or increased loads, turbines respond to overloading by slowing down. It can be seen from Figure 10.5 that the turbine efficiency drops quickly at lower speed after the speed ratio falls below 0.39 or so. The lower efficiency further reduces power output and exacerbates the problem of the mismatch in supply and demand of power. The resulting low output voltage manifests in visibly dim or flickering lights and burnt out motors.

The most effective, immediate action to improve the performance of a turbine operating at an inefficient speed due to overloading is often on the demand side. Requiring all incandescent lamps to be replaced with high-quality, efficient CFL or LED lamps, for example, and scheduling the use of rice cookers away from evening peak hours have proven to be effective. In extreme cases, rotational planned outages during peak demand hours have also been used to manage demand. In the long run, power output may need to be increased either by investing in a larger, more efficient turbine or by impounding water during the day to generate more power during peak hours.

10.1.3.3 Jet Diameter as a Function of Head and Flow

The flow out of a particular nozzle of a Pelton turbine is the product of the cross-section area of the jet and the velocity of the jet.

$$Q_j = A_j \cdot V_j$$

$$A_j = \frac{\pi d^2}{4}$$

where "d" is the diameter of the jet.

$$Q_j = \frac{\pi d^2}{4} \cdot \sqrt{2 \cdot gH}$$

$$d_j = \sqrt{\frac{4Q_j}{\pi \cdot \sqrt{2 \cdot g \cdot H}}}$$

$$d_j = \frac{0.54}{H^{\frac{1}{4}}} \cdot \sqrt{Q_j} \tag{10.9}$$

Equation 10.9 shows how the jet diameter can be calculated for the required flow, Q, at a particular net head. It also means that at a higher head the same nozzle can accommodate a larger flow than at a lower head.

Additional nozzles can be used if a single nozzle cannot accommodate the full design discharge. The maximum number of nozzles that can be used with a horizontal shaft Pelton turbine without interference between jets is only two. With a vertical shaft turbine, however, the number of nozzles can be increased to four, and even up to six on very large turbines (see Figure 10.6).

For multiple jets of the same size,

$$Q_j = \frac{Q}{n_j}$$

where Q_j is the flow out of single nozzle, and n_j is the number of nozzles.

In such a case, the diameter of the jet when there are multiple nozzles, n_j, can be calculated as

$$d_j = \frac{54}{H^{\frac{1}{4}}} \cdot \sqrt{\frac{Q}{n_{jet}}} \tag{10.10}$$

where, d_j = jet diameter (cm), Q = total flow through the turbine from "n" jets (m^3/s), H = net head (m), and n_j = number of nozzles.

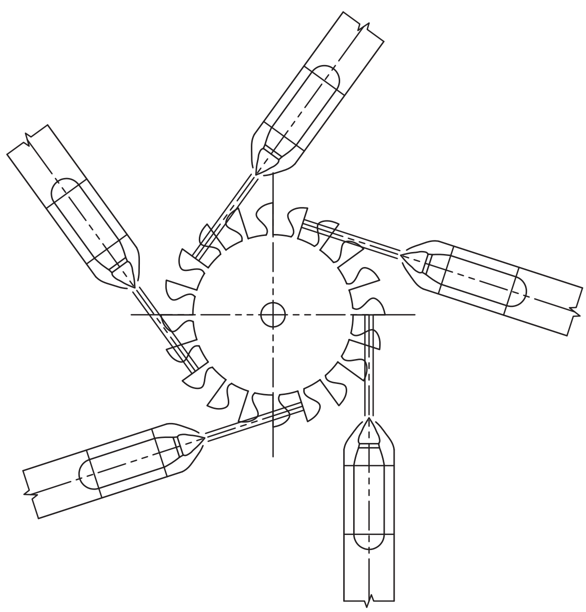

FIGURE 10.6 A five-jet Pelton.

Alternatively, the number of nozzles n_j of a certain diameter d_j required for the flow Q is given by

$$n_j = \frac{2963 \cdot Q}{\sqrt{H} \cdot d_j^2} \tag{10.11}$$

10.1.3.4 Relationship between Jet Diameter and Runner Diameter

A small-diameter runner has the advantages of high RPM and compact turbine size overall. On the other hand, the minimum width of the bucket, which can still accommodate the design flow, sets a limit for what the minimum runner diameter can be. Figure 10.2 shows how water flows into and out of the Pelton bucket without interference as long as the jet diameter is small compared to the bucket. Experience shows that the bucket width must be at least three times as large as the diameter of the jet to avoid interference between the incoming jet and the water leaving the bucket. In turn, the diameter of the runner (PCD) needs to be at least three times as large as the width of the bucket.

Bucket width $w \geq 3 \cdot d_{jet}$, and $PCD \geq 3 \cdot w$.

This implies that $PCD \geq 9 \cdot d_{jet}$.

For most bucket designs, the jet diameter can be no larger than 10%–11% of the runner PCD without reduction in efficiency [2].

In theory, there is no upper limit to the ratio of the PCD to the jet diameter, $m = \frac{D}{d_{jet}}$. However, in practice, it is almost always less than 20. The typical range of "m" lies between nine and 20.

A small-diameter runner limits the maximum size of jet as per the relationship above. When the size of the jet cannot be further increased and remains too small to accommodate the design flow, the designer has the option to use a larger PCD runner or to increase the number of nozzles and divide the flow between them.

10.1.3.5 Relationship between Runner Diameter and Number of Buckets

The runner requires the right number of buckets to operate efficiently. Too few buckets would result in part of the jet passing through the runner without hitting the buckets. Too many buckets result in interception of the jet too early and interference with water as it leaves the buckets.

The optimal number of buckets n_b can be estimated as [3]

$$n_b = \frac{m}{2} + 15 \tag{10.12}$$

Because "m" ranges from nine to 20, the number of buckets on a Pelton runner generally ranges from 20 to 25 with the larger number of buckets on runners on which the size of the bucket is small compared to the runner diameter. The minimum number of buckets required on a runner can be confirmed by simulating the positions of consecutive buckets to make sure that there is no instance when the jet travels between two buckets without hitting either one.

10.1.3.6 Matching Runner Diameter and Flow

The relationships developed above can be utilized to size a Pelton turbine for the specific application described earlier in Example 10.2.

Example 10.3

The most appropriate size of turbine required for a flow of 100 lps, operating at net head of 100 m, can be calculated building on Example 10.2.

There is a preference for the 250-mm diameter runner at this head because, as shown, the speed is around 1500 RPM, and this allows for a direct drive for a four-pole 50-Hz alternator.

The first step will be to calculate "d_j" to see if a single nozzle can sufficiently convey the design flow.

$$d = \frac{0.54}{H^{\frac{1}{4}}} \cdot \sqrt{Q_j}$$

$Q = 0.1\ m^3/s$
$H_{net} = 100\ m$
$d_j = 0.054\ m$

A 54-mm diameter jet is required for a flow of 100 lps at 100 m net head. Because the maximum jet size suitable for use with the 250-mm diameter is 0.11·250 mm = 27.5 mm, the required 54-mm jet is clearly too large for the 250-mm diameter runner. One alternative is to increase the number of nozzles so that the size of each jet is small enough to be used with the 250-mm PCD runner. Four jets each of 27-mm diameter would allow the same flow as a 54-mm jet. A vertical shaft Pelton runner with four nozzles could be used.

The second alternative would be to use a runner with a larger PCD.

If a runner with a diameter of 400 mm is used, for example, the maximum size of the jet allowed would be 44 mm. The number of jets can be calculated by computing the square of the ratio of jet diameters.

$$\left(\frac{54}{44}\right)^2 = 1.5$$

The formula given in Equation 9.18 gives the same result.

$$n_j = \frac{2963 \cdot Q}{\sqrt{H} \cdot d_j^2}$$
$$= \frac{2963 \cdot 0.1}{\sqrt{100} \cdot 4.4^2} = 1.5$$

Thus, two jets would be adequate to handle the flow. Having two jets allows for the use of a simpler horizontal shaft runner arrangement.

There are costs to using a larger diameter runner, however. Not only does it make the turbine more expensive, but the use of a larger runner also means a lower speed and would thus require a drive system to increase the RPM to match the requirement of the alternator.

$$N = 38 \cdot \frac{\sqrt{H}}{D}$$

N is now equal to 950 RPM and requires a drive system to increase the speed to 1500 RPM.

Example 10.3 shows that, as the discharge becomes larger, the Pelton turbine will require multiple nozzles and/or have lower than desired speed. This makes it relatively more expensive to use a Pelton at a lower head. When used at a higher head site, the same Pelton runner operates at higher speed and fewer nozzles can accommodate the same discharge because more water can flow at a higher velocity from the same size nozzle.

Building on a better understanding of interaction between jets, vertical shaft Pelton turbines are now available to handle larger flows through up to six nozzles. Figure 10.6 shows a large 4.9-m diameter Pelton being used at 885 m head to accommodate the significant discharge of 39.59 m^3/s and operating at a low speed of 300 RPM. Prior to the ability to use five or six jets, two Pelton turbines would have been needed for this site (see application chart in Figure 9.10).

Example 10.4

Equations 10.6 to 10.12 can be used to verify some of the coefficients and ratios stated above to be typical of Pelton turbines for the turbine in Figure 10.6.

Net head = 885 m
Flow = 39.59 m^3/s
Power = 316.4 MW
Turbine efficiency = 91.66%
Speed = 300 RPM
PCD = 4060 mm
Number of buckets = 22

Assuming that the coefficient of velocity of the nozzles C_v = 0.99,

$$V_j = C_v \cdot \sqrt{2gH_{net}} = 0.99 \cdot \sqrt{2 \cdot 9.81 \cdot 885} = 130.4 \text{ m/s}$$

$$\omega = 2 \cdot p \cdot f = 2\pi \cdot \frac{300}{60} = 31.4 \frac{\text{radians}}{\text{s}}$$

Peripheral velocity of the runner:

$$u = \frac{D}{2} \cdot \omega = \frac{4.06}{2} \cdot 31.4 = 63.8 \text{ m/s}$$

The ratio of the peripheral velocity to the jet velocity $= \frac{u}{V_j} = \frac{63.8}{130.4} = 0.49$

Equation 10.10 can be used to calculate the jet diameter:

$$d_j = \frac{0.54}{H^{\frac{1}{4}}} \cdot \sqrt{\frac{Q}{n_j}}$$

$$d_j = \frac{0.54}{885^{\frac{1}{4}}} \cdot \sqrt{39.59/4} = 279 \text{ mm}$$

Ratio of diameters: $\frac{D}{d_j} = \frac{4060}{279} = 14.6$, which is well above the lower limit of nine.

10.2 TURGO TURBINES

The Turgo is an impulse turbine similar to the Pelton in that one or more nozzles direct jet(s) at cups mounted on a runner that rotates freely at atmospheric pressure. The size of the jet in both turbine types can be controlled by a spear valve. The cups on the Turgo runner are shaped like shallow bowls that can be thought of as half Pelton buckets (see Figure 10.7). The jet of water enters the Turgo runner from the side at an angle of around 20°, traversing the cup before exiting from the other side.

FIGURE 10.7 Turgo runner. (From Gilkes product literature, Cumbria, UK. http://www.gilkes.com/user_uploads/turgo%20paper2.pdf.)

The Turgo is generally classified as a medium head and medium discharge turbine with application in the small hydro range. Its peak efficiency is around 85%.

The Gilkes company turbine application chart reproduced in Figure 10.8 shows how the Turgo extends the application of impulse turbines into medium head regimes, unsuitable for Pelton turbines, particularly for power output below 5 MW.

The Turgo has a higher specific speed than the Pelton and increases the range of impulse turbines before having to resort to the Francis for small hydropower projects. The Turgo has many of the same benefits as the Pelton. Both turbines are relatively low cost, easily installed and repaired, and are less prone to cavitation. Because their runners operate at atmospheric pressure, both these turbines are less susceptible to reduction in performance from wear, which can increase critical clearances, compared to Francis turbines. Both turbine designs have high part-flow efficiency and thus relatively constant efficiency over a range of flows as is typical of impulse turbines.

The major advantage of the Turgo over the Pelton is that because it has a smaller runner diameter, it can operate at a higher speed for the same power output and head. Alternatively, it can be said that the Turgo is able to accommodate a larger flow of water than the Pelton for the same diameter runner. Whereas the Pelton is constrained by the water volume that the runner can efficiently manage with larger discharge with the jet diameter being limited to around one third of the width of the bucket to avoid interference between the incoming jet and exiting water, the Turgo runner

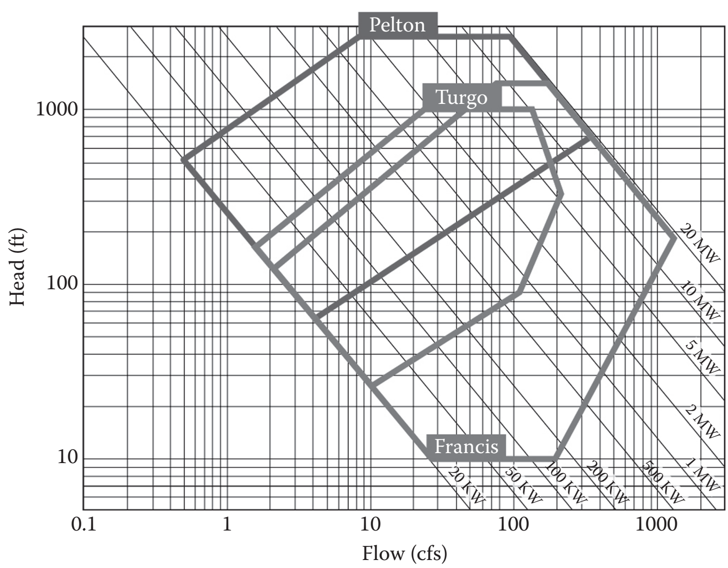

FIGURE 10.8 Turgo application chart. (From Gilkes product literature, Cumbria, UK. http://www.gilkes.com/user_uploads/turgo%20paper2.pdf.)

avoids this problem by having the water exit from a different side of the bucket than the incoming jet. This arrangement allows a Turgo runner with a similar diameter to accept flow from a jet two times larger in area than is possible for a Pelton runner. The Turgo can thus produce the same power output as a Pelton with a smaller runner diameter. The greater runner speed that comes with the smaller runner diameter allows for direct coupling of a Turgo runner with an alternator and thus avoids the need for using a lower speed generator or the need of a drive system to increase the speed.

The main disadvantage of the Turgo is the need for its shaft bearing to withstand a large axial load produced by the oblique angle of the jet entering the buckets. Turgo turbines require heavy duty thrust bearings on the runner shaft to withstand this axial force. The shape of its runner means that the Turgo runner is also more challenging to fabricate compared to the Pelton, particularly in workshops found in developing countries.

The basic calculations of the Turgo are similar to that of the Pelton:

The jet velocity V_j depends only on the head and can be computed as

$$V_j = C_v \cdot \sqrt{2 \cdot g \cdot H}$$

And the relationship between the runner speed "N" and the pitch circle runner diameter "D" is approximately the same as for the Pelton.

$$N = 38 \frac{\sqrt{H}}{D}$$

The jet diameter "d" for the Turgo can be as large as 15.6% of the runner diameter. This compares with a maximum nozzle size of 11% of the runner diameter for a Pelton. This factor of $\sqrt{2}$ times the larger jet diameter for the Turgo translates to a cross-section jet area and flow two times larger than for a Pelton runner of the same PCD.

Example 10.5

Building on Example 10.2 above, in which the design flow for the turbine is 100 lps, and in which there is a preference for the 250-mm diameter runner to produce a speed of around 1500 RPM allowing for a direct drive for a four-pole 50-Hz alternator.

From Example 10.3, the diameter of the jet required to accommodate 0.1 m^3/s of water flow at 100 m head is

$$d = \frac{0.54}{H^{\frac{1}{4}}} \cdot \sqrt{Q} = 0.054$$

The jet diameter was calculated to be d = 0.054 m—that is, a 54-mm jet would be needed to convey a flow of 100 lps at net head of 100 m. Because such a large jet would flood the buckets of a 250-mm PCD Pelton, it had been concluded that it would take four smaller nozzles, each of 27 mm size if a 250 mm Pelton was to be used for this site to directly drive an alternator rated at 1500 RPM.

The maximum jet size that can be used with a 250-mm runner diameter Turgo runner, however, can be as high as 250 mm · 0.156 = 39 mm.

From Equation 10.10, the required diameter of each jet when two jets are used to carry the flow would be

$$d_j = \frac{0.54}{100^{\frac{1}{4}}} \cdot \sqrt{\frac{0.1}{2}} = 38.2 \text{ m}$$

Thus, two jets of 39-mm diameter can convey the design flow of 0.1 m^3 and be accommodated by a 250-mm horizontal Turgo turbine for this site.

10.3 CROSS-FLOW TURBINE

The cross-flow turbine has a rectangular nozzle and a drum-shaped runner with horizontal curved blades rather than buckets, which are welded to parallel disks at the two ends and along additional disks along the length for longer runners. For applications not requiring the highest efficiency, the blades can be cut from sections of commercially available steel pipes and welded into grooves cut into the circular end plates. As shown in Figure 10.9, the nozzle discharges the water jet across the full length of the runner with the flow controlled by a guide vane. Although the cross-flow turbine is categorized as an impulse turbine, it operates with a degree of reaction, particularly when operating at larger valve openings [4].

The development of the cross-flow is credited to Michell and Bánki in the early part of the 20th century, and it is variously called a Michell, Bánki, or Mitchell-Bánki turbine. Ossberger Turbinenfabrik in Germany has been manufacturing this turbine design for more than 90 years, and the name Ossberger used to be synonymous with the cross-flow. Since 1976, mainly on account of its simplicity and ease of fabrication, several thousand simplified cross-flow turbines have been manufactured by workshops in developing countries to be used in local micro hydropower projects. As a result, the cross-flow has become the most widely used turbine for micro hydro systems around the world. This was especially helped by the practical designs and fabrication drawings prepared by the company Entec and the Swiss Center for Appropriate Technology, SKAT, for a series of cross-flow turbines based on the experience of manufacturing turbines for use in the mountains of Nepal (see Box 10.1). A number of organizations have developed their own version of the cross-flow to suit local conditions and manufacturing capabilities.

In addition to availability of simplified models for local manufacture, remote communities find the cross-flow turbine relatively easy to operate and maintain. Its rectangular nozzle and the gap between the blades makes the turbine particularly tolerant of leaves, vegetation, twigs, and other organic debris, which enters between the blades and are flushed out by the exiting flow, after half a revolution, with help from the centrifugal force of the runner.

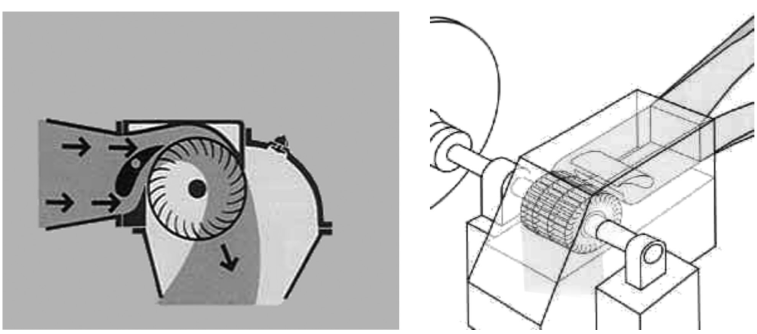

FIGURE 10.9 Cross-flow turbine. (Images from GFA Entec AG.)

BOX 10.1 DEVELOPMENT AND DISSEMINATION OF CROSS-FLOW TURBINES

1903: Australian engineer A. G. M. Michell invents the cross-flow turbine principle.
1917: Hungarian-born Professor Donát Bánki publishes various papers on the subject.
1920: German company Ossberger is awarded patents for its technical improvements and markets turbines in large numbers.
1949: Mockmore and Merryfield, from Oregan State University, publish a comprehensive work on the Bánki water turbine theory and results obtained using their prototype.
1976: Swiss Center for Appropriate Technology (SKAT) constructs the first prototype of the T-1 cross-flow turbine in Balajyu, Nepal, and drafts construction plans for a series of cross-flow turbines designed for technology transfer to other developing countries (T-Series subsequently extends to T1, T3, T7, T8, T12, T14).
1976: Development and Consulting Services (DCS), supported by the United Mission to Nepal, tests its own design of cross-flow turbines in Butwal, West Nepal, to drive agricultural machinery and supports local companies to fabricate more than a thousand units.
1998: International Assistance Mission in Afghanistan develops its version of the cross-flow and transfers technology to local workshops—more than 2000 units fabricated by 2012. Upgraded designs are currently promoted by Remote Hydro Light [5].
2003: Design completed for higher efficiency T-15 under the T-series and Swiss company, GFA Entec, makes licenses available for manufacture of T-15 in Indonesia, Nepal, India, Afghanistan, and Turkey [6].

Source: http://www.jlahydro.be/en/jla-cross-flow-turbines; http://www.entec.ch/entecweb/media/Development_History.pdf; http://www.remotehydrolight.com/LaboratoryTest.pdf

The cross-flow can work under a wide range of flows and heads from under 5 m to more than 200 m. Based on its specific speed (20–80), the cross-flow is a relatively slow turbine and has significant overlap with the Turgo in terms of the head and flow regime it works under. One difference compared with the Turgo is that the cross-flow turbine is sometimes equipped with a draft tube to reduce loss of head, especially for low-head installations when the turbine must be placed considerably above the tailrace water level to be safe from flood risk.

10.3.1 Basic Calculations

The jet of a cross-flow turbine typically enters the wheel at an angle of 16° to the tangent of the periphery of the wheel going radially into the runner from outside. After imparting much of its energy on the first hit, the water passes through the empty space at the center of the runner, and the exiting jet strikes the blades a second time from the inside before it exits the runner radially, imparting additional torque to it before dropping into the tailrace. It is estimated that about 72% of the energy is transferred when the water strikes the blade from the outside and 28% when it strikes the inside periphery [5]. The flow to the runner is controlled by a guide vane, which keeps the shape of the nozzle rectangular across a range of flows.

10.3.1.1 Flow Path and Blade Geometry

Figure 10.10 shows the jet with velocity, V_1, entering the runner at an angle α_1 at the outer rim of the runner. It is assumed that the center of the jet strikes the blade AB. Tracing the path of the water through the turbine, it can be seen that the jet exits the blade AB to travel through the empty space inside the drum of the runner to strike a second blade at point C and finally exit from point D. Standard symbols are used for the inlet and outlet velocity triangles to denote u for the peripheral velocity, V_r, for the relative velocity and β for the blade angle. Indices 1 and 2 are used to signify parameters for the inlet and outlet velocity triangles as water enters and leaves each blade—that is, entry at points A and C and exit at points B and D, respectively. Adapting these symbols to the case of the cross-flow where the water strikes two sets of blades before exiting the runner, prime notation is used for the parameters at the two interior points, B and C, along with the corresponding indices. This allows for distinction between the two sets of inlet and outlet triangles. Thus, the parameters α_2', u_2', V_{r2}', β_2' are used for the outlet triangle at point B of the first blade whereas α_1', u_1', V_{r1}', β_1' are used for the inlet velocity triangle at point C of the subsequent blade.

Absolute velocity of the water jet before it strikes the runner is given by

$$V_1 = C_v \cdot \sqrt{2gH}$$

where C_v is the coefficient of velocity dependent on the nozzle, and H is the net head.

The relative velocity, V_{r1}, and blade angle, β_1, can be drawn for the inlet velocity triangle at point A, once the peripheral velocity, u_1, and angle α_1 are known. As defined in Chapter 9, the blade angle, β_1, is the angle made by the relative velocity with the negative direction of peripheral velocity. Shock is minimized, and maximum efficiency is achieved when the direction of the tangent to the blade at entry point A is the same as the direction of the relative velocity, V_{r1}.

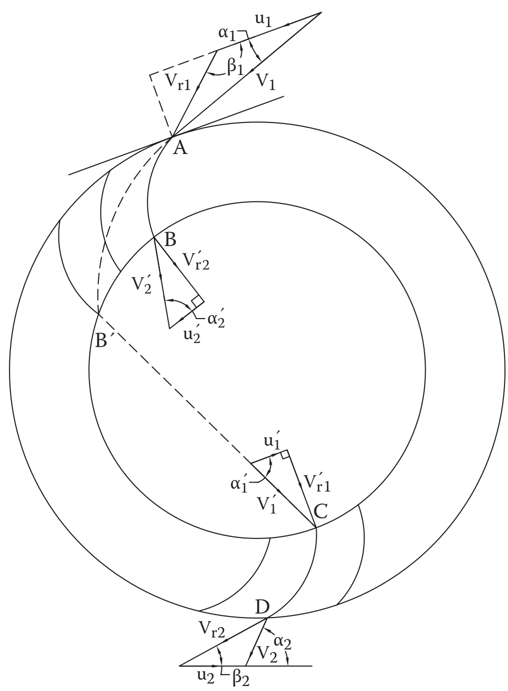

FIGURE 10.10 Path of water through cross-flow turbine.

The absolute velocity, V_2', and angle, α_2', which it makes with the velocity of the wheel, at point B can be determined from V_{r2}', β_2', and u_2' as the water exits blade AB. The blade angle at exit point B is 90°. Assuming negligible friction, $V_{r2}' = V_{r1}$; β_2' is a right angle, and u_2' depends on the inner radius of the runner.

The absolute path of the water as it flows over the moving blade, AB, and the point B′ at which the water leaves the blade are shown by the dotted line in Figure 10.10. Assuming no change in absolute velocity as the water moves through the center of the runner, V_2' becomes V_1' at point C where the water strikes blade CD. This makes the two interim inlet and outlet triangles congruent with corresponding angles $\alpha_1' = \alpha_2'$ and $\beta_1' = \beta_2'$.

Furthermore, $\beta_1 = 180° - \beta_2$ because each of the blades makes the same angle with the peripheral velocity at the rim. The blade angles are supplementary only because they have been defined to be measured against the negative of the peripheral velocity in both the inlet and outlet velocity triangles.

In order to avoid shock at entry at point C, the inlet blade angle must be radial, $\beta_1' = 90°$. One can think of blades AB and CD as forming one continuous S-shaped blade with the jet striking point A and exiting at point D [7]. Given the equivalence of the two internal velocity triangles at points B and C, the velocity vectors between the inlet triangle at point A and the outlet triangle at point D can be compared to compute the work done per second on the runner by the water jet.

The entire jet cannot follow this path, however. A portion of the jet will remain entrained on the periphery of the runner wheel and exit without entering the runner radially at all. Other streams of water will cross inside the wheel impinging on the second blade at a range of angles as well as interfering with each other [7].

Equation 9.12 can be written as

$$P = \rho Q(V_1 \cos \alpha_1 + V_2 \cos \alpha_2)\, u \tag{10.13}$$

From the velocity triangles in Figure 10.10, it can be seen

$$V_{r1} \cdot \cos (180 - \beta_1) = V_1 \cdot \cos \alpha_1 - u_1$$

$$V_2 \cos \alpha_2 = V_{r2} \cos \beta_2 - u_2$$

$$u_1 = u_2 = u$$

$$V_{r2} = \zeta V_{r1}$$

where ζ (zeta) is a friction coefficient of less than 1 if any increase in velocity of the water is considered negligible as a result of gravity between points B and C.

Combining these relationships,

$$V_1 \cos \alpha_1 = V_{r1} \cdot \cos(180 - \beta_1) + u_1$$

$$V_2 \cos \alpha_2 = V_{r2} \cdot \cos \beta_2 - u_2$$

Adding the respective sides of the above equations,

$$V_1 \cos \alpha_1 + V_2 \cos \alpha_2 = V_{r1} (\cos (180 - \beta_1) + \zeta \cos \beta_2)$$

Substituting for V_{r1},

$$V_1 \cos \alpha_1 + V_2 \cos \alpha_2 = (V_1 \cos \alpha_1 - u_1) \cdot (1 + \zeta \cos \beta_2/\cos (180 - \beta_1))$$

Substituting into Equation 10.13 gives

$$P = \rho Qu(V_1 \cos \alpha_1 - u_1) \cdot (1 + \zeta \cos \beta_2/\cos (180 - \beta_1))$$

Because $180° - \beta_1 = \beta_2$,

$$P = \rho Qu(V_1 \cos \alpha_1 - u_1)(1 + \zeta)$$

From the power equation, Equation 9.4,

$$\text{Power Input} = QgH = Qg \cdot \frac{V_1^2}{C_v^2 \cdot 2\ g} = \frac{QV_1^2}{2C_v^2}$$

Efficiency of the runner:

$$\eta = \frac{\text{Power Output}}{\text{Power Input}} = \frac{\rho Qu(V_1 \cos\alpha_1 - u_1) \cdot (1+\zeta)}{QV_1^2/2C_v^2} = (2C_v^2 \cdot u_1/V_1)(1+\zeta)(\cos\alpha_1 - u_1/V_1)$$

By differentiating η with respect to the speed ratio $\frac{u_1}{V_1}$, and setting to zero, the maximum efficiency is found to occur when

$$\frac{u_1}{V_1} = 0.5 \cos\alpha_1 \tag{10.14}$$

and equals

$$\eta_{max} = 0.5C_v^2(1+\zeta)\cos^2\alpha_1 \tag{10.15}$$

To achieve high efficiency, cross-flow turbines require the coefficient of velocity, C_v, of the nozzle and coefficient zeta, ζ, denoting the thinness of the blades and smoothness of their surface to both be as close to unity as possible. The efficiency of the cross-flow turbine depends additionally on the entrance angle, α_1, requiring it to be as close to zero as practical. The limitation in using too small an entrance angle, however, is that the torque and power transfer in the second stage becomes suboptimal. Lower flow velocity results in more of the flow streams being crossed inside the runner and low efficiency on second stage impact. An angle of 16° is usually selected by most cross-flow turbine manufacturers, consistent with what was proposed by Bánki, at least partly because of the convenience of marking a blade angle of 150° on the disk plates for welding blades as explained here.

Assuming $C_v = 0.98$ and $\zeta = 0.98$ at $\alpha_1 = 16°$,

$$\eta_{max} = 87.8\%$$

The question of the optimal entrance angle continues to be debated as researchers attempt to develop models to better understand and control second stage impact and efficiency. Designers have manufactured turbines with entrance angles ranging from 15° to 35° [8].

10.3.1.2 Blade Angle

The blade angle β_1 can be determined once α_1, u_1, and V_1 are known.

From the first inlet velocity triangle in Figure 10.10, it can be seen that the tangent of the complement of the blade angle

$$\tan(180 - \beta_1) = \frac{V_1 \sin\alpha_1}{(V_1 \cos\alpha_1 - u_1)}$$

Substituting $u_1 = 0.5\ V_1 \cos\alpha_1$ from Equation 10.14, for maximum efficiency,

$$\tan(180 - \beta_1) = \frac{V_1 \sin\alpha_1}{(V_1 \cos\alpha_1 - 0.5V_1 \cos\alpha_1)}$$

Therefore,

$$\tan(180 - \beta_1) = 2\tan\alpha_1$$

For $\alpha_1 = 16°$, this gives a blade angle close to 150°:

$$\beta_1 = 180 - 29.83 = 150.17°$$

And the supplement of the blade angle is 30°, which is a convenient angle when cutting the grooves on the disk plates for positioning the blades on the runner.

10.3.1.3 Inlet Curve

An adaptor is used to convert the cross-section of flow from the circular penstock to match the rectangular cross-section of the inlet housing of the cross-flow turbine. Before reaching the runner, the flow is transformed again so that each of the water stream lines striking the turbine blades have constant velocity and the same absolute entrance angle, α_1, despite their different radii.

For water in free flow affected by any kind of guide vane or inlet structure, the law of conservation of velocity momentum requires

$$v_u r = \text{constant}$$

where v_u is the peripheral velocity component of each stream line, and r is the radius measured from the axis. This relationship will be explored in more detail in Chapter 11. Assuming it does hold, this will mean that each stream line will enter the runner at radius R_1 with equal peripheral velocity.

The shape of the inlet curve, which allows a constant entrance angle irrespective of radii, is the logarithmic spiral, expressed by the formula [7]

$$R_\varphi = R_1 e^{k\varphi} \tag{10.16}$$

R_φ is the radius of the inlet curve, R_1 is the radius of the runner, $k = \tan\alpha_1$, and φ ranges from 0° to 90° and is expressed in radians.

This is shown graphically in Figure 10.11.

For example, at $\varphi = 30° = 0.524$ radians, and $\alpha_1 = 16°$, and $\alpha_1 = 16°$,

The ratio between R_φ and R_1 is

$$e^{\tan 16°.0.524} = 1.162.$$

Whereas at $\varphi = 30°$ and 90°, the ratios are 1.0 and 1.569, respectively.

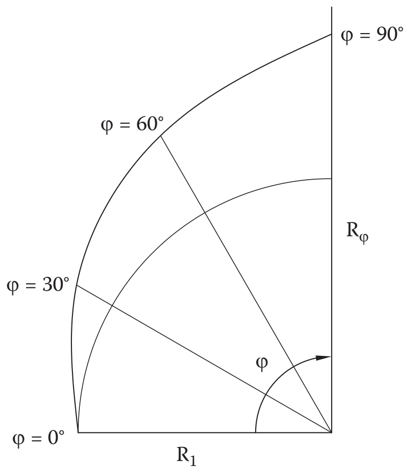

φ	R_φ/R_1
0°	1.0000
30°	1.1620
60°	1.3500
90°	1.5690

FIGURE 10.11 Logarithmic inlet spiral.

10.3.1.4 Runner Diameter

The diameter of the cross-flow runner does not impact the flow that it can accommodate, but it does directly influence its speed.

The angular velocity is related to the peripheral velocity of the runner, u, and its diameter, D by the relationship

$$\omega = 2 \cdot \frac{u}{D}.$$

The angular velocity of the runner is also related to its speed, N, in RPM:

$$\omega = 2\pi f; \text{ where } N = 60 \cdot f.$$

From these relationships, D can be written as

$$D = \frac{u}{\pi N} \cdot 60$$

Assuming that the coefficient of velocity of the nozzle $C_v = 0.98$ and peripheral velocity $u = 0.48\ V_j$,

$$D = \frac{60 \cdot 0.48 \cdot 0.98}{\pi N} \cdot \sqrt{2 \cdot 9.81} \cdot \sqrt{H}$$

$$D_{runner} = 40 \cdot \frac{\sqrt{H}}{N} \tag{10.17}$$

Most manufacturers use standard runner diameters. For example GFA, Entec's T-15 comes in two diameter sizes: 300 mm and 500 mm. Designers can pick from among the available diameter options to achieve the closest turbine speed to that desired.

The jet thickness in a cross-flow turbine is typically between 0.1 and 0.2 times the runner diameter. With information from the manufacturer about the ratio of nozzle thickness to runner diameter, the length of the runner required for the particular site conditions can be calculated to achieve the required flow at the available head.

$$Q = A_{nozzle} \cdot V_{jet}$$

$$A_{nozzle} = t_{jet} \cdot L_{nozzle} = t_{jet} \cdot L_{runner}$$

$$Q = t_{jet} \cdot L_{runner} \cdot C_v \cdot \sqrt{2gH}$$

$$L_{runner} = \frac{Q}{t_{jet} \cdot C_v \cdot \sqrt{2gH}} \tag{10.18}$$

One major advantage of the cross-flow turbine is that the runner length could, in principle, be changed to whatever is required to accommodate the available flow without changing the hydraulic characteristics of the turbine. Twice the flow could be accommodated by doubling the length of the runner, for example, without changing the runner diameter and the corresponding turbine speed. This is different from the Pelton or Turgo with which the runner diameter determines the maximum size of the nozzle. In practice, the longer blades on a larger flow cross-flow turbine shaft will flex more and be susceptible to fracture from metal fatigue. To overcome this problem, it is common practice, for longer runners, to weld additional discs across the length of the runner to keep the unsupported blade lengths short. This reduces the fracture of the blades, but there is a cost in reduced runner efficiency.

The runner diameter does have influence on the maximum flow, however. A larger diameter runner would allow the turbine to accommodate a higher flow for the same runner length because the nozzle thickness could be proportionately larger. The discharge through a cross-flow turbine is proportional to the product of the inlet width of a cross-flow turbine, b_o, and the runner diameter, D. The disadvantage of the larger runner diameter is its lower speed, and the need for gearing up of speed to drive an alternator. This has consequences for both cost and efficiency. If the application is directly driving agricultural milling equipment, which generally operate more slowly than generators, the lower speed of a higher diameter runner is much less of a constraint.

Example 10.6

The workshop in a neighboring town makes cross-flow turbines with fixed size diameter runners of 240 mm and 415 mm. The workshop sizes their nozzles at one fifth the runner diameter. To generate electricity at a site with 16 m head and 200 lps design flow, which diameter cross-flow should the community order, and what would be the runner length?

It is preferable to use a smaller diameter runner with a higher speed because this will require a smaller increase in speed to drive an alternator at 1500 RPM. Let's first try the 240-mm diameter runner.

$$D_{runner} = 40 \cdot \frac{\sqrt{H_{net}}}{N}$$

$$N = 40 \cdot \frac{\sqrt{H_{net}}}{D}$$

$$N = 667 \text{ RPM}$$

The speed of the turbine would need to be increased through the use of a drive system, using pulleys and belts, by a ratio of 1500: 667 = 2.25 to drive the alternator at the required speed.

The next step is to check what the length of 240-mm diameter cross-flow would need to be to accommodate the design flow of 200 lps at the site.

$$t_{jet} = 0.2 \cdot 240 \text{ mm} = 48 \text{ mm}.$$

$$L_{runner} = \frac{Q}{t_{jet} \cdot C_v \cdot \sqrt{2 \cdot g \cdot H}}$$

$$L_{runner} = \frac{0.2}{0.048 \cdot 0.98 \cdot \sqrt{2 \cdot 9.81 \cdot 16}}$$

$$= 0.240 \text{ m} = 240 \text{ m}$$

It is likely that the workshop produces standard length runners, which will be suitable for the site, perhaps 250 mm in this particular case. The 240-mm diameter runner is appropriate for this site.

The 415-mm diameter runner would result in a lower speed of 386 RPM, which would need to be increased by a factor of 3.89 through the use of a drive system to achieve 1500 RPM. The closer the speed ratio is to one, the lower the cost of the drive system due to smaller size of the larger pulley and lower service factor of belts.

10.3.2 Part Flow Efficiency

Commercial crossflow turbines, such as the Ossberger, are specified to be above 80% efficient with their largest machines claiming efficiency as high as 86%. The efficiency of cross-flow turbines built in developing countries range from around 60%–80%. The GFA Entec T-15, the most efficient in the T-series turbines, which are specifically designed to be manufactured in developing countries, claims an efficiency of 75% for smaller machines and above 80% for larger units above 300 kW. Turbine efficiency can be kept almost constant down to around half the maximum design flow through the use of a well-designed guide vane.

Below 50% of maximum flow, efficiency can drop sharply with many designs. For sites that have a significant reduction of water flow in the dry season, the recommended design employs flow partitioning. The turbine is essentially designed with two cells and two guide vanes, one covering one third of the nozzle width, and the second covering the remaining two thirds. By closing the larger guide vane completely and operating only the smaller one, cross-flow turbines with flow partitioning can have fairly constant efficiencies down to around 20% of full design flow. Figure 10.12 shows the superior part flow efficiency of the two-cell Ossberger turbine with flow division of 1:2 between the cells compared with a Francis turbine.

The GFA Entec brochure [9] states that its T-15 series has 70% efficiency at a flow of 40% and maintains 55% efficiency even down to 20% flow (see Figure 10.13). If this range of part flow efficiency is acceptable for the application at hand, it would avoid the additional cost of an additional cell as well as a second guide vane and an additional regulating device.

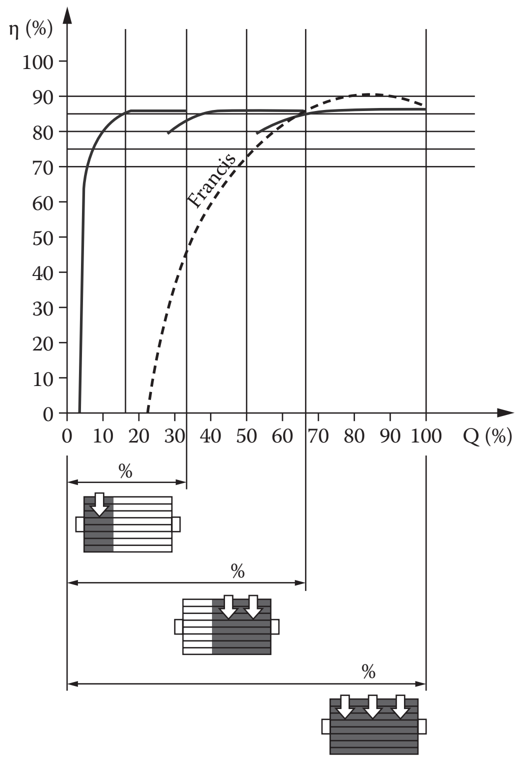

FIGURE 10.12 Part flow efficiency Ossberger.

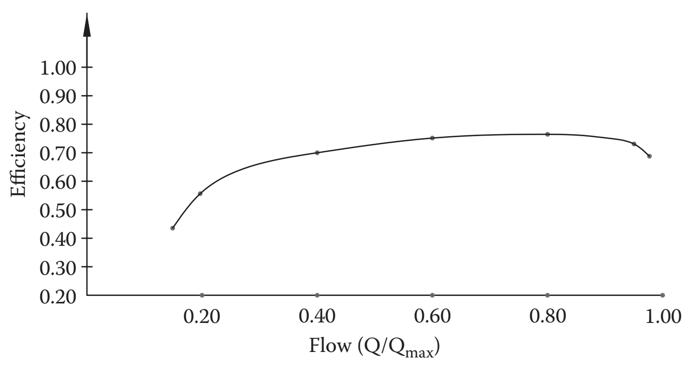

FIGURE 10.13 Efficiency curve of the T-15. (From GFA Entec AG.)

EXERCISES

1. What is the loss in efficiency in the production of a jet of water on account of a nozzle with a coefficient of velocity $C_v = 0.9$? (Answer: 19%.)
2. Estimate the hydraulic efficiency of a Pelton runner with well-polished buckets with a bucket angle of 15°, and the smoothness factor in the bucket $\zeta = 0.98$. (Answer: 97.3%.)
3. What diameter runner is required for a Pelton turbine to perform optimally at a speed of 1550 RPM at a site with a net head of 55 m? What is the largest jet diameter that a runner of this size can efficiently accommodate? What is the maximum flow that a two-jet Pelton turbine can utilize using this runner? Assuming an overall efficiency of 60%, how much

electrical power could this micro hydropower site generate? (Answer: 182 mm, 20.2 mm, 20.4 lps, 6.6 kW.)

4. The manufacturer offers a two-nozzle horizontal axis Pelton turbine with a 200-mm diameter runner. At what speed would the new runner operate most efficiently if used under a net head of 55 m? What is the speed ratio (u/V_{jet}) at which the available runner would operate if the available Pelton were to be utilized at the design speed of 1550 RPM? Estimate the change in relative runner efficiency through the use of a standard sized runner, assuming that the optimal speed ratio is 0.46. What is the maximum flow that the available turbine can accommodate at this site? (Answer: 1409 RPM, 0.51, −1.5%, 24.7 lps.)
5. In Exercise 2, what could the largest jet diameter be if the Pelton turbine were replaced by a Turgo turbine? What maximum flow could a two-jet Turgo accommodate if installed at this same site? How much electrical power could be produced with the Turgo turbine assuming the same overall efficiency of 60%? (Answer: 60.6 mm, 184 lps, 59.5 kW.)
6. A Pelton wheel is operating under a net head of 220 m, and the flow through the nozzle is 35 lps. The deflection angle, ϕ, of the jet by the bucket is 165°. Calculate (a) the power output of the runner and (b) its hydraulic efficiency. Assume that the coefficient of velocity of the nozzle is 0.97, speed ratio is 0.48, and friction factor on the inside of the bucket is 0.90. (Answer: 66.3 kW, 87.8%.)
7. A hydropower site has the following characteristics: available flow 260 lps and net head 9 m. The site is being considered for installation of a locally manufactured cross-flow turbine to power a rice mill and oil expeller during daytime and to drive an induction generator for community lighting in the evening. The available turbine has a runner with a drum diameter of 300 mm and width of 450 mm. According to the manufacturer, the jet thickness of the turbine is 15% of the runner diameter. Verify that the available turbine is able to use all the water flow available at the site. Calculate the maximum mechanical power output of the turbine if its efficiency is specified at 65%. Calculate the RPM of the turbine and the speed ratios required to drive the rice mill, oil expeller, and induction generator using pulleys and flat belts if typical speeds for the equipment are given to be 1000 RPM, 200 RPM, and 1550 RPM, respectively. (Answer: 444 mm turbine width is sufficient to accommodate full flow of 260 lps; 14.9 kW; 400 RPM; speed ratios: rice mill 1:2.5, oil expeller 1:0.5, induction generator 1:3.88.)
8. Due to a conflict over right of way, the mill owner has to dig a new lower canal to convey water to the hydropower site for the mill planned in Exercise 7. If the same cross-flow turbine were to be used to make use of the lower net head available of 7.5 m, what would be the maximum power output of the turbine and its optimal RPM? (Answer: 11.5 kW, 365 RPM.)
9. An unelectrified community receives a donation of a good quality, used Pelton turbine, which is rated 200 kW at an RPM of 1800 under a net head of 350 m. How much power can the turbine produce at a new site with a significantly lower net head of 85 m? What is the speed ratio of the belt drive system that the community has to purchase to use this turbine to drive a 1500 RPM generator? Assume the efficiency of the turbine to be constant in both cases. (Answer: 23.9 kW, drive speed ratio 1.69:1.)
10. A two-jet Pelton turbine must generate 12 MW under a net head of 300 m. Calculate the diameter of the runner if the jet ratio cannot be less than 11, and find the highest speed that the runner can achieve. Assume that the bucket angle is 165°, speed ratio is 0.46, coefficient of velocity is 0.98, and the friction factor on the bucket is 0.95. (Answer: 2.1 m, 310 RPM.)

REFERENCES

1. Thake, J., *The Micro Hydro Pelton Turbine Manual*. Practical Action Publishing, Warwickshire, UK, 2000.
2. Harvey, A. and Brown, A., *Micro-Hydro Design Manual: A Guide to Small-Scale Water Power Schemes*, ITDG Publishing, London, 1993.

3. Inversin, A. R., *Micro-hydropower Source Book*. NRECA International Foundation, Arlington, VA, 1986.
4. Mockmore, C. and Merryfield F., The Banki water-turbine. Engineering Bulletin Series, Number 25, Oregon State University, Corvallis, OR, 1949.
5. Remote Hydro Light. Afghan built water turbine tested in Norway achieves 78.6% efficiency. Jan. 2011. http://www.remotehydrolight.com/LaboratoryTest.pdf.
6. Entec Consulting and Engineering. T15: A new turbine, a long tradition. Jan. 2007. http://www.entec.ch/entecweb/media/Development_History.pdf.
7. Arter, A. and Meier, U., *Hydraulics Engineering Manual. Harnessing Water Power on a Small Scale*, Volume 2. SKAT, Swiss Center for Appropriate Technology; St. Gallen, Switzerland, 1990.
8. Kaunda, C., Kimambo, C., and Nielsen, T., Experimental study on a simplified crossflow turbine. *International Journal of Energy and Environment* 5, 155–182, 2014.
9. Entec Consulting and Engineering, Entec Cross Flow Turbine T-15 brochure, n.d. http://www.entec.ch/entecweb/media/T15_Brochure.pdf.

11 Reaction Turbines

Rotation of the runner in a reaction turbine results from the reaction to its blades changing the direction and momentum of the water flow. The flow in reaction turbines is continuous over the length of the water passage with the runner rotating immersed in water flowing continuously over all its blades. Figure 11.1 shows an example of how all the blades of a reaction turbine, in this case a Kaplan, are in the water and simultaneously interacting with the flow. This is markedly different from impulse turbines with which the runner rotates in the air with a few of the buckets interacting with a high-velocity jet of water at any one time. The simultaneous application of torque on all the blades of a reaction turbine results in significantly more power produced per unit head compared to an impulse turbine using the same sized runner.

Reaction turbine runners are designed to make use of both the pressure energy and kinetic energy of the water flow. The inlet structure, consisting of a spiral casing and a wicket gate with guide vanes designed to introduce swirl or circulation as the water enters the runner, typically transforms only a part of the hydraulic pressure into kinetic energy as the water passes through it. As a result, the flow velocity at the runner inlet is relatively low for reaction turbines compared to impulse turbines. The runner converts the remaining pressure head to kinetic energy and ultimately transforms both the pressure and velocity of the water into mechanical power. To extract the maximum power from the available head, hydraulic pressure is often below atmospheric when the water exits the runner. This is accomplished through the use of a draft tube, described in Section 11.2.

Reaction turbines have higher specific speeds than impulse turbines—that is, for similar head and power output conditions, reaction turbines run at significantly higher speeds. The most widely used reaction turbine designs are the Francis, Kaplan, and propeller. In recent years, compact tubular bulb turbines have become popular for low and very low head applications. Francis turbines, which utilize radial–axial flow, are used across a large range of medium heads (40–700 m) whereas Kaplan and propeller turbines utilize axial flow and are suitable for low head sites (10–80 m).

The higher power capacity per unit head available with reaction compared to impact turbines is demonstrated by the range of large end hydro turbines produced by Andritz Hydro of Austria (see Table 11.1).

Due to its larger range of applicability, the Francis turbine is often referred to as the workhorse of hydropower because 60% of global hydro capacity is generated using this turbine design. Figure 11.2 shows the broad application range of reaction turbines covering medium to low head.

There is overlap between low-power Francis turbines with impulse turbines across the small hydropower range with cross-flow, Turgo turbines and multiple-jet Pelton turbines covering much of the same range as shown in the application chart in Figure 9.14.

11.1 BASIC CALCULATIONS

In place of nozzles, reaction turbines have guide vanes, located in a wicket gate, which direct water flow to the runner. Taking the case of the commonly used radial-flow wicket gate, the velocity vector, $\mathbf{v_0}$, can be divided into its two components:

$$\mathbf{v}_0 = \mathbf{v}_{0r} + \mathbf{v}_{0u} \tag{11.1}$$

where $\mathbf{v}_{0r}$ is the radial component, and $\mathbf{v}_{0u}$ the peripheral component. If α_0 is the angle that $\mathbf{v}_{0u}$ makes with $\mathbf{v}_0$, it can be seen from Figure 11.3 that

$$v_{0u} = v_0 \cos \alpha_0 \tag{11.2}$$

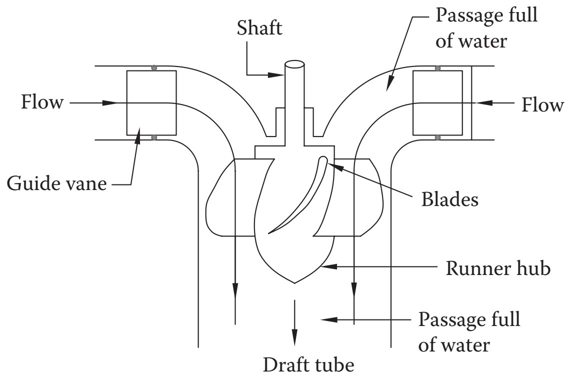

FIGURE 11.1 Water flow through runner of Kaplan turbine.

TABLE 11.1
Power Capacity of Reaction Turbines per Unit Head Compared to Pelton Turbines

	Francis	Kaplan	Bulb	Pelton
Head range	Up to 700 m	10–80 m	1–30 m	Up to 1800 m
Power output per unit	Up to 800 MW	Up to 200 MW	Up to 76 MW	Up to 420 MW

Source: Andritz, Hydro turbines. http://www.andritz.com/index/hydro/hy-others-andritz-hydro/pf-detail?productid=9192.

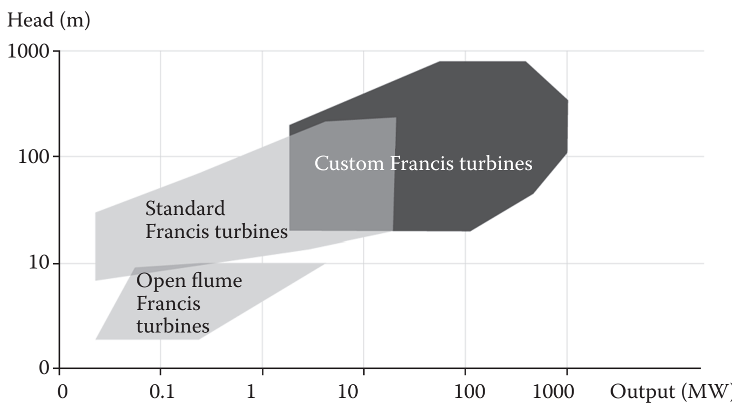

FIGURE 11.2 Application range of Voith Francis turbines. (From http://www.voith.com/en/2013-05-27_voith_francis_turbines.pdf.)

The guide vanes introduce a swirl, indicating that the water flow is rotated about the axis O, which is at a distance $\frac{D_0}{2}$ from the exit end of the guide vane.

The swirl of the water is expressed by the term "circulation" and is denoted by the Greek gamma, Γ, defined as the closed line integral of the dot product between vectors for the velocity and displacement of water:

$$\Gamma = \oint v \cdot ds = \oint v \, ds \cos \alpha \tag{11.3}$$

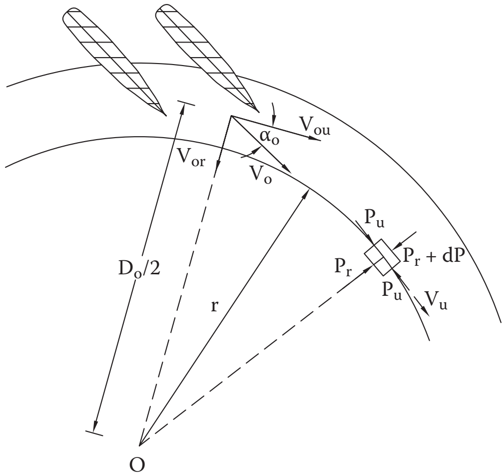

FIGURE 11.3 Swirl created by guide vanes.

S is the closed contour drawn inside the flow, and α is the angle between ***v*** and ***ds*** as shown in Figure 11.4. Circulation, Γ, has units of m²/s and is crucial to generate torque in a reaction turbine.

Integrating along the circle with diameter D_0, immediately downstream of the wicket gate, the Circulation Γ_0 can be expressed as

$$\Gamma_0 = \pi D_0 v_0 \cos \alpha_0 \tag{11.4}$$

where v_0 is the magnitude of the velocity of the water as it comes out of the guide vanes, and α_0 is its angle with the periphery.

It is clear from Equation 11.4 that the guide vanes alone are responsible for creating circulation, Γ_0.

The circulation at any radius r can be written as

$$\Gamma = 2\pi r v_u \tag{11.5}$$

To understand the generation of torque and power by the runner of a reaction turbine, the angular momentum equation can first be used to characterize the free flow of water solely as a result of the action of the guide vanes.

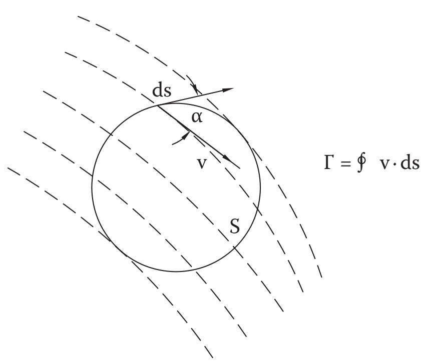

FIGURE 11.4 Circulation.

Consider mass "m" at a radius "r" in the stream line of the velocity, v. The angular momentum equation says that the derivative of the moment for mass "m" around some axis is equal to the sum of the moments of all external forces acting upon this mass about the same axis.

This can be written as

$$\frac{d(mv_u r)_o}{dt} = \sum M_o \tag{11.6}$$

where v_u is the peripheral velocity component of the water acting on the mass, and r is the radius measured from the axis.

$\sum M_o$ reflects the sum of all the moments of external forces acting on the mass about axis O. Analyzing these forces, it can be seen that the main forces acting on mass "m" either cancel each other out, for example, in the case of pressure at each end P_u, or do not contribute to the momentum around the axis in the case of the radial pressures, P_r and $P_r + dP$. The tangential forces, due to liquid friction, are small and can be ignored.

For water in free flow, it can thus be assumed that $\sum M_o = 0$.

In which case,

$$\frac{d(mv_u r)_o}{dt} = 0,$$

which would imply that

$$mv_u r = \text{constant}$$

This gives the important relationship known as the law of conservation of velocity momentum:

$$v_u r = \text{constant} \tag{11.7}$$

Applying Equation 11.7 to radius, $\frac{D_0}{2}$,

$$v_u r = v_{0u}\frac{D_0}{2}$$

Or

$$v_u = \frac{0.5 v_{0u} D_0}{r} \tag{11.8}$$

$v_u(r)$ is seen to be a hyperbola as depicted in Figure 11.5. Equation 11.8 shows that rotational flow consists of fluid elements moving vortex-like on a plane with a common center, with velocity decreasing toward the periphery.

Given the conservation of velocity momentum from Equation 11.7, it can be seen that for a liquid in free flow the circulation is constant for all values of r.

$$\Gamma = \Gamma_0 = \text{constant} \tag{11.9}$$

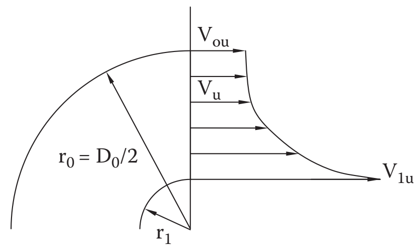

FIGURE 11.5 Velocity distribution of fluid as a function of radius.

Water will, of course, no longer be in free flow once a runner is present in the turbine. However, it can be expected that the circulation created by the guide vanes will be present in the space between the wicket gate and the runner.

11.1.1 Energy Equation

The result of the angular momentum equation, Equation 11.6, is next used to determine how the runner generates power as a reaction to the circulation described above.

The moment of momentum theorem states that in steady-state flow the *torque on the rotor equals the time rate of change of moment of momentum (or angular momentum) of the fluid as it passes through the runner.*

The rate of change of angular momentum can be broken down into two terms:

$$\tau = [\text{Rate of mass flow through the rotor}] \times [\text{Decrease of moment of momentum of the fluid in each blade}]$$

$$\tau = \dot{m}(v_{1u}r_1 - v_{2u}r_2) \tag{11.10}$$

where v_{1u} is the tangential component of the absolute velocity of water at the entry of the runner vane, v_{2u} is the tangential velocity of the absolute velocity of water at the exit of the runner vane, $\dot{m}$ is the rate of mass flow and is equal to the product ρQ where ρ is the density of water and Q is the flow rate in m^3/s.

The sign is important because angular momentum is a vector, and positive means that the runner is spinning in one direction and negative in the opposite direction.

This is a general equation that applies equally to pumps as to turbines. Within turbines, it applies to steam turbines as well as it does to hydropower or wind turbines.

Expanding Equation 11.10 and using the relationships in Equations 11.2 and 11.8 gives

$$\tau = \rho Q(0.5D_{1d}v_1 \cos\alpha_1 - 0.5D_{2d}v_2 \cos\alpha_2) \tag{11.11}$$

The expressions for the circulation at the inlet and outlet of the runner vane can also be written in a similar format using Equation 11.4 as

$$\Gamma_1 = \pi D_{1d}v_1 \cos\alpha_1$$

$$\Gamma_2 = \pi D_{2d}v_2 \cos\alpha_2$$

Equation 11.11 can now be rewritten as

$$\tau = \frac{\rho Q}{2\pi}(\Gamma_1 - \Gamma_2) \tag{11.12}$$

Equation 11.12 can be interpreted as saying that torque is applied to the rotor when its blades change the flow circulation, Γ [1].

Power output of the runner, which is the product of the torque on its shaft and its angular velocity, is also related to the change in the circulation:

$$P = \omega\tau = \omega\frac{\rho Q}{2\pi}(\Gamma_1 - \Gamma_2) \tag{11.13}$$

Combining Equation 11.13 with the power equation, Equation 9.4,

$$P = \rho \cdot Q \cdot g \cdot H \cdot \eta_h$$

It is seen that

$$\rho Q g H \eta_h = \omega \rho Q(0.5D_{1d}v_1 \cos\alpha_1 - 0.5D_{2d}v_2 \cos\alpha_2)$$

and

$$H\eta_h = \frac{\omega}{g}(0.5D_{1d}v_1 \cos\alpha_1 - 0.5D_{2d}v_2 \cos\alpha_2)$$

where H is the head available to the turbine, and η_h is the hydraulic efficiency.

The equation can also be written as

$$H\eta_h = \frac{1}{g}(u_1 v_1 \cos\alpha_1 - u_2 v_2 \cos\alpha_2) \tag{11.14}$$

Because $u_1 = \omega \cdot 0.5D_{1d}$; and $u_2 = \omega \cdot 0.5D_{2d}$.

Combining with Equation 11.12,

$$\rho Q g H \eta_h = \omega\frac{\rho Q}{2\pi}(\Gamma_1 - \Gamma_2)$$

or

$$H\eta_h = \frac{\omega}{2\pi g}(\Gamma_1 - \Gamma_2) \tag{11.15}$$

Equations 11.14 and 11.15 are known as Euler equations. They represent the main energy equations for all reaction turbines. The left side represents the energy received, in Joules, by the runner from 1 Newton weight of fluid flowing through its blades. The right sides in the two equations provide insight into the specific characteristics of the flow before and after the runner that provide the highest efficiency in terms of transferring energy to it.

From Equation 11.15, it can be seen that the maximum efficiency of the runner could, in principle, result if the circulation at the exit, Γ_2, could be negative, thus adding to the Euler head. This situation, which is referred to as reverse circulation or reverse swirl, would, however, require swirl at the runner outlet to be in the direction opposite to the direction of rotation of the runner. In practice, any significant amount of negative swirl causes rapid drop in hydraulic efficiency because this implies residual kinetic energy in the exiting water, which is not available to the runner. Maximum efficiency thus requires Γ_2 to be as small as possible while Γ_1 must be as large as possible, ideally the same as Γ_0. The insight here is that in order to achieve the best efficiency, the reaction turbine runner must ideally fully "use up" the circulation generated by the guide vanes.

This retardation of fluid circulation by the runner blades can also be examined through velocity triangles, introduced in Chapter 9. The runner of the reaction turbine produces torque and is able to generate power when the velocity triangle at the inlet of the runner vane is substantially different from the velocity triangle at its exit. Examining the energy values associated with the three velocity terms from the two triangles, velocity triangles can be used to derive alternate forms of Euler's equation for turbines. Symbols used in Chapter 9 will be used here for consistency.

V_1, V_2 = Absolute velocities as the jet enters and leaves the vane (inlet and outlet)
V_{r1}, V_{r2} = Velocities of the jet relative to the vane velocity at its inlet and outlet
u_1, u_2 = Peripheral velocity of the vane at the inlet and outlet
α_1 and α_2 = Angle of the absolute velocity at inlet and outlet with direction of peripheral velocity
β_1 and β_2 = Angles made by relative velocity vectors with negative direction of u_1 and u_2.

The two other velocities required to complete the velocity triangles are the following:

V_{w1}, V_{w2} = Tangential components of the absolute velocities (= $V_1 \cos \alpha_1$, $V_2 \cos \alpha_2$)
V_{f1}, V_{f2} = Flow components of the absolute velocities (= $V_1 \sin \alpha_1$, $V_2 \sin \alpha_2$)

Using the notation of velocity triangles, Equation 11.14 can also be written as

$$H\eta_h = \frac{1}{g}(u_1 V_{w1} - u_2 V_{w2}) \tag{11.16}$$

From Equation 11.16, the highest value of the head would then be written in the frequently seen equation:

$$H\eta_h = \frac{1}{g}(u_1 V_{w1}) \tag{11.17}$$

Because $V_{w2} = V_2 \cos \alpha_2$, V_{w2} is equal to zero when $\alpha_2 = 90°$, and it can be seen that at maximum efficiency the exit flow has to be radial. Reaction turbines are generally designed to achieve radial exit flow in order to maximize the hydraulic efficiency, and this also implies $V_2 = V_{f2}$.

Equation 11.17 then provides the energy utilized by the rotor per unit weight of water while the energy loss is made up mostly of residual kinetic energy lost to the tailrace.

$$\text{Loss of kinetic energy} = \frac{V_2^2}{2g} = \frac{V_{f2}^2}{2g}$$

The hydraulic efficiency can be seen to equal the ratio of the energy utilized to total energy available.

$$\eta_h = \frac{\frac{1}{g}(u_1 V_{w1})}{H} = \frac{\frac{1}{g}(u_1 V_{w1})}{\frac{1}{g}(u_1 V_{w1}) + \frac{V_{f2}^2}{2g}} = \frac{u_1 V_{w1}}{u_1 V_{w1} + V_{f2}^2/2} \tag{11.18}$$

11.1.2 Euler Equation and Nature of Energy Transfer

From the inlet velocity triangle drawn for a typical Francis turbine runner in Figure 11.6, it can be seen that

$$V_{f1}^2 = V_1^2 - V_{w1}^2$$

$$V_{f1}^2 = V_{r1}^2 - (V_{w1} - u_1)^2$$

Combining these two equations gives

$$V_1^2 - V_{w1}^2 = V_{r1}^2 - (V_{w1} - u_1)^2 = V_{r1}^2 - V_{w1}^2 + 2V_{w1}u_1 - u_1^2$$

From which can be computed

$$V_{w1}u_1 = \frac{1}{2}\left(V_1^2 - V_{r1}^2 + u_1^2\right) \tag{11.19}$$

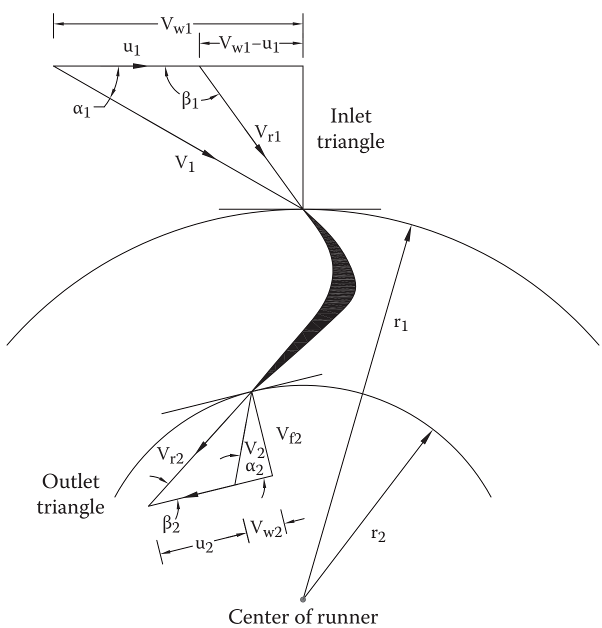

FIGURE 11.6 Velocity triangles for a Francis runner.

From the outlet velocity triangle, it can similarly be seen that

$$V_{w2}u_2 = \frac{1}{2}\left(V_2^2 - V_{r2}^2 + u_2^2\right) \tag{11.20}$$

Substituting for $V_{w1}u_1$ and $V_{w2}u_2$ in Equation 11.16 gives

$$H\eta_h = \frac{V_1^2 - V_2^2}{2g} + \frac{V_{r2}^2 - V_{r1}^2}{2g} + \frac{u_1^2 - u_2^2}{2g} \tag{11.21}$$

Equation 11.21 is an alternative form of the Euler equation and represents how the head extracted by a hydro turbine depends on the difference in velocity triangles at the runner inlet and outlet.

The left side of the equation represents the energy received by the reaction turbine, and the terms on the right side of Equation 11.21 provide insight into how this energy is transferred to the runner [2].

- $\frac{V^2}{2g}$ is known as the velocity head, and the first term on the right hand side, $\frac{V_1^2 - V_2^2}{2g}$, represents the change in kinetic energy between the inlet and outlet of the wheel. This term is also known as the *impulse effect* because it denotes how energy is similarly transferred in an impulse turbine.
- The remaining second and third terms together represent components of the change in pressure head in a reaction turbine, and their total contribution, $\frac{V_{r2}^2 - V_{r1}^2}{2g} + \frac{u_1^2 - u_2^2}{2g}$, is called the *reaction effect*. A convergent passage going from the inlet to outlet results in acceleration of the relative velocity, and $\frac{V_{r2}^2 - V_{r1}^2}{2g}$ represents a corresponding decrease in pressure.
- The third term, $\frac{u_1^2 - u_2^2}{2g}$, represents the remaining change in pressure head resulting from the centrifugal effect. Radial–axial reaction turbines, which are used at relatively higher heads, have a high ratio of diameters, D_1/D_2, and a large resulting difference between u_1 and u_2 accentuating the importance of this third term. Such turbines cover the low specific speed range of reaction turbines. Whereas in axial-flow turbines with high specific speeds, propeller and Kaplan, this third term makes zero contribution to energy transfer because $u_1 = u_2$, and $H\eta_h$ is a function only of the relative and absolute velocities. Because these velocities cannot be high, to avoid excessive losses, axial-flow turbines are limited to lower head sites (see Figure 11.7).

Example 11.1

The peripheral velocity of a Francis runner at inlet is 20 m/s. If the flow and whirl components of the inlet velocity are 5 m/s and 15 m/s respectively, find the following:

a. Inlet guide vane angle, α_1
b. Inlet blade angle, β_1
c. The net head at which the turbine is operating assuming the flow velocity remains constant and there is zero swirl at exit.

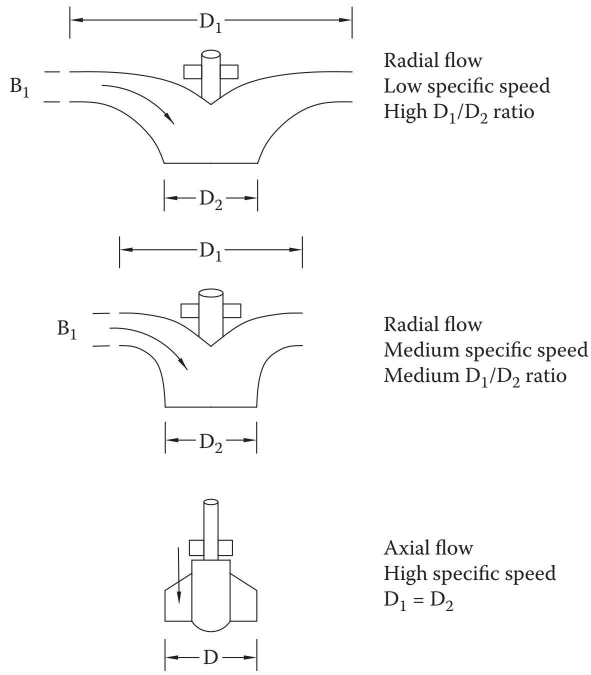

FIGURE 11.7 Profiles of specific speeds and runner diameter ratios of reaction turbines.

Figure 11.8 shows the inlet and outlet velocity triangles for Example 11.1. The blade angle from the inlet triangle is acute as might be expected when the peripheral velocity is larger than the whirl velocity. Zero whirl at exit implies that the guide vane angle in the outlet triangle is 90°, and the jet velocity is equal to the flow velocity.

a. From the inlet velocity triangle in Figure 11.8,

$$\tan\alpha_1 = \frac{V_{f1}}{V_{w1}} = \frac{5}{15} = 0.33$$

$$\alpha_1 = \tan^{-1} 0.33 = 18.42°$$

$$\tan\beta_1 = \frac{V_{f1}}{u_1 - V_{w1}} = \frac{5}{20-15} = 1.0$$

$$\beta_1 = \tan^{-1} 1.0 = 45°$$

b. Equation 11.18 can be used to find the hydraulic efficiency of the rotor:

$$\eta_h = \frac{u_1 V_{w1}}{u_1 V_{w1} + V_{f2}^2/2} = \frac{20\cdot 15}{20\cdot 15 + 5^2/2} = \frac{300}{312.5} = 96\%$$

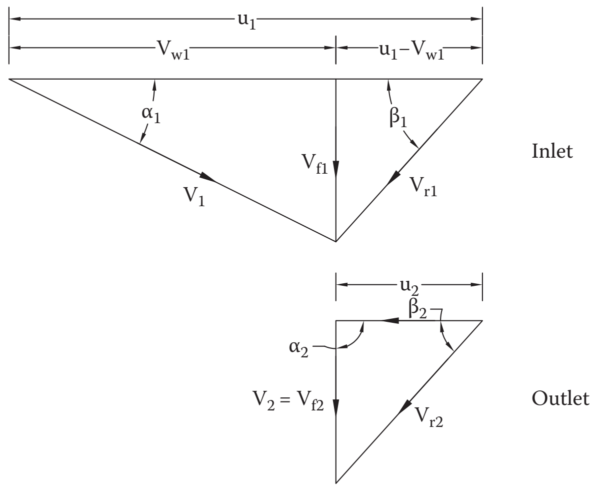

FIGURE 11.8 Inlet and outlet velocity triangles.

From Equation 11.21,

$$H_{net}\eta_h = \frac{1}{g}u_1V_{w1}$$

$$H_{net} = \frac{u_1V_{w1}}{g\cdot\eta_h} = \frac{20\cdot 15}{9.81\cdot 0.96} = 31.9\text{ m}$$

11.1.3 Degree of Reaction

The contribution of the reaction effect to the total head is known as the degree of reaction and is denoted by "R."

$$R = \frac{\dfrac{V_{r2}^2 - V_{r1}^2}{2g} + \dfrac{u_1^2 - u_2^2}{2g}}{H\eta_h} = \frac{H\eta_h - \dfrac{V_1^2 - V_2^2}{2g}}{H\eta_h} \tag{11.22}$$

The reaction effect relies on the development of pressure head, which is contributed by the differences in relative velocity and peripheral velocity between the inlet and outlet of the runner. Reaction turbines must therefore be fully enclosed. Impulse turbines do not rely on any reaction effect because $u_1 = u_2$, and $V_{r1} = V_{r2}$ and their runners operate at atmospheric pressure.

Example 11.2

Find the hydraulic efficiency and degree of reaction of an inward flow reaction turbine with $\alpha_1 = 22°$ and $\beta_1 = 45°$, assuming radial outflow and constant velocity of flow.

From Figure 11.8,

$$V_{f1} = V_{w1}\tan\alpha_1 = V_{w1}\tan 22° = 0.4V_{w1}$$

and

$$V_{f1} = (u_1 - V_{w1}) \tan \beta_1 = (u_1 - V_{w1}) \tan 45° = (u_1 - V_{w1})$$

Combining the two equations,

$$u_1 - V_{w1} = 0.4V_{w1}$$

$$u_1 = 1.4V_{w1}$$

Constant velocity of flow implies

$$V_{f1} = V_{f2} = 0.4V_{w1}$$

a. Substituting for u_1 and V_{f2} in Equation 11.18 for hydraulic efficiency,

$$\eta_h = \frac{u_1 V_{w1}}{u_1 V_{w1} + V_{f2}^2/2} = \frac{1.4V_{w1}^2}{1.4V_{w1}^2 + \dfrac{0.16}{2}V_{w1}^2} = \frac{1.4}{1.48} = 94.6\%$$

b. Using Equation 11.22 for the degree of reaction,

$$R = \frac{H\eta_h - \dfrac{V_1^2 - V_2^2}{2g}}{H\eta_h} = 1 - \frac{V_1^2 - V_2^2}{2gH\eta_h}$$

From the outlet velocity triangle, radial outflow and constant velocity of flow implies

$$V_2 = V_{f2} = V_{f1}$$

$$V_1^2 - V_2^2 = V_1^2 - V_{f2}^2 = V_1^2 - V_{f1}^2 = V_{w1}^2$$

with the last step resulting from the use of the Pythagorean relationship to the inlet velocity triangle.

And $gH\eta_h = u_1 V_{w1}$ from Equation 11.17

So

$$R = 1 - \frac{V_1^2 - V_2^2}{2gH\eta_h} = 1 - \frac{V_{w1}^2}{2u_1 V_{w1}} = 1 - \frac{V_{w1}}{2u_1} = 1 - \frac{V_{w1}}{2 \cdot 1.4V_{w1}} = 1 - 0.36 = 0.64$$

The degree of reaction is hence seen to be 64%.

11.2 DRAFT TUBES

Draft tubes are used with reaction turbines to allow the runner to extract as much as possible of the remaining kinetic energy, which the water still carries as it leaves the runner. The draft tube transforms the available kinetic energy to negative pressure at the outlet of the runner, effectively increasing the total pressure difference between the inlet and outlet of the turbine. After transferring energy to the runner, water is discharged to the tailrace through a closed tube rather than allowing it to fall freely at atmospheric pressure as happens with impulse turbines. In order to recover the remaining kinetic energy efficiently, the draft tube must minimize friction losses while reducing the water velocity. This is achieved by gradually enlarging the cross-sectional area of the draft tube into a conical shape with a maximum angle generally not exceeding 8°.

Along with improving turbine efficiency by utilizing residual kinetic energy, the draft tube allows the turbine to be installed safely above the tailrace while making use of all available head. Being able to place the turbine well above the tailrace also simplifies access and maintenance. The draft tube provides flexibility in locating the turbine between the headrace and tailrace levels by dividing the total available head above and below the turbine. This feature is valuable for low head applications, with which capturing the additional head contributes significantly to the total power available. It is particularly advantageous that higher head can be available to the turbine when the tail water level drops during the dry season, coinciding with when the available water flow is lowest.

The draft tube must reduce pressure at the outlet of the turbine runner to below atmospheric. This requires the draft tube to be full of water at all times to prevent air from being sucked into it, and its open end must always be submerged into the tailrace, below the water surface as shown in Figure 11.9.

Applying Bernoulli's equation to the inlet, 1, and outlet, 2, of the draft tube,

$$\frac{p_1}{\rho g} + \frac{v_1^2}{2g} + z_1 = \frac{p_2}{\rho g} + \frac{v_2^2}{2g} + z_2$$

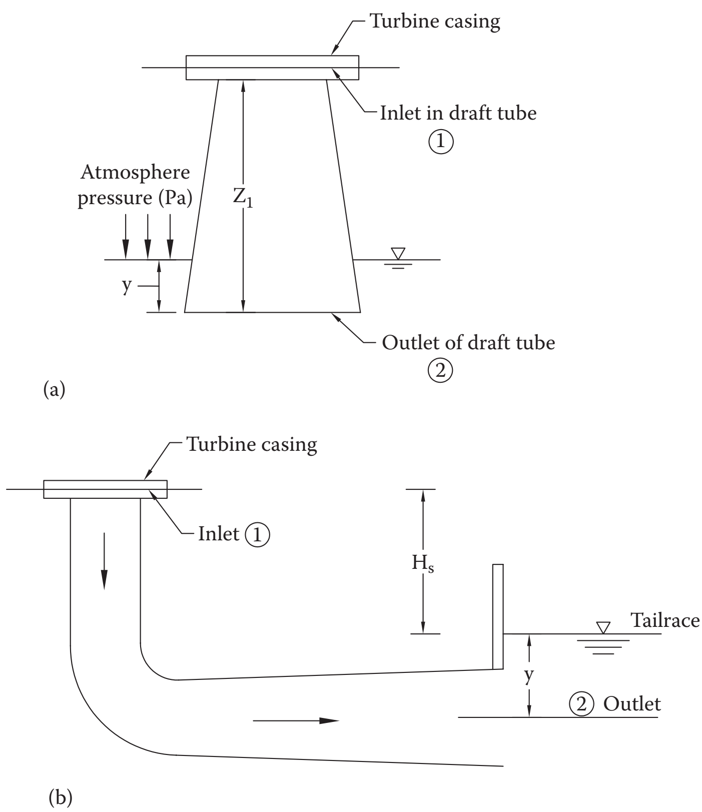

FIGURE 11.9 Draft tubes. (a) Conical and (b) elbow type.

where

p_1 = water pressure at the inlet of the draft tube
p_2 = water pressure at the outlet of the draft tube
v_1 = velocity of the water at the inlet of the draft tube
v_2 = velocity of the water at the outlet of the draft tube
z_1 = height to inlet of the draft tube
z_2 = height to outlet of the draft tube
y = distance between the bottom of the draft tube and the tailrace
p_a = atmospheric pressure at the surface of the tailrace
h_f = the loss of energy from the top to bottom of the draft tube

If z_2 is taken to be zero, z_1 becomes the vertical distance between the inlet and outlet of the draft tube, and Bernoulli's equation can be written as

$$\frac{p_1}{\rho g} + \frac{v_1^2}{2g} + z_1 = \frac{p_2}{\rho g} + \frac{v_2^2}{2g} + 0 + h_f$$

where h_f signifies the loss of energy from friction going from top to bottom of the draft tube.

Rewriting the equation for p_1,

$$\frac{p_1}{\rho g} = \frac{p_2}{\rho g} - z_1 - \left(\frac{v_1^2 - v_2^2}{2g} - h_f\right)$$

Substituting $\frac{p_2}{\rho g} = \frac{p_a}{\rho g} + y$ in the above equation, where p_a is atmospheric pressure, and y is the depth of immersion of the draft tube below the tailrace,

$$\frac{p_1}{\rho g} = \frac{p_a}{\rho g} + (y - z_1) - \left(\frac{v_1^2 - v_2^2}{2g} - h_f\right) \tag{11.23}$$

$(z_1 - y)$ is the vertical distance between the runner exit and the tailwater level and is called the *suction head* of the draft tube and is written as H_s.

$\frac{v_1^2 - v_2^2}{2g}$ is known as the *dynamic head* and is written as H_d.

$$\frac{p_1}{\rho g} = \frac{p_a}{\rho g} - [H_s + (H_d - h_f)] \tag{11.24}$$

$\frac{p_1}{\rho g}$, the pressure at the inlet of the draft tube, can be seen to be less than atmospheric pressure by the sum of the suction head and dynamic head together less the friction loss h_f.

The efficiency of the draft tube, η_d, is defined as the ratio of net gain in pressure head to the velocity head at the entrance of the draft tube.

$$\eta_d = \frac{\text{Net gain in pressure head}}{\text{Velocity head at inlet of draft tube}}$$

$$\eta_d = \frac{\dfrac{v_1^2 - v_2^2}{2g} - h_f}{\dfrac{v_1^2}{2g}} \tag{11.25}$$

For the draft tube to have 100% efficiency it would need to be able to slow down velocity v_2 to zero, and the loss of energy, h_f, would need to be negligible.

Example 11.3

A conical draft tube (Figure 11.10), which has inlet and outlet diameters of 0.85 m and 1.70 m, respectively, discharges water into the tailrace at a velocity of 1.5 m/s. The length of the draft tube is 6.50 m of which 1.50 m is immersed in water.

a. Calculate how much the pressure at the inlet of the draft tube is below atmospheric pressure assuming that loss from friction is equal to 10% of the velocity head at the inlet.

   Flow out of the outlet of the draft tube: $Q = \text{Outlet Area} \cdot V_2 = \pi \cdot \dfrac{1.70^2}{4} \cdot 1.5 = 3.40\ \text{m}^3/\text{s}$.

   The velocity at the inlet of the draft tube: $V_1 = \dfrac{Q}{\text{Inlet Area}} = \dfrac{3.40}{\pi \cdot \dfrac{0.85^2}{4}} = 6.00\ \text{m/s}$

   The friction loss is stated to be 10% of the velocity head at the inlet of the draft tube and can be calculated as $h_f = 0.1 \cdot \dfrac{V_1^2}{2g} = 0.184\ \text{m}$

   Suction pressure head, which is the head provided by the length of the draft tube above the tailrace,

$$H_s = z_1 - y = 6.50\ \text{m} - 1.50\ \text{m} = 5.0\ \text{m}$$

   The gain in pressure head or "dynamic head" as a result of the draft tube slowing down the velocity of water flow is computed as

$$H_D = \frac{V_1^2 - V_2^2}{2g} = \frac{6.0^2 - 1.5^2}{2 \cdot 9.81} = 1.72\ \text{m}$$

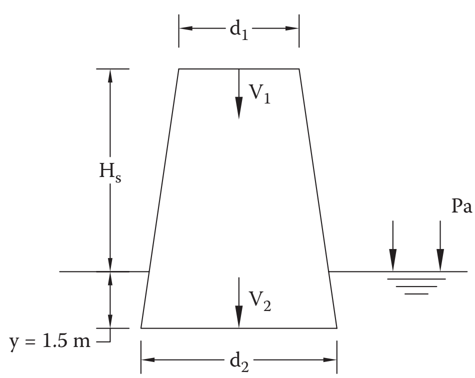

FIGURE 11.10 Conical draft tube.

Net gain in pressure head (the difference between dynamic head and the head loss from friction) = $H_D - h_f$.

From Equation 11.24, the pressure at the inlet of the draft tube is below atmospheric pressure by the sum of the suction head and net gain in pressure head:

$$H_s + H_D - h_f = 5.0 + 1.72 - 0.184 = 6.54 \text{ m}.$$

This corresponds to the extra pressure head that is available to the turbine as a result of having the draft tube.

b. Compute the efficiency of the draft tube.

From Equation 11.25, the efficiency of the draft tube is defined as the ratio of the net gain in pressure head to the velocity head at the inlet of the draft tube:

$$\eta_D = \frac{\text{Net gain in pressure head}}{\text{Velocity head at inlet of draft tube}} = \frac{H_D - h_f}{V_1^2/2g} = \frac{1.54}{1.835} = 84\%$$

11.3 CAVITATION

Reaction turbines are susceptible to damage from the effect of cavitation due to significant change in pressure over runner surfaces. Cavitation results from the collapse of bubbles of water vapor under high pressure on metallic surfaces. The bubbles themselves are created due to localized reduction in liquid pressure, below atmospheric, reaching the vapor pressure of water. The vapor bubbles move to regions of high pressure and get compressed, eventually leading to their collapse. Repeated hammering from intense and irregular localized pressure from the rush of water to fill the space created after a bubble collapses erodes the metal and results in pitting. The most common locations for pitting are at the runner exit surfaces and the inlet of the draft tube, locations where the pressure is negative.

The proper use of a draft tube with reaction turbines requires the designer to take into account its cavitation limits. Thoma suggested a cavitation factor (sigma) to determine the zone where the turbine can work with reduced susceptibility to cavitation.

$$\sigma_{TC} = \frac{\left(\frac{p_a}{\rho g} - \frac{p_y}{\rho g}\right) - H_s}{H} \tag{11.26}$$

where

p_a = Atmospheric pressure
p_v = Vapor pressure at the water temperature at site
H = Net head in meters
H_s = Suction pressure head

The cavitation factor is thus a measure of pressure resulting at the discharge end of the turbine or inlet of the draft tube from the vapor pressure.

Equation 11.26 can also be rewritten as

$$H_{s\,max} = H_a - H_v - \sigma_{TC} \cdot H \tag{11.27}$$

where $H_{s\,max}$, the maximum suction head, gives the maximum height the draft tube can be to avoid cavitation. H_a and H_v represent atmospheric pressure head and vapor pressure head, respectively.

The value of critical Thoma sigma, σ_{TC}, is particular to the type of turbine. A first estimate can be made using the following empirical relations if the specific speed of the turbine is known.

For Francis turbines,

$$\sigma_{TC} = 0.625 \cdot \left(\frac{N_s}{444} \right)^2$$

For propeller turbines,

$$\sigma_{TC} = 0.28 + \left[\frac{1}{7.5} \cdot \left(\frac{N_s}{444} \right)^3 \right]$$

where N_s is the specific speed in metric units.

Manufacturers will be able to provide an accurate value for the critical Thoma Sigma for their turbines, verified by actual model studies.

Example 11.4

Estimate the maximum head of the draft tube that can be used with a Kaplan turbine with the following specifications: net head: 12 m, power output: 25 MW, RPM: 90. Atmospheric pressure at the power station site is 10.0 m of water, and vapor pressure is 0.3 m.

$$N_s = 1.166 \cdot N \cdot \frac{\sqrt{P}}{H^{5/4}}$$

$$N_s = 1.166 \cdot 90 \cdot \frac{\sqrt{25{,}000}}{12^{5/4}} = 742.9$$

$$\sigma_{TC} = 0.28 + \left[\frac{1}{7.5} \cdot \left(\frac{N_s}{444} \right)^3 \right]$$

$$\sigma_{TC} = 0.28 + \left[\frac{1}{7.5} \cdot \left(\frac{742.9}{444} \right)^3 \right] = 0.905$$

$$H_{s\,max} = H_a - H_v - \sigma_{TC}$$

$$H = 10 \text{ m} - 0.3 \text{ m} - 0.905 \cdot 12 = -1.16 \text{ m}$$

The negative suction head means that to avoid cavitation the Kaplan turbine will need to be installed at least 1.16 m below the level of the tailrace.

11.4 FRANCIS TURBINE

The runner of the Francis turbine receives water radially from the perimeter toward its center and produces torque and power as it discharges the flow axially—hence its characterization as

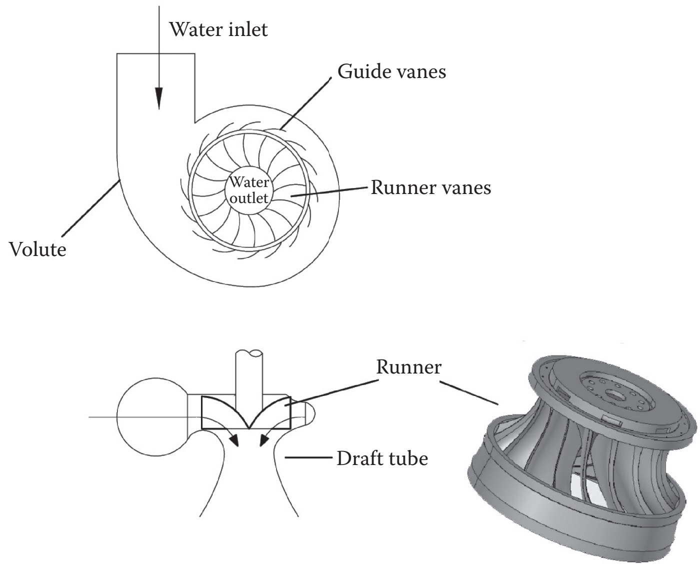

FIGURE 11.11 Francis schematic and runner.

a radial–axial reaction turbine. The runner consists of curved fixed blades, numbering 12 to 17, which are arranged as an annular cascade as shown in Figure 11.11. The blades are rigidly fixed for strength to a crown and to a band at their two ends, and the full runner is typically cast as a single piece. The runner diameter at the inlet edges of the blades, D_1, determines the size of the turbine.

Water from the penstock enters a spiral casing, which is designed with a diminishing cross-sectional area to distribute the water flow uniformly along the outer circumference of the guide vanes. A series of guide vanes, numbering 20 to 24 next direct the water velocity at the required angle into the runner. Being adjustable, the guide vanes are also able to regulate the rate of water flow to achieve high efficiencies over a wide range of discharge, by controlling the size of the opening, α_0. Together the spiral scroll case and guide vanes prerotate the water before it strikes the runner. As the pressurized water passes through the runner with components of both whirl and flow in its velocity, the action of the rotor blades turns it so that the water leaves the runner more or less parallel to its axis and without rotation. Water pressure is reduced dramatically from the inlet to outlet of the runner. As is standard with reaction turbines, a draft tube is used to utilize all the head down to the tailrace and at the same time to allow the runner to extract residual kinetic energy before water is discharged into it. The open end of the draft tube is submerged fully into the tailrace, making the passage of water from the time it enters the Francis turbine to its exit entirely enclosed and isolated from atmospheric pressure.

11.4.1 Power Output and Efficiency of Francis Turbines

The main equations for the computation of power output and efficiency of Francis turbines are summarized below. From Equation 9.15, the power output from the runner of a reaction turbine can be expressed as

$$\text{Power Output} = \rho \cdot Q \cdot (V_{w1} \cdot u_1 \pm V_{w2} \cdot u_2) \tag{11.28}$$

where

ρ = Density of water
Q = Flow through the runner m^3/s
V_{w1} = Velocity of whirl at inlet of runner

u_1 = Peripheral speed at the rim of the runner
V_{w2} = Velocity of whirl of exiting flow
u_2 = Peripheral speed at outlet of runner

When the blades of the Francis turbine are shaped to make the water exit the runner without any circulation to minimize residual kinetic energy of the water, the velocity of whirl, V_{w2}, becomes zero and the power equation simplifies to

$$P = \rho Q(V_{w1} \cdot u_1) \tag{11.29}$$

It is also useful to note that

$$u_1 = \frac{\pi D_1 N}{60} \quad \text{and} \quad u_2 = \frac{\pi D_2 N}{60} \tag{11.30}$$

where
D_1 = diameter of the runner at the inlet
D_2 = diameter of the runner at the outlet
N = speed of the turbine in RPM

The hydraulic efficiency can be expressed by dividing the power output of the runner by the waterpower into the turbine. And it is seen in its two forms:

$$\eta_h = \frac{\text{Power Output of Runner}}{\text{Power of Water Input to Turbine}} = \frac{\rho \cdot Q \cdot (V_{w1} \cdot u_1 \pm V_{w2} \cdot u_2)}{\rho \cdot Q \cdot g \cdot H} = \frac{V_{w1} \cdot u_1 \pm V_{w2} \cdot u_2}{gH}$$

and

$$\eta_h = \frac{V_{w1} \cdot u_1}{gH} \tag{11.31}$$

11.4.1.1 Working Proportions

The following parameters are used in specifying the design of Francis turbines:

a. Speed ratio (K_u) = ratio of peripheral runner speed to the theoretical jet velocity from the change in head across the turbine.

$$K_u = \frac{u_1}{\sqrt{2gH}} \tag{11.32}$$

The value of K_u for Francis turbines ranges from 0.5 to 1.0 with a lower factor for higher head applications and a higher factor for lower head applications. K_u could typically be 0.75 for a Francis turbine to be used for medium head applications. For comparison, the factor of 0.43–0.48 is used for the ratio of bucket speed to jet velocity to achieve maximum efficiency for impulse turbines.

Given that $u = \frac{\pi DN}{60}$, see Equation 11.30; the turbine designer can calculate the diameter of the runner by picking the speed ratio and substituting its desired speed in RPM.

$$D = \frac{60 \cdot K_u}{\pi \cdot N} \sqrt{2gH} \tag{11.33}$$

b. Flow ratio = ratio of velocity of flow at inlet to the theoretical jet velocity

$$K_f = \frac{V_{f1}}{\sqrt{2gH}} \tag{11.34}$$

Typical value of K_f ranges from 0.15 to 0.30.

c. K_t is the vane thickness factor to account for the reduction in available inlet and outlet areas on account of blade thickness and would have a value less than 1 and is typically around 0.95.
d. Relative guide vane passage size, n, is defined as the ratio of width of the runner B_1 to the outer diameter of the runner D_1.

$$n = \frac{B_1}{D_1} \tag{11.35}$$

Typical value of n ranges from 0.10 to 0.45 with higher values corresponding to higher specific speeds.

11.4.2 Design of the Francis Turbine Runner

The discharge equations at the inlet and exit

$$Q = \text{Area of Flow} \times \text{Velocity of Flow}$$

Total area of the outer periphery—that is, at the runner inlet: $A = K_{t1} \cdot \pi \cdot D_1 \cdot B_1$
Similarly, the area of the inner periphery—that is, at the runner exit: $A = K_{t2} \cdot \pi \cdot D_2 \cdot B_2$
Because flows have to be equal at the inlet and outlet,

$$Q = K_{t1} \cdot \pi \cdot D_1 \cdot B_1 \cdot V_{f1} = K_{t2} \cdot \pi \cdot D_2 \cdot B_2 \cdot V_{f2} \tag{11.36}$$

For the given design flow, Q, the velocity of flow,V_{f1}, can be calculated as

$$V_{f1} = \frac{Q}{K_{t1} \cdot \pi \cdot D_1 \cdot B_1} = \frac{Q}{K_{t1} \cdot \pi \cdot n \cdot D_1^2},$$

Combining with the flow ratio,

$$K_f \cdot \sqrt{2gH} = \frac{Q}{K_{t1} \cdot \pi \cdot n \cdot D_1^2}; \because B_1 = n \cdot D_1$$

And the required diameter and width of the runner can be expressed as

$$D_1 = \left(\frac{Q}{K_f \cdot \sqrt{2gH} \cdot K_{t1} \cdot \pi \cdot n} \right)^{0.5} \tag{11.37}$$

Once the diameter, D_1, and the design speed, N, are known, the tangential velocity of the runner u_1 can be calculated as

Tangential velocity, $u_1 = \frac{\pi D_1 N}{60}$

The velocity of whirl at the inlet, V_{w1}, can be computed from Equation 11.31 as

$$V_{w1} = \frac{\eta_h \cdot g \cdot H}{u_1}$$

in the case in which V_{w2} is close to zero.

From the velocity triangles in Figure 11.12, the guide vane angle α and the blade angle, β, can be computed:

$$\tan \alpha_1 = \frac{V_{f1}}{V_{w1}}$$

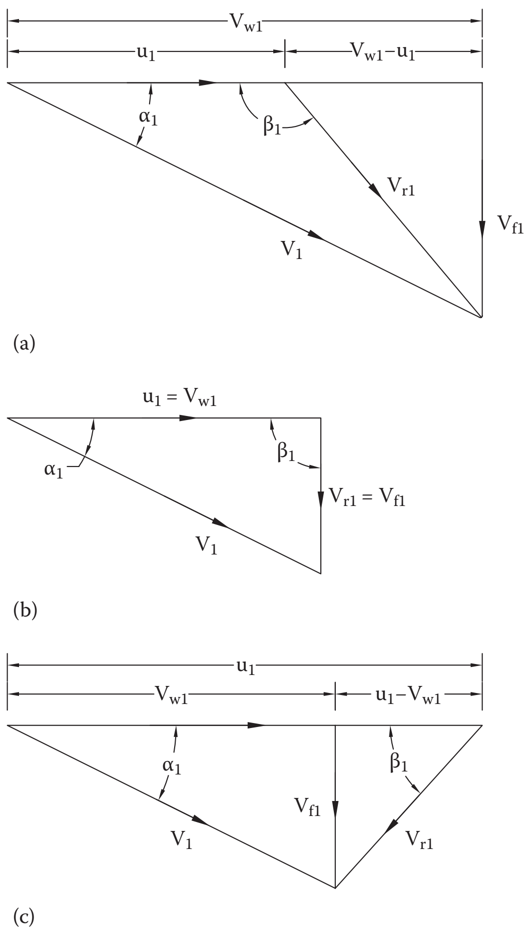

FIGURE 11.12 Velocity triangles by speed of the Francis turbine. (a) Obtuse blade angle, slow Francis, (b) right blade angle, medium speed Francis, and (c) acute blade angle, fast Francis.

$$\tan\beta_1 = \frac{V_{f1}}{u_1 - V_{w1}} \text{ (when } \beta_1 \text{ is acute)}$$

Or

$$\tan\beta_1 = \frac{V_{f1}}{V_{w1} - u_1} \text{ (when } \beta_1 \text{ is obtuse)}$$

Assuming that the runner diameter at the inlet, D_1, is twice as large as the diameter at the outlet D_2, a number of other parameters can be determined,

$$D_1 = 2D_2 \text{ implies that } u_1 = 2u_2.$$

It can also be assumed that $V_{f1} = V_{f2}$ and $K_{t1} = K_{t2}$, which would imply that $B_2 = 2B_1$.

Runner vane angle at exit, β_2, can be computed from the velocity triangle, assuming that the discharge at the runner exit is radial—that is, $\alpha_2 = 90°$

$$\tan\beta_2 = \frac{V_{f2}}{u_2}$$

Example 11.5

A Francis turbine is being considered for a mini hydropower project with the following site specifications:

Net head = 80 m
Speed required = 1000 RPM
Shaft power required: 350 kW
Overall efficiency = 87%

The manufacturer of the turbine provides the following specifications for the turbine runner:

Hydraulic efficiency = 92%
Flow ratio = 0.22
Height ratio = 0.1
Thickness factor = 5% of the circumferential area of the runner
Outer: Inner diameter of runner: 2:1

Assuming that the velocity of the flow is constant inside the turbine and the outlet discharge from the runner is radial, find the following dimensions of the turbine:

a. Diameter of the runner at inlet and outlet
b. Width of the wheel at the inlet and outlet
c. Guide vane angle
d. Blade angles at inlet and outlet

The following parameters are given by site conditions and manufacturer's specifications:

H = 80 m
P = 350 kW

$N = 1000$ RPM
$\eta_h = 92\%$
$\eta_o = 87\%$
$K_f = 0.22$
$\frac{B_1}{D_1} = 0.1$

$\frac{D_1}{D_2} = 2$

$K_t = 1.0 - 5\% = 0.95$

a. To find the diameters of the runner, D_1 and D_2

Using the flow ratio relationship, $K_f = \frac{V_{f1}}{\sqrt{2gH}}$

$$V_{f1} = 0.22 \cdot \sqrt{2gH} = 0.22 \cdot \sqrt{2 \cdot 9.81 \cdot 80} = 8.72 \text{ m/s}$$

$$\text{Area of flow } = K_t \cdot \pi \cdot D_1 \cdot B_1 = 0.95 \cdot \pi \cdot 0.1 \cdot D_1^2 = 0.298 D_1^2$$

Flow through the turbine using the power equation:

$$Q = \frac{P}{\eta_0 \cdot g \cdot H} = \frac{350}{0.87 \cdot 9.81 \cdot 80} = 0.513 \text{ m}^3/\text{s}$$

Because Q = Area of Flow × V_{f1},

$$0.513 = 0.298 D_1^2 \cdot 8.72 \text{ ;}$$

The diameters can be calculated using this equation:

$$D_1 = \sqrt{\frac{0.513}{0.298 \cdot 8.72}} = 0.444 \text{ m}; D_2 = 0.5 \cdot D_1 = 0.222 \text{ m}$$

b. To find the width of the wheel at the inlet and outlet, using the relationship for the relative guide vane passage size,

$$\frac{B_1}{D_1} = 0.1$$

It can be seen that $B_1 = 0.1 \cdot D_1 = 0.044$ m
Assuming $K_{t1} = K_{t2}$ and $V_{f1} = V_{f2}$, $D_1 \cdot B_1 = D_2 \cdot B_2$

$$\therefore B_2 = \frac{D_1 \cdot B_1}{D_2} = \frac{0.444 \cdot 0.0444}{0.222} = 0.089 \text{ m}$$

c. Guide vane angle

Tangential speed of the runner at the inlet,

$$u_1 = \frac{\pi D_1 N}{60} = \frac{\pi \cdot 0.444 \cdot 1000}{60} = 23.25\,\text{m/s}$$

Using the definition of hydraulic efficiency,

$$\eta_h = \frac{V_{w1} \cdot u_1 - V_{w2} \cdot u_2}{g \cdot H},$$

a simplification can be made when the discharge is radial and V_{w2} is equal to zero.

$$\eta_h = \frac{V_{w1} \cdot u_1}{g \cdot H}$$

or

$$V_{w1} = \frac{\eta_h \cdot g \cdot H}{u_1} = \frac{0.92 \cdot 9.81 \cdot 80}{23.25} = 31.06\,\text{m/s}$$

The guide vane angle, α_1, can be calculated from the inlet velocity triangle:

$$\tan\alpha_1 = \frac{V_{f1}}{V_{w1}} = \frac{8.72 \text{ m/s}}{31.06 \text{ m/s}} = 0.281$$

$$\alpha_1 = \tan^{-1}(0.281) = 15.7°$$

d. Runner blade angles at inlet and outlet

The blade angles, β_1 and β_2, can be computed from the inlet and outlet velocity triangles, respectively. As shown in Figure 11.10, for an obtuse vane angle at the inlet (because $V_{w1} > u_1$), the supplement, β_1^1, is calculated first, and β_1 is computed from that.

$$\tan\beta_1' = \frac{V_{f1}}{V_{w1} - u_1} = \frac{8.72}{31.06 - 23.25} = 1.1165$$

$$\beta_1' = \tan^{-1}(1.1165) = 48.2°$$

$$\beta_1 = 180° - \beta_1' = 180° - 48.2° = 131.8°$$

Using the outlet velocity triangle, it can be seen that

$$\tan\beta_2 = \frac{V_{f2}}{u_2} = \frac{V_{f1}}{u_2}$$

V_{f1} has been computed above using the flow ratio.

$$u_2 = \frac{\pi \cdot D_2 \cdot N}{60} = \frac{\pi \cdot 0.222 \cdot 1000}{60} = 11.62$$

$$\tan\beta_2 = \frac{8.72}{11.62} = 0.75$$

$$\beta_2 = \tan^{-1}(0.75) = 36.9°$$

Example 11.6

A Francis turbine runner operating at 600 RPM has an external diameter of 700 mm. The width of the runner at the inlet is 200 mm, vane thickness factor is 0.95, and the velocity of the flow through the runner is 7.61 m/s. The guide vanes make an angle of 28° to the tangent of the wheel, and the discharge at the outlet of the runner is radial. Find the power output of the turbine and blade angles at the inlet.

The main parameters of the Francis runner are given as follows:

$D_1 = 0.7$ m
$N = 600$ RPM
$B_1 = 0.20$ m
$K_{t1} = 0.95$
$V_{f1} = V_{f2} = 7.61$ m/s
$\alpha_1 = 28°$
$\alpha_2 = 90°$
$V_{w2} = 0$

a. First, calculate the tangential velocity of the wheel.
Tangential velocity of the wheel at inlet,

$$u_1 = \frac{\pi D_1 N}{60} = \frac{\pi \cdot 0.7 \cdot 600}{60} = 21.99 \text{ m/s}$$

b. Next, calculate the velocity of the water at the inlet, V_1, and the velocity of whirl V_{w1}.
From the inlet velocity triangle,

$$V_{f1} = V_1 \cdot \sin\alpha_1$$

$$V_1 = \frac{V_{f1}}{\sin\alpha_1} = \frac{7.61}{\sin 28°} = 16.21 \text{ m/s}$$

$$V_{w1} = V_1 \cdot \cos\alpha_1 = 14.31 \text{ m/s}$$

The discharge can be calculated using Equation 11.36:

$$Q = V_{f1} \cdot \pi \cdot K_{t1} \cdot D_1 \cdot B_1 = 3.18 \text{ m}^3/\text{s}$$

Given that V_{w2} is zero,

$$P = \rho Q V_{w1} u_1 = 1000 \text{ kg/m}^3 \cdot 3.18 \text{ m}^3/\text{s} \cdot 14.31 \text{ m/s} \cdot 21.99 \text{ m/s} = 1001 \text{ kW}$$

$$\tan\beta_1 = \frac{V_{f1}}{u_1 - V_{w1}} = \frac{7.61}{21.99 - 14.31} = 0.9909$$

$$\beta_1 = 44.7°$$

11.4.3 Speed of Francis Turbines

The range of specific speeds under which Francis turbines operate is manifested in diverse inlet blade angles and shapes of velocity triangles. As shown in Figure 11.12, an obtuse inlet blade angle indicates a slow Francis whereas a fast Francis turbine is recognized by an acute blade angle with a blade angle of around 90°, indicating a middle speed Francis. In the examples above, β_1 of 131.8° indicates that the Francis turbine of Example 11.5 will have a low specific speed whereas β_1 of 44.7° in Example 11.6 indicates a turbine with high specific speed.

The relationship between specific speed and inlet blade angle can be verified by calculating the specific speed of the turbines in the above examples:

For Example 11.5,

$$N_s = 1.166 \cdot N \cdot \frac{\sqrt{P}}{H^{5/4}} = 1.166 \cdot 1000 \cdot \frac{\sqrt{350}}{80^{1.25}} = 91$$

For Example 11.6, head can be estimated by assuming that the hydraulic efficiency of the turbine is 90%. From the power equation,

$$P = Q \cdot g \cdot H \cdot \eta_h$$

$$H = \frac{P}{Q \cdot g \cdot \eta_h} = \frac{1001}{3.18 \cdot 9.81 \cdot 0.9} = 36 \text{ m}$$

$$N_s = 1.166 \cdot N \cdot \frac{\sqrt{P}}{H^{5/4}} = 1.166 \cdot 600 \cdot \frac{\sqrt{1001}}{36^{1.25}} = 251$$

Example 11.7

Specify the design parameters (D_1, D_2, B_1, B_2, α_1, β_1, β_2) of a Francis turbine to meet the following performance requirements:

Power output: 450 kW
RPM: 750
Head: 45 m
Overall efficiency: 80%
Hydraulic efficiency: 85%

Assume that the flow ratio is 0.22, ratio of width to diameter is 0.25, and the vane thickness factor is 0.95. Also assume that the outlet diameter of the runner is half of the inlet diameter, and the vane thickness factor at the outlet is the same as at the inlet.

The design flow can be computed using the power equation:

$$Q = \frac{P}{H \cdot g \cdot \eta_o} = \frac{450}{45 \cdot 9.81 \cdot 0.8} = 1.27 \text{ m/s}^3$$

Based on the given flow ratio, the flow velocity can be computed:

$$V_{f1} = K_f \cdot \sqrt{2gH} = 0.22 \cdot \sqrt{2 \cdot 9.81 \cdot 45} = 6.54 \text{ m/s}$$

The total inlet area for the flow $A = \pi D_1 B_1 K_{t1}$

$$Q = \text{Velocity of flow} \cdot \text{Area} = V_{f1} \cdot \pi D_1 B_1 K_{t1}$$

Substituting for the width B_1 and putting in the value of K_{t1}, the required diameter of the Francis turbine:

$$B_1 = n \cdot D_1 = 0.25 D_1$$

$$K_{t1} = 0.95$$

$$Q = V_{f1} \cdot 0.25 \cdot 0.95 \cdot \pi D_1^2$$

$$D_1^2 = \frac{Q}{V_{f1} \cdot 0.24 \cdot \pi} = \frac{1.27}{6.54 \cdot 0.75} = 0.26$$

So diameter D_1 = 0.511 m, and width B_1 = 0.1278 m.

On the runner outlet,

$$D_2 = 0.5 D_1 = 0.5 \cdot 0.510 = 0.256 \text{ m}$$

Because the flows have to be same at the inlet and at the outlet, for continuity, the equation below has to hold:

$$V_{f1} \pi D_1 B_1 K_{t1} = V_{f2} \pi D_2 B_2 K_{t2}$$

It can be seen from this equation that if $V_{f1} = V_{f2}$ and $K_{t1} = K_{t2}$, our assumption that $D_1 = 2D_2$ requires $B_2 = 2B_1$ for continuity to hold.

$$B_2 = 0.256 \text{ m}$$

Using the diameter of the runner, the peripheral velocity of the runner can be calculated at its inlet and used to calculate the velocity of whirl from the hydraulic efficiency. With the three velocities, the required angles can be calculated using the relationships from the inlet velocity triangle.

$$u_1 = \frac{\pi \cdot D_1 \cdot N}{60} = \frac{\pi \cdot 0.510 \cdot 750}{60} = 20.08 \text{ m/s}$$

$$u_2 = \frac{\pi \cdot D_2 \cdot N}{60} = 10.04 \text{ m/s}$$

Because $\eta_h = \dfrac{V_{w1} \cdot u_1}{g \cdot H}$, the velocity of whirl at the inlet can be calculated as

$$V_{w1} = \frac{\eta_h \cdot g \cdot H}{u_1} = \frac{0.85 \cdot 9.81 \cdot 45}{20} = 18.68 \text{ m/s}$$

Using the inlet velocity triangle, the guide vane angle, α_1, and the runner blade angles, β, can be calculated. One point to note here is that because $u_1 > V_{w1}$ the inlet blade angle in this example will be acute—that is, smaller than 90°. Figure 11.11 shows that a Francis turbine with an acute inlet blade angle is considered to be relatively fast.

$$\tan\alpha_1 = \frac{V_{f1}}{V_{w1}};\ \alpha_1 = \tan^{-1}\frac{V_{f1}}{V_{w1}} = \tan^{-1}\frac{6.54}{18.76} = 19.3°$$

$$\tan\beta_1 = \frac{V_{f1}}{u_1 - V_{w1}};\ \beta_1 = \tan^{-1}\frac{V_{f1}}{u_1 - V_{w1}} = \tan^{-1}\frac{6.54}{20.02 - 18.76} = 79.0°$$

Using the outlet velocity triangle and assuming that the discharge from the runner is radial,

$$\tan\beta_2 = \frac{V_{f2}}{u_2};$$

$$\beta_2 = \tan^{-1}\frac{V_{f2}}{u_2} = \tan^{-1}\frac{6.54}{10.04} = 33.1°\ .$$

11.5 AXIAL FLOW REACTION TURBINES: PROPELLER AND KAPLAN

Turbines in which the runner rotates with its axis parallel to the water flow, at both inlet and outlet, are known as axial flow turbines. Axial flow turbines have the highest specific speeds among all turbines and are used at sites with low head and high flow characteristics. They are used at heads as low as 2 m but sometimes also find application at sites as high as 60–70 m, overlapping at the higher end with the application range of Francis turbines (see Figure 11.13).

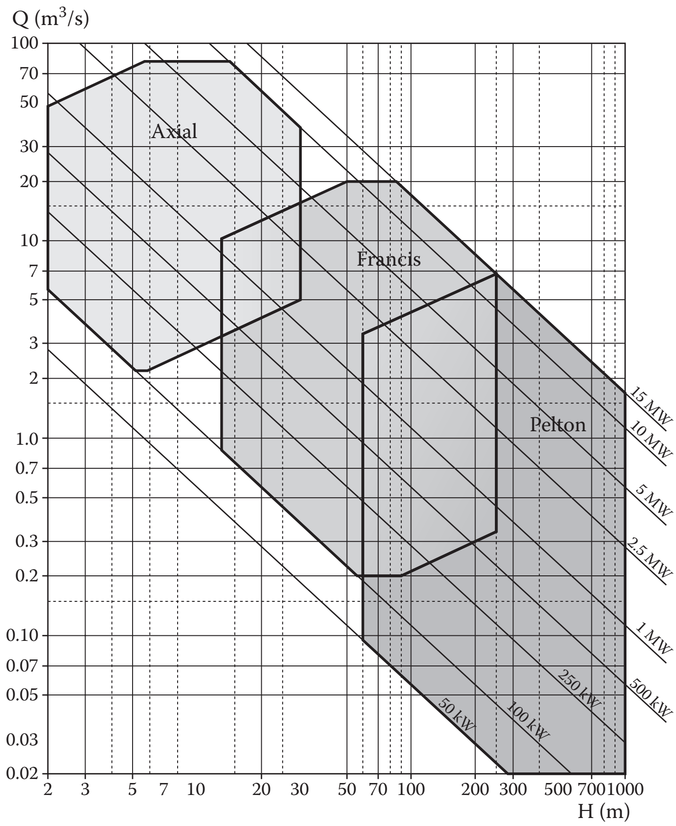

FIGURE 11.13 Application regime for small axial turbines. (From Andritz Hydro.)

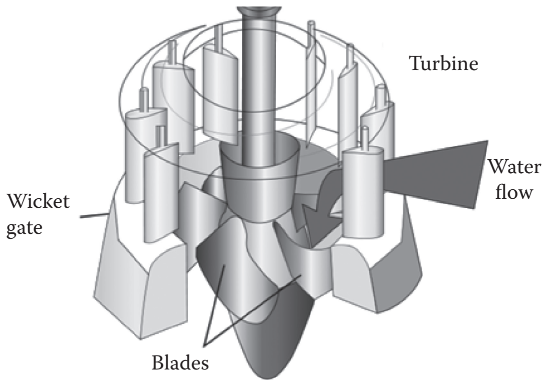

FIGURE 11.14 Kaplan runner and wicket gate. (From US Army Corps of Engineers, https://commons.wikimedia.org/wiki/File:Water_turbine.svg.)

The runner on an axial flow turbine consists of a hub with blades but generally has no outer rim (Figure 11.14). There are typically four to eight blades on the runner, which resembles the propeller on a ship with a higher number of blades generally used for higher head applications. The diameter of the runner characterizes the size of the turbine. As would be expected for a reaction turbine, the flow of water undergoes change in both pressure and velocity as it moves from the inlet to the exit side of the runner and transfers energy to it. Similar to the case of the Francis turbine, water flow is guided to the runner of axial flow turbine by a combination of a fixed stay ring and a wicket gate with movable guide vanes.

Axial flow turbines typically have 20–32 guide vanes with the larger number of vanes used by larger turbines operating at lower heads, which form a circular cascade similar to those used in Francis turbines. The guide vanes are used to regulate flow and power output as well as to induce tangential velocity in the water as it hits the runner blades. The outer housing of large axial flow turbines is generally constructed from reinforced concrete with steel casing being substituted in higher head applications.

The two most widely used axial flow reaction turbines are the propeller and the Kaplan.

11.5.1 Propeller and Kaplan Turbines

The runner blades in propeller turbines are fixed, and their pitch is nonadjustable. This works reasonably well when the turbine is operated within a narrow range of flow where the output remains at or near the optimum range. The part load efficiency of propeller turbines is poor, however, with turbine efficiency falling significantly when used below 80% of rated capacity and to below 70% when used at 50% of rated capacity (Figure 11.15).

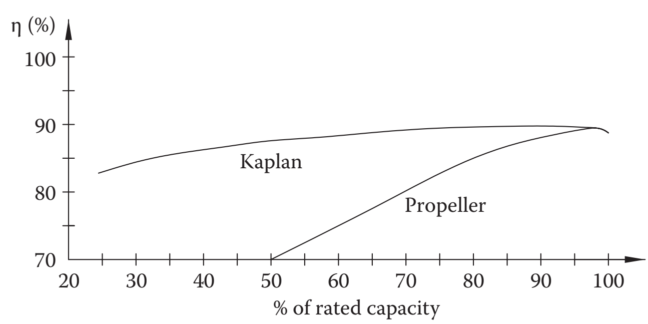

FIGURE 11.15 Part load efficiency of axial-flow turbines.

A Kaplan is a propeller turbine with adjustable blade angles, which result in high efficiency across a range of discharge. It is thus also referred to as a variable pitch propeller turbine. The runner blades are rotated about pivots fixed to the hub of the runner, which allow it to have an efficiency of more than 80% even when it is used at 25% of rated capacity.

Calculations:

$$D_0 = \text{Outer diameter of runner}$$

$$D_h = \text{Diameter of the hub}$$

$V_f = K_f \cdot \sqrt{2gH} = \text{Velocity of flow}$, and K_f is the *flow ratio* and has a typical value of 0.7.

Propeller turbines also have a *speed ratio*, which is defined as

$$K_u = \frac{u}{\sqrt{2gH}} \tag{11.38}$$

where u is the peripheral velocity at the tip of the blade. The speed ratio is defined similarly to the speed ratio of impulse turbines. However, whereas this factor was slightly less than 0.5 for impulse turbines, it is more than 1.0 for Kaplan propeller turbines and typically falls in the range 1.3 to 2.3 with higher speed ratios for higher specific speed turbines.

The area of flow is the area of the full runner minus the area of the hub.

$$\text{Area of flow, } A_f = \frac{\pi}{4} \cdot \left(D_0^2 - D_h^2\right)$$

Discharge through the turbine is the product of the area of flow and velocity of flow.

$$\textit{Discharge} = \textit{Area of flow} \times \textit{Velocity of flow}$$

$$Q = \frac{\pi}{4} \cdot \left(D_0^2 - D_h^2\right) \cdot K_f \cdot \sqrt{2gH}$$

The ratio of the hub diameter to the runner diameter, "n" has a typical value of 0.35.

$$n = \frac{D_h}{D_0} \tag{11.39}$$

$$Q = \frac{\pi}{4} D_0^2 (1 - n^2) \cdot K_f \sqrt{2gH} \tag{11.40}$$

Example 11.8

A Kaplan turbine generates 750 kW under a net head of 20 m. Its flow ratio is 0.65, speed ratio is 1.8, and the ratio of hub diameter to runner diameter is 0.33. Assuming that the overall turbine efficiency is 0.85, find the runner diameter, its speed, and the specific speed of the turbine.

$$K_f = 0.65; \quad K_u = 1.8; \quad n = 0.33$$

Using the relationships above,

$$V_f = K_f\sqrt{2gH} = 0.65\cdot\sqrt{2\cdot 9.81\cdot 20} = 12.88 \text{ m/s}$$

$$u = K_u\sqrt{2gH} = 1.8\cdot\sqrt{2\cdot 9.81\cdot 20} = 35.66 \text{ m/s}$$

Flow through the turbine can be calculated from the power equation:

$$Q = \frac{P}{\eta gH} = \frac{750}{0.85\cdot 9.81\cdot 20} = 4.50 \text{ m}^3\text{/s}\ .$$

Runner diameter can be computed using Equation 11.40:

$$Q = \frac{\pi}{4}D_0^2(1-n^2)\cdot K_f\sqrt{2gH}$$

$$D_0 = \sqrt{\frac{Q}{\frac{\pi}{4}(1-n^2)\cdot K_f\sqrt{2gH}}} = \sqrt{\frac{4.5}{\frac{\pi}{4}(1-n^2)\cdot 12.88}} = 0.707\text{ m}$$

Speed can be computed using the peripheral speed and diameter

$$N = \frac{60\cdot u}{\pi D_0} = \frac{60\cdot 35.66}{\pi\cdot 0.707} = 964 \text{ RPM}$$

$$N_s = 1.166\cdot N\frac{\sqrt{P}}{H^{5/4}} = 1.166\cdot 964\cdot\frac{\sqrt{750}}{20^{1.25}} = 728 \text{ RPM.kW}^{0.5}\text{ m}^{-1.25}$$

Example 11.9

a. Calculate the inlet guide vane angle, the inlet blade angle, and outlet blade angle at the tip of the blade for the Kaplan turbine in Example 11.8. Assume the hydraulic efficiency is 0.92.
b. What will be the inlet and outlet blade angles at the midradius?

a. Hydraulic efficiency,

$$\eta_h = \frac{V_{w1}u_1}{gH};\quad \text{or}\quad V_{w1} = \frac{\eta_h gH}{u_1} = \frac{0.92\cdot 9.81\cdot 20}{35.66} = 5.06 \text{ m/s}$$

The inlet velocity triangle of a Kaplan turbine is similar to that of a fast Francis—that is, it is acute angled with $V_{w1} < u_1$. From Figure 11.12c, it is seen that:

$$\tan\alpha_1 = \frac{V_{f1}}{V_{w1}} = \frac{12.88}{5.06} = 2.5435$$

$$\alpha_1 = \tan^{-1} 2.5435 = 68.5°$$

$$\tan\beta_1 = \frac{V_{f1}}{u_1 - V_{w1}} = \frac{12.88}{35.66 - 5.06} = 0.4209\,;$$

$$\beta_1 = \tan^{-1}(0.4209) = 22.8°$$

Making use of the outlet velocity triangle, which is a right triangle assuming zero whirl at exit, is similar to the outlet triangle in Figure 11.8, $V_{w2} = 0$:

$$\tan\beta_2 = \frac{V_{f2}}{u_2} = \frac{12.88}{35.66} = 0.3611\,;$$

Because $V_{f1} = V_{f2}$ and $u_1 = u_2$

$$\beta_2 = \tan^{-1}(0.3611) = 19.9°$$

b. The velocity triangles for the midradius will be different from the tip because the velocities will be different, and the blade angles at the inlet and outlet can be computed as follows:

$$u_m = \frac{\pi D_m N}{60} = \frac{\pi \cdot \dfrac{D_0 + D_h}{2} \cdot N}{60} = 23.71 \text{ m/s}$$

From Equation 11.7, it is known that the whirl velocity has an inverse relationship with the radius. Velocity of whirl at the hub will be higher than at the tip and can be calculated as

$$V_{w1m} = \frac{V_{w1t} \cdot r_t}{r_m} = \frac{V_{w1t}}{r_m/r_t} = \frac{5.06}{0.665} = 7.61 \text{ m/s}$$

The inlet velocity triangle is acute angled for the midradius because $V_{w1} < u_h$.

From the inlet triangle for the midradius,

$$\tan(\beta_1) = \frac{V_{f1}}{u_1 - V_{w1}} = \frac{12.88}{23.71 - 7.61} = 0.7998\,;$$

$$\beta_1 = \tan^{-1}(0.7998) = 38.7°$$

From the outlet velocity triangle at the midradius,

$$\tan\beta_2 = \frac{V_{f2}}{u_2} = \frac{V_{f1}}{u_1} = \frac{12.88}{23.71} = 0.5430$$

Runner blade angle at exit at the midradius,

$$\beta_2 = \tan^{-1}(0.5430) = 28.5°$$

Compared to the Francis, Kaplan turbines have fewer runner blades and are faster and have less frictional losses. For the same power output, the runners are smaller and more compact in construction. For this reason, Kaplan turbines are sometimes used in place of Francis machines for certain medium head installations. Their use is, however, uncontested for low head sites in conventional hydropower development.

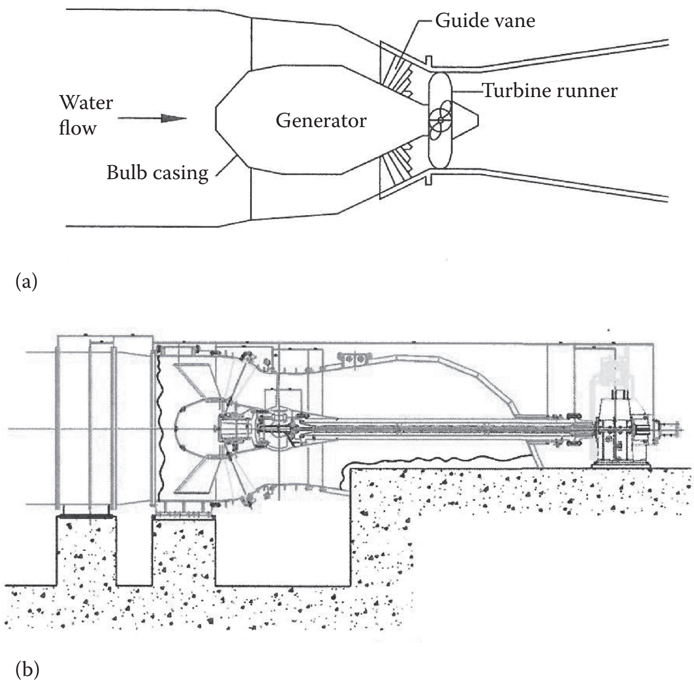

FIGURE 11.16 Schematic of low head (a) bulb turbine and (b) S-type turbine. (From Pentaflo Hydro Engineers.)

11.5.2 Bulb Turbines

A number of compact tubular or "bulb" designs have been developed in recent years in which the combined turbine–generator units can be placed directly in the waterway. The straight water passage in the draft tube both improves the hydraulic behavior and, together with saving in excavation, reduces overall civil works requirements by up to 25%. Single tubular units are available up to 80 MVA in size, and some hydropower companies have come close to replacing the Kaplan turbines for new low head power plants up to heads of 30 m.*

The term "bulb" comes from the shape of the watertight casing upstream of the runner, which contains a generator located on a horizontal axis. A large bulb is centered in the water pipe, which holds the generator, wicket gate, and runner. Tubular turbines are a fully axial design whereas Kaplan turbines have a radial wicket gate (see Figure 11.14). Bulb turbines are available with fixed or variable pitch blades and with or without wicket gates.† For turbines with the variable pitch option, blades are oriented by a moving servomotor cylinder located inside the runner hub.

Pit turbines are bulb turbines with a gearbox. This allows for a smaller generator and reduces the size of the bulb. S-turbines eliminate the need for a bulb housing by placing the generator outside of the water channel with a shaft connecting the runner and generator as shown in Figure 11.16.

11.6 GOVERNORS

The governor maintains the speed of the hydropower turbine within a narrow allowable band in response to changes in load, most basically by regulating the flow of water going to the runner. The governor's two basic components are a control unit and a mechanical actuating system to flow

* http://www.alstom.com/power/renewables/hydro/hydro-turbines/bulb-turbines/
† Hydraulic Turbine Selection and Cost Guidelines (inel.gov)

control devices, such as guide vanes, spear valve needles, and blades. The control unit receives signals corresponding to the speed of the turbine shaft, power output, and water level. It compares these with thresholds set by the operator, and using an algorithm sends corrections to the actuator. Modern-day governors use digital controllers, which are not only very accurate and programmable but can also be controlled remotely.

Francis turbines are governed through regulation of guide vanes. In response to the signal received from the control unit, a servomotor rotates the regulating ring, which connects each of the more than 20 guide vanes. The guide vanes rotate around their axes to change the opening of the flow passages, controlling both the flow to the runner and the guide vane angle to enable the turbine to generate power efficiently over a range of discharge. A relief value is provided next to the inlet of the runner, for contingencies, to reduce the risk of water hammer in case the governor has to direct a sudden closure.

The governor performs an additional critical function for Kaplan turbines. In addition to regulating the discharge into the turbine by controlling guide vane openings, it also changes the angle of the blades, so it can maintain high efficiency even at part load. As can be seen in Figure 11.16, Kaplan turbines have a marked improvement in part load efficiency over the fixed-blade propeller turbine.

11.7 PUMPS AS TURBINES

The centrifugal pump is a radially outward flow machine. During its normal operation, water enters the pump axially through its center. The rotating impeller imparts velocity and pressure to the water, sending it to the circumference of the casing. The casing, which is shaped similar to the spiral case of a reaction turbine, provides for a gradually expanding conduit, which converts the velocity head of the water into the pressure head (Figure 11.17).

Standard, off-the-shelf centrifugal water pumps can be operated in reverse as low-cost turbines. They have the advantage of being readily available as mass produced, low-cost items in market towns across most parts of the world as domestic or municipal supply or irrigation pumps. Pumps and induction motors are often available as an integrated unit, and the motor can be converted to an induction generator as described in Chapter 13.

11.7.1 Suitable Range of Heads and Flows

Before considering the pump as a turbine (PAT), its characteristics as a pump need to be well understood. Figure 11.18 depicts the curve that plots the head that a pump can pump water to and the water flow that it pumps. Two observations from the curve are first that the lower the delivery

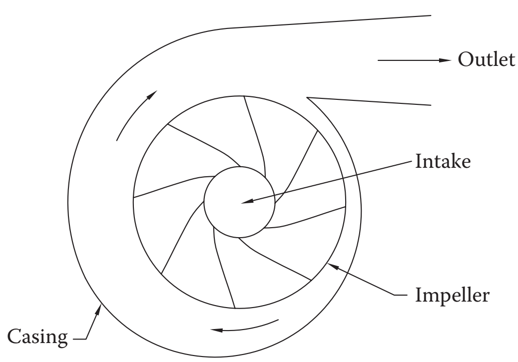

FIGURE 11.17 Schematic of centrifugal pump.

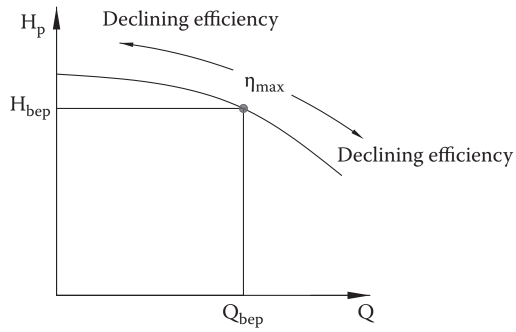

FIGURE 11.18 Pump performance curve.

head, the higher the flow of the water pumped. Second, it shows that there is an optimal combination of head and flow at which the efficiency of the pump is the maximum. At flows and head below or above this point, the pump is working at a lower efficiency [3].

The point at which the turbine is most efficient is known as the *best efficiency point*. The flow and head at this point are Q_{bep} and H_{bep}.

The BEP for a turbine is different than when it functions as a pump. When the pump is being used as a turbine, the higher the pressure head applied, the more the flow increases. Although the percentage efficiency as a turbine is around the same as when it is being used as a pump, the head and flow specifications at BEP for a turbine will be higher than that of the pump. As a pump, friction reduces the actual delivery head and flow. As a turbine, in order to overcome friction, the BEP head has to be quite a bit higher than in the case of the pump.

The following equations are used to predict an estimation for turbine head and flow to operate at the same RPM that the pump is designed for:

$$Q_{tbep} = \frac{Q_{pbep}}{\eta_{max}} \tag{11.41}$$

$$H_{tbep} = \frac{H_{pbep}}{\eta_{max}} \tag{11.42}$$

where

Q_{tbep} is the flow rate "bep" as a turbine
Q_{pbep} is the flow rate "bep" as a pump
H_{tbep} is the head "bep" as a turbine
H_{pbep} is the head "bep" as a pump

η_{max} is the maximum efficiency of the pump and is estimated to be equal to the maximum efficiency of the turbine.

In practice, however, the calculated Q tends to be an overestimation, and the calculated H is often an underestimate. When the turbine speed is the same as the pump speed, the relationship below is generally more accurate in the selection of a pump to be used as a turbine [3].

$$Q_{tbep} = \frac{Q_{pbep}}{\eta_{max}^{0.8}} \tag{11.43}$$

$$H_{tbep} = \frac{H_{pbep}}{\eta_{max}^{1.2}} \tag{11.44}$$

The more practical question that the hydropower designer often asks is what specification pump is required to meet particular hydropower site conditions.

Example 11.10

A hydropower designer is looking for a PAT, which will run at 1500 RPM for a site specification 50 m head and 30 lps flow. What specifications for the pump should the designer look for?

Assuming maximum pump efficiency of 60%, the pump with the following specification might be suitable:

$$Q_{pbep} = Q_{tbep} \cdot \eta_{max}^{0.8} = 30\ \text{lps} \cdot (0.6)^{0.8} = 20\ \text{lps}$$

$$H_{pbep} = H_{tbep} \cdot \eta_{max}^{1.2} = 50\ \text{m} \cdot (0.6)^{1.2} = 27\ \text{m}$$

$$\text{Efficiency} = \frac{H \cdot Q \cdot 9.81}{\text{kW power rating of pump}}$$

From Table 11.2, $\eta_{max} = 0.70$ for the turbine in the 18–20 m head range and 19.7–21.7 lps flow range.

The BEP head and flow specifications for the turbine can be computed as follows for this particular pump:

$$Q_{tbep} = \frac{Q_{pbep}}{\eta_{max}^{0.8}} = \frac{21.7\ \text{lps}}{(0.7)^{0.8}} = 29\ \text{lps}$$

$$Q_{tbep} = \frac{Q_{pbep}}{\eta_{max}^{0.8}} = \frac{19.7\ \text{lps}}{(0.7)^{0.8}} = 26\ \text{lps}$$

$$H_{tbep} = \frac{H_{pbep}}{\eta_{max}^{1.2}} = \frac{18\ \text{m}}{(0.7)^{1.2}} = 28\ \text{m}$$

$$H_{tbep} = \frac{H_{pbep}}{\eta_{max}^{1.2}} = \frac{20\ \text{m}}{(0.7)^{1.2}} = 31\ \text{m}$$

TABLE 11.2
Sample Pump Specification

Pump Model	Power Rating	Total Head in Meters						
		12	14	16	18	20	22	24
		Capacity in Liters per Second						
K-22	5.5 kW	27.0	25.5	23.8	21.7	19.7	17.1	13.8
Efficiency		0.58	0.64	0.68	0.70	0.70	0.67	0.59

Best fit as a turbine would be at a range head: 28–31 m and flow: 26–29 lps.

One important limitation of centrifugal pumps is that the given specifications of the pumps determine fixed head and flow specifications at which the turbine can efficiently be used. The pump used as a turbine cannot therefore accommodate variable flow conditions at the site and is suitable only for a constant flow at all times. Because there is no way to regulate the flow to the PAT, during the dry season when the available flow falls below the design turbine flow, the top section of the penstock pipe becomes empty until the effective head drops to the point at which only available flow is able to pass through the turbine. Power output of the PAT thus falls substantially because, in addition to the lower flow, there is also significant reduction in available head, and on top of which the PAT is operating at below its BEP.

11.8 REVERSIBLE PUMP TURBINES FOR PUMPED STORAGE

Pumped storage hydroelectricity provides a method of storing and producing electricity to supply high peak demands by moving water between reservoirs at different elevations (see Figure 11.19). At times of low power demand, excess electrical capacity is used to pump water into the higher reservoir. When there is higher demand, water is released back into the lower reservoir through a turbine, generating hydroelectricity.

Pumped storage projects are net consumers of energy in that for every kWh of energy generated during peak periods, more than 1 kWh of off-peak energy is required for pumping. Due to evaporation losses from the exposed water surface and electrical and mechanical efficiency losses during conversion, typically 85% of the electrical energy used to pump the water into the upper reservoir can be recovered. However, they easily offset these losses improving the performance of the rest of the grid by flattening out the variations in the load on the power grid, permitting base-load power stations to operate efficiently at full capacity while reducing the need to build special power plants that run only at peak demand times using more costly generation methods.

Low-cost electricity to pump water can increasingly be sourced from intermittent renewables, such as wind and solar energy, as the installed MWs from these technologies continue rapid

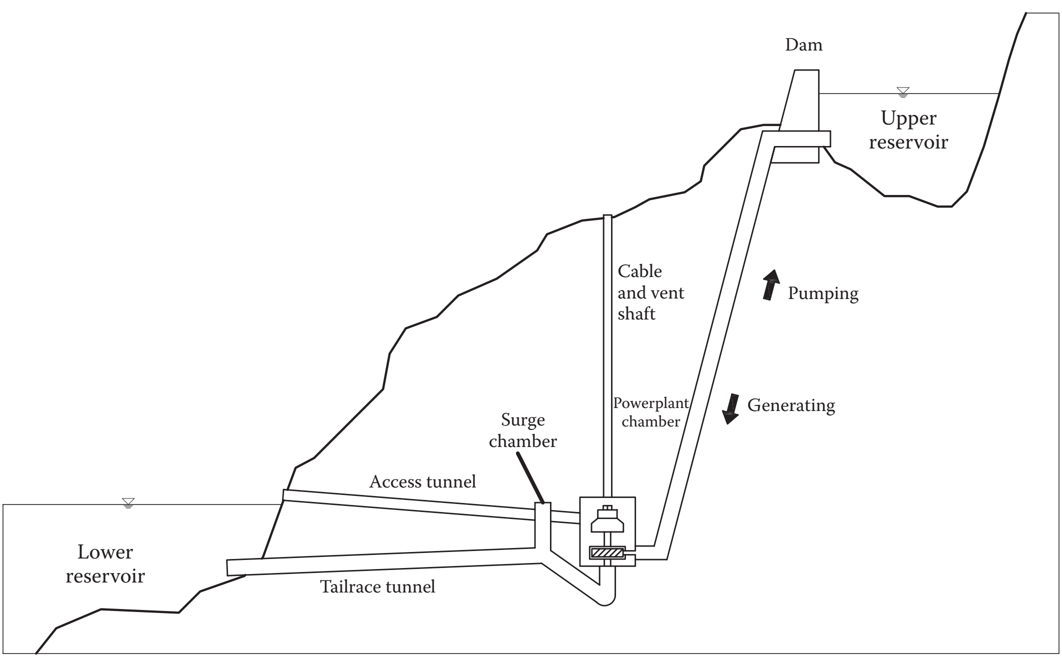

FIGURE 11.19 Pumped hydroelectric storage.

increases. The ability to store energy during periods of oversupply of wind, for example, and generate it when there is high demand makes pumped storage hydro power an excellent complement. The 400 MW Cruachan Power Station in Scotland has been in operation as a pumped-storage hydroelectric plant since 1967. It has a head of 396 m, 8.8 GWh of storage and has a response time 2 minutes from stationary reducing to 30 seconds if spinning (http://www.scotsrenewables.com/blog/distributionandstorage/pumped-storage-hydro-in-scotland/). A number of islands that are looking to significantly increase renewable energy on their grids are seriously examining the option of pumped storage in conjunction with wind generation. In the case of the Canary Islands, Bueno and Carta [4] have proposed the construction of a system consisting of a 20.44 MW wind farm, a 17.80 MW pumping station, and a 60 MW hydro power on the Gran Canaria Island to generate 52.55 GWh of firm renewable power each year.

Reversible pump turbines, usually a Francis turbine design, operate both as a turbine for energy generation and, in the reverse direction, as a pump. The first use of a reversible pump turbine in the United States, which is now standard for pumped storage plants, was at the Tennessee Valley Authority's Hiwassee Dam in North Carolina in 1956.*

The 2010 Technology Summit Meeting on Pumped Storage Hydropower found that although the dominant technology used in pumped storage plants in the United States remains the conventional reversible pump turbine generator, more advanced pump turbine generator technologies are being applied internationally. "In Japan, for more than two decades it has been common practice to incorporate variable speed pump-turbine generators in pumped storage plants. Such units are now in use in other countries especially in Europe. In addition, unidirectional 'three-element' (ternary) machines have been installed wherein there is no change in the rotational direction allowing the units to move rapidly from full pumping to full generation unlike a reversible machine where the machines require a stop before restarting in the opposite direction (and vice versa)."†

EXERCISES

1. A propeller turbine with a hydraulic efficiency of 80% is installed at the base of a reservoir and is placed 2.5 m above the tailrace. The turbine uses a draft tube with an inlet diameter of 1.3 m and efficiency of 70%. If the power output of the turbine is 928.9 kW at a flow of 9.6 m^3/s, how much of the generated power can be attributed to the pressure head above the turbine and to the static and dynamic heads added by the draft tube? What readings would a pressure gauge at the turbine inlet and vacuum gauge at the outlet of the turbine show for the pressure and suction head? (Answer: 600 kW, 188.3 kW, 140.6 kW; 7.97 m, −4.37 m.)
2. In Exercise 2, calculate what the pressure gauges would read if the flow drawn from the reservoir is reduced to 4.8 m^3/s. (Answer: 7.97 m, –2.97 m.)
3. What is the maximum height of a vertical conical draft tube being used with a propeller turbine with an output of 2025 kW and operating at 133 RPM at a net head of 5.8 m. Assume atmospheric pressure at the installation site to be 10.0 m of water and vapor pressure to be 0.2 m of water. (Answer: 4.06 m.)
4. Prove that the degree of reaction of a reaction turbine is a function of α_1 and β_1 only. Assume that the velocity of flow is constant and discharge at exit is radial. (Answer: $R = 1 - \frac{\cot\alpha_1}{2(\cot\beta_1 + \cot\alpha_1)}$.)
5. A Francis turbine runner operating at 250 RPM has an external diameter of 1000 mm. The width of the runner at the inlet is 240 mm, and the velocity of the water flow through the runner is 8.0 m/s. The guide vanes make an angle of 20° to the tangent of the wheel

* http://files.asme.org/asmeorg/Communities/History/Landmarks/5567.pdf

† http://www.esd.ornl.gov/WindWaterPower/PSHSummit.pdf

and the discharge at the outlet of the runner is radial. Find the power output of the turbine assuming a vane thickness factor of 0.95. (Answer: 1649 kW.)

6. A reaction turbine with an inlet runner diameter of 1.2 m and flow area of 0.33 m^2 is operating at a head of 150 m and a speed of 500 RPM. If the guide vane angle and the blade angle at the inlet are 20° and 125°, respectively, find the power produced and hydraulic efficiency. (Answer: 6.7 MW, 90%.)
7. A Francis turbine is used at a head of 196 m. Assuming a speed ratio of 0.76, calculate what its diameter would need to be to drive an eight-pole 60 Hz generator at its synchronous speed. What is the maximum flow this turbine can accommodate if the height of the blades will be limited to 25% of the runner diameter, the flow ratio is 0.25, and the blade thickness factor is 0.95? (1.0 m, 9.25 m^3/s.)
8. A Francis turbine is to be operated at a speed of 450 RPM and is designed for a discharge of 2.5 m^3/s. If $D_1 = 0.8$ m and $\beta_1 = 90°$, blade height B is 10 cm, what should the guide vane angle α_1 be for shock-free entry to the runner? If it is known that $D_2 = 0.5$ m and $\alpha_2 = 75°$, what power can be achieved under these conditions? What is the maximum power with radial exit? (Answer: 29°, 806 kW, 888 kW.)
9. A Kaplan runner develops 12 MW of power, operating under a net head of 15 m and rotating at a speed of 120 RPM. Its dimensions are 5.0 m outer diameter and 2.2 m hub diameter. Assuming hydraulic efficiency of 95% and overall efficiency of 90%, calculate (a) inlet guide vane angle and inlet blade angle at the tip and (b) inlet guide vane angle and inlet blade angle at the hub. (Answer: (a) 52.1°, 12°; (b) 57°, 29.5°.)
10. A hydropower site is being developed to generate 166 MW of power. The head available is 22 m. The designer has to choose between available Francis and Kaplan turbines for the site. If the turbines must operate at a speed of 120 RPM, how many of each type of turbine would be required at this site. Assume that the specific speed of the Francis turbines is limited to 350 and Kaplan turbines to 700. (Answer: Francis 12, Kaplan 3.)
11. A centrifugal pump manufacturer provides curves that show that the highest efficiency of a pump is 60% at a BEP delivery head of 25 m and flow of 10 lps at a speed of 1500 RPM. What site specifications would this pump be most suitable for as a turbine to operate at the same RPM? (Answer: Head: 46 m; Flow 15 lps.)

REFERENCES

1. Krivchenko, G., *Hydraulic Machines: Turbines and Pumps*. CRC Press, Boca Raton, FL, 1994.
2. Subramanya, K., *Hydraulic Machines*. Tata McGraw-Hill Education, New Delhi, 2013.
3. Williams, A., *Pumps as Turbines: A User's Guide*. Practical Action Publishing, Rugby, UK, 2003.
4. Bueno, C., Carta, J. A. 2004. Wind powered pumped hydro storage systems, a means of increasing the penetration of renewable energy in the Canary Islands. *Renewable and Sustainable Energy Reviews* 10, 312–340, 2006.

12 Very Low Head and River Current Turbines

12.1 VERY LOW HEAD TURBINES

Very low head hydropower (VLH) projects, typically defined as having a head of less than 3.2 m,* has generated recent interest for two main reasons. One is that they are environmentally attractive because they can be developed without constructing dams, and the newer turbine designs minimize impacts on fish. Specific characteristics of VLH turbines that reduce fish injury and mortality include (a) relatively larger diameter runner allows fish to keep away from the hub or blade end gaps; (b) lower speed of the runner reduces the impact of blade strikes; (c) smaller pressure gradient between the inlet and outlet of runner reduces pressure-related injury; (d) lower incidence of cavitation reduces associated mortality; (e) smaller shear stresses, which result from rapid changes in velocity over short distances, lowers mortality.†

The second reason VLH sites have become interesting is that most financially attractive, higher head hydropower sites have either been developed already or are prohibited from development for environmental reasons, particularly in OECD countries. See Chapter 15 for environmental considerations, increasingly resulting in limited availability of sites for developing new hydropower projects.

12.1.1 Axial Flow VLH Designs

Standard technology for most installed VLH systems is the pit turbine. As described in Chapter 11, bulb and pit turbines are axial-flow compact units with a horizontal generator held in a watertight casing upstream of the propeller runner. Pit turbines include a gearbox, which allows for use of higher speed generators even at very low heads and hence the use of a smaller bulb casing. The head and flow specifications covered by existing low head bulb turbines are given in Figure 12.1.

One major challenge for developers of conventional VLH sites is that the civil works associated with them can be cost-prohibitive for the amount of power they generate. Figure 12.2 depicts the substantial civil works associated with the vertical siphon Kaplan and bulb turbine, respectively, as examples.

In general, the lower the head, the higher the relative cost of the civil works to generate the same amount of power. For constant output, Leclerc finds from a survey of hundreds of low head sites that, "if the head drops from 3.2 m to 1.4 m, the corresponding concrete volume required to build the power plant is multiplied by 5, while the runner diameter of the turbine is doubled."‡ He concludes that for this reason very low head sites are technically feasible but often unprofitable.

A number of companies have developed special turbine designs and installation arrangements to reduce the civil works for VLH sites. MJ2 Technologies in France (http://www.vlh-turbine.com/) has developed a standardized product called the VLH turbine (see Figure 12.3) with output range between 100 to 500 kW for heads ranging from 1.4 to 4.5 m and flows from 10–30 m^3/s. The VLH turbine comes in five diameter sizes ranging from 3.15 m to 5.00 m.

* http://www.small-hydro.com/Programs/Innovative-Technologies/121-1-Very-Low-Head-Turbine-Generator.aspx; Fraser and Deschenes (2007). http://lamh.gmc.ulaval.ca/fileadmin/docs/Publications_Recentes/VLH_A_New_Turbine_for_Very_Low_Head_Applications.pdf

† http://www1.eere.energy.gov/wind/pdfs/doewater-13741.pdf

‡ http://www.vlh-turbine.com/concrete

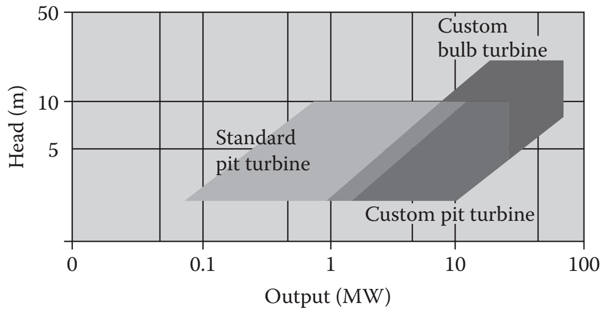

FIGURE 12.1 Application regime for Voith low head pit and bulb turbines. (From http://www.voith.com/en/products-services/hydro-power/turbines/bulbpit-turbines-565.html.)

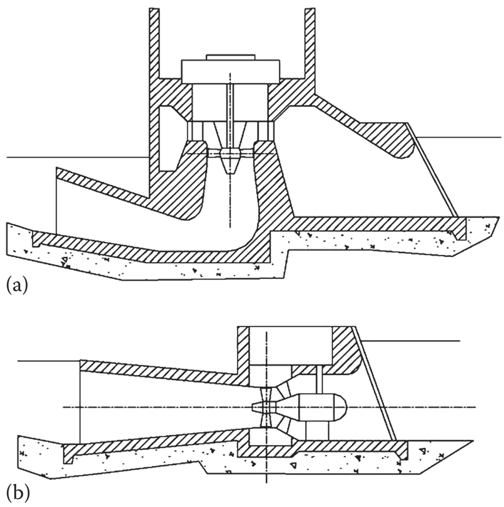

FIGURE 12.2 Civil works for low head turbines (a) civil works for vertical siphon Kaplan, (b) civil works for bulb turbine. (From http://www.vlh-turbine.com/.)

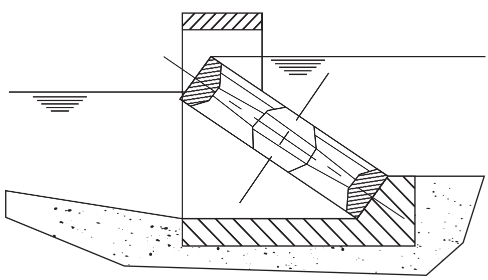

FIGURE 12.3 Schematic of VLH turbine implementation.

As shown in Figure 12.4, the resulting compact unit can be installed with minimal civil construction. The large diameter VLH runner means that no sophisticated civil engineering structures are required for keeping losses low from higher velocity water flow at the inlet to and exit from the runner. Slanted in its mounting, the unit can be removed from the sluice passageway by a lifting device system.

The VLH turbine is an open flow, very low head Kaplan turbine slanted at an angle to the water flow. It has low speed and is fish friendly with tests on eels showing 100% survival rate according to the company. Figure 12.4 shows on the left the VLH in a working position and on the right a 4.5-m runner.

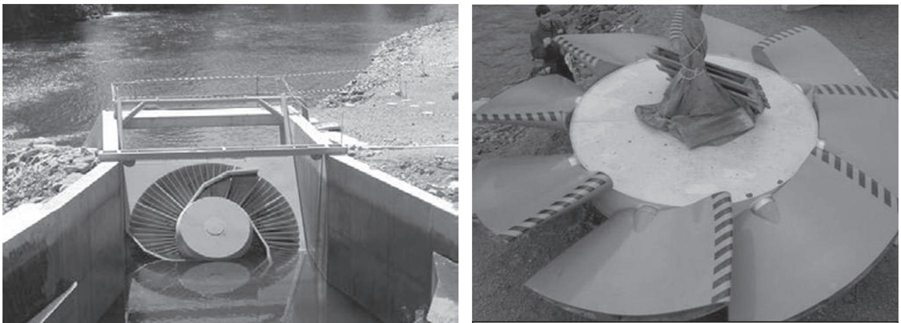

FIGURE 12.4 Installation and runner of VLH turbine.

The VLH unit is an integrated generating set (IGS), incorporating a Kaplan runner with eight adjustable blades and a permanent magnet generator (PMG) directly coupled to the runner shaft. The large diameter runner results in low RPM and significantly reduced danger to fish. Electronic power regulation makes it possible to have a variable speed generator. The adjustable blades and variable speed of the runner allow for high-efficiency operation at sites where both the head and river flow change during different seasons. Housing the runner is a fixed distributor composed of 18 wicket gates with flat bars inserted in between as trashracks and an automatic trashrack cleaner mounted on it.

12.1.2 Natel Energy

Natel Energy from California has introduced a novel two-stage linear flow impulse turbine, named the hydroEngine, which is suitable for use at low head sites between 2 and 20 m of head and can accommodate flows ranging from 0.2 cumec to 13.8 cumecs per unit [1]. The turbine drives a generator via a gearbox or belt drive system. The control panel allows autonomous plant startup and shutdown as well as remote site monitoring and manual override capabilities.

As shown in Figure 12.5, the hydroEngine has two sets of guide vanes and two sets of moving blades; the first set of guide vanes direct water flow to a cascade of moving blades, following which

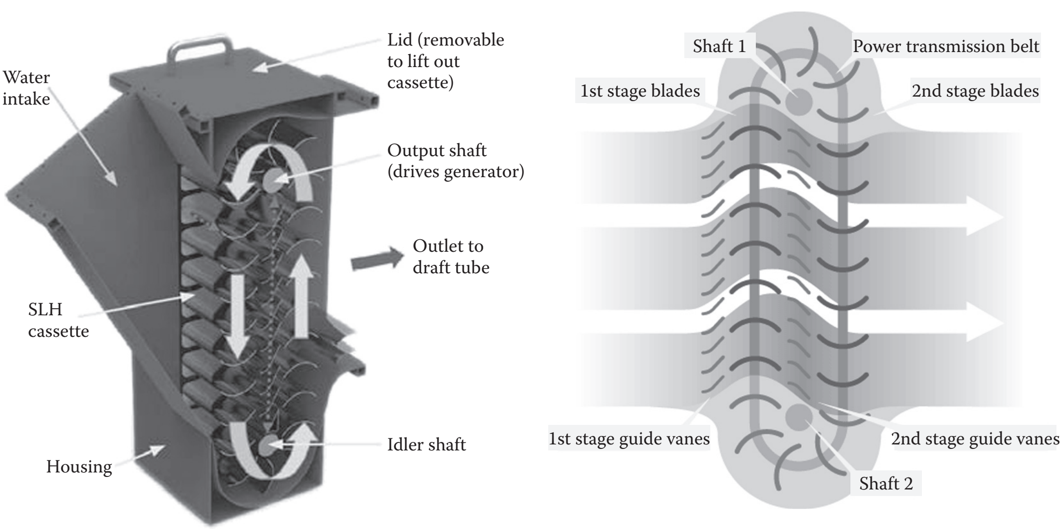

FIGURE 12.5 Natel hydroEngine. (From http://www.natelenergy.com/wp-content/uploads/2015/06/Natel_Product_Brochure_May2015_web.pdf.)

the second set of guide vanes direct water to the second cascade of blades. The guide vanes also control the flow rate to maintain efficiency across a range of flows.

The hydroEngine has similarities with the cross-flow turbine in that it operates as an impulse turbine with the water jet striking blades twice before exiting the runner. Both impulse turbine designs use draft tubes and also share the advantage of being able to utilize a range of blade lengths to accommodate different discharge specifications without changing the diameter of the runner. The hydroEngine embodies several important improvements over the cross-flow, however.

First, the set of guide vanes on the inside of the runner allows the water jet to be more effectively directed at the second set of blades. Inefficiencies in the cross-flow turbine resulting from (a) a portion of the jet being entrained on the periphery of the runner wheel and exiting without entering the runner radially, (b) some of the jet being interrupted by the runner shaft from striking the second blade, and (c) streams of water crossing inside the wheel and interfering with one another as well as impinging on the second set of blades at a range of angles are largely avoided or minimized.

A second improvement over the cross-flow is that by mounting the blades on the power transmission belt and using two shafts, the hydroEngine significantly reduces the effective diameter of the runner. Because the speed of the turbine depends inversely on the runner diameter, this makes for a faster turbine with higher specific speed.

$$N \propto \frac{\sqrt{H_{net}}}{D}$$

The hydroEngine's main power transmission belt operates underwater and would be subject to wear and tear. Scheduled replacement of the critical belt incurs an operating cost, which is likely to be higher than the typical impulse turbine. The company specifies a life of 15,000 hours for the transmission belt at full load corresponding to an average replacement period of 3.5 years if the average load is 50%.

With greater specific speed compared to the cross-flow turbine, the hydroEngine is able to directly compete with small Kaplan turbines, in the <1 MW range, for the low head and high flow application range. Although it has relatively lower efficiency compared to reaction turbines, at between 75% and 80%, the hydroEngine shows promise as an alternative to reaction turbines in the VLH range, requiring substantially less excavation and civil construction to install. According to the company, the hydroEngine's operating costs compare well with Kaplan and propeller turbines, which incur routine repair and maintenance costs due to cavitation.

One important advantange of the hydroEngine is that it is more fish friendly compared to standard Kaplan turbines because it avoids the high speeds of the runner blades, the rapid changes in pressure, or small clearances between the runner and the stationary parts of the housing where fish can get caught.

12.1.3 Archimedes Screw Turbine

The Archimedes screw turbine (Figure 12.6) is a recent addition to the VLH hydropower market having arrived on the scene in the last two decades or so. The same device has been known and used for decades as the Archimedes screw pump with tens of thousands installed worldwide, particularly in sewage treatment works. As its name implies, Archimedes is considered to have invented the screw pump, circa 287–212 BC.

The modern Archimedes screw turbine consists of a fixed outer cylinder on which blades attached on the inner cylinder rotate when water flows through it. The number of blades typically ranges from one to three although in theory there could be an infinite number of them. When the screw is tilted, "buckets" of water are formed between the blades, which rotate the screw as they move down.

Archimedes screw turbine installations share the same benefits as using the screw for pumping: the ability to handle dirty water and widely varying rates of flow at high efficiency. It is not surprising

FIGURE 12.6 Archimedes screw turbine in use in Poland (diameter 3 m; flow of 6 m^3/s; height 1.8 m; maximum power 80 kW). (Courtesy of Pesymista [own work], CCBY-SA 3.0, https://commons.wikimedia.org/wiki/File:Turbina_Archimedesa_MEW_Goryn.jpg#filelinks.)

that the same manufacturers that dominate the screw pump market are also the main suppliers of the screw turbine in the hydropower market as well. Furthermore, the screw turbine inflicts minimal disturbance to the environment. The large opening in the screw allows fish to swim through the turbine without damage. The turbine operates at slow speeds of 10–100 rpm, which reduces risk to the fish at the same time minimizing maintenance costs by preventing premature wear and tear.

Screw turbines are typically available at heads from 1 to 10 m and for discharges from 0.1 to 15 m^3/s, and power outputs are generally below 1 MW. Speed is low for large diameter screws and higher for screws of smaller diameter. The rotational velocity of a screw in revolutions per minute should be no larger than $50/D^{2/3}$, where D is the diameter in meters of the outer cylinder, to minimize turbulence. This would mean that a screw with an outside diameter of 1 m would have a maximum speed of 50 RPM [2].

Guidance on the design of an optimal Archimedes screw is that the ratio of inner to outer radius should be 0.54 [2]:

$$R_i = 0.54\ R_o$$

According to the *Archimedean Screw Handbook* from German manufacturer Ritz-Atro, the pitch of the blades, Λ, or length of one cycle of the screw should range from 1.6 to 2.4 times the length of the outer diameter for optimal performance, depending on the angle of the screw, θ, to the horizontal:

$$\Lambda = 2.4\ R_o\ \mathit{if}\ \theta < 30°$$
$$\Lambda = 2.0\ R_o\ \mathit{if}\ \theta = 30°$$
$$\Lambda = 1.6\ R_o\ \mathit{if}\ \theta < 30°$$

However, the company recommends standardization of $\Lambda = 2.0\ R_o$ to avoid proliferation of different designs and the concomitant manufacturing costs (see Figure 12.7).

Screw turbines can have comparable efficiencies with Francis and Kaplan turbines with efficiency measured in the low 90s. A recent study found mean efficiency of a range of operating plants to be 69% with the best six performing at 75% efficiency [3]. Furthermore, the efficiency of the screw turbine is relatively stable and does not change much with loading conditions. Figure 12.8 gives a comparison of efficiencies between several low head turbines at different discharge levels.

The potential disadvantages of the Archimedes screw turbine are that it is bulky and requires heavy equipment to move the turbine to the site. This limits its use to relatively accessible areas.

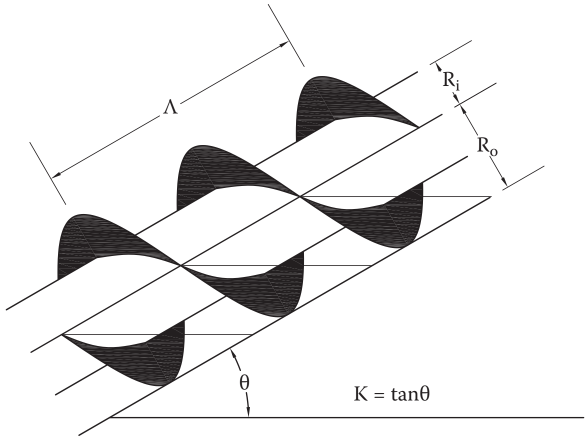

FIGURE 12.7 Pitch of a two-headed Archimedes screw.

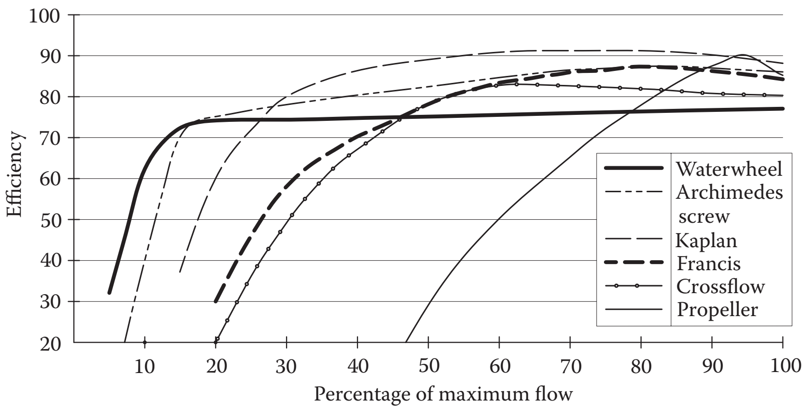

FIGURE 12.8 Efficiency of Archimedes screw at low flow compared to other turbines.

Second, a high ratio gearbox is required to increase its speed to drive the alternator. Together, these two factors can translate into high cost of installation.

12.2 WATER CURRENT TURBINES

Water current turbines (WCT) are "zero head" turbines, which produce power from the kinetic energy of water flowing in a river or a canal. They are used in situations in which it is impractical to create a static head of water through construction of a dam or barrage. Examples are turbines designed to be used on wide irrigation canals or large rivers or to capture energy from marine tides. Much like a wind turbine, the rotor of a WCT extracts kinetic energy from free-flowing fluid. Compared to the energy available from a static head of water, river currents are a diffuse source of energy.

A river speed of 1 m/s, for example, is equivalent to a static head of only 50 mm.

Using Bernoulli's equation,

$$v = \sqrt{2gH}$$

$$H = \frac{v^2}{2g} = 0.05\ \text{m} = 50\ \text{mm}$$

12.2.1 Power Available in Flowing Water

The power available in a mass of water, m, flowing at a velocity, v, can be calculated as

$$\text{Power available} = \frac{\text{Kinetic energy}}{\text{time}} = \frac{0.5mv^2}{t}$$

Considering the volume of water moving inside a cylinder of cross-section area A and length L, the mass, m, of that volume of water can be calculated as

$$\text{Mass: } m = \rho \cdot V = \rho \cdot A \cdot L$$

where ρ is the density of water.

Thus, the power inherent in that flowing water can be expressed as

$$P = \frac{0.5mv^2}{\text{time}} = 0.5 \cdot \rho \cdot A \cdot \frac{L}{t} \cdot v^2 = 0.5 \cdot \rho \cdot A \cdot v^3$$

v = L/t because it is equivalent to the velocity of water that travels through the length of the cylinder.

The power per area or *power density* of the water current can thus be written as

$$\frac{P}{A} = 0.5 \cdot \rho \cdot v^3 \tag{12.1}$$

And can be seen to be proportional to the cube of the velocity.

The water current turbine rotor, which is designed to extract the power from the water current, will produce power output:

$$P_s = 0.5 \rho A_s V_s^3 C_p \tag{12.2}$$

P_s = shaft power
ρ = the density of water 1000 kg/m³
A_s = the sweep area of flow perpendicular to the current direction from which power is to be extracted (m²)
V_s = velocity of water flowing through the area
C_p = coefficient of performance of the rotor

Equation 12.2 shows that the shaft power of the rotor is directly proportional to the area of its sweep. The density of water is around 800 times that of air, and thus water current turbines can produce significant amounts of power at relatively low water velocities compared to wind turbines. Wind speed would need to be more than nine times as high to equal the power density of water. Or, alternatively, water current at 1 m/s would have the same energy content per square meter of sweep area as wind at a speed of 9 m/s.

It is not possible in practice to extract all the energy available in the flowing water. The flowing water cannot give up all its kinetic energy as it passes through the rotor; the flow would have to stop at the rotor exit end for this to happen. As with wind turbines, there is a theoretical limit, known as the *Betz limit* to what the maximum power coefficient C_p can be [4].

C_{pmax} = the theoretical maximum power coefficient = 16/27 = 0.592 or 59%.

The *Betz Law* can be verified as follows:

Assume that the velocities of water current immediately upstream and downstream of the rotor are V_1 and V_2, respectively, and the flow velocity as it goes through the rotor is V_S. A_S is the sweep area of the rotor, and A_1 and A_2 are the cross-sectional areas of water flow immediately upstream and downstream of the rotor.

To be consistent with the principle of conservation of mass, the rate at which mass of water flows through the area of the rotor:

$$\dot{m} = \rho A_1 V_1 = \rho A_S V_S = \rho A_2 V_2 \tag{12.3}$$

It is clear from Equation 12.3 that because the velocity of the water slows as it traverses the rotor ($V_2 < V_1$), the area of flow must increase correspondingly ($A_2 > A_1$).

Power extracted from the water current by the rotor can be computed in two ways:

$$P = F \cdot V_S = m \cdot \frac{dv}{dt} \cdot V_S = \dot{m} \cdot \Delta V \cdot V_S = \rho A_S V_S^2 \cdot (V_1 - V_2) \tag{12.4}$$

after substituting in Equation 12.3. And

$$P = \frac{dE}{dt} = \frac{d\left(0.5 m V_S^2\right)}{dt} = 0.5\dot{m} \cdot \left(V_1^2 - V_2^2\right) = 0.5\rho A_S V_S \cdot \left(V_1^2 - V_2^2\right) \tag{12.5}$$

Combining Equations 12.4 and 12.5 gives the result that

$$\rho A_S V_S^2 \cdot (V_1 - V_2) = 0.5\rho A_S V_S \cdot \left(V_1^2 - V_2^2\right) = 0.5\rho A_S V_S \cdot (V_1 + V_2) \cdot (V_1 - V_2)$$

$$V_S = 0.5(V_1 + V_2) \tag{12.6}$$

The velocity of water as it flows through the rotor is the mean of the upstream and downstream velocities.

Substituting for V_S into Equation 12.4,

$$P = 0.25\rho A_S (V_1 + V_2)^2 \cdot (V_1 - V_2) = 0.25\rho A_S \cdot (V_1 + V_2) \cdot \left(V_1^2 - V_2^2\right)$$

$$P = 0.25\rho A_S \cdot \left(V_1^3 - V_1 \cdot V_2^2 + V_2 \cdot V_1^2 - V_2^3\right) \tag{12.7}$$

The exit flow velocity that results in maximum power for a given V_1 can be computed by differentiating with respect to V_2 and setting to zero:

$$\frac{dP}{dV_2} = 0.25\rho A_S \cdot \left(0 - 2V_1 V_2 + V_1^2 - 3V_2^2\right) = 0$$

This can be solved, by factoring, to give two solutions:

$$(V_1 - 3V_2) \cdot (V_1 + V_2) = 0$$

$$V_1 = 3V_2 \quad \text{and} \quad V_1 = -V_2.$$

Substituting into Equation 12.6 gives possible solutions for $V_S = 2V_2$ and $V_S = 0$ of which only the first can result in power transfer to the turbine.

The maximum power transfer to the river current turbine is seen to result when the exit velocity V_2 is one third of the magnitude of the input velocity, V_1.

The maximum power transfer to the rotor can be computed, when $V_1 = 3V_2$, from Equation 12.7.

$$P_{max} = 0.25\rho A_S \cdot \left(V_1^3 - V_1 \cdot V_2^2 + V_2 \cdot V_1^2 - V_2^3\right) = \frac{16}{27} \cdot \left(0.5\rho A_S V_1^3\right) \tag{12.8}$$

Comparing with Equation 12.2, it can be seen that the maximum coefficient of performance cannot be larger than $\frac{16}{27}$ for any rotor extracting power from a fluid flowing through it at a constant speed.

$$C_{Pmax} = \frac{16}{27} \tag{12.9}$$

In practice, efficiency will be lower than this theoretical maximum because the rotor that converts the kinetic energy to mechanical power is subject to friction and drag forces, which will dissipate some of the available power. The coefficient of performance of the rotor, C_p, accounts for these inefficiencies, and for a small-scale river turbine, the power coefficient is typically around 0.25–0.3.

Example 12.1

A turbine with a swept area of 2.96 m² is placed in a river current moving at 1.5 m/s. Calculate the power available in the flowing water. Assuming that the coefficient of performance of the rotor is 30%, calculate the shaft power available.

Power available in the flowing water:

$$P = 0.5 \cdot 1000 \frac{kg}{m^3} \cdot 2.96\,m^2 \cdot \left(1.5\frac{m}{s}\right)^3$$

$$= 5000 \text{ Watts}$$

Shaft power $P_s = P \cdot C_p = 5\text{ kW} \cdot 0.3 = 1.5\text{ kW}$

12.2.2 Types of Water Current Turbines

Water current turbines can be classified into two types: (a) axial turbines whose axis is aligned with the direction of flow and employs a propeller-type rotor and (b) "cross-axis" type turbines with which the water flow is orthogonal to the rotor axis and which have cylindrical rotating structures. A subtype under the cross-axis is a paddle wheel design that employs impulse blades or buckets.

12.2.2.1 Axial Water Current Turbines

Peter Garman of Intermediate Technology Development Group (ITDG) is credited with developing the first river current turbine in 1978, using an axial design. The design is currently manufactured by the company Thropton Energy Services.* Practical Action† in the UK continues to promote a

* http://www.throptonenergy.co.uk/

† Practical Action (http://practicalaction.org/) is the new name for ITDG.

FIGURE 12.9 River current turbine. (From Practical Action Latin America (Soluciones Prácticas).)

small-scale river current turbine to generate a few hundred Watts, sufficient for charging batteries or pumping water in remote communities (Figure 12.9). One version of the machine is manufactured by the company Tecnologia Energética S.A.C.–Tepersac based in Lima, Peru, and has the following component specifications:

Rotor: The rotor is made up of three fiberglass blades with a nominal diameter of 1.75 m. The axis is placed at an incline to the river flow. Its design turning speed is 45 rpm at 1 m/s speed of river flow. Two stainless steel supporting plates are used for the bucket mounting.

Generator: In order to reduce cost and to be able to manufacture locally, the design uses a permanent magnet generator. The use of magnets allows the speed of generation to be reduced, which, in turn, lowers the cost of the equipment. The generated alternating current is transformed, via a system of rectifying diodes, to 12V DC and the system produces 250 W of power at a speed of 360 rpm.

Transmission: A galvanized steel tube 1.5 inches in diameter is connected directly to the rotor and functions as the transmission shaft. This tube is placed inside a second, similar tube, 2.5 inches in diameter, which serves as protection and support. A fan belt is used to increase the velocity of the rotor to drive the generator.

12.2.2.2 Tidal Marine Turbines

The axial flow water current turbine has in recent years been developed into a tidal marine turbine. Currents that generally move at low speeds of a few cm/s in the open sea can increase to as high as 2–3 m/s when they are channeled through constraining geography, such as straits between islands, bays, and estuaries. In addition to being a large potential source of kinetic energy, if developed to scale, tidal energy would likely have higher value to utilities compared to wind and solar energy in being able to deliver power predictably to a timetable based on well-known cycles of the moon. Tides are essentially long slow waves created by the gravitational pull of the moon and to a lesser scale the sun, on the Earth's surface. The pull forces the ocean to bulge outward on opposite sides of the Earth, causing a rise in the water level in places aligned with the moon. Both the rise and fall in water levels, consistent with diurnal tidal flow and ebb cycle, are accompanied by a horizontal movement of water, which is known as the tidal current.

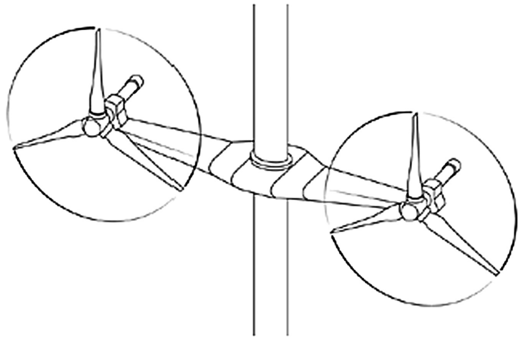

FIGURE 12.10 Marine Current Turbines SeaGen S.

Several locations in the United Kingdom and Channel Islands have been identified as having intense tidal currents over a sufficiently large area to have the potential for exploitation on a multi-gigawatt scale with some estimates put at more than 10 GW.* Other countries in Europe with high potential for tidal energy include France, the Straits of Messina in Italy, and channels between the Greek islands in the Aegean. East Asia and South East Asia, particularly China, the Philippines, Indonesia, Korea, and Japan, have large marine current resources as do Australia, New Zealand, Canada, and South Africa [5]. In the United States, it has been estimated that Florida could potentially meet much of its electricity needs by tapping the Gulfstream off its coast (BOEM†).

Tidal turbines are in their infancy compared to the wind turbines, which they resemble. There are yet no commercial tidal turbine "farms," which are necessary to achieve the economies of scale for cost-competitive generation although several are at advanced stages of planning. Marine Current Turbines (MCT) is working to develop the first tidal energy projects in the United Kingdom. MCT's SeaGen S tidal turbine, among the first commercial tidal energy turbines, uses twin rotors on a cross beam, which can be raised above the water for routine maintenance as shown in Figure 12.10. It is designed for marine environments in water depths up to 38 m and achieves rated power at a tidal current of 2.4 m/s. MCT is working on bringing a 2 MW SeaGen S turbine to market with a rotor diameter of 20 m.

In his opinion piece, "Too Much Torque and Not Enough Action," Peter Fraenkel [5] explains that one of the reasons tidal energy has been slow to develop compared to wind energy is the higher forces tidal turbines have to withstand. The relatively slow speed of tidal turbines, roughly half that of wind turbines, requires a correspondingly higher torque to produce the same power. Because the high torque is a measure of loads that need to be resisted by the device, tidal turbines require stronger blades and more robust structural designs and incur corresponding higher costs.

Table 12.1 shows the speed and torque for typical power-producing turbines and engines in order to produce 1 MW of shaft power.‡

$$P = \tau \cdot \omega = 1000 \text{ kW}$$

The table is instructive in highlighting the large torques that slow turbines, such as tidal and wave turbines, must be designed to withstand to produce significant amounts of power. Fraenkel argues that although the industry is finally close to commercial installations of marine tidal turbines, enormous challenges still remain to design and construct commercial devices in the MW

* http://www.marineturbines.com/Tidal-Energy

† Bureau of Ocean Energy Management, http://www.boem.gov/Renewable-Energy-Program/Renewable-Energy-Guide/Ocean-Current-Energy.aspx

‡ http://www.waterpowermagazine.com/opinion/opiniontoo-much-torque-and-not-enough-action-4190252/

TABLE 12.1
Comparison between Speeds and Torque across Turbine Types

Device	Speed (radians/sec)	Torque (kNm)
Gas turbine	1500	0.67
Diesel engine	150	6.7
Hydro turbines	150–10	6.7–100
Wind turbine	3	335
Tidal turbine	1.5	670
Wave energy device	0.15	6700

Speeds and torques needed to produce 1MW

Source: From Fraenkel (2014) "Too much torque and not enough action."

range to capture wave energy because they must withstand an order of magnitude higher torque than tidal turbines [5].

By comparison, most impulse and reaction turbines discussed in Chapters 10 and 11 have speeds in the range of 10 to 150 radians/sec. The relatively lower torque required for hydraulic turbines to produce power on account of their higher speeds provides one explanation for compact hydropower turbines, capable of producing hundreds of MWs, having been available for more than 150 years (see Table 1.1 for the development history of the water turbine).

12.2.2.3 Cross-Axis Water Current Turbines

Cross-axis turbines are usually of the Darrieus or helical design. These designs are "lift" based and use hydrodynamic lifting surfaces, or hydrofoils, for their blades. Using lift, the blades can move faster than the speed of the water and are hydrodynamically more efficient. Cross-axis turbines rotate in the same direction even with bidirectional water flow. The blades of lift devices typically also use much less material to manufacture than devices based on drag.

A few cross-axis water turbines nevertheless utilize the Savonius or paddle wheel design with impulse blades or buckets. These so called "drag" devices, which rely on blades or buckets being pushed by the water flow, are less efficient than lift devices. They also operate at lower speeds with the rotor speed at the highest efficiency typically at 30% of the speed of the water.

The maximum coefficient of performance of a drag device can be calculated as follows:

Velocity of the water relative to the velocity of the rotating drag device:

$$\mathbf{v_r = v_o - u}$$

where $\mathbf{v_o}$ is the speed of the water, and $\mathbf{u}$ is the speed of the runner.

The rate of work done on the drag device can be calculated similar to the work done by a jet on a plate, using the relative velocity.

As shown in Section 9.1.2, power available to the runner is

$$P = 0.5\rho A(v_o - u)^2 u$$

By differentiating power P with respect to u and setting $\frac{dP}{du}$ to zero, the speed "u" can be calculated for which the power output is either the maximum or minimum.

$$\frac{dP}{du} = 0.5\rho A \frac{d}{du}[(v_0 - u)^2 \cdot u] = 0$$

$$(v_0 - u)^2 \cdot \frac{du}{du} + \frac{d(v_0 - u)^2}{du} \cdot u = 0$$

$$(v_0 - u)^2 + 2u(v_0 - u)(-1) = 0$$

This equation has two solutions:

Either $u = v_0$, which is the case when the runner is rotating at the same speed as the water and offering no resistance to the water flow, no power is being transferred in this situation, and $P = 0$, or $(v_0 - u) - 2u = 0$, in which case $u = \frac{1}{3} v_0$ when the runner is rotating at one third the speed of the water flow. This must be the speed at which power output of the runner is maximum.

Substituting this value for u, gives

$$P_{max} = 0.5\rho A(v_o - u)^2 u = P_w \cdot \frac{4}{27} \tag{12.10}$$

The maximum power out can be written as a function of coefficient of performance C_{Pmax}:

$$P_{max} = C_{P_{max}} \cdot P_w$$

where P_w is the power in the water with velocity v_o, flowing through area A.

Thus

$$C_{P_{max}} = \frac{4}{27} = 0.15 \tag{12.11}$$

Despite their relatively low efficiency, commercial designs are available for river current turbines that utilize drag. Figure 12.11 depicts Hydrovolt's 12 kW Savonius design canal turbine, which is 13 feet long and 6 feet high. Research continues to increase the efficiency of Sarvonius water turbines. Kailash et al. [6] report significant improvement in the coefficient of power in the laboratory through modification of the shape of the blade and especially through the use of a combination of deflector plates on the returning blade sides to obstruct water flow and on the advancing blade side to direct the water flow to the blade.

FIGURE 12.11 Horizontal axis Savonius design. (Hydrovolt C-12 Canal Turbine.)

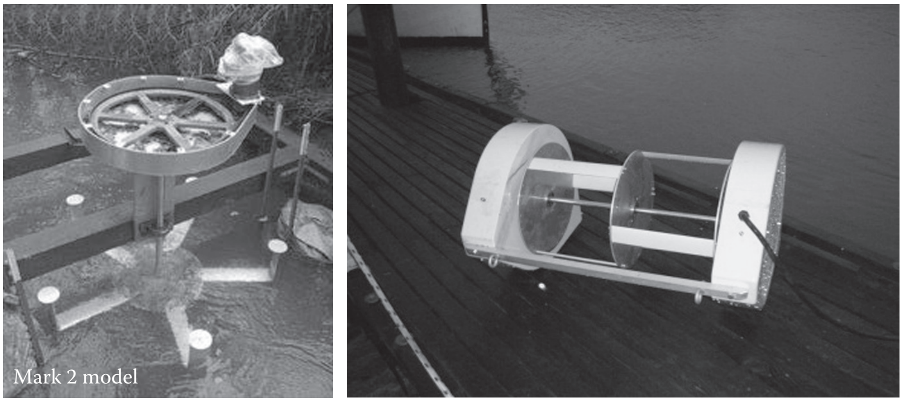

(a) (b)

FIGURE 12.12 Darrieus river current turbines (a) Alternative Hydro Solutions and (b) horizontal design from Hydrovolts.

FIGURE 12.13 Gorlov helical turbine. (From http://www.gcktechnology.com/.)

The maximum efficiency of both the axial water current turbines and the cross-axis turbines with hydrofoil blades is significantly higher than that of the drag devices with their maximum theoretical efficiency limited by the *Betz Limit* to 0.59.

Alternative Hydro Solutions manufactures the vertical axis Darrieus design pictured in Figure 12.12. The turbine is available in several diameters: 1.25 m, 1.5 m, 2.5 m, 3.0 m, and 6.0 m, each available in custom lengths. Hydrovolts offers a horizontal axis Darrieus design, including portable units of less than 1 kW.

The Gorlov helical turbine (GHT), which is a relatively new turbine design developed by Prof. Gorlov in the mid 1980s at Northeastern University, is a cross-axis turbine consisting of helical blades that run along an imaginary cylindrical surface of rotation like a screw thread (Figure 12.13).* The helical twist, which is designed to ensure that the water flow always interacts with the same area of blade surface, is designed to remove the vibrations and dynamic instabilities often associated with Darrieus blades. The helical airfoil blades enable the turbine to rotate at twice the velocity of the water flow. It is self-starting and starts producing power at approximately 0.60 m/s. The standard unit uses three blades and is 1 m in diameter by 2.5 m in length. Multiple units can be installed in parallel to produce more power.

* http://www.gcktechnology.com/GCK/pg2.html

REFERENCES

1. Natel Energy Product Brochure. http://www.natelenergy.com/wp-content/uploads/2015/06/Natel_Product_Brochure_May2015_web.pdf.
2. Rorres, C., The turn of the screw: Optimal design of an Archimedes screw. *Journal of Hydraulic Engineering*, Jan. 2000. https://www.cs.drexel.edu/~crorres/screw/screw.pdf.
3. Lashofer, A., Hawle, W., Kampel, I., Kaltenberger, F., and Pelikan, B., State of technology and design guidelines for the Archimedes screw turbine. *International Journal on Hydropower & Dams*, Hydro 2012—Proceedings, Oct. 2012.
4. Nelson, V., *Wind Energy Renewable Energy and the Environment*. CRC Press, Boca Raton, FL, 2013.
5. Fraenkel, P., Too much torque and not enough action. *International Water Power & Dam Construction*, Mar. 5, 2014. http://www.waterpowermagazine.com/opinion/opiniontoo-much-torque-and-not-enough-action-4190252/.
6. Kailash, G., Eldho, T., and Prabhu, S., Performance study of modified Savonius water turbine with two deflector plates. *International Journal of Rotating Machinery*, 2012, Article ID 679247.

13 Electrical Power

Hydropower was utilized until late in the 19th century as an alternative to steam engines to mechanically drive a range of industrial machinery used in mining and for milling timber, textile, and grain. Although Michael Faraday had invented the electric motor in the 1820s, it took another 70 years for alternating current generators and transformers to be available to allow large-scale generation, transmission, and distribution and industrial utilization of hydroelectricity. All large hydropower turbines and most small hydro systems used in modern times generate electricity. Electricity is versatile and can be transmitted over power lines to be used at locations away from the power plant to power residences, city centers, and industries.

13.1 FUNDAMENTALS OF ELECTRICITY AND MAGNETISM

Maxwell's four equations below summarize the theory of electromagnetism and underlie the generation of electricity, its transmission and distribution, and finally, its use in motors and other electrical devices.

$$\oint E \cdot dA = \frac{q}{\varepsilon_0} \tag{13.1}$$

The electric flux out of any closed surface is proportional to the total charge enclosed within the surface (Gauss's Law for electricity).

$$\oint B \cdot dA = 0 \tag{13.2}$$

The net magnetic flux out of any closed surface is zero (Gauss's law for magnetism).

$$\oint E \cdot ds = -\frac{d\Phi_B}{dt} \tag{13.3}$$

The line integral of the electric field around a closed loop is equal to the negative rate of change of the magnetic flux through the area enclosed by the loop (Faraday's law of induction).

$$\oint B \cdot ds = \mu_0 i + \frac{1}{c^2}\frac{\partial}{\partial t}\int E \cdot dA \tag{13.4}$$

In the case of a static electric field, the line integral of the magnetic field around a closed loop is proportional to the electric current flowing through the loop (Ampere's law).

E = electric field
B = magnetic field
q = electric charge
Φ = magnetic flux
i = electric current
ε_0 = permittivity
c = speed of light

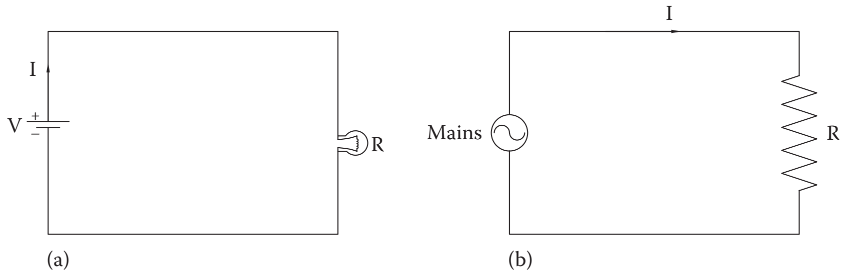

FIGURE 13.1 Electrical circuits. (a) Direct current and (b) alternating current.

In practical application for hydroelectricity, the laws that are useful are the more familiar forms of Faraday's law of induction when it comes to electrical generators, motors, and transformers.

This law states that "induced electromotive force (EMF) in any circuit is equal to the rate of change of the magnetic flux vector through it" and is often written as

$$e = -N\frac{d\Phi}{dt} \tag{13.5}$$

where e is the induced voltage or electromotive force measured in Volts "V" and N is the number of coils. The magnetic flux, Φ, is the magnetic field passing through the coil area normal to it. It is expressed mathematically as the dot product of the magnetic field vector, B, and the coil area **A**: $\Phi = \boldsymbol{B}\cdot\boldsymbol{A}$. The magnetic field, B, is measured in units of Tesla "T" or Wb/m^2.

The minus sign comes from the fact that for the conservation of energy to hold the direction of EMF, current, or flux has to be such that the magnetic field from the induced current must oppose the change in the flux that produced the EMF in the first place. This is also known as Lenz's law.

Electric current is the rate of flow of charge in a conductor. Its symbol is "I," and the unit is Amperes.

$$I = \frac{dQ}{dt} \tag{13.6}$$

Voltage is the potential difference or the electrical equivalent of "pressure," which pushes the current through an element of electrical circuit and is measured in Volts (V).

An important equation in electrical circuits is Ohm's Law, which states that the current through any element of the circuit is directly proportional to the voltage across that element.

$$I \propto V$$

The constant that converts this proportional relationship into an equation is the resistance that the element has to the flow of current and is written as "R" and has units of ohm or Ω.

Ohm's law is written as

$$I = \frac{V}{R} \text{ or } V = IR \tag{13.7}$$

The battery power sources depicted in the circuit above is a source of direct current (DC) whose voltage is of fixed magnitude and current flows in a single direction from the positive pole to the negative. The power from the mains is called alternating current (AC) with voltage and current values changes rapidly over time—changing many times in a second—along with their direction.

13.1.1 Electrical Power

The power consumed by an appliance or produced by a generator can be computed by multiplying the voltage at its terminals and the current flowing into or out of it.

$$P = V \cdot I \tag{13.8}$$

P is in units of Watts, V in volts, and I in amps.

There is a parallel here between the electrical power equation and the hydraulic power equation: The head H is comparable to the voltage, and the water flow Q is comparable to the current I.

In the case of electricity, the same power equation also applies to its utilization in an appliance—that is, the power consumed in the appliance can be computed by multiplying the voltage “V” applied to the appliance by the current “I” drawn by it (see Figure 13.1).

Combining with Ohm’s law, the power equation can also be written as

$$P = \frac{V^2}{R} \text{ and } P = I^2 \cdot R \tag{13.9}$$

which allows computation of the power dissipated in a resistor once the size of the resistance “R” is known, and either V or I is also known.

The voltage and current in direct current, DC, are fixed in time, and in that case, Equation 13.8 describes power that is constant in time as well.

13.1.2 Alternating Current

For ease of transmission over long distances, hydropower is mostly used to generate alternating current (AC) with both voltage and current varying with time in the form of a sinusoid.

$$I = I_p \sin(\omega t) \tag{13.10}$$

and

$$V = V_p \sin(\omega t + \varphi) \tag{13.11}$$

V_p and I_p represent the peak or highest values of the voltage and current waveform, ω is the angular frequency related to the frequency of the waveforms, and φ is the difference in phase angle between the voltage and current waveforms.

$$\omega = 2\pi f \tag{13.12}$$

and

$$f = \frac{1}{T} \tag{13.13}$$

with T being the period of a full cycle of the sinusoid.

The standard frequency used in AC systems is 60 Hz in North and South America and 50 Hz in Europe, Asia, and Africa; 60-Hz systems typically use 100–120 V as their operating distribution voltage, and 220–240 V is used on 50-Hz systems.

Both the voltage and current waveforms oscillate at the same frequency “f” with the phase angle φ showing any misalignment between the voltage and current waveforms as shown in Figure 13.2.

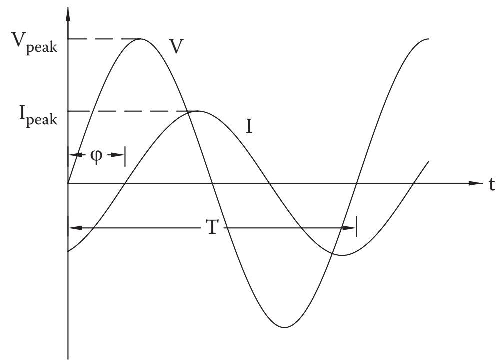

FIGURE 13.2 Sinusoidal variations of AC voltage and current.

13.1.2.1 Root Mean Square (RMS)

The sinusoidal nature of the voltage and current means AC power that is derived from their product also oscillates with time.

$$P(t) = I(t)^2 R \tag{13.14}$$

A sinusoidal cycle is completed within a period T of either 16.67 ms or 20 ms, depending on whether it is a 60-Hz or 50-Hz system. Although power is constantly oscillating, users experience its average rather than instantaneous impact because the time period of the full oscillation cycle is too short for the observer to notice the fluctuations. For example, electrical lights hold a constant brightness because people's eyes can't see rapid fluctuations at these frequencies.

The interest of users in most cases is limited to knowing the average power being used in a device rather than the instantaneous value of power consumption at any time. The average of this oscillating power function can be computed:

$$P_{avg} = \langle I(t)^2 R \rangle = R \cdot \langle I(t)^2 \rangle \tag{13.15}$$

with the symbol, $<I(t)^2>$, signifying the mean of the square of the current I(t), which is multiplied by the constant R.

The mean of an oscillating time function such as current is written mathematically as the root-mean-square where the RMS value of the current, I_{RMS}, is the constant current that would dissipate the same power in a resistor R.

$$P_{avg} = I_{RMS}^2 R \tag{13.16}$$

RMS is defined as the square root of the mean of the squares and can be used for any parameter that varies with time. It provides a particularly useful formulation for sinusoidal waves that vary over positive and negative values and where a simple average would result in a value of zero.

The RMS current can be computed from this definition by substituting I(t) from Equation 13.10:

For a periodic waveform I(t),

$$I_{RMS} = \sqrt{\frac{1}{T}\int_0^T I^2(t) \cdot dt} \tag{13.17}$$

For a sinusoidal waveform, $I = I_p \sin(\omega t)$:

$$I_{RMS} = \sqrt{\frac{1}{T}\int_0^T I_P^2 \sin^2(\omega t)\cdot dt}$$

$$I_{RMS} = \sqrt{\frac{I_P^2}{T}\cdot\left[\frac{t}{2} - \frac{1}{4\omega}\sin 2\omega t + C_1\right]_0^T}$$

$$I_{RMS} = \frac{I_P}{\sqrt{2}} \tag{13.18}$$

The factor $\sqrt{2}$ is known as the crest factor and would be different depending on the shape of the waveform.

The relationship between RMS and peak voltage can similarly be calculated as

$$V_{RMS} = \frac{V_P}{\sqrt{2}} \tag{13.19}$$

Commonly referred to main voltages of 120 V and 220 V are the RMS voltage and the corresponding peak voltages can be calculated using Equation 13.19.

Example 13.1

What are the peak-to-peak height and period of a voltage waveform signifying a 120 V, 60 Hz supply?

$$V_P = \sqrt{2}\cdot V_{RMS} = 1.414\cdot 120\text{ V} = 169.7\text{ V}$$

Peak-to-peak height of waveform = $2 \cdot V_P$ = 339.4 V

$$T = \frac{1}{f} = \frac{1}{60} = 16.67\text{ ms}$$

13.1.2.2 Power Factor

When used in the context of AC power, Equation 13.8 can be written as a function of time:

$$P(t) = V(t)\cdot I(t)$$

The average power over one oscillation cycle is

$$P_{avg} = \frac{1}{T}\int_0^T V(t)\cdot I(t)\,dt \tag{13.20}$$

Substituting, $I = I_p \sin(\omega t)$ and $V = V_p \sin(\omega t + \varphi)$ from Equations 13.10 and 13.11,

$$P_{avg} = \frac{1}{T}\int_0^T V_p \cdot I_p \sin(\omega t) \cdot \sin(\omega t + \varphi)\, dt \tag{13.21}$$

Expanding,

$$\sin \omega t \cdot \sin(\omega t + \varphi) = \sin \omega t (\sin \omega t \cdot \cos \varphi + \cos \omega t \cdot \sin \varphi) = \sin^2 \omega t \cdot \cos \varphi + \frac{1}{2} \sin 2\omega t \cdot \sin \varphi$$

$$P_{avg} = \frac{V_p \cdot I_p}{T} \int_0^T \left(\sin^2 \omega t \cdot \cos \varphi + \frac{1}{2} \sin 2\omega t \cdot \sin \varphi \right) dt$$

$$P_{avg} = \frac{V_p \cdot I_p}{T} \cdot \left\{ \cos \varphi \cdot \left[\frac{t}{2} - \frac{1}{4\omega} \sin 2\omega t + C_1 \right]_0^T - \sin \varphi \cdot \left[\frac{1}{4\omega} \cos 2\omega t + C_2 \right]_0^T \right\}$$

$$P_{avg} = \frac{V_p \cdot I_p}{T} . \frac{T}{2} . \cos \varphi = \frac{V_P}{\sqrt{2}} . \frac{I_P}{\sqrt{2}} . \cos \varphi = V_{RMS} \cdot I_{RMS} \cdot \cos \varphi$$

or

$$P_{avg} = VI \cos \varphi \tag{13.22}$$

with V and I representing RMS values of voltage and current and φ representing the phase angle between V and I. When $\varphi = 0$, the voltage and current are in phase and $P_{avg} = V.I.$ When $\varphi = 90°$, and the voltage and current are out of phase and $P_{avg} = 0$.

Equation 13.22 represents the general power equation for AC.

Cos φ is known as the power factor and signifies what fraction of the power is "real" in that it is based on the actual work done and has to be supplied as the power output of the hydro turbine and how much of the power is "phantom" in that it is used to maintain magnetic or electrical fields in appliances and other parts of the electrical system to make them function but does not dissipate any power. The phantom component of power, which is known as reactive power, is supplied by the generator sitting in the powerhouse, along with real power, but does not directly tax the turbine other than having to provide for losses associated with the additional current.

Reference is generally made to three different components of AC power:

Apparent power (S): the product of RMS values of the voltage and current with units of *volt amperes*: $S = V \cdot I$.

Real power (P): the apparent power corrected for the power factor: $P = VI \cos \varphi$ with units of *Watts*.

Reactive power (Q): the remaining component of apparent power: $Q = VI \sin \varphi$ with units of *volt Ampere reactive* or VAR.

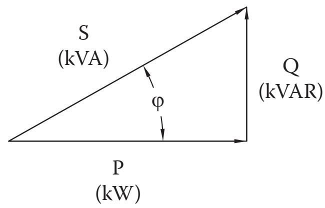

FIGURE 13.3 Power triangle.

A power triangle is used to present the three different components of AC power as phasors, which are vectors used to represent electrical quantities (Figure 13.3).

13.1.2.2.1 Impedance

In a simple AC circuit, in which an alternating voltage is applied across a device, the current flow depends on the applied voltage and its impedance, written as Z.

A general form of Ohm's law can then be written as

$$I = \frac{V}{Z} \tag{13.23}$$

Impedance, Z, is the effective resistance to an alternating current resulting from a combination of ohmic resistance, R, and reactance, X, and is written as a complex number:

$$Z = R + iX \tag{13.24}$$

Both the magnitude of the current and its phase vis-à-vis the voltage is determined by the impedance.

When the appliance is purely resistive, its impedance is equal to its resistance in ohms:

$$Z = R$$

$$I = \frac{V}{Z} = \frac{V}{R}$$

V and I have no phase difference between them. They are drawn in Figure 13.4a as phasors pointing in the same direction.

When the appliance load is purely inductive, impedance is equal to inductive reactance, X_L.

$$Z = X_L = 2\pi fL$$

where inductance, L, is expressed in units of *Henry*, and

$$I = \frac{V}{X_L} \tag{13.25}$$

Inductors slow the current and I lags V by 90° for purely inductive loads as shown in Figure 13.4b.

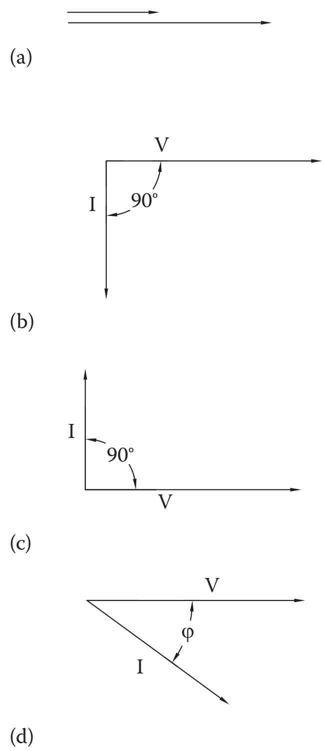

FIGURE 13.4 Phase differences between voltage and current. (a) V, I in phase—resistive load, (b) I lagging V by 90°—purely inductive load, (c) I leading V by 90°—purely capacitive load, and (d) I lagging V by φ—mixed load.

When the load is purely capacitive, impedance is equal to capacitive reactance, X_C.

$Z = X_C = \dfrac{1}{2\pi fC}$ where capacitance, C, is measured in *farads*.

$$I = \frac{V}{X_C} \tag{13.26}$$

Real-life loads are not usually capacitive, but a capacitor added to an AC circuit would cause the opposite effect of an inductor, and the current through it would lead voltage by 90° (Figure 13.4c). Capacitors are used to correct for excessive inductive load in an AC circuit.

When the total load is a mix of resistive, inductive, and capacitive components, its impedance takes on its full complex form:

$$Z = R + i(X_L - X_C) \tag{13.27}$$

with magnitude

$$|Z| = \sqrt{(X_L - X_C)^2 + R^2} \tag{13.28}$$

where the power factor,

$$\cos\varphi = \frac{R}{Z}. \tag{13.29}$$

The current I through the device lags V by this same phase, φ as shown in the phasor diagram in Figure 13.4d.

Each appliance contributes to the power factor, and it is the cumulative power factor resulting from all the connected appliances as well as from the transmission and distribution lines and transformers, which is seen by the generator in the powerhouse. The power factor is close to unity, 1.0, when the cumulative load seen by the hydropower generator is mostly resistive and decreases as the loads with higher reactive power requirements are connected. Synchronous generators are generally designed to supply loads with cumulative power factors as low as 0.8.

There are two main negative impacts on AC circuits from a low, or poor, power factor. First, a low power factor means a higher current draw to do the same amount of work because cos φ is in the denominator when Equation 13.22 is written as

$$I = \frac{P}{V\cos\varphi}.$$

The resulting high current increases the I^2R losses in all parts of the system—generator, transmission, and distribution lines; transformer; and switches—thus lowering the system efficiency.

Second, the generator needs to be able to provide the higher reactive power requirements of a system with low power factor. This puts a strain on the generator and makes it less efficient and in the extreme can cause it to burn out when the power factor is lower than specified by the manufacturer.

Poor power factor is created by excessive inductive loads, which require the supply of additional reactive current to maintain magnetic fields. The most common loads include induction motors, transformers, and fluorescent lamps. Underloaded induction motors are a widespread source of low power factor because the magnetic current drawn by the motor remains almost constant irrespective of the motor loading. Fortunately, in situations in which cos φ is significantly lower than 1.0, power factor can be corrected relatively inexpensively by adding capacitor banks to the system, with equivalent VAR, ideally at the points at which the inductive loads are connected.

From Figure 13.3, it can be seen that

$$P = S\cos\varphi \tag{13.30}$$

$$Q = S\sin\varphi \tag{13.31}$$

$$S^2 = P^2 + Q^2 \tag{13.32}$$

Example 13.2

A single phase 2 kW, 0.8 PF–rated synchronous generator is being evaluated to power lighting load in a village of 70 homes, each of which is to receive 2 CFL lamps rated at 13 W, 0.7 PF. Operating voltage and frequency are 220 V and 50 Hz.

a. Calculate the apparent, real, and reactive power loads that would be placed on the generator by the proposed cumulative lighting load.
b. Calculate the maximum number of lamps that the generator can safely supply.
c. Suggest ways to match the generator specifications to meet the requirements of the load.

a. Total real load: $P = 140 \cdot 13\text{W} = 1820$ Watts
   Apparent load:

$$S = \frac{P}{PF} = \frac{1820}{0.7} = 2600\ \text{VA}$$

Reactive power:

$$Q = \sqrt{S^2 - P^2} = \sqrt{2600^2 - 1820^2} = \sqrt{3,447,600} = 1857 \text{ VAR}$$

It can be checked to see if the apparent and reactive power requirements of the load can be met by the generator.

Maximum apparent power that the generator can generate:

$$S = \frac{P}{PF} = \frac{2000}{0.8} = 2500 \text{ VA}$$

Maximum reactive power that the generator can supply:

$$Q = \sqrt{S^2 - P^2} = \sqrt{2500^2 - 2000^2} = \sqrt{2,250,000} = 1500 \text{ VAR}$$

It is clear that connecting the proposed load will overload the generator. The overloading will happen in two ways. First, the extra 100 VA (2600 VA – 2500 VA) loading will require the main armature coil to carry a higher current than it is rated for. Second, the additional 357 VAR (1857 VAR – 1500 VAR) requirement beyond the generator's rating will mean that the generator's field coil will be seriously overloaded and run the risk of burning out.

b. Each lamp has a VAR requirement

$$Q = \sqrt{S^2 - P^2} = \sqrt{\left(\frac{P}{PF}\right)^2 - P^2} = \sqrt{\left(\frac{13}{0.7}\right)^2 - 13^2} = \sqrt{344.9 - 169} = 13.3 \text{ VAR}$$

Taking into account that the larger source of overloading is in the field coil, because of the poor power factor of the CFL load, one can calculate the maximum number of CFLs possible to be supplied by the generator:

$$\text{Maximum number of CFLs} = \frac{1500 \text{ VAR}}{13.3 \text{ VAR}} = 113$$

The generator can power a total of 113 CFL lamps rated 13 W with a power factor of 0.7.

c. One way to meet the load requirement is to use a larger sized generator.

$$\text{Total VARs required for 140 CFLs} = 13.3 \text{ VAR} \cdot 140 = 1862 \text{ VAR}$$

The size of the generator rated at 0.8 PF required to supply the VARs needed to power this load:

$$S = \frac{Q}{\sin\varphi} = \frac{1862}{\sqrt{1 - 0.8^2}} = 3103 \text{ VA}$$

A less expensive way to meet the requirements of a poor power factor load is to correct the power factor of the load with capacitors with results as shown in Figure 13.5.

Assuming a corrected power factor of 0.95, from Equation 13.22,

$$S = \frac{\text{Watts}}{\text{New power factor}} = \frac{1820 \text{ W}}{0.95} = 1916 \text{ VA}$$

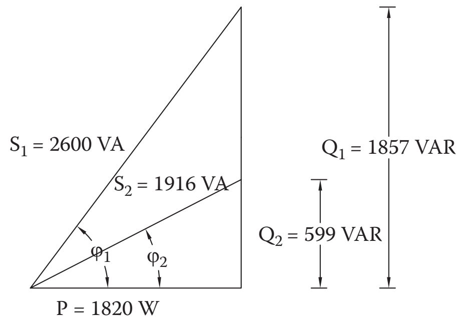

$$PF_1 = \cos\varphi_1 = \frac{1820\ \text{W}}{2600\ \text{VA}} = 0.7$$

$$PF_2 = \cos\varphi_2 = \frac{1820\ \text{W}}{1916\ \text{VA}} = 0.95$$

FIGURE 13.5 Power factor correction.

It can thus be seen that a 2500 VA–rated generator can supply the required 140 CFLs, which will only be drawing 1916 VA of apparent power from the generator.

New, reduced VAR load on the generator is now

$$Q = \sqrt{S^2 - P^2} = \sqrt{1916^2 - 1820^2} = 599\ \text{VAR}$$

The difference between the old and new VAR requirements of the load:

$$1862\ \text{VAR} - 599\ \text{VAR} = 1263\ \text{VAR}$$

These VARs would need to be supplied by a capacitor bank that is specified for power factor correction.

From Equation 13.8 (electrical power equation), the size of capacitors required to provide this correction can be calculated.

$$Q = \frac{V^2}{X_C} = \frac{V^2}{\dfrac{1}{2\pi f C}} = 220^2 \cdot 100 \cdot \pi \cdot C$$

$$C = \frac{Q}{220^2 \cdot 100 \cdot \pi} = \frac{1263\ \text{VAR}}{220^2 \cdot 100 \cdot \pi} = 83 \cdot 10^{-6}\text{Farad}$$

The size of the capacitor required to reduce the PF to 0.95 is 83 microfarads.

The general relationship between reactive power to be mitigated and the power correction capacitance required can be stated as

$$C = \frac{Q}{V^2 \cdot 2 \cdot f \cdot \pi} \tag{13.33}$$

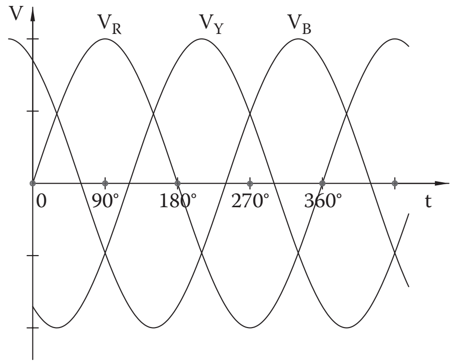

FIGURE 13.6 Three phase voltage waveforms.

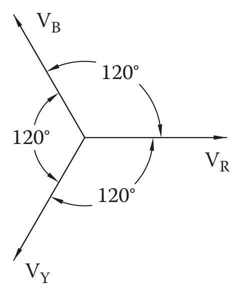

FIGURE 13.7 Phasors representing three phases.

13.1.3 Three Phase AC

To achieve higher efficiency in the use of materials in transmission cables, generators, motors, and other appliances, AC power is normally generated and distributed in three phases. Three-phase AC is equivalent to three single-phase systems that share the same generator, transmission, distribution poles, transformers, and appliances. Each phase is carried on a separate conductor with the voltage and current in each of the phases being offset in time from each other by one third of the oscillation period.

As Figure 13.6 shows, the frequency of all three phases of the voltage or current is the same, but each sinusoidal waveform is offset by a third of the cycle, or 120°, from the next one.

The three phases can be represented by phasors as in Figure 13.7.

13.1.3.1 Three-Phase Circuits

Three-phase loads can be connected in two different configurations (Figure 13.8):

a. Star, which is equivalent to three single-phase connections with three line connections and one neutral
b. Delta with three line connections but no neutral

With star-connected loads, in a three-phase, four-wire system, there are three lines carrying line currents and one neutral carrying the return currents for all three phases. Delta-connected loads have no neutral but have three wires carrying the three line currents. The voltage between any two lines is called the line voltage whereas the voltage between any line and neutral is known as a phase voltage.

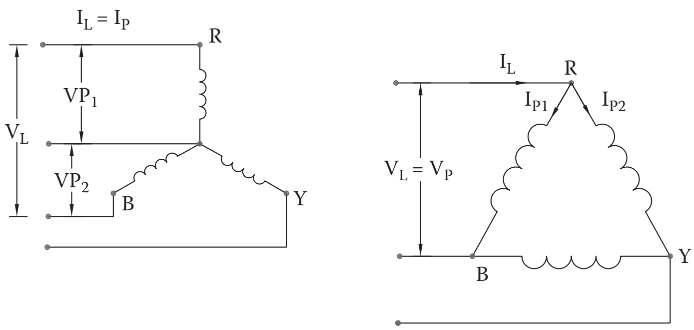

FIGURE 13.8 Star- and delta-connected motor loads.

It is clear for a star-connected load as shown in the diagram above that the phase current and line current are the same:

$$I_L = I_P$$

$$I_N = I_{L1} + I_{L2} + I_{L3}$$

As Figure 13.9 shows, if the three line currents are perfectly balanced in a star connection, the neutral current becomes zero.

The line voltage on the other hand needs to be computed as the difference between adjacent phase voltages.

$$\mathbf{V_L = V_{P1} - V_{P2}}$$

Because the phase voltages have different phases, they need to be added or subtracted as phasors rather than simply as algebraic quantities.

The magnitude of the line voltage can be computed using the law of cosines.

From Figure 13.10, because V_{P1} and V_{P2} are both equal to V_P in magnitude:

$$V_L = \sqrt{V_P^2 + V_P^2 - 2V_P^2 \cos 120°} = \sqrt{2V_P^2 - 2V_P^2 \cdot (-0.5)} = \sqrt{3V_P^2} = \sqrt{3}V_P \quad (13.34)$$

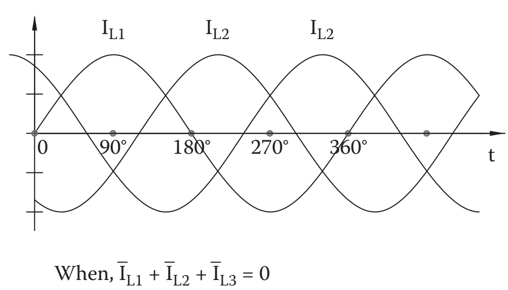

FIGURE 13.9 Balanced currents.

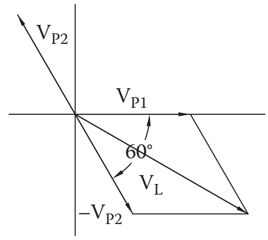

FIGURE 13.10 Phasor subtraction.

TABLE 13.1
Line and Phase Voltages for Star and Delta Connections

	Voltage	Current	Power
Star connection	$V_L = \sqrt{3}V_P$	$I_L = I_P$	$\sqrt{3}V_L \cdot I_L \cos\varphi$
Delta connection	$V_L = V_P$	$I_L = \sqrt{3}I_P$	$\sqrt{3}V_L \cdot I_L \cos\varphi$

With delta-connected loads, the phase voltage and line voltage are the same. However, the line current is the difference between adjacent phase currents:

$$\mathbf{I_L} = \mathbf{I_{P1}} - \mathbf{I_{P2}},$$

and its magnitude can be computed using the law of cosines as

$$I_L = \sqrt{I_P^2 + I_P^2 - 2I_P^2 \cos 120°} = \sqrt{3I_P^2} = \sqrt{3}I_P \tag{13.35}$$

The relationships between line and phase voltages and currents in the star and delta configurations are summarized in Table 13.1.

Example 13.3

For a star-connected motor, the line voltage between phases R and Y is measured at 460 V and the line current into phase R measures 35 A. Assuming the loads are balanced,

a. Calculate the apparent power being drawn by the motor
b. Calculate the expected phase voltage measured between phase R and neutral
c. Calculate the apparent power being drawn by phase R
d. Demonstrate that the power drawn by the motor is equal to the sum of the power consumed in each phase

a. *Apparent power:*

$$S = \sqrt{3}V_L \cdot I_L = 27{,}886 \text{ VA}$$

$$V_P = \frac{V_L}{\sqrt{3}} = \frac{460}{\sqrt{3}} = 265.6 \text{ V}$$

$$S_R = V_R \cdot I_R = 265.6 \cdot 35 = 9295 \text{ VA}$$

b. If the phases are balanced, it follows that $S = 3 \cdot S_R = 27{,}886$ VA

Example 13.4

A 10 hp, a four-pole, three-phase motor connected to 415 V, 50 Hz has a rated full load current of 14 Amps and power factor of 0.85.

a. What would be the apparent, real and reactive power supplied at full load?
b. What would the expected efficiency of the motor be at full load?

$$\text{Apparent power:}\quad S = \sqrt{3}\cdot V\cdot I = 1.732\cdot 415\,V\cdot 14\,A = 10.063\,kVA$$

$$\text{Real power: } P = S\cdot pf = 10.063\,kVA\cdot 0.85 = 8.554\,kW$$

$$\text{Reactive power:}\quad Q = \sqrt{S^2 - P^2} = \sqrt{10.063^2 - 8.554^2} = \sqrt{101.264 - 73.171} = 5.30\,kVAR$$

$$\text{Rated power output} = 10\text{ hp} = 0.746\cdot 10\text{ hp} = 7.46\text{ kW}$$

$$\text{Efficiency: } \eta = \frac{\text{Rated output power}}{\text{Input power}} = \frac{7.46\,kW}{8.554\,kW} = 87.2\%$$

13.2 GENERATORS

Hydropower turbines drive generators to generate electric current. Although the majority of large hydropower systems generate alternating current (AC), smaller systems used to charge batteries generate direct current (DC).

13.2.1 Generator Theory

The magnetic flux through a coil can be changed in two ways to generate the electromotive force, or EMF, as per Faraday's law: the first by holding the flux stationary and moving the coil through it. It can also be done by holding the coil stationary and changing the magnetic flux through it. The flux itself can be generated with a permanent magnet or with an electromagnet using a winding. The part of a generator with windings generating the magnetic flux are known as the "field" and the coil that generates EMF from the changing flux is known as the "armature." Generators can either have a stationary field and a rotating armature or a rotating field and a stationary armature. The rotating part of the generator is generally known as the rotor, and the stationary part is known as the stator.

Figures 13.11a through d demonstrate options for generating EMF:

a. Stationary field generated by a permanent magnet and rotating armature
b. Stationary wound field and rotating armature
c. Stationary armature and rotating field generated by a permanent magnet
d. Stationary armature and rotating wound field

Taking the first simple generator in Figure 13.11a, as the coil rotates at a constant angular velocity in a uniform magnetic field, the flux through the coil will vary sinusoidally.

$$\Phi = \Phi_{max}\sin(\omega t)$$

where Φ_{max} is the maximum flux through the coil, and ωt is the angle that the plane of the coil makes with respect to the flux lines. The maximum flux goes through when the coil is perpendicular to the flux and $\omega t = 90°$, and the flux through it is zero when the coil is parallel to the field and $\omega t = 0°$.

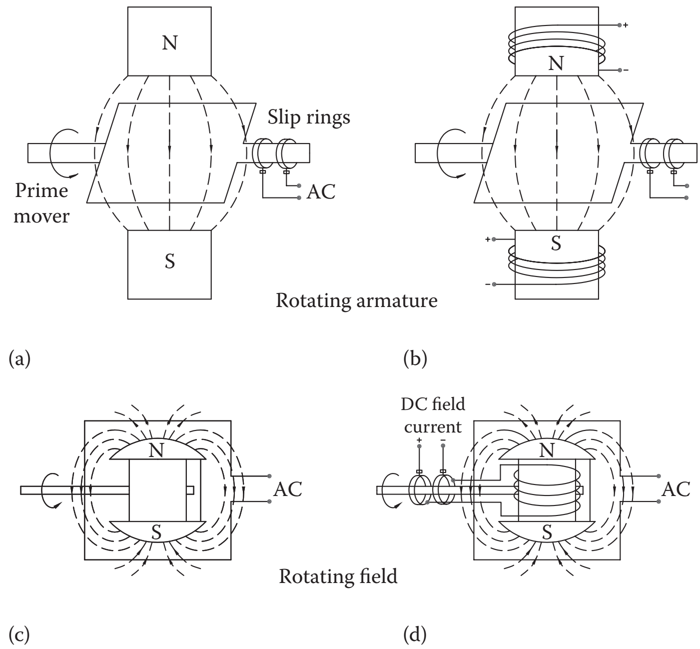

FIGURE 13.11 Options for generating EMF. (a) Stationary field generated by a permanent magnet and rotating armature, (b) stationary wound field and rotating armature, (c) stationary armature and rotating field generated by a permanent magnet, and (d) stationary armature and rotating wound field.

Φ can be differentiated to find the rate of change of flux through the coil as it rotates:

$$\frac{d\Phi}{dt} = \omega\Phi_{max}\cos(\omega t)$$

Substituting into Equation 13.5, gives

$$e = N\frac{d\Phi}{dt} = N\omega\Phi_{max}\cos(\omega t) = E_{max}\cos(\omega t) \quad (13.36)$$

where

$$E_{max} = N\omega\Phi_{max} \quad (13.37)$$

As discussed in Section 13.1.1, it is often more useful to know the RMS voltage rather than the maximum waveform voltage.

Substituting Equation 13.19 gives

$$E_{RMS} = \frac{1}{\sqrt{2}}N\omega\Phi_{max} = \frac{2\pi fN\Phi_{max}}{\sqrt{2}} = 4.44fN\Phi_{max} \quad (13.38)$$

where f = frequency of rotation, and N = number of coils.

Example 13.5

A simple generator using a 10-turn rotor coil is seen to be generating 100 V peak output and a frequency of 10 Hz. Write down its voltage waveform and calculate the maximum pole flux.

a. From the information given,

$$\omega = 2\pi f = 2\pi.10 = 62.8 \text{ radians per sec}$$

The output voltage waveform can be written as e = 100 sin (62.8t)

b. From Equation 13.29, $E_{max} = N\omega\Phi_{max}$

Therefore,

$$\Phi_{max} = \frac{E_{max}}{N\omega} = \frac{100}{10 \cdot 62.8} = 0.159 \text{ Wb}$$

The same answer is arrived at using Equation 13.30 to calculate Φ_{max}:

$$E_{RMS} = \frac{E_{max}}{\sqrt{2}} = \frac{100}{\sqrt{2}} = 4.44 f N \Phi_{max}$$

$$\Phi_{max} = \frac{100}{\sqrt{2} \cdot 4.44 \cdot 10 \cdot 10} = 0.159 \text{ Wb}$$

13.2.2 Direct Current Generators

Similar to a battery, a DC generator has a fixed positive pole and a negative pole. Some DC generators are able to maintain fixed polarity through the use of a commutator. Figure 13.12 demonstrates the use of the commutator for a simple two-pole DC generator with one armature coil. Although the current in the armature coil changes direction, through the use of the commutator, both of the two brushes always maintain their polarity. The commutator is thus able to carry out the function of a mechanical rectifier.

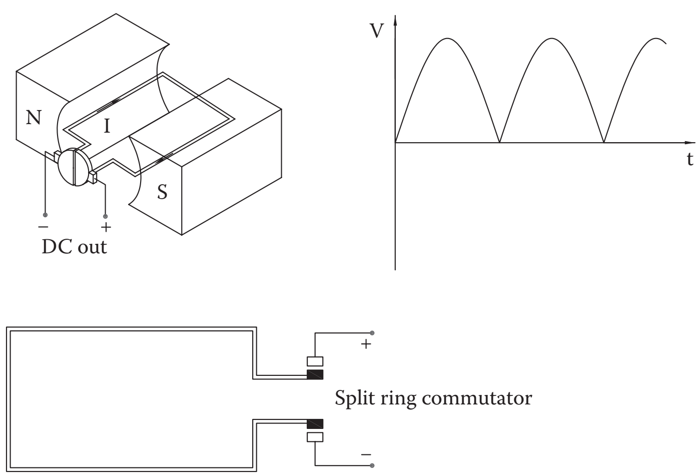

FIGURE 13.12 DC generation using a commutator.

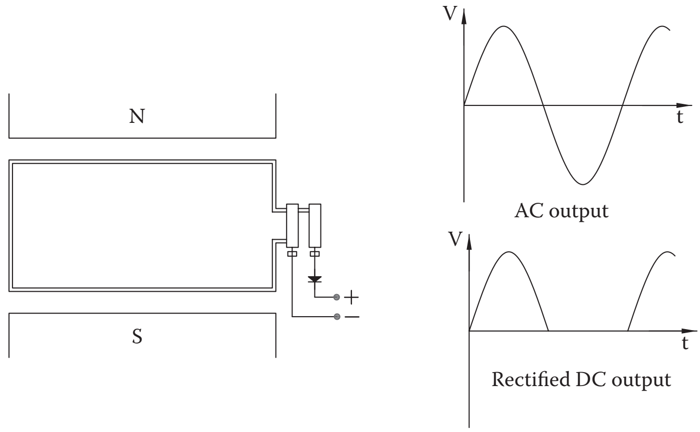

FIGURE 13.13 AC generation with rectified DC output.

Figure 13.13 demonstrates how without the commutator the two terminals would change their polarity as the armature turns, alternating the direction of the current. Most DC generators are really AC generators, which then use semiconductor-based rectifiers to convert the output to DC.

Battery charging is the main application of small DC generators. A voltage regulator is used to limit the current feeding into the batteries after they have reached full charge. The voltage regulator in an automobile provides regulation by controlling the field current available to the spinning rotor inside the alternator. To keep the automobile's lead acid battery charged, the regulator will apply voltage to the field coil and send current through it when the battery terminal voltage drops below 13.5 Volts. To keep the battery from overcharging, the regulator will stop applying voltage to the field when the voltage exceeds 14.5 Volts.

13.2.3 Alternating Current Generators

Alternating current generators generate sinusoidal waveforms as discussed in Section 13.1.1, with the polarity of the terminals changing every half cycle. AC generators are available in single phase or three phase, and the two main categories of generators used in hydropower systems are synchronous and asynchronous.

13.2.3.1 Synchronous Generators

The RPM is directly proportional to the frequency of the output voltage and current in the case of synchronous generators.

RPM = f · 60 sec/min in the case of the simple generator with one pair of magnetic poles as shown in Figure 13.13 because each rotation generates one cycle of the waveform.

The same output frequency can be achieved at lower RPM by increasing the number of magnetic poles. For example, if a second pair of poles were added, in each revolution of the rotor from Figure 13.13, it would generate two voltage cycles rather than one per rotation, and the RPM required to generate a particular frequency would be half. This can be written in an equation as follows:

$$\text{Speed (in RPM)} = \frac{f \cdot 60}{\text{Number of pairs of poles}} = \frac{f \cdot 120}{\text{Poles}} \tag{13.39}$$

Example 13.6

Calculate the speed of a six-pole generator required to generate at 60 Hz.

$$\text{Speed} = \frac{60 \cdot 120}{6} = 1200 \text{ RPM}$$

Increasing the number of poles to 20, for example, would reduce the required RPM to 360 to generate the required 60 Hz. Generators with a large number of poles are used with lower head Kaplan and propeller turbines so that they can directly drive the generator without gearing. Higher head Peltons, on the other hand, typically drive generators with four or six poles.

13.2.3.1.1 Relationship between Output Voltage and Generator RPM

Equations 13.37 and 13.38 show that the voltage output of a generator is directly proportional to both the frequency and the magnetic flux. If the magnetic flux were constant, the output voltage would be directly proportional to the frequency or RPM. So if a four-pole generator was rated to produce 220 V at 50 Hz and 1500 RPM, one would expect that if the RPM of the hydropower turbine went up by 20% to 1800 RPM and the frequency went up correspondingly to 60 Hz, the generator voltage would increase to the dangerous level of 220 V · 1.2 = 264 V. Figure 13.14 shows the relationship between output voltage and generator RPM under no load conditions. To avoid the risk to appliances of being exposed to overvoltage, modern generators use an electronic automatic voltage regulator (AVR) to keep the voltage fixed over a range of RPM by changing the field current and hence the strength of the magnetic field. AVRs are discussed in more detail later in this chapter.

13.2.3.1.2 Single-Phase and Three-Phase Generators

AC generators come in single-phase and three-phase varieties. The three-phase generator is the equivalent of three single-phase generators placed inside the same generator frame but with the output voltages of each phase shifted 120° from each other as depicted in Figure 13.6. Three-phase generators are more efficient in material use because the same frame can generate three times as much power. Synchronous generators are available in three phases starting above a rating of 5 kVA and single-phase generators are generally available up to 25 kVA. Single-phase generators have the advantage of simpler switch gear, controllers, and distribution lines and are used when the loads are close to the generator and are all single phase.

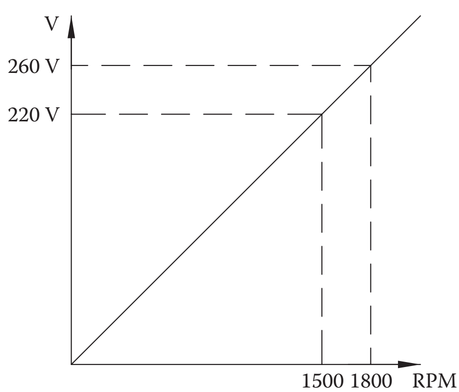

FIGURE 13.14 Generator voltage versus frequency.

13.2.3.1.3 Generator Excitation

As Figure 13.11 shows, the required field flux of the generator can be supplied either by permanent magnets or by windings. The expense and difficulty of acquiring large enough permanent magnets means that most large generators use wound fields.

The magnetic flux, Φ, produced by windings is directly proportional to the number of windings, N, and current, I. The larger the current I, the stronger the flux will be.

$$\Phi = \frac{N \cdot I}{\mathcal{R}} \tag{13.40}$$

The flux is inversely proportional to the reluctance, $\mathcal{R}$, of the magnetic circuit, which provides a measure of opposition that the magnetic circuit offers to the flux. The reluctance is the magnetic equivalent of resistance in an electrical circuit and a function of the magnetic core material as well as the geometry of the field coil.

The current to the field can be provided from an external battery, and a simple arrangement to do this would be to have the battery connected to the field coil through a variable resistor, which would be used to manually control the current to the field.

Most synchronous generators are designed to be "self-exciting" and avoid the need for an external source of current for the field. Self-excitation is achieved by taking a portion of the output AC current, rectifying it, and making that available as field current via a voltage regulator circuit. This regulated DC current flows into the field coil to generate a magnetic field to produce the required AC output voltage when the generator turns at the design RPM. The initial magnetic field required for the device to start up is produced by residual magnetism remaining in the electromagnet's core from the last time the generator was generating. At start up, the small current that is initially generated gets fed back to the field, making the field stronger and allowing a larger current to be generated. This excitation build-up process eventually stabilizes with the voltage regulator sending a controlled current to the field to produce the right voltage at the right RPM.

The residual magnetism of the generator's core may be lost or weakened either by the influence of external magnetic fields from any source or by sitting idle for a long time. If the electromagnet's core loses its residual magnetism, the rotor will spin without producing any output voltage. In such a case, a DC voltage source with the correct polarity can be applied to the field for a short instance, generally after disconnecting the field from the AVR, to get the generator to excite and produce voltage. This so-called "field flashing" reestablishes the residual magnetism to allow the generator to self-excite.

Some older generators had a battery available at start-up so as not to have to rely on the residual magnetism to start the excitation process. In large, modern generators, a small permanent magnet generator (PMG) inside the larger generator is used to provide the large field current that is required.

Two excitation arrangements typically found in synchronous generators are shown in the following figures. Figure 13.15a depicts a self-excited synchronous generator, which draws current for the field winding from the generator output via the AVR. This is typical for generators smaller than 25 kVA. Figure 13.15b shows a three-stage brushless synchronous generator in which a first-stage exciter PMG supplies the field current to a second-stage exciter field via the AVR. The exciter alternator supplies field current to the third stage main field winding. The main armature generates the output power.

By altering the field current, the AVR can produce a relatively constant output voltage over a range of generator RPM and external load conditions. It is the job of the automatic voltage regulator (AVR) to achieve constant voltage output within an acceptable window over the full range of generator loading and even allowing for some variation in frequency. It does so by

a. Increasing field current as the load current increases to keep the voltage constant
b. Increasing field current as the power factor of the load goes down
c. Reducing field current as the frequency increases above design speed
d. Providing under frequency roll-off below a certain frequency

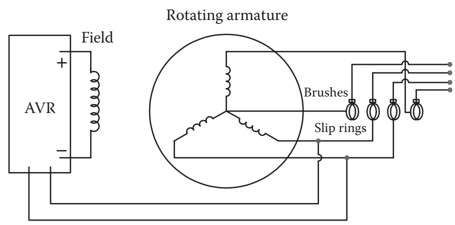

(a)

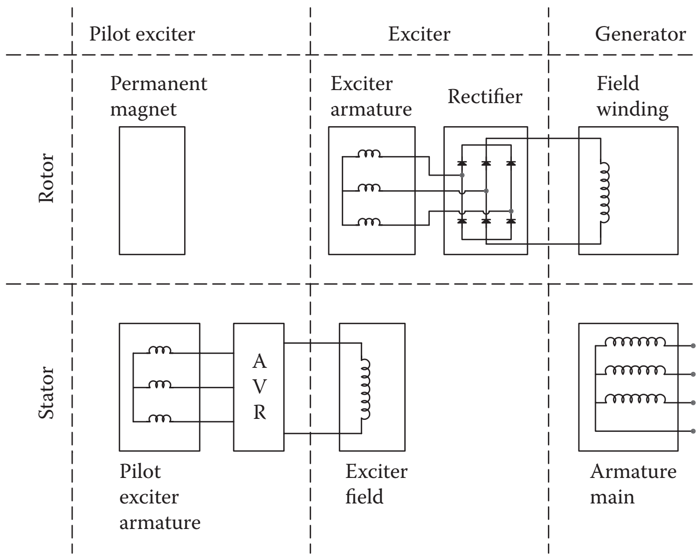

(b)

FIGURE 13.15 Excitation arrangements for synchronous generators. (a) Small generator with brushes and (b) brushless self-excited synchronous generator.

Under frequency roll-off refers to the output voltage needing to come down when the frequency falls below a certain threshold for safety to appliances.

Some older designs of generators use a wound AVR (Figure 13.16), which is able to achieve reasonable regulation of 5% from no load to full load through the use of compounding transformers and without the use of electronics. The compounding transformer sees an increase in flux when the armature current increases and thus pushes proportionately more current to the field coils if either the power factor is low or if the load is high and especially when both are occurring simultaneously. The wound AVR is able to achieve frequency roll-off below design frequencies because the lower generator output voltage reduces the flux in the compounding transformers and thus keeps the field current low. However, the major weakness of the wound AVR is that it is unable to reduce the field current when the voltage and frequency increase above design speed. At runaway generator speed, such a generator would thus generate dangerously high output voltage. For the safety of appliances connected to them, generators with wound AVRs need to be controlled with an overvoltage trip. The trip senses when the output voltage reaches a set threshold and interrupts the field current coming out of the compounding transformers through the use of a relay.

The electronic AVR makes it possible to clamp the output voltage even as the generator overspeeds. By sensing the output voltage and changing the field current, electronic AVRs are able to keep the output voltage constant over a large range of frequencies and to regulate output voltage much more tightly. Although this works very well for high frequencies, this ability to hold the output

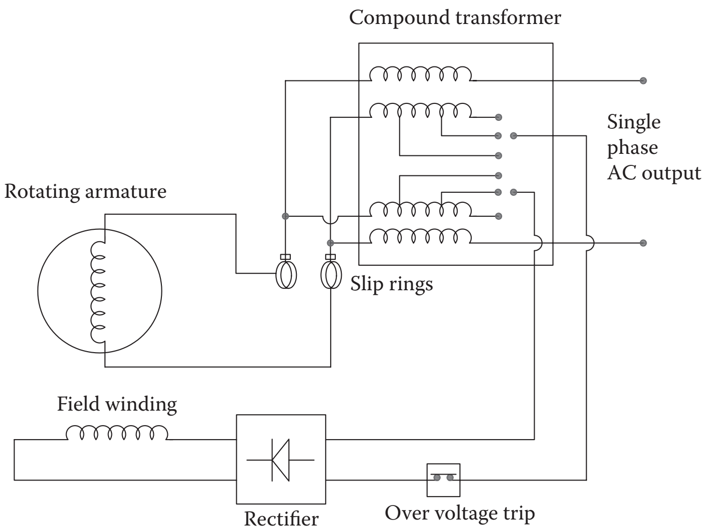

FIGURE 13.16 Wound AVR.

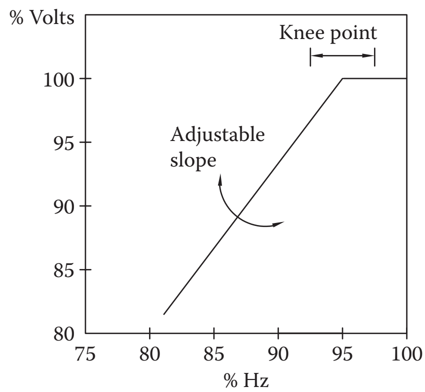

FIGURE 13.17 AVR control and under frequency roll-off.

voltage constant can be dangerous at under frequencies for both the generator and the appliances powered by the generator.

Electronic AVRs build in an under frequency roll-off (UFRO) to allow the voltage to drop at under frequencies. As shown in Figure 13.17, AVRs typically have adjustments to change the slope of the roll-off and the knee point to set the frequency below which the voltage begins to fall.

13.2.3.1.4 Sizing and Derating of Synchronous Generators

In addition to the maximum power output of the hydropower turbine, proper sizing of the synchronous generator must take into account ambient temperature and altitude at the powerhouse. Generators need to be derated if they are to be operated at high altitudes or at high ambient temperatures. Additional derating may be needed if the power factor of the load is expected to be low or for certain types of electronic load controllers that affect the power factor as described.

Air-cooled generators rely on a fan mounted on the rotor to blow ambient air across the length of the gap between the rotor and stator to keep the coils within the allowed temperature range. The lower the temperature of the ambient air, the more effective the cooling. Effective cooling also requires a minimum density of the ambient air. At higher altitudes, where the air is less dense,

TABLE 13.2
Typical Derating Factors for Hydropower Generators

Maximum Ambient Temperature (°C)	20	25	30	35	40	45	50	55
Temperature derating (D_T)	1.10	1.08	1.06	1.03	1.00	0.96	0.92	0.88
Altitude (m)	1000	1500	2000	2500	3000	3500	4000	4500
Altitude derating (D_A)	1.00	0.96	0.93	0.90	0.86	0.83	0.80	0.77
ELC derating (D_E)	0.83							

cooling is less effective. Generator manufacturers typically specify their machines to work at full capacity at 40°C and at an altitude of 1000 m.* Generators can be operated outside these limits but must be derated to take into account the lower effectiveness of the air cooling. Conversely, generators can be rated for higher capacity when used in lower altitudes or cooler climates.

Oversizing of generators is required for use with electronic load controllers, which use a thyristor to direct excess power to a ballast load (see Section 13.3.1.1). The action of the thyristor to direct current flow to the ballast with a phase delay angle forces the current from the generator to effectively lag behind the voltage and thus effectively imposes a low power factor [3]. The lowered power factor combined with anticipated reactive power demands from the connected main load means that the overall power factor seen by the generator may be well below its rating of pf = 0.8. It is generally recommended that the generator should be oversized by 20% if such an electronic load controller is to be used with the generator. This translates to a generator derating factor of 0.83 whenever a phase angle control ELC is used.

Table 13.2 shows typical derating factors for hydropower generators.

The kVA rating of the generator to be used in a particular location can be computed as

$$\text{kVA rating} = \frac{\text{kW}}{\text{PF} \cdot D_T \cdot D_A \cdot D_E} \tag{13.41}$$

Example 13.7

What size of synchronous generator should be specified for use under the following conditions?

Maximum load: 32 kW
Lowest expected power factor of the load: 0.8
Maximum ambient temperature: 40°C
Altitude of operation: 3000 m

Load controlled by an ELC

$$\text{Generator size} = \frac{32\,\text{kW}}{0.8 \cdot 1.0 \cdot 0.86 \cdot 0.83} = 56\ \text{kVA}$$

An additional factor of safety might be needed resulting in the selection of an even larger generator if there is the possibility of the turbine output exceeding the maximum load requirement or if the generator might be required to power large motor loads (single motor > 10% of the generator size).

* https://www.cumminsgeneratortechnologies.com/www/en/download/ratingsbook/RatingsBook.pdf

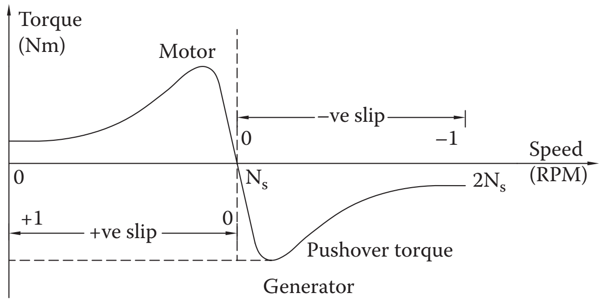

FIGURE 13.18 Torque–speed curve of induction machine.

13.2.3.2 Induction Generators

Induction generators are used for smaller isolated hydropower systems because they are mass-produced, inexpensive, and widely available as squirrel cage induction motors. Larger induction generators can be used for grid-connected hydropower systems.

The equation relating the speed (RPM) of the generator to the number of poles includes the slip, "s" in the case of induction generators.

$$N = \frac{120 \cdot f}{p}(1 - s) \tag{13.42}$$

The slip is positive for an induction motor and negative for an induction generator. This means that an induction motor operates at lower than the synchronous speed with the speed decreasing with loading. An induction generator, on the other hand, rotates faster than the synchronous speed with power output increasing with speed as shown in Figure 13.18.

Slip is defined as the ratio of the slip speed, which is the difference between synchronous speed and the rotor speed, to the synchronous speed:

$$s = \frac{N_s - N}{N_s} \tag{13.43}$$

N_s is the synchronous speed of the rotating field, and N is the speed of the rotor of the induction machine. The slip for an induction motor is very small, less than 0.01, without any load connected and increases with load.

The maximum slip, at full load, ranges in value from less than 0.05 for large machines to up to 0.10 for the smallest induction machines.

Example 13.8

Find the maximum slip of a four-pole, 60 Hz, 50 kVA induction motor which is rated at 1728 RPM. What would be its speed rating as a generator?

As an induction motor

$$N_s = \frac{120 \cdot 60}{4} = 1800$$

$$s = \frac{N_s - N}{N_s} = \frac{1800 - 1728}{1800} = \frac{72}{1800} = 0.04$$

FIGURE 13.19 Induction motor rotor.

As an induction generator

$$N = \frac{120 \cdot 60}{4}(1 - (-4\%)) = 1872 \text{ RPM}$$

The induction generator can be expected to rotate at anywhere from 1800 RPM, with zero power output, to 1872 RPM at maximum power output.

Induction generators have a rotating field, but in place of multiple coils found in synchronous generators, the rotor typically consists of copper or aluminum bars connected by end rings made of the same conductor (see Figure 13.19). Moreover, there is no electrical connection required to the rotor because the transfer of energy from the rotor is by means of electromagnetic induction. Bars in place of coils and the absence of brushes makes induction machines very robust.

13.2.3.2.1 Application of Grid-Connected IG

When the induction machine is connected to the grid as shown in Figure 13.20, closing the circuit breaker without opening the turbine nozzle will result in it operating as a motor driving the turbine runner at slightly less than the synchronous speed. When the turbine nozzle is gradually opened and the jet is directed at the runner, the speed of the motor increases to reach synchronous speed and the slip, s, becomes zero. As the nozzle is opened more and additional power is directed at the runner, the rotor speed exceeds the synchronous speed and the slip becomes negative. There is now active power being transferred across the air gap from the rotor to the stator and into the power bus.

In practice, the procedure to start up the induction generator is to accelerate it slightly above the synchronous speed by opening the nozzle of the hydropower turbine and then to close the circuit

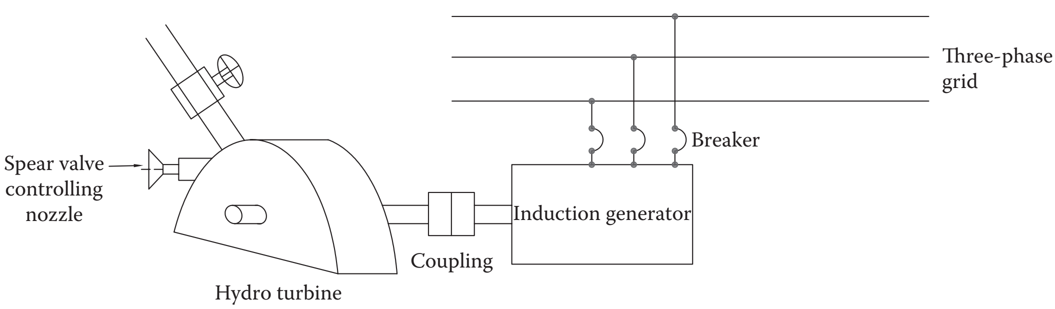

FIGURE 13.20 Grid-connected induction generator.

breaker. Until the breaker is closed, the rotor rotates with no resistance in the absence of a magnetic field. The moment the generator is connected to it, the grid supplies magnetizing current to the stator, which, in turn, creates a rotating field. The interaction of the magnetic flux from the stator and the induced flux from the rotor produces a counter torque to oppose the driving torque of the prime mover [4]. As the turbine nozzle is opened to further increase the power of the jet hitting the turbine runner, the speed of the generator increases as does the electrical power supplied to the grid alongside an increase in counter torque. There is a limit, however, to how much the countertorque can increase together with the speed of the induction generator. If the speed goes over this limit and the so-called pushover torque is exceeded, the power output falls, countertorque or load on the turbine suddenly decreases, and the turbine overspeeds (Figure 13.18). Automatic shutting down of the turbine through the use of jet deflectors or similar devices must be included in the system design to avoid damage to the turbine or generator from overspeeds caused either by opening the nozzle too much and exceeding the pushover torque or a tripping of circuit breakers to the grid.

13.2.3.2.2 Application of Standalone IG

Induction generators are often used as a low-cost alternative to synchronous generators in micro hydropower systems to supply power to communities away from the grid. To operate in a standalone mode, IGs need a substitute source of magnetizing current when it is not available from the grid. Externally connected capacitors can provide the magnetizing current required for the build-up of a rotating magnetic field. Capacitors at the output terminals of an induction motor allows for a voltage build-up when the shaft is rotating.

To understand how the standalone IG achieves excitation, the circuit can be modeled as a simplified equivalent parallel circuit consisting of the magnetizing reactance X_M of the induction motor and external capacitive reactance X_C. The magnetizing current, I_M, is equal to the capacitor current, I_C, with the induction machine and capacitors acting as a resonant circuit at angular frequency, ω, depending on the speed of the shaft. Assuming sufficient capacitance is connected, the current and voltage will keep increasing until the magnetizing impedance is equal to capacitive impedance as can be seen from Equations 13.25 and 13.26 [5].

$$\frac{1}{\omega C} = \omega L_M \tag{13.44}$$

The initial voltage is generated from the residual magnetism remaining in the rotor from the previous operation.

Figure 13.21 shows where the magnetization curve and the capacitance lines cross, which is the operating point, with V_{op} being the output voltage of the IG. Stable operating points exist because magnetic saturation of rotor and stator steel result in current increasing nonlinearly beyond a certain voltage. Magnetizing reactance is seen to decline with increasing current.

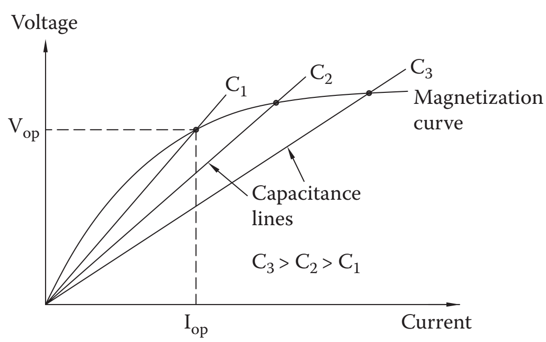

FIGURE 13.21 Magnetization curve versus capacitance lines.

The magnetization curve shows the relationship of the voltage versus the current for magnetizing reactance X_m for the induction motor. The curve can be plotted by increasing the voltage across the terminal of the unloaded motor in steps and measuring the resulting current.

The capacitance line is a plot of Ohm's law:

$$V = IX_C$$

and X_C is the slope of the straight line. Because $X_C = \frac{1}{\omega C}$, a lower capacitance would provide a larger slope, X_C, and hence a steeper line.

The larger the value of C, the lower the slope of the capacitance line and the higher the operating voltage. Using higher capacitance for excitation has one major advantage. By operating further along the magnetizing curve, deeper into the saturation range, the IG is more stable, being able to absorb changes in external loads, including some reactive loads, without a big change in output voltage. However, there are disadvantages of using higher excitation capacitance. One is that more current will flow into the machine, resulting in I^2R losses in the stator. Another is that this loading reduces the IG's power rating as a generator.

Figure 13.22 shows star and delta capacitor connections to convert a star-connected induction motor into a three-phase generator. As the calculations below show, connecting the capacitors in delta requires one third the capacitance of the star connection. The induction generator can supply single-phase loads using the star connection point as the neutral. However, it is not recommended to connect the star point of the capacitors to the system neutral as this will result in waveform distortions and high losses [5].

The voltage rating of available induction motors is an important consideration when converting to standalone IMAGs. In many cases, the motor can be used directly as a generator whereas, in others, modifications may need to be made. Table 13.3 provides standard voltages on available small 50 Hz and 60 Hz induction motors.

Small 60-Hz machines whose nameplates specify 115/200 V indicate that they can be run either in 115 V delta or 200 V star as shown in Figure 13.23. Most manufacturers provide access to all

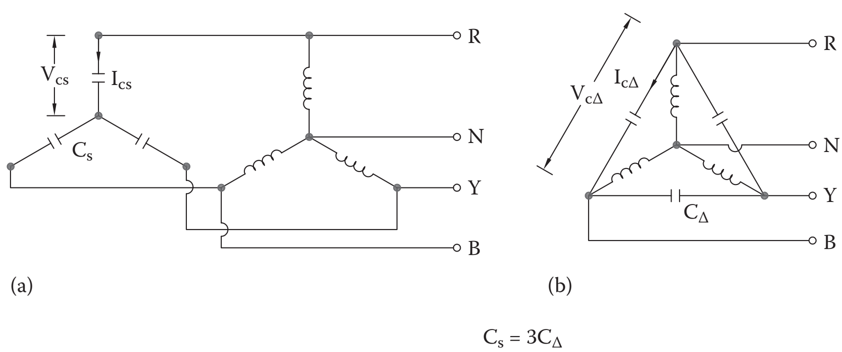

FIGURE 13.22 Excitation capacitor configurations (three-phase generator). (a) Star (s) and (b) delta (Δ).

TABLE 13.3
Standard Induction Motor Voltages in Single and Three Phases

	50 Hz	60 Hz
Single phase	220, 240	115, 277
Three phase	380, 415	200, 480

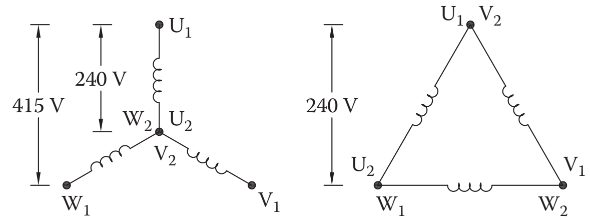

FIGURE 13.23 Star and delta winding configurations.

terminals so that the winding configuration can be altered to suit the needs of the user. The star configuration will be suitable when converting to a 200 V three-phase IMAG. Single-phase, 115 V, loads would utilize the star point as the neutral. The delta winding connection is more suitable when converting to a single-phase 115 V induction generator as described in the section below on "C-2C Connection." Small 50 Hz machines with a voltage rating of 240/415 V and typically less than 3 kW would likewise be connected in star to produce an IMAG in three-phase and in delta to produce a 240 V single-phase IMAG.

Larger induction motors are often designed to be run using a star–delta starter. The windings of these machines are rated to be operated in delta at the higher of the two voltage ratings (e.g., 200 V for 60 Hz and 415 V for 50 Hz machines). Delta-connected 60 Hz motors with a rating of 200 V are not recommended for conversion to three-phase IMAGs because they do not have a star point to serve as a neutral and Earth connection. Without the neutral, they cannot supply single-phase 115 V loads. The same is true for delta-connected, 50-Hz motors with a rating of 415 V, which would not be able to supply single-phase 240-V loads. Utilizing these motors to function as generators would require rewinding to arrive at a 200-V or 415-V star, which is expensive. A less expensive alternative to rewinding could be to reduce the operating voltage by half by reconnecting groups of winding coils to a parallel configuration [5]. The exception, when application of higher voltage IMAGs in delta might be suitable, would be if the transmission distance to the load is long and a step-down transformer is planned to be used as part of the minigrid distribution system. In such a case, generating at higher voltage saves the use of a step-up transformer.

13.2.3.2.3 Calculating the Excitation Capacitance

Calculating the exact capacitance required to generate a particular voltage over a range of loads requires accurate information about the particular induction motor, which needs to be measured using expensive equipment. When IGs are used for smaller micro hydropower systems in which a certain degree of variation of the frequency is acceptable, practical ways to estimate the capacitance include using the manufacturer's published data or taking simple measurements of the operating motor. Starting with this first estimation, the capacitance can be increased or decreased to get the required voltage and frequency relationship over a sufficiently large range of loads.

a. "C" calculated using manufacturer's data

   The important parameters to consider are the full load current and the power factor rating of the motor. These parameters can be used to calculate the reactive power that the induction motor requires to operate at full load.

Using as an example the specifications of Crompton Greaves (India) for a 7.5 kW motor that is required to be converted to a standalone, star-connected induction generator:

Voltage 415, Frequency 50 Hz

Output							Efficiency			Power Factor		
kW	HP	Pole	Frame Size	FL RPM	FLC (Amps)	FLT (Kg-m)	FL	¾ Load	½ Load	FL	¾ Load	½ Load
7.5	10	4	ND160M	1460	14.0	5.00	87.0	87.0	85.0	0.85	0.81	0.73

Apparent, real, and reactive power are calculated at full load:

$$\text{Apparent power: } S = \sqrt{3} \cdot V_L \cdot I_L = \sqrt{3} \cdot 415\ \text{V} \cdot 14.0\ \text{A} = 10{,}063\ \text{VA}$$

$$\text{Real power: } P = S \cdot PF = 10{,}063 \cdot = 8554\ \text{W}$$

The reactive power can be calculated from the power triangle:

$$\text{Reactive power: } Q = \sqrt{S^2 - P^2} = \sqrt{10{,}063^2 - 8554^2} = 5301\ \text{VAR}$$

$$\text{Reactive power per phase: } Q_P = \frac{1}{3} \cdot Q = \frac{5301\ \text{VAR}}{3} = 1767\ \text{VAR}$$

If the capacitors are connected in delta as shown in Figure 13.22b, the voltage across each capacitor is the line voltage of 415 V, and the required capacitance can be computed as follows:

$$I_C = \frac{Q_P}{V_L} = \frac{1767}{415} = 4.26\ \text{A}$$

$$C = \frac{I}{2\pi f V} = \frac{4.26}{100\pi \cdot 415} = 32.7\ \mu\text{F}$$

The capacitance can also be computed using Equation 13.33:

$$C = \frac{Q}{V^2 \cdot 2 \cdot f \cdot \pi}$$

However, if the capacitors are connected in star, the phase voltage across each of the capacitors is lower by a factor of $\sqrt{3}$ compared to the line voltage under the delta configuration. Because C is inversely proportional to the square of V, the value of the capacitance required increases by a factor of three.

$$C = \frac{Q}{V^2 \cdot 2 \cdot f \cdot \pi} = \frac{1767}{\left(\frac{415}{\sqrt{3}}\right)^2 \cdot 2 \cdot 50 \cdot \pi} = 98.0\ \mu F$$

The larger capacitance required for the conversion would increase the cost of the IG. At the same time, capacitors with lower voltage rating can be used, in the star configuration, mitigating some of the higher costs.

b. "C" calculated using field measurement

If the specifications of the motor are not available, perhaps because it is an old or used motor without a name plate, another way to estimate the excitation capacitance required for conversion to an IG, is to carry out a "no load" test by measuring the current drawn by the motor without any load connected to it. The apparent power that the motor draws at no load turns out to be a good first estimate of the reactive power that the capacitors must provide for it to run as a generator at full load. To measure the no load current, a three-phase supply will be needed to power the motor and a clamp meter to measure current. It would also be helpful to have a voltmeter and a frequency meter or RPM meter to ensure that the external supply is supplying power at the expected voltage and frequency.

Example 13.9

If the no load line current when starting up a three-phase motor is 4.50 A at 415 V and 50 Hz, it can be calculated that

$$\text{Reactive power as a loaded IG} = \text{Apparent power as "no load" motor} = \sqrt{3} \cdot V_L \cdot I_L$$
$$= \sqrt{3} \cdot 415\ \text{V} \cdot 4.50\ \text{A} = 3235\ \text{VAR}$$

$$\text{Reactive power to be supplied by each capacitor} = \frac{3235\ \text{VAR}}{3} = 1078.3\ \text{VAR}$$

With the capacitors connected in delta for economy, each of the three capacitors would need to be

$$C = \frac{Q}{V^2 \cdot 2 \cdot f \cdot \pi} = \frac{1078.3}{415^2 \cdot 100\pi} = 20\ \mu F;$$

whereas connected in star, the IMAG would need three capacitors of 60 μF.

Although these two methods of estimation provide a starting point for estimating the required excitation capacitance, in practice, capacitance will need to be added or reduced to achieve the best voltage–frequency relationship for the particular IMAG, covering a range of loads. A few considerations are as follows:

- Both of the above methods of estimation will generally result in capacitance that results in generation of lower-than-rated voltage at the rated frequency when the machine is fully loaded. This happens because the capacitors are not able to provide the full current required to maintain the voltage to compensate for saturation when the machine is fully loaded. Increasing the capacitance would correct this, but the cost of doing so is that the resulting higher level of saturation will reduce both the maximum allowed loading of the generator and its overall efficiency. To avoid this, it is thus generally recommended

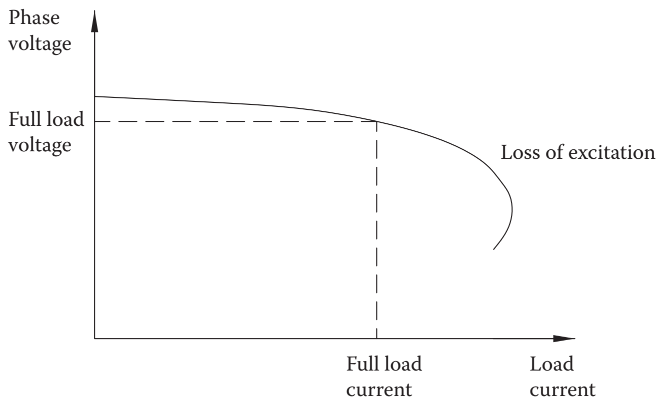

FIGURE 13.24 Voltage changing with load (constant frequency).

that IGs either be operated at higher than synchronous frequency when fully loaded to operate at the required voltage or supply power at a lower than rated voltage at the rated frequency. Higher frequency operation is as a rule safer than lower frequency operation on most appliances likely to be powered by the IG.

- The output voltage of the IG varies with the load when a constant generator frequency is maintained. When the load is fully resistive, it can be seen that the voltage declines slightly with increasing load until the full load is reached—that is, when the generator current equals the current rating as a motor. Further loading of the IG can result in the voltage dropping rapidly, ending with collapse of the excitation.

  When the added load is partially inductive, its reactive current requirement must also be supplied by the excitation capacitors. This effectively reduces the excitation capacitance available to the IG. If the generator RPM is kept constant, a more rapid decline in voltage will be seen with a lower power factor load than when the load is fully resistive. In order for the output voltage to be kept constant, at the same time that the low power factor load is increased, the generator RPM and output frequency must be increased to generate the additional *Ic* required. If the inductive load connected to the IG is too large, for example, if an induction motorload is switched on, the generator risks losing its excitation (see Figure 13.24). Standalone induction generators are generally unsuitable to supply large reactive loads unless the loads come with corrective capacitance to improve the power factor and are furthermore equipped to be soft-started.

13.2.3.2.4 Single-Phase Induction Generators

Small microgrids supplying a few homes in rural areas are often supplied with single-phase power to avoid the expense of three-phase control panels and having to balance loads between different phases of the distribution lines. However, single-phase induction motors are heavier and more expensive than equivalent three-phase motors. They also tend to be less available in larger sizes. Perhaps most importantly, single-phase induction machines are difficult to excite using externally connected capacitors. Fortunately, there are simple configurations for efficiently utilizing a three-phase induction motor as a single phase IMAG.

The simplest way to use a three-phase star-connected induction motor as a single-phase generator is to make use of only one of the phases of a three-phase induction generator as shown in Figure 13.22. Although this works, it tends to be inefficient due to unbalanced loading of the phases. This, in turn, limits the total power that can be generated for a particular size of machine.

13.2.3.2.4.1 "C-2C" Connection A more efficient way to configure a single phase IMAG using a three-phase induction machine is to connect the capacitors in a "C-2C" configuration as shown in Figure 13.25. This conversion requires the use of an induction machine rated 115/200 V connected

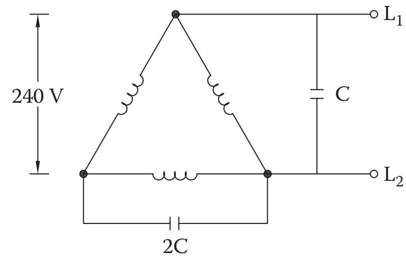

FIGURE 13.25 C-2C configuration (three-phase motor to single-phase generator).

in delta for 60 Hz (or 240/415 V rated motor connected in delta for 50 Hz). The equivalent per-phase excitation capacitance C is connected across one phase, twice this capacitance or "2C" is connected across the adjacent phase and no capacitance is connected across the third phase. As shown in the figure, the external load is connected on the phase connected to the C.

It turns out that with the C-2C configuration, the unbalanced excitation capacitance across the phases are balanced out by the external load such that the generator can be loaded on the single phase, up to 80% of the rating of the full three-phase motor [5]. One important condition for the balance to hold is that the direction of rotation of the generator should be such that the "C phase" should be ahead of the "2C phase." Whether or not the machine is balanced can be checked by measuring current into each winding. If the direction of rotation is incorrect, the windings will be loaded unevenly, leading to overheating and inefficiency. Fortunately, this can easily be corrected by changing the position of the two capacitors.

13.3 ELECTRONIC CONTROL OF HYDROPOWER SYSTEMS

Electrohydraulic governors, which remain in widespread use in hydropower plants, use the principle of proportional–integral–derivative (PID) control. Any variation from the desired output generator frequency is corrected through a feedback loop, which utilizes three key inputs—"P" for the immediate delta change from the set value, "I" for the integral of the small variations accumulated from the past, and "D" for the rate of change—to accurately arrive at the new rate of discharge, which needs to be directed to the runner. The ability of the PID-controller to incorporate the derivative "D" term enables electrohydraulic governors to minimize oscillations and is a marked improvement over the earlier hydraulic–mechanical governor.

Digital governors were developed in the late 1980s and are based on microprocessors. They utilize PID through software algorithms rather than through the use of analog electronic circuitry [5]. Digital governors are the default for new commercial hydropower installations given their higher versatility, thorough programmability, and often lower cost. Several electronic controllers have been developed in recent years for village power minigrids using both digital and analog circuits. They are a less expensive alternative to mechanical governors.

13.3.1 Electronic Load Control

In the case of isolated micro hydropower projects, it is often preferable, for cost and performance reasons, to allow the turbine to produce a fixed amount of power and keep the output frequency and/or voltage constant by controlling the load seen by the generator. This can be accomplished by substituting for the governor at the turbine end with an electronic load controller (ELC) placed right after the generator (Figure 13.26). The ELC senses the output voltage and/or the frequency of the generator and changes the size of the ballast load to keep them within an acceptable range. The sensing and varying of the ballast load can typically be accomplished within a single sine

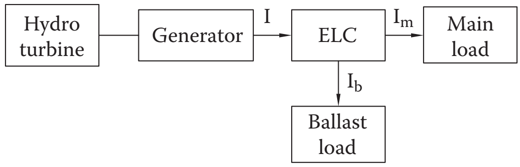

FIGURE 13.26 Electronic load control.

wave cycle following the change in external load and allows the ELC to provide voltage and frequency regulation with no noticeable delay. This speed of response is a major advantage of the ELC over the governor. Additionally, removing the need to change the discharge of water through the turbine as is done by governors to regulate power output, removes risk to the penstock pipe from water hammer.

Electronic load controllers are a popular choice for micro hydropower systems up to around 250 kW, especially for run-of-river systems without water storage. An ELC can still be used to control loads in situations in which it is important to conserve water in a head pond reservoir by lowering the power output of the turbine to conserve water during times of low power demand.

The three main ways that ELCs are designed to control the ballast load to keep the total load to the generator constant, involve (a) phase angle control, (b) relay switch on loads, and (c) mark–space ratio control.

13.3.1.1 Phase Angle Control

The current to the resistive ballast load is varied by controlling the point in the cycle at which the triac or thyristor is switched on. As shown in Figure 13.27, the ELC is able to decrease or increase the effective size of the ballast load by switching on the power to it later or earlier in each sinusoidal cycle. ELCs based on phase angle control sense the frequency from the output voltage waveform and vary the phase angle, α, sometimes also known as the firing angle, so as to change the RMS voltage to the ballast to keep the generator frequency constant. The phase angle α can range from 0° to 180° and is equal on both halves of the cycle. The ballast load typically consists of air heaters or water heaters designed to be around 20% larger aggregated over the three phases than the maximum generator output, to avoid losing control in case output of the generator exceeds the system design.

The main advantage of phase angle control is the ability of the ELC to keep the generator frequency constant within a narrow band without instability.

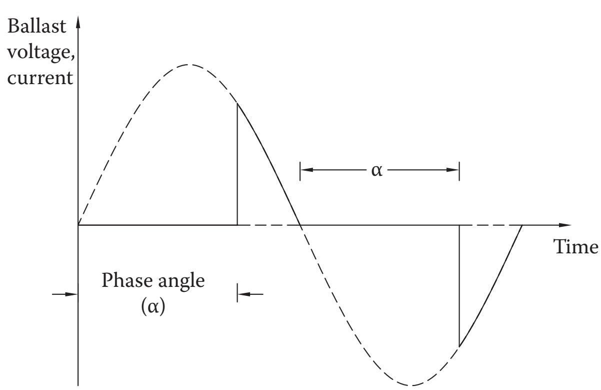

FIGURE 13.27 Phase angle control.

There are a number of disadvantages of phase angle control:

a. Switching on current to the ballast load through part of the cycle results in a variable lagging power factor. ELC's utilizing phase angle control are thus limited to use with synchronous generators. They are not used with induction generators due to the lack of suitability of IMAGs for use with significant lagging power factor loads. Furthermore, the lag in current resulting from use of the ELC reduces the amount of reactive loads that a synchronous generator can supply and still keep within its rated power factor.
b. The switching in and out of the ballast load twice in the middle of every cycle creates high frequency harmonics and waveform distortion, which, in turn, results in heating of the windings. As discussed in Section 13.2.3.1, it is recommended that generators be oversized by 20% when used with phase angle control ELCs to both compensate for the waveform distortion and to enable the generator to supply the required reactive load.
c. Distortion in the waveforms when using the ELC means that for a three-phase generator, the neutral current is not zero and the neutral cables used between the generator, ELC, and ballast load need to be as large as the other cables.

13.3.1.2 Relay Switched on Loads

ELCs can vary the ballast load by using solid-state relays to switch on and off load elements. The major advantage of relay switched ELCs is that there is no waveform distortion and no lagging power factor as a result of the electronic load control.

Some designs use binary weighted loads to arrive at different combinations of discrete resistive loads. Binary weighting of loads allows the maximum number of load steps with the fewest number of discrete loads connected.

For example, a single phase controller with four loads, 0.5 kW, 1 kW, 2 kW, and 4 kW can arrive at 15 equal load steps, from 0.5 kW to 7.5 kW at increments of 0.5 kW (Table 13.4).

TABLE 13.4
Relay Switched-On Loads

0.5 kW	1 kW	2 kW	4 kW	Total Ballast Load (kW)
1	0	0	0	0.5
0	1	0	0	1.0
1	1	0	0	1.5
0	0	1	0	2.0
1	0	1	0	2.5
0	1	1	0	3.0
1	1	1	0	3.5
0	0	0	1	4.0
1	0	0	1	4.5
0	1	0	1	5.0
1	1	0	1	5.5
0	0	1	1	6.0
1	0	1	1	6.5
0	1	1	1	7.0
1	1	1	1	7.5

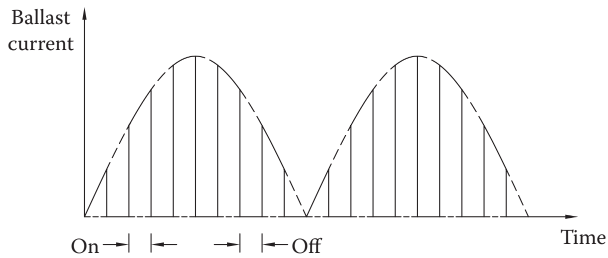

FIGURE 13.28 Mark–space ratio control.

Controller designs sometimes use fixed size loads for simplicity and ease of keeping spares. Powerflow* in New Zealand uses eight loads in its system, seven of which are sized 1 kW each and the eighth is 0.5 kW to arrive at the same 15-step control of a 7.5 kW system as above.

The major advantage of relay switched-on loads is that the generator does not need to be oversized to account for losses from waveform distortion and to compensate for a lagging power factor. The main disadvantage of relay-switched ELCs is that controlling ballast load in fixed steps means that the frequency and voltage cannot be controlled precisely but are maintained within a window. The size of this frequency window can be larger than the 1/15th (7%), in the case above, during times when actual power generation is lower than design power output, such as during the dry season when available discharge is significantly below design levels. Other inconveniences are the need to find ballast loads with accurate resistance values and the complexity of wiring multiple ballast loads, particularly for three-phase systems.

Most ELCs employing phase angle control use relays to switch on additional ballast loads to extend the size range of their controllers. This has the additional advantage of minimizing waveform distortions and lowering power factor impacts. These fixed loads can also be programmed to switch on by order of priority, which is particularly useful when the ballast loads are themselves useful appliances (see Thomson and Howe in Canada†).

13.3.1.3 Mark–Space Ratio Controller

A variation on the phase angle control ELC, which uses the mark–space ratio design, overcomes many of its drawbacks. As with phase angle control, a single ballast load can be used with a mark–space ratio controller. The controller turns the ballast load "on" (mark) and "off" (space) numerous times within a cycle to distribute the load across the cycle, thereby avoiding the problem of the lagging power factor. The switch stays on longer when the ballast load must be increased and for a shorter duration when the ballast needs to be decreased. The switching is typically done by an insulated gate bipolar transistor (IGBT) and requires the power going to the ballast to be rectified.

Figure 13.28 shows the waveform of the current from a mark–space ratio controller going into the ballast load with roughly equal time on and off.

This controller has similar advantages as phase angle control of good voltage regulation and simple configuration of the ballast load. Its major drawback is high-frequency harmonics and waveform distortion. Simple assembly, relatively low cost, little impact on power factor, and easy conversion to a three-phase controller makes mark–space ratio controllers the preferred design for controlling induction generators.

ELCs used with synchronous generators are designed to sense and regulate their frequency. Synchronous generators come with voltage regulators, and most modern generators come with automatic voltage regulators (AVR). It would be redundant for the ELC to also be trying to keep the voltage constant and could instead lead to instability. It is, however, important to make sure for lower

* http://www.powerflow.co.nz/
† http://www.smallhydropower.com/thes.html#no4

cost generators being used with an ELC that voltage regulation is sufficiently accurate such that the voltage output remains at a safe level at the ELC set frequency.

In the case of an induction generator controller (IGC), it is the voltage, rather than frequency, that the controller typically controls because IMAGs are not equipped with independent voltage regulators. When the main load is purely resistive, controlling the voltage results simultaneously in control of frequency. The moment an inductive load is applied, however, the reduced effective excitation capacitance will result in the output voltage first momentarily dropping, leading the controller to reduce the effective ballast load by reducing the width of the mark. The reduction in load on the turbine will increase its speed, and the frequency will rise until the voltage reaches the same level as before the load was applied.

13.4 TRANSMISSION AND DISTRIBUTION

Because hydropower is in widespread use for supplying power to single homes, village power applications, and to feed electricity to the end national grid, a range of systems are in place to transmit and distribute power among users. Depending on the application and size, the systems can utilize direct current or alternating current for transmission and distribution.

13.4.1 Battery Charging Systems

DC generation is selected when the system design calls for power to be generated from the hydropower site 24 hours a day and stored in batteries to be used as required. Most small-scale battery charging hydropower systems come with charge control modules, which are designed to taper off the charge current as the batteries reach full charge and dump the remaining power into ballast loads. Platypus Power from Australia describes how its charge controller improves battery life:

> The heart of the PM1000 Charge Control module is the innovative and proven B-SR50 constant voltage taper current regulator. It allows adjustable boost for maximum battery life. The Charge Control Module comes wired complete with finned dump load elements, circuit breaker, battery voltage meter, charge current meter and dump amp meter for easy installation (http://platypuspower.com.au/).

DC generation can also be preferable when hydropower is used in a hybrid arrangement with solar photovoltaic to supply a home or a community. Both sources of power are used to charge batteries with solar panels providing the bulk of the energy during the dry season and the hydro being responsible for generating energy during periods when there is sufficient flow available in the water supply. A diesel genset is used as a backup during periods when energy consumption exceeds generation from the renewable energy sources.

Figure 13.29 shows an example of a solar–hydro–diesel hybrid used to power a minigrid.

13.4.2 AC Transmission and Distribution

The majority of minigrids for hydropower-based village power systems use alternating current. The reasons for this are, first, that the most easily available appliances continue to be AC and, second, that AC is easily stepped up to higher voltages for transmission and can be stepped down for distribution through the use of transformers. Transmission lines are used to carry generated hydropower to distant loads unless the power plant is located in close proximity to the village, in which case power can immediately be distributed. The main components of the transmission and distribution (T&D) system are conductors, insulators, transformers, towers, and poles. Additional components are guy wires and lightning arresters.

Given the distances that often exist between the powerhouse and the beneficiary community, and high prices of copper and aluminum, conductors used in hydropower minigrids can constitute a

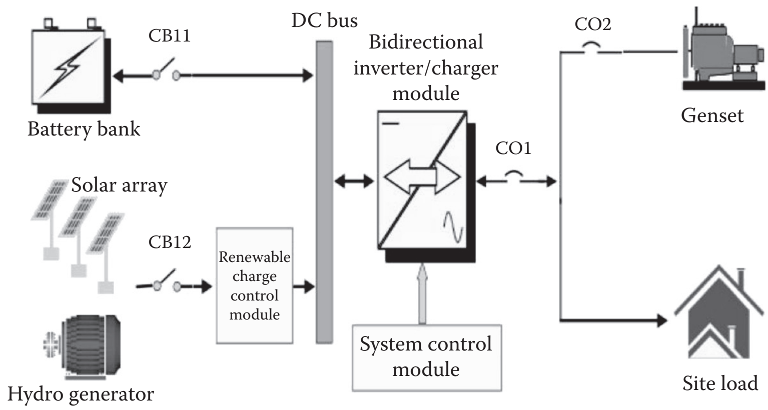

FIGURE 13.29 DC hydro generator as part of a solar–hydro–diesel hybrid. (Courtesy of Optimal Power Solutions, Australia.)

large percentage of the total project cost. It is not unusual for these costs to be a third or higher of the total project cost. As a result, a number of design considerations go into optimizing AC transmission and distribution system. The main choices in design components are the following:

a. Single-phase or three-phase transmission/distribution
b. Voltage level of transmission
c. Copper or aluminum conductors

There are four line configurations most commonly used for distributing AC power.

13.4.2.1 Single Phase Two Wire

This is the simplest and most common form of distribution when a small amount of power, typically less than 10 kW, is required to be distributed within a small radius to power domestic loads limited to lighting and small appliances. A pair of lines, phase and neutral, carry equal current to the load and back (see Figure 13.30). The neutral is grounded for safety (see Section 13.4.7). Power from a three-phase alternator or transformer is sometimes distributed to different communities through three separate single-phase networks.

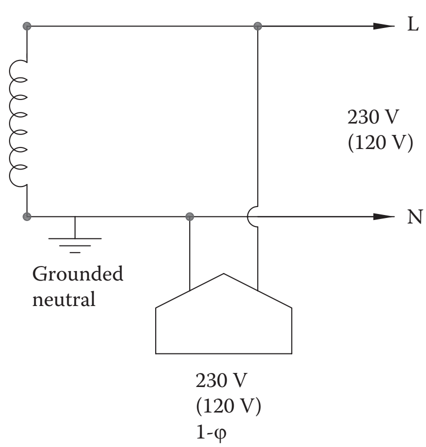

FIGURE 13.30 Single phase, two wire.

TABLE 13.5
Conductor Weight Comparison by Line Configuration

	Relative Conductor Weight Required
1-ϕ 2-wire	1.0
1-ϕ 3-wire (split phase)	0.375
3-ϕ 4-wire (wye)	0.333
3-ϕ 3-wire (delta)	0.75

If a large amount of power has to be conveyed any significant distance, however, single-phase turns out to be expensive based on required conductor weight. Table 13.5 shows that rather counter-intuitively, the three-phase, four-wire wye distribution configuration actually results in the lowest amount of conductor needed to distribute the same amount of power and by a significant margin over single-phase, two-wire distribution. Cables with higher cross-section area are required with the single-phase, two-wire distribution configuration to account for the fact that there is equal voltage drop on both the phase and neutral.

13.4.2.2 Split-Phase (Single-Phase, Three-Wire)

To overcome lower efficiency in conductor material use of single-phase, two-wire distribution, the single-phase three-wire system (120-0-120) is used in North America and Latin America as well as countries such as Japan and the Philippines. Two ends of the winding of a 240 V generator or transformer supply the phases, and the neutral is drawn from the center tap (Figure 13.31). The neutral is grounded for safety. This arrangement is referred to as a split-phase configuration. Significant reduction in conductor weight is achieved when transmitting and distributing power using this configuration. When loads are balanced on the two sides, currents that are 180° apart from each other cancel each other out, resulting in close to zero current going back on the common neutral cable. This means that the "IR" voltage drop results from the resistance on the phase cables and not from the neutral, effectively cutting down the total voltage drop, in the ideal case, to half. Additional savings come from the fact that the two halves of the circuit share a single neutral cable. As Table 13.5 shows, to achieve the same voltage drop, the weight of the cable required for the split-phase configuration can be as low as 37.5% of that required to supply the same load at the same distance using single-phase, two-wire supply.

The split-phase configuration offers the option of a low-cost enhancement to the distribution system to accommodate an increase in load over time. A single-phase, two-wire distribution system can be upgraded to a split-phase configuration to transmit 2.67 times the power without increasing the voltage drop with the addition of a third cable of the same size on existing poles. The upgraded

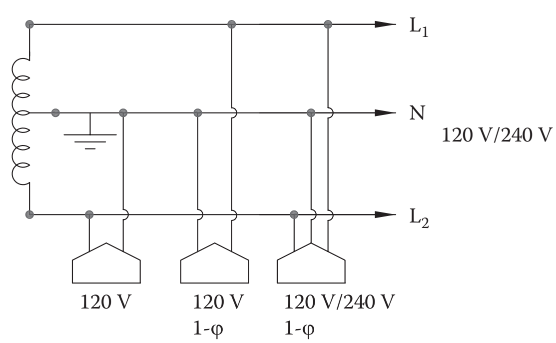

FIGURE 13.31 Split-phase: single phase, three wire.

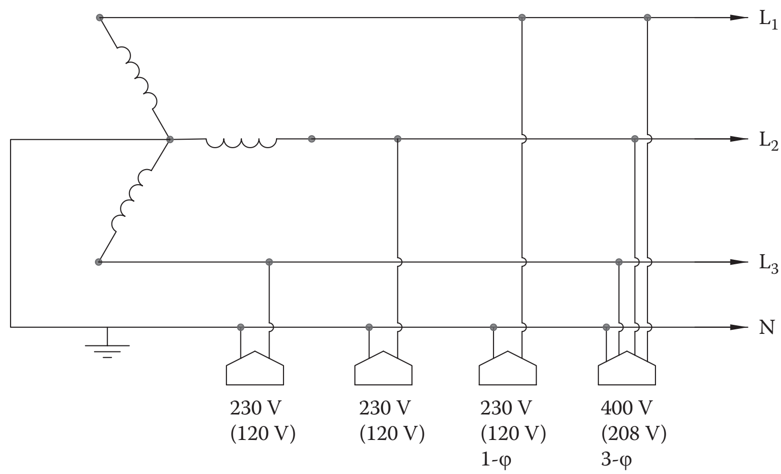

FIGURE 13.32 Three-phase wye.

split-phase configuration would have the additional advantage over the single-phase 120-V supply of being able to power larger loads such as motors at 240 V by connecting them to the two split phases. These larger loads connected to 240 V would draw half has much current in comparison to similar-sized loads being connected at 120 V. This changeover would have to be accompanied by a changeover to a higher capacity generator or transformer with a new rating for 240 V output with a center tap, to supply the new power demand.

13.4.2.3 Three-Phase Star (Four Wire)

The most widely used configuration for low-voltage, three-phase distribution and also the one that requires the least amount of conductor to transmit power, is the star configuration (Wye), using voltage levels of 230/400 V or 120/208 V as shown in Figure 13.32.

The reasons for the lower amounts of conductor required by the Wye configuration are similar to that for the split phase. Under balanced load conditions, a low neutral current means that the "IR" voltage drop is largely limited to the phase conductor, and the configuration further saves on cable by sharing a single neutral conductor for all three phases. If the load were always to be balanced between the phases, the neutral cable could actually be of smaller cross-sectional area than the phase cables. In practice, the same-sized cable is normally used for all four wires both to allow for inevitable imbalances and to also ensure that the neutral cable has equal tensile strength as the phase conductors.

Table 13.5 compares the relative amounts of conductor required for four distribution line configurations designed to result in identical percentage voltage drops. The table shows that using the single-phase, two-wire network as the basis for comparison, the three configurations with the larger number of cables actually require less conductor overall although by varying amounts. The ratios listed are calculated under ideal conditions in which loads between the phases are balanced. Unbalanced loads in real life reduce the advantage in conductor weight of the split-phase and three-phase alternatives. Furthermore, the ratios assume cables are available in a continuous range of sizes; in practice, they are available in a limited number of discrete sizes.

13.4.2.4 Three-Phase Delta (Three Wire)

Three-phase delta configuration consists of transmission/distribution lines that use three phase cables without a neutral (see Figure 13.33). The most common use of this configuration is for high-voltage transmission between transformers. The three-phase delta configuration is not as frequently used for low voltage power distribution compared to the wye.

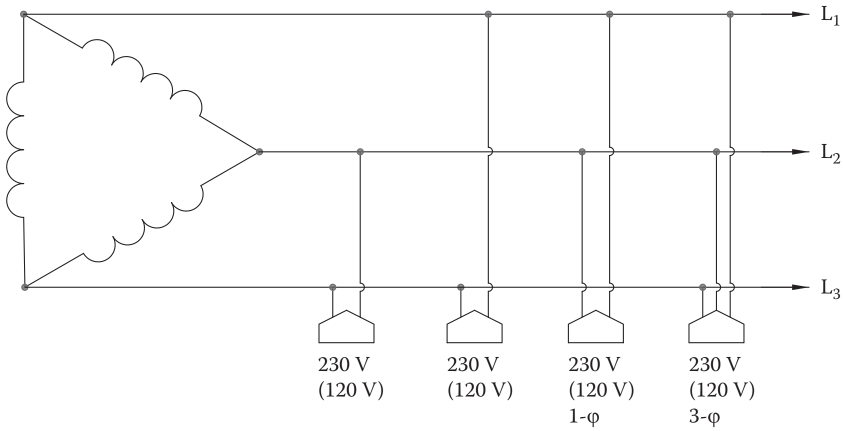

FIGURE 13.33 Three-phase delta.

As can be seen from Table 13.5, at a relative conductor weight of 0.75, the savings in conductor cost is not significant with the delta line configuration compared to the single phase two wire. The reason for larger cables for the delta configuration is that, similar to the two-wire system, there is a voltage drop in cables carrying current in both directions. Furthermore, the voltage drop is larger because line current is higher than phase current in this configuration by a factor of $\sqrt{3}$ as shown in Table 13.1. The main savings in conductor weight result from avoiding the neutral for each of the phases.

In those situations in which the power to be transferred from the hydropower project to the load is more than 50 kW or when the distances are more than a few kilometers, the voltage at which power is transmitted must be increased above the standard distribution voltage, through the use of transformers, in order to limit voltage drop and energy lost in the distribution lines while keeping the weight of the conductors affordable. In the case of hydropower minigrids, transmission voltages higher than the 230/400 V distribution voltages are typically used when the product of kVA and km exceeds 50. This threshold would be around 25 kVA.km in situations in which the distribution voltage is 120/208 V.

Medium line voltages—7.2 kV, 12.47 kV, 25 kV, and 34.5 kV—are commonly used for rural electrification in the United States, and 11 kV and 33 kV are commonly used outside the Americas. Because the best site to locate the hydro powerhouse is close to a waterfall or where the river has the highest gradient, it is seldom that the community using the power also happens to be in the same location. Transmission and distribution lines can be a major cost of the village power system, so it is important to select the system to achieve a reasonable cost without compromising the quality of power supplied or safety.

13.4.3 Transformers

Transformers are used to step AC voltage up and down depending on need. In the case of hydropower minigrids, in which the load centers are at a distance from the powerhouse, the typical configuration is to use a step-up transformer to increase the voltage output of the generator to a medium voltage for transmission and lower the voltage to the distribution voltage at each of the load centers using step-down transformers. A small hydropower system that is supplying the grid requires a step-up transformer to increase the output voltage of the generator to the voltage of the grid bus bar.

The diagram in Figure 13.34 shows the layout for a 100 kW mini hydropower project with which the power is being transmitted to clusters of communities at 11 kV and smaller step-down transformers are used to distribute the power at 230/400 V.

A transformer is able to transfer alternating current between isolated windings, coupled by magnetic induction. Figure 13.35 shows a simple transformer configuration with primary and secondary windings on the same core.

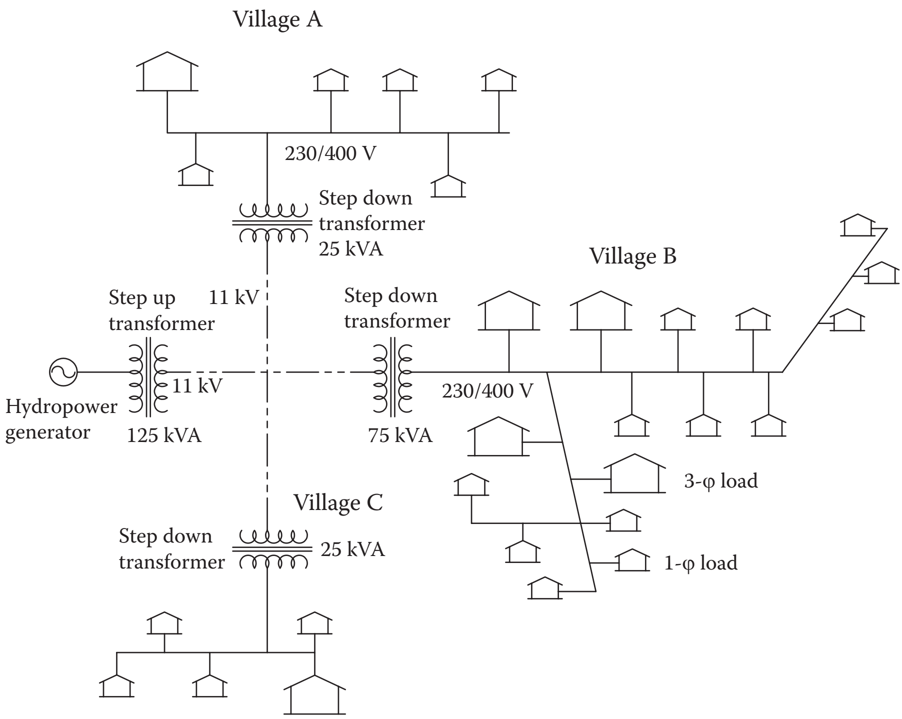

FIGURE 13.34 Transformers used in minigrid.

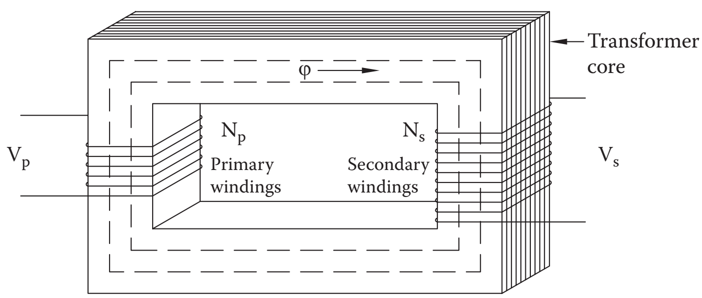

FIGURE 13.35 Simple transformer.

Applying Farday's law of induction, Equation 13.5, to the two windings, it can be seen that on the primary side:

$$V_P = -N_P \frac{d\Phi}{dt}$$

where V_P is the primary voltage, and N_P is the number of primary windings.

Similarly, on the secondary side,

$$V_S = -N_S \frac{d\Phi}{dt}$$

where V_S is the secondary voltage, and N_S is the number of windings on the secondary.

Because the magnetic flux, Φ, carried by the transformer core is the same for both windings,

$$\frac{V_S}{V_P} = \frac{N_S}{N_P} \text{ and } V_S = \frac{N_S}{N_P} \cdot V_P .$$

It can be seen that the secondary voltage can be derived by multiplying the primary voltage by the *turns ratio:* $\frac{N_s}{N_p}$. Step up transformers would thus have $N_s > N_p$, and for step-down transformers: $N_s < N_p$.

13.4.4 Conductors

Conductors are sized for the following:

a. To carry required current with an acceptable voltage drop and without overheating
b. To be strong enough to hold up their own weight and to withstand wind forces even when weighed down by ice

Although copper has higher conductivity, aluminum cables are generally favored for transmitting and distributing larger amounts of power because they are cheaper than copper conductors and are also easier to transport as they have around half the weight for the same resistance per meter. Aluminum conductor steel reinforced (ACSR) is the standard for high-capacity, high-strength stranded cable used for overhead cables. The strand of galvanized steel at the center of the bundled cable provides the high tensile strength required to both hold its weight and withstand forces from wind (see Figure 13.36). Fortunately, however, the steel strand does not impact the conductivity of the ACSR cable significantly because of what is known as the "skin effect." The skin effect refers to a nonuniform distribution of alternating current in a conductor with the current density being highest close to the surface and decreasing with depth into the core of the conductor. Because the inner steel strand of the ACSR is required to carry little current because of the skin effect, the high resistivity of steel compared to aluminum does not significantly impact the resistance of the ACSR cable.

The conductor must be sized such that the voltage drop that would result between the hydropower plant and the final users' residence is within the allowed specification. The drop in voltage between the supply at the powerhouse and the load at the end of the line is a result of both resistance and reactance of the conductor. Another factor that affects voltage drop is the power factor of the load. A low power factor results in a higher voltage drop first because of the larger current needed to supply the load and second due to a stronger contribution of the line reactance to voltage drop. Excessive voltage drop results in low power quality to consumers and can result in malfunction of equipment. Voltage drop in conductors also results in significant losses of power in the system. The anticipated voltage drop and power loss is calculated using the following steps:

a. Calculate the current at the expected power factor:

$$I = \frac{\text{Power}}{V \cdot \cos\phi}$$

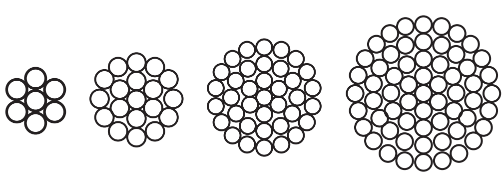

FIGURE 13.36 Stranding of ACSR cables.

b. Calculate the resistance and reactance of the conductor separately.
c. Calculate approximate voltage drop at the point of the final load:

$$\text{Voltage drop} = I \cdot (R\cos\phi + X_L \sin\phi) \tag{13.45}$$

where R is the resistance of the conductor, and X_L is its reactance. ϕ is the phase difference by which current lags voltage and can be calculated from the power factor, $\cos\phi$.

d. Power loss is simply the I^2R loss in the conductor:

$$\text{Power loss} = I^2R$$

Example 13.10

Assume a 220-V, single-phase load of 5 kW, PF = 0.8 at a community 1.0 km away from the hydro powerhouse. Because the power factor is 0.8, the current can be calculated as

$$I = \frac{5\ \text{kW}}{220\ \text{V} \cdot 0.8} = 28.4\ \text{A}$$

If Dog ACSR conductor is selected as the transmission conductor, the resistance "R" can be computed using Table 13.6:

$$R = 0.2733\frac{\Omega}{\text{km}} \cdot 1.0\ \text{km} \cdot 2 = 0.5466\ \Omega$$

The factor of two is needed to account for the total length of conductor in which the current flows, including both the line and neutral cables.

The reactance per unit length of cable is calculated using the formula [2]:

$$X = 2\pi f\left(19 + 46\log_{10}\left(\frac{s}{d}\right)\right)10^{-5}\frac{\Omega}{\text{km}} \tag{13.46}$$

where f is the frequency, s is the distance between the conductors, and d is the overall physical diameter of the conductor, both in units of meters.

It can be seen from the formula that the reactance does not depend on the material of the conductor but rather on its size and spacing from other conductors. Using the values of f = 50 Hz; s = 0.3 m and taking the value for ACSR Dog cable from Table 13.6 of $d = 14.15 \cdot 10^{-3}$ m,

$$X = 100\pi\left(19 + 46\ \log_{10}\left(\frac{0.3}{14.15 \cdot 10^{-3}}\right)\right)10^{-5}\frac{\Omega}{\text{km}} = 0.2514\ \frac{\Omega}{\text{km}}$$

The reactance of the full length of cable

$$X_L = 0.2514\ \frac{\Omega}{\text{km}} \cdot 1.0\ \text{km} \cdot 2 = 0.5027\ \Omega$$

$$\text{Voltage drop} = I(R\cos\phi + X_L\sin\phi)$$

TABLE 13.6
ACSR Specifications ASTM and British Standards

Name	Nominal Aluminum Area (mm^2)	Equivalent Copper Area (mm^2)	Stranding and Wire Diameter (no./mm)		Overall Diameter (mm)	Total Area (mm^2)			Weight (kg/km)			Calculated Breaking Load	Maximum DC Resistance at 20°C
			Alum	Steel		Alum	Steel	Total	Alum	Steel	Total	kN	Ω/km
						ASTM Sizes							
Turkey	13.3	8.39	6/1.68	1/1.68	5.04	13.30	2.22	15.52	36.5	17	54	5.28	2.1499
Swallow	26.69	16.77	6/2.38	1/2.38	7.14	26.69	4.45	31.14	73.0	35	108	10.21	1.0712
Partridge	134.90	85.03	26/2.57	7/2.00	16.28	134.90	21.99	156.90	373	172	545	50.23	0.2141
						British Sizes							
Gopher	25	16.1	6/2.36	1/2.36	7.08	26.25	4.37	30.6	72	34	106	9.6	1.0930
Rabbit	50	32.3	6/3.35	1/3.35	10.05	52.88	8.81	61.7	145	69	214	18.4	0.5426
Dog	100	64.5	6/4.72	7/1.57	14.15	105	13.55	118.6	288	106	394	32.7	0.2733

Substituting

$\cos \phi = 0.8$
$\sin \phi = 0.6$

$$\text{Voltage drop} = 28.4 \cdot (0.5466 \cdot 0.8 + 0.5027 \cdot 0.6) = 21 \text{ V}$$

The percentage voltage drop is thus $VD\% = \frac{21}{(220+21)} \cdot 100 = 8.7\%$ of the supply voltage at the powerhouse.

$$\text{Power loss} = I^2R = (28.4)^2 \cdot 0.5466 = 441 \text{ W}$$

Figure 13.37 shows the voltage drop in the single-phase distribution line while delivering 5 kW of power to a load 1 km away.

If a 8.7% voltage drop is acceptable with the corresponding power loss, Dog ACSR is sufficiently sized cable for supplying this load. If the voltage drop and power loss are deemed to be too high, a larger size cable would be selected and the calculations repeated.

Maximum voltage drops are often specified in the country's electrical code. In the United Kingdom, for example, the maximum allowable voltage drop is 6%. The trade-off in the case of a hydropower minigrid is between the extra expenditure required for a larger sized cable versus the value of energy lost each year due to power loss. If a higher voltage drop would be within the allowable threshold in the country where the project is being proposed, reducing the cost of the conductor is a priority, and the savings in energy is small in comparison with calculations carried out for utilizing a smaller size conductor. In many developing countries, a voltage drop of up to 10% of nominal voltage is acceptable at the end of the longest distribution line for hydropower minigrids, for example, *Nepal's Guidelines for Detailed Feasibility Study of Micro-Hydro Projects* [1].

The choice of conductors would be different if the same community were to be supplied in three phases. This would be possible, for example, if the micro hydropower project is electrifying a 5-kW load divided over 30 homes located in close proximity. If each home consumes roughly the same power, 10 houses could be linked to each phase. An added advantage of the three-phase supply is that the system could also accommodate a three-phase load in the community, such as an electric motor to power a rice mill.

As Example 13.11 shows, and consistent with Table 13.5, three-phase supply will lower the voltage drop and will, at the same time, reduce the total weight of conductor required and thereby minimize the total cost of the transmission line.

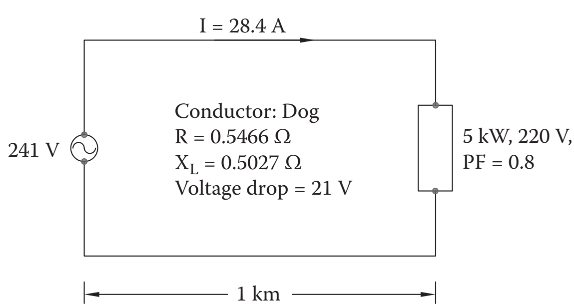

FIGURE 13.37 Voltage drop in single-phase distribution line.

Example 13.11

For a three-phase load of 5 kW rated at 220/380 V and 0.8 PF, 1.0 km away from the hydro powerhouse, select the cable required, using a three-phase, four-wire system, to keep the voltage drop below 5% and compare the total conductor required to Example 13.10 above.

The phase current for each phase:

$$I = \frac{5\ \text{kW}/3}{220\ \text{V} \cdot 0.8} = 9.47\ \text{A}$$

Because it can be expected that the new conductor to be selected can have at least three times the resistance of the ACSR conductor used for a single-phase supply, a Gopher conductor is picked to calculate the resulting voltage drop.

$$R = 1.0930 \frac{\Omega}{\text{km}} \cdot 1.0\ \text{km} = 1.0930\ \Omega$$

Note that the length of the phase conductor alone is used in a three-phase supply to calculate the total resistance because the current in the neutral cable should be close to zero provided the three phases are fairly balanced.

The reactance will change because the value of the spacing s changes. The effective spacing can be calculated as

$$s = \sqrt[3]{s_1 \cdot s_2 \cdot s_3} \tag{13.47}$$

Where s_l, s_2, and s_3 are the distances between the first and second, second and third, and third and first conductors.

$$s = \sqrt[3]{0.3 \cdot 0.3 \cdot 0.6} = 0.38\ \text{m}$$

for four vertically placed conductors.

From Equation 13.46,

$$X = 100\pi\left(19 + 46\ \log_{10}\left(\frac{0.38}{7.08 \cdot 10^{-3}}\right)\right)10^{-5}\ \frac{\Omega}{\text{km}} = 0.3097\ \frac{\Omega}{\text{km}}$$

$$X_L = 0.3097\ \frac{\Omega}{\text{km}} \cdot 1.0\ \text{km} = 0.3097\ \Omega$$

$$\text{Voltage drop} = I(R\cos\phi + X_L \sin\phi) = 9.47 \cdot (1.093 \cdot 0.8 + 0.3097 \cdot 0.6)$$

$$\text{Voltage drop} = 10\ \text{V}$$

$$\text{VD\%} = \frac{10}{(220 + 10)} \cdot 100 = 4.3\%$$

The use of three-phase transmission has resulted in improvement in the percentage of voltage drop by over a factor of two even when the weight of conductor is reduced by an amount calculated below:

Comparing the weight of conductors in the two examples:

$$\text{Weight of Dog cable (single phase)} = 1\,\text{km} \cdot 2 \cdot 394\,\frac{\text{kg}}{\text{km}} = 788\,\text{kg}$$

$$\text{Weight of Gopher cable (three phase)} = 1\,\text{km} \cdot 4 \cdot 106\,\frac{\text{kg}}{\text{km}} = 424\,\text{kg}$$

The weight of conductor required for three-phase transmission is seen to be reduced by a factor of around 1.9.

Even with roughly half the weight of the conductor being used, power loss is reduced using three-phase supply to an estimated

$$\text{Power loss per phase} = I^2 \cdot R = 9.47^2 \cdot 1.093 = 97.2\ \text{Watts}$$

$$\text{Total power loss} = 3 \cdot \text{Power loss per phase} = 3 \cdot 97.2 = 291.6\ \text{W}$$

This is around two thirds of the power loss compared to using single-phase transmission.

Two factors contribute to reduced conductor requirements and lower losses in three-phase transmission. First, only one neutral conductor is required for three phases, and second, the low neutral current means that the effective resistance comes from only the phase conductors.

Examples 13.10 and 13.11 have examined how voltage drop and power loss can be calculated to properly size conductors when the power plant is at one end and the load is concentrated at the end of the line. For the more general case, one finds when designing minigrids with which the distribution lines may have several branches, voltage drop can be calculated, using Equation 13.45, for each of the branches separately and added. Another simplification that can be made is that when consumers are distributed fairly evenly along a line, the voltage drop on that branch will be half compared to when the full load might be at the end of the line.

13.4.5 Insulators

Insulators must be able to support the conductor cable mechanically and at the same time also withstand electrical stress, including from surges from switching and lightning. They are made of porcelain, composite polymer materials, or glass and are rated for both mechanical strength and voltage. Spool or shackle insulators are used on vertical conductors with no crossbars for low-voltage distribution. Pin-type insulators, which are used for medium voltage, support conductors on a crossbar as shown in Figure 13.38. Suspension-type insulators have the conductor hanging below them, and strain insulators are designed to withstand mechanical tension from the pull of the conductor. Both suspension and strain insulators are made of insulation discs connected in series by metal links with the number of discs increasing linearly for higher voltage applications.

13.4.6 Poles and Transmission Towers

The simplest structures to carry conductors overhead for transmission and distribution lines are wood, steel, or concrete poles. Insulators are either placed along the sides of the poles or on a cross arm. High-voltage transmission lines are mostly carried on steel lattice towers.

Minimum clearance from the ground is specified for different situations to ensure safety to people and vehicles and to the power lines themselves. The pole height and spacing of poles need to be selected to conform to these clearances. The clearance needs to be significantly higher in areas traversed by vehicular traffic to make sure that loaded trucks and other tall vehicles can safely pass under the lines. Table 13.7 gives the minimum vertical clearance for low-voltage distribution lines set by NESC in the United States.

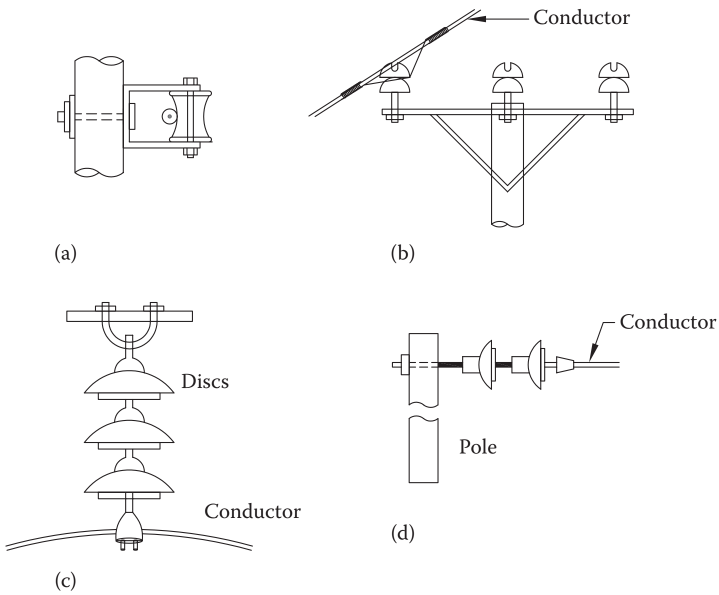

FIGURE 13.38 Insulators. (a) Spool insulator, (b) pin type insulators, (c) suspension type insulator, and (d) strain insulator.

TABLE 13.7
Low-Voltage Conductor Clearances

Clearance Category	Neutral Conductor	Insulated Phase Conductor	Bare Phase Conductor
Areas traversed by vehicular traffic	4.7 m	4.8 m	5.0 m
Areas accessible only to pedestrians	2.9 m	3.6 m	3.8 m

Source: ESMAP, *Mini-Grid Design Manual*, ESMAP Technical Paper Series 007, The Word Bank. 2000.

To calculate the length of the pole required, in addition to the ground clearance, the designer needs to take into account:

- Depth that the pole has to be entered into the ground
- Sag of the conductor
- Spacing between the conductors

The rule of thumb in general use is that the depth of the pole into the ground should be at least 0.6 m plus 10% of the length of the pole. A 7-m pole should be buried 1.3 m into the ground, for example.

The sag of the conductor depends on its weight, its span between poles, and the tension applied to it. The sag can be minimized by increasing the tension on the conductor in order to achieve the required ground clearance with a shorter and hence lower cost pole. This must be done without exceeding the strength of the conductor, however. The factors to be considered are the temperature of the conductor, its weight and additional mechanical loading from wind and ice, and the span, compared to the breaking load specification of the conductor. A rule of thumb is that the tension should not exceed 35% of the ultimate strength of the conductor at 16°C. This safety margin allows for additional forces on the conductor from the wind. The minimum sag conforming to this requirement can be computed mathematically by approximating the catenary curve of the cable as a parabola for short distances which results in the formula:

$$S = \frac{w \cdot L^2}{8H} \tag{13.48}$$

where S is the sag, w is the weight of the conductor per unit length (N/m), L is the span between the poles, and H is the horizontal force at the pole in N and is close to the tension in the conductor.

Assuming that poles are spaced 60 m apart, it can be calculated that the minimum sag that might be allowed for the Dog ACSR cable in Example 13.10 above at 16°C is the following:

From Table 13.6, it can be seen that

$$w = 0.394 \frac{\text{kg}}{\text{m}} \cdot 9.8 = 3.86 \text{ N/m}$$

To keep within the 35% limit,

$$H = 0.35 \cdot 32.7 \text{ kN} = 11{,}445 \text{ N}$$

$$S = \frac{w \cdot L^2}{8H} = \frac{3.86 \cdot 60^2}{8 \cdot 11{,}445} = 0.152 \text{ m}$$

Considering the strength of the cable as the major limitation rather than that of the pole, the Dog ACSR cable can sustain sag as low as 15 cm at 16°C when the span is 60 m. In practice, tables are available from the cable manufacturer showing the minimum allowed sag for each conductor size at different spans and for different conductor temperatures.

13.4.7 Grounding for Safety and Lightning Protection

Grounding or "earthing" an electrical system is required for safety of the system and protection of operators and users. Grounding is based on the principle that the Earth can be a reasonably good electrical conductor from point to point by virtue of the conductivity of the large cross-sectional area of soil in between and can provide an alternative pathway for dangerous currents that might otherwise flow through equipment or persons. The cross-sectional area of the soil is small in the immediate vicinity of the grounding electrode, however, and measures must thus be taken to reduce the resistance there for grounding to be effective.

A grounding rod can be driven into the ground without excavation and can prove effective as an electrode because it is likely to reach deeper, moist soil with lower electrical resistance. Grounding rods are typically 2 m long, at least 16 mm in diameter, and made of steel core for strength with thick copper plating or copper cladding for higher conductivity and resistance to corrosion compared to steel. Multiple connected rods are often used to lower ground resistance by increasing the effective surface area of the electrode. This turns out to be more effective than using a single electrode of a larger diameter. Alternatively, electrodes made of copper or cast iron plates can be used to achieve a larger surface area, in cases when the soil is shallow, but this method requires significant excavation for installation.

Voltage spikes from charge clouds and lightning discharge in the vicinity of distribution and transmission lines can travel along conductors and damage insulation of generator and transformer windings, create arcs between electronic components in powerhouse controls, or burn out appliances in residences. A low resistance electrode can convey damaging currents into the ground. Although they can't protect against a direct lightning strike, protection from short-duration high-voltage spikes can be achieved through the use of lightning arresters mounted on transmission and distribution poles and on transformers. Arresters are found on top of the pole immediately outside the powerhouse in the case of low-voltage minigrid distribution systems. Transformers are typically equipped with holders for lightning arresters. An arrester is connected to each of the phases with its other terminal connected to a common ground. Arresters are made using either metal-oxide varistors or spark gaps. High voltages induced by lightning reduce the resistance inside the varistor allowing the arrester to convey large currents directly to the grounding rod. Spark gaps work by allowing current to jump across them at high voltages to be conveyed to the ground. After the peak voltage passes, the arrester no longer allows current to flow through it, and normal voltage can resume on the phases.

The generator housing as well as other equipment enclosures and metallic surfaces inside the powerhouse need to be interconnected reliably together and bonded to the system ground. Grounding of equipment in this way ensures that all exposed surfaces are at the same potential with each other and with the ground. This reduces the likelihood of a shock to the operator, from touching surfaces at different voltage levels. At the same time, the earthing cable temporarily conveys ground fault current from any of the equipment directly to the ground, ideally tripping the associated circuit breaker and protecting the particular device if wired properly.

Electrical codes in most countries, including the National Electrical Code (NEC) in the United States, require the neutral conductor of a small hydro generator supplying a minigrid to be connected to the grounding system. The neutral conductor would also be grounded in the case of a minigrid supplied from a regional grid through a transformer. When the system neutral is grounded in this way, it is important to ground it at multiple points through the minigrid system. Consumers should also ground the housing of their equipment by bonding them to the grounded neutral conductor and ideally install a grounding rod at their own premises to provide an additional ground.

Some experts believe that where it is not specifically demanded by the country's electrical code it may be safer not to ground the neutral conductor of an isolated low-voltage minigrid used primarily for lighting and entertainment loads with little chance of users touching an energized surface [2]. They argue that such a floating system lowers the magnitude of current that might flow through someone accidentally touching a live component. In a system in which the neutral is not grounded, all conductors, phase and neutral, should be treated as live and adequately insulated. Multipole circuit breakers, which open all conductors including the neutral, should be used in case of a fault in any phase.

EXERCISES

1. Write the equation of the expected sinusoidal waveform out of a single phase AC generator rated 120 V, 60 Hz. Calculate the peak-to-peak voltage and period of each cycle seen on an oscilloscope. (Answer: V = 169.7 sin (377t); 339.4 V, 16.7 ms.)
2. If the total electrical load connected to the generator above is measured to be R = 8.0 Ω and X_L = 4.2 Ω, calculate (a) the current I, (b) the phase difference between V and I, (c) the power factor as seen by the generator. (Answer: 13.3 A, 27.7°, 0.89.)
3. A three-phase generator in a micro hydro powerhouse shows a measurement of 400 V for the line voltage and the current on phase R measures 22.8 A. Assuming that power factor is 0.85 and that the loads are balanced, calculate (a) apparent power being supplied by the generator, (b) expected voltage between phase R and neutral, (c) real and reactive power being delivered by the generator. (Answer: 15.80 kVA, 230.9 V, 12.64 kW, 9.48 kVAR.)

4. A 10-turn coil is in the path of flux, which changes in time as $\Phi = 0.6 \sin (22t)$. What is the RMS voltage and frequency generated in the coil and how does voltage change with time? (Answer: 93.3 V, 3.50 Hz; $e = 132 \cos (22t)$.)
5. How many poles will a synchronous generator need to have to produce 60 Hz AC power when it is directly driven by a Francis turbine operating at a speed of 600 RPM? (Answer: 12.)
6. What minimum kVA rating should a synchronous generator have to be to operate without overheating under the following conditions:
   Maximum load: 350 kW, 0.8 PF, controlled by a phase angle control ELC
   Maximum ambient temperature: 45°C; Altitude of operation: 1500 m. (Answer: 572 kVA.)
7. A four-pole, 50 Hz, 40 kVA induction motor has a slip of 0.05. What would its speed rating likely be as an IMAG? (Answer: 1575 RPM.)
8. A three-phase induction motor has nameplate ratings of 415 V, 50 Hz, PF = 0.80, and full load current = 12.5 amps. Estimate the capacitance required to convert this motor to an induction generator when capacitors are connected in star and delta. (Answer: three times 99.6 μF; three times 33.2 μF.)
9. The line current of an unloaded three-phase 60 Hz motor is measured to be 4.32 A at 200 V when connected in star. Estimate the "C" and "2C" capacitance required to convert this motor to a single phase 115 V induction generator. (Answer: 100 μF, 200 μF.)
10. Select the ACSR cable from Table 13.6 required to transmit 4 kW power at a 0.9 PF from a micro hydropower plant to a load 1.4 km away using line configuration: (a) 208/120 V three-phase wye; (b) 120/240 V split phase. In each case, ensure that the voltage drop is below 7 V. (Answer: (a) Dog (100 mm^2), 5.6 V; (b) Partridge (134.9 mm^2), 7.0 V.)

REFERENCES

1. AEPC, *Guidelines for Detailed Feasibility Study of Micro-Hydro Power*. Energy Sector Assistance Program, AEPC/DANIDA, 2004.
2. ESMAP, *Mini-Grid Design Manual*. ESMAP Technical Paper Series 007. The World Bank, 2000.
3. Harvey, A. and Brown, A., *Micro-Hydro Design Manual: A Guide to Small-Scale Water Power Schemes*, ITDG Publishing, London, 1993.
4. Hubert, C., *Electric Machines*. Prentice Hall, New Jersey, 2002.
5. Mesa Associates and Oak Ridge National Laboratory, Hydropower Advancement Project, Best practice catalog—Governor, 2011.
6. Smith, N., *Motors as Generators for Micro-Hydro Power*. ITDG Publishing, London, 1994.

14 Economic Analysis of Infrastructure Projects

Economic analysis is defined as a systematic approach to determining the optimum use of scarce resources, involving comparison of two or more alternatives in achieving a specific objective under the given assumptions and constraints. Economic analysis takes into account the opportunity costs of resources employed and attempts to measure in monetary terms the private and social costs and benefits of a project to the community or the nation.

In an economic analysis, the viewpoint of the entire society or the country is taken in order to improve the quality of life of the residents while providing the benefits of a particular project. In the case of a hydropower plant, the objective would be to increase the national income while providing electricity to the citizens and industries.

The economic analysis of any infrastructure project including hydropower is complex because of the following reasons:

- There are a number of intangible benefits from hydropower plants that are difficult to quantify (in terms of monetary value). For example, the availability of electricity may lead to establishment of a number of industries, which, in turn, would create demand for various raw materials, provide employment opportunities to the population (in the industries established and the power plant). It is generally difficult to predict what new industries will be established and their corresponding labor demand during the initial planning phase, especially for large hydropower projects.
- Establishment of large hydropower projects often improves local infrastructure, such as roads and communication facilities. Such infrastructure are also used by local residents who are not directly associated with the hydropower project. Furthermore, other industries established in the area will also benefit from such improved infrastructure.
- Availability of hydropower plants along with improved infrastructure will encourage more investments and may lead to establishment of better facilities, such as hospitals, schools, universities, and other facilities. These, in turn, can increase the real estate prices in the area.

The benefits that occur in an economy due to the establishment of an infrastructure project (such as hydropower) but does not increase the income of the project itself is referred to as intangible benefits. The benefits discussed above, such as increase in employment, establishment of industries, and better facilities, all positively impact the region where the project is located. However, such benefits will not increase the income of the newly constructed hydropower plant.

14.1 FINANCIAL ANALYSIS OF INFRASTRUCTURE PROJECTS

Financial analysis on the other hand tries to determine what the total cost of a project is and what the monetary benefits are over the lifetime of the project. In financial analysis, the viewpoint of the developer of the project in question is taken with an objective to earn a profit and maintain the financial soundness of the developer. Financially viable projects are often hard to come by because making a profit is the major issue, and no other factors matter unless a profit is made. For this, the developer needs to review a number of projects, conducting a financial analysis on each of them, before deciding on the one that yields maximum profit for the investment made.

An investor (or an investment company) may not be interested in the intangible benefits as these do not increase the returns on investment made on the project. However, the investor should be interested in the benefits that accrue from the project through sales of electricity generated.

Financial analysis compares revenue and expenses (investment, maintenance, and operation costs) in each project alternative and calculates the corresponding financial return ratios.

Compared to financially viable projects, economically viable projects are easy to come by as other factors (e.g., social) are also factored into the analysis. For public investment projects in the power sector, the economic soundness is a fundamental criterion for deciding whether or not to invest public funds whereas financial viability is required to ensure a sustainable project.

This chapter focuses on how financial analysis for hydropower projects is performed. As discussed earlier, economic analysis is a more complex exercise and is beyond the scope of this chapter.

14.2 BASIC CONCEPTS IN FINANCIAL ANALYSIS FOR HYDROPOWER PROJECTS

Before performing financial analysis of a hydropower plant, it is important to first understand some basic concepts. These are the following:

14.2.1 Equivalence of Kind

In the construction of a hydropower plant there are various resources involved. For example, human resources from the chief design engineer to unskilled laborers are engaged in the construction works. Summarily, concrete mixing and batching plants, excavators and dump trucks, and other machineries as well as construction materials, such as cement, reinforcement steel, and aggregates are required. All these resources have certain costs associated with them. Thus, such commensurable units used in implementing a hydropower plant needs to be converted to cost.

14.2.2 Production

Production refers to the final product (goods or services rendered) that comes out from the investment. In a hydropower project, the production is the energy (kWh) that is generated from the completed power plant.

14.2.3 Equivalence of Time

Investment in a hydropower project occurs in the beginning when the power plant is being constructed whereas the benefits will occur in the future (after construction completion) throughout the lifetime of the power plant. Thus, costs and benefits need to be brought to a similar time frame (present time or some period in the future). Converting monetary value from one time period to another is done using discounting techniques. The inherent assumption in discounting techniques is that a unit of money (say \$100) at present is worth more than the same amount sometimes in the future. Thus, \$100 a year from now is worth less than \$100 now. In other words \$100 in the future would have a discounted (lower) value at present depending on various factors, such as how far in the future will this money be realized, investment opportunities available, and the strength of the currency among others. Because money gets discounted over the years, the banks offer a certain interest rate on deposits to customers. Discounting is further discussed later in this chapter.

Because financial evaluation compares costs incurred (i.e., investments) in present time with future consequences of projects and their alternatives, its reliability depends on the ability to predict financial parameter accurately. There will always be some uncertainties with models that require predictive parameters.

14.2.4 Whose Viewpoint?

Financial analysis is generally carried out from the investor's viewpoint. The investor needs to know whether his investment in the hydropower project yields reasonable returns. If the financial analysis shows that the benefits over the lifetime of the project outweigh the investments made, then the investor may decide to implement such project. On the other hand, economic analysis is often done from the perspective of a region or the entire country where the project is situated.

14.2.5 Incremental Costs and Benefits

Sometimes, financial analysis is also done for certain components of a project. For example, if the penstock pipe diameter is increased, the total head loss would decrease, thereby generating more power (and more annual energy). However, more costs will have to be incurred to fabricate and install a larger diameter pipe. In such case, the marginal (or incremental) cost required to increase the pipe diameter versus incremental benefits from additional energy sold are compared. And if the incremental benefits (brought to present value) outweigh the incremental costs, it will make financial sense to increase the pipe diameter. This exercise is repeated until the incremental costs outweigh incremental benefits at which point the decision is made not to increase the pipe diameter further. With such incremental costs, benefit comparison is done to optimize the dimensions of all major components as well as the installed capacity of a hydropower plant. Another example in the case of a large dam project is to perform an incremental cost–benefit analysis to decide whether building an extra 10 m high dam is justified.

14.3 METHODS OF FINANCIAL ANALYSIS

For a thorough financial analysis of any project, the following comparisons have to be made:

1. Present worth comparison
2. Future worth comparison
3. Benefit–cost ratio comparison
4. Internal rate of return on investment comparison
5. Benefit–cost ratio comparison

Note that sometimes instead of present worth comparison, annual worth or future worth comparisons are also made. The results from the three analyses will be similar—that is, once the criteria for investment is set, the decision on whether to invest or not will be the same.

14.3.1 Present Worth Comparison

This comparison requires converting all cash flows to an equivalent present worth value. In order to convert cash flows of different time periods to present value, discounting factors are used.

The concept of discounting is applicable to the following:

- Cost streams (in monetary terms)
- Revenues streams (in monetary terms)
- Physical quantities, such as kWh, for a hydropower plant

When comparing multiple projects, it is extremely important to have equivalent periods of analysis (project life or the discounting period).

DISCOUNTING

Discounting is defined as the process of adjusting future values to the present. The adjustment takes place by applying a discount rate to the future value. By discounting, one finds the present worth of future amounts.

Discounted value calculation:

$$\mathbf{PV = Fx[1/(1 + i)^n]}$$

where PV = present value, i = discount rate, n = number of years, F = future value
Note: $[1/(1 + i)^n]$ is also referred to as the discount factor.

WHY DO WE HAVE TO DISCOUNT?

Discounting has to be performed in order to accurately compare and evaluate multiple long-term projects that have different cost shapes and benefit streams.

Example 14.1

A hydropower plant that has been recently commissioned is expected to earn a revenue of \$50,000 from sales of electricity in five years. Calculate the present worth of this revenue at 10% discount rate.
Solution:
Given:

F = \$50,000, n = 5, I = 10% or 0.10

$$PV = Fx[1/(1 + i)^n]$$

or

$$PV = 50{,}000\ [1/(1 + 0.10)^5]$$

or

$$PV = 50{,}000 \cdot 0.6209$$

or

$$PV = \$31{,}046.$$

Therefore, \$50,000 revenue from the power plant five years later is worth only \$31,046 at present. In other words, if \$31,046 is deposited in a bank at 10% interest rate compounded annually, the depositor would receive \$50,000 at end of the fifth year.

In a hydropower plant, revenues occur on a regular basis. The power plant may receive monthly revenue from the utility (or the consumers if it is an isolated scheme) on a regular basis. In such cases, each expected monthly revenue amount should be brought to present value using the present value equation.

Often, a power plant's revenue will be uniform, especially on an annual basis—that is, the power plant will generate about the same electrical energy (kWh) annually because the installed capacity is fixed, and long-term available flow for power generation (hydrology) should not vary significantly.

In hydropower projects, often a quick estimate of present worth of benefits is estimated assuming uniform income over the power plant's economic life. The following formula is used for this calculation

$$PV = A\left[\frac{(1+i)^n - 1}{i(1+i)^n}\right],$$

where A, in this case, is the uniform annual income received from the power plant. Other terms are as defined earlier in this chapter. Note that "A" is defined as the end-of-period cash receipt or disbursement in a uniform series continuing for n periods.

Example 14.2

An isolated micro hydropower plant that has been recently commissioned is expected to earn a net revenue of $20,000 from sales of electricity annually (after deducting annual operating costs). This power plant is expected to last 25 years. Calculate the present worth of benefits from this power plant at 8% discount rate for the entire 25 years of its operation.

Solution:

Given:

A = $20,000, n = 25, I = 8% or 0.08

$$PV = A\left[\frac{(1+i)^n - 1}{i(1+i)^n}\right]$$

or

$$PV = 20{,}000\left[\frac{(1+0.08)^{25} - 1}{0.08(1+0.08)^{25}}\right]$$

or

$$PV = 20{,}000 \cdot 10.67$$

or

PV = $213,496 (rounded to the nearest dollar)

Therefore, the present worth of benefits from the micro hydropower project is $213,496.

Example 14.1 assumed a discount rate of 10% whereas Example 14.2 assumed 8%. The question that may come up is what discount rate should one use in financial analysis? The discount rate is effectively a desired return or the return that an investor would expect to receive on some other typical proposal of equal risk. For example an investor who expects to receive 15% return on his investment in the real estate sector may not want to invest in a hydropower project if the returns are lower. Thus, such an investor would use a 15% discount rate to convert future benefits to present value. The discount rate typically includes the following:

- The “rate of time preference.” Most people prefer consumption undertaken now rather than later. Thus, a dollar available now is more highly valued than one received later.
- Uncertainty/risk. There is necessarily some degree of uncertainty as to whether a future dollar will actually be received. Its value is lessened in proportion to the expected size of this uncertainty/risk factor.

There is no single rate of return that is appropriate for every project. Therefore, discount rates used in financial analysis depend on investment opportunities in the region and the risks (physical, financial, political, security, etc.) perceived by the investor.

Once the present worth of benefits is estimated for an assumed discount rate, the decision on whether or not to invest in a project will depend on costs. If the present worth of costs is less than the present worth of benefits, then the investor may decide on implementing the project.

Net present value (NPV) is defined as the difference between the present value of benefits (PVB) and present value of costs (PVC). A positive NPV is also referred to as net present value of benefits.

$$NPV = PVB - PVC.$$

Generally, costs are incurred in a project in the present time. Therefore, unlike benefits that occur in the future, costs are not discounted, especially if the project can be constructed within a year. However, in large hydropower projects for which the construction work takes several years, then the costs would also have to be discounted. In such cases, both present work of benefits and present worth of costs are brought to the same base year.

Example 14.3

If the investment in the isolated micro hydropower plant in Example 14.2 was \$100,000 and the construction period was one year, calculate the net present value of this project.

Solution:

Recall that in Example 14.2 present value of benefits (PVB) = \$213,496

Costs have occurred within one year from start of construction and hence these do not need to be discounted. Therefore, present value of costs (PVC) = \$100,000

$$NPV = PVB - PVC = \$213{,}496 - \$100{,}000 = \$113{,}496.$$

At minimum, NPV needs to be positive for the investor to decide on implementing the project. With an investment of \$100,000, if the NPV is \$113,496, this may be a project worth investing in. The investor would most likely compare this NPV with similar investment (\$100,000) in other projects of similar risk and then reach a decision on whether or not to invest.

14.3.2 Future Worth Comparison

Unlike present worth, future worth comparison requires converting all cash flows that have occurred in the past or present to an equivalent future worth value. This is similar to the concept that when a customer deposits money in a bank account, the bank provides some interest on the deposit.

The future worth of any investment is calculated using the following formula:

$$F = P(1 + i)^n$$

where F is the future worth of the amount P invested for n years at a discount rate of i. Note that F and P are also referred to as FV and PV to denote future value and present value.

Example 14.4

If the $100,000 investment in the isolated micro hydropower plant in Example 14.3 was spread over three years as follows, calculate the net present value of this project.

Year 1: $20,000
Year 2: $50,000
Year 3: $30,000

Solution:

It is useful to make a cash flow diagram showing costs and benefits. Then all costs and benefits should be brought to a base year, which is year "0" in this case. It is assumed that the project is completed in year 0, and revenue from sales of electricity for the first year of operation (between year 0 and year 1) are booked at the beginning of year 1.

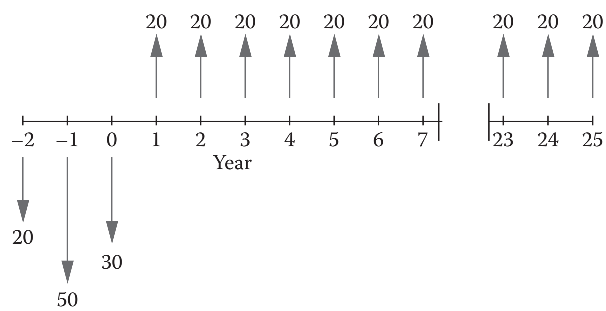

Note: all values above are in $1000

Calculations for PV costs:

For the third year of construction, which is year 0, the costs do not have to be discounted because this is the base year (or present year):

$$\text{Base year cost for year 3} = \$30{,}000$$

For costs incurred in the second year of construction, as the base year is year 0, these costs have to be brought to the future by one year. Therefore, the future worth formula should be used. In this case n = 1, I = 0.08

$$\text{Base year cost for year 2} = 50{,}000 \cdot [(1 + 0.08)^1] = \$54{,}000$$

Similarly, for the first year of construction or year 1, n = 2, I = 0.08

$$\text{Base year cost for year 1} = 20{,}000 \cdot [(1 + 0.08)^2] = \$23{,}328$$

Therefore, total costs brought to year 0 (or PV costs at year 0) = 30,000 + 54,000 + 23,328 = \$107,328

or PV costs at year 0 = \$107,328

Now PV benefits at year 0 = \$213,496 (Example 14.2)

Net present value of benefits = 213,496 − 107,328 = \$106,128

Note that in Example 14.3, when the cost of \$100,000 was incurred within one year (or benefits were realized one year after this cost), the net present value is NPV \$113,496. When the same costs were spread over three years, the net present value decreased slightly. In other words, Example 14.4 is similar to the case in which the developer burrows money from the bank and pays back both the loan and interest due in year 0.

In hydropower projects, as the developer cannot pay back the loans during the construction period (because the revenues have not yet started coming in), any interest incurred during construction (referred to as interest during construction or IDC) is capitalized at the end of construction period. The loan and the capitalized interest together are then treated as a single loan amount, which the developer pays back with interest annually from the revenue stream.

14.3.3 Benefit–Cost Ratio Comparison

The ratio of present value of benefits over present value of costs is defined as benefit–cost ratio.

Benefit cost (BC) ratio = PV benefits/PV costs. In Example 14.4, the BC ratio is 213,496/107,328 = 1.99. Obviously, it would only make sense for the developer to consider investing in a project if the BC ratio is larger than 1.0—that is, NPV is positive. Based on other investment opportunities and project implementation risks perceived, the developer needs to decide on a minimum BC ratio for investment.

14.3.4 Equivalent Uniform Annual Worth Comparison

Instead of computing equivalent present or future worth of a project, the equivalent annual costs or benefits can also be computed. In this analysis, money is converted into an equivalent uniform annual cost or benefit for a given discount rate and time period.

If the present value is known, the uniform annual worth is calculated as follows:

$$A = PV\left[\frac{i(1+i)^n}{(1+i)^n - 1}\right],$$

where A is the equivalent uniform annual worth and PV is the present value of cost or benefit.

On the other hand, if the future value is known, the equivalent uniform annual worth is calculated as follows:

$$A = FV\left[\frac{i}{(1+i)^n - 1}\right],$$

where FV is the future value of cost or benefit.

Example 14.5

Convert the net present value of benefits in Example 14.4 to an equivalent uniform annual benefit.
Solution:

Recall that in Example 14.4 net present value of benefits (NPV) = $106,128,

$$I = 0.08 \quad \text{and} \quad n = 25$$

Using the equation

$$A = PV\left[\frac{i(1+i)^n}{(1+i)^n - 1}\right]$$

or

$$A = 106{,}128\left[\frac{0.08(1.08)^{25}}{(1.08)^{25} - 1}\right]$$

or

$$A = \$9942 \text{ (rounded to nearest dollar)}$$

Therefore, a net present value of $106,128 when converted into an equivalent uniform annual benefit for a period of 25 years at 8% discount rate will be $9942.

Such equivalent uniform annual worth analysis becomes useful when two or more projects that require different investment costs (but are within the developer's investment capability) and yield different benefits over their economic lives need to be compared. Then the project that yields the highest annual worth benefit (for fixed i and n) is selected.

14.3.5 Internal Rate of Return Comparison

The internal rate of return (IRR) of an investment is the discount rate at which the present value of benefits equals the present value of the costs of the investment. Sometimes IRR is also referred to as rate of return (RoR).

IRR is therefore the discount rate at which NPV = 0 or PVB = PVC.

IRR is one of the analyses used to evaluate the desirability of investments. The higher a project's IRR, the more desirable it is to undertake the project. For example, if several projects require the same amount of investment, then the project with the highest IRR would be considered the best and undertaken first.

To calculate IRR of a project, present value of costs and present value of benefits for the same base year are calculated using various discount rates. The discount rate at which they are equal (PVB = PVC) is the IRR. When the cash flows (both costs and benefits) over the years are different, IRR calculations become lengthy. Such complex IRR calculations are done using spreadsheets or computer programs.

Example 14.6

Calculate the IRR for Example 14.4.
Solution:

Recall that in Example 14.4, for a discount rate of 8%, PVC = \$107,328 and PVB = \$213,496 and NPV = 213,496 − 107,328 = \$106,128.

Because NPV is not 0, PVB is higher than the PVC, a higher discount rate should be tried.

Try

$$I = 15\%$$

If the calculations are repeated as in Example 14.4 at i = 0.15, PVB = 129,282, PVC = \$113,950, at a 15% discount rate, the present value of benefits is still higher than the present value of costs.

Therefore, a higher discount rate should be used.

By trial and error, it can be found that at 17% discount rate,

$$\text{PV benefits} = \$115{,}324$$

$$\text{PV costs} = \$115{,}878$$

Because the PV benefits and PV costs are almost equal at a 17% discount rate, the IRR in this example is around 17%. Note that at the 17% discount rate, PV costs are slightly higher than PV benefits, and thus, the actual IRR should be somewhat lower than 17% (16.92%).

IRR is one of the analyses used to evaluate the desirability of investments. The higher a project's IRR, the more desirable it is to undertake the project. For example, if several projects require the same amount of investment, then the project with the highest IRR would be considered the best and undertaken first. When there are multiple investment opportunities, say in hydropower projects, and all of them require about the same capital investment but have different benefit streams, then the project that yields the highest IRR should be selected. Although the initial investments made are similar, due to site conditions, hydrology, and the buy back rates offered by the utility, the benefits can be different for different projects.

14.4 INVESTMENT CRITERIA

A private developer with a certain amount of investment available will try to maximize returns on his investments. As discussed earlier, the developer will invest in a certain project (such as a hydropower plant) only if the returns on his investments are at least equal (if not higher) compared to other alternatives requiring similar investment. The following financial criteria are generally used to decide whether or not investment should be made in a project:

1. *Net present value*
   a. To accept a project, its net present value should be at least positive. Based on investment opportunities available and the investment amount, the developer would decide on how high this net present value should be.
   b. Projects that have higher present value of costs than present value benefits or negative net present value should be outright rejected
2. *Internal rate of return (IRR)*
   a. The minimum criterion for investing in a project is that the IRR should be greater than the ongoing interest offered by banks on deposits—that is, as long as the IRR is equal to or less than the ongoing commercial bank interest rate, the developer

would opt to deposit his investment in a bank and earn relatively risk-free interest as the benefits. In practice, developers would compare IRR for investments in various projects (i.e., real estate or hydropower plant) and select the one that yields the highest IRR.

3. *Benefit–cost ratio (B/C ratio)*
   a. The B/C ratio should be at least greater than one to accept the project. Based on investment opportunities available and the investment amount, the developer would decide on how high this ratio should be.
   b. If the B/C ratio is less than one, the costs are higher than the benefit of the project, and therefore investment is not viable.
4. *Sensitivity analysis*

   The project cost during construction can increase for several reasons. In hydropower projects with more than two or three years of construction, the cost of materials, such as cement, reinforcement steel, or diesel, can increase, thereby increasing construction costs. Similarly, the design of certain components may have to be changed due to site conditions (e.g., geology) that were not known during the earlier stage. Such design changes may also increase the cost of the project. If part of the project's construction cost is financed through a bank loan and the interest rate increases during the loan tenure period, the total project cost will also increase. Private sector developers generally invest only part of the cost required (equity) for project construction and seek bank loans for the balance.

On the other hand, benefits from a hydropower project can also reduce due to various reasons. For example, the hydrology of the region can change, resulting in lower river flows available for power generation. Damages to the intake site due to high floods may result in having to shut down the power plant more frequently and for longer periods than planned.

Because the cost of a hydropower project (or any infrastructure project) may increase during construction and the expected benefits over its lifetime may decrease, sensitivity analysis is performed as part of financial analysis. Sensitivity analysis includes verifying the financial parameters as follows:

- If the project cost increases by a certain percentage (e.g., 10%), will the parameters such as NPV, B/C ratio or IRR still be in an acceptable range? Although these parameters will be less attractive than in the case in which the project is completed within the estimated cost, they still need to demonstrate financial viability. For example, the B/C ratio should be greater than 1.0, and NPV should be positive. Some developers may also have minimum IRR criteria in case of cost overrun.
- If the benefits from the project decrease by a certain percentage, will the above parameters still be in an acceptable range? For example, if part of the construction cost is to be bank financed, then the developer needs to make sure that the revenue generated is adequate even when the benefits decrease.
- What maximum increase in project costs together with maximum decrease in benefits can still make the project financially viable? Generally, in hydropower projects, a 10% increase in costs together with 5%–10% decrease in revenue (throughout the economic life) should still render them financially viable—that is, NPV should be positive and B/C ratio should be at least 1.0. It should also be feasible to payback any loans (with interest) taken to finance the project construction.

An example of simple financial analysis of typical small hydropower project is shown in the table below.

Example 14.7

Financial Evaluation of ABC Hydropower Project

Installed capacity	22.00 MW	Annual inflation rate	3%
Capital cost	40 MUSD	Discount rate	10.0%
Annual energy production	124.00 GWh	Sales royalty	2%
Construction period	3.00 years	Capacity royalty	USD 3
Annual cost of O and M	1.50% of the total projects cost	Income tax on net income	20.0%
Annual cost of insurances	0.80% of the total projects cost	(net income as per financial regulation of the state)	
Energy sales rate	6.50 US cents/kWh	Interest rate on bank loan	10%

	Costs			Revenue							
Year	Capital	O&M+ Insurance	Annual Cost	Gross Sales Revenue	Royalty Sales	Royalty Capacity	Sales Revenue	Income Tax	Net Cash-Flow (Total Investment)	Loan Repayment	Net Cash-Flow (Equity Investment)
2015											
2016	12.36		12.36						**(12.36)**		**(3.71)**
2017	12.73		12.73						**(12.73)**		**(3.82)**
2018	17.48		17.48						**(17.48)**		**(5.25)**
2019	–	0.60	0.92	8.06	0.16	0.07	7.83	0.02	6.89	4.56	2.33
2020	–	0.62	0.94	8.06	0.16	0.07	7.83	0.15	6.74	4.56	2.18
2021	–	0.64	0.96	8.06	0.16	0.07	7.83	0.28	6.60	4.56	2.04
2022	–	0.66	0.98	8.06	0.16	0.07	7.83	0.39	6.47	4.56	1.91
2023	–	0.68	1.00	8.06	0.16	0.07	7.83	0.49	6.34	4.56	1.79
2024	–	0.70	1.02	8.06	0.16	0.07	7.83	0.60	6.22	4.56	1.66
2025	–	0.72	1.04	8.06	0.16	0.07	7.83	0.70	6.10	4.56	1.54
2026	–	0.74	1.06	8.06	0.16	0.07	7.83	0.80	5.98	4.56	1.42
2027	–	0.76	1.08	8.06	0.16	0.07	7.83	0.90	5.86	4.56	1.30
2028	–	0.78	1.10	8.06	0.16	0.07	7.83	1.00	5.73	4.56	1.17

(Continued)

Example 14.7 (Continued)

	Costs			Revenue							
Year	**Capital**	**O&M+ Insurance**	**Annual Cost**	**Gross Sales Revenue**	**Royalty Sales**	**Royalty Capacity**	**Sales Revenue**	**Income Tax**	**Net Cash-Flow (Total Investment)**	**Loan Repayment**	**Net Cash-Flow (Equity Investment)**
2029	–	0.81	1.13	8.06	0.16	0.07	7.83	1.10	5.60		5.60
2030	–	0.83	1.15	8.06	0.16	0.07	7.83	1.12	5.56		5.56
2031	–	0.86	1.18	8.06	0.16	0.07	7.83	1.14	5.52		5.52
2032	–	0.88	1.20	8.06	0.16	0.07	7.83	1.15	5.48		5.48
2033	–	0.91	1.23	8.06	0.16	0.07	7.83	1.16	5.44		5.44
2034	–	0.93	1.25	8.06	0.16	0.07	7.83	1.17	5.41		5.41
2035	–	0.96	1.28	8.06	0.16	0.07	7.83	1.18	5.37		5.37
2036	–	0.99	1.31	8.06	0.16	0.07	7.83	1.18	5.34		5.34
2037	–	1.02	1.34	8.06	0.16	0.07	7.83	1.19	5.30		5.30
2038	–	1.05	1.37	8.06	0.16	0.07	7.83	1.19	5.27		5.27
2039	–	1.08	1.40	8.06	0.16	0.07	7.83	1.19	5.24		5.24
2040	–	1.12	1.44	8.06	0.16	0.07	7.83	1.19	5.21		5.21
2041	–	1.15	1.47	8.06	0.16	0.07	7.83	1.19	5.17		5.17
2042	–	1.18	1.50	8.06	0.16	0.07	7.83	1.19	5.14		5.14
2043	–	1.22	1.54	8.06	0.16	0.07	7.83	1.19	5.11		5.11
			46.50				**58.76**		7.17		
NPV (total investment)			7.17					NPV (equity investment)			10.90
IRR (total investment)			12.2%					IRR (equity investment)			17.1%
B/C ratio (total investment)			1.26								

The above financial analysis example is for a 22-MW hydropower plant. The monetary figures are in millions of USD. The assumptions are given in the start of the table. For example, the capital cost is 40 million USD, and the construction period is 3 years. Average annual energy generation is 123.92 GWh (124 million units). The state levies an energy sales royalty at USD 2% of gross sales and a capacity royalty of USD 3 per kW of installed capacity ($66,000/year) along with a 20% income tax on net income (gross revenue less total royalty). The project will sell electricity at 6.5 US cents per kWh throughout its lifetime (i.e., there is no price escalation factor in annual sales of electricity). The developer has invested 30% of the total project cost, and the balance is being financed by a commercial bank at 10% interest rate. This loan is to be repaid annually in equal installments in 10 years. Note that in column 2 (Capital) and column 10 (Net cash flow on total investment) the sum of annual costs is 43 million USD whereas the total project cost is 40 million USD. This is because the annual costs also include 3 million USD for interest incurred during the construction period. The bank will apply interest (at 10% per year) for the loan provided during the construction period. Because the annual loans cannot be repaid during construction, they are capitalized, and the developer pays back (with interest) from the first year of operation. Thus, the capital cost of the project is construction cost plus interest incurred during the construction period.

Based on the above parameters, the annual sales of electricity (column 4), annual royalty paid to the state, gross annual revenue (annual sales—total annual royalty paid) are calculated. Then sales revenue in column 8 is calculated as gross revenue less annual costs. As can be seen, the annual costs are high for the first three years of the construction period and then these values are lower for the subsequent operation years. During plant operation years, annual operation and maintenance costs (consumables, staff salaries, etc.), cost of insurance, and other recurring costs are included. Such annual costs increase over the years due to an increase in market price for consumables and staff salaries. An annual inflation rate of 3% is applied to increase these costs.

Net cash flow on total investment (column 10) is then calculated by deducting annual costs and 20% income tax from sales revenue. Note that annual tax is not applicable during the project construction period as there is no income during these years. Based on net cash flow on total investment column, financial parameters, such as NPV (17 million USD), IRR (12.2%), and B/C ratio (1.26) are calculated.

For the first 10 years of plant operation, the bank loans need to be repaid with interest (in equal installment). This repayment schedule is shown in column 11. The developer's investment during construction is shown in column 12 for the years 2016–2018. These values are 30% of annual costs required for construction (i.e., 70% is being financed through bank loans). The subsequent rows in column 12 are arrived at by deducting the bank loan repayment amount for the first 10 years of operation. Thereafter, the figures in column 12 are the same as those in column 10: net cash flow on total investment.

The cash flow in column 12 is referred to as net cash flow on equity investment as it presents the cash flow from the developer's perspective. For example, the first three rows of column 12 show the cost incurred by the developer during project construction phase. Similarly, the subsequent rows in column 12 are the annual benefits that the developer receives—that is, any annual benefits after paying back the bank loan with interest is the developer's profit.

As can be seen from the table, the financial parameters (NPV and IRR) are more attractive for net cash flow on equity investment. This is because the IRR on total investment is based on 25 years of plant operation whereas the interest rate applicable is 10% on 70% of the total investment for 10 years of the debt servicing period. In other words, the developer has invested only 30% of the project cost and becomes the owner of 100% of the investment after servicing the debt.

14.5 OPTIMIZATION OF INSTALLED CAPACITY BASED ON HYDROLOGY AND FINANCIAL ANALYSIS

The installed capacity of a grid-connected hydropower plant (i.e., from which all of the generated energy can be sold) is often optimized by comparing the flow hydrology along with the capital cost of the project and expected annual revenue for various installed capacities.

Once the layout of the hydropower project is tentatively fixed, then the gross head is also fixed. Thus, the installed capacity will depend mostly on the selected design discharge. Although the net head can differ based on head losses along the penstock pipe (which depend on the pipe diameter), this effect can be ignored at the initial stage when determining the installed capacity.

For a given hydropower project, as the design discharge is increased, the percentage of time the installed capacity can be generated will decrease. As the availability of flows for power generation is dictated by the river hydrology, the higher the design discharge, the less percentage of time this will be available in a given year (recall the flow duration curve or FDC that was discussed in the earlier chapters). Therefore, beyond a certain installed capacity, as the design discharge is increased, the rate of increase in annual energy generation (i.e., marginal energy generation) will start lowering. On the other hand, as the installed capacity is increased, the capital cost of the project will also increase. Thus, by comparing various installed capacities of the project with corresponding capital costs and annual energy generation and thus the annual revenue, an optimum installed capacity can be reached. The following example illustrates this process.

Example 14.8

Recall "Sizing of Tinekhu small hydropower project" in Chapter 3. In the example below, its installed capacity has been sized based on capital costs, flow hydrology, and expected annual revenue. In the table below, the second column presents the river discharge available for various months of the year. Then, the monthly generation at design discharge varying from 250 l/s to 500 l/s have been calculated at 50 l/s intervals. For each design discharge considered, the annual energy generation and installed capacity have also been calculated on the basis of the following assumptions:

Gross head = 402 m (see Chapter 3) and overall efficiency = 72%.

Furthermore, February is assumed to have 28 days and the rest of the months have 30 days.

		Energy (GWh) for Design Discharge at					
Month	**River Flow (l/s)**	**250 l/s**	**300 l/s**	**350 l/s**	**400 l/s**	**450 l/s**	**500 l/s**
Jan	236	0.482	0.482	0.482	0.482	0.482	0.482
Feb	175	0.334	0.334	0.334	0.334	0.334	0.334
Mar	122	0.249	0.249	0.249	0.249	0.249	0.249
Apr	146	0.298	0.298	0.298	0.298	0.298	0.298
May	231	0.472	0.472	0.472	0.472	0.472	0.472
Jun	1200	0.511	0.613	0.716	0.818	0.920	1.022
Jul	2400	0.511	0.613	0.716	0.818	0.920	1.022
Aug	3300	0.511	0.613	0.716	0.818	0.920	1.022
Sep	1700	0.511	0.613	0.716	0.818	0.920	1.022
Oct	700	0.511	0.613	0.716	0.818	0.920	1.022
Nov	427	0.511	0.613	0.716	0.818	0.873	0.873
Dec	325	0.511	0.613	0.664	0.664	0.664	0.664
Annual energy (GWh)		**5.414**	**6.130**	**6.794**	**7.407**	**7.974**	**8.485**
Installed capacity (KW)		**720**	**852**	**990**	**1136**	**1278**	**1420**

For each design discharge/installed capacity, the capital costs have been estimated separately. Similarly, the annual revenue and the net present value of such revenue have been estimated based on the following assumptions:

Economic life of power plant: 30 years after start of operation
Discount rate 10%
Average tariff: NPR 5.40/kWh and no escalation on tariff provided

The results of the financial analysis are provided in the table below.

Design Discharge (l/s)	Installed Capacity (kW)	Capital Cost (MNPR)	Annual Energy (GWh)	Annual Revenue (MNPR)	PV Annual Revenue (MNPR)	NPV = PV Revenue – Capital Cost (MNPR)
250	710	153	5.414	29.24	275.61	122.61
300	852	183	6.130	33.10	312.03	129.03
350	994	206	6.794	36.69	345.86	139.86
400	1136	236	7.407	40.00	377.08	141.08
450	1278	262	7.974	43.06	405.91	143.91
500	1420	291	8.485	45.82	431.92	140.92

As the design discharge (and installed capacity) increases, the annual generation will also increase up to a certain discharge. However, as the flow duration curve (FDC) indicates, as the design discharge increases, the availability of the larger flows will be for a lower percentage of time. Therefore, as the design discharge increases, the rate of increase in annual energy generation and thus the annual revenue will not continue to increase proportionally. The rate of increase in annual energy generation will start to be lower beyond a certain design discharge. In the above example, when the design discharge is increased from 250 l/s to 300 l/s the annual energy increases by 0.716 GWh (or 716 MWh). However, when the design discharge increases from 300 l/s to 350 l/s, the annual energy generation increases by 0.664 GWh. Similarly, when the design discharge increases from 450 l/s to 500 l/s, the annual energy generation increases by 0.0.511 GWh. Thus, the rate of increase of annual energy generation as a result of increase in design discharge decreases gradually.

In the financial analysis above, the present value of the annual revenue is calculated assuming a 10% discount rate and 30 years of economic life. The difference between the present value of annual revenue and the capital cost for the various design discharge range considered is shown in the last column in the table. This value is the net present value (NPV) of the project (at 10% discount rate and 30 years of economic life). As can be seen from the table, the NPV of the project is maximum at a design discharge of 450 l/s or 1278 kW of installed capacity.

Based on the NPV, what should be the design discharge or the installed capacity? As can be seen from Example 14.8, the project will yield different NPV based on what the design discharge is. The NPV gradually increases until 450 l/s design discharge and then starts to decrease. If the criteria to be adopted is to maximize the NPV, then the installed capacity should be around 1278 kW. However, if the NPV figures are further scrutinized in the table, it becomes obvious that the NPV figures do not change significantly between a design discharge of 350 l/s to 450 l/s corresponding to an installed capacity of 994 kW to 1278 kW. There is less than a 3% difference in NPV as the installed capacity changes from 994 kW to 1278 kW. On the other hand, with this change in installed capacity, the capital costs increase by 56 million NPR or around 27%. In this case, the developer may decide that it is not worthwhile to invest an additional 56 million USD to gain 3% additional NPV from the project, especially if investment capital is limited. Thus, once the financial analysis is performed, the developer may consider additional factors, such as availability of capital costs in order to decide on the installed capacity. If this evaluation is also performed on the basis of IRR (one of the exercise questions), a more complete financial picture would emerge. Furthermore, other factors such as availability of standard electromechanical equipment may also influence the installed capacity. If a 994 kW turbine generator set is not available, the developer may have to opt for 990 kW or 1000 kW installed capacity. Similarly, instead of 1278 kW installed capacity, the equipment available may dictate the capacity to be 1250 kW or 1275 kW.

14.5.1 What If a Project Is Economically, but Not Financially, Viable?

In terms of a power project, this case arises when the country is facing a power crisis, and needs immediate power in accordance with the demand, but the development of the project will negatively affect the financial situation of the developer. The solution is then to seek to modify the operating environment of the utility (revise the power purchase agreement rates, modify other government regulations). It might also be worth revisiting the project design to see if any changes can be made to decrease costs.

14.5.2 Some Complications in Financial Analysis

Because financial analysis is based on predicting benefits that occur in the future for projects that are constructed now, such analysis may not, at times, forecast financial parameters accurately. Some complications that occur in financial analysis are the following:

- Assuming a constant discount rate for future years. The investment climate can change in the future, and therefore, the discount rate assumed now may not be valid in the future.
- Similarly, an attractive project now may become marginal in the future as investments in other sectors could yield higher returns.
- Financial analysis does not consider inflation of the currency. If high inflation occurs in the currency (in which the revenue of the project is based), the project may cease to be financially attractive.
- With changes in technology, the project (hydropower or others) implemented now could become redundant prior to the end of its economic life. Other technology could provide the same output at lower costs. For example, with the introduction of digital cameras, those requiring "films" have become redundant. Similarly, postal services are shrinking worldwide as a result of people sending emails over the Internet.

EXERCISES

1. Discuss why discounting techniques are used to evaluate the financial indicators of a hydropower project.
2. An investor invests 20 million USD in year 1 and earns 6 million USD in year 2, another 7 million USD in year 3, 6 million USD in year four, and 5 million USD in year 5 (refer to Table 14.1). Calculate the NPV and IRR for this investment.
3. The capital expenditure of a hydropower project is 640 million USD at commissioning of the project. The project then starts to generate electrical energy at a rate of 2050 million units (i.e., million kWh) annually for a period of 25 years.
   a. What will be the unit cost of the electricity produced over the period at a 10% discount rate?
   b. What will be the unit price of the electricity produced if the period of operation is extended to 50 years?

TABLE 14.1
Cash Flow

Year	1	2	3	4	5
Cash flow (MUSD)	−20.0	6.0	7.0	6	5

4. If the project in Example 14.3 is delayed by 1 year and the capital cost increases by 25 million USD, and one unit of electricity generated is sold at 6.5 US cents, what is the NPV at 7% discount rate? What is the IRR of the project? Do the NPV and IRR indicate that the project is worth investing in? Why?
5. In Example 14.8, propose the installed capacity of the power plant (using the same design discharge range—that is, 250 l/s to 500 l/s) on the basis of IRR instead of NPV. Should you decide the installed capacity on the basis of NPV or IRR in this case? Discuss the difference in the results.

15 Participatory Processes in Hydropower Development

15.1 ENVIRONMENTAL AND SOCIAL IMPACTS OF HYDROPOWER DEVELOPMENT

In recent years, a number of large hydropower projects, especially those that are reservoir-based, have been mired in controversy. The issues have included social ones around displacement of populations, including indigenous people, by dams and reservoirs; negative impacts on livelihoods of downstream populations; environmental problems resulting from destruction of riparian habitat and breeding grounds of fish and dolphins and inundation of forests and loss of biodiversity; considerations relating to lost revenue from alternative economic activities, such as fisheries and whitewater rafting and canoeing; and lack of accountability and transparency, corruption, and poor governance in general. Controversies that became well known internationally toward the end of the 20th century include the Sardar Sarovar Project on the Narmada River in India, Pak Mun in Thailand, Arun III in Nepal, the Lesotho Highlands Water Project, and the Three Gorges in China. Estimates put at between 40 and 80 million the numbers of people worldwide displaced by dams and around 60% of the world's rivers as having been affected by dams and diversions.

After having dammed the majority of their rivers in the early 20th century for hydropower and irrigation development, industrialized countries have increasingly adopted legislation and witnessed movements to protect the free-flowing character of the remaining pristine rivers. The Canadian Heritage Rivers System (CHRS) is a fast-growing voluntary program established in 1984 to conserve and protect the best examples of Canada's river heritage. The Swedish government has declared four rivers as national rivers protected from any development. The Wild and Scenic Rivers Act of the United States, adopted in 1968, states the following:

> *It is hereby declared to be the policy of the United States that certain selected rivers of the Nation which, with their immediate environments, possess outstandingly remarkable scenic, recreational, geologic, fish and wildlife, historic, cultural or other similar values, shall be preserved in free-flowing condition, and that they and their immediate environments shall be protected for the benefit and enjoyment of present and future generations.*

As of 2009, the Act had protected more than 12,000 miles of 252 rivers across the United States. By comparison, more than 75,000 large dams across the country have modified at least 600,000 miles of American rivers [1]. The United States also has an active dam decommissioning movement, and hundreds of small and medium dams have been dismantled in recent years either for safety reasons, in the case of old dams, or in an attempt to revive fisheries in these rivers.*

In response to the escalating international controversies over large dams, the World Commission on Dams (WCD) was established in May 1998 with a mandate to do the following:

- Review the development effectiveness of large dams and assess alternatives for water resources and energy development
- Develop internationally acceptable criteria, guidelines, and standards for the planning, design, appraisal, construction, operation, monitoring, and decommissioning of dams

* http://www.americanrivers.org/our-work/restoring-rivers/dams/

The World Commission on Dams published its final report, entitled *Dams and Development: A New Framework for Decision-Making* in November 2000 [2]. Commentators have called the WCD a unique experiment in global policy making, using a multistakeholder process to bring together high profile commissioners representing constituencies ranging from grassroots antidam protestors to global engineering firms engaged in dam construction [3]. The report recommends that "decisions on major infrastructure developments take place within a framework that recognizes the rights of all stakeholders, and the risks that each stakeholder group is asked, or obliged to sustain." By advocating for this "rights and risks" approach, the WCD placed human rights at the center of the global dams debate and significantly reframed it in the process.

The commission proposed seven strategic priorities to provide guidance on translating the rights and risks framework into practice and offered 26 specific guidelines to assist in decision-making in weighing options for water and energy projects and for planning and operating dams. The seven priorities listed below are designed to "move from a traditional, top-down, technology-focused approach to advocate significant innovations in assessing options, managing existing dams—including processes for assessing reparations and environmental restoration, gaining public acceptance and negotiating and sharing benefits" [2].

The full report and the extensive WCD knowledge base are meant to be used by all parties involved with dams as the starting point for discussions, debates, internal reviews, and reassessments of existing procedures. The recommendations of the WCD are not binding, however [4]. In fact, several agencies responsible for dam building have rejected the report. Although no country government or bilateral/multilateral funding organization has adopted the full sets of recommendations

BOX 15.1 THE WCD'S SEVEN STRATEGIC PRIORITIES FOR DECISION-MAKING ON DAMS

- Gain public acceptance: Recognize rights, address risks, and safeguard the entitlements of all groups of affected people, particularly indigenous and tribal peoples, women, and other vulnerable groups
- Comprehensive options assessment: Identify appropriate development responses based on a comprehensive and participatory assessment of water, food, and energy needs, giving equal significance to social and environmental *and* economic and financial factors
- Address existing dams: Optimize benefits from existing dams, address outstanding social issues, and strengthen environmental mitigation and restoration measures
- Sustain rivers and livelihoods: Understand, protect, and restore ecosystems at the river basin level
- Recognize entitlements and share benefits: Use joint negotiations with adversely affected people to develop mutually agreeable and legally enforceable mitigation and development provisions that recognize entitlements and ensure affected people are beneficiaries of the project
- Ensure compliance: Ensure that governments, developers, regulators, and operators meet all commitments made for the planning, implementation, and operation of dams
- Share rivers for peace, development, and security: Initiate a shift in focus from the narrow approach of allocating a finite resource to the sharing of rivers and their associated benefits

Source: Summary from Dubash, N. et al., Multi-Stakeholder Processes: The Legacy of the World Commission on Dams. *World Resources Institute, Washington, D.C., 2003.*

and guidelines recommended by the WCD, the strategic priorities have been incorporated by a number of countries that have reviewed their procedures, and most donor organizations have substantially incorporated these priorities into their operations and investment decisions.

15.2 GAINING PUBLIC ACCEPTANCE AND SHARING BENEFITS OF HYDROPOWER WITH LOCAL COMMUNITIES

One conclusion of the WCD is that although large dams did mostly provide substantial and quantifiable economic benefits in a regional or national context, these benefits were often provided at significant cost to local people.

> The WCD Case Studies show that the direct adverse impacts of dams have fallen disproportionately on rural dwellers, subsistence farmers, indigenous peoples, ethnic minorities, and women. [2]

Large hydropower dams are constructed to generate power that is transmitted to beneficiaries who often live far from the water resources. One contributor to the WCD report observes:

> Dams are unique among large infrastructure projects in the scope and manner in which they affect the pattern of access to resources, and their distribution across space, time, and societal groups: *dams take a set of resources—a river and the lands along its banks, generating food and livelihood for local people; and transform them into another set of resources—a reservoir, hydro power and irrigation, providing benefits to people living elsewhere. There is a sense, therefore, in which large dams export rivers and lands, removing them from the productive domain of one community to make them available to another* [2].*

Two of the seven strategic priorities are particularly relevant to strengthen the participation of local people in decision making preceding dam construction and in their sustainable operation: (a) gaining public acceptance and (b) recognizing entitlements and sharing benefits.

15.2.1 Gaining Public Acceptance

Public acceptance of a proposed dam is essential if it is not to be mired in controversy and conflict during construction. The WCD observes that broad acceptance can only emerge from recognizing rights, addressing risks, and safeguarding the entitlements of all groups of affected people, particularly indigenous and tribal peoples, women, and other vulnerable groups.

The WCD highlights that public acceptance can be achieved by applying the following policy principles:

- Recognition of rights and assessment of risks are the basis for the identification and inclusion of stakeholders in decision making on energy and water resources development.
- Access to information, legal, and other support is available to all stakeholders, particularly indigenous and tribal peoples, women, and other vulnerable groups, to enable their informed participation in decision making processes.
- Demonstrable public acceptance of all key decisions is achieved through agreements negotiated in an open and transparent process conducted in good faith and with the informed participation of all stakeholders.
- Decisions on projects affecting indigenous and tribal peoples are guided by their free, prior, and informed consent achieved through formal and informal representative bodies [2].

* Reference 112: Brody, Contributing Paper for WCD Thematic Review I.1 Social Impacts, Section 5.5.

BOX 15.2 SHARING OF HYDROPOWER BENEFITS

In Brazil, Law No. 7990, dated December 28, 1989, requires that royalties be paid to the federal government for using water for power generation purposes. The royalties paid by each power plant generating more than 10 MW represent 6% of the value of the power produced. The royalties are distributed as follows: 10% to the federal government, 45% to the state(s) where the venture is located, and 45% to the municipal districts affected by the venture. The total amount paid out by the Tucurui dam in 1996 reached $19 million with the total royalties for 1991 through 1996 topping $103 million. The Itaipu Dam, in the south of Brazil, pays annually about $13 million in royalties. The royalties are among the leading sources of income for some of the municipal districts. However, royalties by themselves will not address social injustice as the way they are used to benefit local government units depends on broader political and social factors. In some cases, the allocation of these resources is done in a non-transparent way. In others, results are visible. A municipality such as Itaipulandia has paved all the roads in the city and provides agricultural supplies to the population. In addition, local young residents are funded to study at Brazilian universities on the condition that they return to the community for five years.

Source: WCD Tucurui Case Study; Itaipu dam in Ferradas, 1999, WCD Contributing Paper for Thematic Review I.1 Social Impacts (WCD, p. 127).

15.2.2 Recognizing Entitlements and Sharing Benefits

Because local residents often suffer the impacts of hydropower development, and yet economic benefits to them from its development cannot be taken for granted, equitable development requires that transparent mechanisms by which they will benefit from the development of hydropower be clearly defined beforehand. A clear set of rules for how hydropower projects will share project benefits with local residents avoids conflict with communities and can win them over from being adversaries to supporters of hydropower investment. It is not sufficient, however, for local authorities to receive financial resources from hydropower developers; it is equally important to have transparency and accountability at the local level so that project-affected populations understand clearly how they will benefit from the project investment.

Brazil and Nepal are among the few counties that have laws and policies that require sharing of hydropower royalty with local residents, but many countries do not.

Similarly, Nepal's Hydropower Policy (2001) requires the government to share 12% of the hydropower royalty paid by developers with affected District and Village Development Committees [5].

15.3 COMMUNITY MOBILIZATION

Smaller hydropower projects, particularly for supply of power to off-grid communities, typically have much smaller environmental problems; in addition, they also have the advantage that people with riparian rights are themselves the primary beneficiaries of the project. Micro hydropower projects are often developed as a community activity. Because the water resources belong to the community, and benefits of the project are often shared by community members. For the project to be constructed in a cooperative atmosphere and managed sustainably, it must be the outcome of a process of participatory decision making. The community mobilization must be a transparent process that assists the community to come to an open, participatory decision on whether or not to develop the energy project; if the decision is positive, this is followed by organizing the community for resource mobilization, construction, and sustainable operation. An effectively implemented community mobilization process should result in building up social capital within the community alongside the construction of the energy project. When executed well, the mobilization process should have a transformative effect such that the community comes out stronger and more cohesive, in the process of project implementation, and enabled to take on bigger development challenges in the future.

Implementation of a micro hydropower minigrid is challenging—both in its technical design and in the required social mobilization. Thus, few rural communities are able to implement these projects by themselves without specialist assistance. Successful community-based hydropower projects have generally been supported by specialist organizations as part of dedicated programs. Community mobilization is generally carried out by a community-based organization (CBO) or a nongovernmental organization (NGO) as part of the program that is helping the community to develop the hydropower project.

Mobilization of the community to commence a micro hydropower project typically follows these steps:

1. Support the community to list their needs and priorities and to select a committee of representatives to act on behalf of the community to execute development projects.
2. If energy is identified as the highest priority for investment, carry out a participatory needs assessment, and an analysis of all energy options available to the community.
3. Carry out a survey and feasibility study after confirming that the decision to proceed with a hydropower project has come after a full discussion of all options.
4. Discuss a detailed terms of partnership with the community representatives that divides up the tasks and responsibilities between the community and the supporting program.
5. Hold a general meeting with all beneficiaries at the conclusion of which the terms of partnership will be signed between the program and the community.

The full process of mobilizing the community can take from a few months to more than a year. It is not uncommon for conflicts to arise over water rights and right of way issues during the dialogue process. The results of the feasibility study can sometimes throw up challenges if the available potential power that can be produced from a particular site is too small to meet the full needs of the community or if the cost estimation comes out to be unaffordable. During step 3, a sustainable tariff that beneficiary households must pay for the energy has to be determined and agreed upon (see Chapter 12 on tariff determination), and this can sometimes present challenges, and community members might find this too expensive.

Community mobilization itself has costs both in financial resources and time. When done well, the benefits almost always outweigh these costs. The time and effort it takes at the start of the project to carry out the above steps is generally paid back in smooth operations. One of the biggest benefits is that this results in an inclusive process and all community members, rich and poor, stand to benefit from the project. Beneficiary households participate in construction through contribution of labor and cash, based on their capabilities, and in return all receive electricity. Tariff tends to be kept lower for households that use little electricity through a life-line tariff.

A number of development projects, which are holistic in their approach and carry out a range of rural development projects in the same communities, have used community hydropower projects as the basis for building up social capital, for example, the Rural Energy Development Program (REDP) in Nepal and Aga Khan Rural Support Program (AKRSP) in Northern Pakistan. These organizations have found that hydropower projects bring communities together because of the attraction of electrification. Compared to other renewable energy technologies, such as solar home systems, which lends itself to individual ownership, hydropower provides both the challenge and a unique opportunity for community participation.

Nepal's Rural Energy Development Program (REDP) follows a four-stage community mobilization process:

BOX 15.3 AKRSP—COMMUNITY DIALOGUE

The project follows a three-part dialogue process with the local communities.

In the First Dialogue, communities are briefed about the nature of the hydropower project, the intended outcomes, and mutual obligations between AKRSP and the communities. Once there is initial agreement, the technical staff of AKRSP work with the community representatives to assess the available water resources, survey potential sites, and prepare cost estimates. The outcome of this informs the Second Dialogue, which consists of the conducting of the feasibility study. Survey results and cost estimates are presented to the full meeting of the Village Organization (VOs), and detailed Terms of Partnership (TOP) are discussed, and agreement reached. A design and cost estimation of the project is completed based on the feasibility study. Following this, a general meeting of the beneficiary community will be called upon in the village premises to initiate the project (Third Dialogue). During the Third Dialogue, terms of partnership (ToP) will be signed between AKRSP and the beneficiary community, and the first installment of the project cost will be paid and deposited in the project account opened by the community.

Stage I: Formation of Community Organizations (COs): REDP appoints a social mobilizer in each village development committee (VDC) in which it is active. The mobilizer visits every household in the VDC and also meets with local community leaders and government representatives, such as the VDC chairperson, to create awareness about the REDP program and its objectives and principles. Public meetings are organized of clusters of households, which could potentially form a community organization* (CO), for which it is mandatory for at least one male and one female member from each beneficiary household to be present. COs are established during the second meeting, and a chairperson and manager are elected.

Stage II: Formation of Micro Hydro Functional Group[†] *(MHFG):* Mature COs are encouraged to organize themselves into micro hydro functional groups (MHFGs). At least two COs, one female and one male, are necessary in order to form a MHFG. All participating beneficiary COs contribute to a representative management committee. Functional groups for alternative energy, such as biogas, solar energy, and improved cooking stoves, can also be established at this time. Additional functional groups are formed in collaboration with COs working in forest, irrigation, drinking water, skills development, etc., according to need and resources available. It is mandatory for all members of the functional group to attend the monthly meetings during which management committees of functional groups submit their progress reports and make decisions about future activities.

Stage III: Legal Recognition: After six months of successful operation of the MH plant, the group is registered as a legal entity. Elected representatives at the district and village levels and community members discuss and decide on a legal registration for the group. Possible

* A community organization (CO) is an organization of people living in close proximity, sharing common interests, and willing to work together for common goals. Separate COs are formed for men and women in each community and require the participation of at least one male and one female member from each beneficiary household. All decisions are made by consensus during weekly CO meetings. This organization also runs adult education classes for the members.

† A functional group (FG) represents collaboration between two or more community organizations to achieve a specific objective, such as the construction of a micro hydropower project. A management committee is formed to operate and maintain the micro hydro project with proportional representation by members of all participating COs. The committee makes decisions about electricity distribution, electricity tariff, employee management, operation, and maintenance of the micro hydro project.

registration options include nongovernmental organizations (NGOs), cottage industries, companies, a multipurpose cooperative, or a micro hydro cooperative. Most functional groups register as a micro hydro cooperative.

Stage IV: Internalization: For long-term sustainability of the MH schemes, communities receive technical and business-related training and are empowered to operate and maintain the scheme by themselves. Responsibilities of the social mobilizers are gradually handed over to the community.

15.4 GENDER ASPECTS OF VILLAGE HYDROPOWER DEVELOPMENT

Hydropower benefits both men and women and sometimes in different ways. Dhanapala in her Sri Lanka study, "Report on the Gender-Related Impact of Micro-Hydro Technology at Village Level," observes that "women tended to see the benefit of electricity largely in terms of reducing their workload, health, and reduced expenditure whereas men saw benefits in terms of leisure, quality of life and education of children" [6].

A number of studies show that benefits of village hydropower to men and women depend on the type of end uses that are promoted alongside the energy investment. Applications that reduce their workload are particularly appreciated by women. The supply of electricity or mechanical power from hydro provides direct benefits to women when it is used to mechanize drudgery-intensive tasks, such as agro-processing—milling rice, grinding grain, pressing oil—which are often women's tasks in traditional societies. In some areas, hydropower has also been used to replace firewood and time spent on collecting firewood has been reduced—often the task of women and girls.

Other applications of hydropower that benefit women are those that are aligned with existing skills and income-generating activities of the type in which women typically invest. In the case of Sri Lankan villages, Dhanapala points to sewing, *beedi* wrapping, incense stick making, and cinnamon peeling as fitting this category [6]. Weaving carpets and making handicrafts are other activities that women often take up with the advent of electricity. She also notes that there is a large difference in the levels of participation by men and women in the development of village hydropower systems. Men participate much more actively in decision making, project planning, construction, and in operation and maintenance of village hydropower systems than women do.

A number of micro hydropower programs have demonstrated that benefits to women can be increased significantly with a more holistic approach to hydropower that included women's empowerment as well as other components, such as support for income generation and adult literacy. The study, "A Report on the Assessment of REDP: Impacts and its Contribution to Achieving MDGs," [7] was able to bring out a number of linkages between the micro hydropower project and empowerment of women as a result of the holistic approach that the project takes in Nepal. The report found positive impacts of the project on (a) increases in girls' education, (b) a more balanced division of work between men and women, (c) increases in women's involvement in community and social activities, (d) increased women's leadership, and (e) more balanced access and control over community resources between women and men. The study attributes these achievements to significant investment into community mobilization, which precedes all micro hydropower investments, under the REDP program and to a key element within community mobilization to encourage women's participation in public life and to provide them a voice in community affairs.

From the project initiation phase, REDP sensitizes the community members to recognize the central role played by women in the household and in the economy. The community mobilization process encourages women's participation in public life and provides them a voice in the affairs of the community. These actions instill confidence, increase self-reliance and self-esteem, encourage leadership, demonstrate women's management capabilities, and enhance the credibility of women. The men realize and accept them as equal partners in family affairs as well as in development activities.

Additional support provides women more confidence and credibility. In the case of REDP, "Literacy classes and saving and credit schemes are taken as prime movers to mobilize and organize women." Once women are empowered, they can participate more strongly and demand those end uses that benefit them most. In addition to increasing the benefits to women from community hydropower projects, projects such as REDP also encourage women to participate in the construction of hydropower projects and in the overall electrification. Holistic development projects provide opportunities for women to be employed as social mobilizers in the formation of community organizations and in mobilizing labor and resources from the community in construction. Women engineers are also increasingly participating in both the design and construction of hydropower plants within hydropower programs that have prioritized gender mainstreaming.

REDP highlights the role of energy in reducing drudgery and saving working time for women. "Reducing the drudgery of rural women and enhancing their livelihoods is one of the stated outputs of the program." Mechanical milling is one of the ways women's workload is reduced. Traditional milling of rice, wheat, and corn and pressing of oil seed is labor-intensive and inefficient and often falls to the task of women in traditional societies. Electrification through hydropower brings milling technology right in the middle of the community. As mechanical milling is typically 50 to 100 times quicker than hand milling (see Chapter 1), the work is done much quicker and the mill provides an opportunity for women to socialize while they wait their turn at the mill. An additional benefit is that men are more ready to transport the load to the mill and thereby share in the work of women. The mill changes the task of milling from drudgery for women to a job that both men and women can perform. Although mills in unelectrified areas are sometimes powered with diesel engines and provide similar benefits, where resources exist, hydropower electrification is a superior alternative as having a diesel mill in the middle of the community comes with attendant noise and pollution in addition to the cost of diesel fuel.

In cultures in which men have been the traditional decision makers, unless targeted efforts are made, women's voices typically go unheard, and their priorities are ignored when it comes to community infrastructure projects. One way this has been, at least partially, addressed for micro hydropower projects is by forming a separate committee for women to get a chance to meet and formulate their priorities. The National Solidarity Program, which has constructed some 7000 energy projects at the community level in rural Afghanistan, most of them micro hydropower, has a methodology for forming women's subcommittees under the Community Development Councils (CDCs). NSP's guidelines state:

> In many communities cultural norms do not make it possible for men and women to meet. Women's voices were largely unheard in the past and their priorities were often ignored. Female members of the CDC's and/or women's subcommittees have given women a forum to meet, exchange ideas and formulate their priorities.*

Formation of separate groupings for men and women has proven to be an effective technique to enhance participation and get women's voices heard in many countries around the world. Nepal's REDP program similarly emphasizes the formation of separate community organizations (CO) for men and women. "Segregation of women and men allows women to speak up and encourages discussions of specific problems faced by women. In mixed groups, women tended to nod their heads in unison rather than genuinely participate in discussions and decisions. A lot of stress has been placed for building women's self-confidence and capability for independent action. To give them a voice in the community affairs, REDP integrates them into the decision making process, and puts them into the mainstream of the development initiatives. It is mandatory that all concerned CO have equal representation in the Functional Groups."

* http://www.nspafghanistan.org/default.aspx?Sel=26#Q6

15.5 FINANCING OF COMMUNITY HYDROPOWER PROJECTS

Isolated hydropower projects that supply remote communities are seldom able to recover the full costs of generation and distribution. The main challenge is that the plant load factor is relatively low (typically in the 25%–40% range) because the unused energy during off-peak hours cannot be sold to the grid. Being able to sell only a portion of the energy that could be produced results in income from tariffs being insufficient to recover the full investment in the power plant and electrification. Communities in unelectrified parts of the country generally have low income and are outside the mainstream economy and so can generally not pay the tariff required for full cost recovery. Countries where the government and supporting NGOs or donor agencies accept that rural people have a right to electricity but should not pay tariffs higher than customers on the national grid typically provide a subsidy to cover a portion of the capital costs of construction. The standard financing modality that is used for community electrification consists of partial grant, contributed labor, and cash by beneficiary households and the remainder as a loan from a development bank. Table 15.1 shows how micro hydropower projects are financed within national or international programs in selected countries.

TABLE 15.1
Financing of Community Micro Hydropower Projects

Country	Name of Program	Financing
Afghanistan	National Solidarity Program	Block grant available for community hydropower systems equivalent to $200 per household.[a] Communities must contribute a minimum of 10% of the total project costs in either labor, funds, or materials. Social mobilization cost of $5000 per community paid to NGO "Facilitating Partners."
Nepal	Alternative Energy Promotion Center [8]	A grant is provided with a range of subsidies[b] depending on remoteness of the district where the power plant is to be built: <5 kW ranging from $1394/kW–$1719/kW 5–10 kW up to $1626–$1951/kW 10–1000 kW up to $2230–$3549/kW Productive end uses powered by micro-hydro can be supported up to $1858 per small and medium enterprise.
Sri Lanka	RERED	Up to $8000 paid to the "Developer" on achievement of defined milestones. Additional incentive up to $1000 paid to the "Developer" on achievement of economic benefit targets. $600/kW to the Electricity Cooperative Society.[c]
Pakistan	Pakistan Poverty Alleviation Fund	Up to 70% subsidy of capital costs. Communities to contribute 30% of the cost in labor and materials. Partner organizations, such as AKRSP, are paid 12% of capital costs for social mobilization and technical support to communities.
Global	UNDP GEF Small Grants	Through the Global Environment Facility (GEF) Small Grants Program, UNDP[d] has provided grants for several hundred community micro hydro projects around the world, often in conjunction with watershed protection projects.

[a] http://www.nspafghanistan.org/default.aspx?Sel=12
[b] http://www.aepc.gov.np/index.php?option=com_content&view=category&layout=blog&id=87&Itemid=116
[c] http://www.energyservices.lk/offgrid/vhintro.htm
[d] http://sgp.dev.undp.org/index.cfm?module=Projects&page=SearchResults&SearchText=hydropower&CountryID=&RegionID=&FocalAreaIDs=&OperationalProgramIDs=&FullGrant=&RecipientType=&SearchByDate=0&StartMonth=1&StartYear=1990&EndMonth=9&EndYear=2011&ShowMap=No&StartRow=41&MaxRows=10

A number of countries in South Asia, including Nepal, Pakistan, Afghanistan, and Sri Lanka have national programs that provide grants for community managed micro hydropower projects. Pakistan's Poverty Alleviation Fund* uses a formula of 70% grant and 30% community contribution in cash or in kind for micro hydropower projects. The grant roughly covers the cost of components that must be purchased from outside the community, including the turbine, generator, and other electromechanical equipment for the powerhouse; transmission and distribution conductors and insulators; and cement and other construction material. Community contribution includes labor and local materials, such as wooden poles and local construction materials such as sand and aggregate. In Afghanistan, the National Solidarity Program (NSP) provides a subsidy of $200 per household toward equipment and construction costs. In Nepal subsidies of between $171 and $214 are provided per household with the maximum subsidy per kilowatt of power capped. Additional subsidies are provided for transportation of equipment and construction materials to remote communities and for promotion of productive end uses.

REFERENCES

1. Dandekar, P., Where rivers run free. *World Rivers Review*, June 2011. http://www.internationalrivers.org/where-rivers-run-free.
2. World Commission on Dams, *Dams and Development: A New Framework for Decision-Making*. Earthscan, London, 2000.
3. Dubash, N., Dupar, M., Kothari, S., and Lissu, T., *Multi-Stakeholder Processes: The Legacy of the World Commission on Dams*. World Resources Institute, Washington, D.C., 2003.
4. UNEP, *Dams and Development, Relevant Practices for Improved Decision Making*. UNEP-DDP Secretariat. Nairobi, Kenya, 2007.
5. Mathema, A., Guragain, S., Sherpa, N., and Adhikari, B. *Can hydropower drive green economy for Nepal: A review. Journal of Environmental Protection*, 4, 732–740, 2013.
6. Dhanapala, K. *Gender Related Impact of Micro Hydro Technology at the Village Level*. ITDG, Sri Lanka, 1995.
7. Winrock International, A report on the assessment of REDP: Impacts and its contribution to achieving MDGs. Unpublished Report. Winrock International, Kathmandu, 2007.
8. Government of Nepal, Renewable Energy Subsidy Policy. Alternative Energy Promotion Center, Ministry of Population and Environment, 2016.

* http://www.ppaf.org.pk/What_We_Do_detail.aspx?component_id=7

Index

Page numbers followed by f and t indicate figures and tables, respectively.

E

H

I

J

K

L

S